CATCHING OUR FUTURE

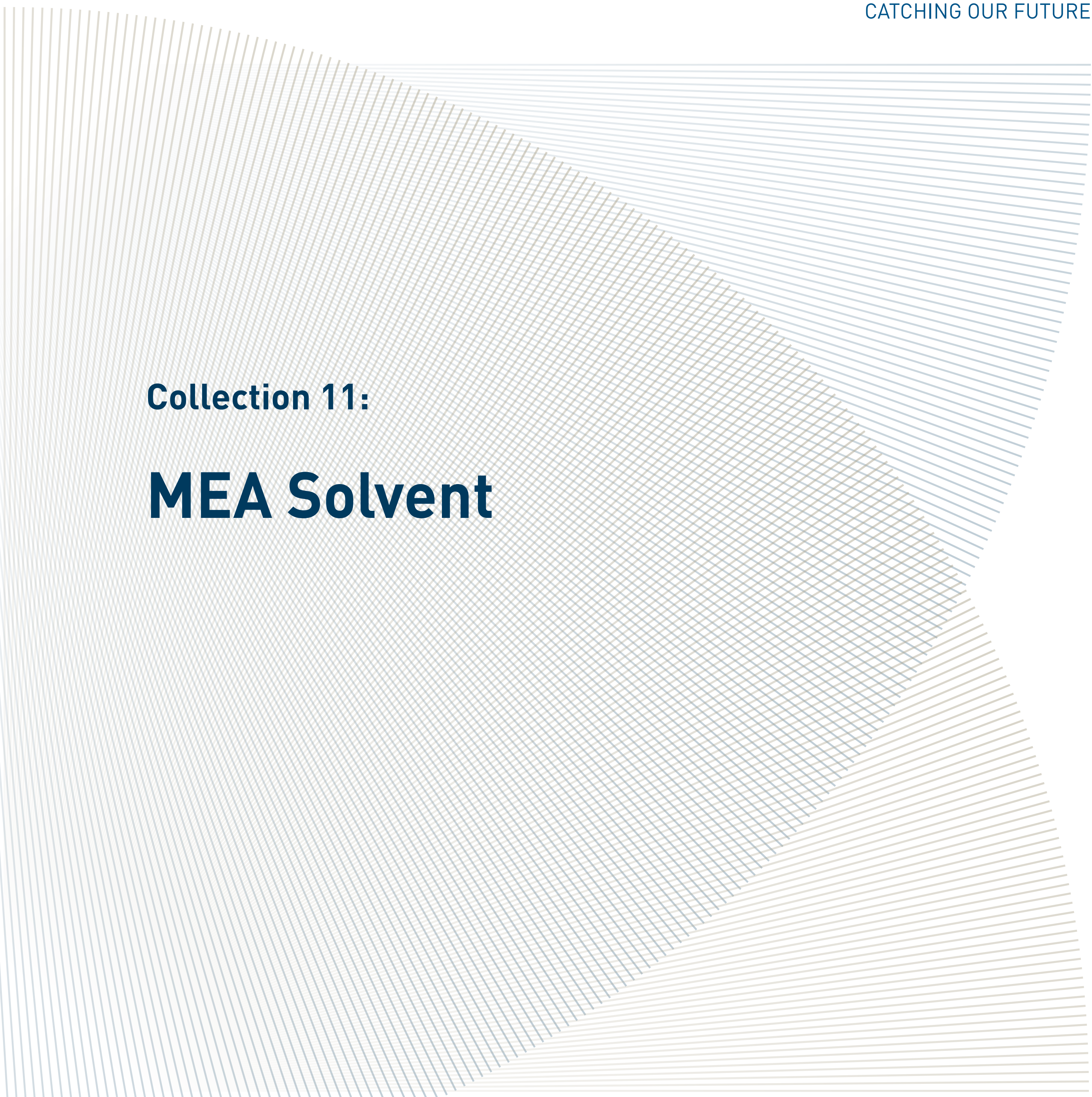

Collection 11:

MEA Solvent

2012-2022
TECHNOLOGY
CENTRE
MONGSTAD

RESEARCH PAPERS BY
TECHNOLOGY CENTRE MONGSTAD (TCM)

11 / 11

At TCM we are committed to promote the competitive deployment of carbon capture technologies to help combat climate change. We do that by supporting technology vendors to derisk at the largest scale before commercialization and by providing invaluable knowledge to project owners throughout their project cycle.

The owners' intentions

«We see an increasing interest for testing at TCM, and we are very pleased that we can continue our important work with testing and research necessary for the deployment of large-scale carbon capture.»

GASSNOVA

«TCM has contributed to maturing the carbon capture supplier market and will remain relevant with the increasing number of technology suppliers lining up for testing.»

equinor

«TCM plays a key role in further developing and reducing the cost of CCS – a crucial technology to help society and economies thrive through the energy transition.»

«In our climate ambition, carbon capture is key. TCM is the best platform to learn, test technologies and accelerate the technology scale up for implementation on our assets.»

TotalEnergies

11

Contents

Contents

11

Contents

CATCHING OUR FUTURE

Results from MEA testing at the CO_2 Technology Centre Mongstad. Verification of Residual Fluid Catalytic Cracker (RFCC) baseline results

(2021)

15th International Conference on Greenhouse Gas Control Technologies, GHGT-15

15–18 March 2021 Abu Dhabi, UAE

Results from MEA testing at the CO_2 Technology Centre Mongstad. Verification of Residual Fluid Catalytic Cracker (RFCC) baseline results

Scott A. Hume[b]*,Muhammad I. Shah[a], Gerard Lombardo[a],Thomas de Cazenove[a], Jane K. Feste[a], Andrew Maxson[b], and Christophe Benquet[a]

[a]CO_2 Technology Centre Mongstad (TCM), 5954 Mongstad, Norway
[b]Electric Power Research Institute, Inc, 3420 Hillview Avenue, Palo Alto, CA 94394, USA

Abstract

Technology Center Mongstad (TCM) houses a pilot-scale test facility for CO_2 capture solvents termed the “amine plant”, where multiple test campaigns have been performed on monoethanolamine (MEA). The third MEA test campaign (MEA-3) was conducted in June 2017 and several subsequent tests on MEA (MEA-4 and MEA-5) were performed, through October 2018. MEA-3, MEA-4, and MEA-5 have been the most significant collaborative test campaigns that the owners of TCM, TCM DA, have conducted since its inauguration in 2012. The large number of public, industrial, research, and academic participants involved in these campaigns have enriched the projects and ensured that the significant results will serve a broad audience. The main objective of these campaigns was to produce knowledge that can be used to reduce the cost as well as the technical, environmental, and financial risks for the commercial-scale deployment of post-combustion CO_2 capture (PCC). This includes demonstration of a model-based control system, dynamic operation of the amine plant, investigating amine aerosol emissions, establishment of residual fluid catalytic cracker (RFCC)—a flue gas emanating from a nearby Equinor refinery that emulates coal in composition—baseline performance with MEA, and specific tests targeted at reducing CO_2 avoided cost. Through the campaigns, both flue gas sources currently available to TCM were used, including the RFCC gas as well as flue gas from a nearby combined-cycle gas turbine (CCGT)-based combined-heat-and-power plant (CHP) that operates off of natural gas.

The Electric Power Research Institute, Inc. (EPRI) assessed the performance of the MEA-based process using an independent verification protocol (IVP) previously developed for the CHP flue gas [1]. The IVP provides a structured testing procedure for assessing the thermal and environmental performance of PCC processes under normal operating conditions. Based on this, methodology results were presented by Faramarzi et al [2]. The IVP was updated for use with the RFCC as this gas contains 13–14 vol% CO_2 content by volume whereas the CHP flue gas has 3.5 vol% CO_2 content. Throughout the RFCC testing, TCM DA manually collected extractive samples from the depleted flue gas and product CO_2 outlets sequentially. As part of the IVP, EPRI also assessed critical plant instrumentation at TCM for accuracy and precision error based on a comparative analysis done during testing operations and against calibration checks.

The MEA baseline process was evaluated during thirteen individual test periods over four days in May 2018. During the tests, extractive samples were taken to measure process contaminants such as aldehydes, ketones, amines, and ammonia. Sulfur oxides

---

* Corresponding author. Tel.: +1-704-595-2978, *E-mail address:* shume@epri.com

Electronic copy available at: https://ssrn.com/abstract=3821037

and nitrogen oxides were continuously monitored using Fourier-transform infrared (FTIR) analysers on the depleted flue gas and product CO_2 streams. TCM DA has installed multiple measurements of the CO_2 concentration (FTIR, non-dispersive infrared sensor, and gas chromatography) allowing comparative confirmation during the test periods. The capture rate was calculated via four methods. CO_2 recovery (overall mass balance) was evaluated and the thermal performance (energy consumption) was assessed based on measured data taken during the tests. The CO_2 capture rate achieved during the MEA RFCC testing was close to 90%, with steam reboiler duties of 3.43–3.51 GJ/tonne-CO_2, and the CO_2 gas mass balance closures were close to 100%. These data and the associated assessments, along with the results of TCM DA sampling during these tests, will be presented in this paper and will provide a new baseline case for 30 wt% MEA solvent in higher concentration flue gas capture cases. Based on this, TCM will now have two baselines covering flue gases with 3.5 vol% CO_2 (Faramarzi et al.) and with 13–14 vol% CO_2 (this project).

Keywords: CO_2 capture; EPRI; MEA; Post-combustion capture; CO_2 Technology Centre Mongstad; TCM

1. Introduction

The CO_2 Technology Centre Mongstad (TCM) is located next to the Equinor refinery in Mongstad, Norway. TCM DA is a joint venture owned by Gassnova representing the Norwegian state, Equinor, Shell, and Total. The test facility, dubbed the “amine plant”, run by TCM DA entered the operational phase in August 2012 and is one of the largest post-combustion CO_2 capture (PCC) test centres in the world. A unique aspect of the facility is that either a flue gas slipstream from a natural gas-fired combined-heat-and-power (CHP) plant or an equivalent volumetric flow from a residual fluid catalytic cracker (RFCC) unit can be used for CO_2 capture. The CHP flue gas contains about 3.5 vol% CO_2 and the RFCC flue gas contains about 13–14 vol% CO_2, the latter of which is comparable to CO_2 levels seen in coal-fired flue gas. The amine plant, designed and constructed by Aker Solutions and Kværner, is a highly flexible and well-instrumented unit that can accommodate a variety of technologies with capabilities of treating flue gas streams of up to 60,000 standard cubic meters per hour. The plant is offered to developers of solvent-based CO_2 capture technologies to test the performance of their solvent technology and to verify technologies aimed to reduce the atmospheric emissions and environmental impact of amines and amine-based degradation products from solvent-based CO_2 capture processes. The objective of TCM DA is to test, verify, and demonstrate CO_2 capture technologies suitable for deployment at full-scale. A significant number of vendors, including Aker Solutions, Alstom (now GE Power), Cansolv Technologies Inc., Carbon Clean Solutions Ltd., Fluor and Ion Engineering have already successfully used the TCM DA facilities to verify their CO_2 capture technologies.

Nomenclature		**Units**	
CHP	combined heat-and-power	barg	bar gauge
EPRI	Electric Power Research Institute, Inc.	g	gram
FTIR	Fourier-transform infrared	GJ/t	gigajoule per tonne
GC	gas chromatograph	kg/hr	kilogram per hour
HP	high pressure	kg/m^3	kilogram per cubic meter
IVP	independent verification protocol	m	meter
LP	low pressure	mg/Sm^3	milligram per standard cubic meter
MEA	monoethanolamine	MJ/hr	megajoule per hour
NDIR	non-dispersive infrared	Sm^3/hr	standard cubic meter per hour
PCC	post-combustion capture	vol%	volume percent
RFCC	residual fluid catalytic cracker	wt%	weight percent
STU	specific thermal use	µ	micro (10^{-6})
TCM	Technology Centre Mongstad		

Multiple tests using monoethanolamine (MEA) have been carried out at TCM to define the baseline performance of the solvent for defined operating conditions using flue gas from the CHP at 3.5 vol% CO_2 content [2]. More recently, the MEA solvent has been tested with the higher CO_2 concentrations from the RFCC flue gas to develop a new baseline

Electronic copy available at: https://ssrn.com/abstract=3821037

for the amine plant, in accordance with an independent verification protocol (IVP), which provides a structured testing procedure, developed by the Electric Power Research Institute, Inc. (EPRI) [1].

2. Amine plant

The schematic of the TCM DA amine plant when treating the CHP flue gas is shown in Figure 1.

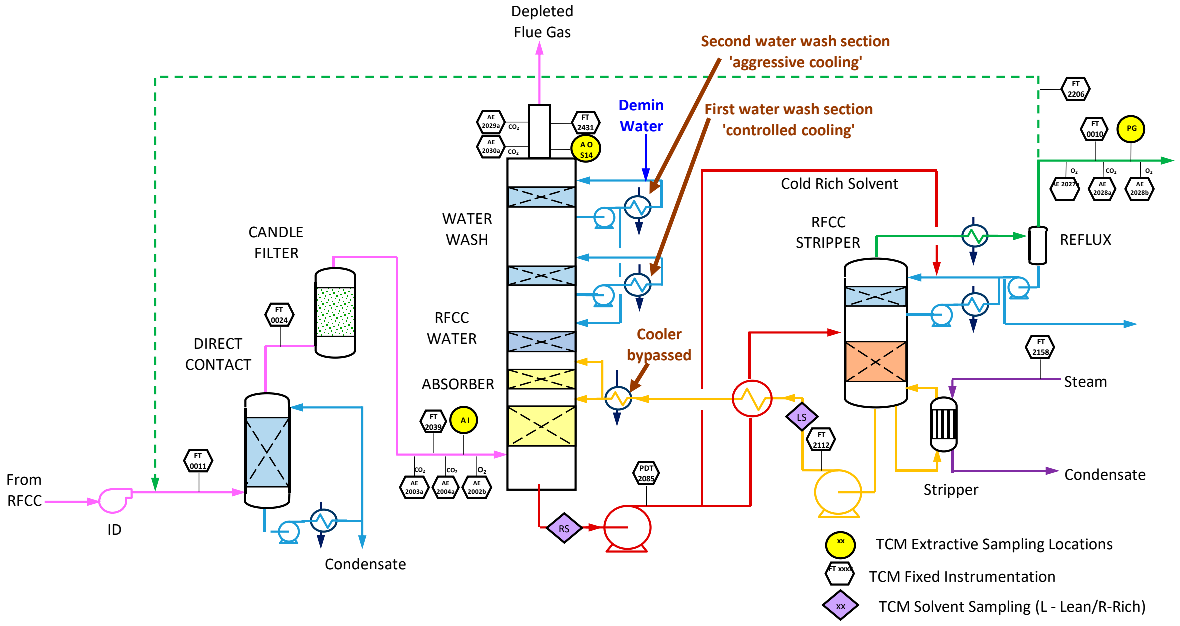

Figure 1. TCM DA amine plant when treating RFCC flue gas

3. IVP overview

The roles and responsibilities of the organizations that conducted the IVP are:

- TCM DA is the prime on the project and its personnel organized the field testing during the test period. They also operated the plant throughout all baseline testing
- EPRI were contracted by TCM DA to develop the IVP during previous MEA baseline testing. EPRI was on site during MEA baseline testing on RFCC flue gas to observe the conduct of the tests and the associated manual extractive sampling. EPRI received the data for the RFCC tests from TCM DA for analysis.

4. Test campaign

The testing of the MEA solvent at TCM was carried out using RFCC flue gas that has CO_2 concentrations of typical coal flue gases. Prior testing with MEA using CHP flue gas was conducted in September 2015. The test periods identified for the RFCC flue gas operation, shown in Table 1, reflect the extractive sampling periods carried out on 28–31 May 2018.

During the testing, personnel from TCM DA manually collected extractive samples from the depleted gas outlet and product CO_2 line downstream of the RFCC stripper. In previous tests, this was sometimes performed by an independent testing contractor. However, TCM DA's competency related to performing this testing was deemed adequate by EPRI, especially since TCM DA is not commercially involved in the outcome and hence can be considered to be unbiased.

Electronic copy available at: https://ssrn.com/abstract=3821037

Data logs for all sampling periods containing pertinent flows, temperatures, pressures, and concentrations measured by permanent plant instruments were supplied by TCM DA for the entire test period.

Table 1. Summary of the test periods

Stream sampled	Date	Start time/Stop time	Sampling Results Reported	Test Period
Depleted Flue Gas	28 May 2018	8:23 / 9:26	MEA, NH_3	C5-1
Depleted Flue Gas	28 May 2018	9:38 / 10:42	MEA, NH_3	C5-2
Depleted Flue Gas	28 May 2018	10:54 / 12:24	MEA, NH_3	C5-3
Depleted Flue Gas	29 May 2018	9:33 / 10:40	MEA, NH_3, Aldehydes, Acetone	C5-4
Depleted Flue Gas	29 May 2018	10:58 / 12:18	MEA, NH_3, Aldehydes, Acetone	C5-5
Depleted Flue Gas	29 May 2018	13:26 / 14:41	MEA, NH_3, Aldehydes, Acetone	C5-6
Depleted Flue Gas/CO_2 Product	30 May 2018	8:29 / 9:33	NO_2, SO_2	C5-7
Depleted Flue Gas/CO_2 Product	30 May 2018	9:42 / 11.18	NO_2, SO_2	C5-8
Depleted Flue Gas/CO_2 Product	30 May 2018	11:41 / 12:41	NO_2, SO_2	C5-9
CO_2 Product	31 May 2018	8:10 / 9:15	MEA, NH_3, Aldehydes, Acetone	C5-10
CO_2 Product	31 May 2018	9:36 / 10:35	MEA, NH_3, Aldehydes, Acetone	C5-11
CO_2 Product	31 May 2018	12:09 / 13:07	MEA, NH_3, Aldehydes, Acetone	C5-12
Depleted Flue Gas	01 June 2018	9:38 / 10:42	MEA, NH_3	C5-13

5. Instrument assessment

To determine the process plant performance, a key component is the quality of the instrumentation installed for measuring the respective compositions and flow rates. Instrumentation quality is determined using two parameters:

- **Accuracy/bias:** This represents the difference between the instrument reading (or average of a set of readings under unchanging process conditions) being assessed and the true value of the parameter being measured. Appropriate determination of the "true value" must be achieved by simultaneous measurement of the parameter using a reference method or instrument with calibration that can be traced to primary standards.
- **Precision:** A determination of the variability of the instrument reading when stream conditions are known to be steady state. Precision is therefore a measure of the random error associated with the measurement.

These measurement errors can be combined to assess the aggregate uncertainty in each measurement. In the absence of a calibration against primary standards for the entire measurement range needed, the uncertainty published by the instrument supplier represents only the precision error.

When the process parameter being measured does not change, precision is a measure of repeatability. In real plant situations, when attempting to operate at steady-state conditions, often process parameters (flow, pressure, and temperature) do vary over the measurement period. Thus, measurements over long periods of time (greater than process time constants) will also include an error term related to process uncertainty.

5.1. Gas-phase compositions

TCM DA has 3 independent Fourier-transform infrared (FTIR) units (Finetech Anafin 2000 and a pair of Gasmet FCX units), facilitating dedicated and continuous FTIR measurements at the absorber inlet, outlet, and CO_2 product gas streams. The CO_2 concentration at the inlet and outlet of the absorber column is also determined by two non-dispersive infrared (NDIR) units at each location, one set to high range (% vol) and one to low range (ppmv) on a dry-gas basis. A dedicated trace O_2 instrument (Teledyne Instruments 3001) is installed to quantify O_2 content of the product CO_2 as this is typically at ppm levels in this stream. A Siemens Maxum Edition II gas chromatograph (GC) unit is also installed, which is capable of measuring the CO_2, O_2, and nitrogen content at all three locations in a near-simultaneous fashion.

Electronic copy available at: https://ssrn.com/abstract=3821037

During the May to June 2018 operations, TCM DA utilized the installed FTIR systems, NDIR analysers, and GC unit to monitor the incoming flue gas and depleted flue gas, as shown in Figure 2 and Figure *3*. It should be noted that the low-range NDIR units could not be used for RFCC testing as the inlet flue gas measurement range is 0–5 vol% (dry) and the outlet depleted flue gas range is 0–1 vol% (dry), both of which are below the gas concentrations measured during these tests.

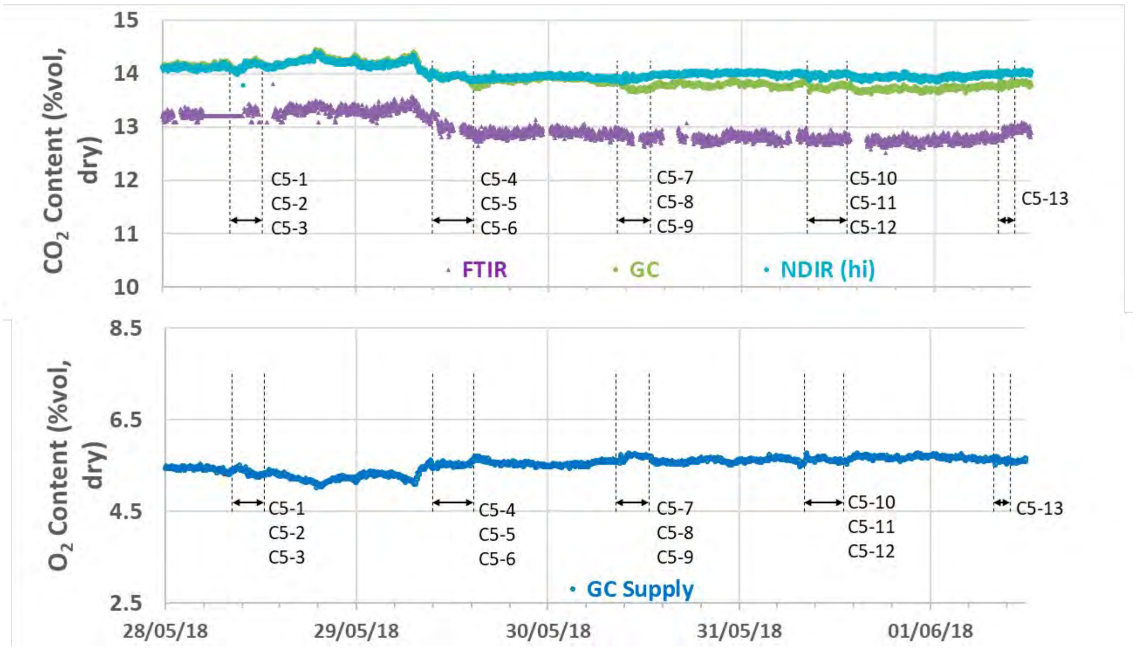

Figure 2. RFCC flue gas supply CO_2 and O_2 data for all analysers

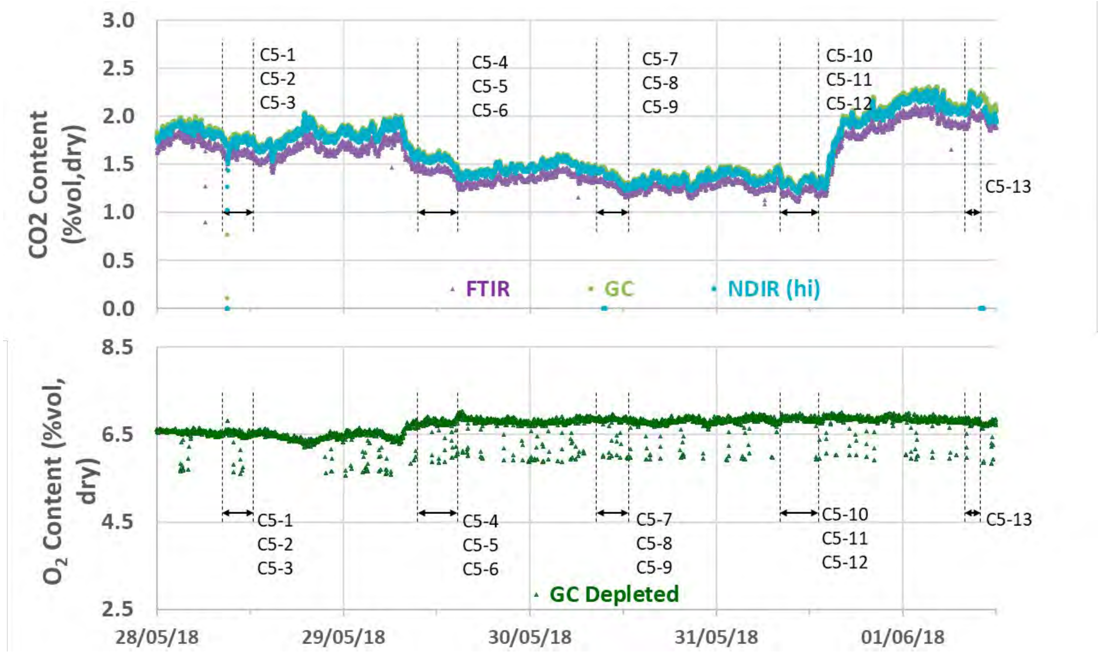

Figure 3. Depleted flue gas CO_2 and O_2 data

Electronic copy available at: https://ssrn.com/abstract=3821037

- Figure 2 displays the RFCC flue gas supply CO_2 and O_2 concentration data over the test campaign. There is good agreement between CO_2 NDIR and the GC CO_2 measurements (<0.2% point difference). The TCM FTIR CO_2 was biased 1% point lower than the other two instruments.
- Figure 3 displays the depleted flue gas CO_2 and O_2 concentration data over the test campaign. The data from all of the TCM instruments show close tracking together, suggesting that the process CO_2 concentration had a degree of variability (±0.2% vol) during that operating period.
- The O_2 content of the product CO_2 was low in the range of 1–2 ppmv, as shown in Figure 4. For the purposes of calculating CO_2 removal and recovery, it is assumed here that the product CO_2 stream is saturated with water at the measured temperature and pressure and contains the small trace quantities of O_2 and N_2 measured. The balance is presumed to be CO_2.

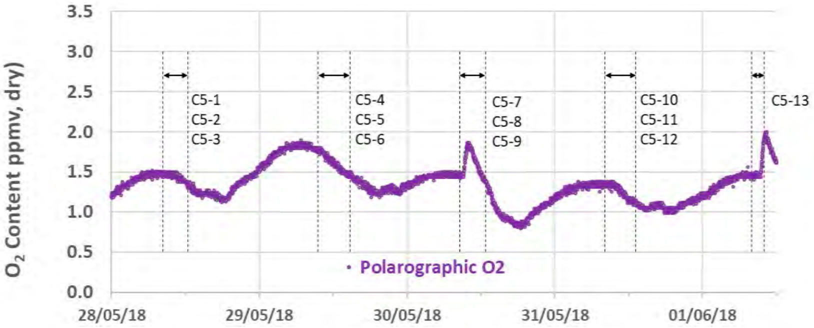

Figure 4. Product gas O_2 data

5.2. *Gas-phase flow rates*

Supply flue gas, depleted flue gas, and the CO_2 product streams were determined by TCM DA plant instrumentation for continuous measurement of the flow rates. In particular, the TCM DA amine plant is well instrumented for determining the RFCC flue gas supply flow rate, with several of the flow meters positioned in series.

- The RFCC flue gas supply flow is measured by two independent multi-pitot-tube flow meter instruments, (FIC-0024 and FT-2039), which are characterized in Table 2. The data from these flow meters are shown in Figure 5. All flow rates are at the defined standard conditions of 15°C and 101.3 kPa. The RFCC flue gas flow was very steady over the entire test period. The test period flow averages used for all calculations are the data reported by the multi-pitot-tube (FIC-0024) as this had a lower precision error.

Table 2. Key flow instrumentations (precision uncertainties are based on internal assessments by TCM DA)

Stream	Tag number	Instrument type	Primary flow measurement	Precision uncertainty
RFCC Flue Gas Supply	FIC-0024	Multi-pitot tube	Differential pressure	2.6%
	FT-2039	Multi-pitot tube	Differential pressure	5.3%
Absorber outlet depleted flue gas	FT-2431	Multi-pitot tube	Differential pressure	5.4%
Product CO_2	FT-0010	Vortex	Flowing volume	1.0%

- The depleted flue gas flow is measured by a single multi-pitot tube flow meter (FT-2431), whose characteristics are listed in Table 2. As observed in prior campaigns, the measured flow has significant transients that are not correlated with any process parameter. Subsequently, the depleted flue gas flow rate was calculated assuming that all O_2 and N_2 entering with the flue gas supply leaves in the depleted flue gas. The performance data reported here use such a calculation for depleted flue gas flow rate.

Electronic copy available at: https://ssrn.com/abstract=3821037

- The product CO_2 flow measured by the vortex flow meter (FT-0010) is the primary flow meter used by TCM DA operators, the characteristics for which are listed in Table 2. Additionally, a Coriolis flow meter is installed (FT-2215), however this instrument has not undergone an accuracy study and so is not used for primary assessment. The data from both flow meters are shown Figure 6. The product CO_2 flow was relatively steady over all periods.

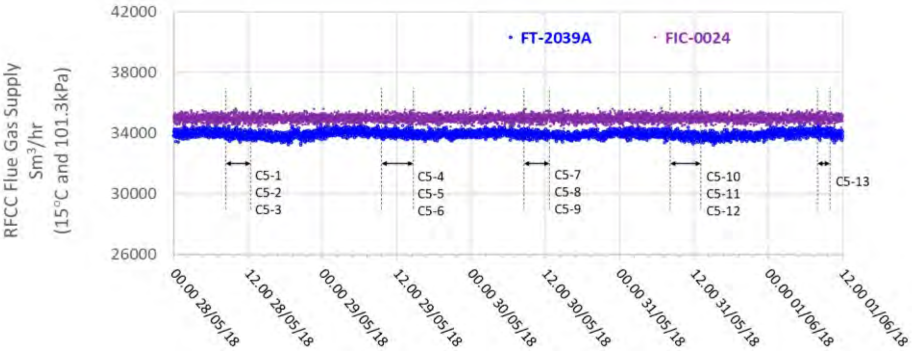

Figure 5. Flue gas supply flow measurements for RFCC testing May-June 2018

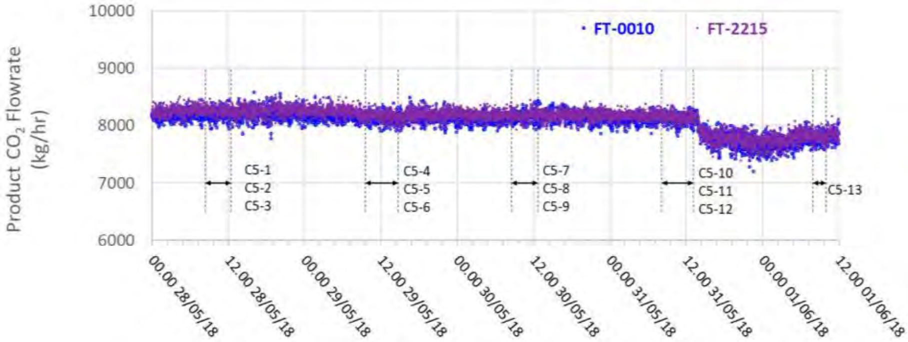

Figure 6. Product flue gas flow rate measurements for RFCC testing May-June 2018

5.3. Steam and condensate flow rates

The TCM DA amine plant receives high-pressure (HP) superheated steam from the neighbouring refinery at a pressure of approximately 30 bar, and a temperature of between 240°C to 310°C. A schematic of the system supplying steam to the stripper reboiler is shown in Figure 7.

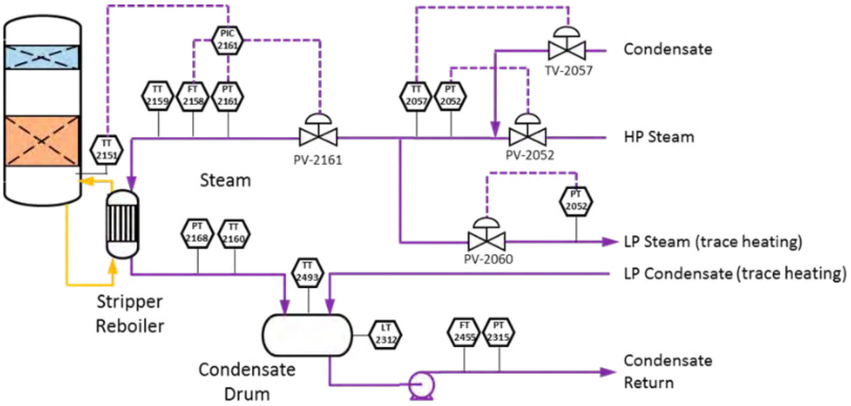

Figure 7. RFCC stripper reboiler steam supply flow schematic

Electronic copy available at: https://ssrn.com/abstract=3821037

The HP steam is throttled near the stripper reboiler to a pressure of approximately 5 bar before being desuperheated with condensate. Following condensation in the stripper reboiler, the steam condensate collects in a receiving vessel before being returned to the refinery.

Steam heat tracing is facilitated using a small amount of medium-pressure steam that is reduced to a lower pressure prior to use. The resultant low-pressure (LP) steam condensate is returned to the same receiver as the stripper reboiler condensate. For thermal energy consumption assessment, the key parameter of interest is the steam flow to the reboiler, shown in Figure 8.

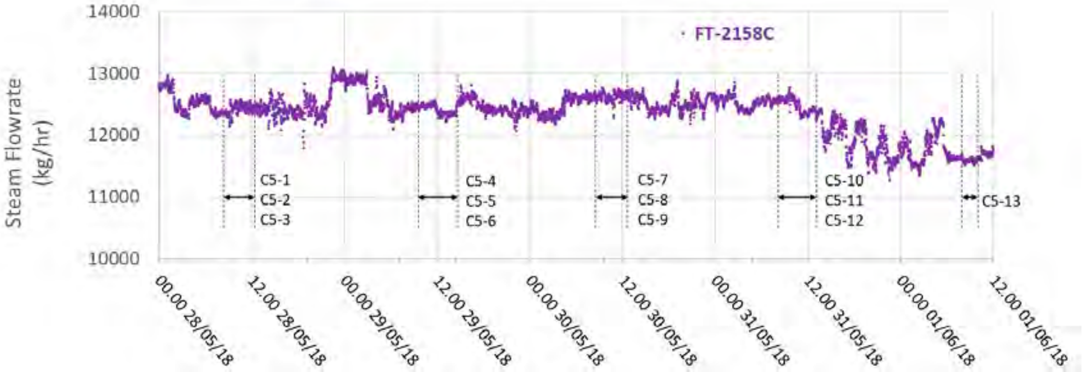

Figure 8. RFCC reboiler steam flow

6. Results and discussion

6.1. CO_2 capture efficiency and recovery

The CO_2 capture efficiency was calculated using the four methods (Methods 1–4) via the formulas detailed in Table 4. In addition, CO_2 recovery is the fraction of CO_2 mass flow in the flue gas supply that is accounted for by measured CO_2 mass flows in the depleted flue gas and product CO_2—it is a measure of the degree to which the CO_2 mass balance is closed.

Table 3. CO_2 capture efficiency and recovery calculation methods

Term	Description	Formula
CO_2 capture efficiency: Method 1	CO_2 product flow as a ratio to the CO_2 flow in the flue gas supply	$=\frac{CO_2(product)}{CO_2(supply)}$
CO_2 capture efficiency: Method 2	CO_2 product flow as a ratio to the sum of the CO_2 product flow and the CO_2 flow in the depleted flue gas	$=\frac{CO_2(product)}{CO_2(product)+CO_2(depleted)}$
CO_2 capture efficiency: Method 3	Ratio of the difference between the CO_2 flow in the flue gas supply and the CO_2 in the depleted flue gas to the CO_2 flow in the flue gas supply	$=\frac{CO_2(supply)-CO_2(depleted)}{CO_2(supply)}$
CO_2 capture efficiency: Method 4	Ratio of the depleted flue gas CO_2 per unit O_2+N_2 to the flue gas supply CO_2 per unit O_2+N_2	$=1-\frac{O_{CO_2}}{(1-O_{CO_2})}\frac{(1-I_{CO_2})}{I_{CO_2}}$
CO_2 recovery	Ratio of the sum of the CO_2 flow in depleted flue gas and the product CO_2 flow divided by the CO_2 flow in the flue gas supply	$=\frac{CO_2(depleted)+CO_2(product)}{CO_2(supply)}$

O_{CO2} = Depleted flue gas CO_2 content, dry I_{CO2} = Flue gas supply CO_2 content, dry

As the depleted flue gas flow measurement was not reliable, it was assumed that the oxygen and nitrogen entering the absorber with the flue gas leaves in the depleted flue gas. The saturated water content of the depleted flue gas was

Electronic copy available at: https://ssrn.com/abstract=3821037

calculated using its temperature and pressure. The CO_2 flow out of the absorber was calculated using the concentration of CO_2 in the depleted flue gas and the calculated mass flowrate. These are essentially the same assumptions as those used for Method 4, which is independent of flowrate and uses a concentration-only approach. Subsequently, Method 3 and Method 4 calculations result in identical CO_2 capture rates.

The CO_2 recovery was then estimated using the calculated flow of depleted flue gas. The calculated CO_2 capture efficiency and recovery are presented in Table 4. For all test periods, the calculated CO_2 captures were quite steady near the 90% capture target and the CO_2 recovery was consistently in the range of 101–104%. Test C5-13 was targeted at the lower 85% capture rate.

Table 4. CO_2 capture results

S = Supply flue gas D= Depleted gas P= Product CO_2	Method 1	Method 2	Method 3	Method 4	CO_2 Recovery
Test Period	$=\frac{P}{S}$	$=\frac{P}{P+D}$	$=\frac{S-D}{S}$	$=1-\frac{O^{i}{}_{CO2}}{\left(1-O_{CO_2}\right)}\frac{\left(1-I^{ii}{}_{CO_2}\right)}{\left(I_{CO_2}\right)}$	$=\frac{D+P}{S}$
C5-1	92.9%	89.9%	89.6%	89.6%	103.7%
C5-2	92.6%	89.6%	89.3%	89.3%	103.8%
C5-3	92.6%	89.6%	89.2%	89.2%	103.8%
C5-4	93.0%	90.4%	90.2%	90.2%	103.2%
C5-5	93.0%	90.5%	90.2%	90.2%	103.1%
C5-6	93.5%	90.9%	90.6%	90.6%	103.2%
C5-7	93.5%	91.2%	91.0%	91.0%	102.7%
C5-8	93.6%	91.6%	91.4%	91.4%	102.4%
C5-9	93.8%	92.2%	92.1%	92.1%	101.9%
C5-10	93.3%	91.9%	91.8%	91.8%	101.6%
C5-11	93.2%	92.3%	92.2%	92.2%	101.0%
C5-12	93.0%	91.9%	91.8%	91.8%	101.4%
C5-13	88.7%	86.9%	86.7%	86.7%	102.3%

[i] *O_{CO2}=Depleted flue gas CO_2 content, dry basis,* [ii] *I_{CO2}=Flue gas supply CO_2 content, dry basis*

The uncertainty calculations and results from calculation Methods 1–3 are shown in Table 5. The following assumptions were used:

- Flow metering uncertainties were calculated by TCM DA for the indicated flow meters based on the specification of the instrument [3].
- Concentration uncertainties for the flue gas flows are those detailed in Table 2.
- Concentration uncertainty for the product CO_2 is assumed to be 1% to allow for CO_2 content as low as 99%.
- CO_2 capture of 90% is representative of that measured during all test periods.
- The uncertainty in CO_2 capture (ECO_2) is almost entirely due to uncertainty in CO_2 content of the RFCC flue gas supply for the assigned total (low) flow uncertainties. The CO_2 capture uncertainty is relatively insensitive to uncertainties in the CO_2 contents of both the product CO_2 and depleted flue gases.

Table 5. Uncertainty in CO_2 capture calculations (nominal CO_2 capture efficiency shown as ECO_2 = 85%)

CO_2 capture calculation method	Stream	Uncertainty in:				CO_2 capture uncertainty Equation
		Total flow	CO_2 content	CO_2 flow	CO_2 capture	
1	Product	1.1%	1%	U_{CO2P}=1.5%	5.4%	$\sqrt{\left(U_{CO2S}\right)^2+\left(U_{CO2P}\right)^2}$
	Supply	1.3%	5%	U_{CO2S}=5.1%		
2	Product	1.1%	1%	U_{CO2P}=1.5%	0.8%	$\left(1-E_{CO2}\right)\sqrt{\left(U_{CO2D}\right)^2+\left(U_{CO2P}\right)^2}$
	Depleted	1.3%	5%	U_{CO2D}=5.2%		
3	Supply	1.3%	5%	U_{CO2S}=5.2%	1.3%	$\frac{\left(1-E_{CO2}\right)}{E_{CO2}}\sqrt{\left(U_{CO2S}\right)^2+\left(U_{CO2D}\right)^2}$
	Depleted	1.3%	5%	U_{CO2D}=5.2%		

Electronic copy available at: https://ssrn.com/abstract=3821037

6.2. Thermal energy consumption

The reboiler thermal duty was calculated as the difference between steam enthalpy at the reboiler inlet temperature and pressure and the saturation enthalpy of water at the reboiler condensate temperature. The specific thermal use (STU) was obtained by dividing the reboiler duty by the product CO_2 flow. The CO_2 product flow was either based on the measured CO_2 product flow (P) or on the difference between the NDIR-measured CO_2 supply flow and the estimated CO_2 depleted flow (S – D). The two corresponding values for STU are shown in Table 6. The results for STU were very consistent during all test periods. The product flow measurements (P) were consistently higher than the using the gas-side difference method (S – D) method, resulting in lower STU values.

Table 6. Stripper reboiler thermal energy consumption

Test period	Reboiler steam flow rate kg/hr	Reboiler duty MJ/hr	Using the product CO_2 flow (P)[i]		Using CO_2 removed (S – D)	
			Product CO_2 Flow kg/hr	Specific Thermal Use GJ/t CO_2	Product CO_2 Flow kg/hr	Specific Thermal Use GJ/t CO_2
C5-1	12,343	28,173	8142	3.46	7849	3.59
C5-2	12,459	28,343	8138	3.48	7843	3.61
C5-3	12,436	28,315	8159	3.47	7863	3.60
C5-4	12,463	28,376	8072	3.52	7824	3.63
C5-5	12,457	28,380	8070	3.52	7827	3.63
C5-6	12,369	28,365	8085	3.51	7835	3.62
C5-7	12,630	28,678	8078	3.55	7865	3.65
C5-8	12,585	28,592	8088	3.54	7902	3.62
C5-9	12,641	28,771	8133	3.54	7984	3.60
C5-10	12,571	28,593	8093	3.53	7962	3.59
C5-11	12,583	28,636	8069	3.55	7988	3.58
C5-12	12,397	28,427	8093	3.51	7984	3.56
C5-13	11,592	26,529	7724	3.43	7548	3.51

[i] *The wet CO_2 flow is obtained by using the FTIR measured moisture content of the product CO_2*

Prior testing with CHP flue gas at approximately an 80 tonnes per day load yielded a regeneration energy range of 3.61–3.66 GJ/tonne-CO_2 using the product CO_2 flow (P) and 3.58–3.60 GJ/tonne-CO_2 using the gas-side difference method (S – D) [2]. The RFCC tests achieved circa 190 tonnes per day load and delivered an average regeneration energy of 3.51 GJ/tonne-CO_2 using product flow (P) and 3.60 GJ/tonne-CO_2 using gas-side difference method (S – D). This represents a 2% reduction in regeneration energy, likely due to the higher inlet CO_2 levels.

6.3. Gas-phase contaminants

Formaldehyde, acetaldehyde, and acetone concentrations were determined by extractive sampling of the depleted flue gas at the absorber outlet during the RFCC test periods as shown in Table 7. The formaldehyde levels are lower than the previous MEA baseline testing values of 720 µg/Sm^3 and 40 g/hr, which were done by an independent, contractor (FORCE Technology) using brought-in instruments. The acetaldehyde levels are considerably lower than the 2015 MEA test samples of 16 mg/Sm^3 and 840 g/h emission levels measured by FORCE Technology. However, acetone levels measured were sufficiently low to be at or below the detection limit of the analysis performed by SINTEF, a similar result to the previous MEA test [2].

Table 7. Depleted gas phase aldehyde concentrations

Test period	Formaldehyde			Acetaldehyde		
	ppmvd	µg/Sm^3	g/h	ppmvd	mg/Sm^3	g/h
C5-4	0.03	43.2	1.19	0.88	1.73	47.8
C5-5	0.03	44.5	1.23	0.82	1.61	44.4
C5-6	0.07	89.1	2.46	0.86	1.69	46.6

For the CO_2 product, shown in Table 8, the formaldehyde levels detected are lower than the manually sampled measurements during the 2015 CHP baseline campaign of 140 µg/Sm^3 and the acetaldehyde levels are considerably lower than the previous level of 150 mg/Sm^3. The 2015 MEA baseline measurements were closer to the levels measured in 2014, where formaldehyde was detected at 190 µg/Sm^3. Although acetone was detected in the CO_2

Electronic copy available at: https://ssrn.com/abstract=3821037

product, these measurements were at or below the detection limit, whereas in the previous MEA baseline all measurements taken were below the detection limit.

Table 8. Product gas aldehyde concentrations

Test period	Formaldehyde			Acetaldehyde		
	ppmvd	µg/Sm^3	g/h	ppmvd	mg/Sm^3	g/h
C5-10	0.06	83.3	0.34	2.90	5.70	23.5
C5-11	0.04	52.5	0.22	3.33	6.55	26.9
C5-12	0.039*	51.9	0.21	3.29	6.46	26.6

* some DNPH cartridges measured below detection limit

TCM DA measured concentrations of MEA and ammonia at the absorber outlet during the RFCC test periods C5-1 to C5-6 and for C5-13 following a modification to the process operating conditions to a lower capture rate target. The results of these manually extracted samples are shown in Table 9.

Table 9. Depleted flue gas stream ammonia and amine concentrations and mass rates as phase contaminants

Test period	MEA			Ammonia		
	ppmvd	mg/Sm^3	g/h	ppmvd	mg/Sm^3	g/h
C5-1	3.16	8.15	231	8.20	5.91	167
C5-2	2.99	7.73	219	7.29	5.25	149
C5-3	2.99	7.72	218	7.74	5.57	157
C5-4	2.67	6.89	195	8.47	6.10	173
C5-5	2.57	6.63	188	7.49	5.40	153
C5-6	2.75	7.11	201	7.67	5.53	157
C5-13	2.93	7.58	216	7.58	5.46	156

The levels detected here for MEA were consistent between samples and are far higher than observed by FORCE Technology during the 2015 CHP gas testing (0.006 mg/Sm^3). Although the levels measured here are higher, previous EPRI experience with coal-derived flue gases has observed comparable single-digit ppm levels of amine at the depleted flue gas location when aerosol levels are low or zero, which TCM DA had achieved using the Brownian demister filter upstream of the absorber. Ammonia levels are lower than the previous CHP tests results, measured at 13 mg/Sm^3. However, it is unknown how degraded the solvent was during these tests in comparison with the previous campaign. TCM DA measured concentrations of MEA and ammonia in the CO_2 product gas during the RFCC test periods C5-10 to C5-12. MEA was not detected, and levels of ammonia were substantially lower at 0.05-0.08mg/Sm^3 than the prior CHP test results [2]. While extractive samples of SO_x and NO_x were not carried out during this test campaign, the FTIR was used to track the relative levels of each component. The RFCC flue gas was expected to have 20–60 ppm (vol, dry) of SO_2 from previous tests, but this couldn't be reliably verified during these tests as the FTIR instrument did not deliver a reliable measurement. The outlet measurements were more consistent, as shown in Table 10. The consistent <1 ppm vol measurement of SO_2 suggests absorption by the MEA solvent.

Table 10. Depleted flue gas SO_2 concentrations and mass rates

Test period	SO_2		
	ppmvd	mg/Sm^3	g/h
C5-1	0.51	1.37	38.9
C5-2	0.56	1.53	43.2
C5-3	0.62	1.69	47.6
C5-4	0.76	2.05	58.1
C5-5	0.69	1.87	53.1
C5-6	0.83	2.25	63.8
C5-7	0.69	1.88	53.1
C5-8	0.77	2.10	59.3
C5-9	0.86	2.32	65.3
C5-10	0.74	1.99	56.2
C5-11	0.77	2.09	58.6
C5-12	1.00	2.71	76.2
C5-13	0.52	1.41	40.3

Electronic copy available at: https://ssrn.com/abstract=3821037

The NO_x quantities passing through the absorber were effectively unchanged, showing only the concentrating effect of the CO_2 removal from the flue gas, where more than 10% of the flue gas volume is removed. As the amine plant operated continuously capturing 90% throughout the test period, the FTIR-measured NO_x data show a consistent increase in concentration at the outlet of the absorber as shown in Figure 9.

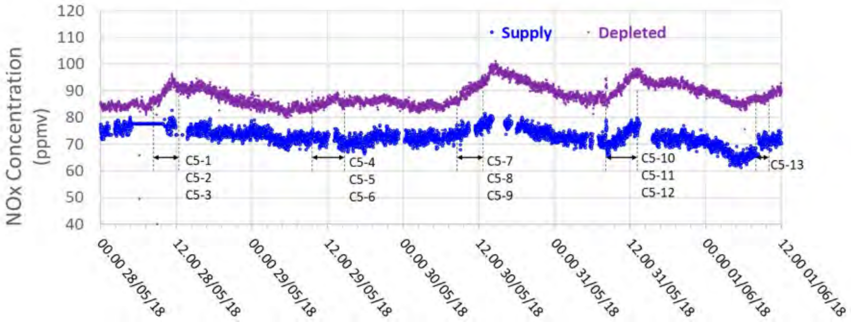

Figure 9. Absorber inlet and outlet NOx values

6.4. New baseline for solvent performance testing

Table 11 presents a portion of the MEA test data obtained at the TCM DA amine plant. Based on these data, a new baseline was established for higher concentration flue gas CO_2 capture.

Table 11. Results of RFCC baseline testing in 2018

Baseline year	**2018**		
Packing height (m)	18	Lean loading	0.23
Flue gas flow (Sm^3/h)	35 000	Rich loading	0.48
Flue gas supply temperature (°C)	31.0	Stripper bottom temperature (°C)	121.0
Flue gas supply pressure (bar)	0.02	CO_2 capture (%)	91
Lean amine flow (kg/h)	133 000	SRD (MJ/kg CO_2)	3.55

7. Conclusions

This baseline represents the performance of the TCM amine plant close to the plant nominal capacity using 5M MEA solvent with higher CO_2 concentration flue gas (13–14 vol%), typical of coal-based thermal plants. Alongside the prior baseline work carried out in 2015 for flue gas with CO_2 concentrations from natural gas-fired CHP units (3–4 vol%) [2], this new baseline will serve as the performance benchmark for other amines tested at the TCM DA amine plant when using RFCC flue gas.

Acknowledgements

The authors gratefully acknowledge the staff of TCM DA, Gassnova, Equinor, Shell, and Total for their contribution and work at the TCM DA facility. The authors also gratefully acknowledge Gassnova, Equinor, Shell, and Total as the owners of TCM DA for their financial support and contributions.

References

[1] Thimsen et al. Results from MEA testing at the CO_2 Technology Centre Mongstad. Part I: Post-Combustion CO_2 capture testing methodology; Energy Procedia 63, 5938–5958; 2014.

[2] Faramarzi et al. Results from MEA testing at the CO_2 Technology Centre Mongstad: Verification of baseline results in 2015; Energy Procedia 114, 1128–1145; 2017.

[3] Flue Gas Composition and Energy & Mass Balance Accuracy Studies at CO_2 Technology Centre Mongstad (TCM DA): Results Related to the Amine Capture Unit." K-E Frøysa and R. Sakariassen. CRM-12-F14016-RA-2: 7 June 2012

Electronic copy available at: https://ssrn.com/abstract=3821037

Application of Sequential Design of Experiments (SDoE) to Large Pilot-Scale Solvent-Based CO_2 Capture Process at Technology Centre Mongstad (TCM)

(2021)

15th International Conference on Greenhouse Gas Control Technologies, GHGT-15

15th 18th March 2021 Abu Dhabi, UAE

Application of Sequential Design of Experiments (SDoE) to Large Pilot-Scale Solvent-Based CO$_2$ Capture Process at Technology Centre Mongstad (TCM)

Joshua C. Morgan[a,b,*], Benjamin Omell[a], Michael Matuszewski[a], David C. Miller[a], Muhammad Ismail Shah[c], Christophe Benquet[c], Anette Beate Nesse Knarvik[c], Thomas de Cazenove[c], Christine M. Anderson-Cook[d], Towfiq Ahmed[d], Charles Tong[e], Brenda Ng[e], Debangsu Bhattacharyya[f]

[a]National Energy Technology Laboratory, 626 Cochrans Mill Road, P.O. Box 10940, Pittsburgh PA 15236-0940, USA
[b] NETL Support Contractor, 626 Cochrans Mill Road, P.O. Box 10940, Pittsburgh PA 15236-0940, USA
[c]CO$_2$ Technology Centre Mongstad, Mongstad 71, 5954 Mongstad, Norway
[d]Los Alamos National Laboratory, P.O. Box 1663, Los Alamos NM 87545, USA
[e]Lawrence Livermore National Laboratory, 7000 East Ave, Livermore CA 94550, USA
[f]West Virginia University, Department of Chemical and Biomedical Engineering, 1306 Evansdale Drive, P.O. Box 6102, Morgantown WV 26506-6102, USA

Abstract

The United States Department of Energy's Carbon Capture Simulation for Industry Impact (CCSI^2) program has developed a framework for sequential design of experiments (SDoE) that aims to maximize knowledge gained from budget- and schedule-limited pilot scale testing. SDoE was applied to the planning and execution of campaigns for testing CO$_2$ capture systems at pilot-scale in order to optimally allocate resources available for the testing. In this methodology, a stochastic process model is developed by quantifying the parametric uncertainty in submodels of interest; for a solvent-based CO$_2$ capture system, these may include physical properties and equipment performance submodels (e.g., mass transfer, interfacial area). This uncertainty is propagated through the full process model, over variable operating conditions, for estimating the resulting uncertainty in key model outputs (e.g., percentage of CO$_2$ capture, solvent regeneration energy requirement). In developing a data collection plan, the predicted output uncertainty is incorporated into an algorithm that seeks simultaneously to select process operating conditions for which the predicted uncertainty is relatively high and to ensure that the entire space of operation is well represented. This test plan is then used to guide operation of the pilot plant at varying steady-state conditions, with resulting process data incorporated into the existing model using Bayesian inference to refine parameter distributions. The updated stochastic model, with reduced parametric uncertainty from data collected, is then used to guide additional data collection, thus the sequential nature of the experimental design.

The SDoE process was implemented at the pilot test unit (12 MWe in scale) at Norway's Technology Centre Mongstad (TCM) in a summer 2018 test campaign with aqueous monoethanolamine (MEA). During the test campaign, the varied operating conditions included the flowrates of circulated solvent, flue gas, and reboiler steam and the CO$_2$ concentration in the flue gas. The process data were used to update probability distributions of mass transfer and interfacial area parameters of a stochastic process model developed by the CCSI^2 team. Two iterations of the SDoE process were executed, resulting in the uncertainty in model predicted CO$_2$ capture percentage decreasing by an average of 58.0 ± 4.7% over the full input space of interest. This work demonstrates the

---

* Corresponding author. *E-mail address:* joshua.morgan@netl.doe.gov

potential of the SDoE process for model refinement through reduction in process model parametric uncertainty, and ultimately risk in scale-up, in CO_2 capture technology performance.

Keywords: post-combustion carbon capture; pilot-scale testing; uncertainty quantification; design of experiments

1. Introduction

The United States Department of Energy's Carbon Capture Simulation for Industry Impact ($CCSI^2$) program is a collaboration of national laboratories, universities, and industrial organizations that provides research and development support for novel CO_2 capture technologies with the objective of reducing risk and accelerating their commercialization. These efforts involve continuing advancements in and applications of the open-source toolset[1] developed as part of its predecessor project, the Carbon Capture Simulation Initiative (CCSI). The CCSI Toolset includes a suite of computational tools and models with the overarching goal of accelerating the development, deployment, and scale-up of CO_2 capture technologies. The toolset includes a rigorous process model, implemented in Aspen Plus®, of the aqueous monoethanolamine (MEA) solvent system, which is the industrial standard for solvent-based CO_2 capture. This model includes quantification of parametric uncertainty for solvent physical property models such as viscosity, density, and surface tension [1], the thermodynamic framework [2], and packing-specific models such as mass transfer, interfacial area, and hydraulics [3]. These submodels combine with a full process model that was validated with process data from the 0.5 MWe pilot test unit at the National Carbon Capture Center (NCCC) in 2014 [4]. In 2017, an additional test campaign for the aqueous MEA system was held at NCCC, incorporating the $CCSI^2$ framework for SDoE. In this methodology, the existing process model is leveraged to inform collection of data that are subsequently used to refine the model and modify the test plan accordingly [5,6]. Over two iterations of the SDoE process, parametric distributions for process submodels were refined through experimental observations of absorber CO_2 capture percentage, resulting in an average uncertainty reduction of approximately 50% for the model prediction of CO_2 capture percentage throughout the input space of interest.

The CCSI aqueous MEA process model was scaled up to 12 MWe for consistency with the pilot test unit at Norway's Technology Centre Mongstad (TCM) and was used in the planning and execution of a test campaign at TCM in summer 2018. TCM is one of the world's largest facilities for testing carbon capture technologies, and previous test results with the MEA solvent system have been reported in the open literature [7-12], including variation in many process variables and both steady-state and dynamic operation. The pilot plant at TCM notably has two sources of flue gas: combined cycle gas turbine (CCGT) based heat and power plant (CHP), with ~3.5 vol% CO_2, and residual fluidized catalytic cracker (RFCC) unit, with ~13-14 vol% CO_2. The TCM plant also contains two stripper columns, each designed for process operation with one of the flue gas sources. This work focused on collecting additional data for the MEA process at TCM with variation in the flowrates of solvent, flue gas, and reboiler steam, the concentration of CO_2 in the flue gas, the packing height of the absorber, and the stripper configuration. During the first three weeks of the test campaign, which are the primary focus of this paper, the SDoE framework was used to guide the collection of process data using the existing MEA process model and multiple test objectives. The data were used to update the model by refining the distributions of parameters in the mass transfer and interfacial area submodels, ultimately resulting in a reduction of predicted uncertainty in the CO_2 capture percentage from 10.5 ± 1.5% to 4.4 ± 0.4%, or an average reduction of 58.0 ± 4.7%, over the full input space of interest. In the final two weeks of the campaign, data were collected for a modified process configuration in which the packing height of the absorber was reduced to 18 meters, and eventually 12 meters, and the stripper configuration was modified so that a fraction (~20%) of the rich solvent exiting the absorber bypasses the lean-rich heat exchanger and is heated in the water wash of the stripper. This work, along with the previous test campaign at NCCC, demonstrates the potential of the SDoE methodology for refining predictions of stochastic process models through strategic data collection. The reduction of model uncertainty effectively reduces expected risk in process design and operation, thus improving confidence when predicting process performance and conducting economic analyses.

---

[1] Available at https://github.com/CCSI-Toolset/

2. Methodology

2.1. SDoE Methodology

The SDoE process developed by CCSI[2] uses a stochastic model, with parametric uncertainty quantified in the submodels, to inform collection of process data in order to maximize the value of data obtained during a test campaign. Moreover, it provides a framework for directly reducing uncertainty in model prediction of capture rates based on new process knowledge gained from data collection. The SDoE process is represented schematically in Fig. 1.

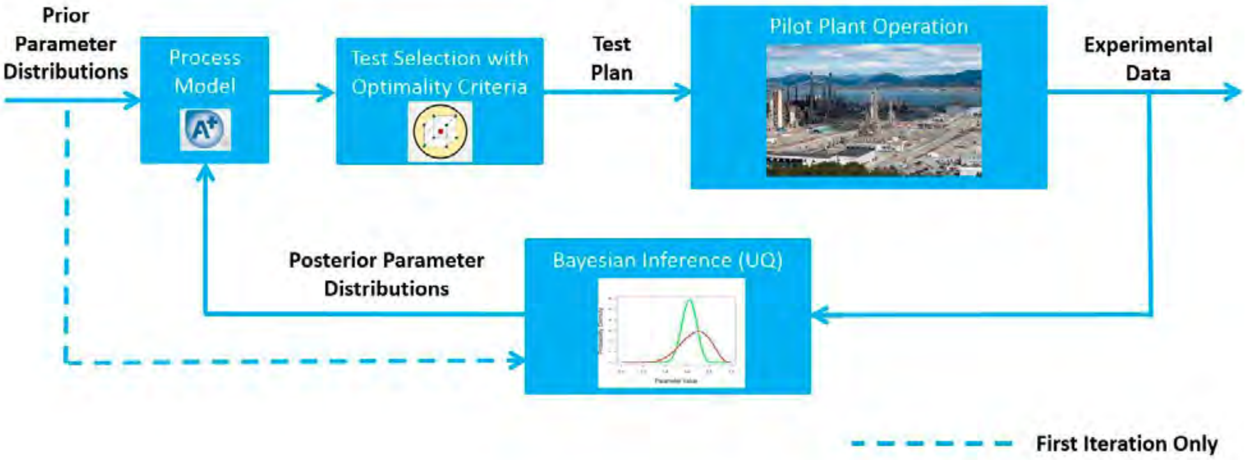

Fig. 1. Schematic representation of SDoE methodology

As shown in Figure 1, *a priori* probability distributions of submodel parameters are propagated through a process model, denoted as $y(\boldsymbol{x}, \boldsymbol{\theta}, \boldsymbol{\theta}^*)$, where $\boldsymbol{x}$ is a set of input variables that can be manipulated in plant operation and $\boldsymbol{\theta}$ and $\boldsymbol{\theta}^*$ are sets of model parameters. These sets differ in that $\boldsymbol{\theta}$ contains parameters for which uncertainty is reduced over the course of executing the SDoE methodology whereas $\boldsymbol{\theta}^*$ has parameters with irreducible uncertainty based on the type of data collected. For the example of a solvent-based CO_2 capture system, $\boldsymbol{\theta}$ includes process specific parameters from submodels such as mass transfer or interfacial area that may be informed through collection of plant data (e.g. CO_2 capture percentage in the absorber column). Conversely, $\boldsymbol{\theta}^*$ includes parameters from physical property submodels, for which uncertainty is readily estimated through direct measurements of the corresponding properties and cannot reasonably be informed from plant level data. If the process model y is sufficiently complex, it may be necessary to replace it with a surrogate model, denoted as $\hat{y}(\boldsymbol{x}, \boldsymbol{\theta}, \boldsymbol{\theta}^*)$, developed and validated over the full input space. For a given point in the input space, a confidence interval for the model prediction are computed by propagating the uncertainty in the full set of parameters ($\boldsymbol{\theta}^{\boldsymbol{T}} = [\boldsymbol{\theta} \quad \boldsymbol{\theta}^*]$) through the surrogate model. The 95% confidence interval, estimated by taking a sample of size M over the full parameter space ($\boldsymbol{\theta}^{\boldsymbol{T},(j)}, \forall\, j = 1, \dots M$), is given as:

$$CI|_{\boldsymbol{x}^{(i)}} = F_{0.975}\left(\left\{\hat{y}\left(\boldsymbol{x}^{(i)}, \boldsymbol{\theta}^{\boldsymbol{T},(1)}\right), \dots, \hat{y}\left(\boldsymbol{x}^{(i)}, \boldsymbol{\theta}^{\boldsymbol{T},(M)}\right)\right\}\right) - F_{0.025}\left(\left\{\hat{y}\left(\boldsymbol{x}^{(i)}, \boldsymbol{\theta}^{\boldsymbol{T},(1)}\right), \dots, \hat{y}\left(\boldsymbol{x}^{(i)}, \boldsymbol{\theta}^{\boldsymbol{T},(M)}\right)\right\}\right) \tag{1}$$

where $\left\{\hat{y}\left(\boldsymbol{x}^{(i)}, \boldsymbol{\theta}^{\boldsymbol{T},(1)}\right), \dots, \hat{y}\left(\boldsymbol{x}^{(i)}, \boldsymbol{\theta}^{\boldsymbol{T},(M)}\right)\right\}$ is the set of values of an output variable calculated from propagating all of the individual $\boldsymbol{\theta}^{\boldsymbol{T},(j)}$ through the surrogate model and F_k represents the k^{th} percentile of this set. The values of $CI|_{\boldsymbol{x}^{(i)}}$ for individual $\boldsymbol{x}^{(i)}$ are considered in the test selection method; the specific optimality criterion used in this work is G-optimality [13], which minimizes the maximum prediction variance. This aim targets experimental settings $\boldsymbol{x}^{(i)}$ for which the predicted uncertainty (i.e., $CI|_{\boldsymbol{x}^{(i)}}$) is relatively large, so that the collection of data at these settings represents high potential for uncertainty reduction. Moreover, the algorithm used in this work for test selection simultaneously seeks to ensure that the full input space is well-represented in the test plan, balancing good representation of design points throughout the region while making locations with large confidence interval widths more likely to be selected.

The test plan is then implemented by running the plant accordingly, resulting in collection of experimental data (denoted *Z*). The data are incorporated into a Bayesian inference framework, using the PSUADE[2] software package. For model parameters of fixed uncertainty, a sample ($\boldsymbol{\theta}^{*,(j)}; \forall\, j = 1, \dots, N$) is drawn from their probability distribution $P(\boldsymbol{\theta}^{*})$. For each sample point $\boldsymbol{\theta}^{*,(j)}$, a posterior distribution for the remaining parameters ($\boldsymbol{\theta}$) is calculated:

$$\pi_j\left(\boldsymbol{\theta}|Z, \boldsymbol{\theta}^{*,(j)}\right) \propto P(\boldsymbol{\theta})L\left(Z|\boldsymbol{\theta}, \boldsymbol{\theta}^{*,(j)}\right) \tag{2}$$

and given in the form of a set of sample points. Here, $L\left(Z|\boldsymbol{\theta}, \boldsymbol{\theta}^{*,(j)}\right)$ represents the likelihood (some metric used to express the distance between simulation predictions and experimental data) of observing a set of experimental data (Z) conditioned on the values of the parameters, $P(\boldsymbol{\theta})$ the prior distribution of the parameters for which uncertainty is updated, and $\pi_j\left(\boldsymbol{\theta}|Z, \boldsymbol{\theta}^{*,(j)}\right)$ the posterior distribution of $\boldsymbol{\theta}$ conditioned on the observed experimental data and the value of $\boldsymbol{\theta}^{*}$ for sample *j*. The overall posterior distribution $\pi\left(\boldsymbol{\theta}|Z, \boldsymbol{\theta}^{*,(j)}\right)$ is obtained through the process of marginalization, combining all individual $\pi_j\left(\boldsymbol{\theta}|Z, \boldsymbol{\theta}^{*,(j)}\right)$. The updated stochastic model, with refined estimates of parameter uncertainties, is then used to re-calculate $CI|_{\boldsymbol{x}^{(i)}}$ throughout the input space. For all subsequent iterations of SDoE, the prior distribution $P(\boldsymbol{\theta})$ is replaced by the posterior distribution $\pi_j\left(\boldsymbol{\theta}|Z, \boldsymbol{\theta}^{*,(j)}\right)$ from the previous iteration.

2.2. Overview of TCM Test Campaign

The TCM test campaign ran for five weeks in summer 2018, in five distinct test phases as outlined in Table 1.

Table 1. Phases of MEA test campaign at TCM

Phase No.	Absorber Packing Height (m)	CO_2 in Flue Gas (vol%)	No. of Data Sets	Stripper Configuration	Description of SDoE Criterion
1	24	8	14	Simple	Space-Filling Design
2	24	8 & 10	10	Simple	Selection of points with optimal economic performance
3	24	8 & 10	41	Simple	Sequential SDoE targeting uncertainty reduction
4	18	10	14	With Bypass	Minimization of specific reboiler duty (SRD)
5	12	10	19	With Bypass	Minimization of SRD

In the first three phases of the campaign, the absorber column was operated with all three packing beds (total height of 24 meters). A conventional stripper configuration was used in which the full amount of rich solvent exiting the absorber is heated in the lean-rich heat exchanger and sent to the top of the stripper column. Throughout the test campaign, flue gas from the CCGT plant (3.5 vol% CO_2) was combined with recycle of the captured CO_2, increasing the flue gas concentration to 8 or 10 vol% CO_2 as required by the test plan. Due to the increased CO_2 concentration in the flue gas, and the corresponding increase in the required solvent circulation rate for capturing CO_2, the larger stripper intended for use with RFCC flue gas was used during this campaign in lieu of the smaller stripper intended for CCGT flue gas. In Phases 4-5, the packing height of the absorber was reduced by changing the number of beds and the stripper configuration was modified so that approximately 20% of the rich solvent exiting the absorber column bypassed the lean-rich heat exchanger and was instead heated with hot vapor leaving the top of the stripper. This portion of the test campaign, also guided with use of the process model, was focused on identifying the optimal solvent circulation for minimizing the specific reboiler duty for the process. Other process variables were fixed for this portion of the test campaign, including a flue gas flowrate of 50,000 sm^3/hr with 10 vol% CO_2 and 85% CO_2 capture. For the purpose of brevity, the details of Phases 4-5 are not included in this paper.

---

[2] Problem Solving Environment for Uncertainty Analysis and Design Exploration (https://computing.llnl.gov/projects/psuade-uncertainty-quantification)

The first three phases differed in the choice of criteria used for developing the test plan. Phase 1 used a space-filling design to ensure that the process model predicts key outputs such as CO_2 capture and specific reboiler duty with reasonable accuracy. Phase 2 focused on collecting data in regions where the model predicts optimal economic performance. Phase 3 focused on collecting data to target regions where the model predicts high uncertainty based on the SDoE procedure in Section 2.1. For all three phases, a desired region of process operation was established based on ranges of operation for flue gas flowrate (G), CO_2 capture percentage (CAP), CO_2 loading in the lean solvent entering the absorber column (α_{lean}), and the volume fraction of CO_2 in the flue gas (y_{CO_2}), with ranges:

$$G \in [36{,}000 - 75{,}000]\ kg/hr \tag{3a}$$

$$CAP \in [80 - 95]\ \% \tag{3b}$$

$$\alpha_{lean} \in [0.10 - 0.25]\ mol\ CO_2/mol\ MEA \tag{3c}$$

$$y_{CO_2} \in \{0.08, 0.10\} \tag{3d}$$

The first three variables are treated as continuous whereas the CO_2 fraction in the flue gas is treated as a categorical variable with two process operation levels. For each value of CO_2 fraction, a test set consisting of candidate experiments with a unique combination of variables $\{G, CAP, \alpha_{lean}\}$ is generated by sampling independently from uniform distributions for each variable with upper and lower limits based on the ranges given in Eq. 3. An Aspen Plus simulation is run for each point in the candidate set to estimate the corresponding values of lean (L_{lean}) and rich (L_{rich}) solvent flowrate, steam flowrate (S) and mass of CO_2 captured ($\dot{m}_{CAP}$). To be included in the final candidate set, a point must satisfy the following conditions based on operational limits for the TCM plant:

$$\dot{m}_{CAP} < 8{,}000\ kg/hr \tag{4a}$$

$$S < 14{,}000\ kg/hr \tag{4b}$$

Separate candidate sets (for $y_{CO_2} = 0.08$ and $y_{CO_2} = 0.10$) were developed using a space-filling approach based on the input vector $\boldsymbol{x} = [G\ S\ \alpha_{lean}]$. These candidate sets were used in Phases 1 and 3, although Phase 1 used a space-filling design on the model input space while Phase 3 incorporated the predicted uncertainty in the model output, using the methodology described in Section 2.1. Moreover, only the candidate set for 8 vol% CO_2 in flue gas was implemented during Phase 1 of the test campaign due to time considerations.

Phase 2, however, was designed based on an optimization problem of the form:

$$\min_{x} f(\boldsymbol{x}) = \frac{CAPEX\left(\frac{A}{P}, i, n\right) + OPEX}{\dot{m}_{CAP}} \tag{5a}$$

$$\left(\frac{A}{P}, i, n\right) = \frac{i(1+i)^n}{(1+i)^n - 1} \tag{5b}$$

$$\boldsymbol{x} = \begin{bmatrix} L_{lean} \\ G \\ \alpha_{lean} \end{bmatrix} \tag{5c}$$

subject to:

$$\boldsymbol{x^L} \le \boldsymbol{x} \le \boldsymbol{x^U} \tag{5d}$$

$$h(\boldsymbol{x}) = 0 \tag{5e}$$

$$g(\boldsymbol{x}) \le 0 \tag{5f}$$

The objective function is the ratio of the equivalent annual operating cost (EAOC) associated with the CO_2 capture to the mass of CO_2 captured. The EAOC is the sum of the capital cost (CAPEX) multiplied by an annuity factor ($\frac{A}{P}, i, n$) and the operating cost (OPEX). Within the annuity factor, $\frac{A}{P}$ is the ratio of annuity to present value, i is the interest rate, and n is the number of years. The vector of decision variables is denoted as $\boldsymbol{x}$ with lower and upper bounds $\boldsymbol{x^L}$ and $\boldsymbol{x^U}$. The equality constraints denoted by $h(\boldsymbol{x})$ includes heat and material balances, and the inequality constraints denoted by $g(\boldsymbol{x})$ includes the constraints for process operation listed in Eq. 4. The optimization was performed separately for the cases with 8 and 10 vol% CO_2 in flue gas. In addition the optimal points in the test plan, additional test points near the optimal points were included. The space surrounding the optimal point can be represented by a cube created by perturbing the input variable values by a chosen amount (10% for this study) from their estimated optimal values. A design that permutes each factor away from this estimated optimum one at a time would require seven test points, or six for the center of each face of the cube (if each factor is manipulated one at a time) and one for the center (optimal) point. As shown in Fig. 2., the design size was reduced to five by considering a fractional factorial structure, which also allows exploration of potential interactions between input factors around the optimum [14].

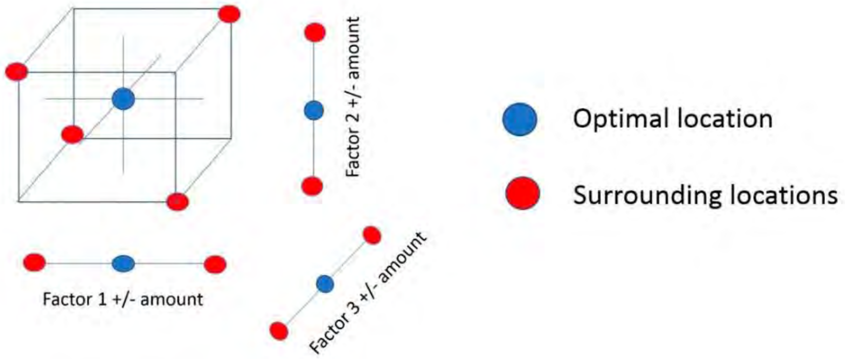

Fig. 2. Space-filling in region around optimal point for Phase 2 test plan

Since two levels of y_{CO_2} were included in the analysis, the reduction of the overall number of points required for the Phase 2 test plan from 14 to 10 was highly beneficial due to the limited amount of time available for the test campaign.

3. Results

3.1 Phase 1

In Phase 1, the test plan was developed using a minimax space-filling methodology [15] to provide an initial data set that was well-representative of the process. For all testing in this phase, the CO_2 concentration in the flue gas was fixed at 8 vol%. The set of input variables included in the test matrix differs from that used for space-filling design in that the input variables for the space-filling design were chosen for modeling convenience whereas the input variables in the test matrix were those directly manipulated in the plant operation. In developing the test matrix, the Aspen simulation was used to estimate the rich solvent flowrate and the flue gas flowrate was converted from mass to volumetric units. The test matrix, which was organized in terms of increasing flue gas flowrate for ease of process operation, for Phase 1 is given in Table 2.

Table 2. Test matrix for Phase 1 design of MEA test campaign at TCM

Test	Rich Solvent Flowrate (kg/hr)	Flue Gas Flowrate (Sm^3/hr)	Steam Flowrate (kg/hr)	CO_2 Capture Percent Estimate
1A	55,300	31,800	5,500	86.1
1B	54,200	36,000	7,200	88.0
1C	92,100	37,300	7,400	92.5
1D	81,400	43,800	7,700	84.9
1E	81,300	45,900	8,900	93.4
1F	120,800	53,700	10,700	92.2
1G	88,900	56,500	12,100	90.4
1H	90,300	57,100	9,800	82.7

When obtaining data for test cases 1A-1B, it was noted that the CO_2 capture percentage was substantially lower than the model predictions. This discrepancy was attributed to solvent maldistribution, or uneven flow through the packing, in the RFCC stripper column, resulting in inefficient performance of the column. This stripper was designed to operate at a solvent flowrate of approximately 200,000 kg/hr, or almost four times higher than the solvent flowrate in cases 1A-1B. Therefore, the lean solvent loading for these test runs was substantially higher than that predicted by the model, and the CO_2 capture percentage lower. This issue was addressed by dividing each subsequent test run into two intervals with distinct operating goals, so that two data sets were collected for test runs 1C-1H. First, the test was executed with the value of steam flowrate specified in the original test matrix. Upon achieving the steady-state, the steam flowrate was manipulated to match the estimated value of CO_2 capture. Parity plots for the model prediction of CO_2 capture percentage in the absorber and steam requirement in the stripper are given in Figure 3.

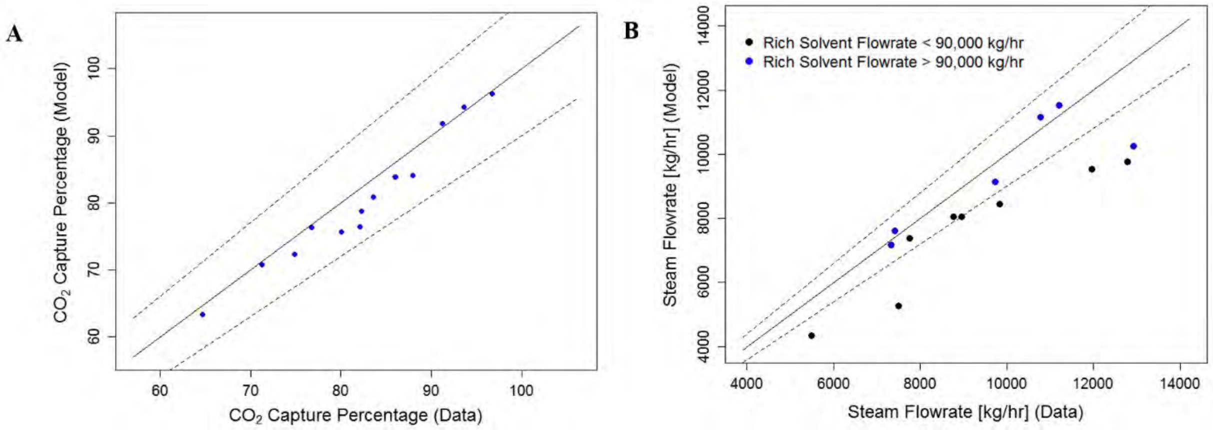

Figure 3. Parity plots for (A) CO_2 capture percentage and (B) steam flowrate required for test runs performed in Phase 1. Dashed lines represent ±10% error.

The original deterministic model, or the model in which all parameters are fixed as point values, predicts the CO_2 capture with a range of ±10% error for all test runs. The average error for CO_2 capture percentage is -2.51 ± 2.29%, with the negative error indicating that the model generally underpredicts the data. The model predicts stripper steam requirement with an average error of -10.83 ± 10.82%, although the error is notably higher for cases in which the solvent flowrate is below 90,000 kg/hr (average error of -16.43 ± 8.49%) than when it is higher than 90,000 kg/hr (average error of -3.67 ± 9.29%). This discrepancy is likely due to liquid maldistribution in the stripper column, as discussed previously. The results obtained in the first phase of the test campaign demonstrated that the initial process model was sufficiently accurate to proceed with the sequential experimental design in subsequent stages.

3.3 Phases 2-3

During the test campaign, data for Phases 2-3 were collected simultaneously and used to update the model parameter distributions through Bayesian inference. The majority of the data for Phase 2 were actually collected after those for Phase 3 due to scheduling convenience. The optimization problem described in Eq. 5 was implemented separately for the 8 and 10 vol% CO_2 cases, and used to develop the test matrix given in Table 3.

Table 3. Test matrix for Phase 2 design of MEA test campaign at TCM

Test	Rich Solvent Flowrate (kg/hr)	Flue Gas Flowrate (Sm^3/hr)	Steam Flowrate (kg/hr)	CO_2 in Flue Gas (vol%)
2A	***107,800***	***40,800***	***10,700***	***10***
2B	107,100	44,100	10,300	8
2C	107,100	44,100	12,500	8
2D	***97,400***	***49,000***	***11,400***	***8***
2E	87,700	53,900	10,300	8
2F	87,700	53,900	12,500	8
2G	97,000	44,900	11,800	10
2H	97,000	44,900	9,600	10
2I	118,600	36,700	9,600	10

In Table 3, the optimal points determined from solving separate optimization problems (Eq. 5) for the $y_{CO_2} = 0.08$ (2A) and $y_{CO_2} = 0.10$ (2D) cases are highlighted, and additional test points were selected by perturbing the variables by ± 10% from the optimal values. Parity plots for the model prediction of CO_2 capture percentage in the absorber and steam requirement in the stripper are given in Fig. 4.

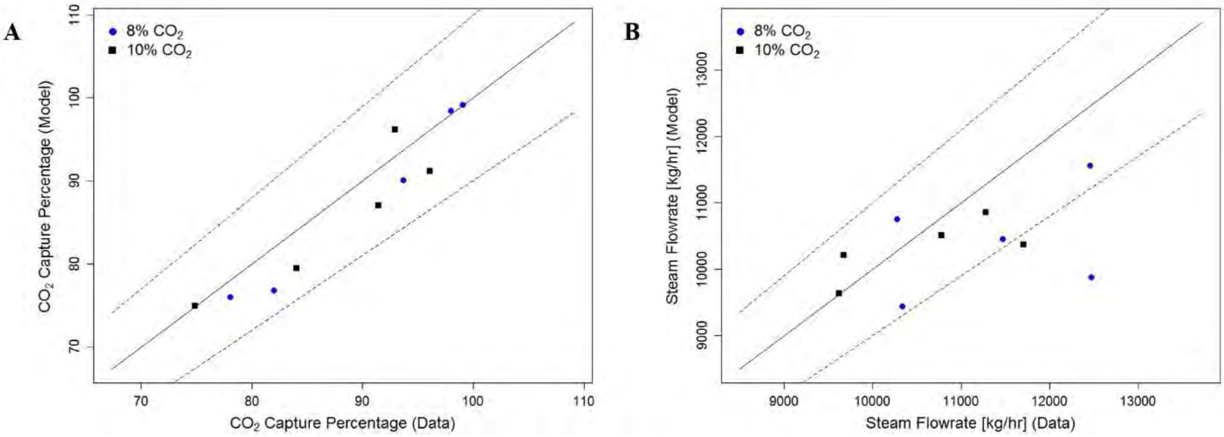

Fig. 4. Parity plots for (A) CO_2 capture percentage and (B) steam flowrate required for test runs performed in Phase 2. Dashed lines represent ±10% error.

As shown in Figure 4, the accuracy of the model for the data collected in Phase 2 is comparable to that in Phase 1. The average percent error for the CO_2 capture prediction and steam requirement prediction is -2.40 ± 3.27% and -5.28 ± 8.00%, respectively. The percentage error for the steam requirement prediction is substantially lower for the data collected in Phase 2 than in Phase 1 due to the absence of test runs with very low (< 85,000 kg/hr) solvent flowrate. Therefore, the model was shown to be sufficiently accurate for the region of the input space likely to be economically optimal.

Phase 3 of the test campaign was focused on data collection in regions where the stochastic model predicts relatively high uncertainty for the absorber CO_2 capture percentage. These data, along with those collected in Phase 2, were used to update the mass transfer and interfacial area model parameter distributions. The test matrix for Phase 3 is shown in Table 4.

Table 4. Test matrix for Phase 3 design of MEA test campaign at TCM (First Iteration)

Test	Rich Solvent Flowrate (kg/hr)	Flue Gas Flowrate (Sm^3/hr)	Steam Flowrate (kg/hr)	CO_2 in Flue Gas (vol%)	CO_2 Capture Percent Estimate
3A	133,900	62,600	11,600	8	85.9
3B	115,400	62,300	10,700	8	81.3
3C	111,900	59,100	11,100	8	89.3
3D	120,200	56,100	10,100	8	84.1
3E	119,500	55,000	9,900	8	83.6
3F	81,500	51,100	10,300	8	90.1
3G	57,500	42,500	8,700	8	81.8
3H	39,300	30,800	6,600	8	80.0
3I	48,300	30,400	8,200	10	80.0
3J	85,600	33,800	7,500	10	85.5
3K	103,100	43,000	9,200	10	82.2

The data collected in Table 4, along with case 2A from Table 3 were used in the Bayesian inference procedure based on Eq. 2. In this work, the parameters contained in $\boldsymbol{\theta}$ included the leading coefficients for the interfacial area and mass transfer submodels developed in previous work [3], and the parameters contained in $\boldsymbol{\theta}^*$ included the thermodynamic model parameters for which distributions were estimated in previous work [2]. Upon obtaining the updated parameter distributions, the refined stochastic model was used to develop a new test matrix, shown in Table 5.

Table 5. Test matrix for Phase 3 design of MEA test campaign at TCM (Second Iteration)

Test	Rich Solvent Flowrate (kg/hr)	Flue Gas Flowrate (Sm^3/hr)	Steam Flowrate (kg/hr)	CO_2 in Flue Gas (vol%)	CO_2 Capture Percent Estimate
3L	96,100	41,300	9,900	10	89.4
3M	94,000	43,500	11,000	10	88.8
3N	119,500	46,500	10,900	10	86.4
3O	150,300	48,200	11,500	10	85.2
3P	130,200	58,400	10,500	8	81.9
3Q	99,900	53,400	10,500	8	90.8
3R	80,800	51,600	12,900	8	88.3
3S	127,500	50,800	10,000	8	88.7
3T	121,200	49,300	9,200	8	85.2
3U	98,200	47,800	8,400	8	81.6
3V	125,500	47,000	9,900	8	94.2

The data collected from the test plan given in Table 5, along with cases 2B-2I in Table 3, were used in a second iteration of the SDoE procedure to update the parameter distributions again. Parity plots for the model prediction of CO_2 capture percentage in the absorber and steam requirement in the stripper for all data collected in both iterations of Phase 3 are given in Figure 5.

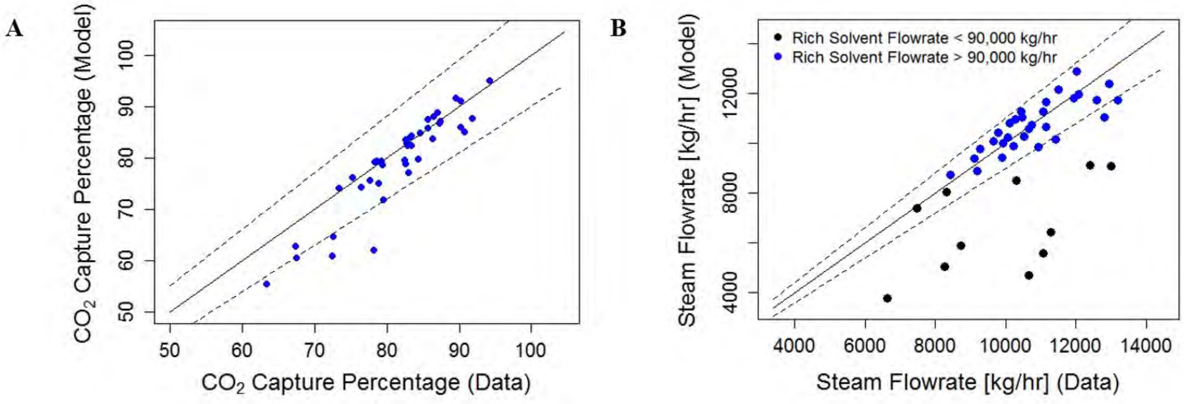

Figure 5. Parity plots for (A) CO_2 capture percentage and (B) steam flowrate required for test runs performed in Phase 3. Dashed lines represent ±10% error.

The average percentage error values for the model predictions of the data collected in Phase 3 are -2.91 ± 5.27% for CO_2 capture percentage and -8.53 ± 17.20% for the steam flowrate. As with the data collected in Phase 1, there is greater discrepancy in the stripper model for cases in which solvent flowrate is low; the average percentage error in the steam requirement is -31.05 ± 17.81% for cases in which the solvent flowrate is below 90,000 kg/hr and -0.27 ± 6.04% when it exceeds 90,000 kg/hr. As previously suggested, the underprediction in steam flowrate is likely due to operation inefficiency of the RFCC stripper caused by solvent maldistribution, as the process is operated at much lower solvent flowrate than the stripper design condition.

The probability density functions of the mass transfer and interfacial area parameters, including the prior and posterior distributions obtained after each SDoE iteration, are given in Fig. 6.

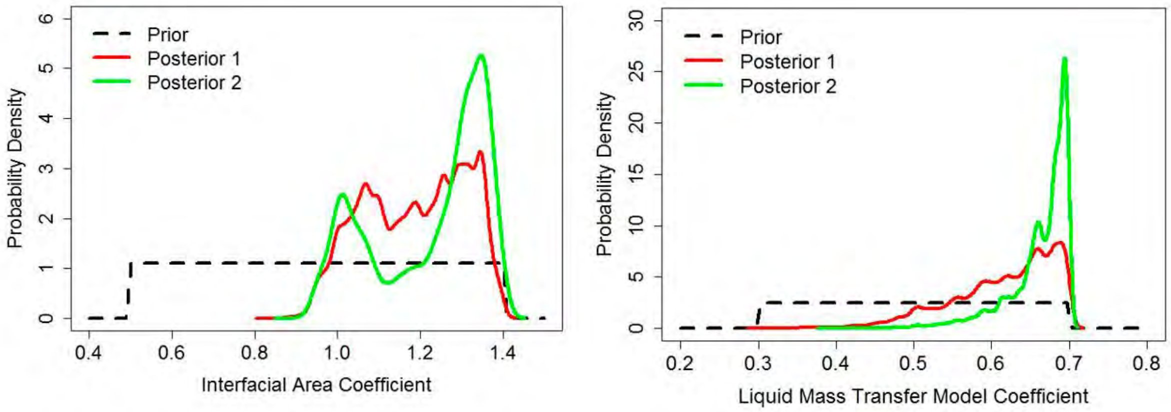

Figure 6. Comparison of prior and posterior distributions of interfacial area and mass transfer model parameters

Uniform prior distributions were initially chosen for the two parameters. The parameter space of plausible values was significantly reduced after incorporating the experimental data from the first iteration of SDoE into the stochastic model through Bayesian inference, with less reduction in the second round of SDoE. The effect of SDoE on model uncertainty reduction is more apparent when considering the model output, namely the CO_2 capture percent in the absorber. The effect of the first iteration of SDoE on reducing model prediction of uncertainty in CO_2 capture percentage is shown in Fig. 7.

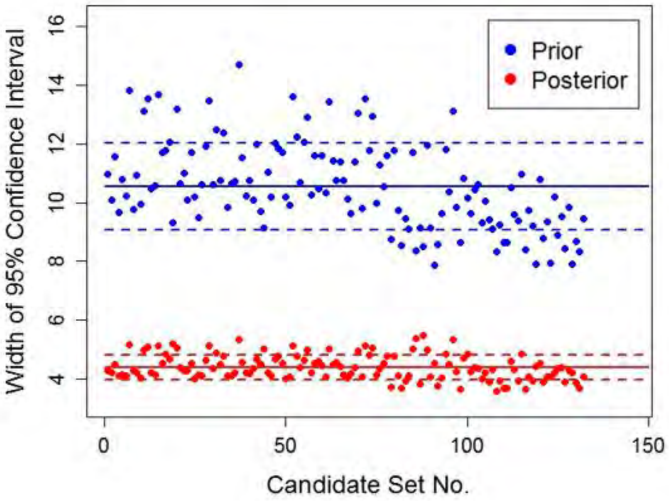

Figure 7. Effect of first round of Bayesian inference on CO_2 capture prediction confidence interval for individual points in candidate set

For the stochastic model prediction using the uniform prior distributions, the average confidence interval width for the CO_2 capture percentage was approximately 10.5% (denoted in Figure 7 by solid line) with standard deviation 1.5% (denoted by dashed lines). For the stochastic model prediction with the posterior distribution obtained after the first iteration of SDoE, the average confidence interval width was approximately 4.4% with standard deviation 0.4%. No further significant reduction in the predicted uncertainty in CO_2 capture percentage was demonstrated in the second round of SDoE. In Figure 7, the candidate set number refers to an index representing a unique combination of input variables (liquid and gas flowrates, CO_2 loading, and CO_2 fraction in flue gas). The percentage of reduction in uncertainty for a given point ($\boldsymbol{x}^{(i)}$) in the candidate set is calculated as:

$$Percent\ Reduction = 100\% \times \frac{[CI|_{\boldsymbol{x}^{(i)}}]_{initial} - [CI|_{\boldsymbol{x}^{(i)}}]_{final}}{[CI|_{\boldsymbol{x}^{(i)}}]_{initial}} \tag{6}$$

where $[CI|_{x^{(i)}}]_{initial}$ and $[CI|_{x^{(i)}}]_{final}$ represent the 95% confidence intervals in the model prediction of CO_2 capture percentage before and after updating the parameter distributions through Bayesian inference, respectively. For the entire candidate set, the average percent reduction in the uncertainty is 58.0 ± 4.7%, which is comparable to the reduction in the previous SDoE-based test campaign executed at NCCC [5,6]. As the ability of the SDoE methodology to reduce parametric uncertainty in a process model for an aqueous MEA system has been demonstrated in multiple campaigns, it may be considered a promising technique for designing future test campaigns to effectively increase fundamental understanding of novel CO_2 capture systems.

4. Conclusions and Future Work

In summary, a sequential design of experiments methodology was implemented for executing a test campaign for aqueous MEA at TCM, guiding collection of process data to refine the parameter distributions in the stochastic process model. This resulted in an average reduction of around 58% in the uncertainty in the prediction of CO_2 capture percentage. The deterministic model, or the model without parameter uncertainty, also predicted the plant performance accurately, with an average error in percentage of CO_2 capture of -2.74 ± 4.47% for the first three phases and an average error of -8.52 ± 14.85% for the reboiler steam requirement. An exception to the accurate performance of the model is for data collected under impractical operating conditions (low solvent circulation rate, in which solvent maldistribution in the stripper column was noted). For data collected when the system was operated with rich solvent flowrate below 90,000 kg/hr, the percent error in the reboiler steam prediction was -23.92 ± 15.70%. However, the percentage error in the steam prediction is -1.17 ± 6.65% for data collected when the rich solvent flowrate was above 90,000 kg/hr. The insights gained during the execution of SDoE guided the development of a new SDoE module with capability for straightforward implementation of the aims used in this experiment [16] that has been implemented in the Framework for Optimization, Quantification of Uncertainty, and Surrogates (FOQUS). This is available as part of the aforementioned CCSI Toolset and will enable the SDoE process to be implemented in a more streamlined manner in future applications. In planned future work, the $CCSI^2$ team will apply the SDoE methodology to novel CO_2 capture technologies with the primary goal of refining initial process models by reducing their uncertainty, and thus the inherent risk associated with preliminary models of new processes, through guided data collection.

Disclaimer

This project was funded by the United States Department of Energy, National Energy Technology Laboratory, in part, through a site support contract. Neither the United States Government nor any agency thereof, nor any of their employees, nor the support contractor, nor any of their employees, makes any warranty, express or implied, or assumes any legal liability or responsibility for the accuracy, completeness, or usefulness of any information, apparatus, product, or process disclosed, or represents that its use would not infringe privately owned rights. Reference herein to any specific commercial product, process, or service by trade name, trademark, manufacturer, or otherwise does not necessarily constitute or imply its endorsement, recommendation, or favoring by the United States Government or any agency thereof. The views and opinions of authors expressed herein do not necessarily state or reflect those of the United States Government or any agency thereof.

Acknowledgement

The authors gratefully acknowledge the staff of TCM DA, Gassnova, Equinor, Shell and Total for their contribution and work at the TCM DA facility. The authors also gratefully acknowledge Gassnova, Equinor, Shell, and Total as the owners of TCM DA for their financial support and contributions.

References

[1] Morgan JC, Bhattacharyya D, Tong C, Miller DC. Uncertainty quantification of property models: methodology and its application to CO_2-loaded aqueous MEA solutions. AIChE J 2015;61(6):1822-39.

[2] Morgan JC, Chinen AS, Omell B, Bhattacharyya D, Tong C, Miller DC. Thermodynamic modeling and uncertainty quantification of CO2-loaded aqueous MEA solutions. Chem Eng Sci 2017;168:309-24.

[3] Chinen AS, Morgan JC, Omell B, Bhattacharyya D, Tong C, Miller DC. Development of a rigorous modeling framework for solvent-based CO_2 capture. Part 1: hydraulic and mass transfer models and their uncertainty quantification. Ind Eng Chem Res 2018;57:10448-63.

[4] Morgan JC, Chinen AS, Omell B, Bhattacharyya D, Tong C, Miller DC. Development of a rigorous modeling framework for solvent-based CO_2 capture. Part 2: steady-state validation and uncertainty quantification with pilot plant data. Ind Eng Chem Res 2018;57:10464-81.

[5] Soepyan B, Anderson-Cook CM, Morgan JC, Tong CH, Bhattacharyya D, Omell BP, Matuszewski MS, Bhat KS, Zamarripa MA, Eslick JC, Kress JD, Gattiker JR, Russell CS, Ng B, Ou JC, Miller DC. Sequential design of experiments to maximize learning from carbon capture pilot plant testing. Comput Aided Chem Eng 2018;44:283-8.

[6] Morgan JC, Chinen AS, Anderson-Cook C, Tong C, Carroll J, Saha C, Omell B, Bhattacharyya D, Matuszewski M, Bhat KS, Miller DC. Development of a framework for sequential Bayesian design of experiments: application to a pilot-scale solvent-based CO_2 capture process. App Energy 2020;262:114533.

[7] Brigman N, Shah MI, Falk-Pedersen O, Cents T, Smith V, De Cazenove T, Morken AK, Hvidsten OA, Chhaganlal M, Feste JK, Lombardo G, Bade OM, Knudsen J, Subramoney SC, Fostås BF, de Koeijer G, Hamborg ES. Results of amine plant operations from 30 wt% to 40 wt% aqueous MEA testing at the CO_2 Technology Centre Mongstad. Energy Procedia 2014;63:6012-22.

[8] Gjernes E, Pedersen S, Cents T, Watson G, Fostås BF, Shah MI, Lombardo G, Desvignes C, Flø NE, Morken AK, De Cazenove T, Faramarzi L, Hamborg ES. Results from 30 wt% MEA performance testing at the CO_2 Technology Centre Mongstad. Energy Procedia 2017;114:1146-57.

[9] Faramarzi L, Thimsen D, Hume S, Maxon A, Watson G, Pedersen S, Gjernes E, Fostås BF, Lombardo G, Cents T, Morken AK, Shah MI, De Cazenove T, Hamborg ES. Results from MEA testing at the CO_2 Technology Centre Mongstad: verification of baseline results in 2015. Energy Procedia 2017;114:1128-45.

[10] Hamborg ES, Smith V, Cents T, Brigman N, Falk-Pedersen O, De Cazenove T, Chhaganlal M, Feste JK, Ullestad Ø, Ulvatn H, Gorset O, Askestad I, Gram LK, Fostås BF, Shah MI, Maxson A, Thimsen D. Results from MEA testing at CO_2 Technology Centre Mongstad. Part II: Verification of baseline results. Energy Procedia 2014;63:5994-6011.

[11] Montañés RM, Flø NE, Nord LO. Dynamic process model validation and control of the amine plant at CO_2 Technology Centre Mongstad. Energies 2017;10:1527.

[12] Bui M, Flø NE, De Cazenove T, Mac Dowell N. Demonstrating flexible operation of the Technology Centre Mongstad (TCM) CO_2 capture plant. Int J Greenh Gas Con 2020;262:114533.

[13] Myers RH, Montgomery DC, Anderson-Cook CM. Practical design optimality. In: Response surface methodology: process and product optimization using design experiments. 4th ed. New York: Wiley Plus; 2016. p. 467-74.

[14] Myers RH, Montgomery DC, Anderson-Cook CM. The one-half fraction of the 2^k design. In: Response surface methodology: process and product optimization using designed experiments. 4th ed. New York: Wiley Plus; 2016. p. 162-174.

[15] Johnson ME, Moore LM, Ylvisaker D. Minimax and maximin distance designs. J Stat Plan Infer 1990;26:131-48.

[16] Lu L, Anderson-Cook CM, Ahmed T. Non-uniform space-filling designs. J Qual Tech 2021; to appear.

CATCHING OUR FUTURE

Cost Reduction Study for MEA based CCGT Post-Combustion CO_2 Capture at Technology Center Mongstad

(2021)

15th International Conference on Greenhouse Gas Control Technologies, GHGT-15

15th 18th March 2021 Abu Dhabi, UAE

Cost Reduction Study for MEA based CCGT Post-Combustion CO_2 Capture at Technology Center Mongstad

Muhammad Ismail Shah[a], Eirik Falck da Silva[b,*], Erik Gjernes[c] and Knut Ingvar Åsen[d]

[a]*Technology Centre Mongstad, 5954 Mongstad, Norway*
[b]*Stavanger Research Center, TOTAL EP Norge AS, 4029 Stavanger, Norway*
[c]*Gassnova SF, Dokkvegen 10, 3920 Porsgrunn, Norway*
[d]*Equinor ASA, PO Box 8500, 4035 Stavanger, Norway*

Abstract

A campaign was carried out by Technology Center Mongstad (TCM) and its owners in the amine capture plant to study various cost saving operating options relevant for combined cycle gas turbine plants. The owners chose MEA as solvent for this test because it is a well-studied solvent system with no commercial constraints regarding sharing of data. Learnings obtained from MEA studies are also expected to be of relevance for other solvent systems.

During this campaign the main focus was on thermal energy optimization at different flue gas flow rates through the absorber column and MEA emissions, with target for reduced CAPEX and OPEX. During the campaign, new options such as a rich solvent bypass to stripper overhead and higher concentration of MEA (up to 38wt%) were tested. Tests were carried out to identify plant configurations and process parameters with the potential for CAPEX and OPEX reduction in a post-combustion carbon capture plant. Significant cost of CO_2 avoided reductions were achieved compared to the previous TCM campaigns for MEA.

Keywords: CO_2 Absorption; Cost Reduction; MEA

1. Introduction

TCM is located next to the Equinor refinery in Mongstad (outside Bergen, Norway) which is the source of the two types of flue gases supplied to TCM. These sources are the combined cycle gas turbine (CCGT) based heat and power plant (CHP) and residual fluid catalytic cracker (RFCC). The owners of TCM started their third monoethanolamine (MEA) test campaign (MEA-3) in June 2017 and continued with MEA-4 and MEA-5 that lasted until October 2018. MEA-3, MEA-4 and MEA-5 have been the most significant collaboration campaigns that TCM has conducted since its inauguration in 2012. The large number of industrial, research and academic participants involved in these campaigns have enriched the projects and ensured that the results will serve a broad range of audiences.

A sub-campaign on cost reduction during MEA-5 was carried out by TCM owners in this capture plant to study various cost saving options. MEA was chosen as solvent for this test because it is a well-studied solvent system with

---

[*] Corresponding author. Tel: +47 948 45 691, *E-mail address:* eirik.silva@total.com

Electronic copy available at: https://ssrn.com/abstract=3821061

no commercial constraints regarding sharing of data. This work follows previous work carried out on the same subject at TCM [1].

2. Test Campaign and Results

The TCM amine plant is shown in Figure 1. The plant has been in operation since 2012 carrying out tests on a number of proprietary and non-proprietary solvent systems. A recent modification to the plant is the addition of a rich solvent partial-bypass upstream of the lean-rich amine heat exchanger to the stripper top. This is intended to improve the energy performance of the plant. A noteworthy feature of the plant is that there are three different feed locations for the lean solvent to the absorber. This allows for testing at different packing height for CO_2 absorption (12m, 18m, and 24m), as shown in yellow in the Figure. Another important feature is that the plant has two strippers with dedicated reboilers, the Combined Heat and Power (CHP) stripper suited for stripping of lower amounts of CO_2 and the Residual Fluidized Catalytic Cracker (RFCC) stripper suited for larger volumes of CO_2. Only CHP flue gas was utilized in the present campaign.

The purpose of the present campaign has been to explore different modes of operation with cost reduction potential. Such as higher flue gas throughput, lower packing height, more concentrated solvent and higher capture rate. Simple configurations such as operating with only one water wash section and higher flue gas inlet temperatures were also investigated. Table 1 summarizes the phases A to F of the test campaign.

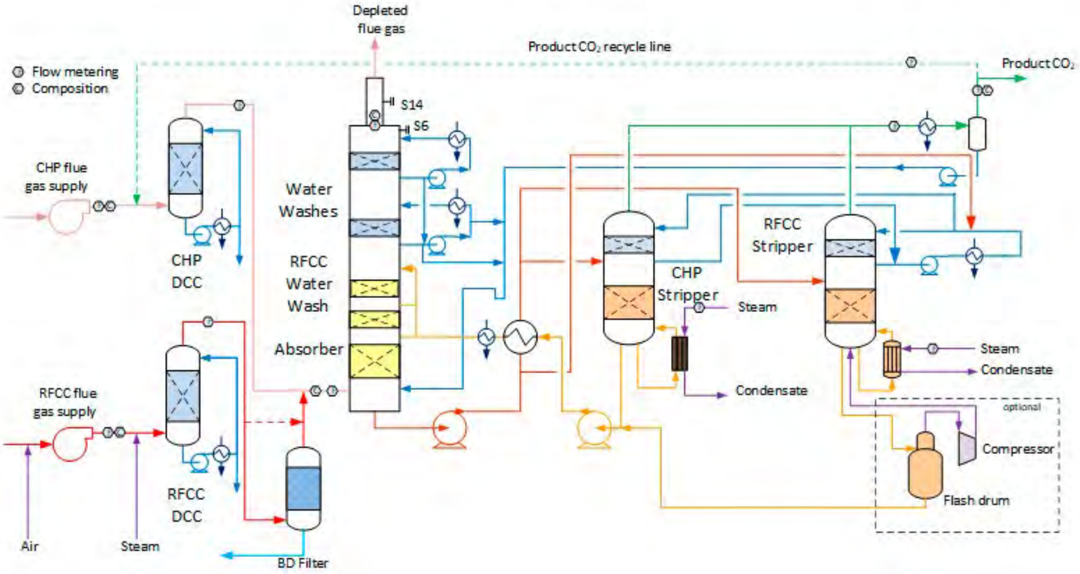

Fig. 1. A process flow diagram of the TCM Amine plant. The diagram illustrates the two different flue gas configurations (CHP and RFCC) as well as the available strippers. The CHP flue gas can be further enriched with CO_2 from a CO_2 recycle line, and the RFCC flue gas can be diluted with air to reach a target CO_2 concentration.

Electronic copy available at: https://ssrn.com/abstract=3821061

Table 1. Phases of the campaign.

Condition	Phase A	Phase B	Phase C	Phase D	Phase E	Phase F
Flue gas flow [Sm^3/h]	40-47,000	50,000	50,000	67,000	67,000	59,000
Absorber packing height [m]	18	18	18	24	24	18
Stripper	CHP	CHP	CHP	RFCC	RFCC	RFCC
CO_2 capture rate [%][1]	85 - 96	90 - 91	89 - 93	95 - 99	98 - 99	90-91
Optimal SRD [GJ/ton CO_2][2]	**3.8** (85)	**3.6** (91)	**3.6** (91)	**3.7** (97)	**4.0** (98)	**3.7** (91)
MEA [wt%]	32	37	34 - 37	35 -36	35 -37	36 -38
CO_2 conc, wet [vol %]	3.6 - 4.2	4.0 – 4.2	3.8 – 4.2	4.0 – 4.2	3.9 – 4.2	4.1 – 4.2
Absorber water wash stages	2	1	1	1/2[3]	1	1
L/G [kg/Sm^3][4]	0.97 - 1.14	0.92 - 1.54	1.13 – 1.74	0.95 – 1.88	1.10 – 1,54	1.12 – 1.47
Flue gas temp [°C]	30	30	45	30	45	30
Rich solvent bypass [%]	0	20	20	20	20	20
Lean solvent temp [°C]	41.2	54.9	54.5	45.0	40.0	44.4
MEA emission [ppmv]	<1	<1	0.6	1.5	2.1	1.1

1: Capture rate is based on method 4 as described in the text. 2: SRD is Specific Reboiler Duty 3 as described in the text. Associated capture rate in parenthesis. 3: Second water wash stage was partially operated to manage emissions. 4: L/G is the ratio of lean solvent flow to flue gas flow into the absorber.

The rich solvent bypass was in operation during all phases of the campaign except phase A. Flue gas CO_2 concentrations varied between 3.6 % and 4.2% during the campaign. The variations in CO_2 concentration were achieved by use of a recycle. Phase A was operated at 32 wt% MEA and was investigating effect of CO_2 concentration and flue gas flow.

Phase A was mainly intended to validate previous work and will not be discussed further. The rest of the cases were operated at MEA concentration up to 38 wt% and with the target of having only the lower absorber water wash section in operation.

Phase B and C were operated at 50,000 Sm^3/h, 18-meter absorber packing, CHP stripper and with flue gas temperature out the absorber of 30 and 45°C, respectively. Operating with higher flue gas temperature could offer potential savings since this will enable the use of a smaller Direct Contact Cooler.

During Phase D and E this temperature variation was intended to be repeated at flue gas flow of 67,000 Sm^3/h, 24-meter absorber packing and RFCC stripper in operation. The flue gas flow of 67,000 Sm^3/h rate is the highest practically possible operating point at TCM and represents 113% of design capacity.

Finally, Phase F was operated at 18-meter absorber packing and 59,000 Sm^3/h flue gas flow at 36-38wt% MEA.

The energy efficiency of the capture process is given by the Specific reboiler duty (SRD), this is defined as the heat delivered to the reboiler from the steam system divided by the amount of captured CO_2:

$$SRD = \frac{\Delta H m_{steam}}{m_{CO2\ cap}} \qquad (1)$$

Electronic copy available at: https://ssrn.com/abstract=3821061

where m_{steam} is the steam flow to the reboiler heat exchanger. ΔH is the enthalpy difference between steam and condensate calculated from measured temperature and pressure, see also reboiler, steam and condensate in Figure 1. Steam pressure is typical around 2.5 barg and up to 160 °C for the tests reported in this paper. CO_2 capture rate is the mass fraction of CO_2 being captured out of the amount of CO_2 flowing into the absorber. The amount of captured CO_2 can be derived from the CO_2 product flow out of the stripper or from difference in CO_2 flow in and out of the absorber. SRD and capture rate are presented utilizing both methods below, while the economical assessment is based on difference in and out of the absorber such that the results can be compared to previous work [1]. This method is in the present paper referred to as “SRD 3”. SRD based on the product flow out of the stripper is referred to as “SRD 1”. The reported results are two-hour averages within a test slot that lasts more than 6 hours. Typically, one liquid solvent sample is taken for each test point.

In the present paper we report CO_2 capture rates based on two methods, Capture Method 1 and Capture Method 4. Method 1 is based on the ratio between the stripper product flow and the absorber inlet flow, while Method 4 is based on the mass balance over the absorber [2].

TCM is equipped with multiple flue gas analyzers and flow meters for each of the main three gas streams. Table 2 shows the ones selected for the current analysis. Water is calculated assuming saturated conditions based on pressure and temperature. Flow out of the absorber is calculated from measured flow into the absorber assuming conservation of all components in and out of the absorber except water and CO_2. Finally, it is assumed that product gas out of the stripper is only CO_2 and water.

Table 2. Measurement of gas flows.

Unit	Property	Method/Principle
Absorber in	H_2O	Calculated from p and T
	CO_2	Infrared spectroscopy (IR)
	Flow	Ultrasonic flow meter
Absorber out	H_2O	Calculated from p and T
	CO_2	Infrared spectroscopy (IR)
	Flow	Calculated from absorber in flow and composition in and out of absorber
Product flow	H_2O	Calculated from p and T
	CO_2	Calculated as: 100 - H_2O
	Flow	Coriolis flow meter

In Figure 2 SRD and capture rate vs. L/G for phase B is shown. At TCM optimum SRD is obtained by varying the lean flow rate (and thereby the L/G) and adjusting the reboiler duty at each solvent circulation point to maintain the required/targeted capture rate. The optimum SRD achieved here was 3.6 GJ/ton CO_2 (based on SRD 3).

Electronic copy available at: https://ssrn.com/abstract=3821061

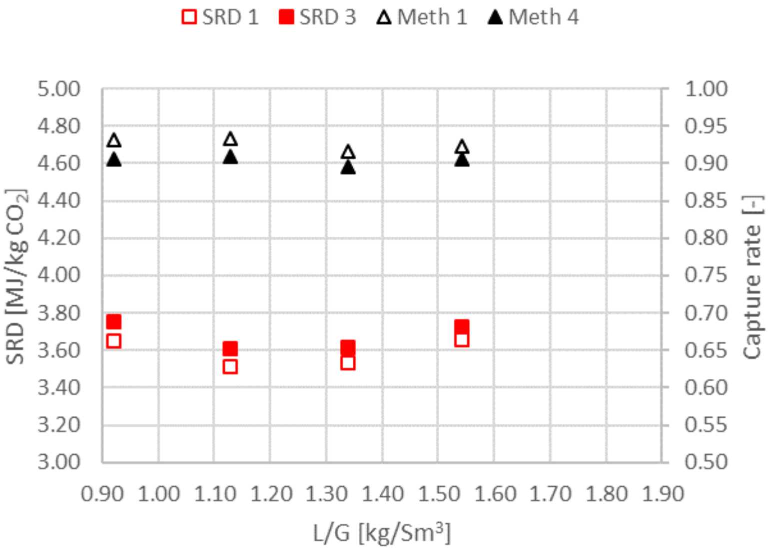

Fig. 2 SRD (left y-axis) and capture rate (right y-axis) for phase B as function of liquid to flue gas ratio (flue gas 50,000 Sm3/h).

One of the best cases demonstrated is “B3-rep” (at L/G of 1.13). The capture rate for this case is a bit above 90%, with SRD of 3.6 GJ/tCO_2 with 18m packing height, 37 wt% MEA, one water wash and MEA emissions below 1 ppm. Flue gas flow is 50,000 Sm^3/h and liquid to gas ratio (L/G) for “B3-rep” is about 1.13 kg solvent/Sm^3 of flue gas. This can result in significant reduction of CAPEX and OPEX, compared to the MEA baseline.

In Figure 3 SRD and capture vs. L/G for phase D is shown. During Phase D 97% CO_2 capture at an SRD of 3.7 GJ/ton CO_2 were achieved. This SRD is perhaps lower than that would have been expected for a very high capture rate. The point at L/G of 1.38 has a high SRD, this is due to high levels of steam being utilized to achieve high capture rates. With Method 4 the capture rate was 99%, with Method 1 it was slightly over a 100% (due to accuracy limitations in calculation). Since the number is over 100% it is not visible in the plot.

Electronic copy available at: https://ssrn.com/abstract=3821061

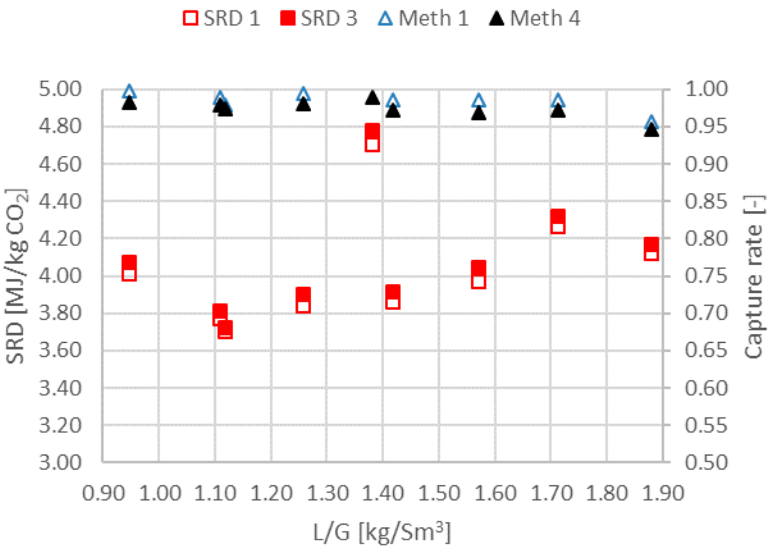

Fig. 3. SRD (left y-axis) and capture rate (right y-axis) for phase D as function of liquid to flue gas ratio (flue gas 67,000 Sm3/h).

Higher flue gas capacity tests at 67,000 Sm^3/h resulted in high amine emission, which is partly due to mechanical entrainment and partly due to only one water wash section being in operation. However high solvent entrainment can be potentially reduced by improving the absorber design by installing a more efficient demister at appropriate location in the absorber. Very high CO_2 capture rate of almost 99% was demonstrated with SRD of 3.8 GJ/tCO_2 with 24 m absorption bed and 67,000 Sm3/h of flue gas capacity. The increase in SRD is about 6% when the capture rate increases from 90% to 99%, however the comparison is not fair as the plant capacity and configuration is not similar in the two cases.

During phase E higher flue gas capacity tests at 67,000 Sm^3/h and flue gas temperature of 45°C resulted in a relatively high SRD and most importantly higher MEA emission as expected.

SRD and capture results from Phase F are shown in Figure 4. Case F2 with 3.8 GJ/ton CO_2 and 90% capture rate was selected for further assessment in the next section.

Electronic copy available at: https://ssrn.com/abstract=3821061

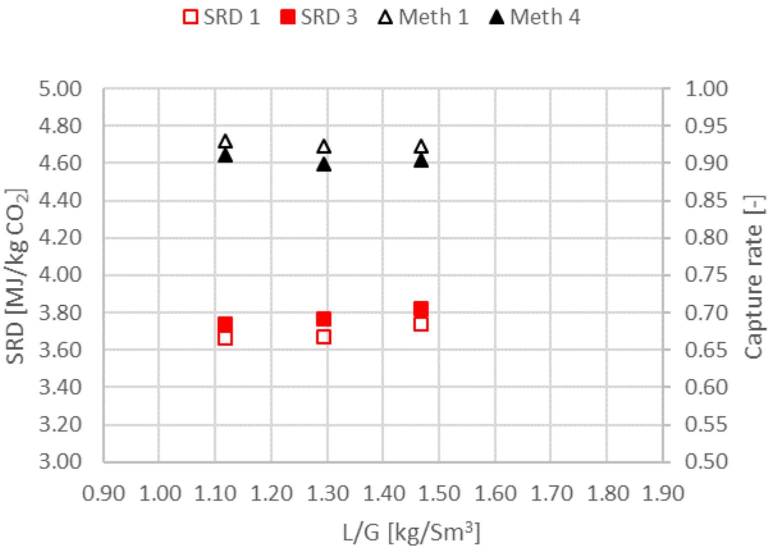

Fig. 4. SRD (left y-axis) and capture rate (right y-axis) for phase F as function of liquid to flue gas ratio (flue gas 59,000 Sm3/h).

In the present campaign the plant was mostly operated with 37 wt% MEA. There have been some relatively short campaigns at TCM in the past where the plant has operated with a concentration slightly higher than 40 wt% MEA [1]. From an energy performance perspective 40 wt% is expected to give better results. There is however a concern that solvent degradation will be more severe for 40 wt% MEA. Degradation can besides being a problem in itself also impact corrosion in the plant. 35 wt% MEA is what TCM is currently comfortable with operating, however long-term continuous test with 37-38 wt% MEA needs to be conducted to better understand degradation, emission and energy performance of the solvent.

Table 3 summarizes the selected cases for economical evaluation along with the reference case named MEA 3 (9-4) [1]. Stripper pressures were maintained at 0.9 barg for all cases. The MEA-3 and B3-rep were operated with CHP stripper while F2 and D3-rep utilized the RFCC stripper. Liquid sample for case D3-rep is taken about 1 hour outside the 2 hours being averaged, but still within the test period.

Electronic copy available at: https://ssrn.com/abstract=3821061

Table 3. Selected cases for economical evaluation [1-3]

#	Abs. pack [m]	MEA[1] [wt%]	Flue gas × 1000 [Sm^3/h]	L/G [kg/Sm^3]	Anti-foam [-]	Stripper bottom temp [°C]	Lean loading [mol/mol]	SRD [GJ/ton CO_2]	CO_2 Capture [%]
MEA-1	24	~ 30	47	1.17	No	119.3	0.23	4.1	~ 85
MEA-2	24	31/30	59	1	Yes	121.0	0.21	3.6	86
MEA-3	18	43/40	51.0	0.98	No	121.7	0.25	3.6	86
F2	18	36/34	59.0	1.29	No	121.0	0.26	3.8	90
B3-rep	18	37/35	50.0	1.13	No	121.4	0.24	3.6	91
D3-rep	24	36/34	67.0	1.12	No	122.5	0.21	3.7	97

1: Number given first is on MEA-water basis, second number is on MEA-water-CO_2 basis.

3. Economic Evaluation

The economic evaluations of power and capture plants in this paper is based on standard "Cost of Electricity" (COE) and "Cost of CO_2 avoided" metrics. These calculations are based on aligned and standardized estimates and assumptions on technology process performance such as energy efficiency, CO_2 generation and capture rates, see e.g. [4]. Cost estimates include CAPEX, operations and maintenance (O&M) including fuel and a set of general price and rate of return assumptions. For each case below, a complete sized capture plant equipment list is established. Aspen In-Plant Cost Estimator (IPCE) V9 is used to estimate equipment cost. Equipment installation factors are then used to estimate total installed costs. Aligned with known projects, including contingency, 30% added to the Aspen Equipment cost and average installation factor of around 5.5. The OPEX can be split in annual cost (of CAPEX), power loss, maintenance, chemicals and fixed operating costs. The gas fired power plant specific cost and performance is based on GTPro simulation of a GE 9HA CCGT plant. 25% contingency is added to the estimated GTPro CCGT CAPEX number. All calculations are furthermore carried out at:

- normalized, per unit (kWh) output from the base industrial (power) plant
- pretax, pre-financing basis
- annual cost basis, applying a capital charge factor corresponding to a standard discount factor and project time horizon

Cost of CO_2 avoided (\$/ton CO_2) is calculated according to Equation below and is based on cost of electricity (COE) and CO_2 emission per kWh (CO_2 emission) for a power plant with capture (cap) and without CO_2 capture (no cap).

$$Cost\ of\ CO_2\ avoided = \frac{COE_{cap} - COE_{no\ cap}}{CO_2\ emission_{no\ cap} - CO_2\ emission_{cap}} \tag{2}$$

The calculated cost of CO_2 avoided implicitly accounts for the capture systems' own energy demand and its inherent CO_2 emissions. The following economic assumptions are applied:

- Fuel gas price: 0.1875 US \$/Sm^3

Electronic copy available at: https://ssrn.com/abstract=3821061

- On-stream hours: 7884 (90 %)
- Discount rate: 5 % real (pretax)
- Time horizon: 30 years

These were chosen to be consistent with a previous economical study [1].

This paper will only report percentage cost reduction and no absolute cost numbers. The main reasons are that the absolute numbers are not useful for the purpose of this work and are partially confidential. In this work one consistent method and one consistent set of assumptions are used for calculating the cost, which is important for a fair comparison.

The experiments targeted lowest possible absorber packing height, lowest possible L/G and SRD while maximizing the captured CO_2 and capture rate. In Table 4 below the experimental data for the selected cases are scaled to a full-scale design at a fixed inlet CO_2 flow of 150 tonnes CO_2/h and measured capture rate case by case.

In order to compare on the same basis in the cost assessment, the CO_2 inlet concentrations for all cases are adjusted to 4.2 % (wet) since the tests was done with close to 4.2 % (wet) CO_2 in the flue gas. Typically, an H class gas-turbine will produce flue gas with at least 4.5% CO_2 which will reduce the CO_2 capture cost further. An increased CO_2 content will impact all the cases in this paper equally (see discussion in previous paper [1]).

The adjusted/scaled absorber packing height and the most important cost parameter, the packing volume, are calculated from the experimental data for the cases selected in the test campaign. The scaled-up absorber volume is based on packing height utilized for each TCM test case and a scaled up cross sectional area. The latter is calculated based on TCM cross sectional area and the ratio of full-scale (150 tonnes CO_2/h, corresponding to 700 MW_{lhv} fuel input) to TCM (case by case) CO_2 inlet flow.

For all scaled up cases the cross-sectional areas are adjusted to fit with a superficial velocity of 2 m/s (at 0 °C, 1 atm). This will secure less differences in pressure drop between the cases and less impact on the flue gas fan duty in a full-scale plant. This means that it is assumed that the CO_2 capture rate depends mainly on the total packing volume and less on the differences in flue gas velocity through the absorber.

Thus, packing height, see Table 4, is adjusted in order to maintain the scaled-up absorber packing volume. The packing volume per captured CO_2 will be equal for each TCM case and corresponding scaled up case. The data are shown in Table 4 including lean solvent flow rate, specific packing volume, amount of captured CO_2 and CO_2 capture rate.

Packing volume is a significant CAPEX element and the most cost-effective packing volume demonstrated in this campaign was 34 m^3/tonne CO_2 capture per hour for the current test conditions. In Case B3-rep and D3-rep a significantly larger stripper (RFCC) was used removing any limits in the stripper process. This had a positive effect in allowing operating with a lower inlet lean loading at an increased solvent flow rate to the absorber (i.e. keeping an optimal L/G) increasing the absorber CO_2 capture capacity and significantly increasing the CO_2 capture rate.

Table 4. Key cost parameters

	Adjusted abs. Pack [m]	Lean solvent flow [kg/kg CO_2 in]	Spec. packing volume [m^3/t CO_2, h]	Captured CO_2 [t/h]	CO_2 capture [%]
MEA-1[1]	~28	~16	~55	128	85
MEA-2[1]	25.5	14.5	50	128	86
MEA-3[1]	18.9	12.5	37	129	86
F2	16.6	17.5	37	135	90
B3-rep	19.5	14.5	36	136	91
D3-rep	19.6	15.5	34	146	97

1: Reference [1].

Electronic copy available at: https://ssrn.com/abstract=3821061

The section above introduced the economic evaluation and cost of CO_2 avoided. In Figure 5 the demonstrated cost reduction for the selected three test cases are compared with the best result from the MEA-3, 2 and 1 campaign [1]. The previous assessment [1] has been revisited and the presented relative cost of CO_2 avoided are updated based a newer gas turbine (H class).

Case D3-rep demonstrates the largest cost reduction contribution, i.e. 4.8 % down relative to MEA-3 and close to 20% relative to MEA 1 The trend is a reduction in CO_2 capture cost with increasing CO_2 capture rate. Since more CO_2 is being captured for a given flue gas stream the total cost (CAPEX) of CO_2 handling will increase somewhat also increasing cost of electricity. For case D3-rep this represents an increased cost of electricity with 3-4% compared to the MEA-3 case. Due to the significantly higher amount of CO_2 captured, the avoided CO_2 cost will still be reduced as shown in Figure 5 below. The cost estimation was done with two water wash stages for the case D3-rep. Results from the campaign did suggest that one stage could have been sufficient, resulting in some additional savings.

Since the cost reduction potential of these measures is experimentally verified in one of the world's largest demonstration plants, the cost reduction should be highly accurate, and hence relevant for future post-combustion plants.

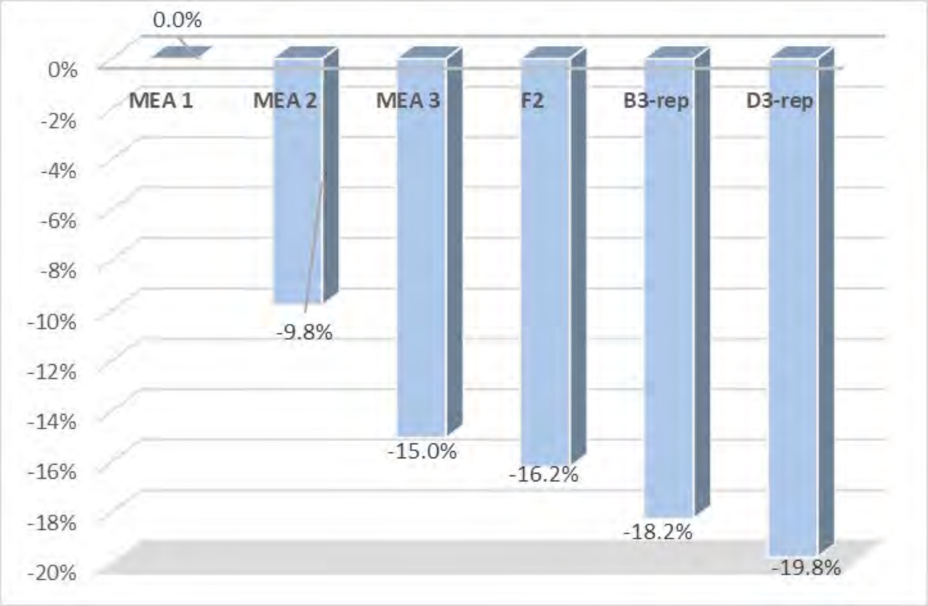

Fig. 5. Demonstrated reduction in cost of CO_2 avoided for the selected cases compared with the earlier MEA campaigns.

4. Conclusions

The results show encouraging cost reduction potential such as lower energy numbers for a more concentrated (35 wt%) MEA solvent and more cost-efficient design of the capture plant. Cost improvements of 4.8% were achieved compared to the previous TCM benchmark (MEA 3) and close to 20% compared to the first campaigns. These results can be viewed as a form of debottlenecking of the amine plant, optimizing its throughput. However, the impact of working with a more concentrated solvent on corrosion, solvent degradation and emissions is something that must be explored further.

Electronic copy available at: https://ssrn.com/abstract=3821061

It is important to notice that these results are generated at one of the world's largest capture demonstration units, and that it is one of the first times such a structured campaign is executed. Similar testing can be carried out with different amine-based solvents. Therefore, these results at TCM scale represent a very relevant basis for scale up and industrial design of amine solvent capture technologies.

Acknowledgements

The authors gratefully acknowledge the staff of TCM DA, Gassnova, Equinor, Shell and Total for their contribution and work at the TCM DA facility. The authors also gratefully acknowledge Gassnova, Equinor, Shell, and Total as the owners of TCM DA for their financial support and contributions.

References

[1] Gjernes E, Pedersen S, Jain D, Åsen KI, Hvidsten OA, de Koeijer G, Faramarzi L, de Cazenove T. Documenting modes of operation with cost saving potential at the Technology Centre Mongstad. GHGT-14, 21st-25th October 2018, Melbourne, Australia

[2] Faramarzi F, Thimsen D, Hume S, Maxon A, Watson G, Pedersen S, Gjernes E, Fostås BF, Lombardo G, Cents T, Morken AK, Shah MI, Cazenove Td, Hamborg ES. Results from MEA testing at the CO2 Technology Centre Mongstad: Verification of baseline results in 2015. Energy Procedia, 114, 2017, 1128-1145

[3] Hamborg ES, Smith V, Cents T, Brigman N, Falk-Pedersen O, de Cazanove T, Chhagnlal M, Feste JK, Ullestad Ø, Ulvatn H, Gorset O, Askestad I, Gram LK, Fostås BF, Shah MI, Maxson A, Thimsen D. Results from MEA testing at the CO2 Technology Centre Mongstad. Part II: Verification of baseline results. Energy Procedia 63, 2014, 5994-6011

[4] Cost and Performance Baseline for Fossil Energy Plants Volume 1a: Bituminous Coal (PC) and Natural Gas to Electricity Revision 3, July 6 2015, DOE/NETL-2015/1723

Electronic copy available at: https://ssrn.com/abstract=3821061

CATCHING OUR FUTURE

A Benchmark for Compact CO_2 Capture Plant Designs by Monoethanolamine Solvent Testing at Technology Centre Mongstad

(2021)

15th International Conference on Greenhouse Gas Control Technologies, GHGT-15

15th 18th March 2021 Abu Dhabi, UAE

A Benchmark for Compact CO_2 Capture Plant Designs by Monoethanolamine Solvent Testing at Technology Centre Mongstad

Gelein de Koeijer[a], Christophe Benquet[bc], Anette Knarvik[ac], Erik Gjernes[d], Steinar Pedersen[a], Odd Arne Hvidsten[ac]

[a]Equinor ASA, P.O. Box 8500, 4035 Stavanger, Norway
[b] Total E&P Norge, Finnestadveien 44, Dusavik, 4029 Stavanger, Norway
[c]Technology Centre Mongstad, 5954 Mongstad, Norway
[d]Gassnova SF, Dokkvegen 10, 3920 Porsgrunn, Norway

Abstract

Technology Centre Mongstad (TCM) is a large and flexible demonstration site for post-combustion CO_2 capture. It is located next to the Equinor refinery at Mongstad (Norway) which is the source of the flue gases supplied to TCM. It has been used for testing CO_2 capture with MEA solvent and a compact design, providing a benchmark for compact CO_2 capture technologies.. The absorber was used with its lowest possible packing height of 12m, and only one of two water washes was used (3m height). The plant was operated with a high flue gas flow rate (67,000 Sm^3/h) and 35 wt% MEA with a sensitivity down to 30 wt%. The CO_2 inlet concentration was 6% mimicking some industrial exhausts, small turbines with exhaust gas recycle or modern turbines with high turbine inlet temperatures. The tests demonstrated that such a low absorber can capture more than 80% of the CO_2 with only a slightly higher steam demand than conventional applications with higher packing heights of 18-24m. The low absorber gave 3.9 MJ/kg CO_2 for the specific reboiler duty, while previous tests at other conditions and with higher absorbers gave 3.5-3.7. Acceptable emissions were observed, while degradation was higher than earlier TCM campaigns due to the choice of running with 35 w% MEA. Overall, a benchmark has been provided for future improved compact capture technologies.

Keywords: CO_2 capture, post-combustion, compact, benchmark, demonstration, monethanolamine

1. Introduction

Technology Centre Mongstad (TCM) is a large and flexible demonstration site for post-combustion CO_2 capture. It is located next to the Equinor refinery at Mongstad (Norway) which is the source of the two types of flue gases supplied to TCM. These sources are the combined cycle gas turbine (CCGT) based heat and power plant (CHP) and residue fluid catalytic cracker (RFCC). TCM is owned by Gassnova (on behalf of the Norwegian state), Shell, Total and Equinor. Various proprietary amine solvents have been tested and matured at TCM since the start-up in 2012. In addition, various campaigns have been executed with a numbered series of open non-proprietary monoethanolamine (MEA). Most of the results have been published. The most significant campaigns were the third monoethanolamine test campaign (MEA-3) in June 2017 and the following MEA-4 and MEA-5 that lasted until October 2018. The large number of public, industrial, research and academic participants involved in these campaigns have enabled that the results served a broad scientific audience. The main objectives of these campaigns were to gain knowledge and information that can be used to reduce the cost as well as technical, environmental and financial risks of commercial scale deployment of post-combustion capture (PCC). This includes demonstration of a model-based control system, dynamic operation of the amine plant, investigating amine aerosol emissions, establishment of residue fluid catalytic cracker (RFCC) baseline performance with MEA, and specific tests targeted at experimentally verifying measures that can reduce the cost of CO_2 avoided [1].

This paper describes a part of the MEA-5 campaign tests relevant for reducing the size of a CO_2 capture plant as the most important driver. Reduced size can be beneficial or even enable CO_2 capture in certain applications. One example is brownfield retrofit of capture on exhausts with very limited spaces, e.g. existing industry near urban areas and refineries. Another example are turbines or engines on offshore oil&gas production unit. Equinor is currently developing its 3CWI concept "CO_2 Capture with Carbonated Water Injection" for greenfield Floating Production, Storage and Offloading (FPSO) units [2]. In this concept CO_2 is captured from a gas turbine, compressed, mixed with produced and/or sea water and injected as dissolved bicarbonate ions. For these examples the main constraints is available space and equipment weight rather than the energy efficiency. As the absorber is the unit of largest mass and volume, experiments that can reduce the uncertainty at low absorber heights are of value for these applications. Not much specific research has been done yet with this motivation.

The tests in this paper are done at elevated CO_2 concentration relative to earlier CHP based campaigns at TCM. 6 vol% was chosen, which reduces the size of the absorber relative to the usual 3.5-4 vol%. The reason for this is that elevated CO_2 concentrations are likely in applications where weight and volume are restricted. One motivation for this choice is the possible use of exhaust gas recycle (EGR) both on turbines and piston engines. Another motivation is the gradual development of increasing the CO_2 content due the higher turbine inlet temperatures in modern turbines allowing for less air cooling of the expander blades. In order to achieve 6 vol% of CO_2 in the flue gas going to the capture plant, the TCM amine plant was operated with flue gas from the Mongstad CCGT plant and with recycling a portion of the captured CO_2.

The absorber packing height was set at 12m, which is the lowest possible at TCM's amine unit. Moreover, one of the two water washes was disabled. This combination simulates the lowest absorber setting possible at TCM, but has significant dry bed height in between. The results will be used for discussing the viability of making post-combustion capture more compact. It is acknowledged that the amine unit at TCM is not specifically designed for testing compact capture. Consequently, the result may not be representative for commercial use as the unit will operate outside the operational window TCM's amine unit is designed for. The data can be utilized as a source for insight, comparison and for benchmarking commercial compact capture technologies.

2. System

TCM's amine unit was used (see e.g. [4][5][6]) and its flexibility was utilized to collect data relevant for a compact capture plant design. This means that the absorber was operated with only the lower packing section (12 m) and with one water wash bed (3 m, Lower (L) in operation, Upper (U) is idle) in service. This is the smallest total amount of packing possible at TCM without modifications. The set-up is illustrated and compared to the full amine plant set-up in Figure 1.

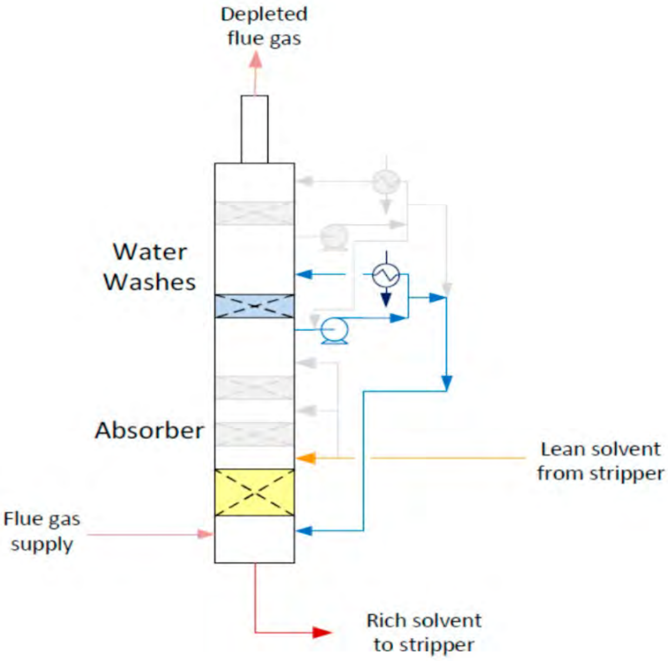

Figure 1. Illustration of the compact flue gas absorber set-up.

The flue gas flow rate was adjusted to its highest practically possible operating point (67,000 Sm^3/h, 113% of design capacity). To mimic higher capacity solvent types, the MEA concentration was increased to 35 wt% from the normally used 30 wt%.

The amine plant has extensive instrumentation with multiple measurements on the streams required for performance assessment. Details on the CHP flue gas characteristics, the main systems in the plant and an assessment of instrumentation quality as well as calculation methods for the main parameters are described in previously published papers, see Gjernes et al [1][7].

3. Method

3.1. Strategy

For this work various test series were executed named by the first letters in the alphabet. The plant was operated with a high flue gas flow rate (67,000 Sm^3/h). An overview of the test series is given in Table 1. The strategy in this work was to start out with the highest achievable capture rate in test series A. Therefore, the steam flow rate to reboiler was maximized and the solvent flow rate was high (106-138 kg/hr). The series B to D were systematic experiments to produce steam demand optimum curves (so-called U-curves) for identifying the lowest specific reboiler duty (SRD) for each series over a selected range of target capture rates (~ 83 to 72 %). In the E and F-series the flue gas temperature into the absorber was higher (45 instead of 30 °C), for assessing potential reduction in the cooling requirement and the equipment size of the direct contact cooler (DCC). As in the A series, the E cases were maximizing the steam flow rate to achieve a high capture rate and the F series was systematic experiments to find the energy optimum. The E case consists only of one test. All these series were run with around 35 w% MEA. Next, some tests were added to put the series A-F in a wider perspective. The cases named B5-1 and B5-2 are two reference runs with MEA at 30 wt% and with lower and upper water wash in operation, respectively. The motivation was to see whether there are differences between the upper and lower water washes. The case named 15-3 is included in the results section to have a comparison against the most compact absorber line-up used in the previous TCM study on modes of operation with cost saving potential back in 2018 [1]. The objectives for the experimental work were to investigate capture rates and specific reboiler duty during parameter testing. Steam flow to reboiler and solvent flow rates were the main variables, while flue gas flow and CO_2 inlet concentration were kept constant.

Table 1. Overview of the tests.

Series	MEA [%]	Flue gas temperature [°C]	Lean x 1000 [kg/h]	Water wash
A	35	30	106-138	L+U
B	35	30	138-98	L
C	35	30	139-83	L
D	35	30	120-72	L
E	35	45	107	L
F	35	45	128-77	L
B5-1	30	30	128	L
B5-2	30	30	128	U

With this strategy, it was the intention to inspire, and stretch the targets for new technology developments of compact and low weight CO_2 capture plants. With more advanced solvents and optimized systems, it is expected that significant improvements beyond what TCM demonstrates here are possible.

The so-called U-curves were produced by variations in the lean amine to gas flow rate ratio (L/G). The cold rich by-pass of the lean rich heat exchanger (17% by-pass) was in operation during all test runs. This variable was left unchanged. It is acknowledged varying it could provide somewhat lower steam demand or higher capture rate, but not significant.

3.2. Measurements

The combination of methods used in the current work is shown in Table 2. The flow out of absorber is based on flow into the absorber assuming all components except water and CO_2 are conserved. Moisture is calculated from temperature and pressure. The product flow is assumed to be CO_2 and moisture only.

Table 2. Selected methods for test performance assessment.

Location	Property	Method
Absorber in	H_2O	Calculated from p and T
	CO_2	Infrared Spectroscopy (IR)
	Flow	Ultrasonic
Absorber out	H_2O	Calculated from p and T
	CO_2	Infrared Spectroscopy (IR)
	Flow	Calculated from absorber in flow and composition
Product flow	H_2O	Calculated from p and T
	CO_2	Calculated as: 100 - H_2O
	Flow	Coriolis

In each test run the plant is first allowed to stabilize over several hours. A set of key performance indicators is used to assess the quality of data. A two-hour stable period is selected for data extraction. Liquid sampling is conducted within this period. All properties except liquid samples (amine concentration and loading) are averaged over the two-hour period. Thus, reported data are based on stable operation with respect to all streams. The total and CO_2 mass balances should be within 100 ± 2%. This procedure allows normally not more than two single test runs per day (24 hours). To make comparisons between the test runs, it is important to maintain stable MEA concentration (35 wt%, CO_2 free) and the absorber inlet CO_2 concentration (6 vol%, dry). MEA concentration, lean and rich loading are calculated from laboratory analysis of the liquid samples. In case there is a missing liquid sample, the lean loading is extrapolated using amine density (only for the following tests: B6-opt, C2, D4 and F2).

The solvent loading is calculated from total inorganic carbon (mole CO_2/kg solvent) and total alkalinity (mole amine/kg solvent):

$$Loading = \frac{total\ inorganic\ carbon}{total\ alkalinity} \tag{1}$$

The specific reboiler duty (SRD) is the heat delivered to the reboiler from the steam flow divided by the amount of captured CO_2:

$$SRD = \frac{\Delta H\ \dot{m}_{steam}}{\dot{m}_{CO2}} \tag{2}$$

In this work the captured CO_2 ($\dot{m}_{CO2}$) is based on the difference in mass flow of CO_2 over the absorber ($\dot{m}_{CO2}$abs, in – $\dot{m}_{CO2}$abs, out). This is chosen in order to aligned with earlier published results (e.g. [1]). Captured CO_2 ($\dot{m}_{CO2}$) based on product flow from stripper will for the present cases result in a lower CO_2 product flow. The steam pressure and temperature are typically around 2.5 barg and 160 °C in this work.

The capture rate is the mass fraction of captured CO_2 and the amount of CO_2 flowing into the absorber.

$$Capture\ rate = \frac{\dot{m}_{CO2,abs\ in} - \dot{m}_{CO2,abs\ out}}{\dot{m}_{CO2,abs\ in}} x100\% \tag{3}$$

The absorber packing volume and thus the absorber size are major CAPEX elements. The absorber packing volume (m^3/ton CO_2, h) was calculated for the cases with highest CO_2 product flow and compared with the previous test case 15-3. The parameter is one metric used for assessing compact absorber designs. The TCM absorber cross section is 7.2 m^2 and packing height applied is 12 m.

The emissions of amine and ammonia were monitored during all test runs. As higher MEA concentration is associated with increased solvent degradation [3] and plant corrosion, degradation and metal content in the solvent were closely monitored. However longer-term testing is expected to be needed to assess the solvent management aspects of higher MEA concentrations. Moreover, the solvent composition was measured before and after for estimating the cumulative degradation.

4. Results and discussion

4.1. Capture rate and steam demand

The observed relation between SRD and capture rate is shown in Figure 2 for all the series A-F and the B5-2 and B5-1 with 30 w% MEA. The lowest SRD value in the U-curves achieved within each test series is shown as transparent squares along with a dashed trend line based on the five selected optimum points. The trend line shows a corresponding decrease in capture rate and SRD from 87% and 4.3 MJ/kg CO_2 down to 73% and 3.7 MJ/kg CO_2. Within each series the capture rates were quite well controlled within the target. The trend line gives a good indication of what is achievable with a compact plant configuration. The results from the F-series (82% capture rate) shows promise also for reducing cooling need and size of the DCC. It is also seen that the SRD is significantly higher for the two test runs with MEA 30wt% (B5-2 and B5-1). The uncertainty at TCM is discussed in other papers [4][5][6] and is assumed not to be significant different in this campaign.

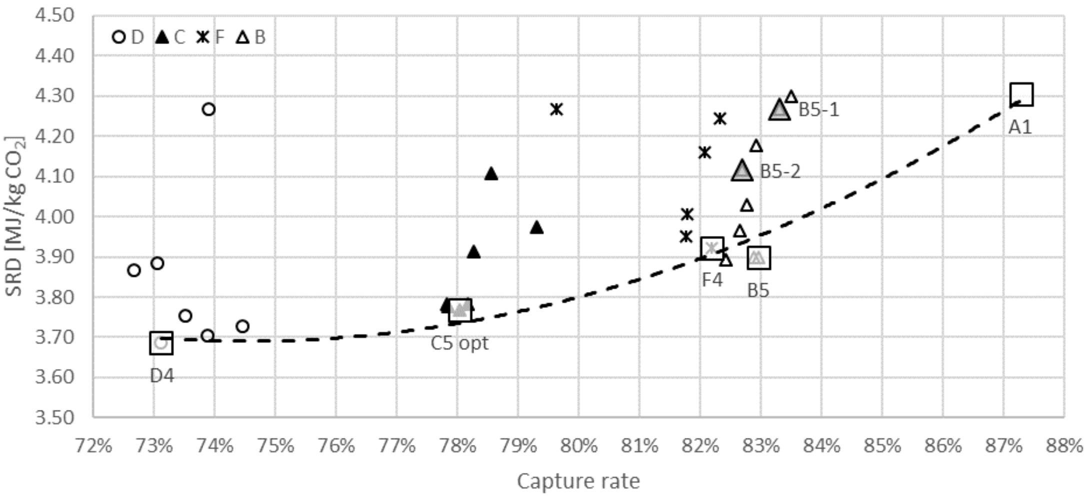

Figure 2. SRD and capture rate for the test series. Optimum points for each series are shown as transparent squares.

As expected with the low absorber height the SRD become higher than TCM has reported earlier for higher absorber heights. For 30 w% MEA Gjernes et al.[1] reports down to 3.6 MJ/kg CO_2 at 86% capture with 3.6 vol% CO_2 in the inlet, while this work shows around 4.0-4.2 MJ/kg CO_2 at 87% capture with 6 vol% CO_2 in the inlet. This increase may not be unacceptable high in situations where energy ample cheap heat is available. Figure 2 also shows that a similar low SRD of around 3.6-3.8 is achievable with a lower capture rate of 70-80%. This decrease may neither be unacceptable in the mentioned applications where space and weight are the limiting factors.

The MEA and wet CO_2 inlet concentrations were aimed to be kept constant for all tests, and the achieved results are shown in Figure 3. There are small variations between the test series and the comparison between the series are representative. There is also good agreement between the two CO_2 measurement methods. The figure also shows MEA concentration close to 31 wt% for the B5-1 and B5-2 cases and the CO_2 concentration in good agreement with the other test series. This means that any differences are likely not to be caused by variations in CO_2 inlet concentration and MEA concentration.

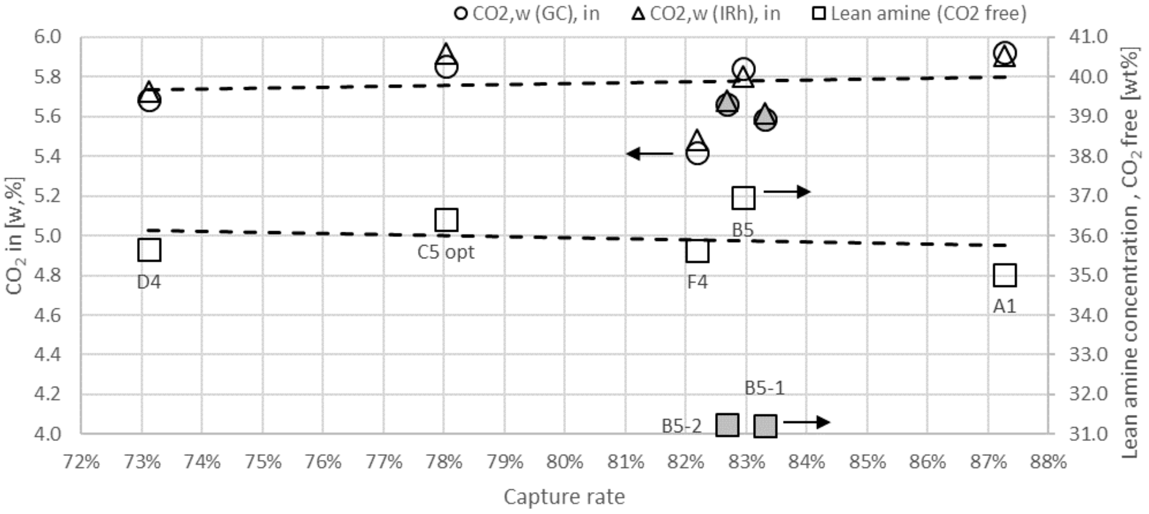

Figure 3. Wet CO_2 inlet concentration and lean amine concentration were maintained at the same level for the selected optimum cases. Grey symbols are for the B5-1 and B5-2 cases that were operated at lower amine concentration.

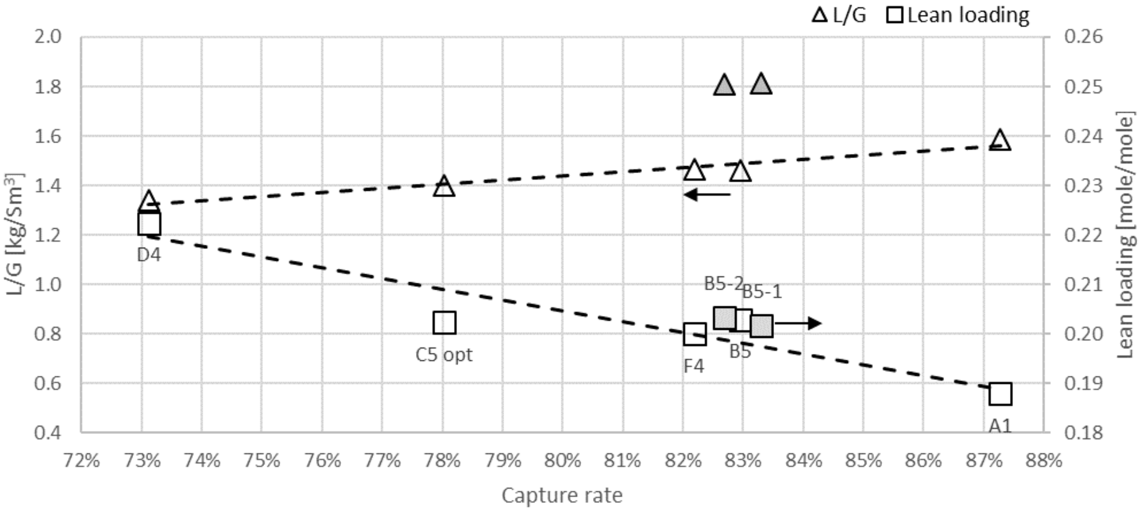

Figure 4. L/G ratio is increasing, and lean loading is decreasing for the optimum cases when plotted versus the targeted capture rate. Grey symbols are for the B5-1 and B5-2 cases that were operated at lower amine concentration.

A graph of the variations in L/G and lean loading versus capture rate is given in Figure 4. There was a wide enough experimental window with respect to lean flow and resulting loading to observe trends. A 14 percentage points higher capture rate (from 73 to 87) demands a 0.03 mole/mole lower lean loading and a 0.3 kg/Sm^3 higher L/G. It is observed that the MEA 30wt% test cases (B5-1 and B5-2) needs a significantly (0.4 kg/Sm^3) higher solvent flow rate to achieve the target capture rate of 82-83% than the results with 35% MEA, while the lean loading is not very different. As mentioned before, all cases are with 67,000 Sm^3/h flue gas flow.

A summary of results from the test series is given in Table 3. The CO_2 captured in the optimum cases shown in Figure 2 are used for calculating the absorber packing volume.

Table 3. Results summary for all test series.

Series #	L/G interval [kg/Sm^3]	Lean loading [mole/mole]	Captured CO_2 Optimum case [tonne/h]	Capture rate interval [%]	SRD interval [MJ/kg CO_2]	Absorber packing volume per tonne captured CO_2 [m^3/tonne CO_2, h]
A	1.6-2.1	0.19-0.24	6.4	84-87	4.3	13
B	1.5-2.1	0.19-0.25	6.0	83-84	3.9-4.3	14
C	1.2-2.1	0.18-0.25	5.8	78-79	3.8-4.1	15
D	1.1-1.8	0.15-0.27	5.2	73-75	3.7-4.3	16
E	1.7	0.19	5.9	87	4.3	15
F	1.2-1.9	0.16-0.24	5.6	80-82	3.9-4.3	15
B5-1/2	1.8	0.2	5.9	82	4.1-4.3	15
15-3	1.4	0.23	3.2	72	4.0	27

The new property added in this Table is the "Absorber packing volume per ton captured CO_2. This is a good property for analyzing the potential for size and weight reductions. Most interestingly, in the A-1 case the CO_2 produced is 6,427 kg/h and the absorber packing volume parameter is 13. The result for the 15-3 case from earlier TCM publication [1] was 27. This shows that there are significant differences in this property and that this campaign had low number ranging from 13-16. The difference with 15-3 up to 27 shows that there should be a significant opportunity for more compact absorber designs and corresponding cost saving for this largest equipment item in post-combustion capture. It is recommended to use this new property in future work for comparison.

A final observation is that no large differences were observed between B5-1 and B5-2. This means that there are likely no big differences between upper and lower water wash (as expected) that can explain any variation or invalidate any conclusions.

4.2. Emissions to air

When changing design of amine based post-combustion one must always keep control of the emissions since these pose of the main HSE risks [8]. Table 4 gives an overview of the measured emissions to air at moments or intervals the results were regarded as reliable and representative. The letter gives which series the measurement is taken from while the number gives which test it is (not reported in detail in this work). Two measurements were done in the C5 test. The online data were 5 min averaged data over an analyzed period of 2 hours.

Table 4 Overview of isokinetic sampling during the period. Note that FTIR values are reported for time slots where isokinetic samplings were not available. In addition to optimum cases, emission results are included from B4, C3 rep, E1 and F3. The FTIR was out of service during case D4 and F4.

Series/Test	Water wash	MEA [ppm]	NH_3 [ppm]	Emission result type
A1	L+U	0.12	9.3	Online (FTIR)
B4	L	0.13	11	Isokinetic
B5	L	0.00	12	Online (FTIR)
C3 rep	L	0.059	9.0	Isokinetic
C5	L	0.047	14	Isokinetic
C5 opt	L	0.37	22	Isokinetic
C5 opt	L	0.52	30	Online (FTIR)
D4	L	-	-	Online (FTIR)
E1	L	5.7	24	Isokinetic
F3	L+U	3.5	26	Isokinetic
F4	L+U	-	-	Online (FTIR)

Except for E1 and F3 the emissions to air were not significantly higher than the ones published earlier on industrially representative operation [9]. In E and F especially the MEA emissions are high, probably higher than most future emission permits will allow. The reason is that the inlet temperature was increased from 30 to 45 °C. So, this seems not to be a favourable measure for compact capture. This indicates that two water washes are likely needed for compact capture if high inlet temperature is unavoidable.

The numbers presented here have a somewhat higher uncertainty than TCM presents in dedicated emission papers, e.g. Morken et al [9]. Some numbers may be somewhat higher than if the plant was operated stable for longer time. Build-up of MEA in water wash can occur. On the other hand, some numbers may be low since they can be impacted by the large amount of dry packing bed above the absorption bed. It must be noted that the quantification limit for the FTIR is 0.5 ppm due to increased instrument noise at low levels. However these uncertainties do not impact the conclusion on the overall low enough levels with 30 °C inlet and the overall too high levels at 45 °C inlet temperature.

4.3. Solvent degradation

When changing design of amine based post-combustion one must also always keep control of the degradation since it can be important for the OPEX and HSE risk. Table 5 gives an overview of metal and heat stable salt (HSS) in the solvent. The compact campaign was done after another campaign of 905 hours. So, the amine was already partly degraded at the start.

Table 5. Overview of metal and heat stable salt (HSS) concentrations after reclaiming and at the beginning and end of the campaign discussed in this paper. All concentrations are mg/kg solvent. Components below the detection limit are marked with "<".

Component	After Reclaiming	Beginning	End
Sum operational hours	0	905	1,230
Sum tons CO_2 captured	0	5,830	7,702
Cr	<0.1	0.30	1.3
Fe	0.2	1.60	11
Ni	0.2	0.5	1.7
Mo	<0.1	<0.1	<0.1
Na	0.9	1.9	4.5
V	<0.1	<0.1	<0.1
Zn	<0.1	<0.1	<0.1
Cu	<0.1	<0.1	<0.1
Sum metals	1.3 - 1.7	4.3 - 4.7	18.5 - 18.9
Formic acid	41.8	285	645
Glycolic acid	<20	54	79
Oxalic acid	<20	84	213
Acetic acid	<20	74	165
Nitrate	37.3	246	510
Nitrite	<30	<35	<35
Sulfate	<35	92	114
Sulfite	<30	<35	<35
Sum HSS	79.1 - 234.1	835 - 905	1,726 – 1,796

The degradation products increase as expected. When deciding to run this campaign with 35wt% a risk of excessive degradation was taken. This risk was mitigated by only running a relative short time of 325 hours. From all the measured concentrations the main discussion in literature focuses on the iron concentration. TCM's own guideline [10] recommends keeping the iron concentration below 5 mg/kg solvent. In the compact campaign it increased from from 1.6 to 11 crossing the recommended value. However, Moser [11] has observed long periods of low degradation above the 5 mg/kg iron. It seems anyhow recommended to have more mitigation actions in place for keeping the degradation under control for using 35 w%. Examples are continuous reclaiming or use any of the new O_2 and/or iron removal technologies.

4.4. Comparison with previous results

Over the years various campaigns have been executed at TCM with MEA on CCGT flue gas, of which the compact campaign in this paper is the latest. From each campaign one representative result was chosen that has most industrial relevance. Table 6 below gives an overview of these representative results enabling a comparison and perspective of what TCM has been achieved at TCM.

Table 6. Comparison of representative results from all MEA campaigns at TCM.

Campaign (literature reference)	CO_2 inlet [vol%]	Gas velocity [m/s]	Absorber packing [m]	MEA [w%]	L/G [kg/Sm^3]	Capture rate [%]	SRD [MJ/kg]	MEA emissions [ppmv]
MEA2 [1]	3.6	2.3	24	30	1.0	86	3.6	< 1
MEA3 [1]	4.2	2.0	18	40	0.98	86	3.6	< 1
MEA5 (B5 this paper)	6	2.7	12	35	1.46	83	3.9	< 1

The results from this compact campaign has as expected the largest SRD as well as the lowest capture rate. The differences with the other cases on variables that are important for cost and HSE are not very large. Hence, we can conclude that the amine unit at TCM can be used to study compact capture, although it is not specifically designed for it. Another result from this Table is a set of data that can be used to tune any overall MEA model. The data give a large enough specter to serve this purpose.

4.5. Discussion on compact capture

The results in this paper give a benchmark for any compact capture technology. Many new ideas and improvements on reducing weight and size can use this work for comparison. Preferably, these should perform better on most variables that are important for cost and HSE. Examples of such more compact but less mature technologies are rotating absorption&desorption, membrane contactors and CO_2 selective gas-gas membranes.

But better results could also be obtained at TCM in the future. One improvement idea for TCM is to use another better solvent. This work already shows that increasing the MEA concentration from 30 to 35% makes compact capture design more attractive. TCM has already tested the solvent CESAR-1 for other motivations [12]. Testing this solvent on compact design like done in this work is a logic next step.

Another idea for TCM is to study in more detail metal build-up and degradation rates in compact design. This work provides a good indication but had not enough hours for industrially relevant conclusions. A final idea is further testing at 45°C and two water washes could also be interesting to be able to find the balance with the size of the direct contact cooler (DCC) upstream the absorber and the lean amine cooler.

5. Conclusions

The amine unit at TCM has been used for testing compact capture for providing a benchmark. The absorber was used with its lowest possible packing height of 12m, and only one of two water washes was used (3m height). The plant was operated with a high flue gas flow rate (67,000 Sm^3/h) and 35 wt% MEA with a sensitivity down to 30 wt%. The CO_2 inlet concentration was 6% mimicking some industrial exhausts, small turbines with exhaust gas recycle or modern turbines with high turbine inlet temperatures. The tests demonstrated that such a low absorber can capture more than 80% of the CO_2 with only a slightly higher steam demand than conventional applications with higher packing heights of 18-24m. The low absorber gave 3.9 MJ/kg for the specific reboiler duty for the low absorber, while the higher absorbers gave 3.5-3.7. Acceptable emissions were observed, while degradation was high due to the choice of running with 35 w% MEA. Overall, a benchmark has been provided for future improved compact capture technologies.

Acknowledgements

The authors gratefully acknowledge the staff of TCM DA, Gassnova, Equinor, Shell and Total for their contribution and work at the TCM DA facility. The authors also gratefully acknowledge Gassnova, Equinor, Shell, and Total as the owners of TCM DA for their financial support and contributions.

References

[1] Gjernes E, Pedersen S, Jain D, Åsen KI, Hvidsten OA, de Koeijer G, Faramarzi L, de Cazenove T, Documenting modes of operation with cost saving potential at the Technology Mongstad, Energy Procedia, 14th Greenhouse Gas Control Technologies Conference Melbourne 21-26 October 2018 (GHGT-14)

[2] Pettersen J, Nilssen OR, De Koeijer G, Approaching Zero CO_2 Emissions for Future Oil and Gas Production Offshore, Abstract and presentation to TCCS-10 conference, June 2019, Trondheim, Norway

[3] Supap T, Idem R, Veawab A, Aroonwilas A, Tontiwachwuthikul P, Chakma A, and Kybett BD, Kinetics of the Oxidative Degradation of Aqueous Monoethanolamine in a Flue Gas Treating Unit, Ind. Eng. Chem. Res. 2001, 40, 16, 3445–3450

[4] Thimsen D, Maxson A, Smith V, Cents T, Falk-Pedersen O, Gorset O, Hamborg ES, Results from MEA testing at the CO_2 Technology Centre Mongstad. Part I: Post-Combustion CO_2 capture testing methodology, Energy Procedia, 63, 2014, 5938-5958,

[5] Hamborg ES, Smith V, Cents T, Brigman N, Falk-Pedersen O, de Cazanove T, Chhagnlal M, Feste JK, Ullestad Ø, Ulvatn H, Gorset O, Askestad I, Gram LK, Fostås BF, Shah MI, Maxson A, Thimsen D, Results from MEA testing at the CO2 Technology Centre Mongstad. Part II: Verification of baseline results, Energy Procedia, 63, 2014, 5994-6011

[6] Faramarzi L, Thimsen D, Hume S, Maxon A, Watson G, Pedersen S, Gjernes E, Fostås BF, Lombardo G, Cents T, Morken AK, Shah MI, de Cazenove T, Hamborg ES, Results from MEA Testing at the CO_2 Technology Centre Mongstad: Verification of Baseline Results in 2015. Energy Procedia, Volume 114, 2017, p 1128-1145.

[7] Gjernes E, Pedersen S, Cents T, Watson G, Fostås BF, Shah MI, Lombardo G, Desvignes C, Flø NE, Morken AK, de Cazenove T, Faramarzi L, Hamborg ES, Results from 30 wt% MEA performance testing at the CO_2 Technology Centre Mongstad, Energy Procedia, Volume 114, 2017, 1146-1157

[8] De Koeijer G, Talstad VR, Nepstad S, Tønnessen D, Falk-Pedersen O, Maree Y, Nielsen C. Health risk analysis for emissions to air from CO2Technology Centre Mongstad, International Journal of Greenhouse Gas Control, 18, 2013, 200–207.

[9] Morken AK, Pedersen S, Kleppe ER, Wisthaler A, Vernstad K, Ullestad Ø, Flø NE, Faramarzi L, Hamborg ES, Degradation and Emission Results of Amine Plant Operations from MEA Testing at the CO2 Technology Centre Mongstad, Energy Procedia, 114, 2017, 1245- 1262

[10] Morken AK, Pedersen S, Nesse SO, Flø NE, Johnsen K, Feste JK, de Cazenove T, Faramarzi L, Vernstad K, CO_2 capture with monoethanolamine: Solvent management and environmental impacts during long term operation at the Technology Centre Mongstad (TCM), International Journal of Greenhouse Gas Control 82 (2019) 175-183.

[11] Moser P, Wiechers G, Schmidt S, Monteiro JGMS, Charalambous C, Garcia S, Fernandez ES, Results of the 18-month test with MEA at the post-combustion capture pilot plant at Niederaussem – new impetus to solvent management, emissions and dynamic behaviour, International Journal of Greenhouse Gas Control, Volume 95, 2020.

[12] Christophe Benquet C, Knarvik A, Gjernes E, Hvidsten OA, Kleppe ER, Akhter S, First Process Results and Operational Experience with CESAR1 Solvent at TCM with High Capture Rates (ALIGN-CCUS Project). To be presented at GHGT-15 Virtual Conference: 15-18 March 2021.

Demonstrating flexible operation of the Technology Centre Mongstad (TCM) CO_2 capture plant

(2019)

This article is behind a paywall.

International Journal of Greenhouse Gas Control 93 (2020) 102879

Contents lists available at ScienceDirect

International Journal of Greenhouse Gas Control

journal homepage: www.elsevier.com/locate/ijggc

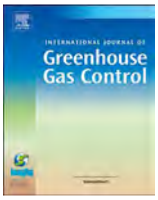

Demonstrating flexible operation of the Technology Centre Mongstad (TCM) CO_2 capture plant

Mai Bui[a,b], Nina E. Flø[c], Thomas de Cazenove[c], Niall Mac Dowell[a,b,*]

[a] Centre for Process Systems Engineering, Imperial College London, South Kensington, London SW7 2AZ UK
[b] Centre for Environmental Policy, Imperial College London, South Kensington, London SW7 1NA UK
[c] Technology Centre Mongstad (TCM), 5954 Mongstad Norway

ARTICLE INFO

Keywords:
CO_2 capture
Dynamic modelling
Flexible operation
Transient operation
Post-combustion capture
Pilot plant
CCGT

ABSTRACT

This study demonstrates the feasibility of flexible operation of CO_2 capture plants with dynamic modelling and experimental testing at the Technology Centre Mongstad (TCM) CO_2 capture facility in Norway. This paper presents three flexible operation scenarios: (i) effect of steam flow rate, (ii) time-varying solvent regeneration, and (iii) variable ramp rate. The dynamic model of the TCM CO_2 capture plant developed in gCCS provides further insights into the process dynamics. As the steam flow rate decreases, lean CO_2 loading increases, thereby reducing CO_2 capture rate and decreasing absorber temperature. The time-varying solvent regeneration scenario is demonstrated successfully. During "off-peak" mode (periods of low electricity price), solvent is regenerated, reducing lean CO_2 loading to 0.16 mol_{CO_2}/mol_{MEA} and increasing CO_2 capture rate to 89–97%. The "peak" mode (period of high electricity price) stores CO_2 within the solvent by reducing the reboiler heat supply and increasing solvent flow rate. During peak mode, lean CO_2 loading increases to 0.48 mol_{CO_2}/mol_{MEA}, reducing CO_2 capture rate to 14.5%, which in turn decreases the absorber temperature profile. The variable ramp rate scenario demonstrates that different ramp rates can be applied successively to a CO_2 capture plant. By maintaining constant liquid-to-gas (L/G) ratio during the changes, the CO_2 capture performance will remain the same, i.e., constant lean CO_2 loading (0.14–0.16 mol_{CO_2}/mol_{MEA}) and CO_2 capture rate (87–89%). We show that flexible operation in a demonstration scale absorption CO_2 capture process is technically feasible. The deviation between the gCCS model and dynamic experimental data demonstrates further research is needed to improve existing dynamic modelling software. Continual development in our understanding of process dynamics during flexible operation of CO_2 capture plants will be essential. This paper provides additional value by presenting a comprehensive dynamic experimental dataset, which will enable others to build upon this work.

For futher information: https://www.sciencedirect.com/science/article/abs/pii/S0098135418303818?via%3Dihub

---

* Corresponding author.
E-mail address: niall@imperial.ac.uk (N. Mac Dowell).

https://doi.org/10.1016/j.ijggc.2019.102879
Received 20 May 2019; Received in revised form 14 October 2019; Accepted 21 October 2019
1750-5836/ © 2019 Elsevier Ltd. All rights reserved.

CO_2 capture with monoethanolamine: Solvent management and environmental impacts during long term operation at the Technology Centre Mongstad (TCM)

(2019)

This article is behind a paywall.

International Journal of Greenhouse Gas Control 82 (2019) 175–183

Contents lists available at ScienceDirect

International Journal of Greenhouse Gas Control

journal homepage: www.elsevier.com/locate/ijggc

CO_2 capture with monoethanolamine: Solvent management and environmental impacts during long term operation at the Technology Centre Mongstad (TCM)

Anne Kolstad Morken[a,b,*], Steinar Pedersen[a,b], Stein Olav Nesse[a,b], Nina Enaasen Flø[a,b], Kim Johnsen[a,b], Jane Karin Feste[a,b], Thomas de Cazenove[a], Leila Faramarzi[a,b], Kai Vernstad[c]

[a] *Technology Centre Mongstad (TCM), 5954 Mongstad, Norway*
[b] *Equinor ASA, P.O. Box 8500, 4035 Stavanger, Norway*
[c] *Sintef Materialer og Kjemi, Avd Bioteknologi, Sem Sælands vei 2, 7034 Trondheim, Norway*

ARTICLE INFO

Keywords:
Monoethanolamine
MEA
CO_2 capture
Emission
Solvent management
Technology Centre Mongstad

ABSTRACT

The owners of the Technology Centre Mongstad (TCM DA) started a monoethanolamine (MEA) test campaign in June 2017. The main objective was to produce knowledge and information that can be used to reduce the cost as well as technical, environmental and financial risks of commercial scale deployment of post-combustion capture (PCC). The campaign covered experimental activities in the amine plant from the 12th of June 2017 until the 30th of July 2018. A wide range of operating conditions were applied, thus giving a unique opportunity to study the impacts on the solvent quality, degradation behavior, corrosion tendency and emissions to the atmosphere. The current work describes how solvent quality and low emissions to atmosphere can be maintained during long-term operation by appropriate solvent management.

For futher information: https://www.sciencedirect.com/science/article/abs/pii/S1750583618307576?via%3Dihub

---

[*] Corresponding author at: Technology Centre Mongstad (TCM), 5954 Mongstad, Norway.
E-mail address: akmo@equinor.com (A.K. Morken).

https://doi.org/10.1016/j.ijggc.2018.12.018
Received 3 October 2018; Received in revised form 11 December 2018; Accepted 27 December 2018
Available online 17 January 2019
1750-5836/ © 2019 Elsevier Ltd. All rights reserved.

Assessment of Material Selection for the CO_2 Absorption Process with Aqueous MEA Solution based on Results from Corrosion Monitoring at Technology Centre Mongstad

(2019)

This article is behind a paywall.

Assessment of Material Selection for the CO_2 Absorption Process with Aqueous MEA Solution based on Results from Corrosion Monitoring at Technology Centre Mongstad

Nina Enaasen Flø[a], Leila Faramarzi[a,b,*], Frank Iversen[a,b], Eirik Romslo Kleppe[a],
Brit Graver[c], Heidi Nornes Bryntesen[d], Kim Johnsen[a,b]

[a] *Technology Centre Mongstad (TCM DA), 5954 Mongstad, Norway*
[b]*Equinor ASA, PO Box 8500, 4035 Stavanger, Norway*
[c]*DNV GL, Veritasvegen 1, 1322 Høvik, Norway*
[d]*Norner AS, Asdalstrand 291, 3962 Stathelle, Norway*

Abstract

In 2017 and 2018, Technology Centre Mongstad (TCM) performed long-term testing of CO_2 capture with aqueous monoethanolamine (MEA) solvent through a series of test campaigns. As part of the test campaigns, a selection of materials was assessed for the CO_2-MEA process by investigation and analysis of material test coupons. The test coupons were exposed to various operating conditions at five different locations in the plant. Both metal and rubber materials were tested in order to detect possible material compatibility issues with the CO_2-MEA process. All metals proved to be suitable, except CS235 which in general showed severe corrosion rates exposed to the MEA solvent. However, a mid-campaign weight loss analysis indicated that CS235 might be acceptable for specific process conditions on the cold rich solvent location. No significant changes were observed on the tested rubber materials, however minor changes in hardness and tensile properties indicated some impact by the MEA solvent environment. In addition to examination of test coupons, the solvent was frequently monitored for typical factors that might indicate or influence corrosion such as the concentration of dissolved metals and heat stable salts (HSS). Some variability in average metal dissolution was observed between specific operational phases, however, the flue gas source did not seem to have significant effect on metal dissolution.

Keywords: Post-combustion CO_2 capture; Technology Centre Mongstad; material testing; material selection; corrosion monitoring

For futher information: https://www.sciencedirect.com/science/article/abs/pii/S1750583618307813?via%3Dihub

---

* Corresponding author. Tel.: + 47 56 34 52 20.
E-mail address: lefar@equinor.no

Results of the fourth Technology Centre Mongstad campaign: LVC testing

(2019)

This article is behind a paywall.

International Journal of Greenhouse Gas Control 89 (2019) 52–64

Contents lists available at ScienceDirect

International Journal of Greenhouse Gas Control

journal homepage: www.elsevier.com/locate/ijggc

Results of the fourth Technology Centre Mongstad campaign: LVC testing

Philip Loldrup Fosbøl[a,*], Randi Neerup[a], Susana Almeida[a], Amirali Rezazadeh[a], Jozsef Gaspar[a], Anette Beate Nesse Knarvik[b], Nina Enaasen Flø[b]

[a] *Center for Energy Resources Engineering (CERE), Department of Chemical Engineering, Technical University of Denmark (DTU), Søltofts Plads, Building 229, DK-2800 Kongens Lyngby, Denmark*
[b] *Technology Centre Mongstad (TCM DA), 5954 Mongstad, Norway*

ARTICLE INFO

Keywords:
Lean vapor compression (LVC)
Specific reboiler duty (SRD)
Monoethanolamine (MEA)
CO_2 capture and storage (CCS)
Technology Centre Mongstad (TCM)
Process optimization

ABSTRACT

The lean vapor compressor (LVC) unit at Technology Centre Mongstad (TCM), Norway has been tested using 30 wt% monoethanol amine (MEA) and flue gas from the combined cycle gas turbine (CCGT) based combined heat and power (CHP) plant. The aim was to study the impact of LVC on the CO_2 capture efficiency and energy profile of the TCM plant. 16 cases have been tested with and without LVC, and with various process parameters such as LVC pressure, solvent flow, inlet flue gas CO_2 concentration, and stripper pressure. Absorber and stripper process conditions were recorded during these tests. The operation of the TCM amine plant was very steady. Standard deviation and reproducibility of the various process parameters were satisfactory. Overall, the LVC results are as expected. A clear trend shows lower operating LVC pressure gives less specific reboiler energy consumption. A maximum thermal energy reduction of 25% was obtained when applying LVC at the expense of a typical LVC electrical energy consumption of 0.1 to 0.2 GJ electric/ton CO_2. Additional results show that the specific reboiler duty (SRD) may have a characteristic non-linear dependence on solvent flow rate. Higher stripper pressure may decrease the specific reboiler duty and be beneficial to the thermal power used in the plant at the expense of increased LVC electrical power consumption. Lower SRD was obtained when increasing the inlet flue gas CO_2 concentrations both with and without LVC. For the LVC cases, no significant indication of additional energy requirement was observed when increasing the CO_2 capture rate. The LVC power consumption in this study was to a large extend conservative due to a specific LVC design chosen. The presented results will help to enhance the accuracy of future CO_2 capture engineering designs.

For futher information: https://www.sciencedirect.com/science/article/abs/pii/S1750583618307552?via%3Dihub

---

* Corresponding author.
E-mail address: plf@kt.dtu.dk (P. Loldrup Fosbøl).

https://doi.org/10.1016/j.ijggc.2019.06.025
Received 3 October 2018; Received in revised form 24 June 2019; Accepted 27 June 2019
Available online 22 August 2019
1750-5836/ © 2019 Elsevier Ltd. All rights reserved.

Demonstration of non-linear model predictive control of post-combustion CO_2 capture processes

(2018)

This article is behind a paywall.

Computers and Chemical Engineering 123 (2019) 184–195

Contents lists available at ScienceDirect

Computers and Chemical Engineering

journal homepage: www.elsevier.com/locate/compchemeng

Demonstration of non-linear model predictive control of post-combustion CO_2 capture processes

S.O. Hauger[a], N. Enaasen Flø[b], H. Kvamsdal[c], F. Gjertsen[a], T. Mejdell[c], M. Hillestad[d,*]

[a] Cybernetica AS, Leirfossv. 27, 7038 Trondheim, Norway
[b] Technology Centre Mongstad (TCM), Mongstad 71, 5954 Mongstad, Norway
[c] Sintef AS, P.O. Box 4760 Torgarden, 7465 Trondheim, Norway
[d] Norwegian University of Science and Technology (NTNU), N-7494 Trondheim, Norway

ARTICLE INFO

Article history:
Received 26 April 2018
Revised 19 September 2018
Accepted 11 December 2018
Available online 27 December 2018

Keywords:
Post-combustion CO_2 capture
Nonlinear model predictive control
Load changes
Pilot plants

ABSTRACT

Nonlinear model predictive control applications have been deployed on two large pilot plants for post combustion CO_2 capture. The control objective is formulated in such a way that the CO_2 capture ratio is controlled at a desired value, while the reboiler duty is formulated as an unreachable maximum constraint. With a correct tuning, it is demonstrated that the controllers automatically compensate for disturbances in flue gas rates and compositions to obtain the desired capture ratio while the reboiler duty is minimized. The applications are able to minimize the transient periods between two different capture rates with the use of minimum reboiler duty.

© 2018 Published by Elsevier Ltd.

For futher information: https://www.sciencedirect.com/science/article/abs/pii/S1750583619303652?via%3Dihub

---

[*] Corresponding author.
E-mail address: magne.hillestad@ntnu.no (M. Hillestad).

https://doi.org/10.1016/j.compchemeng.2018.12.018
0098-1354/© 2018 Published by Elsevier Ltd.

Experimental results of transient testing at the amine plant at Technology Centre Mongstad: Open-loop responses and performance of decentralized control structures for load changes

(2018)

This article is behind a paywall.

International Journal of Greenhouse Gas Control 73 (2018) 42–59

Contents lists available at ScienceDirect

International Journal of Greenhouse Gas Control

journal homepage: www.elsevier.com/locate/ijggc

Experimental results of transient testing at the amine plant at Technology Centre Mongstad: Open-loop responses and performance of decentralized control structures for load changes

Rubén M. Montañés[a],*, Nina E. Flø[b], Lars O. Nord[a]

[a] Department of Energy and Process Engineering, NTNU – Norwegian University of Science and Technology, Kolbjørn Hejes v. 1B, 7491, Trondheim, Norway
[b] Technology Centre Mongstad, 5954, Mongstad, Norway

ARTICLE INFO

Keywords:
Post combustion
Chemical absorption
MEA
CO_2 capture
Dynamic behaviour
Pilot plant
Operational flexibility

ABSTRACT

Flexible operation of combined cycle thermal power plants with chemical absorption post combustion CO_2 capture is a key aspect for the development of the technology. Several studies have assessed the performance of decentralized control structures applied to the post combustion CO_2 capture process via dynamic process simulation, however there is a lack of published data from demonstration or pilot plants. In this work, experiments on transient testing were conducted at the amine plant at Technology Centre Mongstad, for flue gas from a combined cycle combined heat and power plant (3.7–4.1 CO_2 vol%). The experiments include six tests on open-loop responses and eight tests on transient performance of decentralized control structures for fast power plant load change scenarios.

The transient response of key process variables to changes in flue gas volumetric flow rate, solvent flow rate and reboiler duty were analyzed. In general the process stabilizes within 1 h for 20% step changes in process inputs, being the absorber column absorption rates the slowest process variable to stabilize to changes in reboiler duty and solvent flow rate. Tests on fast load changes (10%/min) in flue gas flow rate representing realistic load changes in an upstream power plant showed that decentralized control structures could be employed in order to bring the process to desired off-design steady-state operating conditions within (< 60 min). However, oscillations and instabilities in absorption and desorption rates driven by interactions of the capture rate and stripper temperature feedback control loops can occur when the rich solvent flow rate is changed significantly and fast as a control action to reject the flue gas volumetric flow rate disturbance and keeping liquid to gas ratio or capture rate constant.

For futher information: https://linkinghub.elsevier.com/retrieve/pii/S1750583618300306

---

* Corresponding author at: Department of Energy and Process Engineering, NTNU – Norwegian University of Science and Technology, Kolbjørn Hejes vei 1b, Varmeteknisk * B347, NO – 7491, Trondheim, Norway.

E-mail address: ruben.m.montanes@ntnu.no (R.M. Montañés).

https://doi.org/10.1016/j.ijggc.2018.04.001
Received 16 January 2018; Received in revised form 19 March 2018; Accepted 2 April 2018
Available online 10 April 2018
1750-5836/ © 2018 Elsevier Ltd. All rights reserved.

A compact and easy-to-use mass spectrometer for online monitoring of amines in the flue gas of a post-combustion carbon capture plant

(2018)

This article is behind a paywall.

International Journal of Greenhouse Gas Control 78 (2018) 349–353

Contents lists available at ScienceDirect

International Journal of Greenhouse Gas Control

journal homepage: www.elsevier.com/locate/ijggc

A compact and easy-to-use mass spectrometer for online monitoring of amines in the flue gas of a post-combustion carbon capture plant

Liang Zhu[a], Tomáš Mikoviny[a], Anne Kolstad Morken[b], Wen Tan[a], Armin Wisthaler[a,*]

[a] Department of Chemistry, University of Oslo, P.O. Box 1033, 0315, Oslo, Norway
[b] Technology Centre Mongstad (TCM), 5954, Mongstad, Norway

ARTICLE INFO

Keywords:
Carbon capture
Amines
Emission monitoring
Technology Centre Mongstad
Mass spectrometry
PTR-MS

ABSTRACT

We herein report on the adaptation and deployment of a compact and easy-to-use mass spectrometer for online monitoring of amines in industrial flue gas at ppb to ppm levels. The use of ammonia as a source gas in proton-transfer-reaction mass spectrometry (PTR-MS) greatly simplifies the detection of amines, making it possible to use a low-end commercial instrument version (PTR-QMS 300) for the measurements. We characterized the analytical performance of the instrument (sensitivity, limit of detection, precision, matrix effects) for nine solvent amines (monoethanolamine, dimethylaminoethanol, aminomethylpropanol, methyldiethanolamine, diglycolamine, piperazine, aminoethylpiperazine, methylpiperazine, N-(2-hydroxyethyl)piperazine) and three degradation amines (methylamine, dimethylamine, trimethylamine). The new analyzer was tested and validated in side-by-side measurements with established emission monitoring techniques at the Technology Centre Mongstad (TCM) in Norway. After validation, the instrument was permanently installed on top of the absorber tower to deliver real-time amine emission data to the plant information management system.

Futher information: https://www.sciencedirect.com/science/article/abs/pii/S1750583618304122?via%3Dihub

The Technology Centre Mongstad (TCM) (www.tcmda.com) in

---

[*] Corresponding author.
E-mail address: armin.wisthaler@kjemi.uio.no (A. Wisthaler).

https://doi.org/10.1016/j.ijggc.2018.09.003
Received 12 June 2018; Received in revised form 10 August 2018; Accepted 10 September 2018
1750-5836/ © 2018 Elsevier Ltd. All rights reserved.

CO_2 product quality: assessment of the range and level of impurities in the CO_2 product stream from MEA testing at the Technology Centre Mongstad (TCM)

(2018)

14th International Conference on Greenhouse Gas Control Technologies, GHGT-14

21st -25th October 2018, Melbourne, Australia

CO_2 product quality: assessment of the range and level of impurities in the CO_2 product stream from MEA testing at the Technology Centre Mongstad (TCM)

Kim Johnsen[a,b,*] , Eirik Romslo Kleppe[a], Leila Faramarzi[a,b], Christophe Benquet[a,d], Erik Gjernes[c], Gelein de Koeijer[b], Thomas de Cazenove[a], Anne Kolstad Morken[a,b], Nina Enaasen Flø[a], Muhammad Ismail Shah[a,c], Magnus Aronsson[a], Øyvind Ullestad[a]

[a] Technology Centre Mongstad, 5954 Mongstad, Norway
[b] Equinor ASA, PO Box 8500, 4035 Stavanger, Norway
[c] Gassnova SF, Dokkveien 10, 3920 Porsgrunn, Norway
[d] Total E&P Norge, Finnestadveien 44, Dusavik, 4029 Stavanger, Norway

Abstract

During the recent MEA campaign at the Technology Centre Mongstad (TCM), a broad range of operational conditions have been explored for the post-combustion amine-based CO_2 capture demonstration plant. This paper presents CO_2 product composition data from online gas analyzers, originating from CO_2 capture of two different flue gas sources available at TCM. Detailed composition data obtained by manual sampling and laboratory analysis, both internally at TCM and by Airborne Labs International Inc. is presented. Among the impurities identified and analyzed for, ammonia, formaldehyde and acetaldehyde are the compounds not commonly reported in the literature. The solvent quality, in terms of metal content and amount of degradation products, seemed to be the most influential parameter affecting the concentration of acetaldehyde and ammonia in the CO_2 product gas. In addition, ammonia slip was found to be correlated with operating temperature of the overhead stripper system.

Keywords: MEA; CO_2 product composition; Impurities; Ammonia; Aldehydes

1. Introduction

1.1. MEA campaign at TCM

The Technology Centre Mongstad (TCM) is the world's leading facility for verifying and improving CO_2 capture technologies. TCM is located at Mongstad, one of Norway´s most complex industrial facilities. TCM has been operating since autumn 2012, providing an arena for qualification of CO_2 capture technologies on an industrial scale. In autumn 2017, Gassnova (on behalf of the Norwegian state), Equinor (formerly Statoil), Shell and Total entered into a new ownership agreement securing operations at TCM until 2020. The owners of TCM started their most recent

---

* Corresponding author. Tel.: +47 98 40 68 89;
E-mail address: kim.johnsen@equinor.com

monoethanolamine (MEA) test campaign in June 2017 where a large number of public, industrial, research and academic stakeholders were involved [1]. The campaign included demonstration of a model-based control system, dynamic operation of the amine plant, investigating amine aerosol emissions and specific tests targeted at reducing the cost of CO_2 avoided. Through the testing, both flue gas sources currently available at TCM were used. These sources are the combined cycle gas turbine (CCGT) based heat and power plant (CHP) and the residual fluid catalytic cracker (RFCC). They provide flue gases with a wide range of properties and a CO_2 content from 3.6 to 14%. TCM is located next to the Equinor refinery in Mongstad. The Mongstad refinery is the source of both flue gases supplied to TCM. One of the objectives of the campaign has been to characterize the CO_2 product gas, which is presented in this paper.

1.2. Knowledge gaps

The compounds that make up the CO_2 product stream from a CO_2 capture plant can generally be grouped by their impact on the integrity of downstream transport- and storage systems, health and safety issues or cost impact on overall carbon capture and storage (CCS) value chain. There are several literature references [2,3,4,5,6] discussing the concentration range of compounds expected from the main capture technologies used with fossil-fueled power plants or other industrial sources. The most commonly reported impurities for post-combustion capture technologies, along with their impact on CCS value chain, are listed in Table 1.

Table 1: Reported impact of CO_2 product composition on compression system, transport and storage (incl. EOR) [2-6]

Compound	Corrosion and material	Hydrate formation	HSE issues during venting/accidental release	Operational upsets for re-compression system	Well Integrity (injectivity)	Minimum miscibility pressure (MMP)	Storage/pipeline capacity	Major impact
H_2O	x	x			x			Corrosion and hydrate formation
O_2	x			x		x	x	React with the hydrocarbons within the oil field (EOR), corrosion
N_2/Ar				x	x	x	x	Transport and storage capacity reduction
NO_x			x		x			Reaction with formation and cap rocks, affect injectivity and storage integrity, corrosion, HSE
SO_x			x					Corrosion, HSE
H_2S	x	x	x			x		Hydrate formation & toxicity
CO			x		x			Decrease injectivity and solubility trapping
Total hydrocarbons		x	x			x		Hydrate formation and MMP

References with actual product CO_2 composition data from large scale pilots or demonstration plants operated with amines are rather sparse. In particular, the concentrations of impurities such as amines, ammonia and aldehydes are not easily accessible in the open source literature, although some operational data have previously been reported by TCM during the 2015 MEA baseline tests [7]. Aldehydes, as a possible human carcinogenic by-product of MEA degradation, may represent a HSE risk for CCS facilities if present in high concentrations. Occupational exposure limits are presented by Gentry et al. [8] for both formaldehyde and acetaldehyde. For example, the Health and Safety Executive in the UK has put a long-term exposure limit of 2 and 20 ppm for formaldehyde and acetaldehyde respectively.

The CO_2 product gas composition is likely to vary, depending on plant design, operational parameters and solvent properties. During the recent MEA campaign at TCM, a broad range of operational conditions have been explored for the amine plant. This paper presents CO_2 product composition data from the online gas analyzers installed at TCM, originating from CO_2 capture of both flue gas sources available. Moreover, detailed composition data obtained by manual sampling and laboratory analysis, both internally at TCM and by external labs (Airborne Labs International, Inc.) is presented. The assessment of the CO_2 product composition in this work covers the following operational aspects and sensitivities:

- Composition data from both flue gas sources at TCM;
- Solvent quality;
- Stripper overhead system operation;
- Transient operation.

Nomenclature

BD	Brownian Diffusion (filter)
CCGT	Combined Cycle Gas Turbine
CHP	Combined Heat and Power
CCS	Carbon Capture and Storage
D-mix	Degradation mixture [13]
EOR	Enhanced Oil recovery
FTIR	Fourier-Transform Infrared Spectroscopy
HSE	Health Safety and Environment
HSS	Heat Stable Salts
MEA	Monoethanolamine
MMP	Minimum Miscibility Pressure
PCC	Post combustion capture
RFCC	Residual Fluidized Catalytic Cracker
TCM	Technology Center Mongstad

2. Instrumentation and sampling

2.1. TCM amine plant instrumentation

The major constituents of the CO_2 product stream are measured by different online analyzers (FTIR/GC/IR) downstream the stripper overhead receiver, as shown in Figure 1. In addition, a manual sampling point is located adjacent to the analyzer off-take, enabling sampling and identifications of additional trace compounds. In the 2015 MEA campaign [7] the manual sampling was performed closer to the CO_2 vent stack, and located further downstream of the new sample point, with a larger risk of condensation and non-representative sampling.

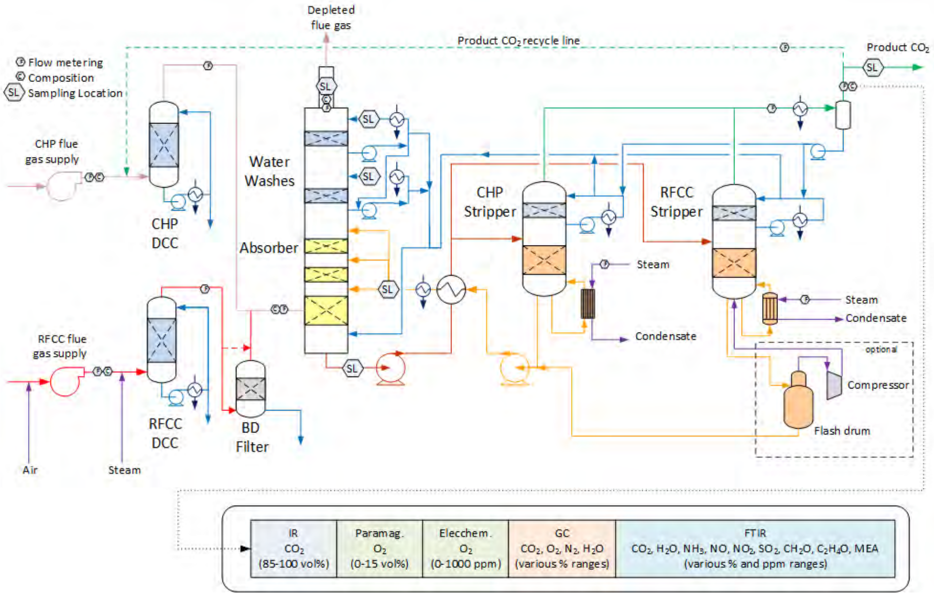

Figure 1: Schematic drawing of TCM amine plant and CO_2 product analysis location

At TCM there are two dedicated strippers for operation with each of the flue gas sources containing different CO_2 concentration levels. Both strippers are equipped with a water wash circulation system in addition to the reflux, as shown in the schematic above. The purpose is to “polish” the gas, reducing traces of soluble impurities in the CO_2 rich gas leaving the stripper. When the stripper water wash system is not in operation, only the reflux from the overhead condenser drum is returned to the stripper.

2.2. Airborne Labs analysis

CO_2 product gas analysis was done by Airborne Labs International, which is an accredited ISO/IEC 17025 laboratory and provider of analytical chemistry testing involving high purity gases and other types of gaseous samples.

Sampling was performed during two periods of MEA campaign in 2017 for both flue gas sources. The sampling was done by TCM lab personnel as instructed by the sample kits provided by Airborne Labs. The complete list of compounds analyzed for by Airborne Labs, including analysis method and uncertainty of analytic readings, is found in Appendix A.

3. Detailed composition data

3.1. Composition data from CHP and RFCC flue gas testing

The CO_2 product gas sampling was conducted at two different time slots during the MEA campaign, operated with CHP and RFCC flue gas respectively. Table 2 shows typical flue gas conditions upstream the absorber at TCM.

Table 2: Typical CHP and RFCC flue gas conditions upstream absorber

	Conditioned CHP flue gas	Conditioned RFCC flue gas
Temperature [°C]	25-50	15-50
Pressure [mbarg]	Up to 250	Up to 250
N_2 [mole%]	73-79	73-79
O_2 [mole%]	13-14	3-8
CO_2 [mole%]	3.6-4.0	13.0-14.5
H_2O [ppmv]	Saturated	Saturated
SO_2 [ppmv]	<0.3	<5
NO_X [ppmv]	<5	100
NH_3 [ppmv]	<5	<1
CO [ppmv]		<10
Particles [parts/cm^3]		$0.3\text{-}0.8\times10^6$

The results from the detailed analysis from Airborne Labs are presented in Table 3. Compounds analyzed for, but not detected are not included the table (the complete list of compounds analyzed for is found in Appendix A). However, some selected impurities of particular interest for CCS, are still reported as not detected (Nd) in the table for the records. The concentrations are reported on an as-is wet basis, except for CO_2 which is on a dry basis.

Three kits for each flue gas source were used during sampling. However, the gas cylinders for two of the sample kits used during the CHP campaign were reported to contain high levels of oxygen and nitrogen, indicating that air contamination may have occurred during the sampling process. Hence, these results are considered to be non-representative and concentrations of CO_2 and non-condensables are not reported for these samples. It should be noted that in the period between the CHP and RFCC campaigns the sample probe was somewhat modified to reduce the risk of condensation in the sample probe.

Table 3 also lists some key operational process parameters during the sampling periods. Solvent quality in terms of metal content and degradation products during the campaign is reported elsewhere [9]. The first product gas sampling during the CHP flue gas campaign in June was performed only one week after the start-up of the amine plant, whereas the two last CHP samples were taken four weeks after the start-up. Sampling with the RFCC flue gas was done over a period of two weeks, four and five weeks after a thermal reclaiming campaign respectively. The impact of solvent quality on the product gas quality is also discussed later in this paper.

A Brownian diffusion (BD) filter is installed downstream the RFCC direct contact cooler (DCC), to control the particle concentration in the RFCC flue gas entering the absorber. A by-pass line is also provided to allow for testing at varying particle concentrations, and sampling was performed both for closed and partly open by-pass line during the RFCC testing. Lombardo et al. [10] provide details on the nature of the aerosols particles and removal efficiency of the Brownian diffusion filter.

The stripper overhead system was operated without the dedicated stripper water wash in operation, i.e. only reflux water returned to the upper stripper packing wash section, throughout all sampling periods.

Table 3: Results from detailed CO_2 product composition analysis by Airborne Labs

Process conditions	21.06.2017	11.07.2017	13.07.2017	07.11.2017	09.11.2017	17.11.2017
Flue gas source	CHP	CHP	CHP	RFCC	RFCC	RFCC
Flue gas rate [Sm^3/h]	59000	35000	35000	35000	35000	35000
Solvent condition						
Fe [mg/kg]	0.4	8.7	-	18	21	28
BD filter operation	N/A	N/A	N/A	By-pass closed	By-pass partly open	
CO_2 content in flue gas [vol%]	3.9	4.1	9.4*	13.7	13.4	14.2
Stripper pressure [barg]	0.9	0.9	0.9	0.9	0.9	0.9
CO_2 product flow rate [kg/h]	3400	2500	5100	7900	7400	7800
Temperature downstream overhead condenser [C]	25	12	12	30	30	21
Stripper overhead reflux rate [kg/h]	1500	1100	1800	3000	2800	3000
CO_2 product analysis						
CO_2 [% v/v]	99.9+	Cont	Cont	99.9+	99.9+	99.9+
Hydrogen [ppmv]	Nd	Cont	Cont	Nd	Nd	Nd
Oxygen + Argon [ppmv]	49	Cont	Cont	28	36	17
Nitrogen [ppmv]	420	Cont	Cont	220	370	310
Carbon monoxide [ppmv]	Nd	Nd	Nd	Nd	Nd	Nd
Ammonia [ppmv]	1.0	Nd	Nd	0.5	Nd	0.5
Oxides of nitrogen (NOx) [ppmv]	Nd	Nd	0.5	0.5	0.5	0.5
Total hydrocarbons, THC [ppmv]	4.8	12	10	11	22	9.3
Acetaldehyde [ppmv]	2.9	6.9	7.1	6.3	6.5	7.7
Formaldehyde [ppmv]	Int	Int	Int	Int	Int	Int
Aromatic hydrocarbon content [ppmv]	Nd	Nd	Nd	Nd	Nd	Nd
Sulfur dioxide [ppmv]	Nd	Nd	Nd	Nd	Nd	Nd
Amines [ppmv]	Nd	Nd	Nd	Nd	Nd	Nd
Ethane [ppmv]	Nd	0.5	Nd	Nd	Nd	Nd
C_6+ [ppmv]	0.7	1.6	1.6	1.7	3.5	1.5
Ethanol [ppmv]	Nd	0.2	0.2	0.3	1.9	0.4
Acetone [ppmv]	Nd	0.2	0.4	0.5	0.4	0.5
Methanol [ppmv]	Nd	0.1	Nd	0.2	Nd	Nd
Ethyl acetate [ppmv]	Nd	Nd	Nd	0.1	0.1	Nd
2-Butanol [ppmv]	Nd	Nd	Nd	0.2	0.1	0.1

Nd= not detected, Int= interference with acetaldehyde spectra, Cont= sample contamination, *obtained by CO_2 recycle operation

3.2. Comparison with online instrumentation

A comparison of the Airborne analysis results with TCM online instrumentation is provided in Table 4 for two selected periods, running with CHP and RFCC flue gas, respectively. For some of the compounds there were additional manual samples and analysis performed by the TCM lab, as noted in the table.

Table 4: Comparison of Airborne analysis results with TCM online instrumentation

	21.06.2017 (CHP)		09.11.2017 (RFCC)	
	Online instrumentation	Manual sampling	Online instrumentation	Manual sampling
MEA [ppmv]	Int	Nd	Nd	Nd[1]
Ammonia [ppmv]	2.2	1.0	6.1	3.4[2]
NO [ppmv]	Nd	Nd	Nd	0.5
NO_2 [ppmv]	Nd		Nd	
SO_2 [ppmv]	0.2	Nd	Nd	Nd
Acetaldehyde [ppmv]	1.7	2.9	5.4	6.5[3]
Formaldehyde [ppmv]	0.3	Int	0.6	0.2[4]
N_2 [ppmv]	220	420	300	370
O_2 [ppmv]	1.8	49[5]	2.0	36[5]

[1] Not detected by neither Airborne nor TCM lab analysis

[2] Not detected by Airborne, reported value in table is from TCM lab analysis

[3] TCM lab analysis gave 7.1 ppmv

[4] Reported value is from TCM lab sampling, Interference in spectra reported by Airborne

[5] Oxygen concentration lumped with argon in Airborne reporting

Nd= not detected, Int= interference in spectra

Neither the online instrumentation nor the analysis from manual sampling could quantify any amines from the CO_2 product gas in the selected periods of comparison. There is fairly good agreement for NO_x and SO_2 between the online FTIR and analysis by Airborne Labs. Moreover, nitrogen concentrations are also comparable, whereas the online electrochemical measurement for oxygen is significantly lower than reported by Airborne Labs. However, these oxygen results are not directly comparable, as Argon is lumped into the reported oxygen concentration from Airborne.

For ammonia, the online FTIR is showing higher values than both analysis performed by Airborne Labs or by the TCM lab. Based on a comparison of a series of ammonia analysis done by the TCM lab throughout the MEA-3 campaign at different point in time, these manual samples are rather consistently and systematically showing approximately 50% of the concentrations found by the FTIR.

For aldehydes the concentrations measured by the FTIR are comparable with manual sampling. Figure 2 shows FTIR measurement of formaldehyde and acetaldehydes in the period of 7th to 9th of November. The results from manual sampling and analysis by Airborne and TCM lab, respectively, are included in the figure.

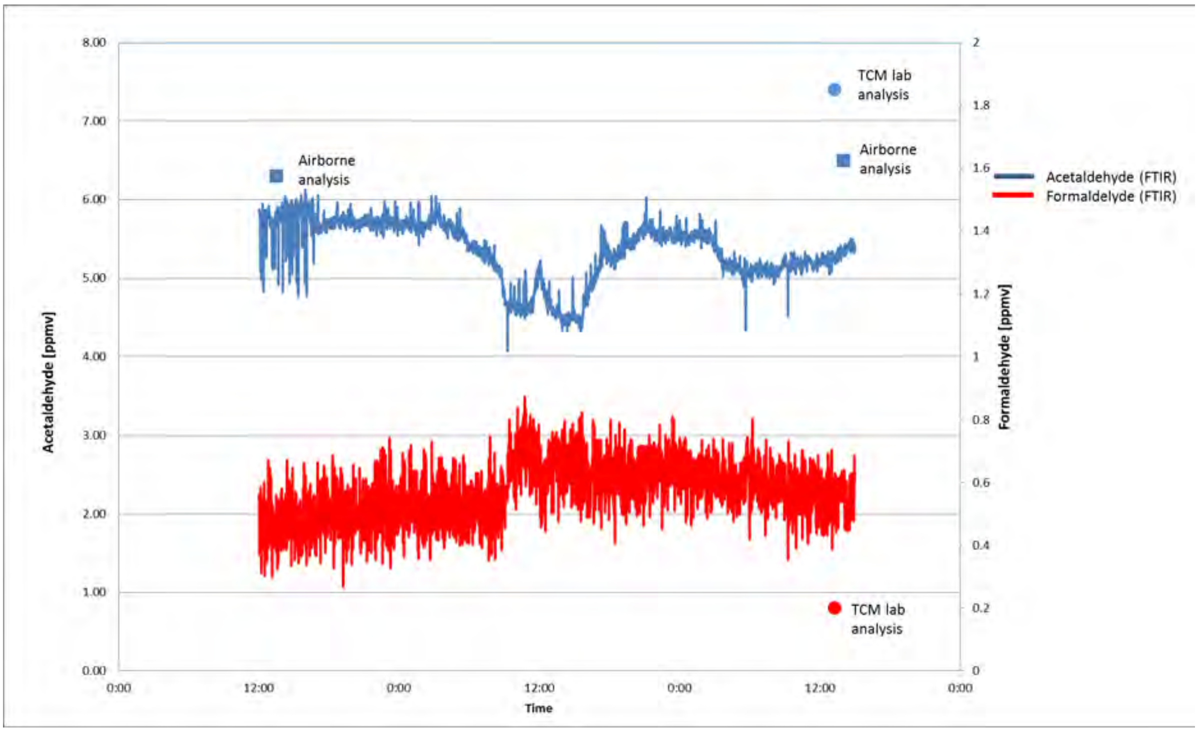

Figure 2: Online FTIR measurement of aldehydes, compared to results from manual sampling and analysis by Airborne TCM/SINTEF for 7th and 9th of November

4. CO_2 product composition sensitivities

4.1. Stripper overhead condensing temperature

The CO_2 product is cooled down in the overhead condenser. The condensed vapor is collected in a reflux receiver drum and returned to the stripper as cold reflux over the upper water wash packing section, as shown in Figure 1. At TCM the CO_2 stripper is also equipped with a stripper water wash circulation system in addition to the reflux. The operational mode of the overhead system will influence the CO_2 quality. In particular, the effect of the condensing temperature and total reflux rate, is of interest with respect to traces and impurities in the CO_2 product stream.

A test with CHP flue gas was performed, where the cooling duty of the condenser was reduced in steps, and consequently increasing the CO_2 product temperature downstream the condenser from 18 to 25 and 35°C in a step-wise manner. The reflux rate was kept stable during the ramps, without operation of the dedicated stripper water wash system. With increased temperature, the water content in the CO_2 product is increased, as an obvious consequence. More interestingly, it was observed that ammonia emissions increased from a steady value of 3 ppmv to almost 6 ppmv, for a condenser outlet temperature of 18 and 35°C, respectively. Reducing the temperature back to 18°C, restored the approximate same concentration of ammonia as prior to the temperature ramp-up, as seen in Figure 3.

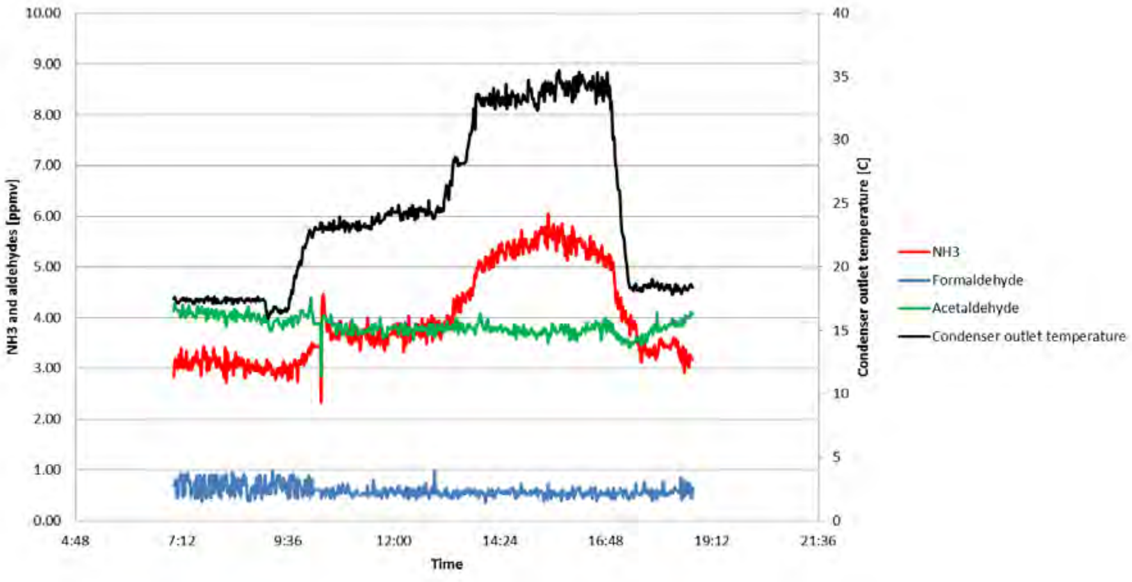

Figure 3: Ammonia and aldehydes concentrations during temperature change of CO_2 product gas

Increasing the CO_2 product temperature will increase the vapor pressure of dissolved ammonium causing higher ammonia slip to downstream re-compression systems and transport system. Also shown in Figure 3 are the formaldehyde and acetaldehyde concentrations, which were not significantly influenced by the temperature changes.

The online FTIR did not detect any amines in the CO_2 product gas for the temperature interval explored during this ramp test.

4.2. Solvent quality

During the MEA campaign both solvent reclaiming and partial or complete inventory replacement have been done to maintain good solvent condition. For certain periods of the campaign the solvent metal content has been higher than usual, as described by Morken et al. [9]. Two selected periods with aged and fresh solvent, denoted F and G respectively, have been assessed for any observable changes in the CO_2 product composition. In period F, the solvent contained relatively high concentrations of metals and degradation products, whereas period G represents a period after a complete solvent inventory replacement and plant wash. More details on the solvent condition in these periods are described elsewhere [9]. For both periods the capture plant was operated with the CHP flue gas. Some key operating conditions for a selected 12-hours window within both periods are listed in Table 5 along with average values for generation of iron, heat stable salts and D-mix.

Table 5: Key operational parameters for comparing CO_2 product impurities for two periods

Period Date	F (09.12.17)	G (18.01.18)
Iron generation [moles/h]	0.26	0.002
Heat stable salts [mole/h]	8.0	0.2
D-Mix [mole/h]	25	3.2
Flue gas flow rate [Sm^3/h]	58000	39000
NO_x in feed gas [ppmv]	1.5	3.0
CO_2 product rate [kg/h]	3600	2500
CO_2 condenser outlet temperature [°C]	19	18
Total reflux rate [kg/h]	1600	1500

Figure 4 shows how ammonia and acetaldehyde in the CO_2 product gas compare for a selected time interval of 12 hours in the two periods. Data points every minute are shown. First, it is evident that the ammonia concentration is significantly higher for period F than G, with concentrations in the region of 50-60 ppmv. This relates to the difference in metal concentration in the solvent for the two periods, as iron has an increased catalytic effect on oxidative degradation of the solvent, resulting in higher ammonia emissions. Also, it is seen that the concentration of acetaldehyde is significantly higher for period F with average of 16 ppmv, compared to approximately 2 ppm for period G. The concentration of formaldehyde, not shown in the figure, does not seem to be correlated to solvent conditions in the same way as acetaldehyde, as both periods show values in the same range of concentrations. Unfortunately, reliable readings of amines from the online FTIR was not available for both the periods under consideration.

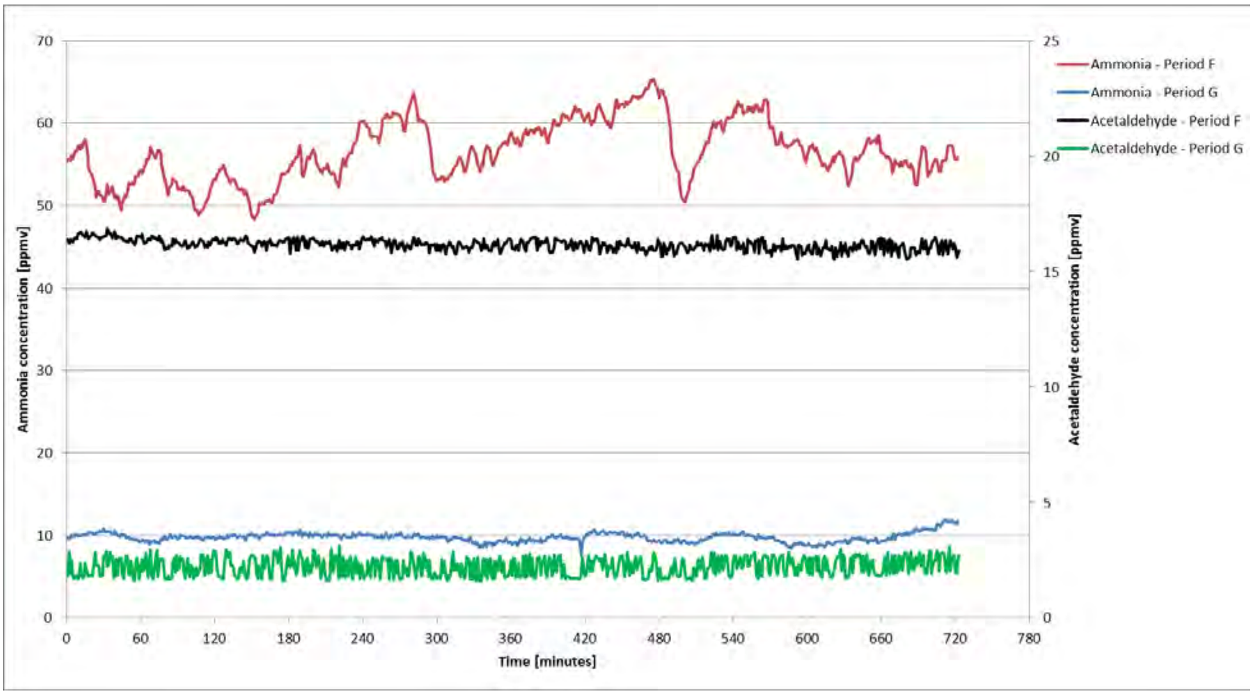

Figure 4: Ammonia and acetaldehyde concentrations (FTIR) in CO_2 product over a 12-hours period for periods F and G. Data points averaged every minute

4.3. Transient operation

A so-called rapid load change test was done by ramping the CHP flue gas rate between 55000 Sm^3/h to 35000 Sm^3/h within 5 minutes, while adjusting solvent circulation rate and reboiler duty to maintain a constant capture rate of approximately 85%. Figure 5 shows the corresponding solvent circulation and CO_2 product flow rates for this test. This test intended to mimic a rapid load change/turn down of the power plant, to study if there were any observable changes in the CO_2 product composition.

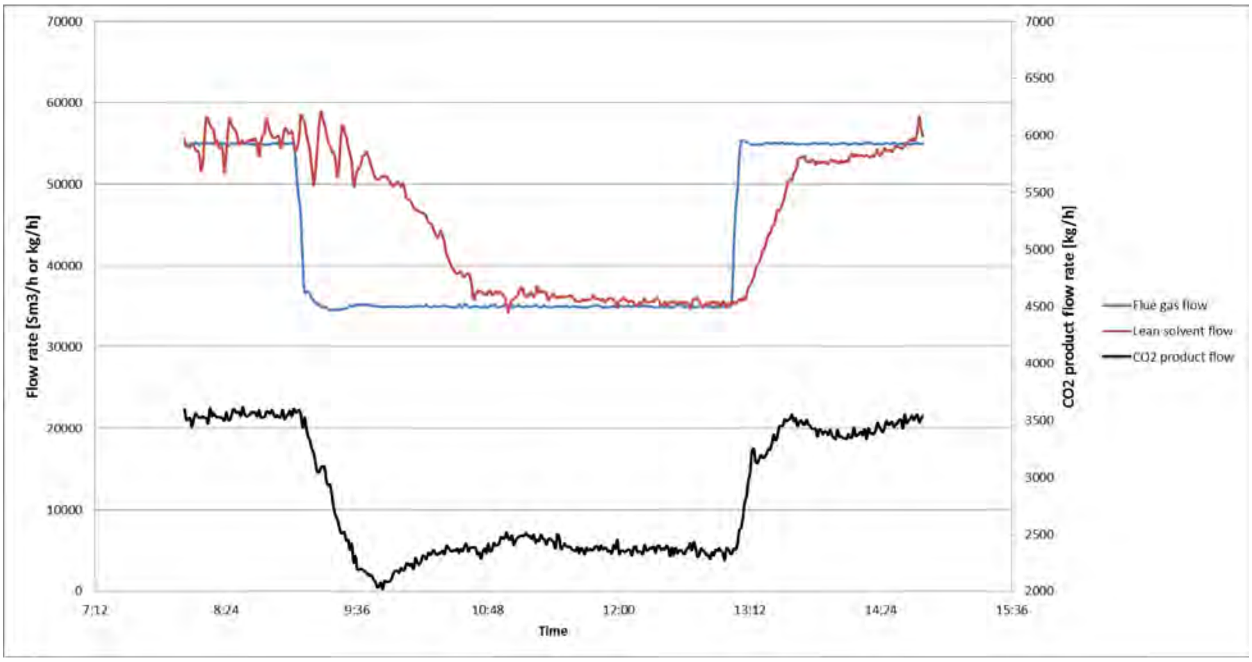

Figure 5: Flow rates of flue gas (CHP), solvent and product gas for transient rapid load change test

For the ramp-down, the stripper outlet temperature is slightly increased during the transient as the total product flow rate decreases, reducing the required cooling duty of the overhead condenser. As the condenser temperature controller was not properly tuned for such a transient, this resulted in a slight increase in CO_2 product temperature and hence ammonia slip, as a seen in Figure 6. The aldehydes concentrations are rather stable during the transients, except for a small peak in acetaldehyde concentration observed during the ramp-up. There was not detected any MEA, NO_X or SO_2 by the online FTIR during this test.

For changes in flue gas and solvent circulation rate, it could be foreseen that contact time for different gas/liquid (G/L) ratios could influence that amount of dissolved trace compounds in the rich amine leaving the absorber sump. In addition, if significant foaming occurs in absorber, the amount of non-condensable that are carried-under as gas bubbles could increase with increased solvent circulation. However, from the online instrumentation no significant changes are seen for the for the O_2 and N_2 concentrations, which remained at approximately 3 ppmv and 100 ppmv, respectively.

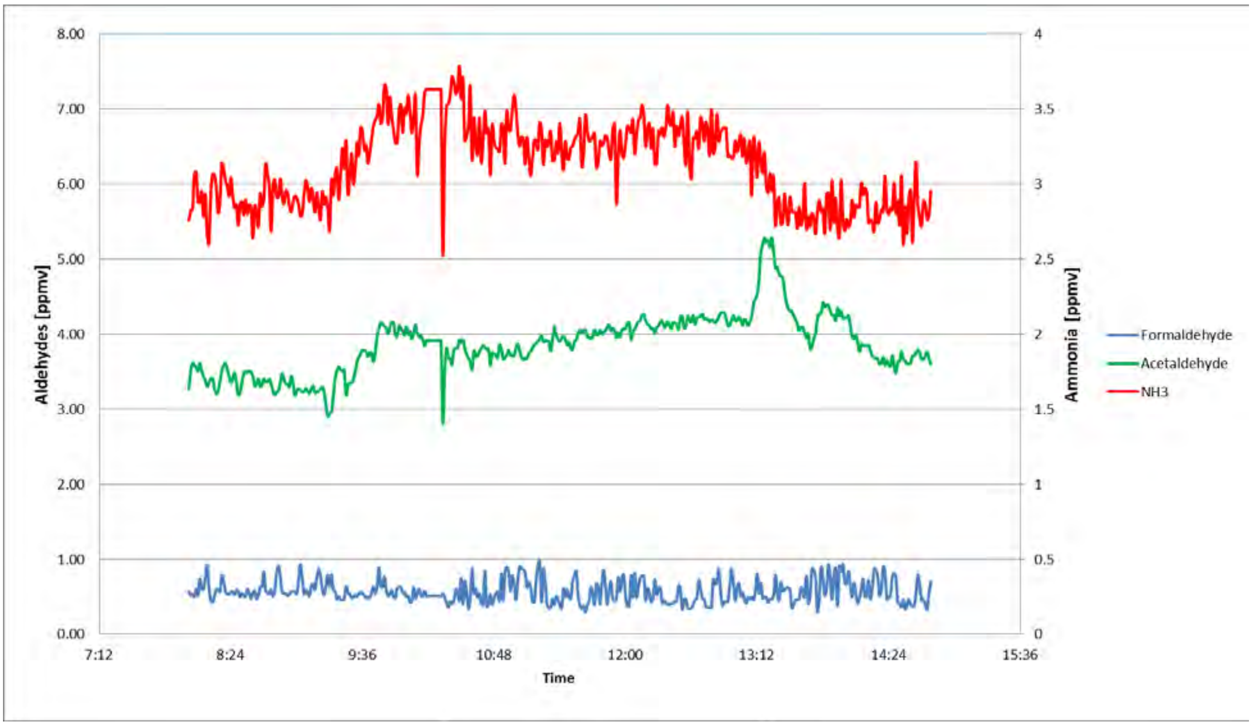

Figure 6: Ammonia and aldehydes concentrations in product gas during rapid load change test

5. Discussions

The reported dry basis purity of CO_2 of 99.9% is very high and in accordance with other references reporting purity of 99.6-99.8% from post combustion capture by chemical absorption processes [3]. The CO_2 product gas leaving the stripper overhead system will always be water saturated at the pressure and temperature in overhead reflux condenser and receiver. For transportation purpose, a drying unit will almost always be required downstream the capture unit. The final saturation degree, dictating the design of the drying system, will be set by compressor and intercoolers configuration. The amount of water to be handled by downstream systems is not an inherent feature of post combustion, but rather a choice of operational settings, and is therefore not reported explicitly as an impurity in this work.

Nitrogen is found to be the impurity with highest level in the product gas, regardless of flue gas source, operational condition or solvent condition with concentrations ranging from 200 to 400 ppmv. Nitrogen can arise from entrainment of gas bubbles in the rich solvent flow from the absorber or possibly from NO_X conversion. Other non-condensables reported from the Airborne analysis were O_2 and Ar, where the sum was ranging from 10-50 ppmv. Presence of non-condensables at higher concentrations could have an adverse effect on operation of rotating equipment in the downstream compression and liquefaction part of the value chain, as they will influence the phase envelope characteristics. In particular, the presence of gas bubbles in liquid CO_2 could cause increased vibration on CO_2 injection pumps.

Ammonia concentration in the CO_2 product gas has during the MEA campaign at TCM varied with the solvent quality. In general, the ammonia levels throughout the campaign has been low (< 10 ppmv). However, in periods where the solvent contained relatively high amounts of degradations products, e.g. prior to reclaiming operation, the ammonia emissions occasionally exceeded 60 ppmv. At these elevated concentrations there is a risk of solids formation downstream the stripper, such as ammonium carbamate, carbonate and bicarbonate as CO_2 reacts with NH_3. This was experienced at TCM, observed by increased pressure drop over the pressure control valve at the outlet of the condenser receiver vessel. Restricted flow and lack of operability of the pressure control valve caused plant shut down. Upon opening the control valve, salt precipitation was evident in the valve trim, restricting the flow and causing the high pressure drop. Such precipitation could also be a safety concern, if salts block impulse and feed lines to pressure safety valves that protect the stripper and overhead system. This is in particular valid for uninsulated and non-heat traced piping. Moreover, ammonia is reported [11, 12] to have an adverse effect on molecular sieve dehydration systems if deployed downstream, as it weakens the binding structure of sieves. No recommended threshold value was found reported in the literature.

Similar to ammonia, acetaldehyde concentration seems to correlate with the solvent quality. Formaldehyde seems to be less sensitive to the solvent condition with reported concentrations smaller than 1 ppmv. In general, the acetaldehyde concentration has been smaller than 10 ppmv throughout the campaign, whereas elevated concentration up to 15-20 ppmv was experienced in periods with increased degradation products and metal concentration in the solvent.

Amines were not detected from the samples analyzed by Airborne Labs, consistent with results from TCM lab analysis and FTIR online instrumentation. Based on analysis of MEA in liquid phase in reflux receiver drum and vapor pressure considerations, the expected MEA vapor phase concentration should be virtually zero. The design of the overhead condenser receiver at TCM is equipped with a wire mesh pad. The overhead receiver drum is common for both stripper configurations, which means that the load and consequently the separation efficiency is excepted to vary and some entrainment cannot be ruled out, although not found by the sampling probes in this study. In general, separation drums will not be 100% efficient and some liquid carry-over is to be expected, and design considerations of downstream systems should be made to include traces of amines. Consequently, trace levels over time will damage and reduce the lifetime of a molecular sieve used for drying, if constant carry-over is experienced.

6. Conclusions

After evaluating several months of operational data from the recent MEA campaign, it is evident that the CO_2 product gas is rather unaffected by flue gas source and process conditions dictating the capture rate. CO_2 concentrations of 99.9 v/v% on dry basis was obtained with nitrogen being the major impurity.

Among the impurities identified and analyzed for, ammonia, formaldehyde and acetaldehyde stand out as compounds not commonly reported in the literature. The solvent quality, in terms of metal content and amount of degradation products, seems to be the most influential parameter on the concentrations of acetaldehyde and ammonia the CO_2 product gas. In addition, the ammonia slip was found to be correlated with temperature of the overhead stripper system.

High ammonia emissions were experienced in periods where plant was operated with a highly degraded solvent. For ammonia concentrations exceeding 60 ppmv, precipitation of salts as ammonia combines with CO_2, caused operational upsets in the stripper overhead system due blocking and extensive pressure drop. Hence, special considerations for solvent quality management should be given with respect to ammonia emissions from CO_2 stripper.

It should be noted that the presented results are only typical and valid for MEA and the process parameters at TCM. The variation of the measurements suggests that the limitation of the trace compounds in the CO_2 product is challenging and sensitive to many parameters. This is also likely to be valid for other amines.

Acknowledgements

The authors gratefully acknowledge the staff at TCM DA, Gassnova, Equinor, Shell and Total for their contribution and work at the TCM DA facility. The authors also gratefully acknowledge Gassnova, Equinor, Shell and Total as the owners of TCM DA for their financial support and contribution.

Appendix A. Airborne Lab International analysis details

Table 6: CO_2 product analysis provided by Airborne labs

Compound	Lower detection limit	Analysis method	Uncertainty of reading
CO_2	5 % v/v	ISBT 4.0 GC/DID	12%
Hydrogen	10 ppmv	ISBT 4.0 GC/DID	12%
Helium	50 ppmv	ISBT 4.0 GC/DID	12%
Oxygen + Argon	10 ppmv	ISBT 4.0 GC/DID	12%
Nitrogen	10 ppmv	ISBT 4.0 GC/DID	12%
Carbon monoxide	2 ppmv	ISBT 5.0 DT (colormetric)	20%
Ammonia	0.5 ppmv	ISBT 6.0 DT (colormetric)	20%
Oxides of nitrogen (NOx)	0.5 ppmv	ISBT 7.1 DT (colormetric)	20%
Phosphine	0.25 ppmv	ISBT 9.0 DT (colormetric)	20%
Total hydrocarbons, THC	0.1 ppmv	ISBT 10.0 THA (FID)	2.7%
Total non-methane hydrocarbons	0.1 ppmv	ISBT 10.1 GC/DID	5.2%
Methane	0.1 ppm	ISBT 10.1 GC/DID	5.2%
Acetaldehyde	0.05 ppmv	ISBT 11.0 GC/FID	6.6%
Formaldehyde	0.05 ppmv	DT	20%
Aromatic hydrocarbon content	2 ppmv	ISBT 12.0 GC/FID	6.2%
Benzene	2 ppmv	ISBT 12.0 GC/FID	6.2%
Toluene	2 ppmv	ISBT 12.0 GC/FID	6.2%
Ethyl benzene	2 ppmv	ISBT 12.0 GC/FID	6.2%
m,p Xylenes	2 ppmv	ISBT 12.0 GC/FID	6.2%
o Xylene	2 ppmv	ISBT 12.0 GC/FID	6.2%
Total Sulfur content	0.01 ppmv	ISBT 14.0 GC/SCD	8.8%
Sulfur dioxide	0.01 ppmv	ISBT 14.0 GC/SCD	20%
Hydrogen cyanide	0.2 ppmv	ISBT SM 1.0 GC/FID	6.6%
Vinyl chloride	0.1 ppmv	ISBT SM 2.0 GC/FID	6.6%
Amines	0.5 ppmv	DT	20%
Speciated volatile hydrocarbonds[1]	0.1 ppmv	ISBT 10.1 GC/DID	5.2%
Speciated volatile sulfur compunds[2]	0.01 ppmv	ISBT 14.0 GC/SCD	8.8%
Speciated volatile oxygenates[3]	0.1 ppmv	ISBT 11.0 GC/FID	6.6%

[1] Ethane, Ethylene, Propane, Propylene, Isobutane, n-Butane, Butene, Isopentane, n-pentane, Hexanes+

[2] Hydrogen sulfide, Carbonyl sulfide, Methyl mercaptan, Ethyl mercaptan, Dimethyl sulfide, Carbon disulfide, t-Butyl mercaptan, Isopropyl mercaptan, n-Propyl mercaptan, Methyl propyl sulfide, 2-Butyl mercaptan, i-Butyl mercaptan, Diethyl sulfide, n-Butyl mercaptan, Dimethyl disulphide

[3] Dimetyl ether, Ethylene oxide, Diethyl ether, Propionaldehyde, Aceton, Methanol, t-Butanol, Ethanol, Isopropanol, Ethyl acetate, Methyl ethyl ketone, 2-Butanol, n-Propanol, Isobutanol, n-Butanol, Isoamyl alcohol, Isoamyl acetate

References

[1] The open-source centre at TCM, https://catchingourfuture.com/

[2] de Visser E, Hendriks C, Barrio M, Mølnvik MJ, de Koeijer G, Liljemark S, Le Gallo Y. Dynamis CO_2 quality recommendations. Int. Journal of Greenhouse Gas Control, Vol. 2, Issue 4, 2008, p. 478-484

[3] Porter RTJ, Fairweather M, Pourkashananian M, Woolley RM. The range and level of impurities in CO_2 streams from different carbon capture sources. Int. Journal of Greenhouse Gas Control, Vol. 36, 2015, p. 161-174

[4] Abbas Z, Mezher T, Abu-Zahra MRM. Evaluation of CO_2 Purification Requirements and the Selection of Processes for Impurities Deep Removal from the CO_2 Product Stream. Energy Procedia, Volume 37, 2013, p. 2389-2396,

[5] DNVGL-RP-F104. Design and operation of carbon dioxide pipelines, 2017

[6] IEA GHG. Impact of CO_2 impurity on CO_2 compression, liquefaction and transportation. Report 2016/01, April 2016

[7] Faramarzi L, Thimsen D, Hume S, Maxon A, Watson G, Pedersen S, Gjernes E, Fostås B, Lombardo G, Cents T, Morken AK, Shah MI, de Cazenove T, Hamborg ES. Results from MEA testing at the CO_2 Technology Centre Mongstad: Verification of baseline results in 2015. Energy Procedia, Volume 114, 2015, p.1128-1145

[8] Gentry PR, House-Knight T, Harris A, Greene T, Campleman S. Potential occupational risk of amines in carbon capture for power generation. Int Arch Occup Environ Health (2014) 87:591–606

[9] Morken AK, Pedersen S, Nesse SO, Flø NE, Johnsen K, Feste JK, de Cazenove T, Faramarzi L, Vernstad K. CO_2 capture with monoethanolamine: solvent management and environmental impact (GHGT-14, 2018)

[10] Lombado G, Shah MI, Fostås B, Hvidsten OA, Faramarzi L, Cazenove TD, Lepaumier H, Rogiers P. Results from aerosols measurement in amine plant treating gas turbine and residual fluidized catalytic cracker flue gases at the CO_2 Technology Centre Mongstad (GHGT-14 ,2018)

[11] Kempra J, Sutherland L, Watt J, Santos S. Evaluation and analysis of the performance of dehydration units for CO_2 capture, Energy Procedia 63 (2014) p. 7568 – 7584

[12] Purcell T. Effects of Contaminants on Molecular Sieves, Hydrocarbon Engineering, 1997

[13] Morken AK, Pedersen S, Kleppe ER, Wisthaler A, Vernstad K, Ullestad Ø, Flø NE, Faramarzi L, Hamborg ES. Degradation and Emission Results of Amine Plant Operations from MEA Testing at the CO_2 Technology Centre Mongstad, Energy Procedia 114, 1245-1262

Results from testing of a Brownian diffusion filter for reducing the aerosol concentration in a residual fluidized catalytic cracker flue gas at the Technology Centre Mongstad

(2018)

14th International Conference on Greenhouse Gas Control Technologies, GHGT-14

21st -25th October 2018, Melbourne, Australia

Results from testing of a Brownian diffusion filter for reducing the aerosol concentration in a residual fluidized catalytic cracker flue gas at the Technology Centre Mongstad

Gerard Lombardo[a,c]*, Muhammad Ismail shah[a,c], Berit Fostås[b], Odd Arne Hvidsten[b,c], Leila Faramarzi[b,c], Thomas de Cazenove[c], Hélène Lepaumier[d], Pieter Rogiers[d]

[a] *Gassnova SF, Dokkvegen 10, 3920 Porsgrunn, Norway*
[b] *Equinor ASA, PO Box 8500, 4035 Stavanger, Norway*
[c] *Technology Centre Mongstad, 5954 Mongstad, Norway*
[d] *Laborelec, Rodestraat 125, 1630 Linkebeek, Belgium*

Abstract

Operation of amine absorbers with a flue gas containing sulfuric acid aerosols and dust particles is a challenge. After the installation of a Brownian diffusion filter upstream the absorber the aerosols are reduced and TCM has been able to operate the amine plant with the residual fluidized catalytic cracker flue gas. The Brownian diffusion filter efficiency is assessed based on the number particle concentration and aerosol size distribution. The tests at TCM demonstrate that more than 95 % of the aerosols were removed. The growth of the aerosols with moisture from the flue gas is fast and is not detected by the instrumentation installed at TCM. The water captured by the Brownian diffusion filter confirms that the mass concentration of the aerosols captured is between 1000 and 5000 mg/Sm^3 of flue gas.

Keywords: CO2 capture; Aerosol; Amine emissions; Brownian diffusion filter

1. Introduction

The Technology Centre Mongstad (TCM) is the world’s leading facility for verifying and improving CO_2 capture technologies. TCM is located at Mongstad, one of Norway´s most complex industrial facilities. TCM has been operating since autumn 2012, providing an arena for qualification of CO_2 capture technologies on an industrial scale. In autumn 2017, Gassnova (on behalf of the Norwegian state), Equinor (formerly Statoil), Shell and Total entered into a new ownership agreement securing operations at TCM until 2020. The owners of TCM started their most recent monoethanolamine (MEA) test campaign in June 2017 where a large number of public, industrial, research and academic stakeholders were involved [1]. The campaign included demonstration of a model-based control system, dynamic operation of the amine plant, investigating amine aerosol emissions and specific tests targeted at

---

* Corresponding author. Tel.: +47 40 00 59 08.
E-mail address: postmottak@gassnova.no

reducing the cost of CO_2 avoided. Through the testing, both flue gas sources currently available at TCM were used. These sources are the combined cycle gas turbine (CCGT) based heat and power plant (CHP) and the residual fluidized catalytic cracker (RFCC). They provide flue gases with a wide range of properties and a CO_2 content from 3.6 to 14 %. TCM is located next to the Equinor refinery in Mongstad. The Mongstad refinery is the source of both flue gases supplied to TCM.

During the MEA campaigns in 2017 and 2018 TCM executed a series of tests to capture CO_2 from residual fluidized catalytic cracker flue gas. It was first of its kind test campaigns at TCM where CO_2 is captured from RFCC flue gas treated with a Brownian diffusion filter. A previous MEA test campaign was conducted while capturing CO_2 from combined cycle gas turbine flue gas mixed with RFCC flue gas and recycled CO_2. A pilot Brownian diffusion filter was tested in this previous campaign. Results of the previous campaign are documented at the GHGT-13 [2]. The new learning's related to the Brownian filter efficiency and aerosol properties are reported in this paper. These learning's are valuable for the design of flue gas treatments upstream or downstream of amine absorbers. The impact of flue gas pretreatment by the BD filter on the MEA emissions is reported separately [3].

Nomenclature

CHP	Combined heat and power plant
BD filter	Brownian diffusion filter
DCC	Direct contact cooler
ELPI$^+$	Electrical low pressure impactor
MEA	Monoethanolamine
RFCC	Residual fluidized catalytic cracker
TCM	Technology Centre Mongstad
WESP	Wet electrostatic precipitator

2. Process description

In December 2016, a Brownian diffusion filter was installed between the RFCC direct contact cooler (DCC) and the amine absorber. The vessel for the Brownian diffusion Filter includes a high efficiency demister and twenty-one filters filled with fibers typically called candles. A simplified sketch of the BD filter unit is given in the figure 1.

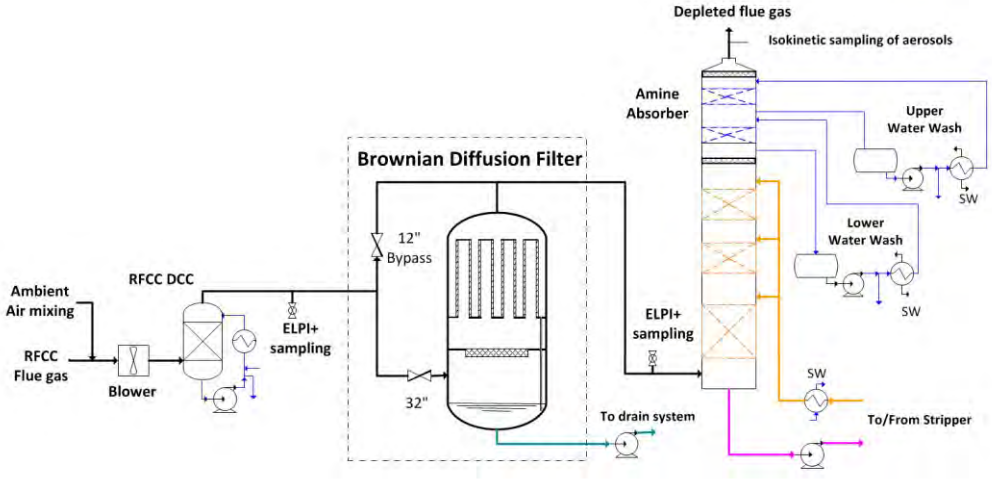

Figure 1. Simplified flow diagram of the Brownian diffusion Filter.

A detailed description of the BD filter unit is given in the following sections.

1.1. Functional description of the BD filter and design capacity

The main design parameters are:

- Design flue gas flow rate: 35,000 Sm^3/h
- Maximum allowable differential pressure of the demister: 12 mbar
- Maximum allowable differential pressure of the candles: 30 mbar

Based on the operation experience acquired since the installation of the filter, a maximum RFCC flue gas flow of 40,000 Sm^3/h to 45,000 Sm^3/h is possible but the filter efficiency is slightly reduced.

The particles are captured by fibers and each particle captured grows by further accumulation until droplets are formed. When the weight of the droplets is sufficient, a water film occurs, flowing down to the bottom of the candles. During operation, the candles are partly filled with the water accumulated. The liquid collected downstream the candles is drained to the bottom of the vessel. A pump controls the level of the vessel.

1.2. Typical aerosol description at TCM

The table 1 describes the total number concentration and weight concentration of aerosols in the flue gas.

Table 1. Typical aerosol parameters at TCM.

Main components	Units	Upstream BD filter	Downstream BD filter	Downstream BD filter with bypass
Number concentration	x 10^6 part./cm^3	15 to 25	0.3 to 0.8	0.3 to 4.6
Size distribution	µm	0.01 to 10	0.01 to 0.5	0.01 to 5
Weight concentration	mg/Sm^3	1000 to 5000	3 to 10	3 to >200
Fly ash/catalyst/non soluble salts	mg/Sm^3	<5	<0.1	<0.1
H_2SO_4 & Salts (mainly ammonium sulfates)	mg/Sm^3	20 to 30 (H_2SO_4: 10 to 20)	<0.6	<0.6 to 5

Upstream the filter, the RFCC flue gas contains a high number of particles between 10 nm and over 5 µm diameter, and the composition is expected to be similar to the flue gas from a coal power plant without fabric filters. As illustrated in figure 2 the particle size distribution is variable upstream the BD filter. The variation of aerosol size distribution is caused by the fluctuations of the operation parameters of the refinery and mainly by the steam injection in the flue gas upstream of the RFCC DCC. At TCM, the steam injection is necessary in order to keep the temperature and moisture constant in the flue gas. The size distribution of the RFCC flue gas has been checked during several campaigns, before the installation of the BD filter, upstream and downstream the RFCC DCC and downstream of the absorber. The similarity between the measured size distributions suggests that a BD filter may be also applicable at the absorber outlet.

The flue gas composition downstream the candles at TCM is expected to be similar to coal flue gas treated with a conventional electrostatic precipitator and an additional flue gas purification unit as a fabric filter or advance purification systems as a wet electrostatic precipitator (WESP). The BD filter bypass allows higher particle concentrations to the absorber.

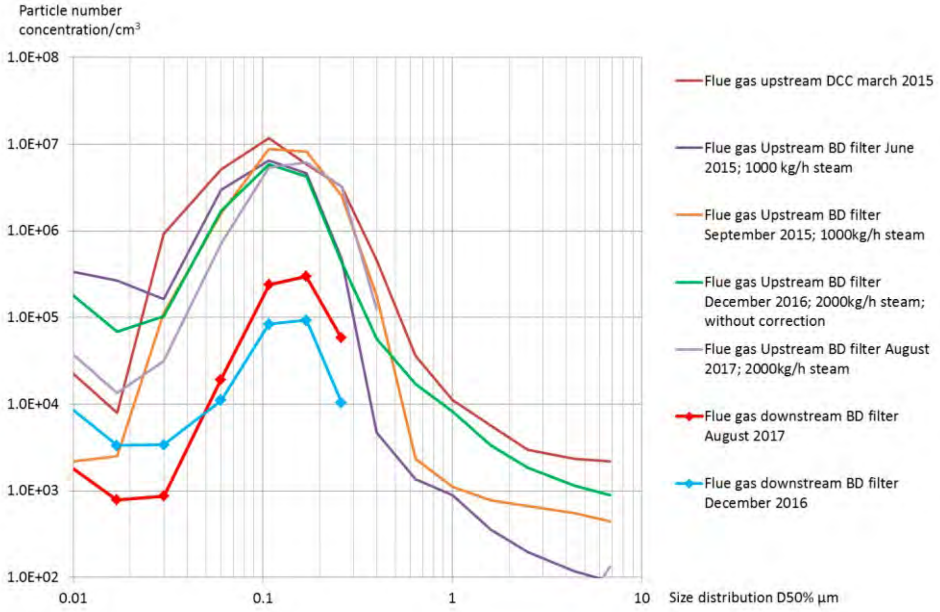

Figure 2. Typical size distribution upstream and downstream the BD filter.

1.3. Installation and mechanical design of the candles

The entire vessel including candles and demister is designed and delivered by Begg Cousland Envirotec Limited (United Kingdom). The candles are fixed to a main support plate as described in figure 3. The flue gas inlet is located at the bottom of the vessel, upstream of the demister and the flue gas is distributed to each candle through the openings in the main support plate.

Figure 3 Installation pictures. To the left: main support plate of the candles. To the right: the flue gas inlet is located at the bottom of the vessel.

An isometric view of the RFCC flue gas treatment system is presented in figure 4. The bypass to the filter is located in the pipe rack. In order to minimize the capture of aerosols above 1 µm to the bypass, the connection of the bypass to the main duct is not isokinetic (branch tee) and the velocity to the bypass is low compared to the main flow to the filter.

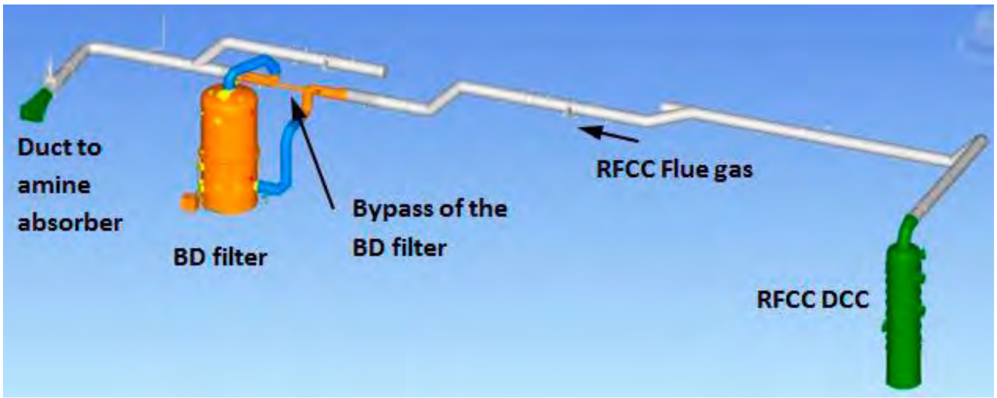

Figure 4. Isometric view of the RFCC flue gas treatment system.

1.4. Candle description

The thickness of the candle bed fibers is 50 mm and the total filtration area of the 21 candles is 135 m^2. The inlet velocity to the filtration area is 7.2 cm/s. The design is optimized, based on the results from the pilot tests from various fiber types and suppliers.

The capture efficiency of the BD filter is approximately 97 % of the particle number based on 35,000 Sm^3/h of flue gas with 20 x 10^6 particles/cm^3. The number concentration downstream the candles is 0.3 x 10^6 particles/cm^3 with clean candles and 0.7 x 10^6 particles/cm^3 with used candles. The capture efficiency of the particles with a diameter between 10 nm and 70 nm is decreasing with higher flue gas flow. The life span of the candles may be reduced by the accumulation of catalyst particles. The life span of the candles shall be confirmed by further tests at TCM.

1.5. Installation and mechanical design of the demister

The demister installed upstream the candles is described in figure 5. The purpose of the demister is to minimize the catalyst particles accumulation in the candles. A Scanning Electron Microscopy with an Energy Dispersive X-ray spectrometer (SEM-EDX) was used to measure the elemental composition of the deposits and catalyst in the aerosols. As the catalyst particles are mainly detected in aerosols of 1 μm or above, a high efficiency demister is required.

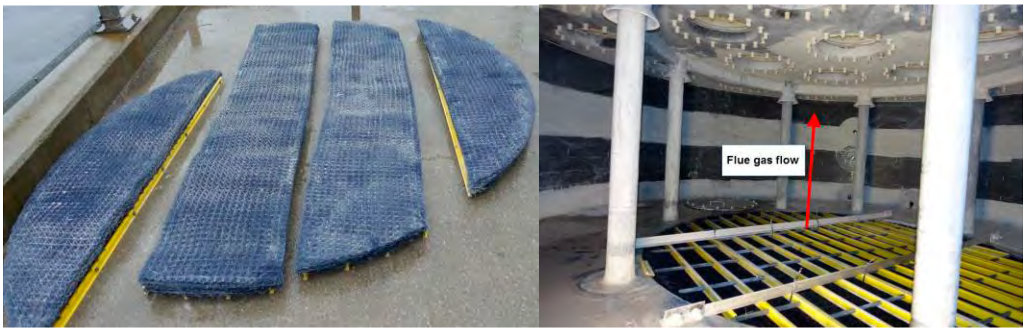

Figure 5. High efficiency demister. To the left: demister pads disassembled for cleaning operation. To the right: the demister pads are located under the yellow support grid. The candle support plate with the openings to the candles is visible at the top of the picture.

The demister is 2.45 m diameter, 120 mm thick and includes several diverse layers of polypropylene mesh. The demister is arranged in five sections and each section divided in a lower and upper bundle. The inlet velocity to the demister is 2 m/s. A demister is usually designed to remove liquid particles, but at TCM the demister is operated with catalyst particles and the demister requires periodic cleaning. At 35,000 Sm^3/h, the mass of catalyst particles captured in the vessel is between 1 and 2.5 kg/day. Dry or accumulated catalyst particles require a disassembling of the demister and a manual cleaning with pressurized water. A cleaning is typically performed after a campaign period of 2 months. The operation parameters of the demister are critical in order to avoid dry areas and accumulation of catalyst. The accumulation of catalyst is likely limited at high water load and flooding conditions in the demister bed. A complete spare part of the demister is available at TCM in order to minimize the shutdown period during cleaning operation. A shutdown of 4 to 6 hours is usually necessary for a replacement of the demister.

3. Campaigns and test summary

A brief overview of the different tests conducted is given below and test results are detailed out in the following sections.

- From 16 to 22 December 2016: BD filter start-up/test and efficiency measurements with the use of $ELPI^+$ (Electrical low pressure impactor: refer to section 6)
- From 24 to 30 January 2017: pressure drop tests of BD filter
- From 21 February to 25 April 2017: BD filter tests and proprietary solvent campaign with RFCC flue gas
- From 24 July to 17 November 2017: BD filter tests, MEA 3 test campaign and efficiency measurements with the use of $ELPI^+$

4. Demister and Candle filter pressure drop

The pressure drop test results for are summarized in the table 2. At constant temperature and gas phase composition, the pressure drop through the candles and the demister is directly proportional to the flue gas flow and increasing with the mass of aerosols captured.

Table 2. Demister and Candle filter pressure drop.

Operation summary	Parameter	Comment
Operation period	18 weeks	7 periods from December 2016 to November 2017
Flue gas flow	35,000 Sm^3/h	Design capacity
Flue gas temperature to filter & absorber	20 ºC to 35 ºC	Controlled by steam injection upstream the RFCC DCC (2000 to 3000 kg/h)
Pressure drop of the demister	5 to 6 mbar (Design: 12 mbar)	Stable pressure drop. Variations due to aerosol mass in the flue gas
Pressure drop of the candles	15 to 17 mbar (Design: 30 mbar)	Stable pressure drop. Variations due to aerosol mass in the flue gas

The efficiency of the demister secures a lower pressure drop of the candles than measured during the pilot tests in 2015. The water load in the demister and the accumulation of catalyst particles establish flooding conditions in the demister and high capture efficiency for aerosols above 1 µm. Due to the flooding conditions, water droplets are entrained from the demister to the candles.

The accumulation of catalyst particles in the candles is confirmed by the inspections of January, April, August and November 2017. However, the accumulation looks limited and no increase of pressure drop is observed. The life span of the candle will be estimated during the future campaigns with RFCC flue gas.

5. Mass of aerosols captured based on the liquid level measurements of the BD filter vessel

The mass of aerosol captured by the demister and the candles is estimated based on the liquid level measurement of the BD filter vessel.

The liquid accumulation in the filter vessel may be caused by:

- Aerosols captured
- Water condensation from the flue gas in the ducts and in the BD filter vessel. Based on the temperature decrease between the DCC and the inlet to the absorber, the maximum water condensation is estimated to 30 kg/h. A water condensation of 10 to 20 kg/h is confirmed during the tests with ambient air instead of flue gas.
- Liquid entrainment from the DCC. The tests with ambient air from 20,000 Sm^3/h to 55,000 Sm^3/h confirm that there is no entrainment of liquid from the DCC if the flow rate is limited to 45,000 Sm^3/h.

At the design flow of 35,000 Sm^3/h, the estimated capture rate is summarized in the table 3. The average concentrations of sulfate salts and sulfuric acid are based on laboratory water analysis from the vessel.

Table 3. Mass concentration of aerosols captured.

	Mass concentration of aerosols captured with steam injection upstream the RFCC DCC (mg/Sm^3)	Mass concentration of aerosols captured without steam injection (mg/Sm^3)
Aerosols captured	1500 to 3000 (up to 100 kg/h)	500 to 900
Sulfate salts	30	Not measured
Sulfuric acid	7	1
Catalyst particles	>1	Not measured

As described in the section 8, the mass concentration of water in the aerosols captured is higher than estimated with the $ELPI^+$ measurements (50 to 500 mg/Sm^3). A substantial number of aerosols with a diameter between 2 and 10 µm are necessary to explain the mass of aerosols captured in the vessel. The capture rate measured by the liquid level of the vessel confirms that the $ELPI^+$ is not designed for the detection of large aerosols mainly composed of water. The salts and sulfuric acid concentrations are in accordance with the previous flue gas measurements between 2013 and 2015. Most of the catalyst particles are eliminated with the vessel drain and the mass cannot be estimated. A mass concentration of 1 to 3 mg/Sm^3 of catalyst particles is estimated based on the previous flue gas isokinetic gravimetric sampling.

6. $ELPI^+$ technology

6.1. Introduction

Based on weight concentration, the high efficiency of Brownian diffusion filters is well established. Most of the authority regulations are based on weight concentration and manual isokinetic sampling. The weight of aerosols under 0.5 µm is insignificant, but these aerosols may grow in the absorber, hence the efficiency based on weight is not satisfactory for amine absorbers. Therefore, the efficiency of the Brownian diffusion filter has been determined based on the particle number concentration and particle size distribution measured upstream and downstream the BD filter unit. The particle number concentration and particle size distribution are estimated with $ELPI^+$ measurements performed by Engie Research and Technologies.

Working principle of the $ELPI^+$:

1. Particle charging
2. Size classification in a cascade impactor (14 size classes)
3. Electrical detection with sensitive electrometers

6.2. ELPI$^+$ description and limitations for the measurements of aerosols with high load of water

As described in the figure 6, the ELPI$^+$ measurements require usually a dilution of the sample with dry air in order to avoid water condensation on the EPLI$^+$ stages. The particle size distribution and number concentration may be modified by this dilution if the aerosols contain large particles with mainly water.

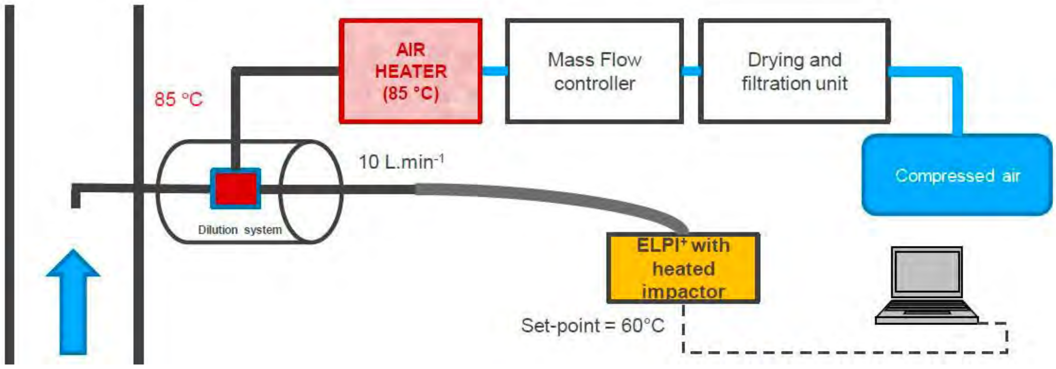

Figure 6. ELPI$^+$ sampling system.

In the range of 10 nm to 1 µm, the ELPI$^+$ (Electrical low pressure impactor) is applicable to estimate the efficiency of the Brownian diffusion filter based on the particles number concentration, but the impact of following limitations shall be evaluated during the measurements:

- Impactor loading: if a measurement continues a long period or sampling is made from a high particle concentration, the high amount of collected particles can have a negative effect on the impactor performance. As a rule of thumb, 1 mg of particles per one impactor stage can be used as an absolute maximum value.
- The sampling to the ELPI$^+$ is not isokinetic upstream the filter. With the dilution system used, an isokinetic sampling to the ELPI$^+$ is not reliable or complex. However, as demonstrated by previous studies [4, 5], the effect of non-isokinetic sampling of aerosols on the observed sizes is not important since most of the aerosol size is smaller than 0.5 µm.
- Fine Particle Correction: diffusion causes the impact of the smallest particles on a too early stage, leading to an overestimation of the particle size. An algorithm is used to correct the ELPI$^+$ readings. It is possible to calculate both uncorrected and corrected particle size distributions.
- Aerosols above 2 µm, composed only of water are unstable and easy to evaporate. This type of aerosols may be a challenge for ELPI$^+$ measurements.

7. Results from ELPI$^+$ measurements just after the first startup of the BD filter

The ELPI$^+$ measurements completed just after the first startup of the BD filter are summarized in the table 4.

Table 4. ELPI$^+$ measurements of December 2016.

Location/Sample	RFCC flow rate (Sm^3/h)	Number conc. All stages ($Part./cm^3$)
Unfiltered RFCC flue gas	25,000	1.61×10^7 to 3.4×10^7
	35,000	1.1×10^8
Pre-filtered RFCC flue gas, downstream Bluefil demister	25,000	1.5×10^7
	35,000	1.5 to 1.9×10^7
Filtered RFCC flue gas, downstream Brownian candles	25,000	2.2 to 2.6×10^5
	35,000	2.6 to 3.3×10^5
	39,000	2.2×10^5

Comments to the results:

- Relatively large variations are measured for the RFCC flue gas, as previously observed since the first measurements in 2015: from 12 to 34 million particles/cm^3
- Due to turbulent weather conditions with outdoor sampling with the ELPI$^+$, unstable measurements are experienced.
- As the particles above 1 µm are not detected; the efficiency of the demister could not be demonstrated for these particles.
- The large number of particles for the unfiltered RFCC flue gas is due to particles of 0.01 µm size.
- As expected, the efficiency of the Brownian diffusion candle filter is decreasing at higher flow rates for the smaller aerosol diameters.

The filter performance has been demonstrated at different flue gas flow rates. Results are summarized in the table 5 below.

Table 5. Filter performance at start up (December 2016).

Flue gas flow (Sm^3/h)	Downstream pre-filter (Particles/cm^3)	Downstream Brownian diffusion filter (Particles/cm^3)	Efficiency (%)
25,000	1.49 x 10^7	1.41 x 10^5	99.1
35,000	1.87 x 10^7	2.13 x 10^5	98.9
39,000	Not measured	2 x 10^5	

An overall efficiency of 99 % is confirmed for the particles > 20 nm. As the candles are new and not saturated with aerosols, a higher efficiency than measured during the pilot test is confirmed (Pilot test efficiency: 98 %). The efficiency is slightly decreasing at higher flue gas flow

8. Results from ELPI$^+$ measurements in August 2017

8.1. Aerosols size distribution of the RFCC flue gas before filtration

Figure 7 shows that for all samplings, the size distribution of the RFCC flue gas before filtration is similar in the range from 0.06 to 0.2 µm. The variation of size under 0.06 µm is caused by the operation at the refinery as well as the ELPI$^+$ sampling system, i.e. the number of small aerosols is varying with dilution effect, algorithm for small particle correction or unstable conditions. Above 0.2 µm, the particle size is increasing quickly with steam injection and temperature control of the flue gas. In addition, the ELPI$^+$ algorithm for small particle correction removes most of the particles detected by the ELPI$^+$.

The mass of aerosols in one cubic of flue gas could be assessed based on the ELPI$^+$ measurements considering:

- The number of particles and size distribution.
- Spherical particles with 1000 kg/m^3 as density.

Based on ELPI$^+$ measurements, the mass concentration of aerosols is estimated at 20 mg/Sm^3 by taking into account small particle correction and 500 mg/Sm^3 without small particle correction. These values are much lower than the actual mass captured by the candles. In August 2017, the average mass concentration captured was 1600 mg/Sm^3. A typical size distribution of 1600 mg/Sm^3 is shown in the figure 7 and addition of 45,000 particles/cm^3 above 1 µm is sufficient to simulate the missing weight. This number is negligible compared to the total number of particle measured (1.5 x 10^7 particles/cm^3).

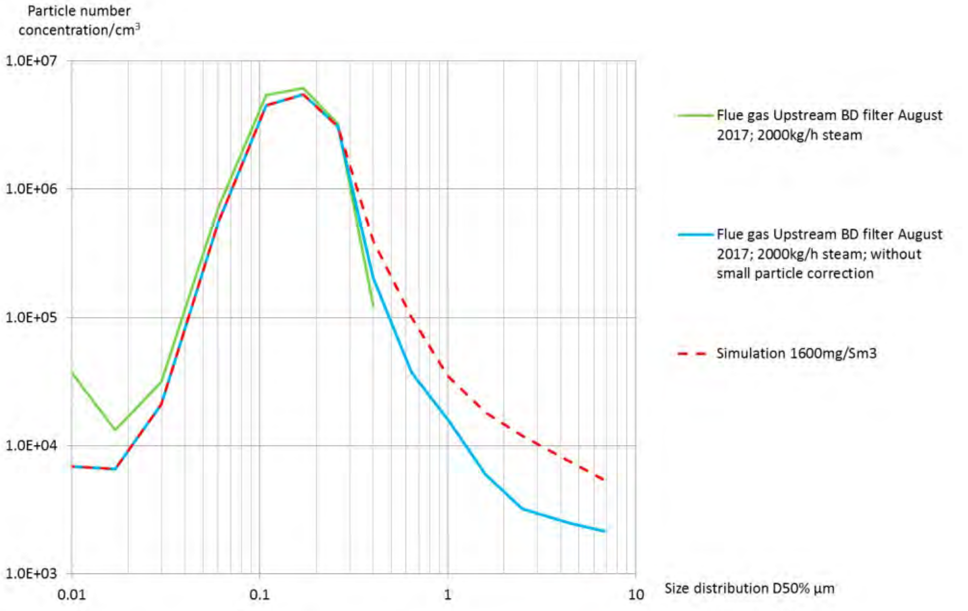

Figure 7. Summary of the measurements of the size distribution upstream the Brownian diffusion candles.

8.2. Particle number concentration of the RFCC flue gas after filtration

As summarized in tables 6, 7 and 8 in order to confirm the filter efficiency, the same test procedure for the ELPI$^+$ measurements as in December 2016 was repeated in August 2017. The bypass of the filter and the impact to the aerosol concentration are also evaluated.

Table 6. ELPI$^+$ measurements in August 2017 with DB filter bypass in operation. The lower particle number at 100 % opening of the bypass is likely caused by the position of the disk of the butterfly valve and a higher pressure drop.

Sample Location	Flue gas flow (Sm^3/h)	Filter Bypass Valve opening (%)	Downstream BD filter (Particles/cm^3)
Unfiltered RFCC flue gas	35,000		1.48 x 10^7 to 1.57 x 10^7
Filtered RFCC flue gas, downstream Brownian filter	35,000	0	6.2 x 10^5
	40,000	0	6.65 x 10^5 to 6.82 x 10^5
	44,000	0	6.84 x 10^5
	48,000	0	9.25 x 10^5
Mixed flow: filtered RFCC flue gas + filter bypass	35,000	0	7.37 x 10^5
	35,000	10	9.38 x 10^5
	35,000	20	1.18 x 10^6
	35,000	30	1.49 x 10^6
	35,000	40	1.92 x 10^6
	35,000	50	2.59 x 10^6
	35,000	60	3.38 x 10^6
	35,000	70	4.24 x 10^6
	35,000	80	4.65 x 10^6
	35,000	90	4.84 x 10^6
	35,000	100	4.15 x 10^6

Table 7. Filter performance in August 2017.

Flue gas flow (Sm^3/h)	Unfiltered RFCC flue gas ($Particles/cm^3$)	Downstream BD filter ($Particles/cm^3$)	Efficiency (%)
35,000	1.5×10^7	6.15×10^5	95.9
40,000	1.5×10^7	6.7×10^5	95.5
44,000	1.5×10^7	6.8×10^5	95.5
48,000	1.5×10^7	9.2×10^5	93.9

Table 8. Comparison of the filter performance to previously measured efficiencies.

Test	Flue gas flow (Sm^3/h)	Efficiency (%)
Pilot 2015	1,000	98.5
New candles 2016	35,000	98.9
Candles August 2017	35,000	95.9

Comments to the efficiency results:

- The stability of the $ELPI^+$ measurements at the BD filter inlet is challenging and variable.
- The inlet concentration is not checked simultaneously with the outlet concentration. The number of particles of the unfiltered RFCC flue gas is assumed based on previous measurements.
- The mass of particles at the filter inlet is highly variable with the steam injection and the number of particles is variable with the refinery operation. Any effect of the steam injection has not been studied.

A lower efficiency after a period of operation with RFCC flue gas is experienced and may be caused by:

- Higher water load to the candles (steam injection and variable efficiency of the demister)
- Progressive accumulation of sulfuric acid in the new candles. The accumulation is normally stabilized by drainage of the candles after several weeks of operation.
- Candles partially blocked by catalyst particles or non-soluble salts: the accumulation is confirmed by inspections, but does not look significant.
- An inspection performed in 2018 confirms that a leakage occurs in the upper part of the bed for some candles. Due to gas flow, operating conditions being above the maximum design rate and the filters being overloaded with liquid being carried over from the lower demister, the fiber beds have compressed. Further tests shall be performed in 2018 after repair the fiber beds.
- Further measurements and periodic inspections are necessary in order to estimate the life span of the candle fibers and confirm the efficiency.

9. Capacity of the BD filter bypass

The purpose of the BD filter bypass, see figures 1 and 4, is to control the aerosol concentration to the absorber in order to test the robustness of solvents for the limitation of emissions. As the flow to the DB filter bypass is not proportional to the valve opening, flue gas flow to the bypass is estimated. Methodology of the calculation is as follow:

- The total flow to the bypass and the filter is measured and controlled by the fan velocity
- At constant temperature and flue gas composition the gas flow rate to the filter is proportional to the pressure drop of the candles. Thus, the flow to the candles can be based on the candle pressure drop.
- The pressure drop of the candles has been verified at various flue gas flows
- The flow to the bypass is estimated based on the total flow and on the flow to the candles

Several tests are performed. The figure 8 describes the average gas flow to the bypass at various bypass valve opening.

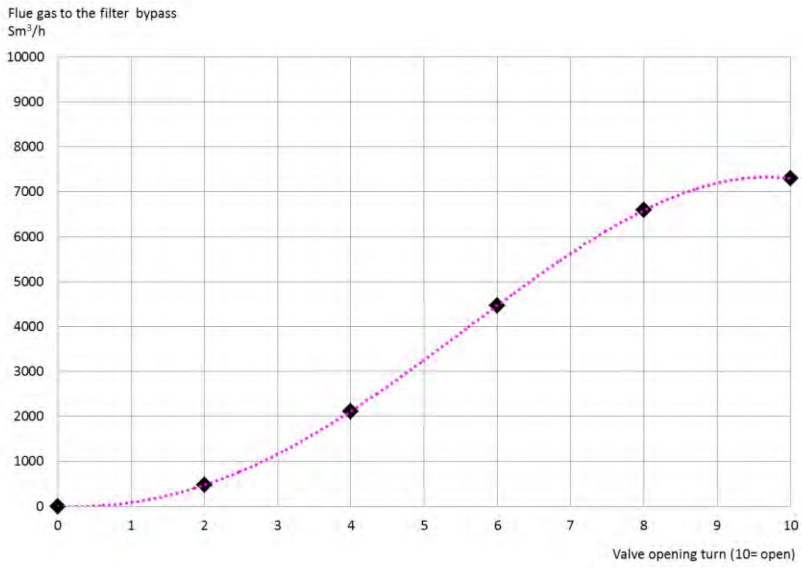

Figure 8. Flue gas flow to the bypass as a function of the butterfly valve opening. The dotted line is a polynomial trend of the test results.

As expected and confirmed by the figure 9, for aerosols under 1µm of diameter, the total particle concentration is proportional to the bypass flow. Several ELPI$^+$ measurements are performed in order to confirm the reliability of the particle concentration in the flue gas upstream the absorber as a function of the flue gas flow to the bypass.

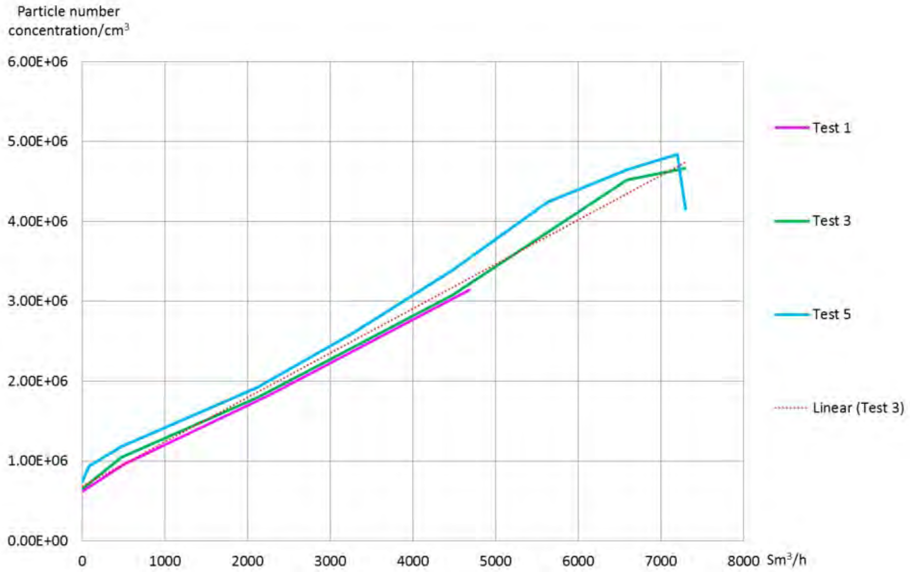

Figure 9. Flue gas flow to the bypass as a function of the particle number concentration.

Figure 10 shows a constant size distribution of the aerosols downstream the BD filter in the most of range measured by the ELPI$^+$. No particles above 0.5 µm are measured. Without small particle correction, even if the number of large particle is overestimated, the number of particles above 0.5 µm is not significant (<1000).

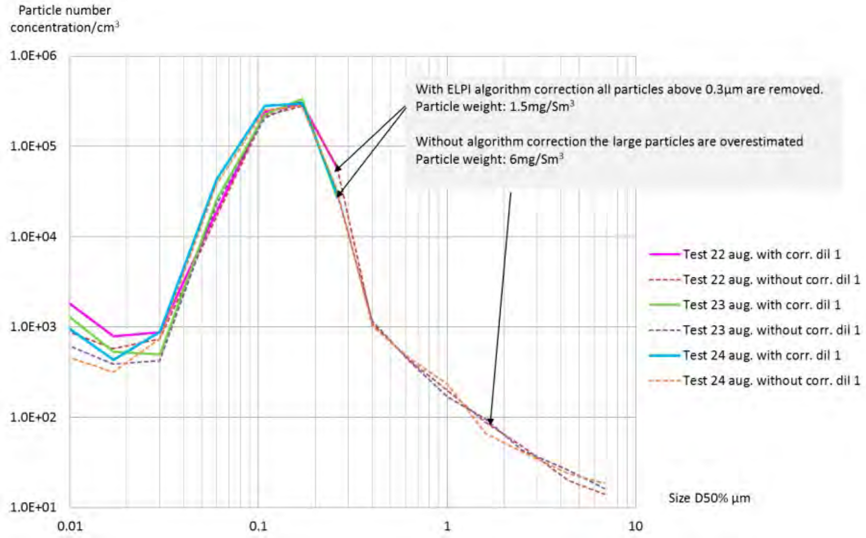

Figure 10. Particle size distribution downstream the BD filter without bypass.

As shown in figure 11, the size distribution of the RFCC flue gas downstream the BD filter and after the open bypass is similar in most of the ranges measured by the ELPI$^+$, but the particle number concentration increases with the valve opening. With small particle correction, no particles above 0.4 µm are measured. Without small particle correction, the number of particles above 0.4 µm is significant (>10,000). Consequently, the number of particles above 0.4 µm cannot be confirmed. At higher flue gas flow to the bypass, it is possible that a higher number of the larger particles are entrained to the bypass.

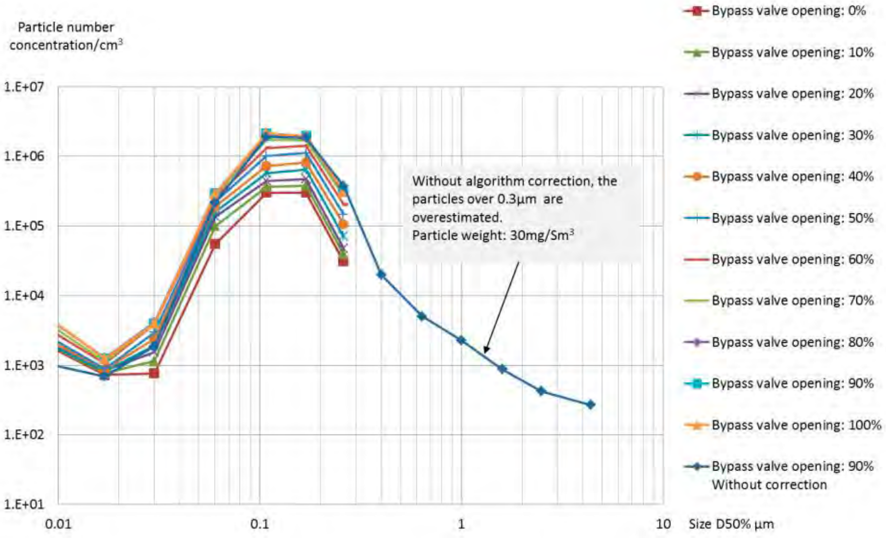

Figure 11. Particle size distribution downstream the BD filter with bypass.

10. Conclusion

The efficiency of the BD filter system installed at TCM allows the operation of the amine absorber with the RFCC flue gas without breaching the TCM amine emission permit. With the BD filter bypass, various particle concentrations may be generated and controlled in order to test the sensibility of the amine solvents to the aerosols. The test flexibility of the Technology Centre Mongstad is increased, allowing the simulation of different flue gas compositions with aerosols. During a test campaign, the efficiency of the filter is stable, even with fluctuations of the flue gas composition and the presence of components like $SO_{2.}$ Furthers tests are necessary in order to confirm the following items:

- Effect of the accumulation of catalyst particles in the BD filter
- Effect of high and variable aerosol mass to the BD filter
- Estimate the life span of the candles
- Demister efficiency

The removal of aerosols and fly ash in a flue gas is usually and preferably performed by electrostatic precipitators (ESP) and fabric filters, but the tests at TCM suggest that a BD filter may be applicable in specific full scale projects. The BD filter may be installed upstream or downstream of the absorber if the fly ash concentration is minimized upstream of the BD filter as achieved at TCM.

The $ELPI^+$ (Electrical low pressure impactor) is reliable to measure the aerosol number concentration. However, in the specific case of aerosols above 2 µm diameter composed only of water, the $ELPI^+$ is not applicable since these aerosols are unstable and easy to evaporate. An assessment of the accuracy of the correction algorithm for the fine particles used to correct the $ELPI^+$ readings may be necessary, especially for aerosols above 1 µm of diameter in a flue gas.

11. Acknowledgements

The authors gratefully acknowledge the staff at TCM DA, Gassnova, Equinor, Shell and Total for their contribution and work at the TCM DA facility. The authors also gratefully acknowledge TCM owners and the Climit Demo project AeroSolve (616125) for their financial support and contributions.

References

[1] The open-source centre at TCM. https//catchingourfuture.com/

[2] Lombardo G, Fostås BF, Shah MI, Morken AK, Hvidsten OA, Mertens J, Hamborg ES. Results from aerosol measurement in amine plant treating gas turbine and Residue Fluidized Catalytic Cracker flue gases at the CO_2 Technology Centre Mongstad. Energy Procedia. Volume 114; 2017. p. 1210-1230.

[3] Shah MI, Lombardo G, Fostås BF, Benquet C, Morken AK. CO2 capture from RFCC flue gas with 30 wt% MEA at Technology Centre Mongstad, process optimization and performance comparison. (to be presented at GHGT-14, 2018, Melbourne, Autralia)

[4] Mertens J, Lepaumier H, Desagher D, Thielens ML. Understanding Ethanolamine (MEA) and ammonia emissions from amine based post-combustion carbon capture: lessons learned from field tests. Internat. J. Greenhouse Gas Control. 2013, 13, 72-77.

[5] Mertens J, Brachert L, Desagher D, Thielens ML, Khakharia P, Goetheer E, Schaber K. $ELPI^+$ measurements of aerosol growth in an amine absorption column. Internat. J. Greenhouse Gas Control. 2014, 23, 44-50.

CO_2 capture from RFCC flue gas with 30 wt% MEA at Technology Centre Mongstad, process optimization and performance comparison

(2018)

14th International Conference on Greenhouse Gas Control Technologies, GHGT-14

21st -25th October 2018, Melbourne, Australia

CO_2 capture from RFCC flue gas with 30 wt% MEA at Technology Centre Mongstad, process optimization and performance comparison

Muhammad Ismail Shah[a]*, Gerard Lombardo[b], Berit Fostås[c], Christophe Benquet[d], Anne Kolstad Morken[a], Thomas de Cazenove[a]

[a]*Technology Centre Mongstad, 5954 Mongstad, Norway*
[b]*Gassnova SF, Dokkvegen 10, 3920 Porsgrunn, Norway*
[c]*Equinor ASA, PO Box 8500, 4035 Stavanger, Norway*
[d]*Total E&P Norge, Finnestadveien 44, Dusavik,* 4029 Stavanger, Norway

Abstract

Aerosol based amine emission from post combustion carbon capture process is very challenging in terms of accurate online measurement, compliance to emission permit and operating cost due to high solvent makeup. At Technology Centre Mongstad (TCM), an advanced process configuration is developed and tested to control and reduce amine emissions in parallel to accurately measure MEA emissions by online FTIR. The advanced configuration consists of a Brownian diffusion filter upstream the absorber, RFCC water wash, special design and operation of online sampling system and a fractional cold rich amine bypass to the stripper. With the flue gas from the Residue fluidized catalytic cracker (RFCC), promising results are achieved by applying the advanced process configuration. MEA emissions are reduced to about 2 ppm and specific reboiler duty of 3.5 GJ/ton CO_2 is demonstrated with a capture rate of about 90%.

Keywords: CO_2 capture, Aerosol, Amine emissions, Advanced process configuration for amine plant, Online monitoring of amine emission,FTIR

1. Introduction

The Technology Centre Mongstad (TCM) is the world's leading facility for verifying and improving CO_2 capture technologies. TCM is located at Mongstad, one of Norway´s most complex industrial facilities. TCM has been operating since autumn 2012, providing an arena for qualification of CO_2 capture technologies on an industrial scale. In autumn 2017, Gassnova (on behalf of the Norwegian state), Equinor (formerly Statoil), Shell and Total entered into a new ownership agreement securing operations at TCM until 2020. The owners of TCM started their most

---

* Corresponding author. Tel.: +47 40 00 59 08.
E-mail address: postmottak@gassnova.no

recent monoethanolamine (MEA) test campaign in June 2017 where a large number of public, industrial, research and academic stakeholders were involved [1]. The campaign included demonstration of a model-based control system, dynamic operation of the amine plant, investigating amine aerosol emissions and specific tests targeted at reducing the specific cost of CO_2 capture. Through the testing, both flue gas sources currently available at TCM were used. These sources are the combined cycle gas turbine (CCGT) based heat and power plant (CHP) and the residue fluidized catalytic cracker (RFCC). They provide flue gases with a wide range of properties and CO_2 content from 3.6 to 14 vol%. TCM is located next to the Equinor refinery in Mongstad. The Mongstad refinery is the source of both flue gases supplied to TCM.

Until 2017, TCM had not been able to operate the amine plant with RFCC flue gas due to very high amine emissions (> 20 ppmv) caused by sulfuric acid aerosol and dust particles present in the flue gas [2]. By installation of a Brownian diffusion (BD) filter upstream the absorber, more than 95% of the aerosol were removed and together with optimization of plant process parameters and configuration, the amine emissions were reduced to levels well below TCM's emission permit (< 6 ppmv for amines.) this allowed for long term testing with RFCC flue gas in the amine plant.

TCM participated in the Climit Demo project AeroSolve (616125) that was led by SINTEF with NTNU, Uniper, Engie, TNO and the Road project as partners. The project aimed to close knowledge gaps related to aerosol emissions from CO_2 capture plants whereas a part of the project TCM conducted a 3 months test campaign treating the RFCC flue gas with MEA under "work package 4" of the project (Testing at industrial demo scale). Based on the learnings gained through this campaign, TCM optimized and modified process configurations and online emission sampling system followed by further testing with the RFCC flue gas and MEA under MEA-4 campaign during Q2-2018. The conventional amine process configuration was modified to an advanced amine process configuration which is able to efficiently capture CO_2 from flue gases containing aerosol, and the sampling system was modified to accurately and reliably measure amine aerosol. Description of the sampling system, optimal TCM amine plant process configuration to minimize aerosol emissions and specific reboiler duty as main results from testing, is presented in the current paper.

Nomenclature

CCGT	Combined cycle gas turbine
CHP	Combined heat and power
RFCC	Residue fluidized catalytic cracker
ppmv	parts per million by volume
UoM	Unit of measure
w	wet basis
Conc.	Concentration
MEA X	TCM owner's MEA campaign, where X=1,2,3,4
WP4	Work package 4
Sm^3/h	Standard cubic meter per hour at 101.325 kPa and 15°C
VOC	Volatile organic components
Meth X	Method where X=1, 2, 3
mill	million
Vol%	Volume percent
LVC	Lean Vapour Compressor
wt%	weight percent

2. TCM's experience with Aerosol based emissions and its control

TCM is regulated under emission permit from the Norwegian environmental authority (Miljødirektoratet). The emission permit regulates amine plant's emissions to air of ammonia (NH_3), Amines (primary, secondary and tertiary) and aldehydes. Table 1 given below shows the allowable emission limits applicable to the amine plant.

Table 1. TCM Amine plant applicable emission permit

Emission component	Emission source	Emission limits	
		Daily average concentration limit	Yearly limit(kg/year)
Ammonia (NH_3)	Amine plant	100 ppmv	6,000
Total Amines	Amine plant	6 ppmv*	2,800
Total Aldehydes	Amine plant		1 g/s

* Maximum hourly averaged emission 15 ppmv

Under normal operation conditions the amine plant capturing CO_2 with 30 wt% MEA from CCGT flue gas has amine emissions to air below 1 ppmv and ammonia emissions about 10-20 ppmv [3] . TCM tested capturing CO_2 with 30 wt% MEA for the first time, from the RFCC flue gas in spring 2013. It was soon found that emissions were very high and shortly further testing with RFCC and MEA were abandoned to avoid violation of the emission permit and to find ways to mitigate high amine emission to air.

To understand and control high amine emissions further tests with CCGT flue gas with recycled CO_2 and controlled addition of RFCC flue gas supported by several manual isokinetic sampling of the depleted flue gas were conducted in autumn 2015 [11]. After through testing, control and repeatability of high amine emission tests, it was concluded that high amine emission is caused by sulfuric acid aerosol in the RFCC flue gas together with process conditions which causes high amine emission in the form of aerosol. From tests in autumn 2015, the need for RFCC flue gas aerosol removal, upgrade of the absorber water wash system and online flue gas sampling systems was deemed necessary to be able to run with RFCC flue gas and 30 wt% MEA in compliance to the applicable emission permit.

During late 2016 a high efficiency Brownian diffusion (BD) filter with flue gas capacity of 35,000 Sm^3/h was installed downstream the Direct Contact Cooler (DCC) and upstream the absorber, followed by upgrade of the water wash systems to increase its cooling capacity to 12 MW (thermal), where 6 MW (thermal) on the lower water wash and 6 MW on the upper water wash system. The later upgrade allows keeping the plant in water balance and allows for flexible operation in terms of lean amine temperature, and selection of the ratio of cooling needed in the water washes.

During period summer-autumn 2017, the amine plant with the new installations was tested with 30 wt% MEA under the AeroSolve project. TCM amine plant's ability to run with RFCC flue gas, 30 wt% MEA and compliance with the emission permit was demonstrated thoroughly and continuously supported by manual isokinetic sampling. During this period it was observed that the online flue gas analysis system was suffering stability issues due to accumulation of aerosol and degradation of amines. The online flue gas sampling system was upgraded and modified by TCM, to overcome aerosol accumulation and degradation of amines in the sampling line.

The upgraded online flue gas sampling system with advanced process configuration to reduce specific reboiler duty (SRD) was thoroughly and successfully tested during spring 2018 with 30 wt% MEA and RFCC flue gas.

2.1 TCM's Amine plant

The amine plant is a generic and highly flexible CO_2 capture plant designed and constructed by Aker Solutions and Kværner. The amine plant can either capture CO_2 from CCGT flue gas or RFCC flue gas with a design CO_2 production capacity of 80 tonnes/day and 200 tonnes/day respectively [4]. Figure 1 given below shows a simplified process flow diagram with online meters and instrumentation.

Flue gas from the blower is conditioned and saturated with water to the required temperature (normally 20-50°C) in the DCC. The CHP DCC system cools the flue gas from about 195°C down to the required temperature while the RFCC DCC saturates the flue gas from 20°C up to 50°C by injecting live steam into the DCC as the RFCC flue gas leaving the upstream (refinery side) flue gas desulfurization unit (FGD) is at around 20°C. Conditioned and water saturated RFCC flue gas enters the high efficiency BD filter where most part of aerosol and catalyst particles from the flue gas are removed. Filtered RFCC flue gas enters the rectangular absorber, where flue gas flows counter currently to lean amine solvent. The lean amine solvent can be fed either at 12m, 18m or 24m to the absorber structured packed bed. In the conventional configuration CO_2 depleted flue gas enters the lower water wash followed by upper water wash to reduce VOC, NH_3 and some amine emission to the air and condition the flue gas to the required humidity and thus keeps the plant in good water balance.

Rich amine from the absorber is pumped through the rich/lean cross plate heat exchanger to the top of either RFCC or CHP stripper depending on the flue gas source and CO_2 amount to be produced. The RFCC stripper is a structured packed bed column equipped with water wash and shell and tube type natural thermosiphon reboiler which utilizes low pressure steam to regenerate rich solvent, CHP stripper is described elsewhere [4]. Stripped CO_2 is cooled to about 20°C in the overhead condenser utilizing sea water. Condensate from cooled CO_2 product is separated in the reflux drum and pumped back into the stripper top, while CO_2 product is vented to the ambient via CO_2 stack. The RFCC stripper is also equipped with a Lean vapor compressor (LVC) system, which can be lined-up with the RFCC stripper if required. In the LVC system, hot lean amine which is at bobble point is throttled to a lower pressure and fed to the flash drum generating steam. In the flash drum steam and lean amine solvent are separated. Steam from the flash drum is compressed to stripper bottom pressure in a compressor by the expense of electrical energy. The superheated steam from compressor is fed to the stripper which provides extra energy to regenerate rich amine and reduces consumption of low pressure steam. Lean amine solvent from the flash drum is pumped back to the absorber through rich/lean cross plate heat exchanger followed by lean amine cooler. The lean amine is cooled to the required feed temperature in the lean amine cooler.

The amine plant is heavily instrumented with dedicated online analyzers and flow meters. Details of the online analyzer and meters are given in Figure 1.

2.2 *RFCC flue gas composition and its challenges for CO_2 capture amine based process*

RFCC flue gas contains high concentration of CO_2, with about 14.7 vol% of CO_2 (wet basis), 3.2 vol% of O_2, 77 vol% N_2 and saturated with water. This makes the RFCC flue gas equivalent to flue gas from coal power plant. Further details of the RFCC flue gas are given in Table 2 below. The concentration of trace elements in the RFCC flue gas fluctuates during normal operation.

Table 2. Typical RFCC flue gas composition upstream and downstream the BD filter

RFCC flue gas composition:		Inlet BD Filter	Inlet of Absorber
N_2	mol%	77.0	77.0
Ar	mol%	0.9	0.9
O_2	mol%	3.2	3.2
CO_2	mol%	14.7	14.7
H_2O	mol%	4.2	4.2
SO_2	ppmv	5	5
NOx	ppmv	100	100
NO_2	ppmv	2.5	2.5
NH_3	ppmv	0.2	0.2
CO	ppmv	10	10
Total Particulates	mg/Sm^3	15-40	<0.5
H_2SO_4 Aerosol	mg/Sm^3	10-25	<0.5
Salts	mg/Sm^3	5-15	<0.5
Non-water soluble (SiO_2,$CaCO_3$,metals)	mg/Sm^3	0-2	<0.1
Particle number concentration	aerosol/cm^3	21* million	300,000 to 500,000**

*Aerosol conc. upstream the BD filter may vary from 15 million to 25 million. ** conc. downstream the BD filter varies between 300,000-800, 000 aerosol/cm^3.

RFCC flue gas contains catalyst fines in the range of a micron to submicron sizes which are different in composition and nature to fly ash contained in coal power plant flue gas. If coal power plant flue gas is filtered for example with a bag house filter to reduce mercury, it will result in very clean flue gas comparable to RFCC flue gas downstream the BD filter. H_2SO_4 aerosol shown on mass basis in table 2 is equivalent to about 21 million aerosol/cm^3 most of them are of submicron size.

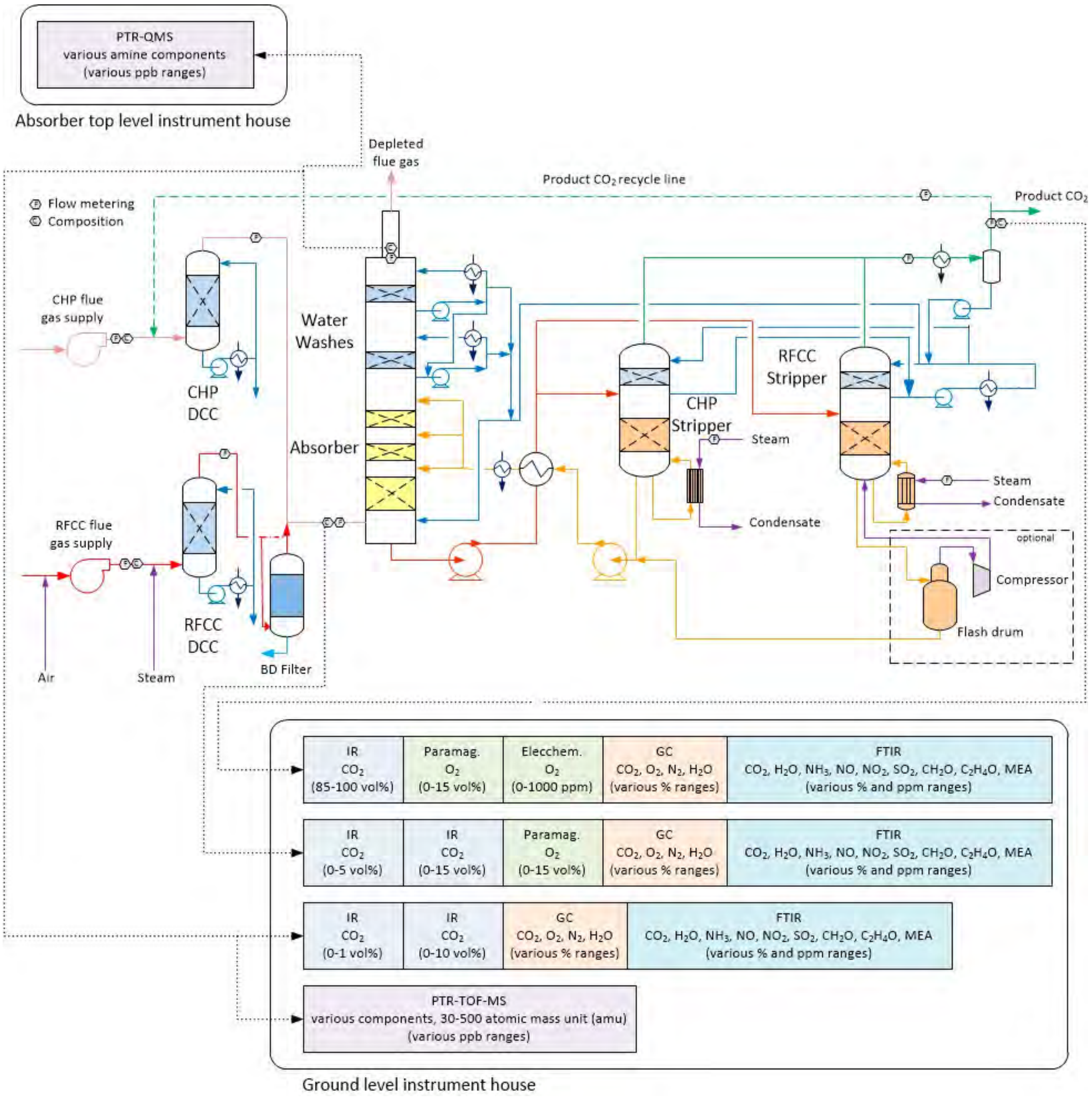

Figure 1. TCM Amine plant with two flue gas sources, CHP and RFCC with corresponding strippers, flue gas analyzers and meters.

BD filter reduces aerosol in the RFCC flue gas from around 21 million aerosol/cm^3 to around 500,000 aerosol/cm^3. Further details on performance of BD filter can be found elsewhere [2]. A bypass over the BD filter allows higher aerosol concentrations to the absorber in order to study its effects on emissions. The sensibility of advance amines may be compared to MEA at various aerosol concentrations and operational parameters. Submicron aerosol larger than 0.1 µm grow in the absorber in the presence of supersaturated water vapor due to exothermic reaction of CO_2 and MEA. The submicron aerosol absorb MEA from the flue gas in the region close to the lean amine inlet and absorber bulge zone, MEA has the highest partial pressure in this region of the absorber. Submicron aerosol from the absorption section will follow the depleted flue gas and will not be removed efficiently by conventional mesh pads or water wash packing bed(s). MEA emission in the form of aerosol can be reduced by reducing the number of aerosol nuclei in the feed flue gas to the absorber and by avoiding/reducing supersaturation in the absorber. At TCM the former is achieved by filtering the flue gas via the BD filter. The latter is achieved by operating the amine plant in such a way to minimize supersaturation in the absorber and water wash sections which allows for maximum MEA removal from the gas phase before the depleted flue gas enters the upper water wash.

Depleted RFCC flue gas containing MEA aerosol poses a great challenge to the online emission monitoring (FTIR, PTR-QMS, PTR-TOF-MS) system installed at TCM as MEA aerosol accumulate in the sampling system (filters, pumps, lines etc.) which makes online analysis erratic.

The existing sampling system for online emission monitoring in the TCM amine plant, which has been verified for gas phase emissions [5], is not suitable when aerosol are present in the sample flue gas. The problem was particularly experienced at higher MEA emissions (> 4-6 ppmv). With emissions around 2 ppmv MEA, the weight of the aerosol is in the range 30-50 mg/Sm^3, while at 6 ppmv MEA, the weight of the aerosol may be up to 100 mg/Sm^3 due to the increased diameter. The aerosol, which mainly consist of water, accumulate in the sampling system despite that sampling line has filters and is heat traced. The sampling system was designed for homogenous gas phase emissions and it has been proven to function very well when there are no aerosol present. In previous campaigns with CHP flue gas there has been good agreement between online measurements and manual isokinetic sampling and laboratory analysis [5].

In contrast aerosol carrying amines in the depleted RFCC flue gas accumulated in the sample line and associated filters, pump, and fittings resulting in erratic analysis and unreliable behavior. Upon occurrence of such problems, the sampling system was flushed several times but helped only for a short time. To ensure reliable measurements, proper design of online sampling system is required to avoid condensation, degradation and accumulation of aerosol and flue gas components. TCM's online flue gas sampling was therefore modified to be able to efficiently evaporate aerosol, avoid accumulation, degradation and reliably and to accurately measure emissions. µm

2.3 Modified online flue gas sampling system

During tests with RFCC flue gas and 30 wt% MEA regular manual isokinetic sampling were collected and analyzed to make sure that the online emission monitoring system is working properly. The data was also used to properly design a robust online emission monitoring system. Several modifications to the online emission monitoring system were made during the period (2017-2018). This resulted in a robust and reliable emission monitoring system capable of accurately analyzing flue gas even in the presence of aerosol.

The modified online flue gas sampling system as shown in Figure 2, consists of an electric heat traced sampling probe equipped with 6 mm nozzle pointing at 90° to the horizontal plane and placed at 250 mm from the absorber stack's inner wall. The sampling probe is flushed with cold instrument air if needed. The temperature of the heat tracing elements of the probe can be controlled from 40 to 200°C. Flue gas sample via the probe leads to evaporator, the evaporator is a 316ss double pipe type of electric heater, where the flue gas sample travels in the annulus. The flue gas sample in the annulus of the evaporator is heated by 622 W heating elements installed on the outside of shell and the heating elements inside the inner rod located in the center of the evaporator. The rod runs along the length of the evaporator. The annulus of the evaporator is 12.5 mm wide and 670 mm long. A suction pump sucks 1 m^3/h of flue gas sample through the probe resulting in a flue gas sample velocity similar to the velocity in stack, which makes it isokinetic. The flue gas has a residence time of ~4 seconds in the evaporator. Flue gas sample from the pump is filtered with several filters ranging in sizes from 0.1 µm to 10 µm located in the filter house.

The filtered flue gas sample delivers a feed of 0.4 m^3/h to the online FTIR over a flowmeter while rest of the sample is routed back to the absorber. The FTIR analyzer is located in the analysis house close to the bottom of the absorber. A sampling line of 110 m length in sulfonated and polished stainless steel which is heat traced and insulated carries the flue gas sample to the FTIR analyzer. This arrangement avoids accumulation of aerosol and condensable components on the surfaces. To avoid chemical degradation of the sample the flue gas sample is not overheated and kept close to 80°C.

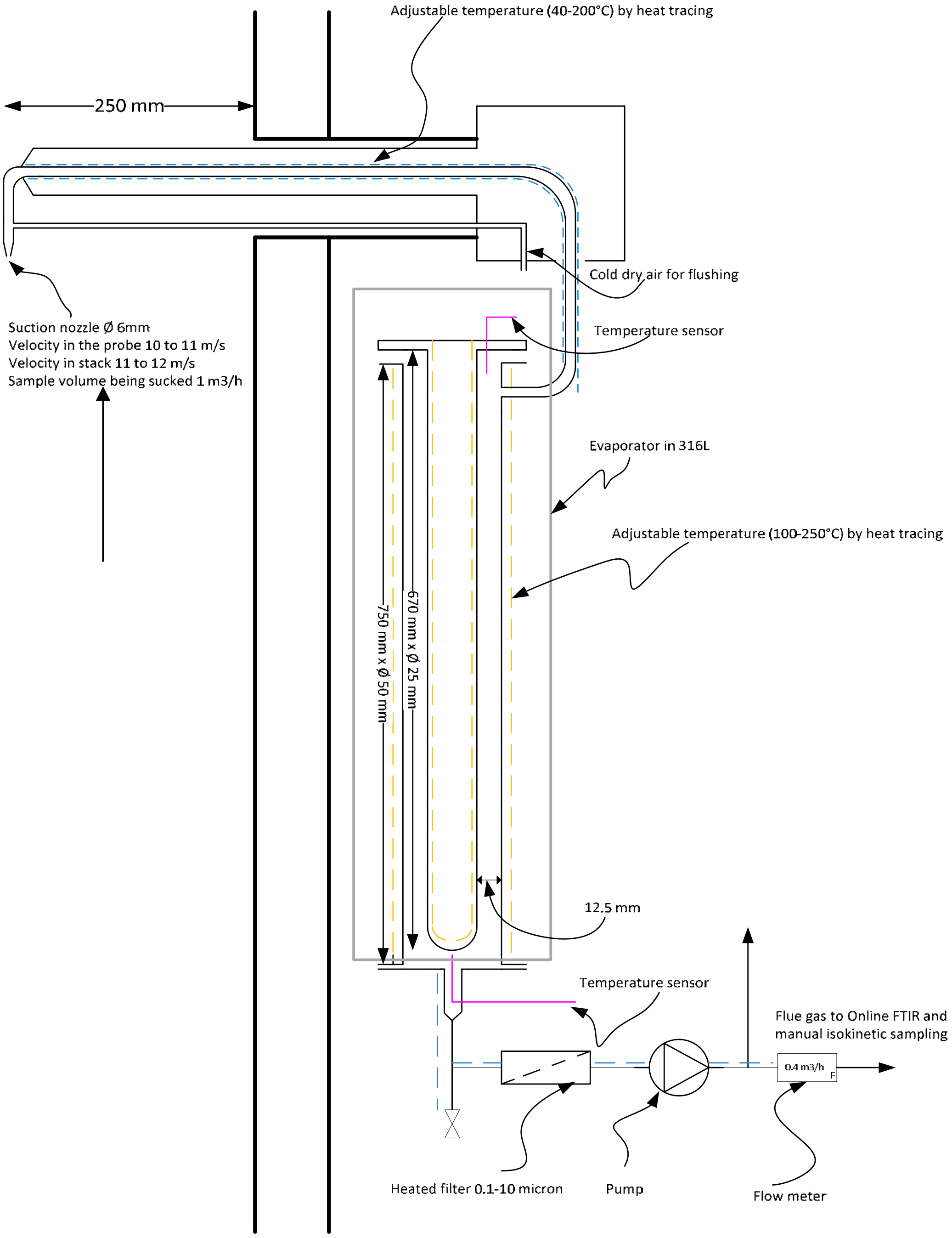

Figure 2. Sketch of TCM modified online flue gas sampling system able to accurately analyze flue gas containing aerosol.

2.4 Isokinetic sampling sketch and description

To verify online sampling system, manual isokinetic sampling of the absorber depleted flue gas for quantification of the concentration of emitted chemical components, were planned to be taken several times on weekly basis and more frequent in demanding periods during testing with RFCC flue gas.

In 2016, TCM further developed the existing method for isokinetic sampling to enable capturing very fine liquid droplets and aerosol. Up to then, the amine plant had mainly been used for capturing CO_2 from the CCGT flue gas with very low to almost negligible concentration of SO_2 and no aerosol. The development resulted in a modified manual sampling method for amine emission in presence of aerosol. Figure 3 illustrates a sketch of the modified manual isokinetic sampling method. The sampling train consists of a cold probe, a condenser, a dry impinger with jet inlet design, distribution manifold and 0.05 M H_2SO_4 impinger train. The method has been further optimized since 2016, and the mist trap now consists of only one bottle with jet inlet and no glass wool. The jet-formed inlet of the bottle accelerates the gas containing particles/aerosol/droplets and over a fixed distance lets the particles impinge against a flat glass surface at higher velocity. During this operation droplets gets broken and agglomerated to bigger droplets which are less prone to further re-entrainment.

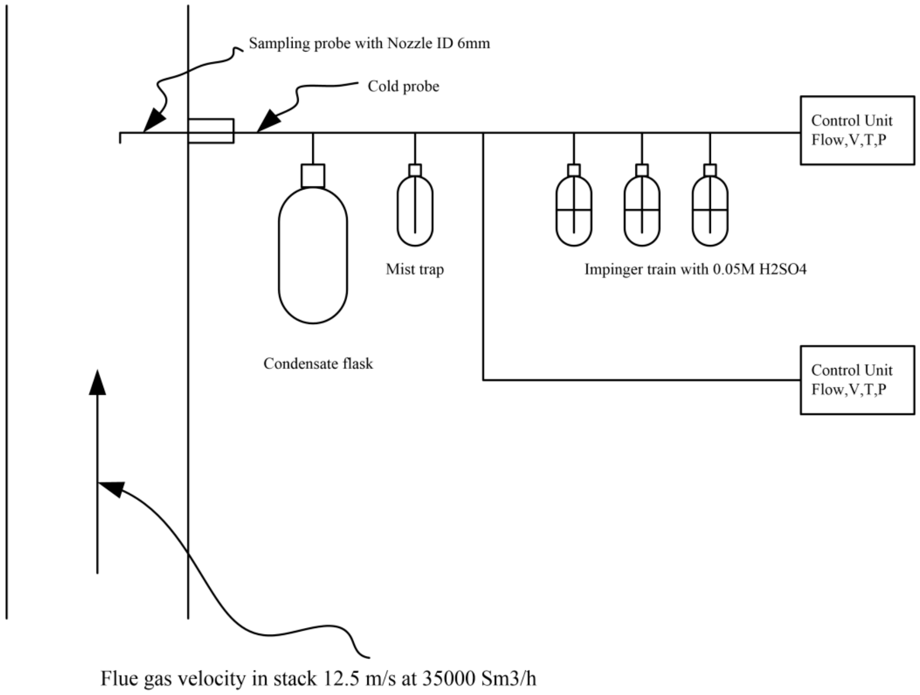

Figure 3. Modified manual sampling train configurations at TCM for collection of mist and flue gas sample. This method has been further optimized and the mist trap now consists of only one bottle with jet inlet and no glass wool.

2.5 Comparison of manual isokinetic and online emission results

While running with RFCC flue gas the TCM online emission monitoring system was suffering from severe aerosol accumulation resulting in erratic emission numbers. Erratic functioning of the online emission monitoring system was monitored by comparing water concentration in the depleted flue gas reported by FTIR to calculated water concentration from steam table based on the actual temperature and pressure of the depleted flue gas. Fluctuations or discrepancies between the measured water concentration and calculated concentration reveal problems with online emissions monitoring system. Figure 4a shows such an example.

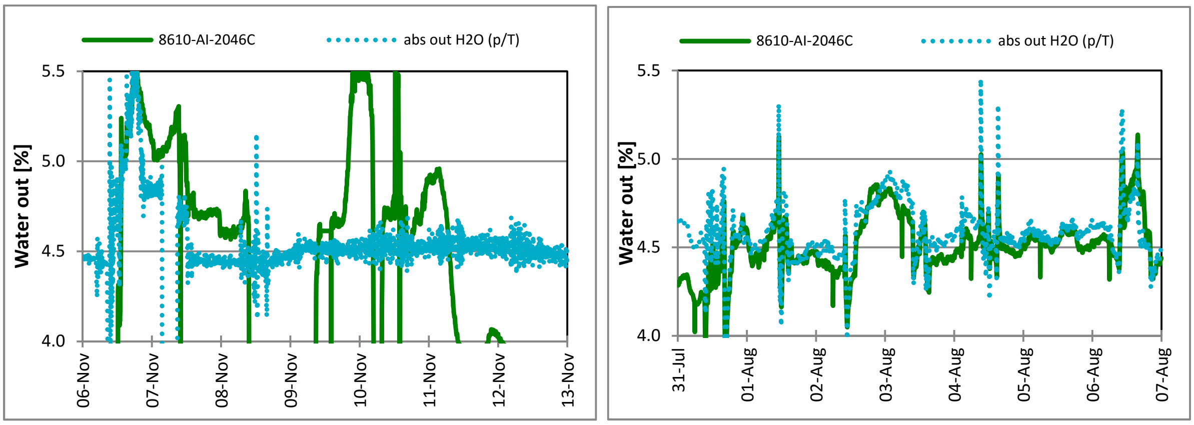

Figure 4a (left) Water measured by online FTIR (Green solid line) showing fluctuations and discrepancy problems with the sampling system. water concentration from FTIR does not match with calculated water concentration (dotted line in light blue) in the depleted flue gas. All process parameters were kept unchanged during this period. Figure 4b (right), shows good agreement between water concentration both from the FTIR and calculated.

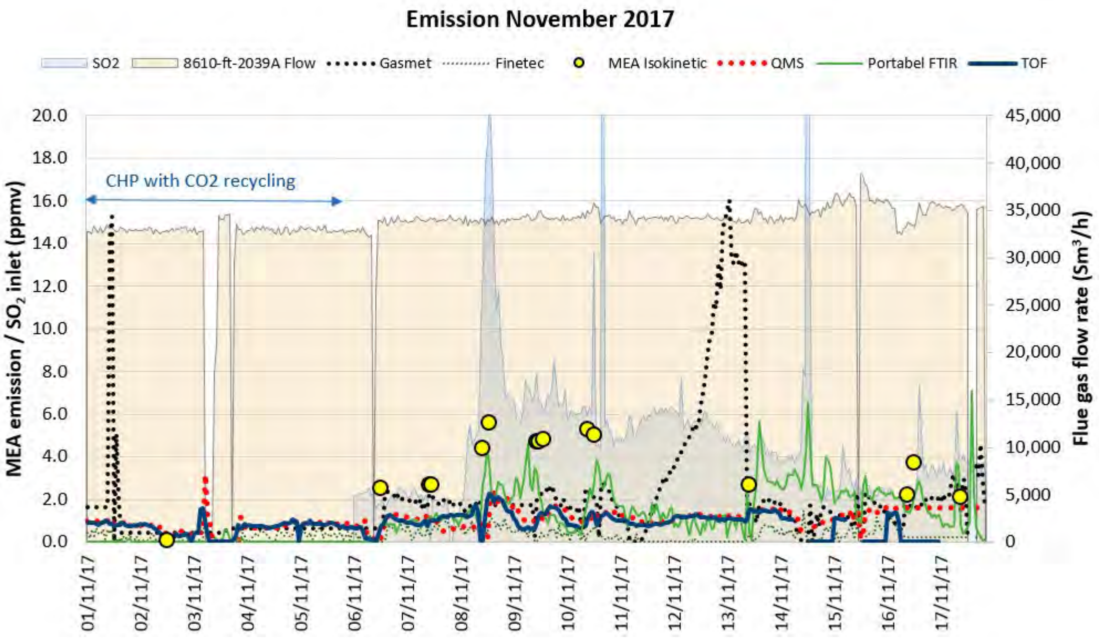

Figure 5 Comparison of isokinetic sampling results to the non-modified online sampling system.

Figure 5 shows comparison of FTIR (Gasmet) and isokinetic results from November 2017, before modification of the sampling system. FTIR mentioned in this paper is FTIR (Gasmet) and will be denoted by FTIR for reference. In Figure 5, on left side, FTIR results compared to manual isokinetic show good agreement during this period the plant was running with CHP flue gas with CO_2 recycle having similar CO_2 conc. as RFCC flue gas but free of aerosol and has less SO_2. From 6th of November the flue gas source is switched to RFCC. During the first couple of days differences in results from FTIR and Isokinetic is not very pronounced. From the 8th of November the difference in results from isokinetic and FTIR begins to increase this can also be noticed from Figure 4a showing mismatch between the water conc. measured by FTIR and calculated. This instance reveals accumulation of aerosol in the sampling system and perhaps enhanced by non-representative sample due to the fact that the probe for FTIR was installed at location S6 as shown in Figure 11. S6 is located in the concrete absorber wall where the probe may not have received a representative sample due to its non-optimal design. This was verified by manual sampling at S6 which does not match manual isokinetic results at S14 (shown in Figure 11). From 11th of November the deviation in results from FTIR to isokinetic gets very large, the behavior renders the online system inadequate for flue gas containing aerosol. Therefore, it was deemed necessary to modify the existing online sampling system to be able to analyze accurately and reliably in the presence of aerosol in the flue gas.

The objective of the TCM modified online sampling system is to be able to measure total amine emission in the depleted flue gas both in the form of aerosol and gas phase, and to increase the online systems availability and reliability with challenging flue gases.

Figure 6 shows comparison of results from the modified online sampling system with FTIR installed at S14 and manual isokinetic samples. All process parameter (i.e.) flue gas flow rate, CO_2 concentration in the inlet flue gas, lean amine temperature, water wash(s) process parameters, CO_2 capture rate, and lean amine flow rate were kept unchanged while performing manual isokinetic sampling and collecting data from the online FTIR.

It is obvious from Figure 6 that isokinetic and online FTIR results from the modified sampling system are in good agreement and is not suffering from aerosol accumulation and degradation. The modified system is tested thoroughly for more than two months with RFCC without any problems of aerosol accumulation.

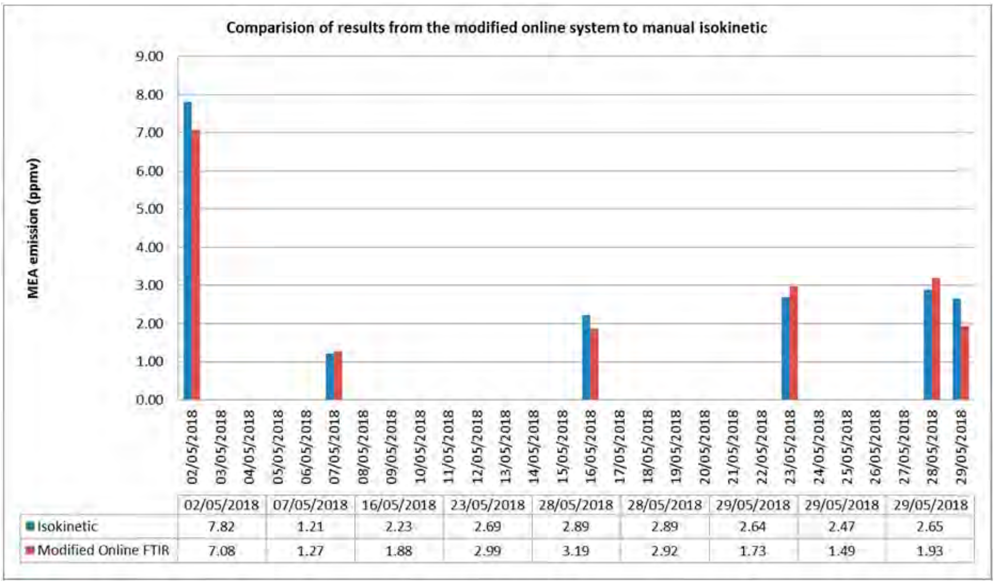

	02/05/2018	07/05/2018	16/05/2018	23/05/2018	28/05/2018	28/05/2018	29/05/2018	29/05/2018	29/05/2018
■ Isokinetic	7.82	1.21	2.23	2.69	2.89	2.89	2.64	2.47	2.65
■ Modified Online FTIR	7.08	1.27	1.88	2.99	3.19	2.92	1.73	1.49	1.93

Figure 6. Comparison of results from the modified online sampling system with FTIR and isokinetic.

3. Process optimization for energy consumption and low emission

During the AeroSolve Climit project (August-November 2017), testing with RFCC flue gas and 30 wt% MEA was conducted to find optimal process conditions resulting in low emissions and optimum SRD. Some of the tests conducted during AeroSolve project were revised and further optimized with the modified online sampling system in operation during spring 2018 under TCM owner's MEA-4 test program. During all these tests caustic soda solution was injected in the RFCC DCC to reduce SO_2 in the flue gas entering the absorber.

Some of the process parameters and plant configuration which were optimized in the AeroSolve project are:

- Lean amine temperature

- Lean amine loading for minimum Specific reboiler duty (SRD)
- Process plant configuration to result in minimum emissions

As a result, an advanced process plant configuration together with the mentioned modified online sampling system was developed which results in lower SRD and low emissions. Details of the optimized process parameters are given below.

3.1. Lean amine temperature optimization

CO_2 absorption in chemical solvents like MEA, MDEA or MEA+AMP etc. is an exothermic process resulting in temperature increase of the absorbing solvent and flue gas in mutual contact. The temperature increase is largest in the absorber bulge zone as shown by the temperature profile of the TCM amine absorber in Figure 7. Due to heat generation and temperature increase in the absorber bulge zone water is evaporated from the bulk of the solvent to the gas phase and thus saturates the flue gas at a given temperature, pressure and composition. The saturation of gas phase with water can be further increased to supersaturation, S as given by equation (1), by creation of aerosol (including both homogenous and heterogeneous aerosol) due to rapid quenching with cold lean amine and in presence of large amount of submicron foreign nuclei. Aerosol formation and its growth in gas-liquid contactors such as absorbers and scrubbers has been extensively studied for quenching of acid gases [6], [7], [8].

$$S = \frac{Total\ partial\ pressure\ of\ condensable\ components}{Equilibrium\ partial\ pressure\ of\ condensable\ components} \quad (1)$$

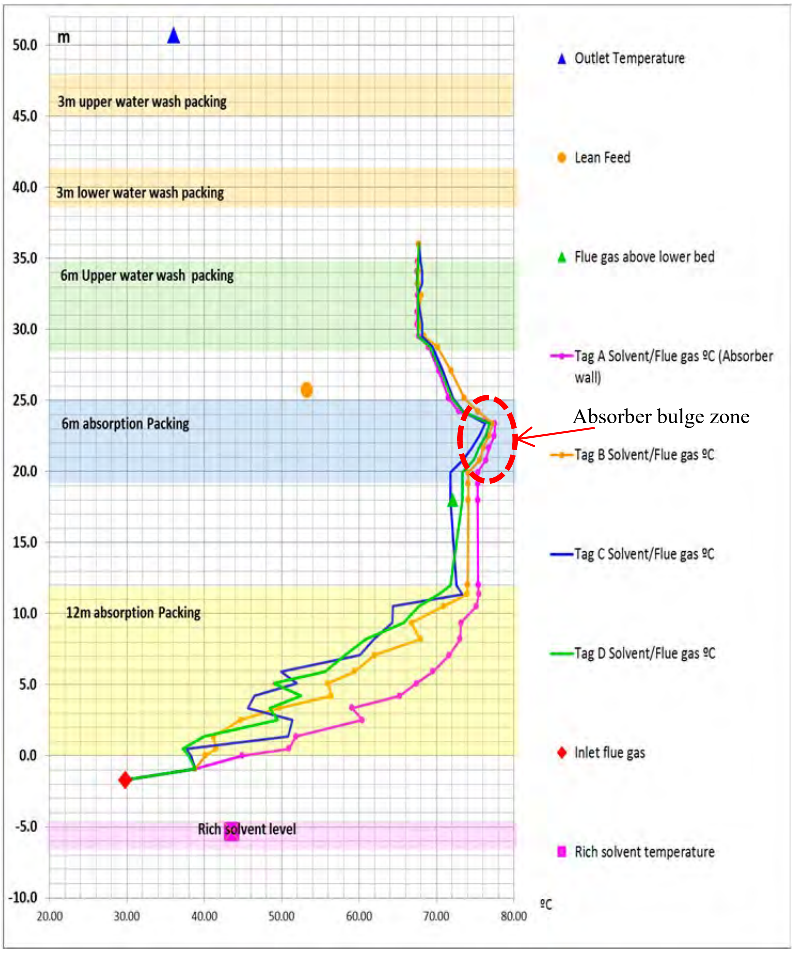

Figure 7. Absorber temperature profile, running with RFCC flue gas. CO_2 capture of 85%.

For homogenous supersaturation a higher degree of saturation is required S>2 [9], depending on temperature and composition. For heterogeneous aerosol formation, the degree of supersaturation required could be as low as close to S~1 due to presence of large number of nuclei available in the gas phase. The aerosol formed in the absorber bulge zone will follow the flue gas stream to the downstream water wash system(s). The aerosol may grow further due to condensation, coalescence and process parameters which favor rapid quenching.

Lean amine entering the absorber is typically around 35-40°C where the highest bulge temperature in the absorber is around 50-55°C for CCGT type of flue gas at 85% CO_2 capture [5], while for RFCC or coal flue gas having around 14% CO_2 the bulge temperature is around 75-78°C for 85% CO_2 capture with 30 wt% MEA. The environment for creation and growth of aerosol due to supersaturation will be favorable if the temperature difference between the lean amine and absorber bulge (ΔT_{bl}) is large.

$$\Delta T_{bl} = \text{Bulge temperature} - \text{Lean amine inlet temperature} \qquad (2)$$

Therefore, keeping small difference between the lean amine temperature and bulge temperature will help reducing aerosol formation and hence reduce amine aerosol emissions. On the other hand running CO_2 capture plants with high lean amine temperature to reduce the ΔT_{bl} may lead to increased SRD due to the fact that less energy from hot lean amine is recovered in the rich lean cross heat exchanger. As a result more energy is lost to cooling water in the water wash system. To reduce the energy loss in a conventional amine plant configuration, ΔT_{bl} needs to be kept largest possible to allow for optimal SRD and acceptable amine emission in compliance to the applicable emission permit.

Several tests were conducted during the testing at TCM within the AeroSolve project to optimize the lean amine temperature in terms of reducing emissions. Figure 8 shows MEA emission as function of ΔT_{bl}.

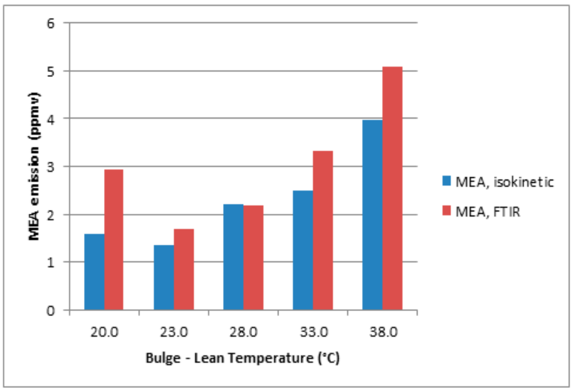

Figure 8 shows reduction in MEA emissions by reducing ΔTbl.

From Figure 8 it is obvious that MEA emissions are reduced by reducing ΔT_{bl}. This supports the theory of reducing supersaturation in the gas phase reduces MEA emissions. During tests with RFCC flue gas TCM targeted to run the plant with less than 1-2 ppm of MEA emissions. Based on the results it was decided to keep ΔT_{bl} below 25°C for tests with RFCC flue gas at 87% CO_2 capture rate which allows keeping MEA emissions below 2 ppm.

3.2. Lean amine loading for minimum Specific reboiler duty (SRD)

The plant performance was optimized for 18 m absorber packed height, with about 14% CO_2 by varying lean solvent flow rate and manipulating steam flow rate to stripper reboiler to find process conditions resulting in 87% CO_2 capture with lowest SRD. As the online sampling system during the AeroSolve project was not able to accurately and reliably measure MEA emissions resulting from tests with RFCC flue gas, it was decided to run SRD optimization tests with CHP and CO_2 recycle flue gas to avoid any breach of emission permit. CHP flue gas with

CO_2 recycle flowrate from the stripper overhead was adjusted, to achieve CO_2 concentration in the flue gas at absorber inlet similar to RFCC flue gas CO_2 concentration.

Table 3 given below summarizes range of process parameters tested during SRD optimization tests. At each solvent flow rate, the steam pressure was manipulated and hence the steam flow rate to achieve 87% CO_2 capture. At stable conditions, lean and rich solvent samples were collected for analysis of MEA and CO_2 concentration. After every 24 hours, the solvent flow rate was changed to the next set point and the procedure was repeated at each solvent flow rate.

Table 3. List of process parameters during SRD optimization tests.

Parameter	UoM	Range
Number of test cases		10
Absorber Packing height	m	18
Flue gas flow into absorber	Sm^3/h (w)	35,000
Flue gas composition:		
CO_2	mole%	13.1-13.5
H_2O	mole%	4.0 – 4.2
O_2	mole%	12.2 – 13.5
Flue gas inlet temperature	°C	29 – 30
Conc. of MEA in lean solvent (CO_2 loaded)	wt%	28-30.2
Lean solvent flow rate	kg/h	100,000 – 165,000
Lean solvent temperature	ºC	50 to 55
Liquid to Gas ratio	kg/Sm^3	2.8-4.6
Stripper bottom temperature	°C	119.5 – 122.6
CO_2 capture rate	%	86-89
Stripper pressure	barg	0.95-0.96

Figure 9 shows results for the SRD optimization tests. Capture rate during these tests was within 86-88% as denoted by red david (*) stars in the figure. For the targeted 86-89% CO_2 capture, a minimum SRD of 3.67 GJ/ton CO_2 was achieved. For optimal SRD, a lean solvent circulation rate of 120,000 kg/h with 30 wt% MEA is required while utilizing 18 m packing height of the absorber bed. Table 4 summarizes some more details for tests reported in Figure 9. More details about SRD(Meth 1) and SRD(Meth 3) as shown in figure 9. can be found elsewhere [10].

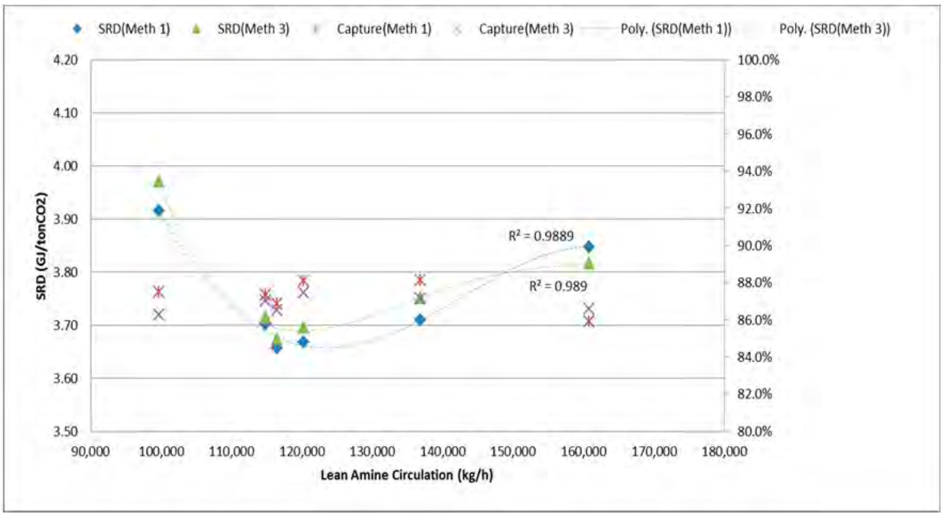

Figure 9. U-curve for SRD optimization, CHP flue gas with CO_2 recycle and 30 wt% MEA.

Table 4. List of process parameters during SRD optimization tests

Case ID	Flue gas flow rate (Sm^3/h)	Lean amine flow rate (kg/h)	Lean amine loading(mol CO_2/mol MEA)	CO_2 Capture rate (%)*	SRD (GJ/ton CO_2)*
2C-CHP-6C Recy	33,908	99,670	0.160	88.3%	3.92
2C-CHP-6A Recy	33,900	114,873	0.19	87.3%	3.70
2C-CHP-5C Recy	33,934	116,455	0.204	87.3%	3.67
2C-CHP-8A Recy	33,918	120,360	0.199	87.4%	3.67
2C-CHP-3 Recy	33,699	136,867	0.251	88.1%	3.71
2C-CHP-4 Recy	33,874	160,821	0.273	85.9%	3.85

*Tabulated Capture rate and SRD is based on Meth 1.

4. Advanced process configuration for reduction and control of amine aerosol emission

TCM developed and tested an advanced novel concept to reduce and control amine aerosol emission and improve the energy efficiency of the overall CO_2 capture process. The advanced process configuration was tested for an extended period during spring 2018 under TCM owner's MEA-4 campaign. The advanced process configuration's performance was independently verified by a third party, Electric Power Research Institute (EPRI) in May 2018. The independent verified advanced process configuration's performance with RFCC flue gas will serve as baseline for bench marking other amine based technologies. The independent verified RFCC baseline will be published later. Following modifications were made to the amine plant prior to running tests with RFCC flue gas under the MEA-4 campaign, in order to allow for accurate and reliable online emission monitoring, amine aerosol emission reduction, and improve the energy efficiency of the overall process.

- Modification of online emission monitoring system
- Modification of the 3rd absorption bed to "RFCC water wash"
- Installation of cold rich by pass line to the stripper
- Installation of Brownian diffusion (BD) filter

Brownian diffusion filter was installed in December 2016 and thoroughly tested with RFCC flue gas during 2017 and 2018. Details about performance of TCM BD filter can be found elsewhere [2]. Modification of online emissions monitoring system with FTIR is described in section 2.3 while rests of the modifications are described below.

4.1. Modification of the 3rd absorption bed to RFCC water wash

The RFCC flue gas downstream the BD filter contains around 500,000-800,000 aerosol/cm^3, most part of the aerosol are submicron (0.1-0.5 μm) [11]. In absorber the submicron aerosol grow by condensation of water and coalescence followed by absorption of MEA present in vapor phase in the bulge zone. Majority of aerosol carrying amine from the absorber bulge zone will follow the supersaturated depleted flue gas to downstream sections of the absorber (i.e) water wash(s) and demisters.

A conventionally designed amine plant treating flue gas which contains aerosol and particulates cannot remove submicron aerosol. This is due to the fact that in a conventional absorber system, the depleted flue gas from absorption section is quenched abruptly to keep the plant in water balance and recover some amines and ammonia. Abrupt quenching in the presence of nuclei generates and grows more aerosol due to heterogeneous supersaturation which results in increased emissions. Therefore, abrupt quenching of the depleted flue gas needs to be avoided when amine are present in the gas phase. At TCM a three stage water wash system is tested in order to mitigate the aerosol emissions. The system is tested with up to 2000,000 aerosol/cm^3 in the flue gas at the absorber inlet.

Abrupt quenching of the depleted flue gas containing aerosol at TCM is avoided by a special designed water wash which is termed “RFCC water wash” utilizing the pre-existing 6 m deep upper absorption bed. As suggested by its name the RFCC water wash is operated when capturing CO_2 from RFCC flue gas. The purpose of the RFCC water wash is to remove as much as possible of the amines in gas phase with hot and relatively clean water from the upper water wash [12]. Simultaneously, large aerosol above 5 µm generated above the bulge area are captured in the RFCC water wash. In the future, a demister shall be installed upstream of the RFCC water wash in order to capture larger aerosol and increase the RFCC water wash efficiency.

The lower water wash is operated at the highest possible temperature in order to capture the remaining amines in gas phase and to avoid water condensation on aerosol.

- The upper water wash cools down the flue gas for the plant water balance.
- The RFCC water wash consists of 6 m Flexipac 2X (SS) structured packing with equivalent diameter similar to the absorber equivalent diameter and a special distributor.

The special distributor has a capacity corresponding to the total clean water condensed in the upper water wash. This is about 6-8 m^3/h of water during normal conditions. Hot water at around (60-70°C) either from the upper or lower water wash, preferably from the upper water wash together with inherent leakage of about 1 m^3/h of water from the lower water wash collector tray is fed to the RFCC water wash. Water fed to the RFCC water wash distributor irrigates the packing and aerosol in the depleted flue gas counter currently contacts hot water. Aerosol in the depleted flue gas grow to a larger size which makes it possible to be removed from the flue gas in the RFCC water wash. Major part of aerosol containing amine is recovered here. Water from the RFCC water wash containing removed aerosol flow down to the absorber packing and eventually to absorber sump. Figure 10. shows details of the RFCC water wash configuration.

The amine captured in each water wash is estimated based on the laboratory analysis of the water wash circulation water and the flow meters of each water wash drain. The tests confirm that more than 90% of the amines are captured in the RFCC water wash. 5% to 8% are captured in the lower water wash. Less than 2% are captured in the upper water wash. The total amines captured in the three water washes correspond to a concentration up to 2,000 ppmv of MEA in the flue gas upstream the water washes. As the theoretical MEA concentration in the gas phase is lower than 400 ppmv, it is deducted that most of the amines captured in the RFCC water wash are caused by MEA condensed on aerosol.

A different water wash configuration is tested elsewhere [12] with a limited water flow to the lower water wash further operation parameters are not available in the public domain.

At TCM depleted flue gas from RFCC water wash continues to lower water wash where the flue gas is cooled by removing about 1 MW of heat. From the lower water wash the depleted flue gas leads to upper water wash and cools down to a temperature just above the flue gas inlet temperature in order to keep the plant in water balance.

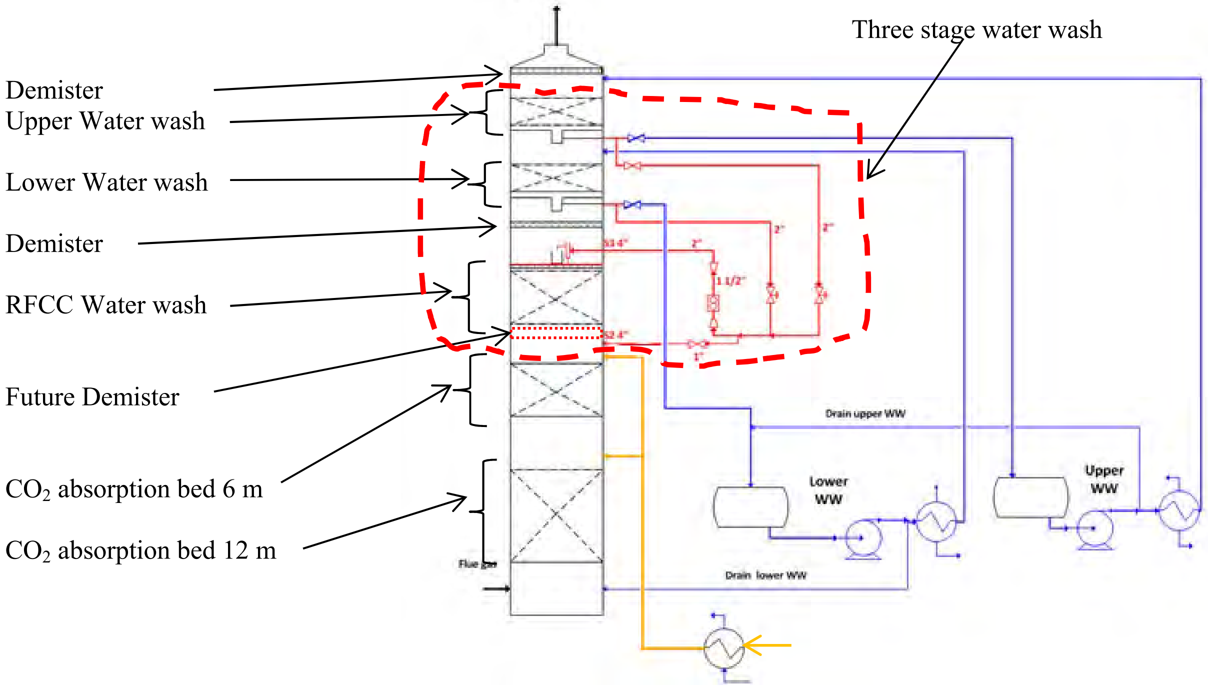

Figure 10. Water wash configuration for the TCM amine plant absorber.

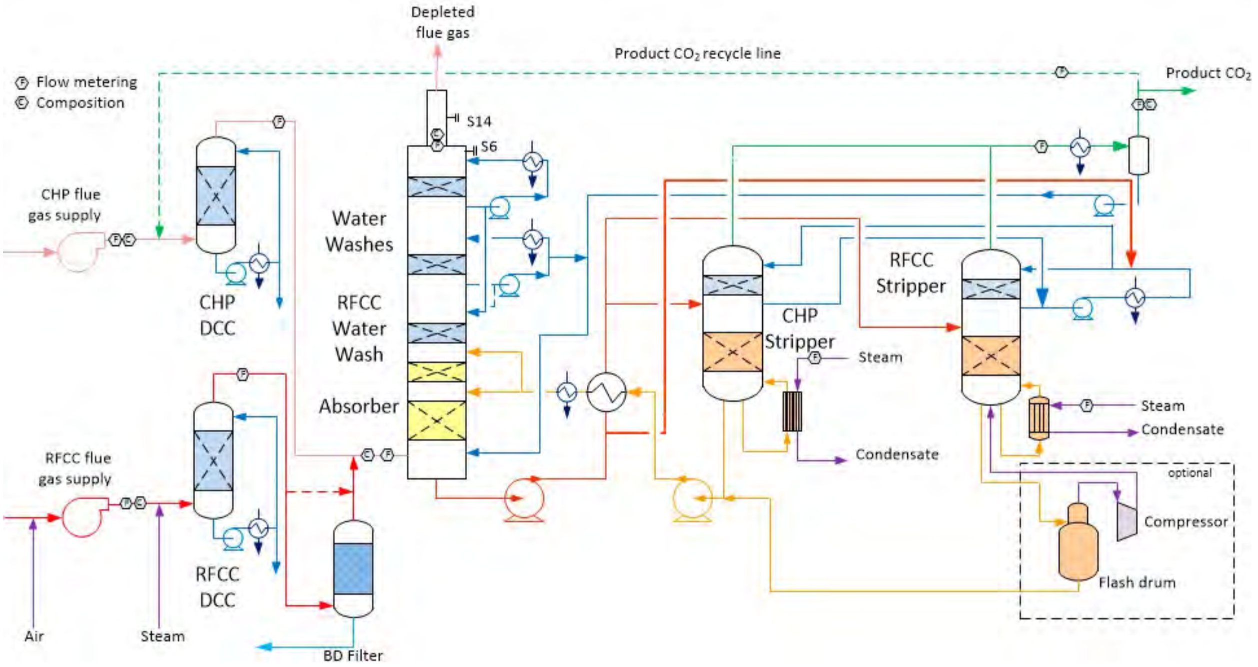

Figure 11. TCM Advanced process configuration for emissions control and optimal SRD. RFCC WW and rich amine bypass over cross heat exchanger is shown in the figure.

4.2. Installation of cold rich by pass line

As discussed in section 3.1, lean amine inlet temperature to absorber needs to be kept around 55°C while capturing CO_2 from RFCC flue gas, this gives a ΔT_{bl}~ 23°C. Lean amine temperature of 50°C or above can be achieved by two ways:

- Bypassing a fraction of hot lean amine over rich-lean cross heat exchanger
- Bypassing a fraction of cold rich amine over rich-lean cross heat exchanger

By applying the first approach a fraction of hot lean amine bypasses over the rich-lean cross exchanger, the bypass hot lean is mixed with cold lean amine exiting the cross heat exchanger and fed to the absorber without further cooling in the downstream trim cooler. Bypassing a fraction of hot lean amine increases SRD because the available recoverable heat in the cross heat exchanger reduces and the extra heat in the bypass stream is transferred to flue gas and thus lost in the cooling water.

By applying the second approach a fraction of cold rich solvent downstream the rich pump bypasses the cross rich-lean heat exchanger and fed to the stripper overhead system. Via the stripper overhead system, the rich bypass stream enters the stripper water wash section and functions as extra reflux by condensing water from the gas phase in the stripper top section accompanied by further cooling in the stripper top section. The energy from condensation of water in the stripper top section is recovered in the cold rich stream running down the stripping section thus reduces the energy lost in the overhead condenser. Around 2/3 of water in the stripper top section is condensed by the cold rich amine stream. While 1/3 of the water in the hot stripper gas stream is condensed in the overhead sea water cooled condenser. This reduces SRD from 3.67 to 3.5 GJ/ton CO_2 at similar conditions. The second approach as described above was implemented to the TCM amine plant as illustrated in Figure 11 and tested thoroughly. The advanced configuration consisting of BD filter, three stage water wash system, cold rich bypass to stripper and modified online emission monitoring system was tested successfully over a long period and enabled TCM to run amine plant with RFCC in compliance with the applicable emission permit in an efficient manner. Table 5 summarizes results achieved with the advanced configuration and RFCC flue gas.

Table 5. Performance of advanced process configuration of amine plant

Aerosol in Flue gas downstream BD filter	Aerosol/cm^3	500,000 to 2 000,000*
Absorption parameters	CO_2 conc. in flue gas (vol%)	13-14
	CO_2 capture (%)	~90
	Lean amine MEA (wt%)	30
	Lean amine temperature (°C)	55
	RFCC water wash in operation (yes/no)	Yes
	Lower water wash duty	1/4th of total cooling duty
	Upper water wash duty	3/4th of total cooling duty
Absorber MEA emissions	ppm(v)	1.5 to 3
SRD without Cold rich bypass	GJ/ton CO_2	3.67
SRD with Cold rich bypass	GJ/ton CO_2	3.5

*2 000,000 aerosol/cm^3 in the flue gas were achieved with bypassing a small amount of RFCC flue gas over the BD filter.

Conclusion

TCM has developed and tested an advanced amine plant process configuration for RFCC flue gas with 30 wt% MEA. The advanced configuration in addition to conventional configuration consists of a Brownian diffusion filter, three stage water wash system, online sampling system tolerating aerosol, fractional bypass of cold rich amine stream and operational parameters which enables to reduce aerosol based amine emissions to around 2 ppm and SRD of 3.5 GJ/ton CO_2. To avoid MEA emissions above 2 ppmv the flue gas entering the absorber should have no more than 1000,000 aerosol/cm^3, the ΔT_{bl} needs to be kept within 25°C and any abrupt quenching of aerosol containing depleted flue gas needs to be avoided. The latter is achieved by operating the RFCC water wash with the special procedure described in this paper. To reduce SRD a fraction of rich stream should be bypassed over the lean rich cross heat exchanger and fed to the stripper, this helps to reduce steam demand and thus lowers SRD. The sampling line for the online analysis and monitoring should be designed to avoid accumulation and degradation of chemical species and should be able to evaporate all chemical species and keep it in gaseous form.

Acknowledgements

The authors gratefully acknowledge the staff of TCM DA, Gassnova, Equinor, Shell and Total for their contribution and work at the TCM DA facility. The authors also gratefully acknowledge TCM owners and the Climit Demo project AeroSolve (616125) for their financial support and contributions.

References

[1] The Open-source Centre at TCM, https://catchingourfuture.com/

[2] Lombardo G, Shah MI, Fostås B, Hvidsten OA, Faramarzi L, Cazenove TD, Lepaumier H, Rogiers P. Results from aerosol measurement in amine plant treating gas turbine and residue fluidized catalytic cracker flue gases at the CO_2 Technology Centre Mongstad (GHGT-14 ,2018)

[3] Morken A.K, Pedersen S, Kleppe ER, Wisthaler A, Vernstad K, Ullestad Ø, Flø NE, Faramarzi L, Hamborg ES. Emission results of amine plant operations from MEA testing at the CO_2 Technology Centre Mongstad, Energy Procedia 63(2014), 6023-6038

[4] Gjernes E,Pedersen S,Cents T, Watson G, Fotås BF, Shah MI, Lombardo G, Desvignes C, Flø NE, Morken AK, Cazenove TD, Faramarzi L,Hamborg ES. Results from 30 wt% MEA performance testing at the CO_2 Technology Centre Mongstad, Energy Procedia 114(2017)1146-1157

[5] Faramarzi L,Timsen D,Hume S,Maxon A,Watson G,Gjernes E,Fostås BF,Lomarado G,Cents T,Morken AK,Shah MI,Cazenove TD,Hamborg ES. Results from MEA testing at the CO_2 Technology Centre Mongstad: Verification of baseline results in 2015. Energy Procedia 114(2017)1128-1145

[6] Gretscher, H., Schaber, K., Aerosol formation by heterogeneous nucleation in wet scrubbing processes, Chem. Eng. Process. Process Intensif., 38, 541–548, 1999.

[7] Wix, A., Schaber, K., Ofenloch, O., Ehrig, R., Deuflhard, P. Simulation of Aerosol Formation in Gas-Liquid Contact Devices, Chem. Eng. Commun., 194, 565–577, 2007.

[8] Brachert, L., Kochenburger, T., Schaber, K., Facing the Sulfuric Acid Aerosol Problem in Flue Gas Cleaning: Pilot Plant Experiments and Simulation, Aerosol Sci. Technol.,47, 1083–1091, 2013.

[9] Purvil Khakharia. Aerosol-based Emission, Solvent Degradation, and Corrosion in Post Combustion CO_2 capture (PhD thesis 2015)

[10] Hamborg ES, Smith V, Cents T, Brigman N, Pedersen OF, Cazenove TD, Chhaganlal M,Feste JK, Ullestad ØmUlvatn H,Gorset O,Askestad Inga,Gram LK, Fostås BF, Shah MI, Maxon A, Thimsen D. Results from MEA testing at the CO_2 Technology Centre Mongstad. Part II: Verification of baseline results, Energy Procedia 630(2014) 5994-6011

[11] Lombardo G, Fostås BF, Shah MI, Morken AK, Hvidsten OA, Mertens J, Hamborg ES. Results from aerosol measurement in amine plant treating gas turbine and Residuel Fluidized Catalytic Cracker flue gases at the CO_2 Technology Centre Mongstad. Energy Procedia 114(2017) 1210-1230

[12] Moser P, Schmidt S, Stahl K, Vorberg G,Lozano GA, Stoffregen T, Røsler F. Demonstrating Emission Reduction-Results from the Post combustion Capture Pilot Plant at Niederaussem. Energy Procedia 63(2014) 902-910.

CATCHING OUR FUTURE

Documenting modes of operation with cost saving potential at the Technology Centre Mongstad

(2018)

14th International Conference on Greenhouse Gas Control Technologies, GHGT-14

21st -25th October 2018, Melbourne, Australia

Documenting modes of operation with cost saving potential at the Technology Centre Mongstad

Erik Gjernes[a]*, Steinar Pedersen[b], Divya Jain[c], Knut Ingvar Åsen[b], Odd Arne Hvidsten[b,d], Gelein de Koeijer[b], Leila Faramarzi[b,d], Thomas de Cazenove[d,e]

[a]Gassnova SF, Dokkvegen 10, 3920 Porsgrunn, Norway
[b]Equinor ASA, PO Box 8500, 4035 Stavanger, Norway
[c]Shell Global Solutions International B.V., PO Box 663, 2501CR The Hague, The Netherlands
[d]Technology Centre Mongstad, 5954 Mongstad, Norway
[e]A/S Norske Shell, Tankveien 1, P.O.Box 40, 4098 Tananger, Norway

Abstract

From December 2017 to February 2018 the Technology Centre Mongstad (TCM DA), operated a test campaign capturing CO_2 by use of monoethanolamine (MEA) in a 80 to 200 ton CO_2 per day demonstration unit. The primary objective was to provide experimental evidence for reducing operational as well as capital costs of CO_2 capture. For cost assessment a selection of the test cases has been used as a basis for estimating cost of full scale amine based CO_2 capture for a large combined cycle gas turbine based (CCGT) power plant. The cost of CO_2 avoided is presented for these cases and the case with the lowest cost of CO_2 avoided has been furthered investigated by a parameter study. The cost assessment is presented relative to two earlier MEA campaigns at TCM. A reduction in cost of CO_2 avoided up to 18% was justified by experiments while further improvements were made plausible theoretically.

Keywords: MEA; post-combustion capture; cost of CO_2 avoided; CO_2 Technology Centre Mongstad; TCM DA

1. Introduction

The Technology Centre Mongstad (TCM) is the world's leading facility for verifying and improving CO_2 capture technologies. TCM is located at Mongstad, one of Norway´s most complex industrial facilities. TCM has been operating since autumn 2012, providing an arena for qualification of CO_2 capture technologies on an industrial scale. In autumn 2017, Gassnova (on behalf of the Norwegian state), Equinor (formerly Statoil), Shell and Total entered into a new ownership agreement securing operations at TCM until 2020. The owners of TCM started their most recent monoethanolamine (MEA) test campaign in June 2017 where a large number of public, industrial, research and academic stakeholders were involved [1]. The campaign included demonstration of a model-based control system, dynamic operation of the amine plant, investigating amine aerosol emissions and specific tests targeted at reducing the

---

* Corresponding author. Tel.: +47 40 00 59 08.
E-mail address: postmottak@gassnova.no

cost of CO_2 avoided. Through the testing, both flue gas sources currently available at TCM were used. These sources are the combined cycle gas turbine (CCGT) based heat and power plant (CHP) and the residual fluidized catalytic cracker (RFCC). They provide flue gases with a wide range of properties and a CO_2 content from 3.6 to 14 %. TCM is located next to the Equinor refinery in Mongstad. The Mongstad refinery is the source of both flue gases supplied to TCM.

The part of the test campaign addressing cost of CO_2 avoided will be reported in the current paper where the aim is to estimate the potential for cost reduction of some known measures based on experimental data from TCM's amine unit. This means that these estimates will be experimentally verified. It is the first time such a structured cost reduction test campaign has been executed on such a large test unit. Hence the results are expected to be useful for large scale plants. Besides an experimental verification of known measures, this paper will also use this methodology to estimate other cost reduction measures on a theoretical basis using extrapolation of the verified results.

The performance of TCM's amine plant was presented in 2014 [2] along with an independent verification protocol developed by Electric Power Research Institute (Epri) [3]. The performance was reported with a specific reboiler duty (SRD) of 4.1 GJ/ton CO_2 for a case with 47,000 Sm^3/h flue gas flow at 3.7 % CO_2 and a capture rate around 85 %. CO_2 concentration in the flow in and out of the absorber as well as in the product flow was measured by use of one FTIR unit that cycled between the three flows. One cycle lasted more than one hour, thus simultaneous gas composition measurements could not be presented. In 2015 performance was revisited after a major upgrade of the gas phase measuring system. The upgrade included multiple gas phase analyzers at each of the three flows, i.e. in and out of the absorber and out of the stripper. The use of anti-foam significantly improved the performance and resulted in an SRD of 3.6 GJ/ton CO_2 [4] for operation at 59,0000 Sm^3/h flue gas flow with 3.6 % CO_2. The 47,000 Sm^3/h case was also revisited in 2015 [5] with a test program for energy optimization based on maintaining 85 % capture rate for various combinations of stripper bottom temperature and corresponding lean CO_2 loading (mole CO_2 per mole amine). This resulted in SRDs for the cases without and with the use of anti-foam of 3.9 and 3.6 GJ/ton CO_2, respectively. These results were used for establishing a baseline. This work takes the next step: how can the cost of capture based on this baseline be reduced through a structured test campaign?

Nomenclature

Abs. pack	Absorber packing height
CAPEX	Capital expenditure
CCGT	Combined cycle gas turbine
CHP	Combined heat and power plant
L/G	Liquid to gas ration, i.e. ratio of solvent flow and flue gas flow
MEA	Monoethanolamine
MEA-1	Test campaign at TCM on MEA (2013-2014)
MEA-2	Test campaign at TCM on MEA (2015)
MEA-3	Test campaign at TCM on MEA (2017-2018)
OPEX	Operational expenditure
RFCC	Residual fluidized catalytic cracker
Sm^3/h	Standard cubic meter per hour at 15 °C and 101.325 kPa
SRD	Specific reboiler duty
ton	1,000 kg,
TCM	Technology Centre Mongstad
wt%	Concentration on weight basis

2. Overview of the tests program

The test program that is reported in this paper was executed at TCM from December 2017 to February 2018. The main elements investigated were:

- Absorber configurations with packing heights at 24, 18 and 12 meter
- Solvent concentration with MEA at 30 and 40 wt%

In addition to this, most of the tests were operated at slightly elevated CO_2 concentration in the flue gas to be treated, i.e. from 3.6 to 4.2 % CO_2 (wet), and during last part of the campaign anti-foam was injected based on experience from the test program in 2015 [5]. The test program contains 18 test series and the main operational parameters are listed in Appendix A.

The operation in December 2017 was stopped due to signs of corrosion i.e. increasing iron content in the solvent and high levels of ammonia emissions to air. Results from corrosion monitoring at TCM is reported in e.g. [6]. After inspection and a comprehensive plant washing operation, the test program was started up again week 3, 2018. The following two months different modes of operation were investigated. Before presenting the experimental results and cost assessments, the definitions of specific reboiler duty, capture rate and CO_2 loading will be discussed.

Figure 1 shows the TCM amine plant in CHP mode. It is a flexible plant that enables testing of CO_2 capture in several configurations and offers a wide range of flue gas flow rates as well as flue gas compositions [2 to 5]. In the current campaign injection of lean amine is made at three different heights in the absorber and thus utilising 24, 18 and 12 meter absorber packing (yellow boxes in figure), respectively. The CO_2 recycle line has been in operation for most of the campaign in order to maintain a CO_2 level of 4.2 % (wet) in the flue gas into the absorber.

Specific reboiler duty (SRD) is defined as the heat delivered to the reboiler from the steam system divided by the amount of captured CO_2:

$$SRD = \frac{\Delta H \, \dot{m}_{steam}}{\dot{m}_{CO_2 cap}} \tag{1}$$

where $\dot{m}_{steam}$ is the steam flow to the reboiler heat exchanger. ΔH is the enthalpy difference between steam and condensate calculated from measured temperature and pressure, see also reboiler, steam and condensate in Figure 1. Steam pressure is typical around 2.5 barg and up to 160 °C for the tests reported in this paper.

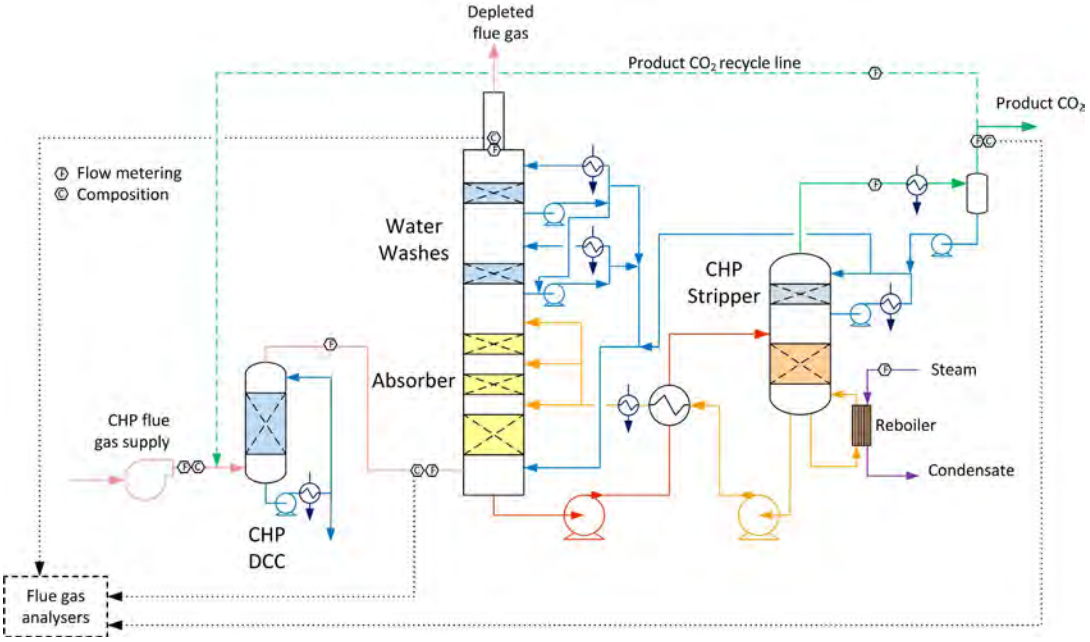

Figure 1. The TCM amine plant in CHP mode (up to 80 ton CO_2 per day). Flow meters and flue gas analysers are located at absorber inlet, outlet/depleted flue gas and product flow. Captured CO_2 can be recycled, see green dotted line, to increase the CO_2 concentration in the flue gas flow into the absorber.

CO_2 capture rate is the mass fraction of CO_2 being captured out of the amount of CO_2 flowing into the absorber:

$$\varepsilon = \frac{\dot{m}_{CO_2 cap}}{\dot{m}_{CO_2\, in}} \tag{2}$$

Captured CO_2 ($\dot{m}_{CO_2 cap}$) in (1) and (2) can be based on CO_2 in product flow ($\dot{m}_{CO2,prod}$) leaving the stripper or on difference in mass flow of CO_2 over the absorber ($\dot{m}_{CO_2 abs,in} - \dot{m}_{CO_2 abs,out}$). There are several ways of calculating CO_2 capture rate [4]. In addition to this and as outlined in more details in [4,5] TCM is equipped with multiple flue gas analysers for measuring composition in and out of the absorber and out of the stripper, see Figure 1. This also includes moisture which alternatively can be calculated based on thermodynamics using temperature and pressure of the gases in question. The flow meter at the absorber outlet is unreliable and flow out of absorber is calculated from flow into the absorber assuming that all components except moisture and CO_2 are conserved. The current analysis will be based on the selection of composition analysers, flow meters and calculation methods presented in Appendix B.

Lean and rich solvent loading (mole CO_2/mole amine) are calculated from laboratory analysis of liquid solvent samples that provide total inorganic carbon (mole CO_2/kg solvent) and total alkalinity (mole amine/kg solvent):

$$loading = \frac{Total\ inorganic\ carbon}{Total\ alkalinity} \tag{3}$$

3. Optimising performance: energy

Most of the MEA-3 program was conducted with CO_2 concentration at 4.2 % (wet) in the flue gas into the absorber. This was maintained by recycling captured CO_2 back to the absorber inlet. This secured stable CO_2 concentration in the flue gas since recycled CO_2 could top the initial CO_2 concentration of 3.5 to 3.9 % up to 4.2 % (wet). This CO_2 level is typical for state of the art CCGT plants. Selected test series that will be discussed below are presented in Table 1.

Figure 2 shows to the left the MEA-3 test series 3 with black filled symbols and series 11 with black open symbols. These two series were operated at 47,000 Sm³/h, 24 meter absorber packing and without use of anti-foam. Compared to results from the MEA-2 campaign in 2015 [5] these two new test series resulted in a lower optimum SRD, but this may be due to several aspects and in addition the CO_2 concentration in the flue gas into absorber was higher. However, during this part of the campaign the amine plant could be operated at rather high stripper bottom temperature and corresponding low lean solvent CO_2 loading without the use of antifoam. Thus, the resulting optimum point was found at a higher stripper bottom temperature and lower lean CO_2 loading compared to MEA-2 results, i.e. 118.1 °C /0.29 mole/mole for MEA-2 versus 121.0 °C/0.21 mole/mole for MEA-3. Results down to 3.6 GJ/ton CO_2 was not achieved at 24 meter absorber packing when operated without the use of anti-foam and as will be presented below the effect anti-foam was not at all as pronounced as in the MEA-2 campaign. We acknowledge this difference in performance which could be due to several factors, however, this has not yet been concluded.

Table 1. Selected test series from MEA-3 campaign at 24 and 18 meter absorber packing, the latter operated at 30 and 40 wt% MEA. The liquid-to gas ratio (L/G) is the ratio of lean amine- to flue gas flow. SRD is based on thermal energy, see equation 1.

#	Abs. pack [m]	MEA [wt%]	Flue gas × 1000 [Sm³/h]	Anti-foam [-]	Lean × 1000 [kg/h]	L/G [kg/Sm³]	Stripper bottom temp [°C]	SRD [GJ/ton CO_2]	CO_2 capture [%]
3	24	30	47.0	No	42.0–55.0	0.89–1.17	119.8–121.5	3.8-4.4	86
11	24	30	47.0	No	45.0–60.0	0.96–1.28	119.7–121.4	3.8-4.4	83-86
13	18	30	47.0	Yes	47.5–55.0	1.01–1.17	120.6–121.4	3.9-4.1	84-86
17	18	30	47.0	Yes	52.2–55.1	1.11–1.17	121.5–121.9	3.8-3.9	85-89
B	18	30	47.1-47.2	No[1]	52.5–52.7	1.11–1.12	120.8–120.9	3.8-3.9	87
9	18	40	51.0	No	44.8–55.0	0.88–1.08	121.0–122.8	3.6	82-86

[1] Test series B is made after reclaiming and with no use of anti-foam.

All SRDs and capture rates presented in Figure 2, Table 1 and Table 2 are calculated based on that captured CO_2 ($\dot{m}_{CO_2 cap}$) in equation (1) is derived from the difference in mass flow of CO_2 over the absorber. Earlier reported data from MEA-2 campaign [5] was based on measured product mass flow of out of stripper. The discussion below is based on a reassessment of these data using mass flow of CO_2 over the absorber. The data points presented are made from averaging process data over a two hour time slot. This time slot also includes liquid solvent samples such that solvent CO_2 loading can be calculated according to equation (3).

Performance at 18 meter absorber packing height was investigated at both 30 and 40 wt% MEA. Figure 2 shows to the right the MEA-3 test series 13 and 17 with filled and open brown symbols, respectively. The blue filled symbols are test series B without anti-foam that was executed after solvent reclaiming. The best SRDs were obtained around 3.8 GJ/ton CO_2 for test series 17 which is a bit below the 24 meter tests in MEA-2 without anti-foam. The red filled symbols in Figure 2 right hand side shows MEA-3 series 9 which was operated with 51,000 Sm^3/h flue gas flow, 40 wt% MEA and without the use of anti-foam. The optimum SRD is similar as the best performance from MEA-2, however, the absorber packing required was reduced from 24 meter (MEA-2) to 18 meter (MEA-3) and no use of anti-foam. Test series 9 was stopped before completion due to increasing ammonia emission and signs of corrosion i.e. increasing iron content in solvent. Thus only a limited number of parameter variations was conducted during operation at 40 wt% MEA and there might still be a potential for obtaining even lower SRDs. Another observation was that the use of anti-foam had limited effect on performance which can be seen from the brown (with anti-foam) and the blue symbols (without anti-foam) in Figure 2 to the right. Case 9-4 that was operated at 40 wt% MEA without the use of anti-foam resulted in the lowest SRD in this campaign.

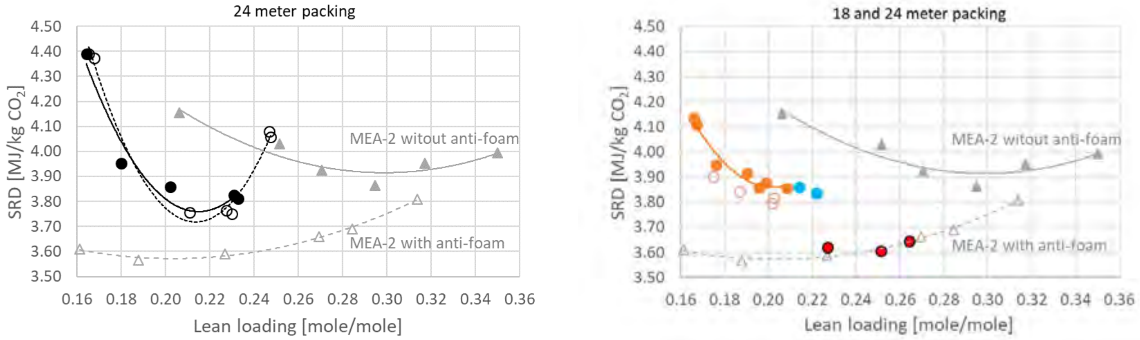

Figure 2. To the left SRD for tests utilising 24 meter absorber packing compared to results from MEA-2 in 2015 (grey symbols and lines). MEA-3 series 3 is with black filled symbols and series 11 is with black open symbols. To the right SRD for tests at 18 meter absorber packing compared to the same results from MEA-2 in 2015 (grey symbols and lines). Series 13 is with brown filled symbols, series 17 with brown open symbols, series B with blue symbols and series 9 which is with 40 wt% MEA, is with red symbols. SRDs are calculated based on difference in mass flow of CO_2 over the absorber. All plots except series 9 are with 30 wt% MEA. The right and left figure present the same MEA-2 results utilising 24 meter absorber packing. Table 1 and Table 2 provide more information about the test series.

Table 2. With ref to Figure 2 operational data, SRD and capture rate for the three cases at lowest SRD values during MEA-3. SRD is based on thermal energy, see equation 1.

#	Abs. pack [m]	MEA [wt%]	Flue gas × 1000 [Sm^3/h]	L/G [-]	Anti-foam [-]	Stripper bottom temp [°C]	Lean loading [mole/mole]	SRD [GJ/ton CO_2]	CO_2 Capture [%]
11-1	24	30	47.0	1.07	No	121.0	0.21	3.8	85
17-5	18	30	47.0	1.11	Yes	121.6	0.20	3.8	88
9-4	18	40	51.0	0.98	No	121.7	0.25	3.6	87

4. Modes of operation

Based on previous work [4,5] it was interesting to further investigate the trade-off between capital expenditure (CAPEX) and operational expenditure (OPEX) parameters for operating conditions relevant for various CCGT- and exhaust gas recycling systems with the aim of providing experimental evidence on how total capture cost can be minimized.

The flexibility of the TCM amine plant was utilized in test series with large variations in absorber packing height, flue gas flow rate, liquid- to gas flow ratio (L/G), solvent CO_2 loading and inlet CO_2 concentration. This experimental set-up covered a range of operating modes. Data collection and performance results such as mass balance, CO_2 recovery, capture rate and SRD are according to methods described in section 2 above. Table 3 gives operational parameters and performance results for selected cases used in the cost evaluation described in section 6 below. Data from previous campaigns, MEA-1 and MEA-2 [2,4], are also included in the table for comparison.

Table 3. Test cases selected for further investigation. Case 11-1 and 9-4 are optimum modes of operation selected from Figure 2. The liquid- to gas ratio (L/G) is the ratio of lean amine- to flue gas flow. SRD is based on thermal energy, see equation 1.

#	Abs. pack [m]	MEA [wt%]	Flue gas × 1000 [Sm^3/h]	CO_2 wet [%]	L/G [-]	Lean loading [mole/mole]	SRD [GJ/ton CO_2]	$\dot{m}_{CO_2 cap}$ [kg/h]	CO_2 capture [%]
11-1	24	30	47.0	4.2	1.07	0.21	3.8	3,160	85
5-1	24	30	59.0	4.1	0.92	0.20	4.0	3,480	77
8-1	18	30	51.0	4.3	1.07	0.21	3.9	3,360	82
9-4	18	40	51.0	4.2	0.98	0.25	3.6	3,430	86
13-2	18	30	47.0	4.3	1.12	0.20	3.9	3,180	84
15-0	12	30	47.0	4.2	1.18	-	4.1	2,700	73
15-3	12	30	47.0	5.0	1.38	0.23	4.0	3,170	72
MEA-1	24	30	47.0	3.7	1.17	0.23	4.1	2,750	~ 85
MEA-2	24	30	59.0	3.6	1.00	0.21	3.6	3,390	86

The initial learning at TCM during the years 2013 and 2014 are represented by the test case MEA-1. At that time the operation was mainly with 24 meter absorber packing height and flue gas flow at 47,000 Sm^3/h (80 % of design flow capacity). For capture rates between 85 to 90 % the specific reboiler duty was measured to 4.1 GJ/ton CO_2.

In the MEA-2 campaign in 2015 learning from several test campaigns were implemented in the test plan. Addition of anti-foam improved especially the stripper performance. This allowed operation with full flue gas load and achievement of both high capture rates and significantly lower SRD values.

In the current MEA-3 campaign, the cases 11-1 and 5-1 are utilizing 24 meter absorber packing height and were run at 47,000 and 59,000 Sm^3/h flue gas flow, respectively. The stripper performance constrained the maximum possible CO_2 capture to 3,480 kg/h in the case with highest flue gas flow. The corresponding capture rate was 77%. However, during the current campaign no energy optimisation was made at 59,000 Sm^3/h flue gas flow and this test was done without the use of anti-foam.

From the three cases run at 18 meter absorber packing height (cases 8-1, 9-4 and 13-2) it is seen that the benefit of 40 w% MEA is lower L/G, lower SRD and still achieving high capture rate. The low L/G and the high lean CO_2 loading indicates a further potential for capturing more CO_2 in this system.

The two cases run at 12 meter absorber packing height achieved rather low capture rates. The benefit of increasing the CO_2 concentration in the flue gas flow into absorber from 4.2 to 5.0 % (wet) is assessed based on results from these two cases.

5. Cost assessment and cost of CO_2 avoided

The economic evaluations of power and capture plants in this paper is based on standard "Cost of Electricity" (COE)- and "Cost of CO_2 avoided" metrics. These calculations are based on aligned and standardized estimates and assumptions on technology process performance such as energy efficiency, CO_2 generation and capture rates, see e.g. [7]. Cost estimates include CAPEX, operations and maintenance (O&M) including fuel and a set of general price and rate of return assumptions. For each case in section 6 below, a complete sized capture plant equipment list is established. Aspen In-Plant Cost Estimator (IPCE) V9 is used to estimate equipment cost. Equipment installation factors are then used to estimate total installed costs. The OPEX can be split in annual cost (of capex), power loss, maintenance, chemicals and fixed operating costs. The gas fired power plant specific cost is based on GTPro and a West Europe scenario. All calculations are furthermore carried out at:

- normalised, per unit (kWh) output from the base industrial (power) plant
- pretax, pre-financing basis
- annual cost basis, applying a capital charge factor corresponding to a standard discount factor and project time horizon

Cost of CO_2 avoided (\$/ton CO_2) is calculated according to (4) below and is based on cost of electricity (*COE*) and CO_2 emission per kWh (*CO_2 emission*) for a power plant with capture (*cap*) and without CO_2 capture (*no cap*).

$$Cost\ of\ CO_2\ avoided = \frac{COE_{cap} - COE_{no\ cap}}{CO_2\ emission_{no\ cap} - CO_2\ emission_{cap}} \tag{4}$$

The calculated cost of CO_2 avoided implicitly accounts for the capture systems' own energy demand and its inherent CO_2 emissions. The following economic assumptions are applied:

- Fuel gas price: 0.1875 US \$/Sm^3
- On-stream hours: 7,884 (90 %)
- Discount rate: 5 % real (pretax)
- Time horizon: 30 years

This paper will only report percentage cost reduction and no absolute cost numbers. The main reasons are that the absolute numbers are not useful for the purpose of this work and are partially confidential. In this work one consistent method and one consistent set of assumptions are used for calculating the cost, which is important for a fair comparison.

6. Cost evaluation of selected cases

The experiments targeted lowest possible absorber packing height, lowest possible L/G and SRD while maximizing the captured CO_2 and capture rate. In Table 4 below the experimental data for the selected cases are scaled to a full-scale design at a fixed inlet CO_2 flow of 150 ton CO_2/h and measured capture rate case by case.

In order to compare the MEA-1 and MEA-2 to MEA-3 on the same basis in the cost assessment, the CO_2 inlet concentrations for these two cases are adjusted up to 4.2 % (wet) and the flue gas flow rates are reduced correspondingly, reducing the size and cost of flue gas blower, DCC and absorber. The superficial gas velocity is held constant in the DCC and absorber, reducing the diameter of these units.

The adjusted/scaled absorber packing height and the most important cost parameter, the packing volume, are calculated from the experimental data for the cases selected in the MEA-3 campaign. The scaled-up absorber volume is based on packing height utilised for each TCM test case and a scaled up cross sectional area. The latter is calculated based on TCM cross sectional area and the ratio of full-scale (150 ton CO_2/h) to TCM (case by case) CO_2 inlet flow. For all scaled up cases the cross sectional areas are adjusted to fit with a superficial velocity of 2 m/s (at 0 °C, 1 atm).

Thus, packing height, see Table 4, is adjusted in order to maintain the scaled-up absorber packing volume. The packing volume per captured CO_2 will be equal for each TCM and corresponding scaled up case. The data are shown in Table 4 below together with calculated lean solvent flow per kg CO_2 into absorber, CO_2 loading in lean and rich amine. The rich CO_2 loading is calculated based on solvent flow rate and captured CO_2.

Packing volume is a major CAPEX element and for operation with 30 and 40 wt% MEA the most cost-effective packing volume demonstrated at TCM was about 37 m^3/ton CO_2 capture per hour for the current test conditions. This result is however, design and site specific. In case 9-4 with 40 wt% MEA the main cost reduction parameters are reduced enthalpy to reboiler (low SRD) and reduced solvent flow rate.

The case 11-1 had more packing than needed and very little CO_2 is captured in the upper 6 m packed bed. The cases 11-1, 8-1 and 13-2 performed close to the MEA-2 results, while the case 5-1 was performing poorer. The flue gas flow rate was very high in this case resulting in high CO_2 flow into the absorber. The rich CO_2 loading was high, indicating that the solvent flow rate was too low to achieve high capture rate. Solvent flow rate was 12.02 kg solvent per kg CO_2 in comparison to at least 13.50 kg solvent per kg CO_2 into absorber for the best cases. In new campaigns some of the cases could be further improved if higher capture rates are obtained.

The cases 15-0 and 15-3 with 12 m absorber packing achieved the lowest packing volume per kg CO_2 captured. On the other hand, the capture rate was low and the solvent flow rate was higher. This resulted in higher capture cost. These cases had in fact a too low packing volume.

In MEA-1 the packing volume was slightly higher than for the 11-1 case, solvent flow was higher and the rich loading was lower. In MEA-2 with 24 meter absorber packing height, the packing volume of 50 m^3 per ton CO_2 captured is on the high side compared to the MEA-3 results.

Table 4. The test cases selected for further investigation are scaled up to 150 ton of CO_2/h in the flue gas into the absorber base on 2 m/s superficial velocity (at 0 °C, 1 atm) in the absorber. Case 11-1 and 9-4 are optimum cases in Figure 2 while rest of the tests documents different modes of operation.

#	Adjusted abs. pack [m]	Packing Volume [m^3/ton CO_2, h]	Lean solvent flow [kg/kg CO_2 in]	Lean loading [mole/mole]	Rich Loading [mole/mole]	Captured CO_2 [ton/h]	CO_2 capture [%]
11-1	27.3	54	13.48	0.21	0.51	128	85
5-1	22.4	49	12.02	0.20	0.51	115	77
8-1	18.5	38	13.31	0.21	0.51	123	82
9-4	19.0	37	12.48	0.25	0.50	129	86
13-2	20.2	40	13.94	0.20	0.50	127	84
15-0	13.7	32	15.07	0.21	0.45	110	73
15-3	13.7	27	14.74	0.23	0.47	108	72
MEA-1	~28	~55	~16	0.23	0.48	128	85
MEA-2	25.5	50	14.5	0.21	0.50	128	86

Section 5 above introduces the economic evaluation and cost of CO_2 avoided. In Figure 3 to the left the demonstrated cost reduction for the seven test cases selected from MEA-3 is presented relative to the cost of CO_2 avoided of MEA-1. The demonstrated effect of increasing the CO_2 concentration in flue gas into absorber from 4.2 to 5.0 % (wet) is shown by cases 15-0 and 15-3. When scaled to 150 ton CO_2/h the cost reduction for 15-0 to 15-3 is mainly due to the reduced resulting flow of flue gas, impacting the cost of the DCC, flue gas blower and absorber. Case 9-4 demonstrates the largest cost reduction contribution, i.e. 13.5 % down relative to MEA-1. This case is also presented in Figure 3 to the right (MEA-3) along with MEA-2 and a theoretically case based on 9-4 assuming 5 % CO_2 (wet) in the flue gas. The latter improves the case 9-4 by about 5 % points.

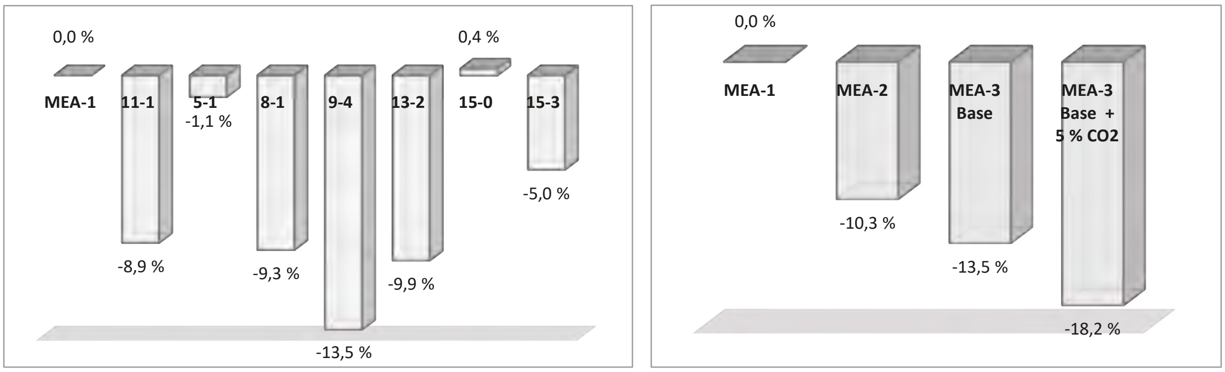

Figure 3. To the left: Demonstrated reduction in cost of CO_2 avoided for seven selected MEA-3 cases. To the right: Lowering cost of CO_2 avoided in campaigns MEA-1 to MEA-3. The MEA-3 is also presented with its theoretically potential if CO_2 content in flue gas is 5 % (MEA-3 Base + 5 % CO_2). Results are presented relative to assessment made for MEA-1 in 2014. Note that case 9-4 in the left plot is presented as "MEA-3 base" in the right plot.

The measures in Figure 3 do not represent radical new ways of operating or new technologies. They can rather be categorized as learning-by doing. They are typically measures relevant for the first few plants, also called FOAK – first of a kind. Since the cost reduction potential of these measures is experimentally verified in one of the world's largest demonstration plants, the cost reduction should be highly accurate, and hence relevant for future post-combustion plants.

Based on the experience from the test campaign other reduction measures have been studies on a theoretical basis in order to investigate future potential for reducing cost of CO_2 avoided. A theoretical parameter study has been made based on case 9-4, referred as "MEA-3 Base" in Figure 4. The following elements have been assessed:

- Reduce from 2 × 3 meter wash section to 1 × 3 meter wash section
- Reduce solvent consumption from 1.6 kg/ton CO_2 down to 0.3 kg/ton CO_2 [8,9]
- Increase CO_2 capture rate from 86 to 90 %
- Reduce steam consumption to achieve SRD of 3.1 GJ/ton CO_2 (other solvents than MEA)
- Increasing CO_2 content in flue gas from 4.2 up to 5 %

These measures are considered to be realistic. Most of the numbers are reported in the post-combustion literature and seem reasonable. In addition to these measures reduced manning is also included in the parameter study for illustration:

- Reduced manning from 4 operators per shift to 1 operator per shift

Figure 4 shows the cumulative effect for cost of CO_2 avoided from these 6 elements. Solvent and process development relates to the first five items. The assumptions on operators before and after reduction is not based on TCM experience. The second last element corresponds to state of the art CCGT plants that are expected to be operated at 5 % CO_2. The five first elements improves the "MEA-3 Base" by 17.1 % while utilizing all six elements results in 21.5 % improvement.

All in all, these initiatives will represent a reduction in cost of CO_2 avoided of the order of 30 % when compared to MEA-1. However, note that these measures are not necessary cumulative, i.e. all combinations may not be possible at the same time.

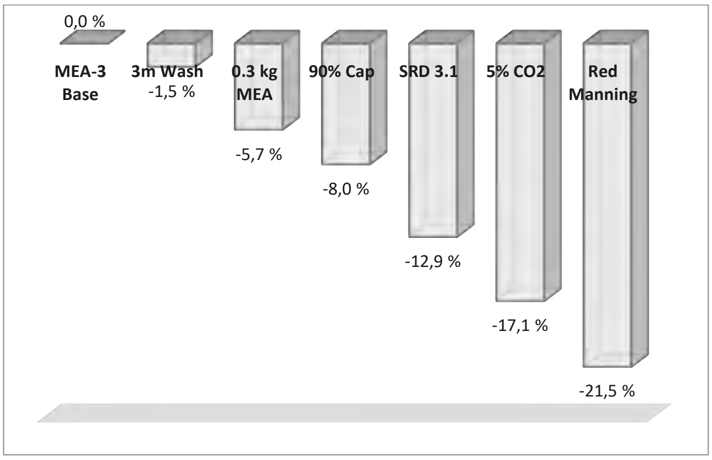

Figure 4. Relative cost of CO_2 avoided based test case 9-4 (MEA-3 Base) and a theoretical parameter study involving 6 cost reduction initiatives introduced on top of each other.

7. Conclusion

Different modes of operation with cost saving potential were executed as part of the MEA-3 campaign at TCM from December 2017 to February 2018. The target was to explore learning from five years of operation at TCM with respect to overall cost reduction potential using the relative cost of CO_2 avoided metric. The new results were therefore compared to those reported from the MEA-1 and MEA-2 campaigns. The investigation of optimum energy performance identified that SRD values below 3.6 GJ/ton CO_2 for MEA are challenging to achieve with 30 wt% MEA and a CCGT like flue gas. This performance is achieved at TCM with a conventional amine plant and may be optimized with an advance process plant. In the cost reduction part of the investigation the level of 10 % cost reduction in cost of CO_2 avoided as achieved in MEA-2 was confirmed with the new experiments. Packing volume is a major CAPEX element and the most cost-effective packing volume demonstrated based on TCM equipment, was about 37 m^3/ton CO_2 capture per hour for the current test conditions. The lowest cost of CO_2 avoided was demonstrated when using MEA at 40 wt% and 18 meter absorber packing height. Compared with MEA-1 results a cost reduction of 13.5% was demonstrated. There is likely a further cost reduction potential of 5 %-points for this case. This is based on results from tests when the flue gas CO_2 concentration was increased from 4.2 to 5.0 % (wet). Finally, a theoretical parameter variation showed a potential cost reduction of around 20 % compared with MEA-3 Base. Compared to MEA-1 this amounts to a reduction potential of the order of 30 %. However, all combinations may not be possible at the same time.

It is important to notice that these results are generated at one of the world's largest capture demonstration units, and that it is the first time that such a structured campaign is executed. Similar testing can be carried out with different amine-based solvents. Therefore, these results at TCM scale represent a very relevant basis for scale up and industrial design of amine solvent capture technologies.

Acknowledgements

The authors gratefully acknowledge the staff of TCM DA, Gassnova, Equinor, Shell and Total for their contribution and work at the TCM DA facility. The authors also gratefully acknowledge Gassnova, Equinor, Shell, and Total as the owners of TCM DA for their financial support and contributions.

Appendix A

Table A1. The test series during MEA-3, 2017-2018.

#	Abs. pack [m]	MEA [wt%]	Flue gas × 1,000 [Sm^3/h]	Anti-foam [-]	Lean × 1,000 [kg/h]	L/G [-]	Stripper bottom [°C]	Lean loading [-]	CO_2 wet %
1[1]	12-18	30	40.0-60.0	No	39.4-66.0	0.82-1.11	119.2-121.5	0.15-0.23	3.5-3.9
2	12-24	30	40.0-47.0	No	40.5-44.1	0.94-1.10	120.0-120.5	0.18-021	3.8-3.9
3	24	30	47.0	No	42.0–55.0	0.89–1.17	119.8–121.5	0.16-0.23	4.1-4.3
4	24	30	50.5-53.0	No	54.5-54.6	1.03-1.08	120.2-120.4	0.20-0.21	4.1-4.2
5	24	30	59.0	No	54.4	0.92	120.5	0.20	4.1-4.2
6	Test of max flue gas flow vs. pressure drop in the absorber								
7	24	30	51.0	No	54.8	1.07	120.8	0.21	4.1-4.2
8	18	30	51.0	No	54.1-73.9	1.06-1.45	118.5-120.6	0.21-0.28	4.2-4.3
9[2]	18	40	51.0	No	44.8–55.1	0.88–1.08	120.5–122.8	0.23-0.28	4.1-4.4
10	18	30	51.0	No	55.2-60.1	1.08-1.18	120.6-121.2	0.22-0.25	4.1-4.2
11	24	30	47.0	No	45.0–60.0	0.96–1.28	119.7–121.4	0.17-0.25	4.2-4.3
12	18	30	47.0	No	49.6-54.7	1.06-1.16	120.5-121.1	0.19-0.21	4.1-4.3
13	18	30	47.0	Yes	47.5–55.0	1.01–1.17	120.6–121.4	0.17-0.21	4.1-4.3
14	12	30	47.0	Yes	54.2-65.2	1.15-1.39	120.8-121.7	0.18-0.22	4.1-4.3
15[3]	12	30	47.0	Yes	55.3-65.0	1.18-1.38	120.5	0.23	4.2-5.0
16	12	30	40.0	Yes	35.2	1.14	121.2	0.20	4.2
17[4]	18	30	47.0	Yes	52.2–55.1	1.11–1.17	121.0–121.9	0.17-0.21	4.2
B	18	30	47.1-47.2	No	52.5–52.7	1.11–1.12	120.8–120.9	0.21-0.22	4.2-4.3

[1] Tests in week 49 and 50 2017. Rest of the test series were executed in 2018.
[2] Full range of parameters reported, but 9-1 and 9-3 were at capture rate below 80% and are not included in Table 1 (section 3).
[3] Includes test at elevated CO_2, i.e. 5% CO_2 (wet).
[4] Full range of parameters reported, but 17-1 was at capture rate below 80% and is not included in Table 1 (section 3).

Appendix B

Table B1. Selected instruments and calculation methods for analysing test data.

Unit	Property	Method	Tag/comment
Absorber in	H_2O	Calculated f(T,p)	8610-TT-2041, 8610-PT-2040
	CO_2	IR-high	8610-AI-2004A
	Flow	Ultrasonic	8610-FT-0150
Absorber out	H_2O	Calculated f(T,p)	8610-TT-2035, 8610-PT-2430
	CO_2	IR-high	8610-AI-2030A
	Flow	Calculated	Based on flow: "Absorber in"
Product flow	H_2O	Calculated f(T,p)	8615-TT-2210, 8615-PT-2213
	CO_2	Calculated	100 – f(T,p)
	Flow	Coriolis	8615-FT-2215

With ref to Table B1 the volume flow out of the absorber ($\dot{V}_{out}$) is calculated from volume flow into ($\dot{V}_{in}$) the absorber assuming all components except water (C_{H_2O}) and CO2 (C_{CO_2}) are conserved:

$$\dot{V}_{out} = \dot{V}_{in}\frac{100-C_{H_2O}^{in}-C_{CO_2}^{in}}{100-C_{H_2O}^{out}-C_{CO_2}^{out}} \tag{B-1}$$

References

[1] The Open-source Centre at TCM, https://catchingourfuture.com/

[2] Hamborg ES, Smith V, Cents T, Brigman N, Falk-Pedersen O, de Cazenove T, Chhaganl M, Feste JK, Ullestad Ø, Ulvatn H, Gorset O, Askestad I, Gram LK, Fostås BF, Shah MI, Maxson A, Thimsen D. Results from MEA testing at the CO_2 Technology Centre Mongstad. Part II: Verification of baseline results. Energy Procedia, Volume 63, 2014, p. 5994-6011.

[3] Thimsen D, Maxson A, Smith V, Cents T, Falk-Pedersen O, Gorset O, Hamborg ES. Results from MEA testing at the CO_2 Technology Centre Mongstad. Part I: Post-Combustion CO_2 capture testing methodology. Energy Procedia, Volume 63, 2014, p. 5938-5958.

[4] Faramarzi L, Thimsen D, Hume S, Maxon A, Watson G, Pedersen S, Gjernes E, Fostås BF, Lombardo G, Cents T, Morken AK, Shah MI, de Cazenove T, Hamborg ES, Results from MEA Testing at the CO_2 Technology Centre Mongstad: Verification of Baseline Results in 2015. Energy Procedia, Volume 114, 2017, p 1128-1145.

[5] Gjernes E, Pedersen S, Cents T, Watson G, Fostås BF, Shah MI, Lombardo G, Desvignes C, Flø NE, Morken AK, de Cazenove T, Faramarzi L, Hamborg ES. Results from 30 wt% MEA performance testing at the CO_2 Technology Centre Mongstad. Energy Procedia, Volume 114, 2017, p 1146-1157.

[6] Flø NE, Faramarzi L, Iversen F, Kleppe ER, Graver B, Byntesen HN, Johnsen K. Assessment of material selection for the CO_2 absorption process with aqueous MEA solution based on results from corrosion monitoring at Technology Centre Mongstad. To be presented at GHGT-14, 2018, Melbourne, Australia.

[7] Cost and Performance Baseline for Fossil Energy Plants Volume 1a: Bituminous Coal (PC) and Natural Gas to Electricity Revision 3, July 6, 2015, DOE/NETL-2015/1723.

[8] Morken, AK, Pedersen S, Kleppe ER, Wisthaler A,Vernstad K, Ullestad Ø, Flø NE, Faramarzi L, Hamborg ES. Degradation and Emission Results of Amine Plant Operations from MEA Testing at the CO_2 Technology Centre Mongstad. Energy Procedia, Volume 114, 2017, p 1245-1262.

[9] Gorset O, Knudsen JN, Bade OM, Askestad I. Results from Testing of Aker Solutions Advanced Amine Solvents at CO_2 Technology Centre Mongstad. Energy Procedia, Volume 63, 2014, p 6267-6280.

Monitoring real time, in-line variations of noble gas concentrations during CO_2 capture operations by means of a portable mass spectrometer

(2018)

14th International Conference on Greenhouse Gas Control Technologies, GHGT-14

21st -25th October 2018, Melbourne, Australia

Monitoring real time, in-line variations of noble gas concentrations during CO_2 capture operations by means of a portable mass spectrometer

Anja Sundal[1]*, Ulrich W. Weber[1, 2], Matthias S. Brennwald[2], Philip Ringrose[3, 4], Nina Enaasen Flø[4, 5], Kim Johnsen[4, 5], Leila Faramarzi[4, 5], Per Aagaard[1], Rolf Kipfer[2]

[1]*Department of Geosciences, University of Oslo, Sem Saelands vei 1, 0371Oslo, Norway*
[2]*Swiss Federal Institute of Aquatic Science and Technology, Dübendorf, Switzerland*
[3]*Norwegian University of Science and Technology, Trondheim, Norway*
[4]*Equinor, Norway*
[5]*Technology Centre Mongstad, Norway*

Abstract

In the ICO$_2$P-project the overall aim is to develop an innovative and cost-effective monitoring scheme for CO_2 capture and storage operations, implementing new methods for in situ noble gas measurements. The first step is to establish a basis for fluid source identification by recording temporal variance of noble gas composition in CO_2 product. Studies of noble gases related to CCS typically include few, single point samples. In ICO$_2$P, a portable mass spectrometer (i.e. miniRUEDI) is utilized to directly measure real time variability of the noble gas content in CO_2 gas streams at operating CCS facilities. The first study was performed at the Technology Centre Mongstad (TCM) in Norway, a large-scale test facility for post-combustion CO_2 capture operations. During an open scientific test campaign for amine-based capture (TSA-MEA), noble gases (He, Ar, Kr) as well as CO_2, N_2, O_2 concentrations in the CO_2 product stream were recorded every 10 to 15 minutes during a 5-day period. He concentrations (<0.001ppm)were depleted post-capture and too low for temporal variation measurements in the CO_2 product line. Ar concentrations (0.15 – 0.65 ppm) were significantly higher and temporal variation was successfully recorded in the CO_2 product line. Ar was found to be sensitive to capture operations, e.g. CO_2 recycling ratio. This new approach will provide knowledge of the uniqueness and variability of inherent noble gas fingerprints and depletion/absorption during CCS operations and provide grounds for comparison between fluid origins needed in leakage detection schemes at CO_2 storage sites.

Keywords: CO_2 storage; CO_2 capture; CCS; noble gases; monitoring;

---

* Corresponding author. Tel.: +47 22856652
E-mail address: anja.sundal@geo.uio.no

1. Introduction

During a recent feasibility study [1], to assess the potential for real-time, semi-continuous noble gas monitoring, data were collected from CO_2 capture operations at the Technology Centre Mongstad (TCM) in Norway (Fig. 1), using a novel method for quantitative gas composition measurement. The overall aim has been to contribute towards developing innovative and cost-effective monitoring schemes for CO_2 capture and storage operations, work that is now part of an ongoing research project - the ICO_2P-2 project [1] during 2018-2021.

By recording temporal variance of noble gas composition in CO_2 capture products, the inherent geochemical fingerprint can be evaluated with respect to the potential for source identification at prospective storage sites (i.e. differentiation of sources at CO_2 seepage sites or natural variations in marine and terrestrial environments). Studies so far typically include only a few, single point samples, and there is a clear need for more background data on gas compositions and better sampling strategies to ensure safe storage and reliable leakage detection. The miniRuedi [2] portable mass spectrometer has the capacity to measure low concentrations (i.e. partial pressures) of He, Ar and Kr, as well as CO_2, CH_4, O_2 and other relevant chemical substances with high accuracy at sample intervals of < 15 minutes. This technology proved suitable for monitoring fluctuations in some components of the CO_2-product composition, as tested during an open scientific test campaign for post-combustion capture processes; amine-based temperature swing absorption (TSA), at TCM in summer 2017.

This data set, and further work, will provide important knowledge on absolute variability in CO_2 product from complex and mixed sources. During capture operations and before storage of CO_2 can commence, there is a need to document variability, and to evaluate the inherent compositional signature (and the potential need for adding tracers). This approach will allow for source-specific identification of fluids; differentiating injected (anthropogenic) CO_2 from natural (methanogenic / biogenic) CO_2 rich gases at potential leakage points.

Fig. 1. Technology Centre Mongstad (TCM), Norway [Photo © Equinor] DA amine plant with CHP flue gas inlet from the front, and the high absorber tower in the middle. “Captured” CO_2 product outlet and sample point towards the right.

2. Noble gases as tracers in CCS (and EOR)

Reliable monitoring is a prerequisite for safe, long-term storage and public acceptance of CCS. Terrestrial noble gases (i.e. He, Ne, Ar, Kr, Xe) appear to be suitable natural tracers for monitoring and understanding CO_2-rich gas systems [3]. They are chemically inert and non-degradable. And in contrast to several commonly applied chemical tracers (e.g. PerFluoroCarbons), inherent noble gases are not harmful to the environment and bring no additional cost. The concept of using noble gases for monitoring CO_2 projects has been demonstrated at small-scale onshore facilities, and noble gas data proved to be crucial evidence to rule out an alleged leakage incident at the Weyburn project [4].

However, there are still knowledge gaps: studies so far typically include only a few, single-point samples, and there is a clear need for better data on gas compositions and variability.

To understand large-scale reservoir dynamics and fluid mixing at CO_2 injection sites and along possible leakage paths, experience from research related to multi-phase hydrocarbon systems have to be used and adapted to the scientific case of CCS. Formation water in deep, saline aquifers will have a unique noble gas signature based on a blend of an atmospheric component (stable contents of ^{20}Ne, ^{36}Ar, ^{84}Kr), a deep mantle component (mostly supplying ^{3}He) and a crustal radiogenic component (production of ^{4}He, ^{21}Ne, ^{40}Ar). The signature is a function of time and dependent on the in-situ lithology [5]. Crustal ^{4}He is supplied from radiogenic decay of U and Th in minerals, and ^{40}Ar is produced by radioactive decay of ^{40}K. The mixing ratios of meteoric, mantle and crustal components may yield information about residence times and fluid mixing. E.g., it was found that seepage of methane causes depletion of ^{20}Ne and ^{36}Ar relative to ^{4}He by partitioning, as the heavier noble gas species are more soluble in methane than in water [5]. Exchange between groundwater and oil phase may also be detected as increased ^{20}Ne and ^{36}Ar abundance in oil, as described for the Magnus Field in the British North Sea [6]. Injected CO_2-rich fluid will also interact with formation water and/or hydrocarbon phases present in a storage reservoir. A recent tracer test at the Cranfield enhanced oil recovery (EOR) field in the US, adding Kr and Xe, showed noble gases to be stripped from formation water and into the CO_2 phase [7]. Mapping of the background noble gas abundance before injection is of utmost importance to characterize the natural gas composition and spatial distributions prior to CO_2 injection. This will improve the understanding of CO_2 trapping mechanisms and oil/water/gas partitioning in reservoirs, and form the grounds for comparison needed in leakage detection schemes.

2.1. Compositional variability in captured CO_2

Norway is currently at the forefront in developing CCS, along with Canada, Australia, USA and China. With two active storage sites and a national plan to establish another, larger-scale offshore storage site at Smeaheia, there is an imminent need to prepare reliable, cost-effective and long-term monitoring programs. Noble gas finger-printing can provide an applicable solution, but there is a significant knowledge gap concerning the inherent signature of CO_2 from various capture processes.

At the operative Sleipner and Snøhvit sites, inherent CO_2 from fossil sources (natural gas reservoirs) is captured (as part of the gas processing) and re-injected into a storage formation (saline aquifer). Such single-source storage schemes are expected to display the least degree of temporal variation in the noble gas compositions of injected gas. The noble gas signature of a given natural gas accumulation is related to long-term, slow accumulation rates of e.g. ^{3}He, ^{4}He, ^{21}Ne, ^{40}Ar in a given geological setting. Lateral or vertical compositional gradients in reservoirs related to the lithology and contact time with fluids in traps and along migration paths, may be documented as compositional changes during production. However, these changes are expectedly subtle, compared to complex mixed-source and post-combustion schemes. At the Technology Centre Mongstad (TCM) the source is mixed, and natural gas from several reservoirs are combusted before CO_2-rich flue-gas enters the capture facility. CO_2 is captured from a combination of flue gases; (1) from a combined cycle gas turbine (CCGT) based heat and power plant (CHP) or (2) the residual fluid catalytic cracker (RFCC) at the Equinor refinery at Mongstad. At the CHP plant large quantities of gases from different fossil sources are combined, but after initial mixing and combustion, the signature of the flue gases are expected to become relatively homogenous within a few days. Then, with addition of residual refinery gas, the compositional variability is expected to increase. Further, the combustion process will add an atmospheric component.

Depletion of the radiogenic/nucleogenic components of reservoir derived noble gases occurs during combustion and capture [8]. In the product line recirculation rates, addition of different solutes with given solubilities for the gases and their isotopes under varying pressure and temperature conditions will affect noble gas contents. In this study, we attempt to document temporal changes, and the next step is to interpret and decipher the relative effects of capture processes on noble gas fingerprinting. Additionally, documenting variation in the fossil gas feed is highly relevant in evaluating the traceability of mixed-source gas in future storage schemes, involving captured CO_2 also from other industries (e.g. cement, ammonia, waste incineration, biogas). E.g. the presented storage scheme for Smeaheia involves storage of CO_2 from mixed sources, after post-combustion capture.

3. Methodology

3.1. Capture processes at TCM

The Technology Centre Mongstad (TCM) is a large-scale test facility for CO_2 capture operations. This study was conducted in July 2017 during an open scientific test campaign for post-combustion capture processes, using amine-based temperature swing absorption (TSA) [e.g. 9, 10, 11]. Monoethanolamine (MEA) is used as solvent for CO_2. The combined cycle gas turbine and power plant is run with reservoir gas from different fields in the North Sea mixed with a fraction (up to 50 %) of residual gases from the nearby refinery. Flue gas is fed into the TCM plant, cooled, run through the absorber, before CO_2 is stripped off by heating the solvent and vented to a safe location in a dedicated vent stack (Fig. 2). During the test period, the capture plant was run with flue gas from the CHP plant, with a CO_2 concentration of approximately 4 vol%. In addition, recycling (i.e. return of CO_2 product back to feed gas upstream absorber) was performed, increasing the CO_2 content to mimic concentrations similar to coal combustion capture (Fig. 2).

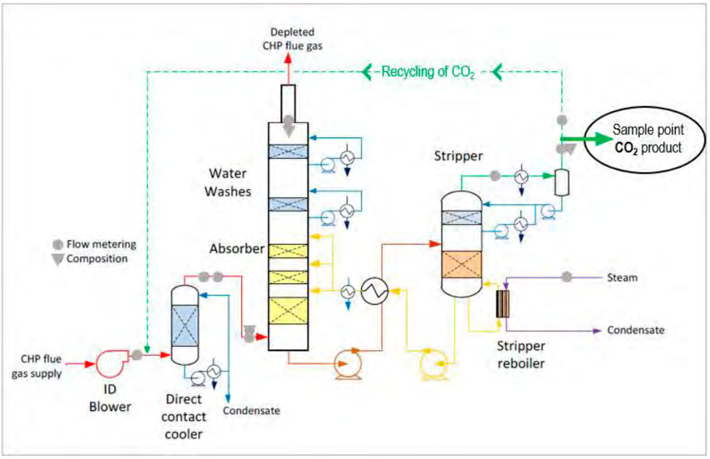

Fig. 2. Post-Combstion CO_2 capture at the Technology Centre Mongstad during TSA-MEA test campaigns. A mobile mass spectrometer was connected to the CO_2 product line. Modified from Thimsen et a. [9]

3.2. Portable mass spectrometer

The adapted mass spectrometric technology for analyzing extremely low concentrations and the isotopic fractionations of He, Ne, Kr, Xe, Ar in water and gas is available only in few laboratories worldwide, with the research laboratory at Eawag/ETH (Zürich) being one of the pioneers in this field.

The miniRuedi (Fig. 3) allows for semi-continuous gas analysis (i.e. partial pressures), and may be used to measure noble gas concentrations. It consists mainly of two vacuum pumps (DP, TP) and a quadrupole mass spectrometer (QMS) with two detectors (Faraday and Multiplier) with different sensitivities. In contrast to fixed laboratory units, no purification by e.g. cryogenics is carried out, which reduces the detection limits, but allows for on-site measurements and smaller instrument units [2]. The instrument has several inlet ports such that a standard gas for calibration and multiple samples can be measured subsequently and automatically without changing the setup. The consumption rate of sample gas is negligible low compared to passing gas streams.

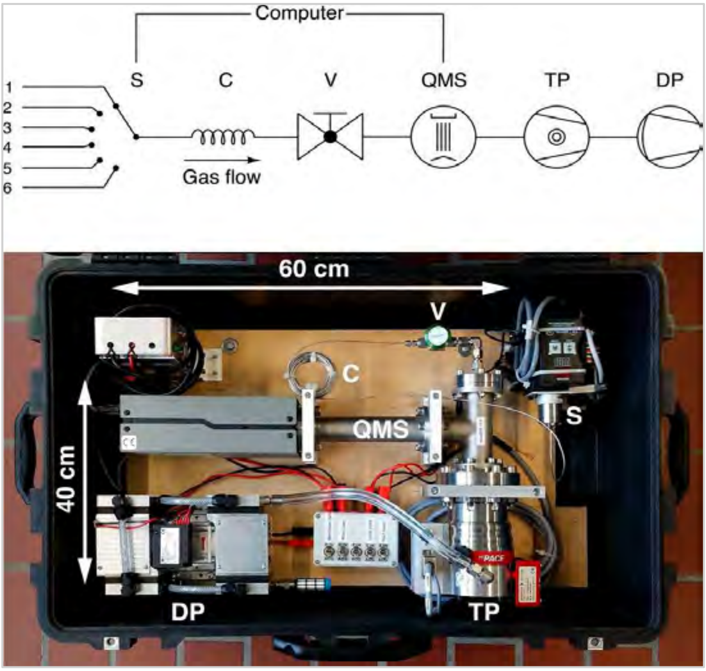

Fig. 3. The miniRuedi portable mass spectrometer (figure from Brennwald et al. [2]) set up with 6-port inlet selector valve (S), capillary (C), inlet valve (V), quadrupole masspectrometer (QMS), turbomolecular pump (TP), and diaphragm pump (DP).

3.3. Sample set-up

A miniRuedi [2] mass spectrometer was connected to the outgoing CO_2 product line, downstream the overhead condenser of the CO_2 stripper (Fig. 2). This stream is water-saturated, and the slip-stream to the instrument was passed through a dryer to avoid the risk of condensation in the instrument. A pressure regulator was mounted between the sample point and the membrane inlet to decrease the inlet pressure to atmospheric pressure. This inlet pressures were fairly constant and recorded with a pressure sensor. The instrument was mounted in less than 1 hour, and ran continuously during a 5-day test period. The analytical sequence was set to repeating cycles of one air-standard analysis block (calibration), followed by three CO_2 output stream sample analysis blocks. An ambient air sample analysis block was added intermittently to remove residual CO_2 from the ion source. The analysis blocks lasted between 10 and 15 minutes depending on the number of components measured. During the test He, H_2O, Ne, N_2, O_2, Ar, CO_2 and Kr were measured. In this way, a unique, semi-continuous data series of gas content was collected and suitable measurement routines were established. Single samples were gathered for lab analysis of noble gas isotopes.

4. Results

The instrument ran steadily throughout the sampling period. However, as this was a feasibility study, parameters such as air-calibration and sampling intervals as well as the selection of analyzed components were tweaked and tested underway. Absolute concentrations of CO_2, O_2 and N_2 were compared with measurements performed by TCM (in-line gas-chromatography). Low concentrations of noble gases throughout the measuring campaign confirm depletion during capture. Kr and Ne were excluded after initial sampling tests, as their partial pressures were below the detection limit. He was too low (< 0.001 ppm) throughout for proper quantification with the miniRuedi, as peak variation could not be deciphered from background. This was confirmed in new, preliminary data analysed after the GHGT poster presentation, and thus He plots are excluded from this final summary. Further studies of single samples and continuous measurement of pre-capture variation (source inlet) are ongoing.

Ar (150 – 650 ppm) contents were significantly higher compared to He, Kr, Ne, and was measured throughout the 5-day sampling period (Fig. 4). Some significant changes were observed (i.e. sudden increase/decrease). The

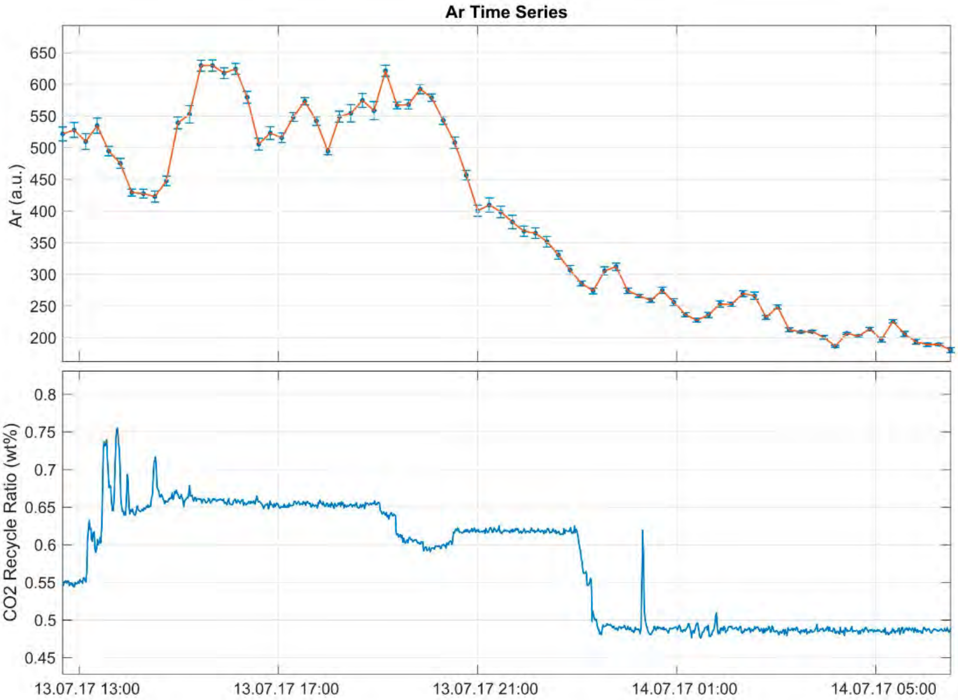

Fig. 4. Measured Ar concentrations (ppm) during the test period 10.07. – 15.07.2017 (upper) displaying co-variance with CO_2 recycle ratio (wt %) at the TCM plant (lower).

analytical error at sampling intervals of 10 - 15 minutes was acceptable, but the standard gas (air) used for calibration was found to be sub-optimal. Ar concentrations appear to be sensitive to changes in the recycle ratio and the capture process (Figs. 4, 5). Preliminary results from single samples confirm that He content is lower in the refinery gas compared to in the natural gas source, and concentrations are expected to vary according to relative contributions from natural gas versus refinery gas (Fig. 6). An observed decline in measured Ar concentrations coincided with reduction of CO_2 recycling in the line, a scheduled process change (Fig. 4).

Fig. 5. Gas flows (kg/h); flue gas, CO_2 product and recycled CO_2.

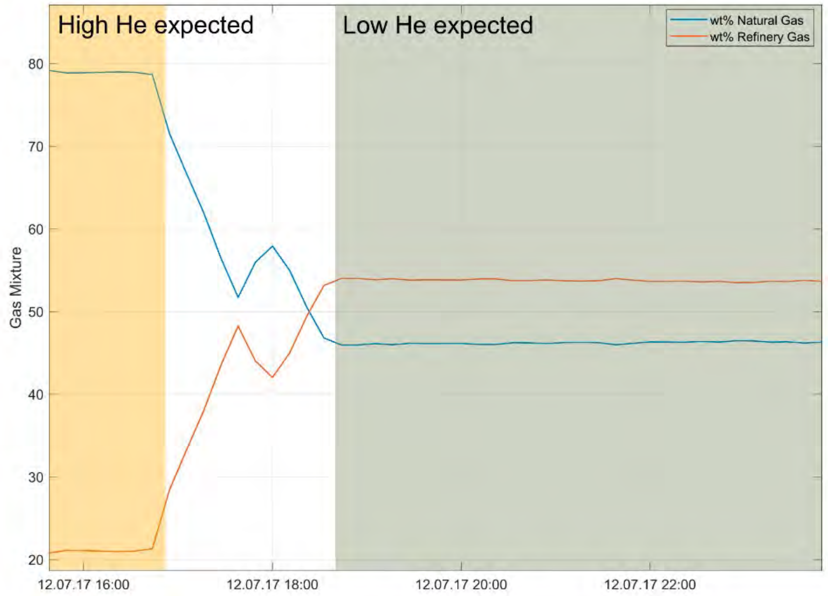

Fig. 6. Change in flue gas composition (wt % refinery gas vs. natural, detail from Fig. 5). Single samples indicate lower He concentrations in RFCC flue gas, such that concentration changes are expected for different mixing ratios.

5. Discussion

The test was successful in that the miniRuedi instrument ran continuously and variation in Ar concentrations were observed and documented. Up to 50 % change in relative concentrations of Ar was observed in the course of 5 days. This shows that there is noble gas variability, and that continuous monitoring is useful to ensure representative sampling in evaluation of inherent fingerprints and traceability. Preliminary single sample results show that concentrations are detectable with our technique before absorption (capture). During gas combustion and in the RFCC process, contamination with air occurs.

Assuming that tests during the capture processing (e.g. recycling) in a regularly working plant are not occurring, variations due to the capture process are expected to be minor. Thus noble gas variation related to source rather than process changes should be measured/detectable at the inlet. This is evaluated in ongoing studies.

The approach of in-line monitoring with a miniRuedi instrument is straightforward. However, optimization is necessary in order to reduce analytical uncertainty. Sample intervals of ~ 10 minutes were found suitable with respect to signal reading time and peak heights, and relative to sample resolution (gradual compositional changes). A customized calibration gas more similar to the CO_2-product should be used in future tests for improved accuracy. Absolute variability in Ar concentrations was registered, and may be used to guide sampling for further chemical analysis and noble gas isotopic signature, ensuring a representative data set of single samples.

TCM is a test facility, and thus the CO_2 product is not stored. There are, however, plans to establish a full value CCS chain in Norway, including storage of CO_2 captured post-combustion [12]. Storage of CO_2 from multiple sources (e.g. fossil fuels, cement, waste incineration) and different capture operations are challenging. Semi-continuous noble gas analysis may allow for pre-injection gas fingerprinting. With regards to detectability at potential leakage sites and separation of different anthropogenic type sources in reservoirs, however, some additional tracer gas may have to be added. At single-source sites (e.g. Snøhvit, Utsira), inherent fingerprints may suffice for source identification. For evaluation of source variability and the effect of the capture process on noble gas signatures, both the flue gas supply (inlet) and CO_2 product (outlet) should be monitored simultaneously. Multiple capillary inlets to the miniRuedi instrument allows for semi-continous monitoring of several sample points. Total variation estimates are useful to guide sampling for isotopic analysis.

Ar concentrations displayed significant variation. During the Ar decrease shown in Fig. 4 the recycling rate was adjusted. Even though this is a change that may not occur in a running large-scale capture site, the dramatic decrease emphasizes that there is a response in the noble gas assembly related to capture process changes. During the test period measurements indicate that noble gases were heavily depleted after capture. He concentrations are significantly lower than atmospheric concentrations (~ 0.00524 hPa). Alternative sampling techniques, e.g. [13], may be tested in further research for gases currently below detection limit (i.e. He, Ne, Kr). Monitoring in-line variation and correlating with isotopic fractions from previous samples will reduce the need for costly and time-consuming lab analysis.

6. Conclusions

The utilization of noble gases as added and/or natural tracers in the context of CO_2 storage monitoring is rather new. As CCS is being upscaled and put into practice, the need for combined and improved monitoring techniques is becoming evident. This feasibility study found that the miniRuedi [2] allows for frequent and accurate measurements of Ar abundance in captured CO_2 from a *post-combustion* like facility (TCM). Preliminary single sample analyses indicate detectability also for continuous measurements of variation in He in the flue gas supply (source) before absorption and depletion during *post-combustion* capture. At *pre-combustion* sites, however, contamination with air is expected to be significantly lower, and considering He concentrations (enriched during radiogenic production) measured in North Sea gas fields [6], monitoring temporal variations for He in the CO_2 product at *pre-combustion* capture sites is feasible. Documentation of variability in live gas streams and guided follow-up sampling for isotopic analysis in the lab will provide an important basis for consideration of noble gas fingerprints in monitoring schemes and leakage detection. This is a new approach that will provide knowledge of the uniqueness of noble gas fingerprints in the product stream from hydrocarbon production, CO_2 capture operations and in the injection line for CO_2 storage.

Acknowledgements

The ICO2P-project is funded by CLIMIT-Demo under grant #616220. The work was also partially funded by the SUCCES FME research center at the Department of Gesociences under grant 193825/S60 from the Research Council of Norway. The authors gratefully acknowledge the staff at TCM DA, Gassnova, Equinor, Shell and Total for their contribution and work at the TCM DA facility. The authors also gratefully acknowledge Gassnova, Equinor, Shell and Total as the owners of TCM DA for their financial support and contribution. We would also like to thank Eawag/ETH for making a miniRuedi instrument available. The project period is scheduled for 2016-2018. A continuation of this project is granted by RCN (#280551), and ICO2P-2 will continue until 2021, including a Ph.D. project. www.mn.uio.no/geo/english/research/projects/ico2p/

References

[1] CLIMIT-Demo feasibility study "ICO2P" under grant 193825/S60: www.mn.uio.no/geo/english/research/projects/ico2p/

[2] Brennwald, M. S., Schmidt, M., Oser, J., and Kipfer, R. (2016). A portable and autonomous mass spectrometric system for on-site environmental gas analysis. *Env.Science & Technology*, 50(24), 13455–13463.

[3] Gilfillan et al. (2008) The noble gas geochemistry of natural CO_2 gas reservoirs from the Colorado Plateau and Rocky Mountain provinces, USA. *Geochimica et Cosmologica Acta*, *72*(4), 1174-1198.

[4] Gilfillan et al. (2017) Using noble gas fingerprints at the Kerr Farm to assess CO_2 leakage allegations linked to the Weyburn-Midale CO_2 monitoring and storage project. *Int. Jour. of Greenhouse Gas Control*, 63, 215-225.

[5] Lollar, B. S., & Ballentine, C. J. (2009). Insights into deep carbon derived from noble gases. *Nature Geosci. 2*(8), 543.

[6] Ballentine, C. J., O'Nions, R. K., & Coleman, M. L. (1996). A Magnus opus: Helium, neon, and argon isotopes in a North Sea oilfield. *Geochimica et Cosmochimica Acta*, *60*(5), 831-849.

[7] Györe et al. (2015). Tracing injected CO_2 in the Cranfield enhanced oil recovery field (MS, USA) using He, Ne and Ar isotopes. *Int. Jour. of Greenhouse Gas Control*, *42*, 554-561.

[8] Flude, S., Johnson, G., Gilfillan, S. M., & Haszeldine, R. S. (2016). Inherent tracers for CCS in sedimentary formations: composition and applications. *Env. Science & Technology*, *50*(15), 7939-7955.

[9] de Koeijer, G., Enge, Y., Sanden, K., Graff, O. F., Falk-Pedersen, O., Amundsen, T., & Overå, S. (2011). CO2 Technology Centre Mongstad–Design, functionality and emissions of the amine plant. *Energy Procedia*, *4*, 1207-1213.

[10] Thimsen et al. (2014). Results from MEA testing at the CO_2 Post-Combstion CO_2 capture testing. Part I: Post-Combstion CO_2 capture testing methodology. *Energy Procedia*, *63*, 5938-5958.

[11] Flø, N. E., Faramarzi, L., de Cazenove, T., Hvidsten, O. A., Morken, A. K., Hamborg, E. S., ... & Fostås, B. F. (2017). Results from MEA degradation and reclaiming processes at the CO2 Technology Centre Mongstad. *Energy Procedia*, *114*, 1307-1324.

[12] Gassnova (2018) Feasibility study for full scale CCS in Norway: www.gassnova.no/en/Documents/Feasibilitystudy...

[13] Manning, C. C., Stanley, R. H., & Lott III, D. E. (2016). Continuous measurements of dissolved Ne, Ar, Kr, and Xe ratios with a field-Deployable gas equilibration mass spectrometer. *Analytical chemistry*, *88*(6), 3040-3048.

CATCHING OUR FUTURE

Dynamic Process Model Validation and Control of the Amine Plant at CO_2 Technology Centre Mongstad

(2017)

energies

Article

Dynamic Process Model Validation and Control of the Amine Plant at CO_2 Technology Centre Mongstad

Rubén M. Montañés [1,*], Nina E. Flø [2] and Lars O. Nord [1]

[1] Department of Energy and Process Engineering, NTNU—Norwegian University of Science and Technology, NO-7491 Trondheim, Norway; lars.nord@ntnu.no
[2] CO_2 Technology Center Mongstad, NO-5954 Mongstad, Norway; nflo@tcmda.no
[*] Correspondence: ruben.m.montanes@ntnu.no; Tel.: +47-73-5073722

Received: 24 August 2017; Accepted: 26 September 2017; Published: 1 October 2017

Abstract: This paper presents a set of steady-state and transient data for dynamic process model validation of the chemical absorption process with monoethanolamine (MEA) for post-combustion CO_2 capture of exhaust gas from a natural gas-fired power plant. The data selection includes a wide range of steady-state operating conditions and transient tests. A dynamic process model developed in the open physical modeling language Modelica is validated. The model is utilized to evaluate the open-loop transient performance at different loads of the plant, showing that pilot plant main process variables respond more slowly at lower operating loads of the plant, to step changes in main process inputs and disturbances. The performance of four decentralized control structures is evaluated, for fast load change transient events. Manipulation of reboiler duty to control CO_2 capture ratio at the absorber's inlet and rich solvent flow rate to control the stripper bottom solvent temperature showed the best performance.

Keywords: pilot plant; transient data; dynamic simulation; flexibility; post-combustion; decentralized control; process dynamics; chemical absorption; CO_2 capture

1. Introduction

Carbon capture and storage (CCS) is a group of technologies that can significantly contribute to the reduction of anthropogenic CO_2 emissions from thermal power generation and other carbon-intensive industries [1]. There are two commercial-scale coal-fired power plants with post-combustion CO_2 capture (PCC) using amines being operated today, at Boundary Dam in Canada [2] and at Petra Nova project at the Parish Power Station in the US [3]. These projects prove the technical feasibility of the technology at commercial scale. Among the different options and technologies for CO_2 capture in thermal power generation, post-combustion CO_2 capture with chemical absorption is considered the more mature technology that can contribute to significantly reducing the carbon intensity ($kgCO_2/kWh_{el}$) of fossil-fueled thermal power plants. In future energy systems with a high penetration of renewable energy sources, the variability in demand and generation will introduce a change in the operating patterns of thermal power generation plants, which will have to change operating conditions [4–6]; there will also be a higher frequency of significant transient events including load changes, and start-up and shut-down events [7,8]. In this regard, Boot-Handford et al.'s carbon capture and storage update 2014 concludes that the financial case for CCS requires that it operates in a flexible manner and that load-following ability is extremely important to the long-term economics [9].

Among the different features of flexible operation of power plants with CCS, an important aspect is the transient behavior of the system when varying operating conditions. This means that efficient operation and emissions and the related operational costs during transient operation will gain importance. However, the operational experience from commercial-scale power plants with post combustion CO_2 capture is scarce and the published transient pilot plant data from test campaigns is limited. Therefore, there is a need for the development of dynamic process models. Dynamic process models can contribute to developing the learning curve for flexible operation of PCC plants. These tools can assist in evaluating the feasibility of flexible operation strategies as well as design process configurations and operational strategies that can lead to the reduction of operational costs and increased revenue during power plant operation. The study of the transient performance with dynamic process models can contribute to identifying process bottlenecks and ease the process scale-up.

Dynamic process models allow the study of the open-loop transient performance of the plant [10], the evaluation of different process configurations and designs [11], the development and implementation of optimal control strategies [12–20], as well as the study of the plant behavior under different operational flexibility scenarios [21,22]. In addition, the power plant and the PCC unit can be treated as an integrated system and dynamic process models can be utilized to analyze the response of the capture unit to changes that occur upstream in the power plant [12,15,19,23–25]. Furthermore, the operational flexibility of the PCC plant can be improved with plant design or using control strategies [26–29]. The core purpose of dynamic process models is to capture the time-dependent behavior of the process under transient conditions. However, the validation of dynamic process models with experiments and pilot plant data is necessary in order to assess the reliability of simulation results.

Kvamsdal et al. [30] developed a dynamic process model of a CO_2 absorber column and used steady-state data from a pilot plant to validate liquid temperature profiles, capture ratio % and rich loading. That work highlighted the necessity of building up a dynamic process model of the integrated system (including stripper, lean/rich heat exchanger, mixing tank and main process equipment), to understand the complexities of dynamic operation of the plant. Gaspar and Cormos [31] developed a dynamic process model of the absorber/desorber process and validated with steady-state plant data. Several publications are available, in which the models were validated only with steady-state pilot plant data [11,32–35]. Biliyok et al. [36] presented a dynamic model validation study where transient data was driven by decrease in solvent flow rate to the absorber, fluctuating concentration of CO_2 at absorber inlet and a varying absorber's feed flue gas stream temperature to the absorber. A dynamic process model developed in Modelica language was validated with transient data from the Esbjerg pilot plant by Åkesson et al. [37]. That data consisted of the transient performance after one step-change in flue gas mass flow rate. An extensive review work by Bui et al. [38] concluded that research efforts are required on producing transient pilot plant data.

More recent works have included validation of dynamic process models with transient plant data from pilot plants. A K-Spice model by Flø et al. was validated with pilot plant data from the Brindisi pilot plant [39]. Flø et al. [40] validated a dynamic process model of CO_2 absorption process, developed in Matlab, with steady-state and transient pilot plant data from the Gløshaugen (Norwegian University of Science and Technology (NTNU)/SINTEF) pilot plant. Van de Haar et al. [41] conducted dynamic process model validation of a dynamic process model in Modelica with transient data from a pilot plant located at the site of the coal-fired Maasvlakte power plant in the Netherlands. Gaspar et al. [42] conducted model validation with transient data from two step changes in flue gas volumetric flow rate from the Esbjerg pilot plant. Other works include the validation of equilibrium-based models such as that of Dutta et al. [43]; or the work by Chinen et al. [44] which conducted dynamic process model validation of a process model in Aspen Plus® with transient plant data from the National Carbon Capture Center (NCCC) in the US. Manaf et al. [45] developed a data-driven black box mathematical model, based on transient pilot plant data, by means of system identification. In addition, dynamic process models have been developed to study the transient behavior of the chemical absorption CO_2 capture process using piperazine (PZ) as chemical solvent [19,20]. It should be noted that the majority of work has been conducted for typical flue gas compositions from coal-based power plants with CO_2 concentration around 12 vol % [38].

From the literature review it can be concluded that dynamic process model validation is a challenging process due to:

- The scarce availability of transient or dynamic pilot plant data.
- Most available data is found from small-scale pilot plants. That has implications for the reliability of simulation results when applying dynamic process models to scaled-up applications.
- The works involving transient data generally include the response of the plant to disturbances in a few process variables.
- Most of the validation work was done for flue gas with a typical CO_2 content from coal-based power plants.

Flexible operation of PCC plants has been studied with pilot plant test facilities in test campaigns. Faber et al. [46] conducted open-loop step change responses at the Esbjerg pilot plant; this type of analysis helps in understanding the transient performance of the process. They concluded that the overall system acts as a buffer to perturbations at the plant inlet and that the coupled operation of the absorber/desorber unit led to fluctuations in the system when all parameters—flue gas and solvent mass flow rates and reboiler duty—are changed simultaneously. Bui et al. [47] presented a flexible operation campaign conducted at the Commonwealth Scientific and Industrial Research Organization (CSIRO)'s PCC pilot plant in Australian Gas Light Company (AGL) Loy Yang, a brown-coal-fired power station in Australia. The generated transient data included step changes in flue gas flow rate, solvent flow rate and steam pressure. The purpose of the study was to generate a set of data for validation of dynamic process models, and to gain insight into process behavior under varying operating conditions. A different approach was taken by Tait et al. [48] who conducted experiments that simulated flexible operation scenarios on a pilot plant to treat synthetic flue gas with a CO_2 concentration of 4.3 vol%, typical of a natural gas combined cycle (NGCC) plant. Tests for transient operation have been conducted at the amine plant at CO_2 Technology Center Mongstad (TCM DA). De Koeijer et al. presented two cases: a first case with controlled stop-restart of the plant, driven by a controlled stop of flue gas and steam sent to the PCC plant; and a second case with sudden stop of the blower upstream of the absorber [49]. Nevertheless, a limited amount of transient testing can be conducted during test campaigns. A thoroughly validated dynamic process model can help to study the transient performance, controllability, and flexible operation of the plant and process dynamics via dynamic process simulation.

In this work, a suitable set of steady-state and transient plant data, collected from a MEA campaign at CO_2 Technology Center Mongstad, is selected for dynamic process model validation purposes. The plant was operated with flue gas from a natural gas fueled combined heat and power plant. The selected data is utilized to validate a dynamic process model of the amine-based CO_2 absorption-desorption process at TCM DA. Then, the validated model is employed to carry out two case studies on the process dynamics of the TCM DA amine plant. In the first case study, the open-loop transient response of the pilot plant at different operating loads of the plant is analyzed. In the second case study, the performance of four decentralized control structures of TCM DA amine pilot plant is evaluated for fast disturbances in flue gas volumetric flow rate.

2. Materials and Methods

2.1. Plant Description

CO_2 Technology Center Mongstad test site has a pilot-scale amine-based chemical absorption process plant. The amine plant can be configured to treat flue gas from a catalytic cracker from the Mongstad refinery, with CO_2 content of around 13–14 vol%, typically found in flue gas from coal-fired power plants, and also to treat exhaust gas coming from a combined cycle gas turbine combined heat and power plant (CHP), with CO_2 content of around 3.5 vol%. A fraction of the product CO_2 mass flow rate can be re-circulated back upstream of the direct contact cooler (DCC) to increase the CO_2 content, so CO_2 concentrations of between 3.5 and 13–14 vol% could be fed to the plant to simulate the effects of exhaust gas recirculation [50]. Table 1 presents data of the main process equipment of TCM DA amine plant when configured to treat CHP flue gas, which has a total flue gas capacity of

60,000 Sm^3/h and can capture around 80 ton CO_2/day. Figure 1 shows a simplified process flow sheet of the amine plant at TCM DA when configured for CHP gas. A slipstream of exhaust gas is extracted from the CHP plant placed next to the TCM DA facility, and it consists of about 3% of the total exhaust gas. An induced draft blower is utilized to blow the flue gas flow. It has variable speed drives that allow the flue gas volumetric flow rate fed to the absorber column to be manipulated. Upstream the absorber column, a direct contact cooler cools down and saturates the flue gas with water, by means of a counter-current flow stream of water.

Table 1. Size and materials of main process equipment at the amine plant at TCM DA with CHP stripper configuration.

Absorber	
Column cross sectional area (m^2)	3.55 × 2
Column height (m)	62
Packing height (12 + 6 + 6) (m)	24
Water wash section height (3 + 3) (m)	6
Absorber packing type	Koch Glitsch Flexipac 2X
Absorber washer packing type	Koch Glitsch Flexipac 2Y HC
CHP Stripper	
Column cross sectional area (m^2)	1.33
Diameter (m)	1.3
Packing height (m)	8
Water wash section height (m)	1.6
Absorber packing type	Koch Glitsch Flexipac 2X
Absorber washer packing type	Koch Glitsch Flexipac 2Y HC
Heat Exchanger L/Rich	
Duty (kW)	10358
Heat transfer area (m^2)	308
Material	SS 316L
Reboiler	
Duty (kW)	3365
Heat transfer area (m^2)	142
Material	SS 316L
Lean Amine Cooler	
Duty (kW)	5182
Heat transfer area (m^2)	78.8
Material	TITANIUM

A chemical absorption process occurs in the absorber column, where the chemical solvent, flowing from top to bottom, meets the flue gas flowing in counter-current. The absorber column consists of a rectangular polypropylene-lined concrete column with a height of 62 m and a cross-section of 2 × 3.55 m. The absorber-packed sections consisting of Flexipac 2X (Koch-Glitsch Italia, Vimercate, Italy) structured stainless-steel packing are distributed from bottom to top in three sections of 12 m, 6 m and 6 m. Two water-wash systems are installed in the top of the absorption column, consisting of two sections of Flexipac 2Y HC (Koch-Glitsch Italia, Vimercate, Italy) structured stainless-steel packing. The water-wash sections limit emissions and are used to keep the water balance of the plant. The upper water-wash sections can be operated as acid wash [51]. In addition, the plant can be configured to use different packing heights in the absorber column resulting in 12, 18 or 24 m. This can be implemented at TCM plant by introducing all the lean solvent flow at 12 m of absorber packing, 18 m of absorber packing (12 + 6) m or 24 m of absorber packing (12 + 6 + 6) m.

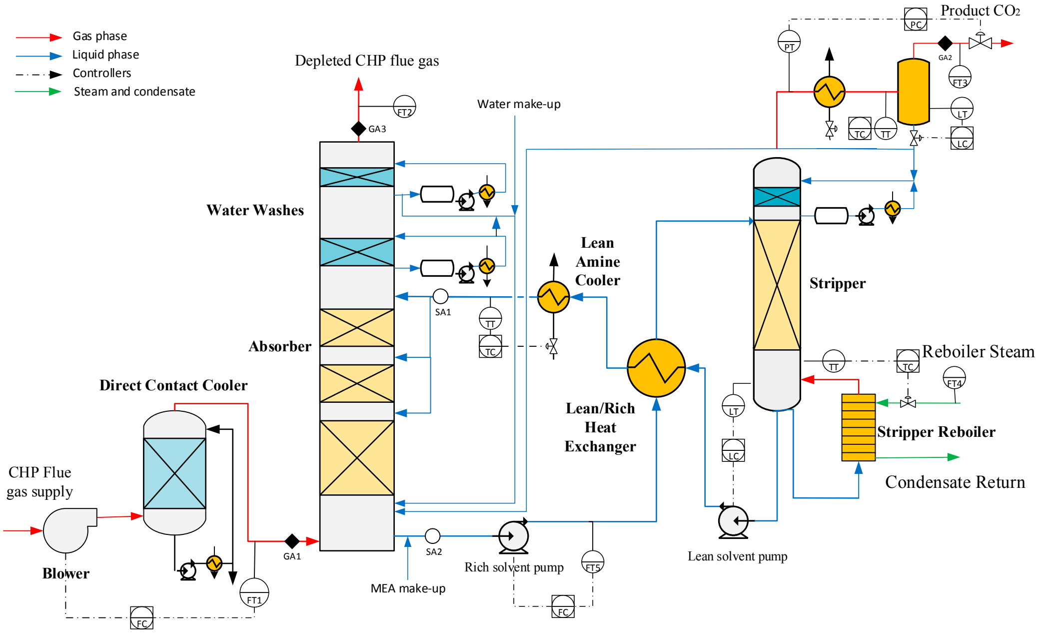

Figure 1. Simplified process flow sheet of the amine plant at CO_2 Technology Center Mongstad, when configured to treat flue gas from a natural gas-fired power plant. The figure shows the location of some gas analyzers (GA), solvent analyzers (SA), flow transmitters (FT), pressure transmitters (PT), temperature transmitters (TT) and level transmitters (LT). The main process controllers of the regulatory control layer are shown, including flow controllers (FC), temperature controllers (TC), pressure controllers (PC) and level controllers (LC).

A 10.4 MW plate and frame heat exchanger is present at the plant where the cold rich amine solution coming from the absorber sump cools down the hot lean amine solution coming from the stripper. In addition, a 5.2 MW lean amine cooler is utilized to set the temperature of the lean solvent conducted to the top of the absorber packing sections, by using a stream of cooling water. The rich solvent is pumped to the top of the stripper column, where it meets the stripping vapors generated in the reboiler. The CHP stripper with overhead condenser system consists of an 8 m column of Koch Glitsch Flexipac 2X structured stainless-steel packing of 1.3-m-diameter, and a water-wash system with Koch Glitsch Flexipac 2Y HC structured stainless-steel packing of 1.6 m of height. The stripper reboiler consists of a 3.4 MW thermosiphon steam-driven system that supplies the heat required for the desorption process. The steam supplied to the reboiler comes from the refinery situated next to the TCM DA facility. Details on the steam supply system can be found in Faramarzi et al. [51].

2.2. Pilot Plant Configuration and Instrumentation

The TCM DA amine plant can be utilized to test various chemical solvents. In this work, the tests were conducted with 30 wt. % aqueous monoethanolamine (MEA). During the tests conducted in the test campaign, the responses and performance of the pilot plant were logged and extracted every 30 s. Gas composition was logged with gas analyzers at the inlet of the absorber, outlet of the absorber, and the product CO_2. A gas chromatograph (GC) installed at TCM DA plant can measure concentrations of CO_2, N_2, H_2O and O_2 at the three locations in a nearly simultaneous manner, which is a desired feature for transient tests; refer to GA1, GA2 and GA3 in Figure 1. Details on gas analyzers and instrumentation at TCM DA plant can be found in [51].

Gas phase flow rates were measured at the plant during the tests. The flue gas volumetric flow rate fed to the absorber is measured with an ultra-sonic flow meter (FT1). As discussed by Faramarzi et al. in [51], the depleted flue gas flow meter (FT2) had a higher degree of variability than FT1, and some transients were observed on the FT2 measurement that were not explained by changes in process parameters at the plant. Therefore the depleted flue gas flow rate was calculated in the test campaign by considering that all O_2 and N_2 fed to the absorber goes out of the plant with the depleted flue gas. The cooled product CO_2 discharge flow (FT3) was measured with a vortex flow meter. Other flow rates measured at the plant include the steam fed to the reboiler, the lean amine flow rate at the absorber inlet and the rich amine flow rate at the absorber outlet. For flue gas flow meters, the standard conditions are 15 °C and 101.3 kPa [51].

Pressures and pressure drops at different components of the plant were logged. In addition, main process temperatures were logged. For process model validation, it is common to assess the model prediction of the absorber and stripper temperature profiles. Within the absorber and stripper columns of TCM DA's amine plant there are four temperature sensors distributed in the radial plane per meter of packing in the axial direction. Thus, there are 96 temperature sensors within packed segments of absorber column and 28 temperature sensors within the packed segment in the stripper column. These measurements allow the creation of clear temperature profiles of the absorber and stripper columns in the axial direction (at each column height, the resulting temperature value is the average of the four measurements distributed in the radial plane).

Online solvent analysis measurements (SA) were taken at the inlet (SA1) and outlet of the absorber (SA2); refer to Figure 1. The measurements include pH, density and conductivity. In addition, solvent samples were regularly taken manually and analyzed onsite. These analyses allow MEA concentration and CO_2 loadings to be calculated at the sampling points on a periodic basis. The actual reboiler duty was estimated as suggested in Thimsen et al. [52]. Equation (1) shows the calculation of the actual reboiler duty, where F_{steam} is the logged measurement data of steam mass flow rate (refer to FT4 in Figure 1), T_c is the condensate temperature, T_g is the superheated steam inlet temperature, p_g is the steam pressure at inlet, and p_c is the condensate pressure. Enthalpy was calculated with the use of accurate steam tables, with the condensate at the reboiler outlet assumed to be saturated liquid at T_c or p_c. The specific reboiler duty (SRD) in kJ/kgCO_2 is calculated as in Equation (2), where F_{prod} is the CO_2 rich product mass flow rate; refer to FT3 in Figure 1.

$$\dot{Q}_{reb} = F_{steam}\left(h_g\left(T_g, p_g\right) - h_c\left(T_c, p_c\right)\right) \tag{1}$$

$$SRD = \frac{\dot{Q}_{reb}}{F_{Prod}} \tag{2}$$

During the tests presented in this work, the averaged total inventory of aqueous MEA was around 38.2 m^3. Averaged values of liquid hold-ups and its distribution at different components of the plant during the steady-state tests included in this work are presented in Table 2. Detailed data on solvent inventory distribution throughout the plant is of importance in order to obtain suitable dynamic process simulation results. The regulatory control layer of the plant was active during the tests conducted in the MEA campaign. The main control loops of the regulatory control layer are presented in Figure 1. Note that the actual regulatory control layer of the amine plant at TCM DA is more complex and includes more control loops for auxiliary equipment, stable and safe operation of the plant, and start-up and shut-down sequences. The control loops included here are those the authors found relevant for the purposes of dynamic process modeling and simulation of this plant during online operation, and considering the time scales of interest for process operation.

Table 2. Averaged values of total solvent inventory and its distribution within the main components of the TCM plant.

PCC Plant Main Components	Solvent Inventory (m^3)
Absorber sump	8.1
Absorber packing	8.4
CHP stripper packing	1.0
CHP stripper sump	2.3
CHP reboiler	0.4
Cold rich solvent pipe	2.2
Cold lean solvent pipes	5.2
Hot rich solvent pipe	1.1
Hot lean solvent pipes (including reboiler pipes)	8.2
Lean/rich hx—lean side	0.5
Lean/rich hx—rich side	0.5
Lean cooler	0.3
TOTAL	38.2

2.3. Dynamic Process Model

Dynamic process modeling was carried out by means of the physical modeling language Modelica [53]. Modelica allows development of systems of differential and algebraic equations that represent the physical phenomena occurring in the different components of the system. The process models of the equipment typically found in a chemical absorption plant were obtained from a Modelica library called Gas Liquid Contactors (Modelon AB, Lund, Sweden) [54], and the commercial tool Dymola (Dassault Systèmes, Vélizy-Villacoublay, France) [55] was utilized to develop the models and carry out the simulations. The component models include absorber and stripper columns, sumps, lean and rich heat exchanger, stripper reboiler, overhead condenser, condensers, pipe models, pumps, valves, measurements and controllers. The dynamic process model of the amine plant at TCM DA presented in Figure 1 was developed by parameterizing, modifying and connecting the different models. For this purpose, the main process equipment, size, geometry and materials were considered; refer to Table 1. A key aspect for obtaining suitable dynamic simulation results is the consideration of the distribution of solvent inventory at the different equipment of the plant. Therefore, solvent inventory distribution was implemented in the dynamic process model; refer to Table 2. Finally, the equivalent regulatory control layer of the plant was applied in the dynamic process model; discussed later in Section 5.2. The models contained in the library have been presented elsewhere [56,57]; therefore only an overview of the models is presented in the following. Numerical integration of the resulting system of differential and algebraic equations was carried out in Dymola with the differential algebraic system solver (DASSL) implemented in Dymola [55]. The main assumptions applied are [56]:

- All chemical reactions occur in the liquid phase and are assumed to be in equilibrium.
- The flue gas into the absorber contains only CO_2, O_2, H_2O and N_2.
- MEA is non-volatile and not present in the gas phase.
- The total amount of liquid in the column is defined as the packing hold-up and the sump liquid hold-up.
- The reboiler is modeled as an equilibrium flash stage.
- The liquid in the column sumps and other large volumes are assumed to be ideally mixed.
- Mass and heat transfer between liquid and gas phase is restricted to packed section.
- Negligible temperature difference between the liquid bulk and interface to gas phase.
- No storage of mass and energy in the gas phase.
- All liquid from the packing bottom in the stripper is fed to the reboiler with a constant liquid level.
- Constant target packing hold-up.

The models of the absorber and stripper columns are developed based on the two-film theory; therefore, at the gas and liquid interface thermodynamic equilibrium is assumed. Interface mass transfer phenomena is modeled in packed sections with a rate-based approach with enhancement factor E [30], which takes into account the enhanced mass transfer due to chemical reactions; refer to Equations (3) and (4), where $c_{i,if}$ and $c_{i,b}$ are molar concentrations at liquid bulk and interface, A_{if} is the contact area, k_i are the mass transfer coefficients by Onda [58], T is the bulk phase temperature, and p_i are the partial pressures of the species in the gas phase. The pseudo-first order enhancement factor E is calculated as in Equation (5), where k_{CO_2} is the overall reaction constant for CO_2 and C_{MEA} the molar free MEA-concentration taken from [59], the diffusivity D_{CO_2} of CO_2 in aqueous MEA is calculated by the Stokes-Einstein relation and the diffusivity of CO_2 in water from [60]. C_{ef} is a pre-multiplying coefficient for calibration of enhancement factor. The packing characteristics of Koch Glitsch Flexipac 2X were considered for parameterizing the packing segments of the dynamic process model for absorber and stripper columns, with a surface area of 225 m^2/m^3 and a void fraction of 0.97.

$$\dot{n}_{i,l} = A_{if} k_{i,l} E \left(c_{i,b} - c_{i,if} \right) \qquad i = CO_2 \tag{3}$$

$$\dot{n}_{i,v} = \frac{A_{if} K_{i,v} \left(p_{i,b} - p_{i,if} \right)}{RT} \qquad i = CO_2,\ H_2O \tag{4}$$

$$E = C_{ef} \frac{\sqrt{C_{MEA} k_{CO_2} D_{CO_2}}}{k_{i,l}} \qquad i = CO_2 \tag{5}$$

Phase equilibrium at the gas-liquid interface is calculated as in Equations (6) and (7), where the solubility of CO_2 in water is considered by Henry's law, with He_i from [61]; activity coefficients γ_i are implemented from [61]; chemical equilibrium is assumed at the interface and liquid bulk, and the chemical equilibrium constants K_i implemented in the process model are obtained from Böttinger [61]. The Van't Hoff equation is utilized in order to infer the heats of reaction ΔH_r from the equilibrium constant; refer to Equation (8). The Chilton-Colburn analogy was employed to correlate sensible heat transfer between phases with the gas phase mass transfer coefficient. Latent heat connected to the transferred mass flow from one phase to the other is considered in the specific enthalpies of the individual species. The heat of evaporation and heat of solution are a function of temperature but are considered constant with solvent CO_2 loading. The gas phase model assumes ideal gas law, and the pressure of the column p is determined by the gas phase pressure drop.

$$y_i p = \gamma_i x_i \, He_i \; i = CO_2 \tag{6}$$

$$y_i p = \gamma_i x_i \, p_{i,sat}(T) \; i = H_2O \tag{7}$$

$$\frac{dlnK}{dT} = \frac{\Delta H_r}{RT^2} \tag{8}$$

The lean-rich heat exchanger is modeled as a static heat exchanger model with the ε-NTU (effectiveness—number of thermal units), and pure transport delay models are used to account for dead times included by the solvent hold-up within piping' volumes.

At the top of the absorber column a washer model is implemented, consisting of a volume model with phase separation that saturates the gas with water at the targeted temperature. A make-up stream of water is injected in the absorber sump to keep the H_2O mass balance of the system. MEA is assumed non-volatile in the model and therefore it is only present in the liquid phase. However, in the actual plant make-up MEA is required for operation and it is injected upstream the rich amine pump; refer to Figure 1.

3. Steady-State Validation of Dynamic Process Model

3.1. Steady-State Operating Cases

A test campaign was conducted at the amine plant at TCM DA using MEA, operated from 6 July until 17 October 2015. Table 3 shows the steady-state cases generated during the test campaign that were used in this work for dynamic process model validation purposes. The plant was operated with 30 wt. % MEA for all cases. The objective was to select a set of steady-state cases from the MEA campaign that could represent a wide range of steady-state operating conditions, including data from full capacity of volumetric flow rate fed to the absorber column. The steady-state cases were generated by varying the set points of the main pilot plant inputs, namely solvent circulation flow rate F_{solv} (refer to FT5 in Figure 1), reboiler duty ($\dot{Q}_{reb}$), and flue gas volumetric flow rate (F_{gas}). The steady-state cases represent a variation in operating conditions of the plant, especially on the flue gas volumetric flow rate load of the absorber, CO_2 capture rate, L/G ratio in the absorber and absorber packing height. Cases 1 to 5 are operated at absorber full flue gas capacity of around 60,000 Sm^3/h. A similar mass-based L/G ratio, of around 0.89, is kept in the absorber column during the steady-state operating cases with full capacity, with the exception of Case 4, where it is changed to 0.8, by varying the rich solvent mass flow rate. The main process variability in these cases is the change in reboiler duty, with CO_2 capture rate ranging from 85 to 68%. CO_2 capture rate was calculated with the method 1 described by Thimsen et al. [52]; refer to Equation (9), where F_{prod} refers to the product CO_2 flow rate (FT3 in Figure 1), and X_{CO_2} is the mass fraction of CO_2 in the absorber inlet (measured at GA1 in Figure 1). Note that here CO_2 capture rate has been named *Des* as it defines the desorption ratio utilized in Section 5.2. In addition, Cases 2 to 5 were operated with 18 m absorber packing, i.e., the uppermost absorber-packing segment is kept dry. Cases 6 to 10 are operated with 24 m absorber packing and the absorber column at 80% volumetric flue gas flow rate capacity. The mass-based L/G ratios on the absorber range from 1.34 to 0.75 for Cases 6 to 10, by varying solvent circulation mass flow rate. The capture rate is kept constant at around 85% by varying the reboiler duty.

Table 3. A selection of steady-state data cases obtained from the test campaign conducted at TCM plant during autumn 2015. The plant was operated with 30 wt. % aqueous MEA.

Case	1	2	3	4	5	6	7	8	9	10
Gas flow rate (Sm^3/h)	59,461	59,468	59,442	59,499	59,544	46,973	46,973	46,973	46,973	46,973
Rich solvent flow rate (kg/s)	17.33	17.31	17.22	15.50	17.24	20.56	17.50	16.11	12.74	11.46
L/G ratio (kg/kg)	0.89	0.89	0.89	0.80	0.89	1.34	1.14	1.05	0.83	0.75
Reboiler duty (kW)	3417	3159	2664	2397	3056	2745	2669	2667	2659	2682
Absorber inlet gas CO_2 (vol%)	3.64	3.61	3.59	3.58	3.59	3.60	3.62	3.62	3.62	3.62
Absorber inlet gas O_2 (vol%)	15.52	15.54	15.55	15.46	15.35	15.30	15.48	15.49	15.51	15.52
Absorber inlet gas H_2O (vol%)	3.98	3.92	3.93	4.01	4.22	3.80	3.36	3.46	3.52	3.43
Absorber inlet gas N_2 (vol%)	79.09	79.02	78.85	78.57	78.20	78.18	78.88	78.94	79.06	78.96
Loading rich (mol/mol)	0.490	0.485	0.498	0.500	0.495	0.475	0.488	0.486	0.493	0.491
Loading lean (mol/mol)	0.280	0.294	0.333	0.341	0.314	0.342	0.329	0.310	0.260	0.229
Stripper bottom temperature (°C)	120.9	121.1	119.1	118.9	120.1	116.6	118.3	119.1	121.4	121.8
CO_2 product flow (kg/s)	0.95	0.89	0.75	0.68	0.84	0.74	0.74	0.75	0.77	0.76
CO_2 capture rate (%)	85	80	68	-	75	85	85	85	85	85
Absorber packing height (m)	24	18	18	18	18	24	24	24	24	24

The first series of tests during the MEA campaign were dedicated to verification of mass balances of the plant [50]. CO_2 mass balance gives results close to 100%, and Gjernes et al. [50] conclude that CO_2 mass balance based on gas phase can be maintained at a level better than 100 ± 5%. In this work, the suggested method in [50] was used during data selection in order to ensure that the steady-state data cases presented in Table 3 have acceptable CO_2 mass balance.

In order to develop the overall dynamic process model of the plant, the steady-state data for Case 1, refer to Table 3, was used as a reference to calibrate the dynamic process model, and the main outputs from the model simulations were compared with the plant data. This data set was chosen since it represents the baseline operating conditions of the amine plant at TCM DA when using aqueous MEA as chemical solvent, as presented in Faramarzi et al. [51]. The models of the different subsystems of the plant consisting of (i) absorber column; (ii) lean/rich heat exchanger; and (iii) stripper column with overhead condenser and reboiler were calibrated separately, and then linked to form the overall dynamic process model. The model was calibrated by tuning a pre-multiplying coefficient C_{ef} for the enhancement factor E. It was set to 0.28 in absorber packed segments and 0.01 in stripper packed segments. The validation section included in this work extends on work conducted previously [62].

$$Des = \frac{F_{prod}}{F_{gas} \cdot X_{CO_2}} \tag{9}$$

3.2. Validation Results of Dynamic Process Model with Steady-State Plant Data

The results from the simulated dynamic process model for the steady-state operating cases, described in Section 3.1, are displayed in Table 4. The results shown are for main process variables during pilot plant operation, namely CO_2 lean (L_l) and rich (L_r) loadings, product CO_2 flow rate (F_{prod}), specific reboiler duty (SRD) and stripper bottom temperature T_{str}. Possible deviations in dynamic process model prediction arise from errors related to measurement uncertainty and to modeling uncertainty, the latter being related to the fact that a physical model is always a simplification of reality. This means that it is natural to observe some deviation in the prediction of the dynamic process model simulation. Therefore, it is of importance to quantify these errors so that they are kept within reasonable bounds. The absolute percentage errors (AP) and the mean absolute percentage errors (MAP) are calculated as in Equations (10) and (11), where x_m is the value of the process variable predicted by the process model simulation, x_p is the value of the process variable measured at the pilot plant at the given steady-state operation case, and n is the number of steady-state cases studied.

$$AP = 100 \cdot \left| \frac{(x_m - x_p)}{x_p} \right| \tag{10}$$

$$MAP = 100 \cdot \sum_{i}^{n} \frac{\left| \frac{(x_{m,i} - x_{p,i})}{x_{p,i}} \right|}{n} \tag{11}$$

The results for lean CO_2 loading are presented in Figure 2 with a parity plot, where ±5% and ±10% error lines are also shown. It is clear that the dynamic process model under-predicts lean loading for most of the cases, with a $MAP < 6.6\%$. In addition, Figure 2 shows the parity plot for CO_2 product flow rate; in this case, the CO_2 product flow rate is also under-predicted by the dynamic process model, with a $MAP < 5.3\%$. Figure 3 shows the parity plot for stripper bottom temperature, with the ±2% error lines plotted; stripper bottom temperature T_{str} presented a $MAP < 1\%$. From the parity plots, one can observe that, despite the errors found in the absolute values predicted by the dynamic process model with respect to the reference plant data, the dynamic process model can predict the variability in the main process variables for a wide range of steady-state operating conditions.

Table 4. Results from dynamic process simulation of the amine plant at TCM for the 10 steady-state operation cases. The pilot plant data for solvent CO_2 lean loading (L_l), solvent CO_2 rich loading (L_r), CO_2 product flow rate (F_{prod}), specific reboiler duty (*SRD*) and stripper bottom temperature (T_{str}) are shown. In addition, the model prediction during steady-state simulation for the same process variables is shown. Calculated absolute percentage errors (*AP*) and mean absolute percentage errors (*MAP*) between pilot plant measurements and simulated model predictions for the 10 steady-state operating cases are presented.

Case		1	2	3	4	5	6	7	8	9	10
Rich loading L_r (mol/mol)	Pilot plant	0.489	0.485	0.498	0.500	0.495	0.475	0.488	0.486	0.493	0.491
	Model	0.514	0.513	0.514	0.514	0.513	0.512	0.513	0.514	0.514	0.514
	AP	5.01	5.58	3.19	2.91	3.55	7.81	5.17	5.62	4.43	4.70
	MAP										4.80
Lean loading L_l (mol/mol)	Pilot plant	0.282	0.294	0.333	0.341	0.314	0.342	0.329	0.310	0.260	0.229
	Model	0.257	0.273	0.309	0.306	0.279	0.343	0.312	0.292	0.241	0.224
	AP	8.93	7.24	7.16	10.06	11.34	0.35	4.98	5.94	7.10	2.35
	MAP										6.55
CO_2 Product flow F_{prod} (kg/sec)	Pilot plant	0.95	0.89	0.75	0.68	0.84	0.74	0.74	0.75	0.77	0.76
	Model	0.90	0.84	0.72	0.65	0.82	0.70	0.71	0.72	0.70	0.67
	AP	4.97	4.72	5.18	4.38	1.96	4.65	3.50	3.44	8.46	11.42
	MAP										5.27
Specific reboiler duty *SRD* (kJ/kg)	Pilot plant	3602	3562	3533	3509	3651	3727	3613	3561	3463	3538
	Model	3791	3739	3726	3670	3724	3909	3744	3688	3783	3994
	AP	5.23	4.95	5.46	4.58	2.00	4.88	3.63	3.56	9.24	12.89
	MAP										5.64
Stripper bottom temperature T_{str} (°C)	Pilot plant	120.9	121.1	119.1	118.9	120.1	116.6	118.3	119.1	121.4	121.8
	Model	121.0	119.8	117.2	117.2	119.4	114.7	117.0	118.3	121.0	121.8
	AP	0.08	1.06	1.63	1.42	0.61	1.62	1.10	0.71	0.31	0.04
	MAP										0.86

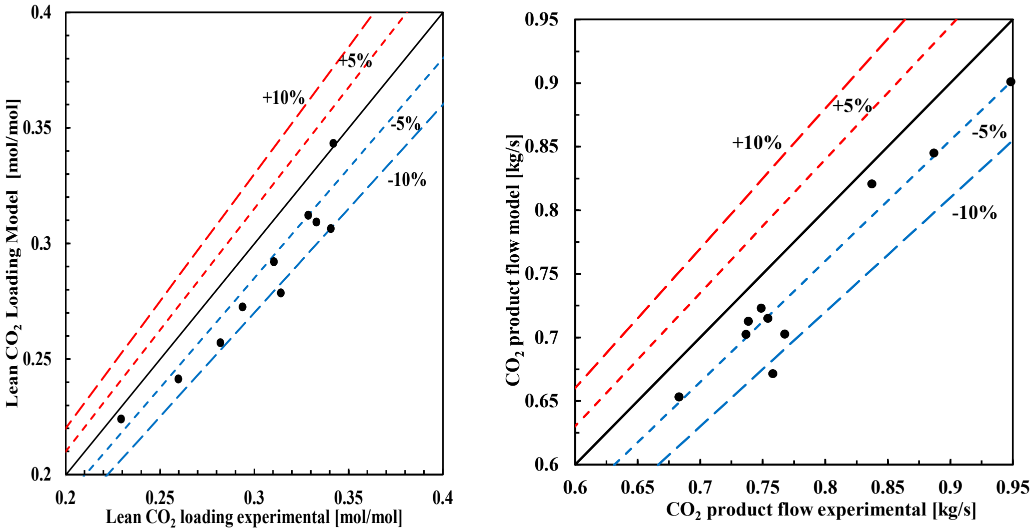

Figure 2. Parity plots of lean CO_2 loading (**left**) and CO_2 product flow rate (**right**). Lines for +10%, +5%, −5% and −10% percentage error are shown. The mean percentage error is <6.6% for CO_2 lean loading and <5.3% for product CO_2 flow rate (F_{prod}).

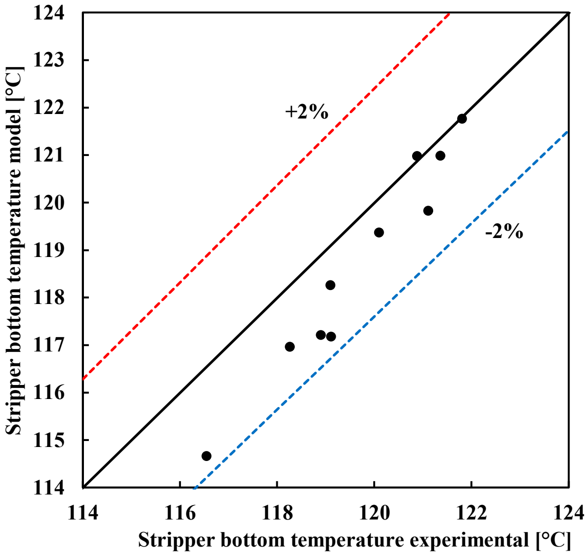

Figure 3. Parity plot for stripper bottom temperature for the 10 steady-state operation cases. Lines for +2% and −2% percentage errors are shown. The mean percentage error is 0.86 for stripper bottom temperature.

Temperature within absorber and stripper column is an important process variable since it affects phase equilibrium at liquid and gas-liquid interface. Some important model parameters and thermophysical properties depend on temperature, including heat capacity, water heat of condensation, heats of reaction, equilibrium constants and CO_2 solubility. Therefore, it is desirable that the dynamic process model can predict with good accuracy absorber and stripper columns' temperature profiles. Figure 4 shows the comparison between the pilot plant temperature profiles of the absorber and desorber columns with the predictions from the simulation of the dynamic process models. Two steady-state operating cases are presented: Case 1 (Table 3) with absorber flue gas volumetric capacity of 100%, mass-based L/G ratio of 0.89 and capture target of 85%; and Case 6 (refer to Table 3) with 80% flue gas volumetric capacity, mass-based L/G ratio of 1.34 and capture target of 85%.

Both cases were operated with 24 m of wet absorber packing, and represent two operating cases with different flue gas capacities and L/G ratios.

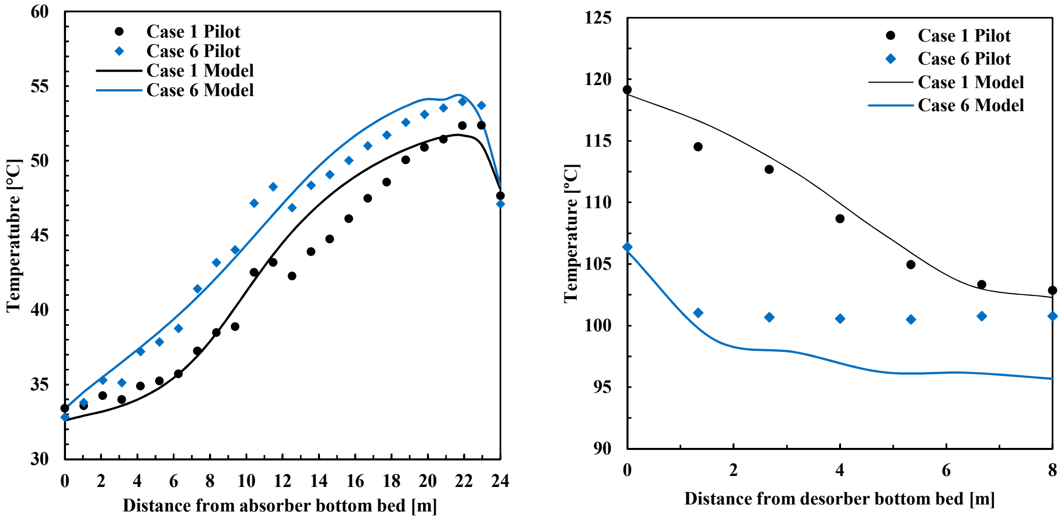

Figure 4. Temperature profiles for absorber column (**left**) and stripper column (**right**) for steady-state cases 1 and 6. In both steady-state operation cases, 24 m of absorber packing were utilized.

Validation of absorber and stripper temperature profiles is normally considered a challenging task for several reasons. At TCM DA the temperature profiles are the resulting averaged values of the 4 measurements distributed radially in a given axial position within the column; refer to Section 3. A given pilot plant temperature value presented in Figure 4 is the resulting average over time during one hour of steady-state operating conditions, of the averaged 4 temperature measurements radially distributed within the absorber or stripper column, at the given axial position of the column. The individual temperature measurements are considered reliable and the resulting temperature profiles are reasonable. However, some sensors are located closer to the center of the packing while others closer to the wall. This results in a maximum variation (<6 °C) which is observed between the measurements in the same radial plane, which depends on operating conditions and is different at different radial planes. Based on the results presented in Figure 4, the dynamic process model can properly predict absorber and stripper column temperature profiles with sufficient accuracy considering the purpose of application. Absorber temperature profiles predicted by the model show a good agreement with the experimental pilot plant data, and the model is capable of properly predicting the trends in temperature along the column. The absorber temperature profiles have a mean absolute percentage error (<2.5%) for Case 1 and (<2.1%) for Case 6, which is within the observed maximum variability of the temperature measurements in a given radial plane. In addition, desorber temperature profiles have a mean average error (<0.6%) for Case 1 and (<3.6%) for Case 6. It is the desorber temperature profile for Case 6 that presents the less accurate prediction. In addition, it can be concluded that the process model is capable of properly predicting the variation of temperature profiles for various steady-state operating conditions.

4. Validation of Dynamic Process Model with Transient Plant Data

For dynamic process model validation purposes transient tests are conducted by means of open-loop step changes in the main process inputs to the plant. The transient behavior occurs between the initial steady-state operating conditions until the new steady-state operating conditions are reached. In this work, the experiments consist of set-point changes in rich solvent flow rate, flue gas volumetric flow rate fed to the absorber and reboiler duty. The output trajectories of main process variables are observed and compared with the model output trajectories. In order to obtain good sets of data for validation, it is desired to apply the step changes in plant inputs in a non-simultaneous manner. However, this is not normally easy to implement in practice. In order to compare the pilot plant experimental output trajectories with the output trajectories predicted by the dynamic process models, input trajectories were utilized in the dynamic simulations. This means that the measured time series of the inputs applied to the pilot plant during the tests were applied as disturbances or inputs to the dynamic process model; refer to Figures 5a, 6a and 7a. During the three tests, the regulatory control layer of the plant was active. In Figures 5 and 6, the time $t = 0$ corresponds to the point from which the set point of flue gas volumetric flow rate was changed. In Figure 7 the time $t = 0$ is the point from when the set point of rich solvent flow rate was changed.

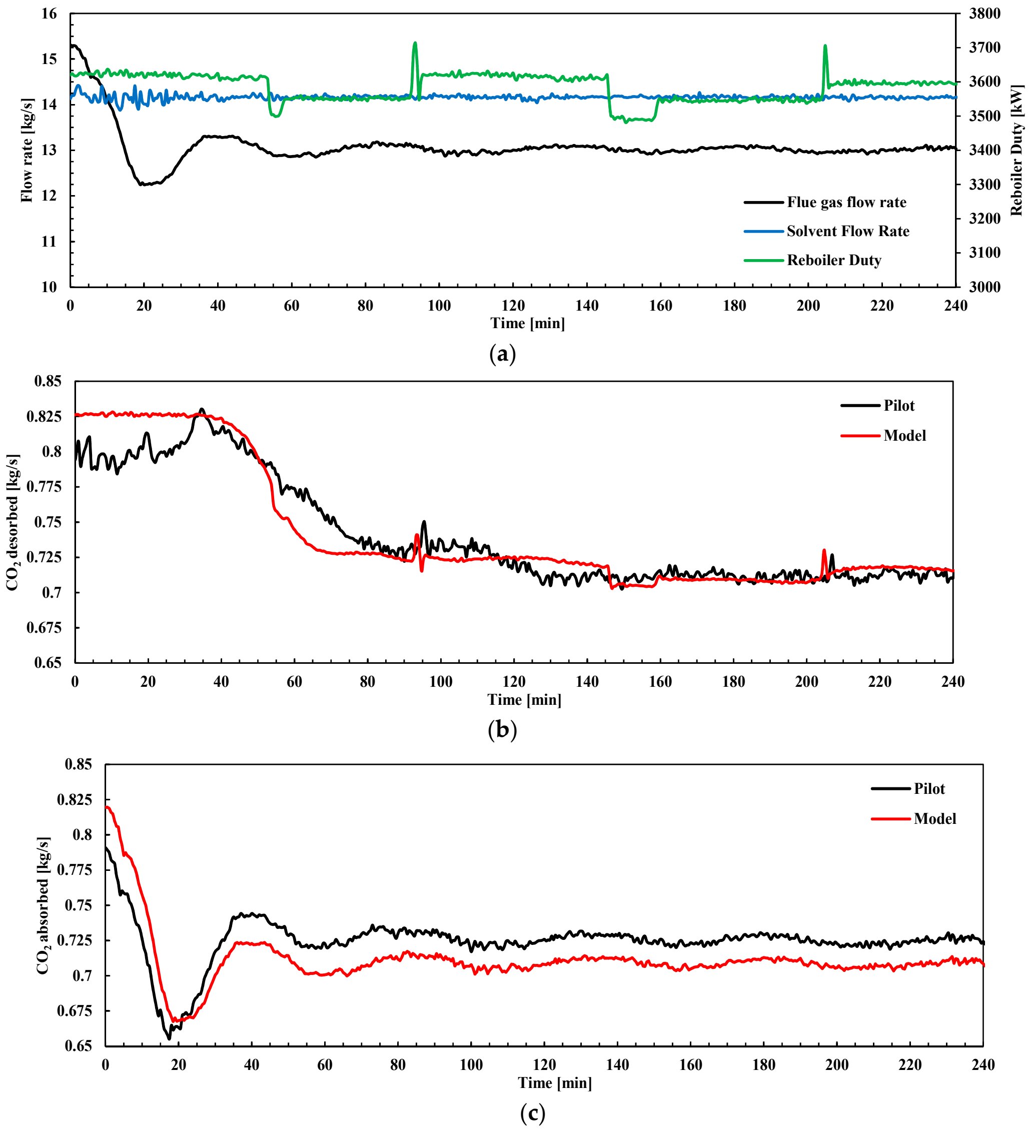

Figure 5. (**a**) Main inputs to the plant for test with flue gas flow rate set-point reduction (kg/s). Rich solvent flow rate from absorber (kg/s) and reboiler duty (kW); (**b**) Pilot plant transient response and model output trajectory for CO_2 product flow rate F_{prod} or CO_2 desorbed (refer to FT3 in Figure 1); (**c**) Pilot plant transient response and model output trajectory for CO_2 absorbed in absorber column, refer to Equation (11). The time $t = 0$ corresponds to the point from which the set point of flue gas volumetric flow rate was changed.

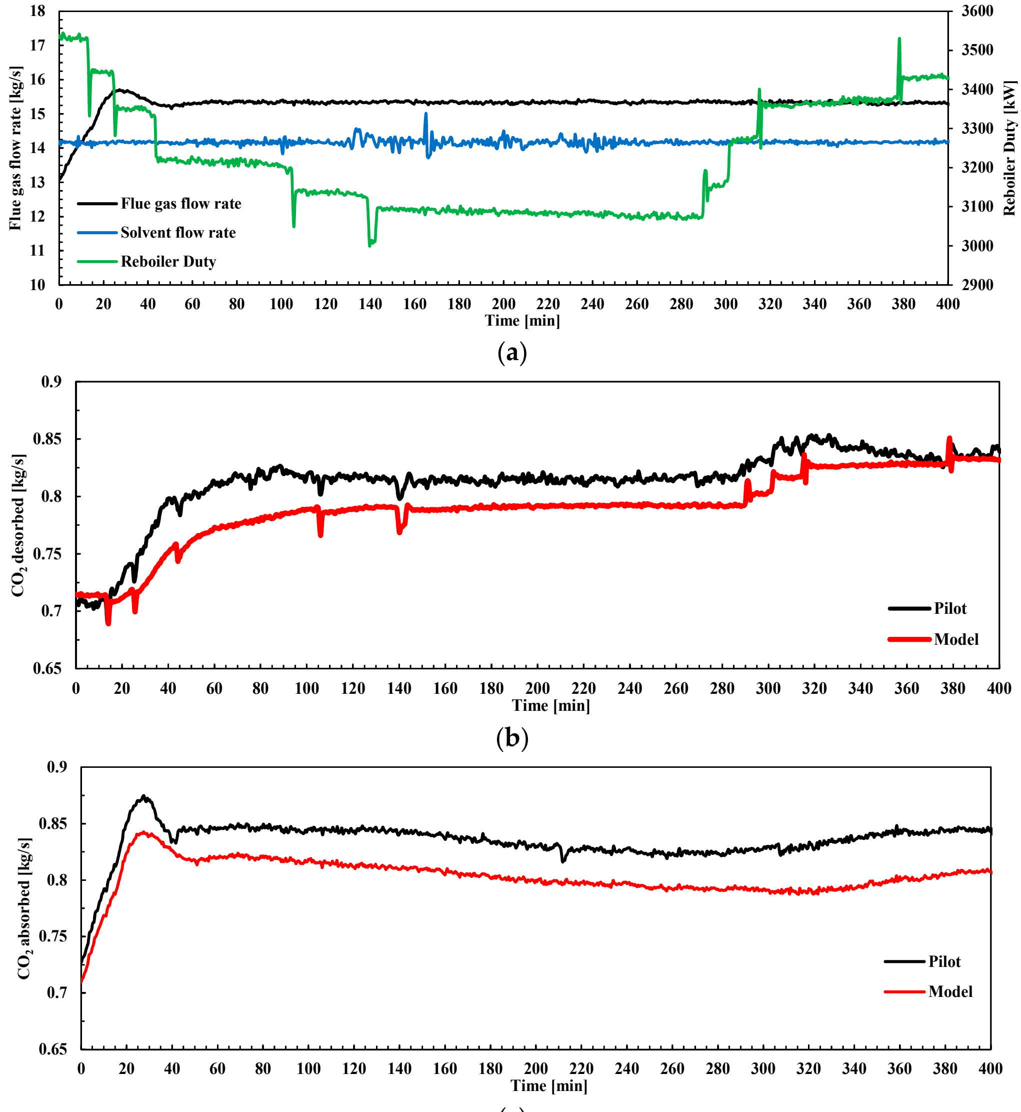

(**a**)

(**b**)

(**c**)

Figure 6. (**a**) Main inputs to the plant for test with flue gas flow rate set-point increase (kg/s). Rich solvent flow rate from absorber (kg/s) and reboiler duty (kW); (**b**) Pilot plant transient response and model output trajectory for CO_2 product flow rate F_{prod} or CO_2 desorbed (refer to FT3 in Figure 1); (**c**) Pilot plant transient response and model output trajectory for CO_2 absorbed in absorber column, refer to Equation (11). The time $t = 0$ corresponds to the point from which the set point of flue gas volumetric flow rate was changed.

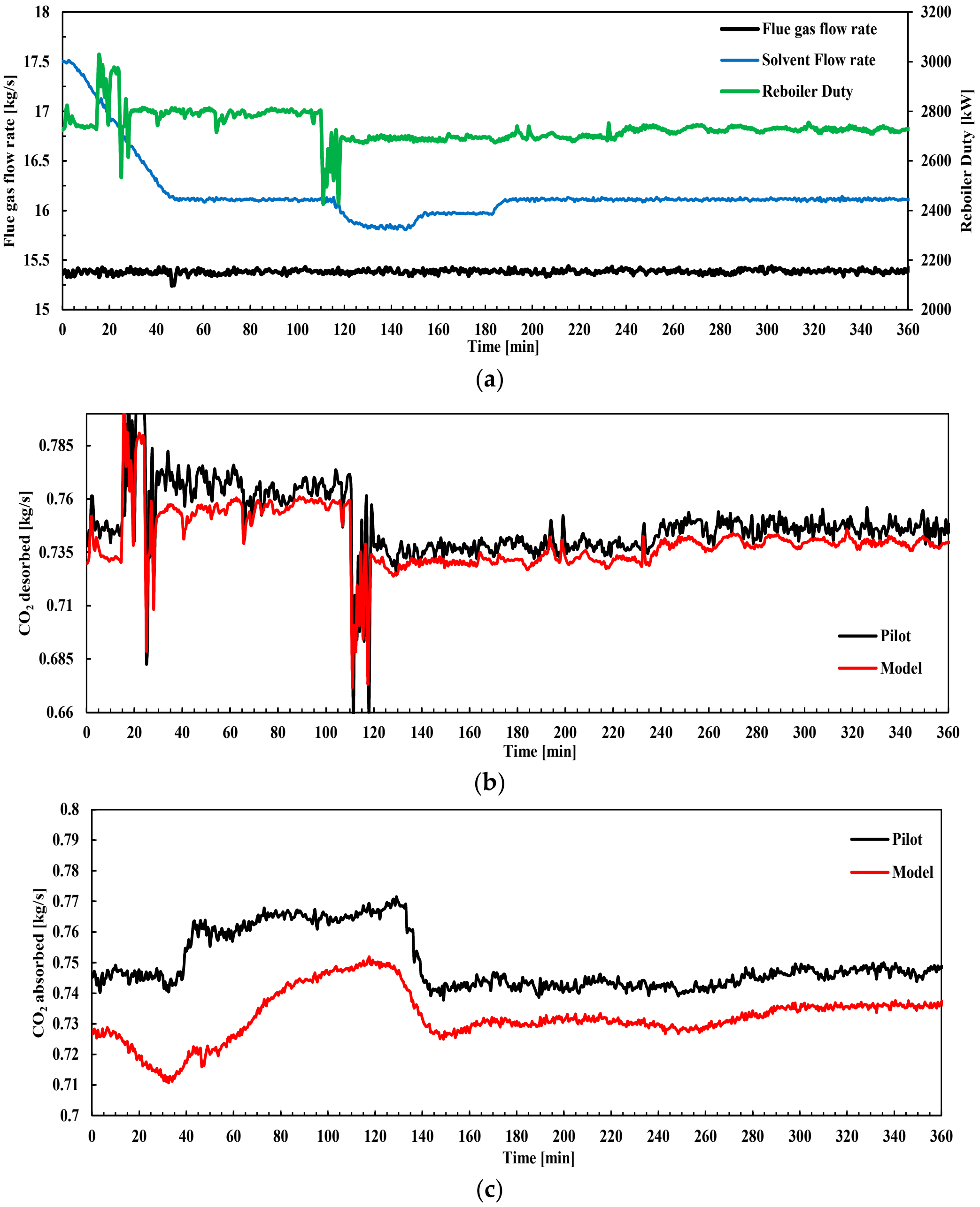

Figure 7. (**a**) Main inputs to the plant. Flue gas volumetric flow rate set-point change increase (kg/s). Rich solvent flow rate from absorber (kg/s) and steam flow to reboiler (kg/s); (**b**) Pilot plant transient response and model output trajectory for CO_2 product flow rate F_{prod} or CO_2 desorbed (refer to FT3 in Figure 1); (**c**) Pilot plant response in CO_2 absorbed mass flow rate (kg/s). The time $t = 0$ corresponds to the point from which the set point of rich solvent flow rate was changed.

4.1. Flue Gas Flow Rate Ramp-Down

The main disturbance applied in this transient test consisted of a reduction in flue gas volumetric flow rate at the inlet of the absorber. It was implemented at TCM DA pilot plant by changing the set point of the blower cascade controller from 47,000 Sm^3 to 40,000 Sm^3; refer to FT1 in Figure 1. This corresponds with flue gas volumetric flow capacities in the absorber column of 80% and 67% respectively. Figure 5a shows the three main inputs of the plant for this test. During the test, reboiler duty was changed in steps around the value of 3550 kW; this might be due to the effects of the regulatory control layer on steam mass flow rate. The solvent mass flow rate had small amplitude oscillations around the set point.

$$CO_{2,abs} = F_{gas} \cdot X_{CO_2} - F_{depleted} \cdot X_{CO_{2,out}} \tag{12}$$

Figure 5b,c show the output trajectories of CO_2 product flow rate (or CO_2 desorbed) and CO_2 absorbed to the disturbance applied in this test. CO_2 absorbed is calculated as the difference between CO_2 mass flow rate at the absorber inlet and the CO_2 mass flow rate leaving the absorber with the depleted flue gas at the top of the absorber; refer to Equation (12). In Figure 5b, a dead time of around 40 min was observed, i.e., no significant changes are found in the CO_2 desorbed until around 40 min after the disturbance was applied to the pilot plant. In addition, the plant did not reach steady-state operating conditions until around 4 h later. As shown in Figure 5c, there is not significant dead time in the response of CO_2 absorbed. The difference observed between the output trajectories is characteristic of the coupled transient performance of the absorber and stripper columns. Figure 5b,c shows that the process model is capable of predicting the main process dynamics for CO_2 product mass flow rate (CO_2 desorbed), including an adequate prediction of dead times and stabilization time. In addition, the CO_2 absorbed transient performance trends are predicted in a satisfactory manner.

4.2. Flue Gas Flow Rate Ramp-Up and Step Changes in Reboiler Duty

These tests consist of combined input changes to the plant in terms of flue gas volumetric flow rate and reboiler duty. A set-point increase of the flue gas volumetric flow rate fed to the absorber from 40,000 to 47,000 Sm^3/h was applied. This corresponds with 67% and 80% of the absorber column capacity, respectively. In addition, step-changes in reboiler duty were applied during the transient test. Figure 6a shows the three main inputs of the plant during the test. Figure 6b,c show the CO_2 product flow and CO_2 absorbed for the model and the pilot plant data. In this test a dead time of around 20 min in the response of CO_2 desorbed was observed. This confirms the buffering effect by the chemical process in terms of the response of CO_2 desorbed when the flue gas volumetric flow rate is changed. There is evidence to support this observation in previous pilot plant studies [46–48]. The delay in the response is partly attributed to solvent circulation time and the redistribution of liquid. Despite the steady-state offset shown on CO_2 absorbed in Figure 6b, a good prediction of the main transient response is seen. It is possible that the reduction in reboiler duty at around 10 min flattens out the response in CO_2 product flow rate.

4.3. Solvent Flow Rate Ramp-Down

In this test, the plant is operated in steady-state until the rich solvent mass flow rate set point is ramped down from around 17.5 kg/s to around 16.1 kg/s; refer to FT5 in Figure 1. The reboiler duty and flue gas volumetric flow rate were intended to be kept constant. Figure 7a shows the three main inputs of the plant during this transient test. In addition, the pilot plant performance in terms of product CO_2 mass flow F_{prod} (or CO_2 desorbed) and absorbed CO_2 flow rate are presented, together with the dynamic process model simulations for this test. Again, a satisfactory agreement is found between the plant trajectories and the output trajectories predicted by the dynamic process model.

From the three transient tests presented above, it can be concluded that the dynamic process model predicts the transient trends of the main output trajectories of the process for different inputs to the plant. In addition, the dead times and stabilization times of the process are properly predicted by the dynamic process models, despite the steady-state deviations observed and already quantified in Section 3.2. This means that the dynamic process model is suitable for simulation studies at the plant scale, including dynamic process simulations to analyze the plant transient performance, and for control tuning and advanced control layer design, including control structure studies.

5. Case Study: Open-Loop Performance and Decentralized Control Structures

5.1. Open-Loop Step Responses at Different Plant Flue Gas Capacities

A power plant operated in a power market with a high penetration of renewables will most likely be operated in load-following mode [7,63]. This means that the power plant with PCC will be operated during a significant amount of its lifetime at part loads. In the case of a natural gas combined cycle power plant with post-combustion CO_2 capture it means that, at part-load operation, the gas turbine (GT) load will be reduced, generating a reduced mass flow rate of flue gas that would be conducted to the PCC unit. The purpose of this case study is to investigate the transient performance of the PCC pilot plant via dynamic process simulation by implementing open-loop step changes to the dynamic process model, and to compare the response of the plant at different part-load operating points, defined by different mass flow rates of flue gas to be treated. The analysis will assess the transient response of the plant to multiple and non-simultaneous step changes in three key inputs to the plant, namely (i) flue gas flow rate F_{gas} (ii) solvent flow rate F_{solv}; and (iii) reboiler duty $\dot{Q}_{reb}$, at different flue gas mass flow rate capacities of the plant. In order to define the part-load operating points, a decentralized control structure was utilized, in which reboiler duty was the manipulated variable to control stripper bottom temperature T_{str} to 120.9 °C, and the solvent flow rate was the manipulated variable to control CO_2 capture ratio Cap to 0.85, as defined in Equation (13). When operating the plant at different flue gas mass flow rates, corresponding to 100%, 80% and 60% of nominal mass flow rate, this results in the three steady-state operating points presented in Tables 5 and 6. The control structure is defined as control structure A in Table 7.

$$Cap = \frac{F_{gas} \cdot X_{CO_2} - F_{depleted} \cdot X_{CO_{2,out}}}{F_{gas} \cdot X_{CO_2}} \tag{13}$$

Table 5. Simulated pilot plant inputs' set points for the three operating points to be studied, corresponding to 100%, 80% and 60% of flue gas mass flow rate capacity of the pilot plant. With $Cap = 0.85$ and $T_{str} = 120.9$ °C for all cases.

Pilot Load (%)	F_{gas} (kg/h)	F_{solv} (kg/s)	$\dot{Q}_{reb}$ (MW)
100	19.3	17.6	3.5
80	15.3	13.2	2.7
60	11.6	9.5	2.1

Table 6. Simulated pilot plant values for the process variables, lean CO_2 loading L_l, rich CO_2 loading L_r, CO_2 capture ratio Cap and CO_2 product flow rate, at three different operating points of the plant, corresponding to 100%, 80% and 60% of flue gas mass flow rate capacity of the pilot plant. With $Cap = 0.85$ and $T_{str} = 120.9$ °C for all cases.

Pilot Load (%)	L_l (mol/mol)	L_r (mol/mol)	Cap	F_{prod} (kg/s)
100	0.280	0.501	0.85	0.91
80	0.246	0.514	0.85	0.72
60	0.228	0.514	0.85	0.55

Table 7. Control structures for the supervisory control layer of the TCM amine plant. Key manipulated variables (MVs) are solvent flow rate F_{solv} and reboiler duty Q_{reb}. Controlled variables are CO_2 capture ratio *Cap* to 85%, defined in Equation (12), and stripper bottom temperature T_{str} to 120.9 °C. Control structure D controls *Cap* via a feed forward FF controller.

	Pairing 1		**Pairing 2**	
Control Structure	**Manipulated Variable**	**Controlled Variable**	**Manipulated Variable**	**Controlled Variable**
A	F_{solv}	*Cap*	Q_{reb}	T_{str}
B	Q_{reb}	*Cap*	F_{solv}	T_{str}
C	F_{solv}	*L/G*	Q_{reb}	T_{str}
D	F_{solv}	*Cap, with FF*	Q_{reb}	T_{str}

The open-loop response was studied for the process variables (i) CO_2 absorbed $CO_{2,abs}$, in Equation (11); (ii) CO_2 desorbed $CO_{2,abs}$ (or F_{prod}); (iii) lean CO_2 loading L_l at the inlet of the absorber; and (iv) rich CO_2 loading L_r at the outlet of the absorber. To characterize the transient response, dead time θ, settling time t_s, total stabilization time t_t, and relative change (*RC*) were calculated:

- Dead time θ: it is the time that takes before a process variable starts to change from the initial steady-state conditions as a response to the disturbance or input.
- Settling time: The 10% settling time t_s is the time taken from when the process variable begins to respond to the input change (dead time) until it remains within an error band described by 10% of the change in the process variable Δy and the final steady-state value of the process variable y_∞, i.e.: $-0.1\ \Delta y + y_\infty < y_\infty < 0.1\ \Delta y + y_\infty$.
- Total stabilization time: the sum of the dead time θ and the settling time t_s is the resulting total stabilization time t_t.
- Relative change *RC:* Change in the observed process variable from initial steady-state conditions y_0 to the final steady-state conditions; refer to Equation (14).

$$RC(\%) = 100 \cdot \frac{y_\infty - y_0}{y_0} \tag{14}$$

The detailed results of the process simulations are presented in Tables A1–A3 in Appendix A. Figure 8 shows the total stabilization times for the selected process variables at the three operating points, for step changes in solvent flow rate and reboiler duty. The responses for step changes in flue gas flow rate are not presented, since it is shown in Table A1 that the relative change *RC* in the output process variables is very small or negligible (*RC* ranges from −0.81% to 0.21%). This can be explained by the highly diluted nature of the CO_2 in the flue gas (ca. 3.5 vol%). The results show the non-linear behavior of the plant, with different transient responses to step change set-point increase and decrease in key plant inputs, and at different loads of the plant.

Figure 8a shows the total stabilization time for lean CO_2 loading L_l at the inlet of the absorber, which ranges from 25 to 45 min in all cases. The results show that the required time for total stabilization increases when the plant is operated at lower loads. As shown in Appendix A (Tables A1 and A2), a general trend was that the dead time θ in the response of L_l to step changes in reboiler duty and rich solvent mass flow rate increases at part-load points. This could be explained by the fact that at lower loads the solvent mass flow rate is smaller (refer to F_{solv} in Table 6), resulting in longer residence times of the solvent through each equipment hold-up, piping, and recycle loop, this is, larger circulation time. This can also explain why dead times are generally larger when decreasing solvent flow rate than when increasing it; refer to Table A2 in Appendix A.

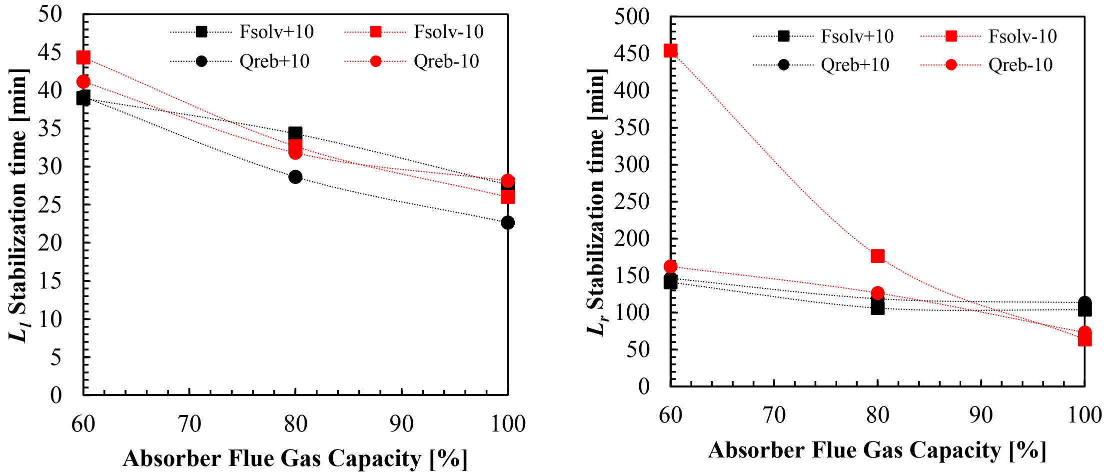

(**a**) Lean CO2 loading (**b**) Rich CO2 loading

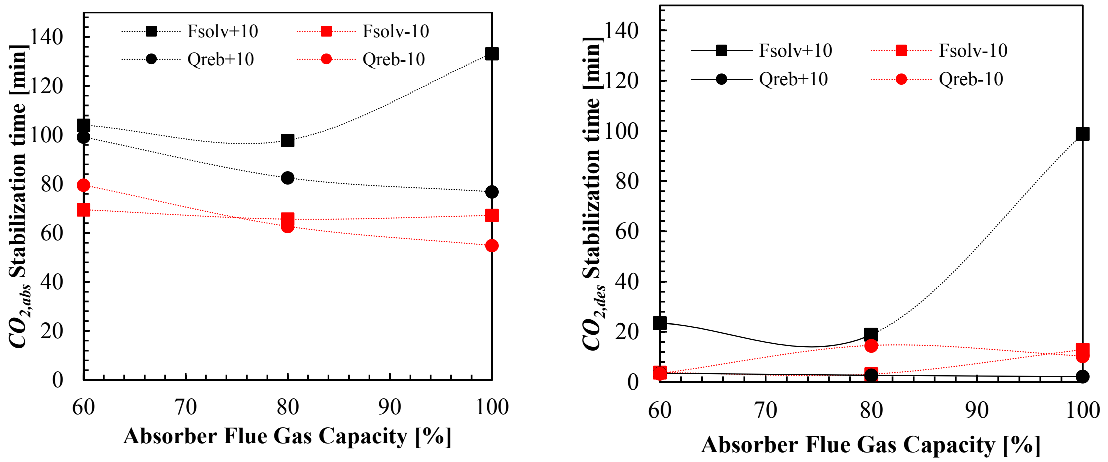

(**c**) CO2 absorbed flow rate (**d**) CO2 desorbed flow rate

Figure 8. Simulation results. Total stabilization times t_s for open-loop ± 10% step changes in solvent flow rate and reboiler duty for the process variables (**a**) Lean CO_2 loading L_l; (**b**) rich CO_2 loading L_r; (**c**) CO_2 absorbed $CO_{2,abs}$ and (**d**) CO_2 desorbed $CO_{2,abs}$. Stabilization times are calculated for the response when the plant is operated at three different operating points in terms of flue gas mass flow rate, 100%, 80% and 60% of nominal capacity; refer to Tables 5 and 6.

Figure 8b shows the total stabilization times for rich CO_2 loading L_r at the outlet of the absorber sump. In this case, the stabilization times range from 60 to 450 min. It should be mentioned that the relative change RC in rich CO_2 loading is also small or negligible for the disturbances studied (see Appendix A), due to the fact that the solvent is operated close to its maximum loading capacity of 0.51 mol/mol CO_2 loading. The total stabilization times of the responses of rich CO_2 loading L_r to disturbances in solvent flow rate and reboiler duty are larger at lower plant loads. At 60% flue gas capacity, a very slow response is found in L_r when the solvent flow rate is decreased by a −10% step change; however, the relative change RC of L_r in this process variable is negligible for this plant disturbance; refer to Table A2 in Appendix A.

The total stabilization times for CO_2 absorbed $CO_{2,abs}$ response to disturbances in rich solvent mass flow rate F_{solv} and reboiler duty $\dot{Q}_{reb}$ are shown in Figure 8c. Total stabilization times range from 55 to 135 min. When the rich solvent mass flow rate is increased by 10%, this results in an increase in CO_2 absorbed with a relative change RC of 0.35% to 4.18% (refer to Table A2), due to the increased L/G ratio in the absorber column. However, since the reboiler duty is kept constant, the lean loading will increase (see RC values of L_l in Table A2). Due to the residence time in the hot solvent piping, lean/rich heat exchanger and lean amine cooler of the recycle loop, it takes time for the solvent to be distributed towards the inlet of the absorber. A dead time in CO_2 lean loading L_l at the inlet of the absorber of 11 to 22 min is observed (see Table A2). This results in it taking a long time for the $CO_{2,abs}$ to stabilize. When the rich solvent mass flow rate is decreased by 10%, it is observed that the CO_2 absorbed $CO_{2,abs}$ decreases (relative change RC between −3.14% and −5.59% in Table A2). This is a result of the combination of the reduction in L/G ratio and the decrease in lean loading L_l. $CO_{2,abs}$ requiring time for stabilization (stabilization time of 65 to 69 min). When reboiler duty $\dot{Q}_{reb}$ is increased by 10%, the lean loading L_l is decreased significantly (RC ranging from 6.75 to 8.59%), which results in increase of $CO_{2,abs}$ (relative change RC of 4.0% to 6.07%). The change in lean loading L_l is observed at the absorber inlet with a dead time of 13 to 23 min (due to circulation time of the solvent in the recycle loop), and the total stabilization time for $CO_{2,abs}$ for increase in reboiler duty ranges from 76 to 99 min. When reboiler duty $\dot{Q}_{reb}$ is decreased by 10%, the solvent lean loading increases (RC of 6.63% to 8.46%), resulting in less CO_2 being absorbed. Relatively slower response in $CO_{2,abs}$ to disturbances in solvent flow rate and reboiler duty were found when the PCC was operated at lower loads (55 to 99 min). An exception is found for the case when the solvent flow rate is increased at 100% mass flow rate operating conditions of the plant.

Figure 8d shows the stabilization times for CO_2 desorbed $CO_{2,abs}$. For disturbances in rich solvent flow rate and reboiler duty, the desorbed CO_2 stabilizes slightly faster at lower loads (ranging from 2 to 100 min). In general, it was found that the desorption rate stabilized faster than the absorption rate $CO_{2,abs}$ for the disturbances in solvent flow rate and reboiler duty applied to the process. When solvent flow rate is decreased, this results in smaller L/G ratio in the absorber column and less CO_2 being desorbed in the stripper column. Since the rich CO_2 loading does not change significantly (RC in L_r from 0 to 0.08%), the CO_2 desorbed $CO_{2,des}$ stabilizes faster than the CO_2 absorbed (circulation time through the recycle loop is not affecting the stabilization of $CO_{2,abs}$). When the reboiler duty $\dot{Q}_{reb}$ is increased by 10%, the relative change in CO_2 desorbed is large (4 to 6.07% in Table A3), and with fast total stabilization time (2 to 3 min in Table A3). A change in reboiler duty results in a fast response in the produced stripping vapors, which also results in a fast response in CO_2 product flow rate (CO_2 desorbed). The longest stabilization time for CO_2 desorbed is found when the solvent flow rate is increased at 100% operating conditions. It is notable that there is a big difference in total stabilization times for solvent flow rate increase at different loads of the plant.

5.2. Decentralized Control Structures

In this section, four control structures for the TCM DA amine plant were tested via dynamic process model simulations. The scenario considers realistic load changes on the power plant, by changing flue gas flow rate feed to the absorber column. From a control analysis perspective, flue gas flow rate change can be considered as a disturbance applied to the PCC process. A load change event would result in a significant change in flue gas flow rate, at a ramp rate given by GT operation and controls. Fast ramp rates are the goal of power plant operators, since a fast power plant can respond to the variability in costs in a day-ahead power market [7,64]. For a NGCC power plant, a fast ramp rate is considered to be around 10%/min GT load [4,65]. Two tests were considered and simulated:

- Test 1: Ramping down flue gas flow rate from 100 to 70% in 3 min. The transient event starts at $t_0 = 0$ min, and sufficient simulation time is allowed for the plant to reach the new steady-state.
- Test 2: Flue gas flow rate is ramped up from 70 to 100% in 3 min. The transient event starts at $t_0 = 0$ min, and sufficient simulation time is allowed for the plant to reach the new steady-state.

The supervisory or advanced control layer of the TCM DA amine plant has three main degrees of freedom, consisting of set point of flue gas volumetric flow rate F_{gas}, set point of rich pump solvent flow rate F_{solv}, and steam flow rate to feed the reboiler duty $\dot{Q}_{reb}$; refer to FT1, FT5 and FT4, respectively in Figure 1. Under normal and stable operation of the pilot plant at TCM DA, such degrees of freedom are changed manually by the operators to bring the plant to different operating conditions. If flue gas flow rate is considered to be a disturbance, there are two degrees of freedom left for operation. Note that here we do not consider the degrees of freedom available to the operators in the stabilizing or regulatory control layer, or for other auxiliary operations of the plant, or start-up procedures. Several studies in the literature suggest that keeping the capture ratio *Cap* and a temperature in the stripper column constant can lead to efficient operation of the process for varying loads of the PCC absorber-desorber process [13]. In this analysis, four control structures were tested, as presented in Table 7. All the feedback control loops are PI controllers, and were tuned with the simple internal model control (SIMC) tuning rules [66].

- **Control structure A** uses F_{solv} to control capture ratio at the top of the absorber *Cap* defined by Equation (13) to the set point of 0.85, and reboiler duty $\dot{Q}_{reb}$ to control the solvent temperature at the stripper bottom T_{str} to the set point of 120.9 °C. This control structure has been previously proposed in the literature in different studies including [14,16], where it shows a fast response and the capability to reject disturbances.
- **Control structure B** uses F_{solv} to control the solvent temperature at the stripper bottom T_{str} to the set point of 120.9 °C, and reboiler duty $\dot{Q}_{reb}$ to control capture ratio at the top of the absorber *Cap* to the set point of 0.85. Note that changes in reboiler duty result in a big change in solvent lean CO_2 loading (large relative change *RC*; see Appendix A). A similar version was suggested by Panahi and Skogestad [14], where it was found that this control structure showed similar dynamic behavior, in response to disturbances in flue gas flow rate, compared with a model predictive control scheme (MPC).
- **Control structure C** utilizes solvent flow rate F_{solv} to control the mass-based L/G ratio in the absorber column at the same value as that in the close-to-design-point operating conditions. This control structure has been studied previously in [12,15]. This control loop is implemented via ratio control. In addition, reboiler duty is manipulated to control T_{str} to 120.9 °C. The control structure leads to different final steady-state operating conditions when ramping down the plant load than the other three alternatives.
- **Control structure D** is a modification of control structure A. In this control structure, the solvent flow rate set point is changed via a feed forward (FF) action to control the capture ratio *Cap* at 0.85; in addition, the stripper bottom temperature is controlled by manipulating the reboiler duty. The feed forward controller is implemented by a set-point ramp change in the solvent flow rate with the same total duration as the flue gas flow rate ramp change, to the final value that gives a *Cap* of 0.85 under final steady-state conditions.

Figure 9 shows the simulated time input trajectories during the test with flue gas flow rate reduction. The manipulated variables F_{solv} and $\dot{Q}_{reb}$ are shown for the different control structures evaluated. Figure 10 shows the output trajectories of CO_2 capture ratio *Cap*, desorption ratio *Des*, CO_2 absorbed and CO_2 desorbed for the transient tests of flue gas flow rate reduction. Figure 11 shows the trajectories of lean loading L_l and stripper bottom solvent temperature T_{str} for flue gas flow rate reduction. In addition, Figure 12 shows the simulated time input trajectories during the test with flue gas flow rate increase. Figure 13 shows the output trajectories of CO_2 capture ratio *Cap*, desorption ratio *Des*, CO_2 absorbed and CO_2 desorbed for the transient tests of flue gas flow rate increase, and Figure 14 shows the trajectories of lean loading L_l and stripper bottom solvent temperature T_{str} for flue gas flow rate increase. In order to compare the different control structure performances during transient load change, the total stabilization times of the selected process variables are shown in Table 8. These will indicate how fast the plant achieves stabilization of the different floating (not controlled) process variables when moving from one operating condition to the next one. In addition, three transient performance indicators have been considered and presented in Table 9. Note that, for this analysis auxiliary consumptions of the plant are not considered.

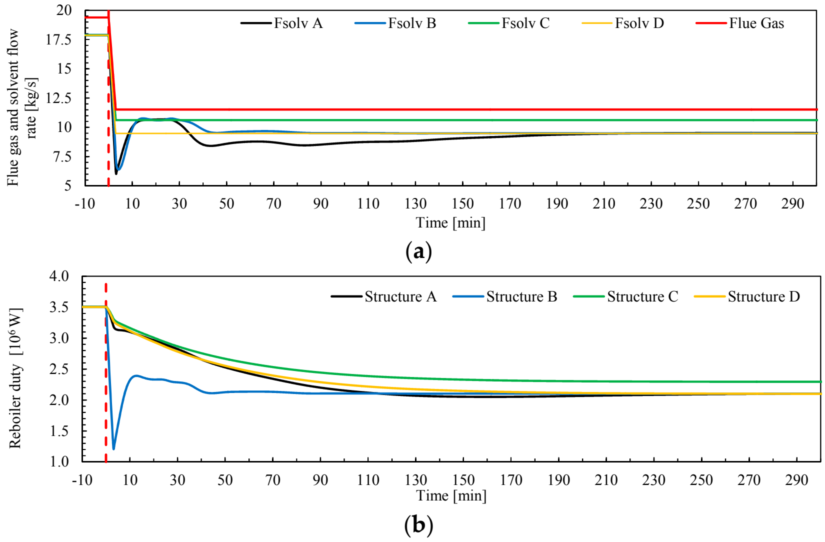

Figure 9. Inputs to the pilot plant during simulations for load change ramp-down (Test 1) from 100 to 70% with a ramp rate of 10%/min reduction in flue gas flow rate, for control structures A, B, C and D. (**a**) Flue gas flow rate (kg/s), as a disturbance, and solvent flow rates (kg/s) of the rich pump as manipulated variables (MVs); (**b**) Reboiler duty (W) as MV. The red vertical dotted line shows when the transient event starts at t_0.

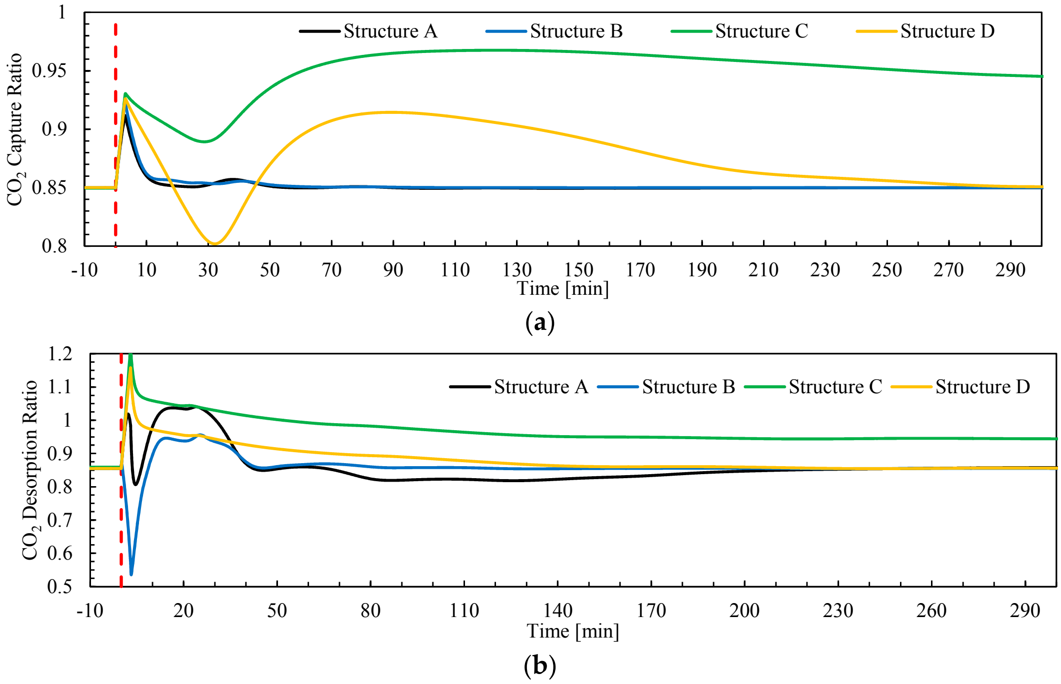

Figure 10. *Cont*.

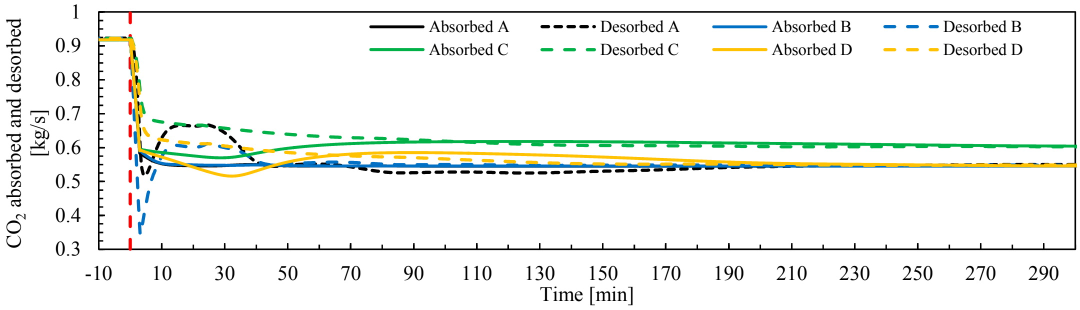

(**c**)

Figure 10. Outputs from pilot plant model during simulations for load change ramp-down (Test 1) from 100 to 70% with a ramp rate of 10%/min reduction in flue gas flow rate, for control structures A, B, C and D. (**a**) CO_2 capture ratio *Cap*, as controlled variable (CV); (**b**) CO_2 desorption ratio *Des*; (**c**) CO_2 absorption and desorption rates (kg/s). The red vertical dotted line shows when the transient event starts at t_0.

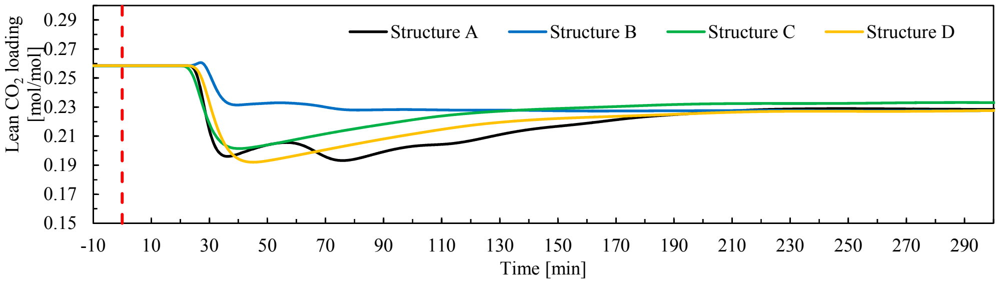

(**a**)

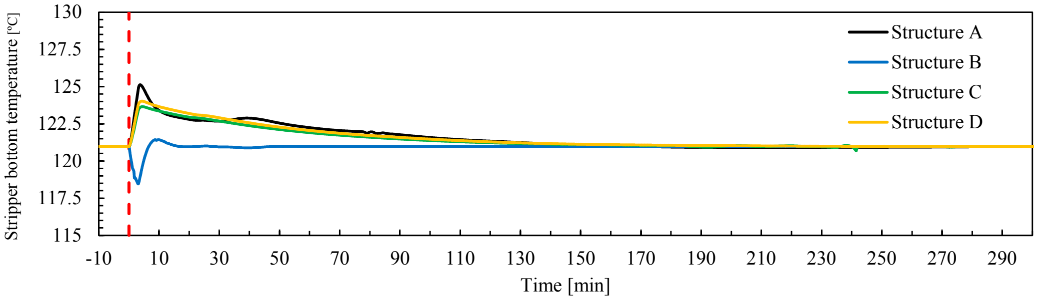

(**b**)

Figure 11. Outputs from pilot plant model during simulations for load change ramp-down (Test 1) from 100 to 70% with a ramp rate of 10%/min reduction in flue gas flow rate, for control structures A, B, C and D. (**a**) Lean CO_2 loading at the inlet of the absorber; (**b**) Stripper bottom temperature as controlled variable (°C). The red vertical dotted line shows when the transient event starts at t_0.

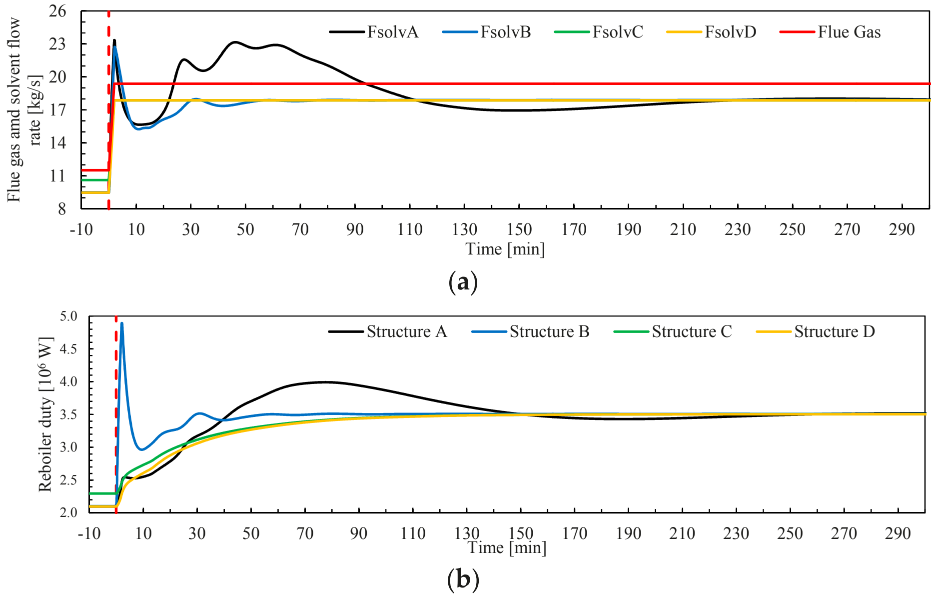

(**a**)

(**b**)

Figure 12. Inputs to the pilot plant during simulations for load change ramp-up (Test 2) from 70 to 100% with a ramp rate of 10%/min increase in flue gas flow rate, for control structures A, B, C and D. (**a**) Flue gas flow rate (kg/s), as a disturbance, and solvent flow rates (kg/s) of the rich pump as manipulated variables (MVs); (**b**) Reboiler duty (W) as MV. The red vertical dotted line shows when the transient event starts at t_0.

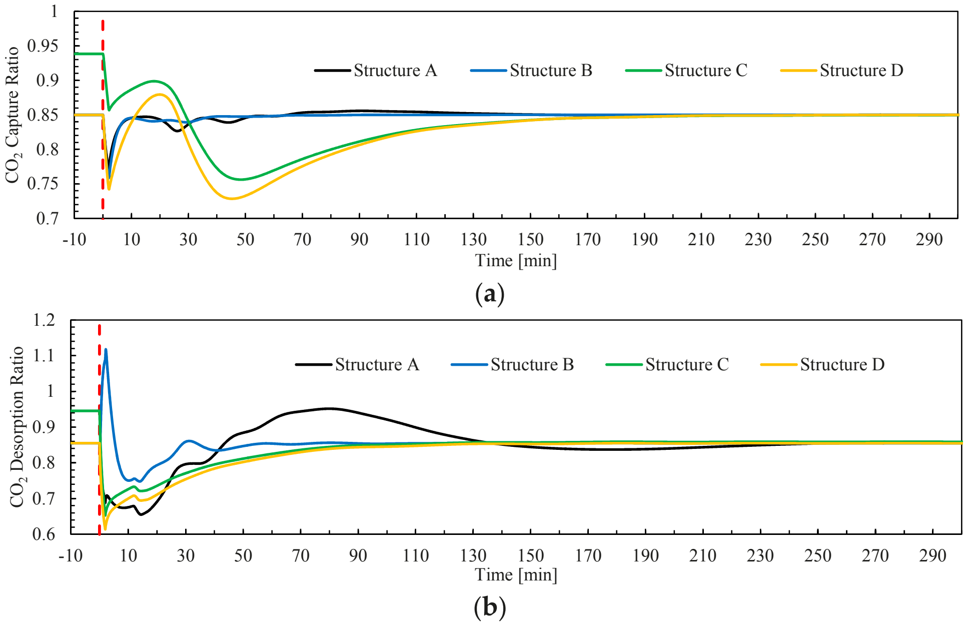

(**a**)

(**b**)

Figure 13. *Cont*.

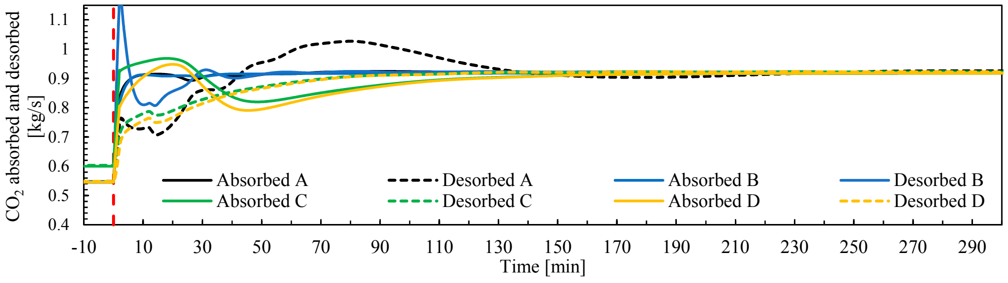

(**c**)

Figure 13. Outputs from pilot plant model during simulations for load change ramp-up (Test 2) from 70 to 100% with a ramp rate of 10%/min increase in flue gas flow rate, for control structures A, B, C and D. (**a**) CO_2 capture ratio *Cap*, as controlled variable (CV); (**b**) CO_2 desorption ratio *Des*; (**c**) CO_2 absorption and desorption rates (kg/s). The red vertical dotted line shows when the transient event starts at t_0.

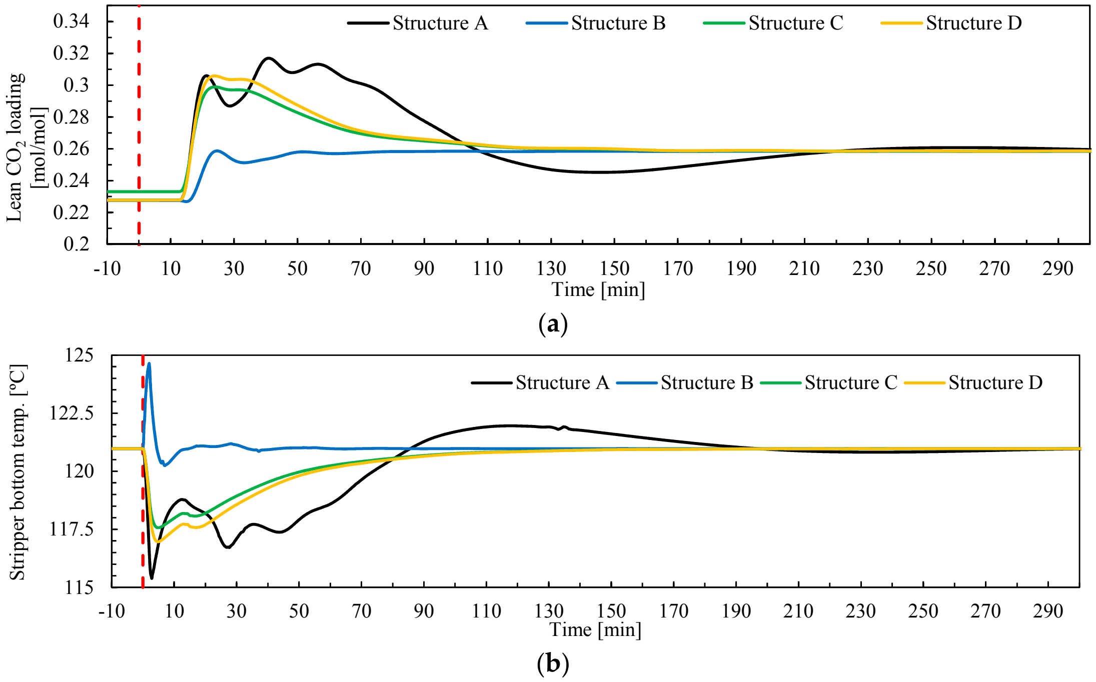

Figure 14. Outputs from pilot plant model during simulations for load change ramp-up (Test 2) from 70 to 100% with a ramp rate of 10%/min increase in flue gas flow rate, for control structures A, B, C and D. (**a**) Lean CO_2 loading at the inlet of the absorber; (**b**) Stripper bottom temperature as controlled variable (°C). The red vertical dotted line shows when the transient event starts at t_0.

Table 8. Total stabilization times of the floating process variables for the different control structures, when ramping down the plant $t_{t,down}$ from 100% flue gas mass flow rate to 70%; and when ramping up the plant $t_{t,up}$ from 70% flue gas mass flow rate to 100%.

Control Structure	Process Variable	$t_{t,down}$ (min)	$t_{t,up}$ (min)
A	CO_2 Absorbed	3.3	71.0
	CO_2 Desorbed	36.3	112.7
	L_l	187.7	201.0
B	CO_2 Absorbed	4.0	5.2
	CO_2 Desorbed	35.3	27.5
	L_l	68.2	46.7
C	CO_2 Absorbed	3.6	97.7
	CO_2 Desorbed	56.5	63.7
	L_l	172.2	115.5
D	CO_2 Absorbed	6.2	96.8
	CO_2 Desorbed	50.3	59.2
	L_l	185.0	113.8

Table 9. Simulation results for accumulated reboiler energy consumption Q_{reb} (MJ), accumulated CO_2 emitted $CO_{2,em}$ and accumulated CO_2 captured $CO_{2,cap}$ during the transient event (8 h) for the different control structures A,B, C and D (refer to Table 7), when ramping up and down the plant (between 100% and 70% of flue gas mass flow rate). Static plant refers to an ideal static plant that changes from the initial operating conditions to the final operating conditions instantaneously at time t = 0. An integration time of t_f = 480 min was utilized to calculate the values for the ideal static plant.

Transient Event	Indicator	Static Plant	A	B	C	D
Ramp down	Q_{reb} (MJ)	60,441	63,353	60,926	69,045	64,046
	$CO_{2,em}$ (tons)	2.66	2.64	2.65	0.96	2.39
	$CO_{2,cap}$ (tons)	15.70	15.76	15.75	17.44	16.01
Ramp up	Q_{reb} (MJ)	100,924	100,898	100,655	98,973	98,667
	$CO_{2,em}$ (tons)	4.49	4.51	4.53	4.77	4.94
	$CO_{2,cap}$ (tons)	26.41	26.39	26.37	26.13	25.96

- **Accumulated reboiler energy input Q_{reb} (MJ)**: see Equation (15). This is calculated by integration of the $\dot{Q}_{reb}$ trajectory under the transient event, from the initial time t_0 = 0 min to the final time t_f = 480 min (8 h). The final time was defined to ensure that the plant was already under steady-state conditions at the final operating point. This value Q_{reb} represents the main energy consumption of the process during the transient event of load change. In addition, the consumption of an ideal static plant is included for comparison (see Table 9). The ideal static plant is assumed to change from initial to the final steady-state operating conditions instantaneously at time t_0, and would operate until t_f. The static plant value represents the minimum value when ramping down and a maximum value when ramping up.

$$Q_{reb} = \int_{t_0}^{t_f} \dot{Q}_{reb}(t)dt \qquad (15)$$

- **Accumulated CO_2 emitted $CO_{2,em}$ (tons)**: see Equation (16). This is calculated by integration of the $\dot{m}_{CO_2}$ trajectory under the transient event, from the initial time t_0 = 0 min to the final time t_f = 480 min; this represents the CO_2 emitted at the absorber stack. The final time was defined to ensure that the plant was already under steady-state conditions at the final operating point. This measure represents the CO_2 emitted during the transient event of load change.

For comparison, the CO_2 emitted by an ideal static plant is calculated (considered as the maximum value when ramping down and a minimum value when ramping up), shown in Table 9.

$$CO_{2,em} = \int_{t_0}^{t_f} \dot{m}_{CO_2}(t)dt = \int_{t_0}^{t_f} \dot{m}_{depleted}(t) \cdot X_{CO_2}(t)dt \tag{16}$$

- **Accumulated CO_2 captured $CO_{2,cap}$ (tons)**: see Equation (17). This is calculated by integration of the CO_2 absorbed $CO_{2,abs}$ trajectory (Equation (12)) under the transient event, from the initial time $t_0 = 0$ min to the final time $t_f = 480$ min. The final time was defined to ensure that the plant was already under steady-state conditions at the final operating point. This measure represents the CO_2 captured during the transient event of load change. For comparison, the CO_2 captured by an ideal static plant is calculated (considered as the minimum value when ramping down and a maximum value when ramping up), shown in Table 9.

$$CO_{2,cap} = \int_{t_0}^{t_f} \left(F_{gas}(t) \cdot X_{CO_2}(t) - F_{depleted}(t) \cdot X_{CO_{2,out}}(t) \right) dt \tag{17}$$

Figure 10 shows that the CO_2 capture ratio *Cap* had similar trajectories for control structures A and B during Test 1 (flue gas ramp-down), and that *Cap* reached stabilization conditions faster (20–50 min) than control structures C and D (around 270 min). *Cap* had also larger excursions from the set point than when control structures A and B are utilized. The same trends are found for Test 2 with flue gas flow rate ramp-up (Figure 13). When ramping up, control structures C and D stabilize faster (around 160 min) than when ramping down. This showed that the utilization of close-loop feedback control (structures A and B) allows shorter stabilization times to be reached for the controlled variable CO_2 capture ratio *Cap*. The desorption ratio *Des* trajectories in Figure 10 show that the plant requires the shortest stabilization time for this process variable when employing control structure B (around 60 min), followed by control structure A and C (around 200 min). This can be explained by the fact that for a change in reboiler duty the response of CO_2 desorbed has a fast total stabilization time and a large static relative change *RC* (where *RC* ranges from 4 to 6.29% and total stabilization time range from 2.2 to 3.5 min for a +10% step in reboiler duty); refer to Table A3. When it comes to the stabilization time required for *Des* for Test 1, structures C and D presented a poorer performance as the trajectories for *Cap* and *Des* deviate from the set point significantly. For control structure A, *Des* showed slow performance for Test 2 (around 210 min total stabilization time) with significant oscillations around set point; refer to Figure 13.

When ramping down the plant, CO_2 absorbed and CO_2 desorbed require similar stabilization times for control structures A and B (around 3 min for $CO_{2,abs}$ and 36 min for $CO_{2,abs}$), while the control structures C and D require longer stabilization times for CO_2 desorbed (around 50 to 57 min); refer to Table 8. The trajectory of CO_2 lean loading again shows shorter stabilization time for control structure B. This can be explained by the large static relative change *RC* of the response of CO_2 lean loading to changes in reboiler duty (where *RC* ranges from −6.29% to −4.97% and total stabilization time range from 22.7 to 39.2 min for a +10% step in reboiler duty); refer to Table A3. This contributes to the tight control of CO_2 capture ratio *Cap* achieved by control structure B, since the CO_2 lean loading L_l is a key process variable that connects the operation of the stripper and the absorber columns via the recycle loop. In addition, control structure B shows the shortest stabilization times and smaller excursions of the stripper bottom temperature T_{str} (around 15 to 30 min), in Figures 11 and 14.

When the plant load is ramped up from 70 to 100% (Test 2), the control structure B in general showed a faster dynamic performance with significantly shorter stabilization times required for the floating process variables considered (5.2 min for $CO_{2,abs}$, 27.5 min for $CO_{2,abs}$ and 46.7 min for L_l), see Table 9; followed by C, D and A. Note that control structure B presented a faster dynamic performance towards stabilization while ramping up (L_l stabilizes in 46.7 min) than when ramping down the process (L_l stabilizes in 68.2 min). Control structures A, C and D required shorter stabilization times for CO_2 absorption and CO_2 desorption when ramping down the process load, while CO_2 lean loading stabilized faster when ramping up the plant load; refer to the stabilization time values in Table 9. When the plant is operated under control structure C, the optimum solvent flow rate F_{solv} and lean loading L_l are not reached at the 70% absorber capacity steady-state operating conditions; refer to time >250 min in Figures 9a and 11a, and time <0 min in Figures 12a and 14a. This leads to a higher *Cap* than specified (refer time $t > 290$ min in Figure 10a and time $t < 0$ min in Figure 13a), and therefore higher reboiler duty (time $t > 290$ min in Figure 9b and time $t < 0$ min in Figure 12b), even though the stripper bottom temperature T_{str} criterion is satisfied.

During the ramp-down transient event of the plant (i.e., period of 8 h from the time change was implemented), the least energy-intensive performance measured by Q_{reb} in Table 9 was observed for control structure B. In addition, this structure shows the largest CO_2 emissions during the transient event, albeit still lower than the ideal static plant. The fast stabilization time of the plant process variables achieved by control structure B provides a transient performance that is the closest to the ideal static plant. Control structures C and D showed the largest CO_2 captured during the transient event. However, when ramping down the plant load, this means that the plant is emitting less CO_2 during the transient event with control structures A, B, C and D than that established by the operational objective and represented by the ideal static plant case. Consequently, when ramping down the plant load, CO_2 emissions will always be lower than those of the equivalent ideal static plant. In addition, the plant is capturing more CO_2 than the ideal static plant. Figure 10a shows how there are periods of time in which the capture ratio *Cap* is above the target of 0.85, leading to more CO_2 being captured than the ideal static plant during the transient event. Control structures A and B showed the largest CO_2 emitted when compared with the ideal static case. Despite control structure A presenting a similar amount of CO_2 emitted during the transient event, it requires a larger amount of energy input during this period than control structure B. Therefore, control structure B shows the best performance in terms of energy consumption and CO_2 emissions during the transient load change event of ramping down the PCC plant load. When ramping up the plant load the most energy-intensive control structure is control structure B. However CO_2 emissions are the lowest, being closer to the minimum established by the static plant. This means that, when ramping up the plant load, CO_2 emissions will always be higher than those of the equivalent ideal static plant. While control structure D is the least energy-intensive process during the transient event of load change increase, it is the control structure with the largest CO_2 emissions during this transient event.

6. Conclusions

The pilot plant data obtained in this work from an MEA campaign at TCM DA amine plant includes ten steady-state operating data sets. The data sets consist of a wide range of steady-state operating conditions of the chemical absorption process in terms of L/G ratio in the absorber column, different absorber packing heights, CO_2 capture ratios, reboiler duty and flue gas flow rate fed to the absorber. The data is considered reliable and valid and can be used for process model validation purposes. In addition, the three transient data sets presented in this work represent transient operation of the pilot plant driven by set-point changes in flue gas flow rate, solvent circulation flow rate and reboiler duty. The transient data sets are considered reliable and suitable for dynamic process model validation purposes, provided that input trajectories can be applied to the dynamic process model.

The validation of the dynamic process model with the steady-state and transient data shows that the process model has a good capability of predicting the steady-state and transient behavior of the plant for a wide range of operating conditions. The validation included in this work proves the capacities of dynamic process modeling applied to large-scale experimental data. The model is considered suitable for studies including transient performance analysis and control structure evaluation studies at the plant scale. In addition, it provides confidence towards using the dynamic process model for analysis of larger-scale PCC plants.

The case study carried out in this work via dynamic process simulations with the validated model shows that, generally, the plant responds more slowly at lower operating loads (the load being defined by the flow rate fed to the absorber). A general trend is observed, in which it takes a longer time to stabilize the main process variables of the pilot plant under open-loop step changes in the main inputs of the process, namely solvent flow rate, flue gas flow rate and reboiler duty. From the process simulations, it is found that, in general, the desorption rate stabilizes faster than the absorption rate for set-point step changes in solvent flow rate and reboiler duty. In addition, $\pm 10\%$ step changes in flue gas flow rate around a given operating point do not cause a large relative change in the main process variables of the process (RC ranges from -0.81% to 0.21%).

The evaluation of the decentralized control structures shows that by adding closed-loop controllers on the two main degrees of freedom of the plant—solvent flow rate and reboiler duty—to control two other process variables, including CO_2 capture ratio and stripper bottom solvent temperature, the plant can be stabilized faster and more efficiently under varying loads. The control structure that showed the best performance was control structure B, in which the reboiler duty is manipulated to control CO_2 capture ratio at the inlet of the absorber and the rich solvent flow rate to control the stripper bottom solvent temperature. It was observed that control structure B provides the fastest stabilization times for the main process variables under scenarios when the plant load is ramped down and up, with ramp rates typically found in NGCC power plants with fast-cycling capabilities. When reducing the PCC process load, this control structure is the least energy-intensive of those evaluated in this work. When increasing the plant load, this control structure is the one with the lowest accumulated CO_2 emissions imposed by the process inertia during load-change transient operation.

Acknowledgments: The authors acknowledge the Department of Energy and Process Engineering at NTNU-Norwegian University of Science and Technology and TCM DA owners Gassnova, Shell, Statoil and Sasol, for funding this project. The funds for covering the costs to publish in open access were provided by the Norwegian University of Science and Technology—NTNU.

Author Contributions: Rubén M. Montañés contributed to the selection of experimental data; processed the experimental data; developed the models; carried out the calibration, validation and simulation of the dynamic process models; defined and carried out the case studies; analyzed the results; and wrote the manuscript. Nina E. Flø contributed to the experimental data selection; contributed to the critical analysis of the results; and reviewed the manuscript. Lars O. Nord contributed to the critical analysis of the results; reviewed the manuscript; and supervised the work.

Conflicts of Interest: The authors declare no conflict of interest.

Abbreviations and Symbols

A_{if}	Contact area
AP	Absolute percentage error
Cap	CO_2 capture ratio
CHP	Combined heat and power
CCS	Carbon capture and storage
CO_2	Carbon dioxide
$CO_{2,em}$	CO_2 emitted (kg/s)
c_i	Molar concentration
C_{ef}	Pre-multiplying coefficient
DCC	Direct contact cooler
Des	Desorption ratio
D_{CO2}	Diffusivity of CO_2 in aqueous monoethanolamine
E	Enhancement factor
F	Mass flow rate (kg/s)

FB	Feedback
FC	Flow controller
FF	Feed-forward
FT	Flow transmitter
GA	Gas analyzer
GC	Gas chromatograph
GT	Gas turbine
He_i	Henry's constant
H_2O	Water
HX	Heat exchanger
k_i	Mass transfer coefficient
K_i	Equilibrium constant
LC	Level controller
L_l	Lean CO_2 loading
L_r	Rich CO_2 loading
L/G	Mass-based liquid to gas ratio (kg/kg)
LT	Level transmitter
MAP	Mean absolute percentage error
MEA	Monoethanolamine
MPC	Model predictive control
N_2	Nitrogen
NCCC	National carbon capture center
NGCC	Natural gas combined cycle
O_2	Oxygen
p	Pressure (Pa)
PC	Pressure controller
PCC	Post-combustion CO_2 capture
PT	Pressure transmitter
PZ	Piperazine
$\dot{Q}_{reb}$	Reboiler duty (W)
Q_{reb}	Reboiler energy input (J)
RC	Relative change
SA	Solvent analyzer
SIMC	Simplified internal model control
SRD	Specific reboiler duty (kJ/kgCO_2)
T	Temperature (K)
TC	Temperature controller
TCM DA	CO_2 Technology Cener Mongstad
t_s	Settling time
t_t	Total stabilization time
TT	Temperature transmitter
X	Mass fraction
x_p	Value measured at pilot plant
x_m	Value simulated model
y_∞	Steady-state final value
θ	Dead time
γ_i	Activity coefficient
ΔH_r	Heat of reaction
Δy	Change in process variable
ε-NTU	Effectiveness number of thermal units

Appendix A

Tables A1–A3 show the simulation results in terms of the dead time θ, 10% settling time t_s, total stabilization time t_t and relative change RC %, for the open-loop response to step-changes in the main inputs to the plant. The step changes are applied to the plant when it is operated at three different steady-state operating conditions defined by three different mass flow rate capacities of the absorber column. The inputs are:

- Flue gas mass flow rate ±10% step-change.
- Solvent mass flow rate ±10% step-change.
- Reboiler duty ±10% step-change.

The output process variables studied are:

- CO$_2$ lean loading L_l (mol/mol).
- CO$_2$ rich loading L_r (mol/mol).
- CO$_2$ absorbed $CO_{2,abs}$ (kg/s).
- CO$_2$ desorbed $CO_{2,abs}$ (kg/s).

Table A1. Open-loop response to ±10% step-changes in flue gas mass flow rate for three different operating points of the pilot plant. Responses in CO$_2$ lean loading L_l, CO$_2$ rich loading L_r, CO$_2$ absorbed, and CO$_2$ desorbed.

	Input	F_{gas} **+10%**				F_{gas} **−10%**			
Plant Load	**Process Variable**	*θ (min)*	*t_s (min)*	*t_t (min)*	*RC (%)*	*θ (min)*	*t_s (min)*	*t_t (min)*	*RC (%)*
100%	L_l	40.5	296.5	337.0	0.01	33.5	133.2	166.7	−0.35
	L_r	0.0	41.7	41.7	0.09	19.0	116.3	135.3	−0.76
	$CO_{2,abs}$	0.0	95.2	95.2	0.05	0.0	168.7	168.7	−0.81
	$CO_{2,abs}$	22.2	244.3	266.5	0.04	22.7	128.7	151.3	−0.80
80%	L_l	50.3	260.8	311.2	−0.03	42.7	442.0	484.7	0.04
	L_r	0.0	53.3	53.3	0.21	67.2	117.5	184.7	−0.15
	$CO_{2,abs}$	0.0	61.8	61.8	−0.03	0.0	334.5	334.5	−0.06
	$CO_{2,abs}$	25.5	393.7	419.2	−0.03	23.8	364.7	388.5	−0.06
60%	L_l	51.9	424.9	476.8	−0.03	53.7	318.5	372.2	0.08
	L_r	0.0	96.1	96.1	0.00	0.0	192.8	192.8	−0.05
	$CO_{2,abs}$	0.0	113.7	113.7	−0.05	0.0	141.2	141.2	0.09
	$CO_{2,abs}$	27.7	363.4	391.1	−0.05	25.6	369.9	395.5	0.09

Table A2. Open-loop response to ±10% step-changes in solvent mass flow rate for three different operating points of the pilot plant. Responses in CO$_2$ lean loading L_l, CO$_2$ rich loading L_r, CO$_2$ absorbed, and CO$_2$ desorbed.

	Input	F_{solv} **+10%**				F_{solv} **−10%**			
Plant Load	**Process Variable**	*θ (min)*	*t_s (min)*	*t_t (min)*	*RC (%)*	*θ (min)*	*t_s (min)*	*t_t (min)*	*RC (%)*
100%	L_l	11.8	15.8	27.7	8.59	14.5	11.5	26	−7.50
	L_r	14.2	89.7	103.8	−0.10	0	63.83	63.83	0.08
	$CO_{2,abs}$	0.0	133.2	133.2	0.35	0	67.16	67.16	−3.14
	$CO_{2,abs}$	0.0	98.8	98.8	0.35	0	12.83	12.83	−3.15
80%	L_l	15.8	18.5	34.3	7.85	19.5	13.16	32.66	−6.87
	L_r	0.0	106.3	106.3	−0.04	0	176.66	176.66	0.02
	$CO_{2,abs}$	0.0	97.8	97.8	2.09	0	65.66	65.66	−4.38
	$CO_{2,abs}$	0.0	18.8	18.8	2.09	0	3.16	3.16	−4.39
60%	L_l	22.0	17.0	39.0	6.75	27	17.33	44.33	−6.28
	L_r	0.0	141.0	141.0	−0.02	0	454	454	0.00
	$CO_{2,abs}$	0.0	104.0	104.0	4.18	0	69.5	69.5	−5.59
	$CO_{2,abs}$	0.0	23.5	23.5	4.18	0	3.8	3.8	−5.59

Table A3. Open-loop response to ±10% step-changes in reboiler duty for three different operating points of the pilot plant. Responses in CO_2 lean loading L_l, CO_2 rich loading L_r, CO_2 absorbed, and CO_2 desorbed.

	Input	$\dot{Q}_{reb}$ **+10%**				$\dot{Q}_{reb}$ **−10%**			
Plant Load	**Process Variable**	θ *(min)*	t_s *(min)*	t_t *(min)*	*RC* (%)	θ *(min)*	t_s *(min)*	t_t *(min)*	*RC* (%)
100%	L_l	13.0	9.7	22.7	−6.29	12.7	15.5	28.2	8.46
	L_r	31.8	81.5	113.3	−0.22	29.5	43.3	72.8	0.00
	$CO_{2,abs}$	6.0	70.8	76.8	6.07	5.0	49.8	54.8	−8.48
	$CO_{2,abs}$	0.0	2.2	2.2	6.07	0.0	10.3	10.3	−8.48
80%	L_l	17.0	11.7	28.7	−5.60	17.0	14.8	31.8	7.78
	L_r	40.7	78.0	118.7	−0.03	38.3	88.0	126.3	0.02
	$CO_{2,abs}$	7.8	74.7	82.5	5.19	5.7	57.0	62.7	−7.16
	$CO_{2,abs}$	0.0	2.7	2.7	5.19	0.0	14.5	14.5	−0.05
60%	L_l	23.2	16.0	39.2	−4.97	23.8	17.3	41.2	6.63
	L_r	47.0	99.3	146.3	−0.01	47.8	114.7	162.5	0.00
	$CO_{2,abs}$	9.5	89.6	99.1	4.00	7.5	72.0	79.5	−5.30
	$CO_{2,abs}$	0.0	3.5	3.5	4.00	0.0	3.3	3.3	−5.30

References

1. The International Energy Agency (IEA). *CO_2 Capture and Storage: A Key Carbon Abatement Option*; International Energy Agency: Paris, France, 2008.
2. Singh, A.; Stéphenne, K. Shell Cansolv CO_2 capture technology: Achievement from first commercial plant. *Energy Procedia* **2014**, *63*, 1678–1685. [CrossRef]
3. Laboratory, N.E.T. Petra Nova Parish Holdings. W.A. Parish Post-Combustion CO_2 Capture and Sequestration Project. Available online: https://www.netl.doe.gov/research/coal/project-information/fe0003311-ppp (accessed on 28 September 2017).
4. Hentschel, J.; Babić, U.A.; Spliethoff, H. A parametric approach for the valuation of power plant flexibility options. *Energy Rep.* **2016**, *2*, 40–47. [CrossRef]
5. Mac Dowell, N.; Staffell, I. The role of flexible CCS in the UK's future energy system. *Int. J. Greenh. Gas Control* **2016**, *48*, 327–344. [CrossRef]
6. Gaspar, J.; Jorgensen, J.B.; Fosbol, P.L. Control of a post-combustion CO_2 capture plant during process start-up and load variations. *IFAC-PapersOnLine* **2015**, *48*, 580–585. [CrossRef]
7. Montañés, R.M.; Korpås, M.; Nord, L.O.; Jaehnert, S. Identifying operational requirements for flexible CCS power plant in future energy systems. *Energy Procedia* **2016**, *86*, 22–31. [CrossRef]
8. Johnsson, F.; Odenberger, M.; Göransson, L. Challenges to integrate CCS into low carbon electricity markets. *Energy Procedia* **2014**, *63*, 7485–7493. [CrossRef]
9. Boot-Handford, M.E.; Abanades, J.C.; Anthony, E.J.; Blunt, M.J.; Brandani, S.; Mac Dowell, N.; Fernandez, J.R.; Ferrari, M.-C.; Gross, R.; Hallett, J.P.; et al. Carbon capture and storage update. *Energy Environ. Sci.* **2014**, *7*, 130–189. [CrossRef]
10. Flø, N.E.; Kvamsdal, H.M.; Hillestad, M.; Mejdell, T. Dominating dynamics of the post-combustion CO_2 absorption process. *Comput. Chem. Eng.* **2016**, *86*, 171–183. [CrossRef]
11. Karimi, M.; Hillestad, M.; Svendsen, H.F. Investigation of the dynamic behavior of different stripper configurations for post-combustion CO_2 capture. *Int. J. Greenh. Gas Control* **2012**, *7*, 230–239. [CrossRef]
12. Garđarsdóttir, S.Ó.; Montañés, R.M.; Normann, F.; Nord, L.O.; Johnsson, F. Effects of CO_2-absorption control strategies on the dynamic performance of a supercritical pulverized-coal-fired power plant. *Ind. Eng. Chem. Res.* **2017**, *56*, 4415–4430. [CrossRef]
13. Panahi, M.; Skogestad, S. Economically efficient operation of CO_2 capturing process part i: Self-optimizing procedure for selecting the best controlled variables. *Chem. Eng. Process. Process Intensif.* **2011**, *50*, 247–253. [CrossRef]
14. Panahi, M.; Skogestad, S. Economically efficient operation of CO_2 capturing process. Part II. Design of control layer. *Chem. Eng. Process. Process Intensif.* **2012**, *52*, 112–124. [CrossRef]

15. Montañés, R.M.; GarÐarsdóttir, S.Ó.; Normann, F.; Johnsson, F.; Nord, L.O. Demonstrating load-change transient performance of a commercial-scale natural gas combined cycle power plant with post-combustion CO_2 capture. *Int. J. Greenh. Gas Control* **2017**, *63*, 158–174. [CrossRef]
16. Nittaya, T.; Douglas, P.L.; Croiset, E.; Ricardez-Sandoval, L.A. Dynamic modelling and control of MEA absorption processes for CO_2 capture from power plants. *Fuel* **2014**, *116*, 672–691. [CrossRef]
17. Zhang, Q.; Turton, R.; Bhattacharyya, D. Development of model and model-predictive control of an MEA-based postcombustion CO_2 capture process. *Ind. Eng. Chem. Res.* **2016**, *55*, 1292–1308. [CrossRef]
18. International Energy Agency Greenhouse Gas R&D Programme (IEAGHG). *Evaluation of Process Control Strategies for Normal, Flexible, and Upset Operation Conditions of CO_2 Post Combustion Capture Processes*; July 2016; IEAGHG: Cheltenham, UK, September 2016.
19. Walters, M.S.; Edgar, T.F.; Rochelle, G.T. Regulatory control of amine scrubbing for CO_2 capture from power plants. *Ind. Eng. Chem. Res.* **2016**, *55*, 4646–4657. [CrossRef]
20. Gaspar, J.; Ricardez-Sandoval, L.; Jørgensen, J.B.; Fosbøl, P.L. Controllability and flexibility analysis of CO_2 post-combustion capture using piperazine and MEA. *Int. J. Greenh. Gas Control* **2016**, *51*, 276–289. [CrossRef]
21. Mac Dowell, N.; Shah, N. The multi-period optimisation of an amine-based CO_2 capture process integrated with a super-critical coal-fired power station for flexible operation. *Comput. Chem. Eng.* **2015**, *74*, 169–183. [CrossRef]
22. Flø, N.E.; Kvamsdal, H.M.; Hillestad, M. Dynamic simulation of post-combustion CO_2 capture for flexible operation of the brindisi pilot plant. *Int. J. Greenh. Gas Control* **2016**, *48 Pt 2*, 204–215. [CrossRef]
23. Ceccarelli, N.; van Leeuwen, M.; Wolf, T.; van Leeuwen, P.; van der Vaart, R.; Maas, W.; Ramos, A. Flexibility of low-CO_2 gas power plants: Integration of the CO_2 capture unit with CCGT operation. *Energy Procedia* **2014**, *63*, 1703–1726. [CrossRef]
24. Wellner, K.; Marx-Schubach, T.; Schmitz, G. Dynamic behavior of coal-fired power plants with postcombustion CO_2 capture. *Ind. Eng. Chem. Res.* **2016**, *55*, 12038–12045. [CrossRef]
25. Olaleye, A.K.; Oko, E.; Wang, M.; Kelsall, G. Dynamic modelling and analysis of supercritical coal-fired power plant integrated with post-combustion CO_2 capture. In *Clean Coal Technology and Sustainable Development, Proceedings of the 8th International Symposium on Coal Combustion, Beijing, China, 19-22 July 2015*; Yue, G., Li, S., Eds.; Springer: Beijing, China, 2016; pp. 359–363.
26. Mechleri, E.; Lawal, A.; Ramos, A.; Davison, J.; Dowell, N.M. Process control strategies for flexible operation of post-combustion CO_2 capture plants. *Int. J. Greenh. Gas Control* **2017**, *57*, 14–25. [CrossRef]
27. Mechleri, E.; Fennell, P.S.; Dowell, N.M. Optimisation and evaluation of flexible operation strategies for coal- and gas-CCS power stations with a multi-period design approach. *Int. J. Greenh. Gas Control* **2017**, *59*, 24–39. [CrossRef]
28. Sanchez Fernandez, E.; Sanchez del Rio, M.; Chalmers, H.; Khakharia, P.; Goetheer, E.L.V.; Gibbins, J.; Lucquiaud, M. Operational flexibility options in power plants with integrated post-combustion capture. *Int. J. Greenh. Gas Control* **2016**, *48*, 275–289. [CrossRef]
29. Dutta, R.; Nord, L.O.; Bolland, O. Selection and design of post-combustion CO_2 capture process for 600 MW natural gas fueled thermal power plant based on operability. *Energy* **2017**, *121*, 643–656. [CrossRef]
30. Kvamsdal, H.M.; Jakobsen, J.P.; Hoff, K.A. Dynamic modeling and simulation of a CO_2 absorber column for post-combustion CO_2 capture. *Chem. Eng. Process. Process Intensif.* **2009**, *48*, 135–144. [CrossRef]
31. Gaspar, J.; Cormos, A.-M. Dynamic modeling and absorption capacity assessment of CO_2 capture process. *Int. J. Greenh. Gas Control* **2012**, *8*, 45–55. [CrossRef]
32. Harun, N.; Nittaya, T.; Douglas, P.L.; Croiset, E.; Ricardez-Sandoval, L.A. Dynamic simulation of MEA absorption process for CO_2 capture from power plants. *Int. J. Greenh. Gas Control* **2012**, *10*, 295–309. [CrossRef]
33. Jayarathna, S.A.; Lie, B.; Melaaen, M.C. Amine based CO_2 capture plant: Dynamic modeling and simulations. *Int. J. Greenh. Gas Control* **2013**, *14*, 282–290. [CrossRef]
34. He, Z.; Sahraei, M.H.; Ricardez-Sandoval, L.A. Flexible operation and simultaneous scheduling and control of a CO_2 capture plant using model predictive control. *Int. J. Greenh. Gas Control* **2016**, *48*, 300–311. [CrossRef]
35. Luu, M.T.; Abdul Manaf, N.; Abbas, A. Dynamic modelling and control strategies for flexible operation of amine-based post-combustion CO_2 capture systems. *Int. J. Greenh. Gas Control* **2015**, *39*, 377–389. [CrossRef]
36. Biliyok, C.; Lawal, A.; Wang, M.; Seibert, F. Dynamic modelling, validation and analysis of post-combustion chemical absorption CO_2 capture plant. *Int. J. Greenh. Gas Control* **2012**, *9*, 428–445. [CrossRef]

37. Åkesson, J.; Laird, C.D.; Lavedan, G.; Prölß, K.; Tummescheit, H.; Velut, S.; Zhu, Y. Nonlinear model predictive control of a CO_2 post-combustion absorption unit. *Chem. Eng. Technol.* **2012**, *35*, 445–454. [CrossRef]
38. Bui, M.; Gunawan, I.; Verheyen, V.; Feron, P.; Meuleman, E.; Adeloju, S. Dynamic modelling and optimisation of flexible operation in post-combustion CO_2 capture plants—A review. *Comput. Chem. Eng.* **2014**, *61*, 245–265. [CrossRef]
39. Enaasen, N.; Zangrilli, L.; Mangiaracina, A.; Mejdell, T.; Kvamsdal, H.M.; Hillestad, M. Validation of a dynamic model of the brindisi pilot plant. *Energy Procedia* **2014**, *63*, 1040–1054. [CrossRef]
40. Enaasen Flø, N.; Knuutila, H.; Kvamsdal, H.M.; Hillestad, M. Dynamic model validation of the post-combustion CO_2 absorption process. *Int. J. Greenh. Gas Control* **2015**, *41*, 127–141. [CrossRef]
41. Van De Haar, A.; Trapp, C.; Wellner, K.; De Kler, R.; Schmitz, G.; Colonna, P. Dynamics of postcombustion CO_2 capture plants: Modeling, validation, and case study. *Ind. Eng. Chem. Res.* **2017**, *56*, 1810–1822. [CrossRef] [PubMed]
42. Gaspar, J.; Gladis, A.; Jørgensen, J.B.; Thomsen, K.; von Solms, N.; Fosbøl, P.L. Dynamic operation and simulation of post-combustion CO_2 capture. *Energy Procedia* **2016**, *86*, 205–214. [CrossRef]
43. Dutta, R.; Nord, L.O.; Bolland, O. Prospects of using equilibrium-based column models in dynamic process simulation of post-combustion CO_2 capture for coal-fired power plant. *Fuel* **2017**, *202*, 85–97. [CrossRef]
44. Chinen, A.S.; Morgan, J.C.; Omell, B.P.; Bhattacharyya, D.; Miller, D.C. Dynamic data reconciliation and model validation of a MEA-based CO_2 capture system using pilot plant data. In Proceedings of the 11th IFAC Symposium on Dynamics and Control of Process Systems, Including Biosystems, Trondheim, Norway, 6–8 June 2016.
45. Abdul Manaf, N.; Cousins, A.; Feron, P.; Abbas, A. Dynamic modelling, identification and preliminary control analysis of an amine-based post-combustion CO_2 capture pilot plant. *J. Clean. Prod.* **2016**, *113*, 635–653. [CrossRef]
46. Faber, R.; Köpcke, M.; Biede, O.; Knudsen, J.N.; Andersen, J. Open-loop step responses for the MEA post-combustion capture process: Experimental results from the esbjerg pilot plant. *Energy Procedia* **2011**, *4*, 1427–1434. [CrossRef]
47. Bui, M.; Gunawan, I.; Verheyen, V.; Feron, P.; Meuleman, E. Flexible operation of CSIRO's post-combustion CO_2 capture pilot plant at the AGL Loy Yang power station. *Int. J. Greenh. Gas Control* **2016**, *48*, 188–203. [CrossRef]
48. Tait, P.; Buschle, B.; Ausner, I.; Valluri, P.; Wehrli, M.; Lucquiaud, M. A pilot-scale study of dynamic response scenarios for the flexible operation of post-combustion CO_2 capture. *Int. J. Greenh. Gas Control* **2016**, *48*, 216–233. [CrossRef]
49. De Koeijer, G.M.; Aasen, K.I.; Steinseth Hamborg, E. *Scale-Up and Transient Operation of CO_2 Capture Plants at CO_2 Technology Centre Mongstad*; Society of Petroleum Engineers: Abu Dhabi, UAE, 2014.
50. Gjernes, E.; Pedersen, S.; Cents, T.; Watson, G.; Fostås, B.F.; Shah, M.I.; Lombardo, G.; Desvignes, C.; Flø, N.E.; Morken, A.K.; et al. Results from 30 wt % MEA performance testing at the CO_2 Technology Centre Mongstad. *Energy Procedia* **2017**, *114*, 1146–1157. [CrossRef]
51. Faramarzi, L.; Thimsen, D.; Hume, S.; Maxon, A.; Watson, G.; Pedersen, S.; Gjernes, E.; Fostås, B.F.; Lombardo, G.; Cents, T.; et al. Results from MEA testing at the CO_2 Technology Centre Mongstad: Verification of baseline results in 2015. *Energy Procedia* **2017**, *114*, 1128–1145. [CrossRef]
52. Thimsen, D.; Maxson, A.; Smith, V.; Cents, T.; Falk-Pedersen, O.; Gorset, O.; Hamborg, E.S. Results from MEA testing at the CO_2 Technology Centre Mongstad. Part I: Post-combustion CO_2 capture testing methodology. *Energy Procedia* **2014**, *63*, 5938–5958. [CrossRef]
53. Modelica Association. Available online: https://www.Modelica.Org/ (accessed on 28 September 2017).
54. Modelon. Post-Combustion Capture with Amine Solutions. Available online: http://www.Modelon.Com/industries/energy-process/carbon-capture-and-sequestration/ (accessed on 28 September 2017).
55. Dassault Systems, Dymola. Available online: http://www.3ds.Com/products-services/catia/products/dymola (accessed on 28 September 2017).
56. Prölß, K.; Tummescheit, H.; Velut, S.; Åkesson, J. Dynamic model of a post-combustion absorption unit for use in a non-linear model predictive control scheme. *Energy Procedia* **2011**, *4*, 2620–2627. [CrossRef]
57. Garðarsdóttir, S.Ó.; Normann, F.; Andersson, K.; Prölß, K.; Emilsdóttir, S.; Johnsson, F. Post-combustion CO_2 capture applied to a state-of-the-art coal-fired power plant—The influence of dynamic process conditions. *Int. J. Greenh. Gas Control* **2015**, *33*, 51–62. [CrossRef]

58. Onda, K.; Takeuchi, H.; Okumoto, Y. Mass transfer coefficients between gas and liquid phases in packed columns. *J. Chem. Eng. Jpn.* **1968**, *1*, 56–62. [CrossRef]
59. Versteeg, G.F.; Van Dijck, L.A.J.; Van Swaaij, W.P.M. On the kinetics between CO_2 and alkanolamines both in aqueous and non-aqueous solutions. An overview. *Chem. Eng. Commun.* **1996**, *144*, 113–158. [CrossRef]
60. Holst, J.V.; Versteeg, G.F.; Brilman, D.W.F.; Hogendoorn, J.A. Kinetic study of CO_2 with various amino acid salts in aqueous solution. *Chem. Eng. Sci.* **2009**, *64*, 59–68. [CrossRef]
61. Böttinger, W. *Nmr-Spektroskopische Untersuchung der Reaktivabsorption von Kohlendioxid in Wässrigen Aminlösungen*; VDI-Verlag: Düsseldorf, Germany, 2006.
62. Montañés, R.M.; Flø, N.E.; Dutta, R.; Nord, L.O.; Bolland, O. Dynamic process model development and validation with transient plant data collected from an mea test campaign at the CO_2 technology center mongstad. *Energy Procedia* **2017**, *114*, 1538–1550. [CrossRef]
63. International Energy Agency Greenhouse Gas R&D Programme (IEAGHG). *Operating Flexibility of Power Plants with CCS*; IEAGHG: Cheltenham, UK, June 2012.
64. Christopher, H.J.; James, K. How to Determine a Unit Ramp Rate (MW/min) for Lowest Total Production Cost. Available online: http://www.heatrate.com/docs/Value-of-Ramp-Rate-1987.pdf (accessed on 28 September 2017).
65. Genrup, M.; Thern, M. *Ny Gasturbinteknik 2012–2014: Gas Turbine Developments*; Report 2012; ELFORSK: Stockholm, Sweden, 2013.
66. Skogestad, S.; Grimholt, C. The SIMC method for smooth PID controller tuning. In *Pid Control in the Third Millennium: Lessons Learned and New Approaches*; Vilanova, R., Visioli, A., Eds.; Springer: London, UK, 2012; pp. 147–175.

© 2017 by the authors. Licensee MDPI, Basel, Switzerland. This article is an open access article distributed under the terms and conditions of the Creative Commons Attribution (CC BY) license (http://creativecommons.org/licenses/by/4.0/).

CATCHING OUR FUTURE

Ambient Measurements of Amines by PTR-QiTOF: Instrument Performance Assessment and Results from Field Measurements in the Vicinity of TCM, Mongstad

(2016)

Available online at www.sciencedirect.com

ScienceDirect

Energy Procedia 114 (2017) 1017 – 1021

Energy Procedia

213th International Conference on Greenhouse Gas Control Technologies, GHGT-13, 14-18 November 2016, Lausanne, Switzerland

Ambient Measurements of Amines by PTR-QiTOF: Instrument Performance Assessment and Results from Field Measurements in the Vicinity of TCM, Mongstad

Tomáš Mikoviny[a], Claus J. Nielsen[a], Wen Tan[a], Armin Wisthaler[a]*, Liang Zhu[a], Anne Kolstad Morken[b], Terje Niøten Nilsen[b]

[a]*Department of Chemistry, University of Oslo, P.O. Box 1033 Blindern, 0315 Oslo, Norway*
[b]*CO_2 Technology Centre Mongstad (TCM DA), 5954 Mongstad, Norway*

Abstract

A PTR-QiTOF instrument was deployed in the field in the vicinity of the CO_2 Technology Center Mongstad (TCM) for measuring amines in ambient air. The observed single-to-double-digit pptv levels of dimethylamine (DMA) and trimethylamine (TMA) are comparable to natural background values reported in the literature for these species. No indication was found that these small alkylamines stem from industrial activities at Mongstad. Monoethanolamine (MEA) was observed at single-digit pptv levels, but further analytical work is needed to validate measurements at such low concentrations. No indication was found that small enhancements in ambient MEA levels were caused by emissions from TCM. No other industrial amines (2-amino-2-methylpropanol, diethylamine and piperazine) were detected in ambient air. According to the current state of knowledge, the observed levels of amines pose no harm to human health or the environment.

© 2017 The Authors. Published by Elsevier Ltd. This is an open access article under the CC BY-NC-ND license (http://creativecommons.org/licenses/by-nc-nd/4.0/).
Peer-review under responsibility of the organizing committee of GHGT-13.

Keywords: amines, post-combustion CO_2 capture, PTR-MS, baseline measurements

---

* Corresponding author. Tel.: +47-22859139
E-mail address: armin.wisthaler@kjemi.uio.no

1876-6102 © 2017 The Authors. Published by Elsevier Ltd. This is an open access article under the CC BY-NC-ND license (http://creativecommons.org/licenses/by-nc-nd/4.0/).
Peer-review under responsibility of the organizing committee of GHGT-13.
doi:10.1016/j.egypro.2017.03.1246

1. Introduction

Amine-based capture of carbon dioxide (CO_2) results in the release of trace amounts of amines to the atmosphere. While amines are nowadays routinely monitored in stack gas, the detection of amines under highly diluted atmospheric conditions remains an analytical challenge [1]. Proton-Transfer-Reaction Mass Spectrometry (PTR-MS) has been successfully used for on-line monitoring of amines in stack gas [2,3] and in atmosphere simulation chambers [4,5,6]. Recently, the ultra-sensitive proton-transfer-reaction quadrupole ion guide time-of-flight mass spectrometer (PTR-QiToF-MS) has become available [7], which is capable of detecting trace gases at single-digit pptv levels (1 pptv = 1 pmol mol^{-1} = 10^{-12} v/v). In the present study, we have used this novel analytical tool for carrying out exploratory measurements of amines in ambient air in the vicinity of the CO_2 Technology Center Mongstad (TCM).

2. Methods

Ambient air measurements were carried out at Sunsbø (60°46'10.1"N, 5°09'08.6"E), Sande (60°50'56.6"N, 5°00'21.0"E) and Mongstad West (60°48'45.7"N, 5°00'43.4"E) from Aug 6 - 28, Aug 28 - Sept 10 and Sept 10 – 25, 2015, respectively. The geographic location of the three measurement sites and of TCM is shown in Figure 1.

Fig. 1. Geographical map showing the locations of the measurement sites at Sunsbø, Sande and Mongstad West and of the Technology Center Mongstad (TCM).

PTR-MS is an on-line chemical ionization (CI) technique for atmospheric trace gases that has been routinely deployed in atmospheric chemistry field studies over the past decade [8]. Only recently, the ultra-sensitive PTR-QiTOF-MS instrument version has become available which detects gaseous analytes at single-digit pptv-levels [7].

We operated the PTR-QiTOF instrument in the routine mode of operation recommended by the manufacturer (H_3O^+ CI; drift tube pressure 3.8 mbar, drift tube temperature 60 °C, reduced electric field strength 120 Td with 1 Td = 10^{-17} V cm^2). Mass spectra were recorded in the m/z 15 to m/z 510 range, but only selected signals corresponding to protonated methylamine, dimethylamine (DMA) and ethylamine, trimethylamine (TMA), monoethanolamine (MEA), 2-amino-2-methylpropanol (AMP), diethylamine and piperazine, respectively, were analyzed in detail. The list of target amines was taken from a previous study [1]. The PTR-TOF Data Analyzer v4.44 was used for data analysis [9]. 2-minute and 1-hour averages were generated from the data output.

An optimized inlet system was used for minimizing inlet losses of amines. Ambient air was sampled at a flow rate of 12 liters per minute trough a passivated stainless steel tube (material: SilcoNert® 2000, outer diameter: 6.35

mm, length: 115 cm, temperature: 60 °C). The PTR-QiTOF instrument sub-sampled a flow of 0.5 liters per minute through a heated capillary (material: PEEK, outer diameter: 1.59 mm, temperature: 60 °C). No evidence for inlet losses was found when ambient air was spiked with known amounts of DMA and TMA at pptv levels.

Amine-free air generated from compressed and catalytically cleaned (Pt/Pd at 325 °C) ambient air was periodically (every 12 hours for 30 minutes) fed to the inlet system for instrumental background determination.

Instrumental response factors for DMA, TMA and MEA were calculated from ion-molecule reaction kinetics using the molecular properties reported previously [4,5,6]. The estimated accuracy of the reported volume mixing ratios is ±20% for volume mixing ratios above 10 pptv.

TCM is part of a large industrial complex (refinery, power plant, oil terminal) at Mongstad which is located in a pristine coastal environment. Oil and gas tracers were used for distinguishing between periods when the outflow from the Mongstad complex was advected to the sampling sites and periods when natural background air was sampled. TCM was in operation during the ambient air measurement campaign, with MEA being used for CO_2 capture.

3. Results

AMP, diethylamine and piperazine were not detected at levels above 10 pptv in the recorded mass spectra. It was not possible to measure these species at single-digit pptv levels due to mass spectral interferences. The PTR-QiTOF instrument, in its routine mode of operation, was not capable of detecting methylamine. The abundant O_2^+ signals distorted the mass spectrum in the region where methylamine is detected.

The hourly average time series of DMA, TMA and MEA are shown in Figures 2a, 2b and 2c, respectively. The color-coded data points identify the time periods when the outflow from the Mongstad industrial complex was advected to the sampling site.

DMA was observed at single-digit pptv levels, which is at or close to the instrumental detection limit. The detection of amines at such low concentrations is an analytical challenge and all single-digit pptv data reported herein should be taken with caution. More analytical validation work is needed in this concentration regime. The 2-minute average data show episodic short-term enhancements in the 10 to 22 pptv range at all three measurement sites. These enhancements were found both in natural background air and in the outflow from the Mongstad complex.

TMA levels were typically close to zero, with the exception of an episode lasting from Sept 1 to 12 when hourly average volume mixing ratios up to 49 pptv were recorded. Enhanced levels of TMA were observed at the Sande and the Mongstad West site, both in natural background air and in the outflow from the industrial site.

MEA levels were also in the single-digit pptv range. Yet again, these concentrations should be interpreted with caution. A 1-2 pptv enhancement was observed in the period from Aug 31 to Sept 10, both in natural background air and in the Mongstad outflow. This comes as a surprise as MEA is not believed to have natural sources. Further research is warranted to confirm these findings and exclude potential signal interferences for MEA.

The time series data indicate that amine levels were not enhanced in the Mongstad outflow as compared to natural background conditions. This is also reflected in the overall statistical analysis summarized in Table 1.

4. Discussion and Conclusions

A PTR-QiTOF instrument was successfully deployed in the field for the first time to measure amines in ambient air. The observed single-to-double-digit pptv levels of DMA and TMA are comparable to coastal background values reported in the literature for these species [10]. No indication was found that these small alkylamines stem from industrial activities at Mongstad. According to the current state of knowledge, the observed levels of alkylamines pose no direct or indirect harm to human health or the environment.

TCM was operating on MEA during the ambient measurements. Single-digit pptv levels of MEA were observed in ambient air, but no indications were found that these small enhancements were caused by emissions from TCM. Further analytical work is, however, needed to validate MEA measurements at such low concentrations. No other industrial amines (AMP, diethylamine and piperazine) were detected.

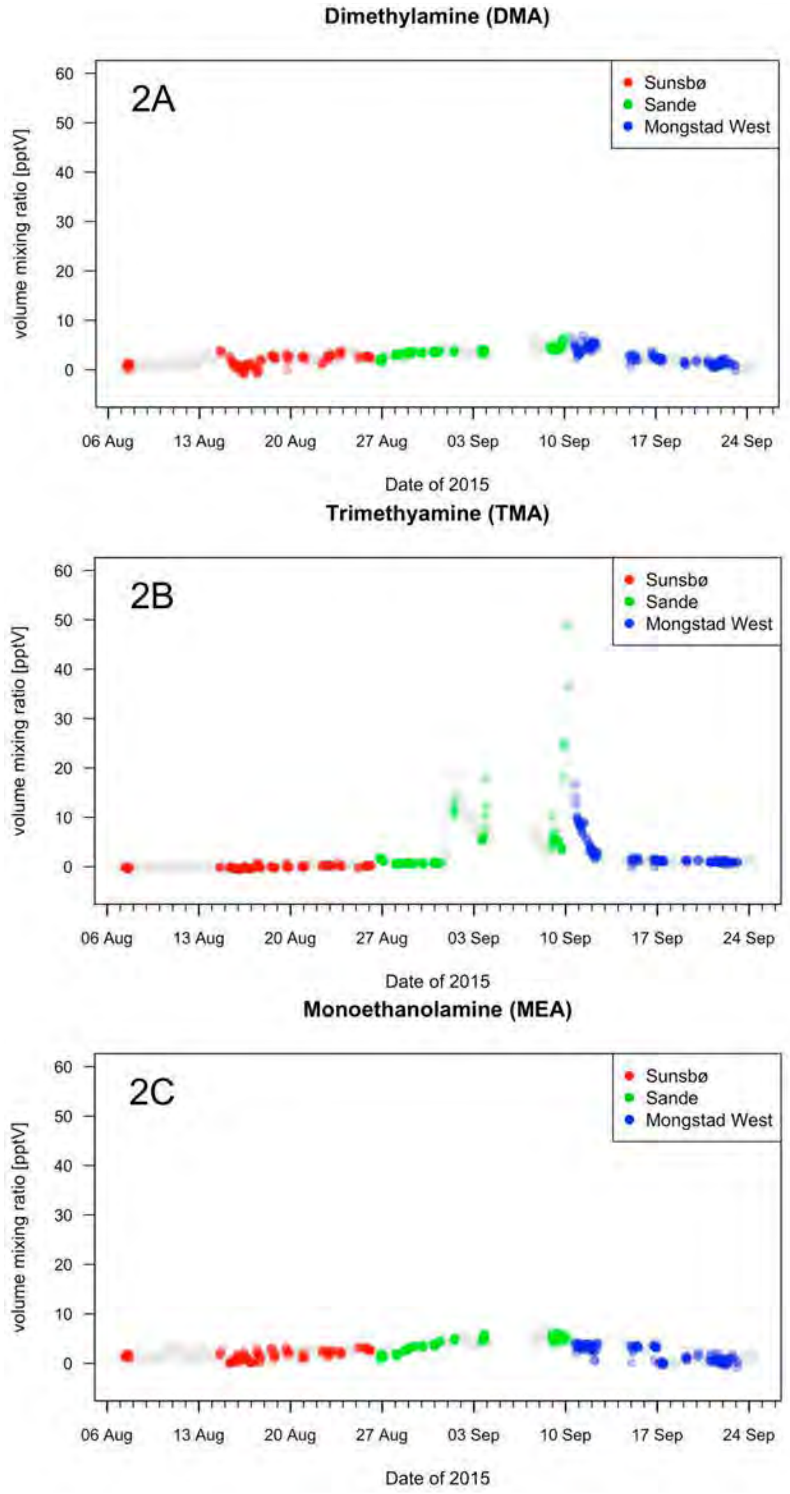

Fig. 2. Hourly average time series of DMA, TMA and MEA amine as measured at Sunsbø, Sande and Mongstad West in August and September of 2015. The color-coded data points identify the time periods when the Mongstad outflow was advected to the sampling sites.

Table 1. Average mixing ratios (in pptv) of DMA, TMA and MEA as observed at the Sunsbø, Sande and Mongstad West sites, respectively, when the Mongstad plume was advected and under natural background conditions. No statistically significant enhancement of amines was found in the outflow from the Mongstad industrial complex as compared to natural background conditions.

	DMA		TMA		MEA	
	TCM	baseline	TCM	baseline	TCM	baseline
Sunsbø	1.2 ± 1.8	1.6 ± 1.9	0.5 ± 0.6	0.5 ± 0.7	0.2 ± 1.9	0.5 ± 1.9
Sande	3.3 ± 1.9	3.4 ± 1.7	5.2 ± 7.9	5.7 ± 7.1	2.4 ± 2.2	2.5 ± 1.8
Mongstad west	0.9 ± 2.1	0.6 ± 1.8	0.7 ± 1.1	1.0 ± 1.1	0.1 ± 2.1	0.5 ± 2.2

References

[1] Vik AF, Rostkowski P. Amines in ambient air at TCM - Monitoring program May 2012 – April 2013, NILU Report OR 31/2015 (2015)

[2] Zhu L, Schade GW, Nielsen CJ. Real time monitoring of emissions from monoethanolamine-based industrial scale carbon capture facilities. Environ Sci Technol. 2013; 47, 14306-14314

[3] Morken AK, Nenseter B, Pedersen S, Chhaganlal M, Feste JK, Tyborgnes RB, Ullestad Ø, Ulvatn H, Zhu L, Mikoviny T, Wisthaler A, Cents T, Bade OM,GKnudsen J, de Koeijer G, Falk-Pedersen O, Hamborg ES. Emission results of amine plant operations from MEA testing at the CO2 Technology Centre Mongstad. Energy Procedia 2014; 63, 6023–6038

[4] Nielsen CJ, D´Anna B, Bossi R, Bunkan AJC, Dithmer L, Glasius M, Hallquist M, Hansen AMK, Lutz A, Salo K, Maguta MM, Nguyen Q, Mikoviny T, Müller M, Skov H, Sarrasin E, Stenstrøm Y, Tang Y, Westerlund J, Wisthaler A. Atmospheric Degradation of Amines (ADA). Summary report from atmospheric chemistry studies of amines, nitrosamines, nitramines and amides, University of Oslo, Oslo, Norway 2012; ISBN 978-82-992954-7-5, http://urn.nb.no/URN:NBN:no-30510

[5] Nielsen CJ, D'Anna B, Karl M, Aursnes M, Boreave A, Bossi R, Bunkan AJC, Glasius M, Hansen AMK, Hallquist M, Kristensen K, Mikoviny T, Maguta MM, Müller M, Nguyen Q, Westerlund J, Salo K, Skov H, Stenstrøm Y, Wisthaler A. Atmospheric Degradation of Amines (ADA). Summary report: Photo-oxidation of methylamine, dimethylamine and trimethylamine, NILU Report OR 2/2011

[6] Nielsen CJ, D'Anna B, Dye C, George C, Graus M, Hansel A, Karl M, King S, Musabila M, Müller M, Schmiedbauer N, Stenstrøm Y, Wisthaler A. Atmospheric Degradation of Amines (ADA). Summary report: Gas phase photo-oxidation of 2-aminoethanol (MEA), NILU Report OR 8/2010

[7] Sulzer P, Hartungen E, Hanel G, Feil S, Winkler K, Mutschlechner P, Haidacher S, Schottkowsky R, Gunsch D, Seehauser H, Striednig M, Jürschik S, Breiev K, Lanza M, Herbig J, Märk JL, Märk TD, Jordan A. A Proton Transfer Reaction-Quadrupole interface Time-Of-Flight Mass Spectrometer (PTR-QiTOF): High speed due to extreme sensitivity. Int J Mass Spectrom 2014; 368:1–5

[8] De Gouw J, Warneke C. Measurements of volatile organic compounds in the earth's atmosphere using proton-transfer-reaction mass spectrometry, Mass Spectrom Rev 2007; 26, 2:223–257

[9] Müller M, Mikoviny T, Jud W, D'Anna B, Wisthaler A. A new software tool for the analysis of high resolution PTR-TOF mass spectra, Chemom Intell Lab Syst 2013; 127:158–165

[10] Ge X, Wexler AS, Clegg SL. Atmospheric amines - Part I. A review, Atmos Environ 2011; 45:524-546

Results from MEA testing at the CO_2 Technology Centre Mongstad: Verification of baseline results in 2015

(2016)

Available online at www.sciencedirect.com

ScienceDirect

Energy Procedia 114 (2017) 1128 – 1145

Energy Procedia

13th International Conference on Greenhouse Gas Control Technologies, GHGT-13, 14-18 November 2016, Lausanne, Switzerland

Results from MEA testing at the CO_2 Technology Centre Mongstad: Verification of baseline results in 2015

Leila Faramarzi[a,b,]*, David Thimsen[c], Scott Hume[c], Andrew Maxon[c], Guillaume Watson[d], Pedersen S[a], Erik Gjernes[e], Berit F. Fostås[b], Gerard Lombardo[e], Toine Cents[f], Anne Kolstad Morken[a,b], Muhammad Ismail Shah[a,e], Thomas de Cazenove[a], Espen Steinseth Hamborg[a,b]

[a] *CO_2 Technology Centre Mongstad (TCM DA), 5954 Mongstad, Norway*
[b] *Statoil ASA, P.O. Box 8500, 4035 Stavanger, Norway*
[c] *Electric Power Research Institute, Inc., 3420 Hillview Avenue, Palo Alto, CA 34304, USA*
[d] *Shell Global Solutions International B.V., PO Box 663, 2501CR The Hague, The Netherlands*
[e] *Gassnova SF, Dokkvegen 10, 3920 Porsgrunn, Norway*
[f] *Sasol Technology, P.O. Box 5486, Johannesburg 2000, South Africa*

Abstract

In 2015, the CO_2 Technology Center Mongstad (TCM DA) operated a post-combustion CO_2 capture test campaign using aqueous monoethanolamine solvent at 30 weight%. The main objective was to demonstrate and document the performance of the TCM DA amine plant located in Mongstad, Norway.

During the treatment of flue gas from the natural gas-fired combined heat and power plant at Mongstad, a revised baseline was established for the TCM DA amine plant in accordance to the verification protocol developed by the Electrical Research Institute, Inc. This paper presents the revised baseline, which can be considered as a reference case for the solvent-based CO_2 capture processes applied to natural gas-based flue gases.

© 2017 The Authors. Published by Elsevier Ltd. This is an open access article under the CC BY-NC-ND license (http://creativecommons.org/licenses/by-nc-nd/4.0/).
Peer-review under responsibility of the organizing committee of GHGT-13.

Keywords: CO_2 capture; EPRI; Verification; Monoethanolamine; CO_2 Technology Centre Mongstad; TCM DA

---

* Corresponding author. Tel.: +47-56 34 52 20.
E-mail address: leila.faramarzi@tcmda.com

1876-6102 © 2017 The Authors. Published by Elsevier Ltd. This is an open access article under the CC BY-NC-ND license (http://creativecommons.org/licenses/by-nc-nd/4.0/).
Peer-review under responsibility of the organizing committee of GHGT-13.
doi:10.1016/j.egypro.2017.03.1271

1. Introduction

The CO_2 Technology Centre Mongstad (TCM) is located next to the Statoil refinery in Mongstad, Norway. TCM DA is a joint venture set up by Gassnova representing the Norwegian state, Statoil, Shell, and Sasol. The facility run by TCM DA entered the operational phase in August 2012 and is one of the largest post-combustion CO_2 capture (PCC) test centres in the world. A unique aspect of the facility is that either a flue gas slipstream from a natural gas-based combined heat and power (CHP) plant or an equivalent volumetric flow from a residual fluid catalytic cracker (RFCC) unit can be used for CO_2 capture. The CHP flue gas contains about 3.5% CO_2 and the RFCC flue gas contains about 13-14% CO_2, the latter of which is comparable to CO_2 levels seen in coal-fired flue gas. One of the main test plants at TCM DA is a highly flexible and well-instrumented amine plant. The amine plant was designed and constructed by Aker Solutions and Kværner to accommodate a variety of technologies, with capabilities of treating flue gas streams of up to 60,000 standard cubic meters per hour. The plant is being offered to vendors of solvent-based CO_2 capture technologies to, among others, test: (1) the performance of their solvent technology; and (2) technologies aimed to reduce the atmospheric emissions and environmental impact of amines and amine-based degradation products from solvent-based CO_2 capture processes. The objective of TCM DA is to test, verify, and demonstrate CO_2 capture technologies suitable for deployment at full-scale. A significant number of vendors, Aker Solutions, Alstom (now GE Power), Cansolv Technologies Inc., and Carbon Clean Solutions Ltd. have already successfully used the TCM DA facilities to verify their CO_2 capture technologies.

From 6 July to 17 October 2015 TCM DA, in collaboration with partners, operated a monoethanolamine (MEA) campaign with the main objective to document and demonstrate the amine plant performance.

TCM DA investigated the stripper performance and concluded that the use of anti-foam made it possible to utilise the full flue gas supply capacity of 60,000 standard cubic meters per hour. At the full CHP flue gas capacity, the CO_2 capture rate was about 85% when MEA at 30 weight% (wt%) was used. The corresponding specific reboiler duty (SRD) was about 3.6 GJ/ton CO_2. Total and CO_2 mass balance closures were near 100 %. Emission levels of MEA, NH_3, aldehydes, nitrosamines, nitramines, and other compounds were also measured during extractive samples for the defined time periods and were all below the permissible levels set by the Norwegian Environment Agency (Miljødirektoratet).

During the treatment of the CHP flue gas at full capacity, a revised baseline was established for the TCM DA amine plant. The revised CHP baseline was verified by the Electric Power Research Institute, Inc. (EPRI).

EPRI has developed a structured CO_2 capture testing methodology for characterizing PCC processes. EPRI's methodology is designed to provide relevant information for baselining and comparing technologies, referred to as an independent verification protocol (IVP). This methodology has been tailored to the TCM DA amine plant facility and is presented in detail elsewhere [1].

The amine plant is planned and equipped for conducting research and development activities and TCM DA has recently installed a number of additional gas-phase analysers to improve the speed and accuracy of measurements. The IVP methodology has therefore been updated by EPRI to reflect these recently installed instruments.

The revised CHP baseline was verified by EPRI, following their requirements including the use of third-party gas phase and emission measurements done by FORCE Technology. FORCE Technology performed comprehensive measurements on flow rates, temperatures, and compositions on the absorber inlet, the absorber outlet (depleted flue gas), and the stripper outlet.

This paper will present the revised baseline for the TCM DA amine plant, in accordance to the IVP developed by EPRI.

Nomenclature		**Units**	
ASME	American Society of Mechanical Engineers	barg	bar gauge
CEMs	continuous emissions monitors	count/cm^3	count per cubic centimetre
CHP	combined heat and power	g/hr	grams per hour
ELPI+	electrical low pressure impactor	GJ/t	giga joule per ton
EPRI	Electrical Power Research Institute, Inc.	kg/hr	kilogram per hour
FTIR	Fourier transform infrared	kg/m^3	kilogram per cubic meter
GC	gas chromatograph	m	meter
IVP	independent verification protocol	mg/Sm^3	milligram per standard cubic meter
NDIR	non-dispersive infrared	MJ/hr	mega joule per hour
PCC	post-combustion CO_2 capture	Sm^3/hr	standard cubic meter per hour
RFCC	residual fluid catalytic cracker	vol%	volume percentage
TCM	Technology Centre Mongstad	wt%	weight percentage
TVOC	total volatile organic carbon	µm	micrometre

2. Amine plant

The schematic of the TCM DA amine plant when treating the CHP flue gas is shown in Figure 1.

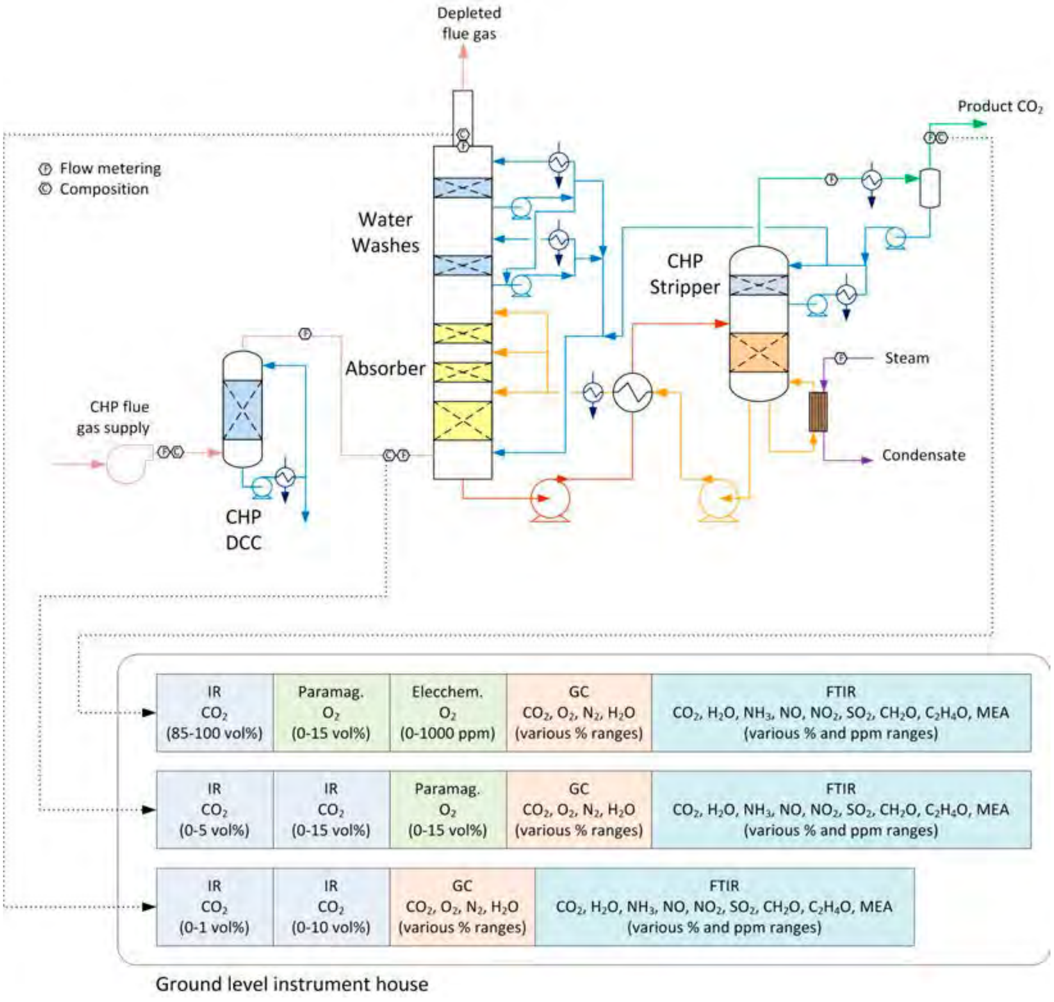

Figure 1. The TCM DA amine plant when treating the CHP flue gas.

The nominal CHP flue gas characteristics along with the existing instrumentations are specified elsewhere [2]. The main systems in the plant are also explained in detail in a previously published paper [1].

3. IVP project overview

The roles and responsibilities of the organizations that conducted the current IVP project are as follows;

- **TCM DA** is the project owner and organized the field testing during the test period. The test program for the baseline testing was developed by the owners of TCM DA. TCM DA personnel operated the plant throughout the testing and collected lean and rich liquid samples for laboratory analysis during the test period.
- **FORCE Technology** was contracted by TCM DA to collect and analyse samples from the CHP flue gas supply, depleted flue gas, and product CO_2 streams. Two crews from FORCE Technology conducted the sampling sequentially with a single set of continuous emissions monitors (CEMs). FORCE Technology also collected gas samples for off-site analysis of particulate, SO_2, SO_3, amine, and degraded amine components.
- **Laborelec** carried out particulate concentration and size distribution measurements during the baselining period. Laborelec characterized the size of and the number of particles formed at different points through the absorber tower by using an electrical low-pressure impactor (ELPI+) device.
- **EPRI** was contracted by TCM DA to apply the IVP during the MEA baseline testing. Two EPRI engineers were on-site during the testing to observe the conduct of the tests. EPRI also led analyzing the results from the IVP project.

4. IVP

4.1. Approach

A detailed description of the IVP approach was previously reported [1]. A summary of the approach is provided here.

The purpose of the IVP is to measure and report key performance indices of the PCC process (those indices critical to up-scaling the process). Key performance indices (dependent parameters) include CO_2 capture, CO_2 production, emission, utility usage (steam, power and cooling), and trace constituents of the depleted flue gas and product CO_2. The key performance indices depend on a number of independent parameters including: the overall process design, physical characteristics (and operating conditions) of process equipment, flue gas supply conditions and flow rate, lean and rich solutions conditions and flow rate, and stripper pressure.

Many of the dependent parameters can be modeled using commonly available chemical engineering computer process modeling tools. Field measurement of these key performance indices (along with the uncertainty in the measurements) can be used to calibrate the computer process models. Other dependent parameters (such as trace components in the depleted flue gas and product CO_2) are difficult to model with currently available tools. Field measurements of these parameters will serve as primary data for up-scaling process designs.

The IVP approach to field performance testing is generally consistent with the approach taken by others for performance testing of a number of power processes [3]. The IVP specifies procedures for collecting composition, temperature, pressure, and flow data at TCM DA sufficient to calculate and report key performance indices and the corresponding numerical uncertainty in the values reported. Industry-accepted standard reference test methods are specified for the collection of composition, temperature, pressure, and flow data. Procedures for reducing the data are also specified. The IVP focuses on campaign-style testing in which days are dedicated to testing at previously selected optimum process operating conditions, but the IVP principles can also guide parametric testing undertaken to identify optimum process conditions.

4.2. MEA 2015 test campaign conduct

The second campaign of base-case testing of the performance of the TCM DA amine plant using a nominal 30% MEA as the solvent was conducted the week of 7 September 2015 after approximately eight weeks of operating the amine plant with the 30 wt% MEA solution. The plant was operated at steady state throughout the week.

FORCE Technology was on-site to manually collect contemporaneous samples from the flue gas supply, depleted flue gas, and product CO_2. Laborelec was also on-site to manually collect samples for particulate and aerosol size distribution analysis at different locations through the absorber tower.

During all sampling periods the following data were collected:

- CO, CO_2, NO_X, O_2, SO_2, and N_2 (by difference) concentrations in volume percent (vol%)
- Flow rate, pressure, and temperature.

The sampling time periods and sampling period designators are shown in Table 1 along with additional sampling undertaken on each day. Data logs for all sampling periods containing pertinent flows, temperatures, pressures, and concentrations measured by permanent plant instruments were supplied by TCM DA.

Table 1. FORCE Technology and Laborelec sampling periods.

Stream sampled	Date	Start time / Stop time	Sampling results reported	Test period
Depleted flue gas	9 September 2015	12:50 / 15:37	Flow	C3-4
		13:08 / 15:44	H_2SO_4, SO_2, HCl, HF, HCN, particulates, CEMs	C3-1
		17:07 / 19:18	Acetone, aldehydes, amides, amines	C3-2
Depleted flue gas	10 September 2015	9:07 / 11:05	NH_3, total N, H_2S, mercaptans, TVOC[*]	C3-3
Product CO_2	9 September 2015	13:08 / 15:45	H_2SO_4, SO_2, HCl, HF, HCN, particulates, CEMs	C3-1
		13:09 / 14:59	Flow	C3-4
		17:10 / 19:19	Acetone, aldehydes, amides, amines	C3-2
Product CO_2	10 September 2015	9:04 / 11:06	NH_3, total N, H_2S, mercaptans, TVOC	C3-3
Flue gas supply	9 September 2015	11:58 – 15:01	Flow	C3-4
		13:08 / 15:45	H_2SO_4, SO_2, HCl, HF, HCN, particulates, CEMs	C3-1
		17:07 / 19:19	Acetone, aldehydes, amides, amines	C3-2
Flue gas supply	10 September 2015	9:04 / 11:06	NH_3, total N, H_2S, mercaptans, TVOC	C3-3
Post-capture packing	10 September 2015	19:55 / 19:57	Particle size distribution	C3-5
Post-water wash	10 September 2015	18:32 / 18:34	Particle size distribution	C3-6
Post-acid wash	8 September 2015	13:57 / 15:06	Particle size distribution	C3-7
Absorber outlet	11 September 2015	10:47 / 11:32	Particle size distribution	C3-8

[*] *TVOC: total volatile organic carbon*

5. Instrument assessment

An important component in the determination of process plant performance is the quality of the instrumentation installed for measuring the respective compositions and flow rates. Two measures of instrumentation quality are:

- Accuracy/bias: This represents the difference between the instrument reading (or average of a set of readings under unchanging process conditions) being assessed and the true value of the parameter being measured. Appropriate determination of the "true value" must be achieved by simultaneous measurement of the parameter using a reference method or instrument with calibration that can be traced to primary standards.
- Precision: A determination of the variability of the instrument reading when stream conditions are known to be steady state. Precision is therefore a measure of the random error associated with the measurement.

These measurement errors can be combined to assess the aggregate uncertainty in a given measurement. In the absence of a calibration against primary standards for the entire measurement range needed, the uncertainty published by the instrument supplier represents only the precision error.

When the process parameter being measured does not change, precision is a measure of repeatability. In real plant situations, it is often the case that the process parameters (flow, pressure, and temperature) do vary over the measurement period. Thus, measurements over long periods of time (greater than process time constants) will also include an error term related to process uncertainty.

5.1. Gas phase compositions

In the first baseline MEA in 2014, the CO_2 and O_2 content of the flue gas supply, depleted flue gas, and CO_2 product stream were routinely determined by a single Fourier Transform Infrared (FTIR) instrument (Applied Instrument Technologies and Finetech, model: Anafin 2000) along with an O_2 instrument (Siemens, model: Oxymat 6). Since these instruments were shared between the sampling points, a sampling system was installed to extract from the various single points as given by Thimsen et al. [1]. The sample was continuously drawn by a selection system serving the analysers and was diverted to the common analysers in a 90-minute cycle; i.e., the analyser cycles between flue gas supply for 15 minutes, depleted flue gas for 30 minutes, and CO_2 product stream for 15 minutes, and an additional 30 minutes for purging operations.

Following the first MEA baseline campaign, TCM DA has since installed a number of additions to the gas measurement systems to improve the speed and accuracy of the measurements and widen the breadth of measurement techniques. To complement the original FTIR unit, two new additional Gasmet FTIR units (model: FCX) were installed, facilitating dedicated and continuous FTIR measurements at all three locations. Additionally, the CO_2 concentration at the inlet and outlet of the absorber column was also determined by two non-dispersive infrared (NDIR) units (Siemens, model: Ultramat 6) at each location, one set to high range (vol%) and one low range (ppmv) on a dry-gas basis. A trace O_2 instrument [Teledyne Instruments 3001] was installed to quantify O_2 content of the product CO_2. The system has been further complemented with a new Siemens Maxum Edition II gas chromatograph (GC) unit that is capable of measuring the CO_2, O_2, and nitrogen content at all three locations in a near-simultaneous fashion.

During the September 2015 operations, FORCE Technology carried out simultaneous analysis on three process streams (flue gas supply, depleted flue gas, and CO_2 product stream). Comparison of the TCM DA values determined by the FTIR systems (after converting to dry basis assuming saturation at the measured pressure and temperature), NDIR analysers, and GC with the FORCE Technology data are given in Figure 2 and Figure 3. Details include:

- Figure 2 displays the CHP flue gas supply CO_2 and O_2 concentration data over the test campaign. There is good agreement between the FORCE Technology CO_2 NDIR and the TCM GC CO_2 measurements (<0.5% point difference) with the two TCM NDIR units showing a similar offset of 2% of the measured value (<0.08 vol%). The TCM FTIR CO_2 average values compare well with the FORCE Technology measurements, however the instantaneous measurements showed significant scatter from the mean value (7% spread, representing ±0.3 vol%). The TCM FTIR O_2 measurements agree more closely (less than 0.5 vol% dry O_2) than the GC, which is over 1 vol% dry O_2 higher in all measurement points. On the morning of 10 September 2015, the second O_2 measurement period carried out by FORCE Technology has an overall similar offset as observed on 9 September 2015 following a morning calibration of the instrument.

- Figure 3 displays the depleted flue gas CO_2 and O_2 concentration data over the test campaign. The data from all of the TCM instruments closely track together, suggesting that the process CO_2 concentration had a degree of variability (±0.2 vol%) during that operating period. The FORCE Technology measurements showed more variability than the TCM instruments. Data from all four TCM instruments are consistently higher than the FORCE Technology data by 10% to 25% (FTIR is the closest). The consistency in this bias, especially between the TCM NDIR and FORCE Technology NDIR instruments suggests either a difference in the calibrations of the respective instruments during the FORCE Technology campaign or, possibly, an anomaly in the FORCE Technology sampling system that diluted the sample with ambient air. It is also important to note that the FORCE Technology measurements of depleted flue gas CO_2 were at or below the stated limit of detection of 0.5 vol%, although the NDIR was calibrated using "low-range" calibration gases and values down to 0.3 vol% were reported to a single significant figure to reflect the increased uncertainty of the measurements at these low levels.
- The product CO_2 composition data reported by FORCE Technology had an O_2 content of between 5-12 ppmv, far lower than the 1-2 vol% reported by FORCE Technology during the MEA campaign in February 2014 [4], which was thought to be contaminated by air in-leakage and subsequently disqualified. The TCM GC instrument measured nitrogen in the product with an average of 180 ppmv. For the purposes of calculating CO_2 removal and recovery, it is assumed here that the product CO_2 stream is saturated with water at the measured temperature and pressure and contains the small trace quantities of O_2 and N_2 measured. The balance is presumed to be CO_2.

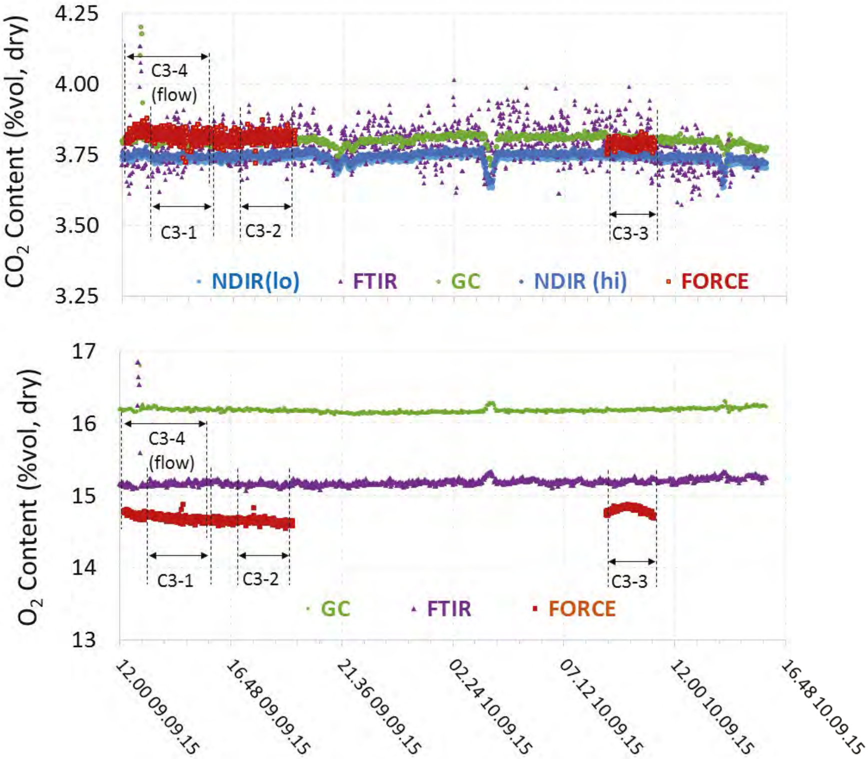

Figure 2. CHP flue gas supply CO_2 and O_2 data for all analysers. Data collected by FORCE Technology on 9 and 10 September 2015 are also shown.

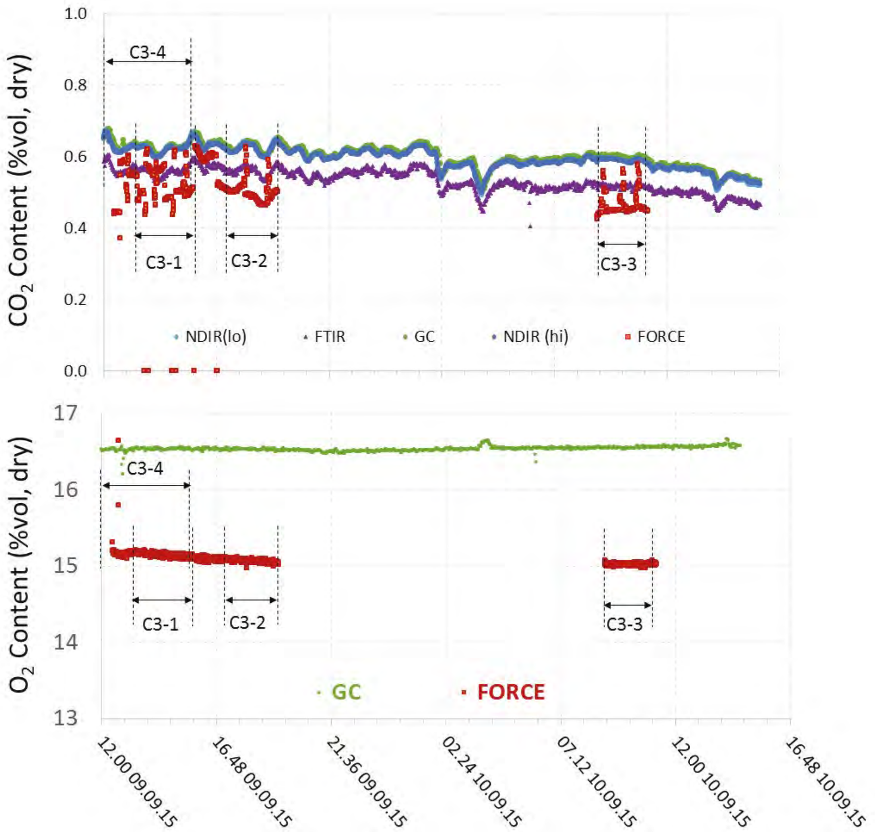

Figure 3. Depleted flue gas CO_2 and O_2 data. Data collected by FORCE Technology on 9 and 10 September 2015 are also shown.

5.2. Gas phase flow rates

Continuous measurement of the flow rates of the supply flue gas, depleted flue gas, and CO_2 product stream were determined by TCM DA plant instrumentation. In particular, the TCM DA amine plant facility is well instrumented for determining the flue gas supply flow rate, with several different types of flow meters positioned in series.

During the base-case operations, pitot-tube traversing of the supply flue gas, depleted flue gas, and CO_2 product stream was carried out by FORCE Technology to determine the flow rates, the results of which are compared to plant instrumentation measurements below:

- The CHP flue gas supply flow is measured by two independent instruments, an ultrasonic flow meter (FT-0150) and a multi-pitot-tube flow meter (FIC-0124), which are characterized in Table 2. The data from these flow meters are shown in Figure 4. All flow rates are at defined standard conditions of 15 °C and 101.3 kPa. The CHP flue gas flow was very steady over the test period on 9 September 2015 when FORCE Technology made independent measurements of flow as indicated in Figure 4. The difference between the values measured by FORCE Technology and that measured by the plant instruments is between 2–6%, well within the reported uncertainty in the FORCE Technology measurement of 10% The test period flow averages used for all calculations are the data reported by the ultrasonic flow meter (FT-0150).
- The depleted flue gas flow is measured by a single multi-pitot tube flow meter (FT-2431), whose characteristics are listed in Table 2. The measured flow had a higher degree of variability than the inlet CHP measurement (spread of 5.9% versus 0.7% for FT-0150) and also has significant transients that are not correlated with any process parameter. The data are, however, fairly consistent over the period during which FORCE Technology

made independent measurements on 9 September 2015 so a comparison is possible. The individual FORCE Technology measurements average to 55,900±10% Sm^3/hr, dry (101.3 kPa, 15°C) at this location. The average flow over the same time period reported by the plant flow meter is 54,200 Sm^3/hr, well within the 10% uncertainty in the FORCE Technology measurement. Nevertheless, the questions associated with this measurement are sufficient to choose to calculate the depleted flue gas flow rate assuming that all O_2 and N_2 entering with the flue gas supply leave in the depleted flue gas. The performance data reported here use such a calculation of depleted flue gas flow rate.

- The product CO_2 flow measured by the vortex flow meter (FT-0010) is the primary flow meter used by TCM operators, whose characteristics are listed in Table 2. The data from this flow meter are shown in Figure 5. The product CO_2 flow was relatively steady over the test period. FORCE Technology made independent measurements of flow on 9 September 2015 as indicated in Figure 5. The difference between the value measured by FORCE Technology and that measured by the plant instruments is approximately 7.5%, within the measurement uncertainty reported by FORCE Technology of 10%.

Table 2. Key flow instrumentations. Precision uncertainties are based on internal assessments by TCM DA.

Stream	Tag number	Instrument type	Primary flow measurement	Precision uncertainty
CHP flue gas supply	FIC-0124	Multi-pitot tube	Differential pressure	2.5%
	FT-0150	Ultra-sonic	Flowing volume	1.3%
Absorber outlet depleted flue gas	FT-2431	Multi-pitot tube	Differential pressure	5.4%
Product CO_2	FT-0010	Vortex	Flowing volume	1.0%

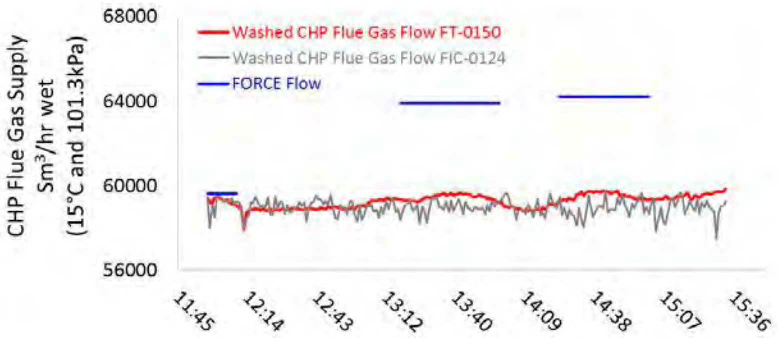

Figure 4. CHP flue gas supply flow measurements measured on 9th September 2016.

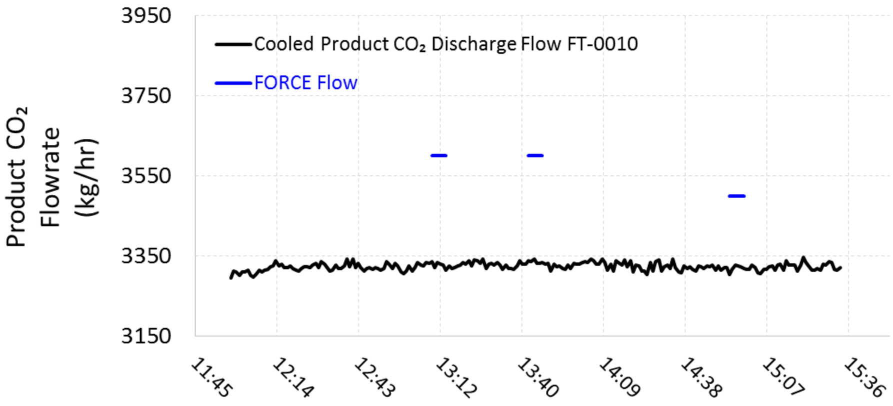

Figure 5. Product CO_2 flow rate and test period averages measured on 9 September 2016.

5.3. Steam and condensate flow rates

The TCM DA amine plant receives high-pressure (HP) superheated steam from the neighbouring refinery at a pressure of approximately 30 bars and a temperature of between 240°C to 310°C. The HP steam is throttled near the stripper reboiler to a pressure of approximately 5 bar before being desuperheated with condensate. Following condensation in the stripper reboiler, the steam condensate collects in a receiving vessel before being returned to the refinery. Steam heat tracing is facilitated using a small amount of medium-pressure (MP) steam that is reduced to a lower pressure prior to use. The resultant low-pressure (LP) steam condensate is returned to the same receiver as the stripper reboiler condensate. A schematic of the system supplying steam to the stripper reboiler is shown in Figure 6.

For thermal energy consumption assessment, the key parameter of interest is the steam flow to the reboiler. The HP condensate flow returned to the refinery can be assessed as a check on this parameter. The condensate return flow should be the sum of the reboiler steam flow and any condensate flow produced in steam heat tracing. Figure 7 shows these two parameters. As a result of higher ambient temperatures experienced in September 2015 the average condensate flow measurement (FT-2455) was either at or slightly lower than the steam flow measurement (FT-2386). (During the first MEA baseline testing in January 2014, condensate measurements exceeded the steam flow measurement due to the contribution of trace heating).

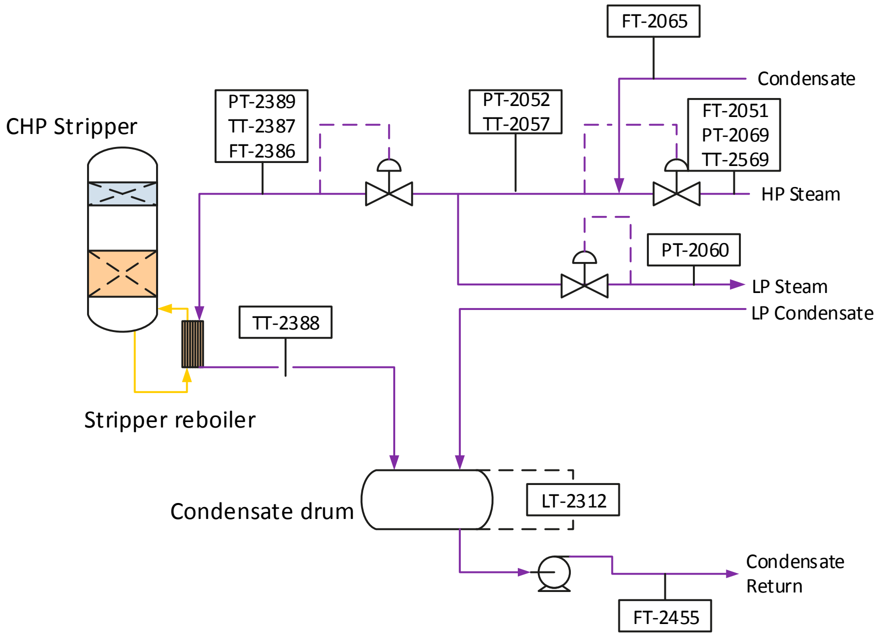

Figure 6. Stripper reboiler steam supply flow schematic.

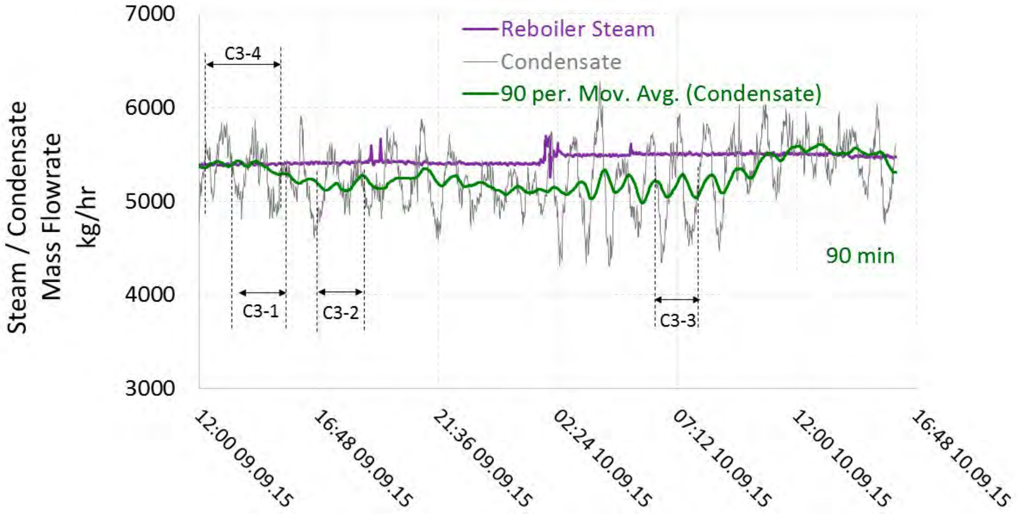

Figure 7. Reboiler steam flow and HP condensate return flow.

6. Results and discussions

6.1. CO_2 capture efficiency and recovery

The CO_2 capture efficiency was calculated using the four methods (Methods 1–4) shown in Table 8 in Appendix A. CO_2 recovery is the fraction of CO_2 mass flow in the flue gas supply that is accounted for by measured CO_2 mass flows in the depleted flue gas and product CO_2; it is a measure of the degree to which the CO_2 mass balance is closed. The formula to calculate the amount of CO_2 recovery from the flue gas supply is also given in Table 8 in Appendix A.

The depleted flue gas flow measurement was not reliable and therefore it was calculated. It was assumed that the oxygen and nitrogen entering the absorber with the flue gas leave in the depleted flue gas. The saturated water content of the depleted flue gas was calculated using its temperature and pressure. The CO_2 flow out of the absorber was calculated using the concentration of CO_2 in the depleted flue gas. These are essentially the same assumptions as those used for Method 4. Therefore, Method 3 and Method 4 calculations result in identical CO_2 capture rates. The CO_2 recovery was then estimated using the calculated flow of depleted flue gas. The calculated CO_2 capture efficiency and recovery are presented in Table 3. For all test periods, the calculated CO_2 capture was quite steady and the CO_2 recovery was about 98–99%.

Table 3. CO_2 capture results.

S= Flue gas supply *D*= Depleted flue gas *P*= Product CO_2	Method 1	Method 2	Method 3	Method 4	CO_2 Recovery
Test Period	$=\frac{P}{S}$	$=\frac{P}{P+D}$	$=\frac{S-D}{S}$	$=1-\frac{O_{CO_2}}{(1-O_{CO_2})}\frac{(1-I_{CO_2})}{(I_{CO_2})}$	$=\frac{D+P}{S}$
C3-1	83.3%	83.7%	83.8%	83.8%	99.4%
C3-2	83.1%	83.7%	83.8%	83.8%	99.2%
C3-3	83.6%	84.5%	84.7%	84.7%	98.7%
C3-4	83.4%	83.7%	83.7%	83.7%	99.6%
C3-5	84.0%	85.3%	85.5%	85.5%	98.3%
C3-6	84.7%	86.0%	86.3%	86.3%	98.2%
C3-7	82.7%	82.9%	83.0%	83.0%	99.7%
C3-8	85.0%	85.8%	85.9%	85.9%	99.0%

O_{CO2}*=Depleted flue gas* CO_2 *content, dry basis and* I_{CO2}*=Flue gas supply* CO_2 *content, dry basis*

The uncertainty calculations and results from each calculation method are shown in Table 4. The following assumptions were used:

- Flow metering uncertainties were calculated by TCM DA for the indicated flow meters based on the specification of the instrument.
- Concentration uncertainties for the flue gas flows are those described in Section 5.2.
- Concentration uncertainty for the product CO_2 is assumed to be 1% to allow for actual CO_2 content as low as 99%.
- CO_2 capture of 85% is representative of that measured during all test periods.
- The uncertainty in CO_2 capture is almost entirely due to uncertainty in CO_2 content of the CHP flue gas supply for the assigned total (low) flow uncertainties. The CO_2 capture uncertainty is relatively insensitive to uncertainties both in the CO_2 contents of both the product CO_2 and the depleted flue gas.

Table 4. Uncertainty in CO_2 capture calculations (nominal CO_2 capture efficiency shown as ECO_2 =85%).

CO_2 capture calculation method	Stream*	Uncertainty in:				CO_2 capture uncertainty Equation
		Total flow	CO_2 content	CO_2 flow	CO_2 capture	
1	*P*	1.1%	1%	U_{CO2P}=1.5%	5.4%	$\sqrt{(U_{CO2S})^2+(U_{CO2P})^2}$
	S	1.3%	5%	U_{CO2S}=5.1%		
2	*P*	1.1%	1%	U_{CO2P}=1.5%	0.8%	$(1-E_{CO2})\sqrt{(U_{CO2D})^2+(U_{CO2P})^2}$
	D	1.3%	5%	U_{CO2D}=5.2%		
3	*S*	1.3%	5%	U_{CO2S}=5.2%	1.3%	$\frac{(1-E_{CO2})}{E_{CO2}}\sqrt{(U_{CO2S})^2+(U_{CO2D})^2}$
	D	1.3%	5%	U_{CO2D}=5.2%		

[*] *P= Product CO_2, S= Supply flue gas, D= Depleted flue gas*

6.2. Thermal energy consumption

The reboiler thermal duty was calculated as the difference between steam enthalpy at the reboiler inlet temperature and pressure and the saturation enthalpy of water at the reboiler condensate temperature. The specific thermal duty (SRD) was obtained by dividing the reboiler duty by the product CO_2 flow. The CO_2 product flow was either based on the measured CO_2 product flow (P) or on the difference between the NDIR-measured CO_2 supply flow and the estimated CO_2 depleted flow (S-D). The two corresponding values for SRD are shown in Table 5. The results for SRD were very consistent during all test periods.

Table 5. Stripper reboiler thermal energy consumption.

Test period	Reboiler steam flow rate kg/hr	Reboiler duty MJ/hr	Using the measured product CO_2 flow (P)*		Using CO_2 removed from the flue gas (S – D)	
			Product CO_2 Flow kg/hr	Specific thermal use GJ/t CO_2	Product CO_2 Flow kg/hr	Specific thermal use GJ/t CO_2
C3-1	5397	11,963	3307	3.62	3326	3.60
C3-2	5421	11,978	3308	3.62	3336	3.59
C3-3	5508	12,185	3332	3.66	3376	3.61
C3-4	5395	11,963	3305	3.62	3318	3.60
C3-5	5417	12,149	3340	3.64	3398	3.58
C3-6	5446	12,204	3339	3.65	3400	3.59
C3-7	5414	12,050	3342	3.61	3351	3.60
C3-8	5525	12,205	3353	3.64	3386	3.60

[*] *The wet CO_2 flow, which is obtained by using the FTIR measured moisture content of the product CO_2.*

6.3. Gas phase contaminants

FORCE Technology measured the gas phase concentration of the compounds listed below in the three gas streams. The data are shown in Table 9-11 in Appendix B.

- SO_2 was simultaneously measured in the three gas streams during test period C3-1. A modest amount of SO_2 was present in the flue gas supply. No SO_2 entering the absorber in the flue gas supplied left the plant in either the depleted flue gas or product CO_2 streams.
- NO_x concentrations and mass flows were measured in the three gas streams during test period C3-1. NO_x concentrations were below the detectable limit during all test periods.
- Acetone, formaldehyde, and acetaldehyde concentrations and mass flow rates were measured during test period C3-2. The aldehydes in the depleted flue gas and product CO_2 do did exist in the supplied flue gas and were, presumably, produced in the absorption process. Acetone was not detected in any gas stream. FORCE Technology's measurements for the acetaldehyde concentrations were not successful and therefore the values measured by TCM DA is shown in Table 10 in Appendix B.
- Amines/Amides concentrations and mass rates were measured during test period C3-2. None of the compounds were detected in the CHP flue gas supply. The only compounds detected in the depleted flue gas and product CO_2 were MEA and methylamine. Traces of ethylamine, dimethylamine, and diethylamine were detected in the depleted flue gas only. Amides were below the detection limits.
- H_2SO_4 concentration was measured in the three gas streams as aggregate sulfate (reported as H_2SO_4 equivalent) during test period C3-1. The concentration of H_2SO_4 was below the respective detection limits.
- Particulates were measured during test period C3-1. The total amount of particulates in the CHP flue gas supply is very low. The amount of particulates in the three gas streams was below the detection limit.
- Ammonia was simultaneously measured in the three gas streams during test period C3-3. Measurable amounts of ammonia were found in the depleted flue gas and in the product CO_2. Ammonia was not detected in the CHP flue gas supply suggesting it resulted from MEA degradation during the process.
- TVOC was measured during test period C3-3. Measurable amounts of TVOC were detected in the product CO_2. The CHP flue gas supply does not contain any TVOC and presumably, it resulted from MEA degradation during the CO_2 capture process.

6.4. Laborelec particle measurements

Laborelec carried out particle size testing using an Electrical Low Pressure Impactor (ELPI+). Four locations of the absorber tower were monitored to investigate the potential formation of particles as the depleted flue gas passes through the washing stages and demisters. The results shown in Table 6 have measurements that were near to the detection limit of the ELPI+ when inserted in the process. The ambient air measurements undertaken during these tests were higher than the process measurements by almost one order of magnitude. The measurements were three to four orders of magnitude lower than similar measurements taken on flue gas from a coal thermal plant, proving the scarcity of particles in the CHP flue gases. The small amount of particles and their small sizes remain largely unchanged as they pass through the absorber.

Table 6. Particle counts and size distribution through absorber sections

Test period	Parameter	Units	Total	50% oversize (μm)	90% oversize (μm)
C3-5	Leaving capture section	count/cm^3	6608	0.040	0.023
C3-6	Leaving lower water wash	count/cm^3	7937	0.025	0.021
C3-7	Leaving upper water wash	count/cm^3	3193	0.015	0.010
C3-8	Absorber stack	count/cm^3	9767	0.020	0.012

6.5. New baseline for solvent performance testing

Table 7 presents a portion of the MEA test data obtained at the TCM DA amine plant. Based on these data which were obtained at about test period C3-4 when flow rates were measured, a new baseline is established. As the instrumentation of the amine plant and therefore the measurements are significantly improved since the previous MEA baseline in 2014 [4], the 2015 MEA results will set the baseline for performance benchmarking of other amines at TCM DA. The 2014 baseline is therefore considered obsolete.

Table 7. Results of baseline testing in 2015

Baseline year	2015
Packing height (m)	24
Flue gas flow (Sm^3/h)	59 000
Flue gas supply temperature (°C)	30.0
Flue gas supply pressure (bar)	0.01
Lean amine flow (kg/h)	57 000
Lean loading	0.20
Rich loading	0.48
Stripper bottom temperature (°C)	121.0
CO_2 capture (%)	83.4
SRD (MJ/kg CO_2)	3.62

Comprehensive process data for the TCM DA baseline testing in 2015 are given in Table 12, Appendix C.

7. Conclusions

The quality of the gas phase measurements at the TCM DA amine plant is significantly improved by installing new online instruments. Using the upgraded instrumentations, a new baseline for the TCM DA amine plant is established which has replaced the 2014 baseline. The new baseline is set up close to the plant nominal capacity and will serve as the performance benchmark for other amines tested at the TCM DA amine plant.

Acknowledgements

The authors gratefully acknowledge the staff of TCM DA, Gassnova, Statoil, Shell and Sasol for their contribution and work at the TCM DA facility. The authors also gratefully acknowledge Gassnova, Statoil, Shell, and Sasol as the owners of TCM DA for their financial support and contributions.

Appendix A.

Table 8. Calculation methods for CO_2 capture efficiency and recovery

CO_2 capture efficiency	Description	Formula
Method 1	CO_2 product flow as a ratio to the CO_2 flow in the flue gas supply	$=\frac{CO_2(\text{product})}{CO_2(\text{supply})}$
Method 2	CO_2 product flow as a ratio to the sum of the CO_2 product flow and the CO_2 flow in the depleted flue gas	$=\frac{CO_2(\text{product})}{CO_2(\text{product})+CO_2(\text{depleted})}$
Method 3	Ratio of the difference between the CO_2 flow in the flue gas supply and the CO_2 in the depleted flue gas to the CO_2 flow in the flue gas supply	$=\frac{CO_2(\text{supply})-CO_2(\text{depleted})}{CO_2(\text{supply})}$
Method 4	100% less the ratio of the depleted flue gas CO_2 per unit O_2+N_2 to the flue gas supply CO_2 per unit O_2+N_2	$=1-\frac{O_{CO_c}}{(1-O_{CO_2})}\frac{(1-I_{CO_2})}{I_{CO_2}}$ O_{CO2} = Depleted flue gas CO_2 content, dry I_{CO2} = Flue gas supply CO_2 content, dry
CO_2 recovery	Ratio of the sum of the CO_2 flow in depleted flue gas and the product CO_2 flow divided by the CO_2 flow in the flue gas supply	$=\frac{CO_2(\text{depleted})+CO_2(\text{product})}{CO_2(\text{supply})}$

Appendix B. Gas phase contaminants measured by FORCE Technology during the 2015 baseline testing

Table 9. Concentration of the contaminants in the gas streams: Test period C3-1.

		Test period C3-1		
Component	Units	Flue gas supply	Depleted flue gas	Product CO_2
NO_X	mg/Sm^3 (dry)	< 10	< 10	< 10
	kg/hr	< 0.6	< 0.5	< 0.02
SO_2	mg/Sm^3 (dry)	0.29	< 0.20	< 0.20
	g/hr	16.6	< 11.1	< 0.4
H_2SO_4	mg/Sm^3 (dry)	0.014	< 0.01	-
	g/hr	0.80	< 0.5	-
Filterable Particulate	mg/Sm^3 (dry)	< 0.08	< 0.08	-
	g/hr	< 5	< 5	-

Table 10. Concentration of the contaminants in the gas streams: Test period C3-2.

		Test period C3-2		
Component	Units	Flue gas supply	Depleted flue gas	Product CO_2
Formaldehyde	mg/Sm^3 (dry)	< 0.4	0.72	0.14
	g/hr	< 23	40	0.25
Acetaldehyde	mg/Sm^3 (dry)	< 0.8	0.43*	15.33*
	g/hr	< 40	-	-
Acetone	mg/Sm^3 (dry)	< 3	< 1	< 0.9
	g/hr	< 172	< 55	< 2
Formamide	mg/Sm^3 (dry)	< 0.04	< 0.04	< 0.03
Acetamide	mg/Sm^3 (dry)	< 0.04	< 0.04	< 0.03
MEA	mg/Sm^3 (dry)	< 0.003	0.0059	0.076
DEA	mg/Sm^3 (dry)	< 0.0004	< 0.0004	< 0.0003
TEA	mg/Sm^3 (dry)	< 0.0004	< 0.0004	< 0.0003
NDELA	mg/Sm^3 (dry)	< 0.0002	< 0.0002	< 0.0001
NDMA	mg/Sm^3 (dry)	< 0.0004	< 0.0004	< 0.0003
NMOR, NMEA, NPYR, NDEA, NPIP, NDPA, NDBA	mg/Sm^3 (dry)	< 0.0002	< 0.0002	< 0.0001
Methylamine	mg/Sm^3 (dry)	< 0.0008	0.030	<0.0006
Ethylamine	mg/Sm^3 (dry)	< 0.0008	0.0012	< 0.0006
Propylamine	mg/Sm^3 (dry)	< 0.0008	< 0.0008	< 0.0006
Dimethylamine	mg/Sm^3 (dry)	< 0.0008	0.029	< 0.00065
Ethylmethylamine	mg/Sm^3 (dry)	< 0.0008	< 0.0008	< 0.0006
Diethylamine	mg/Sm^3 (dry)	< 0.002	0.0097	0.0029
Dipropylamine	mg/Sm^3 (dry)	< 0.002	< 0.002	< 0.001
TONO	mg/Sm^3 (dry)	< 0.002	< 0.002	< 0.001
Sum, all amines	mg/Sm^3 (dry)	< 0.04	0.076	0.079
	g/hr	< 0.1	4.1	0.14
Sum, all amides	mg/Sm^3 (dry)	< 0.08	< 0.08	< 0.06
	g/hr	< 2	< 2	< 0.05
Total N (excluding NH_3, NO_3^-) test period C3-3	mg/Sm^3 (dry)	-	3.6	2.6
	g/hr	-	190	4.7

* FORCE Technology measurements for the acetaldehyde concentration in both depleted flue gas and product CO_2 were not successful. The values given in Table 5 for acetaldehyde were measured by the TCM DA online FTIR analysers.

Table 11 Concentration of the contaminants in the gas streams: Test period C3-3.

		Test period C3-3		
Components	Units	Flue gas supply	Depleted flue gas	Product CO_2
NH_3	mg/Sm^3 (dry)	< 0.30	13	14
	g/hr	< 20	720	24.9
TVOC	mg/Sm^3 (dry)	< 0.50	< 0.50	6
	g/hr	< 30	< 30	10.7

Appendix C. Amine plant 2015 baseline testing results

Table 12 presents the process data for the TCM amine plant averaged for the period C3-4 of baseline testing in 2015 (when flow rates were measured). During that period the plant was running at nearly stable conditions and the process parameters fluctuations were insignificant.

Table 12. Averaged process data for the test period C3-4 of baseline testing in September 2015.

Operating capacity	%	100
CHP flue gas supply rate	Sm^3/h	59 430
CHP flue gas supply temperature	°C	29.8
CHP flue gas supply pressure	barg	0.01
CHP flue gas supply CO_2 concentration (dry)	vol%	3.7
CHP flue gas supply O_2 concentration (wet)	vol%	14.6
CHP flue gas supply water content	vol%	3.7
Depleted flue gas temperature	°C	30.4
Lean MEA concentration (CO_2 free)	wt%	31
Lean MEA concentration (incl CO_2)	wt%	30
Lean CO_2 loading	mol CO_2/mol MEA	0.20
Lean amine supply flow rate	kg/h	57 434
Lean amine supply temperature	°C	37.0
Lean amine density	kg/m^3	1 073
Rich solution return temperature	°C	33.2
Temperature above upper absorber packing	°C	39.7
Wash water 1 (lower) supply flow rate	kg/h	55 005
Wash water 1 inlet temperature	°C	30.4
Wash water 1 withdrawal temperature	°C	44.9
Temperature above Wash Water 1	°C	38.0
Wash water 2 (upper) supply flow rate	kg/h	54 997
Wash water 2 inlet temperature	°C	30.4
Wash water 2 withdrawal temperature	°C	37.3
Temperature above Wash Water 2	°C	30.4

Rich CO_2 loading	mol CO_2/mol MEA	0.48
Rich solution supply flow rate	kg/h	60 775
Rich solution supply temperature	°C	110.7
Lean solution return temperature	°C	121.3
Rich amine density	kg/m^3	1 125
Reboiler steam flow rate	kg/h	5 398
Reboiler steam temperature	°C	156
Reboiler steam pressure	barg	2.04
Reboiler condensate temperature	°C	132.8
Reboiler condensate pressure	barg	1.96
Stripper overhead pressure	barg	0.91
Stripper overhead temperature	°C	96.1
Stripper overhead reflux flow rate	kg/h	1 227
Stripper overhead reflux temperature	°C	17.64
Stripper sump temperature	°C	121.0
Reboiler solution temperature	°C	125.1
Lean vapour compressor system	-	off
Product CO_2 flow rate	kg/h	3 325
Product CO_2 discharge temperature	°C	17.9
Product CO_2 discharge pressure	barg	0.017
Product CO_2 water content	vol%	1.3
Active absorber packing height	m	24
Temperature, upper absorber packing – 6	°C	47.4
Temperature, upper absorber packing – 5	°C	51.7
Temperature, upper absorber packing – 4	°C	51.6
Temperature, upper absorber packing – 3	°C	50.5
Temperature, upper absorber packing – 2	°C	49.9
Temperature, upper absorber packing – 1	°C	48.9
Temperature, middle absorber packing – 6	°C	47.2
Temperature, middle absorber packing – 5	°C	46.0
Temperature, middle absorber packing – 4	°C	44.4
Temperature, middle absorber packing – 3	°C	43.1
Temperature, middle absorber packing – 2	°C	42.2
Temperature, middle absorber packing – 1	°C	40.9
Temperature, lower absorber packing – 12	°C	40.6
Temperature, lower absorber packing – 11	°C	41.6
Temperature, lower absorber packing – 10	°C	37.4
Temperature, lower absorber packing – 9	°C	37.1

Temperature, lower absorber packing – 8	°C	35.9
Temperature, lower absorber packing – 7	°C	34.3
Temperature, lower absorber packing – 6	°C	34.1
Temperature, lower absorber packing – 5	°C	33.8
Temperature, lower absorber packing – 4	°C	32.9
Temperature, lower absorber packing – 3	°C	33.2
Temperature, lower absorber packing – 2	°C	32.5
Temperature, lower absorber packing – 1	°C	32.4
Stripping section packing height	m	8
Temperature, stripper packing – 7	°C	102.7
Temperature, stripper packing – 6	°C	103.1
Temperature, stripper packing – 5	°C	104.5
Temperature, stripper packing – 4	°C	107.7
Temperature, stripper packing – 3	°C	112.1
Temperature, stripper packing – 2	°C	114.7
Temperature, stripper packing – 1	°C	119.4

References

[1] Thimsen D, Maxson A, Smith V, Cents T, Falk-Pedersen O, Gorset O, Hamborg ES. Results from MEA testing at the CO_2 Technology Centre Mongstad. Part I: Post-Combustion CO_2 capture testing methodology Energy Procedia 63 5938-5958; 2014.

[2] Gjernes E, Pedersen S, Cents T, Watson G, Fostås BF, Shah MI, Lombardo G, Desvignes C, Flø NE, Morken AK, de Cazenove T, Faramarzi L, Hamborg ES. Results from 30 wt% MEA performance testing at the CO_2 Technology Centre Mongstad. Energy Procedia (GHGT-13), Forthcoming 2017.

[3] American Society of Mechanical Engineers, New York, NY. PTC-4, Fired Steam Generators, 2008.

[4] Hamborg ES, Smith V, Cents T, Brigman N, Falk-Pedersen O, de Cazanove T, Chhagnlal M, Feste JK, Ullestad Ø, Ulvatn H, Gorset O, Askestad I, Gram LK, Fostås BF, Shah MI, Maxson A, Thimsen D. Results from MEA testing at the CO_2 Technology Centre Mongstad. Part II: Verification of baseline results. Energy Procedia 63, 5994-6011; 2014.

Results from 30 wt% MEA performance testing at the CO_2 Technology Centre Mongstad

(2016)

Available online at www.sciencedirect.com

ScienceDirect

Energy Procedia 114 (2017) 1146 – 1157

Energy Procedia

13th International Conference on Greenhouse Gas Control Technologies, GHGT-13, 14-18 November 2016, Lausanne, Switzerland

Results from 30 wt% MEA performance testing at the CO_2 Technology Centre Mongstad

Erik Gjernes[a]*, Steinar Pedersen[b], Toine Cents[c], Guillaume Watson[d], Berit F. Fostås[b], Muhammad Ismail Shah[a], Gerard Lombardo[a,e], Coralie Desvignes[e], Nina Enaasen Fløe[e], Anne Kolstad Morken[b,e], Thomas de Cazenove[e], Leila Faramarzi[b,e], Espen Steinseth Hamborg[b,e]

[a]*Gassnova SF, Dokkvegen 10, 3920 Porsgrunn, Norway*
[b]*Statoil ASA, PO Box 8500, 4035 Stavanger, Norway*
[c]*Sasol Technology, PO Box 5486, Johannesburg 2000, South Africa*
[d]*Shell Global Solutions International B.V., PO Box 663, 2501CR The Hague, The Netherlands*
[e]*CO_2 Technology Centre Mongstad (TCM DA), 5954 Mongstad, Norway*

Abstract

In 2015, the CO_2 Technology Center Mongstad (TCM DA), operated a test campaign using aqueous monoethanolamine (MEA) solvent at 30 wt%. The main objective was to demonstrate and document the performance of the TCM DA Amine Plant located in Mongstad, Norway. The main elements were: verifying mass balances over the capture plant, revise the performance baseline from 2014, challenge the plant capacity, investigate mist/aerosol induced emission to the air and parameter variation in order to further stretch the plant performance. The current paper presents an overview of the campaign and reports on mass balance and plant performance.

© 2017 The Authors. Published by Elsevier Ltd. This is an open access article under the CC BY-NC-ND license (http://creativecommons.org/licenses/by-nc-nd/4.0/).
Peer-review under responsibility of the organizing committee of GHGT-13.

---

* Corresponding author. Tel.: +47 40 00 59 08.
E-mail address: postmottak@gassnova.no

1876-6102 © 2017 The Authors. Published by Elsevier Ltd. This is an open access article under the CC BY-NC-ND license (http://creativecommons.org/licenses/by-nc-nd/4.0/).
Peer-review under responsibility of the organizing committee of GHGT-13.
doi:10.1016/j.egypro.2017.03.1276

Keywords: CO_2 capture; MEA; Post-combustion capture; CO_2 Technology Centre Mongstad; TCM DA

1. Introduction

The CO_2 Technology Centre Mongstad (TCM DA) is located next to the Statoil refinery in Mongstad, Norway. TCM DA is a joint venture set up by Gassnova representing the Norwegian state, Statoil, Shell, and Sasol. The facility run by TCM DA entered the operational phase in August 2012 and it is one of the largest post-combustion CO_2 capture test centres in the world. A unique aspect of the facility is that either a flue gas slipstream from a natural gas turbine based combined heat and power (CHP) plant or an equivalent volumetric flow from a residual fluidized catalytic cracker (RFCC) unit can be used for CO_2 capture. The CHP flue gas contains about 3.5% CO_2 and the RFCC flue gas contains about 13-14% CO_2. One of the main test plants at TCM DA is a highly flexible and well-instrumented amine plant. The amine plant was designed and constructed by Aker Solutions and Kværner to accommodate a variety of technologies, with capabilities of treating flue gas streams of up to 60,000 standard cubic meters per hour. The plant is being offered to vendors of solvent based CO_2 capture technologies to, among others, test; (1) the performance of their solvent technology, and (2) technologies aimed to reduce the atmospheric emissions and environmental impact of amines and amine based degradation products from such solvent based CO_2 capture processes. The objective of TCM DA is to test, verify, and demonstrate CO_2 capture technologies suitable for deployment at full-scale. Up to now the vendors Aker Solutions, Alstom, Cansolv Technologies Inc. and Carbon Clean Solutions Ltd. have successfully used the TCM DA facilities to verify their CO_2 capture technologies.

2. The 2015 MEA campaign

From July to October 2015 a test campaign capturing CO_2 from flue gas from the CHP plant at Mongstad refinery was executed at TCM. The flue gas has typically 3.5% CO_2 while the solvent comprised 30% aqueous monoethanolamine (MEA). The campaign was a joint project between TCM DA and its owners Gassnova, Statoil, Shell, and Sasol.

The campaign was split in five test series:

1. Verify mass balances
2. Revise the performance baseline
3. Challenge the plant capacity
4. Mist investigation
5. Stretch targets

Series 1: The verification of the mass balances is described in section 4. The flow and composition measurements and methods for calculating total and CO_2 mass balances are explained in detail and performance results are given. This test series (Series 1) was carried out at a flue gas flow rate of about 47,000 Sm^3/h. Data collection was done under stable operating conditions and when the capture rate was 85%.

Series 2: The plant performance for operating conditions very similar to those reported from TCM in 2014 [1] was investigated with the new gas phase composition measurements that provided improved control of the mass balances. This test series (Series 2) used the stripper bottom temperature as the controlling variable and the solvent circulation rate was used to adjust capture rate as close as possible to 85% before experimental data was collected. The optimum performances for operation without and with the use of anti-foam were identified by the obtained u-curves, showing relation between the specific reboiler duty and the stripper bottom temperature or the lean loading. Results are given in section 5.

Series 3: The use of anti-foam improved significantly the plant performance. It also became clear that using anti-foam would allow stable plant operation at the full design flue gas flow plant capacity. Therefore a test series (Series 3) was run with 59,000 Sm^3/h flue gas flow rate. The plant performance was documented according to the independent verification protocol (IVP) [2]. This new baseline is reported in [3] and will replace the TCM baseline published in 2014 [1]. Results from reducing absorber packing is, however, presented in section 6.

Series 4: A two week period of the campaign was used to investigate effect of mist/aerosol particles in the incoming flue gas on emissions to atmosphere (Series 4). This is reported in [4].

Series 5: The test series 5 (stretched targets) was planned to include tests with the use of lean vapor compressor (LVC, see bottom right corner of Figure 1), increased amine concentration (40%) and CO_2 capture from flue gases at elevated CO_2 concentrations. Due to time constraints, only the latter part of test series 5 was implemented. All tests were with the use of anti-foam and section 6 presents results from tests made from 3.6 to and 9% CO_2 in the flue gas flow into the absorber.

The total campaign included close to 2,000 hours of plant operation and results are reported in several papers that cover emissions and degradation [5], reclaiming [6] and corrosion [7].

Table 1 below presents an overview of the test series and main parameter ranges used during the 2015 MEA campaign at TCM.

Table 1. Overall test activities with reference to tests series: 1 Verify mass balances, 2 Revise the performance baseline, 3 Challenge the plant capacity, 4 Mist investigation and 5 Stretch targets. Plant performance documented according to the independent verification protocol [2] is labeled 3-2 (IVP). The test series 5 covered variation in packing height and CO_2 in flue gas into the absorber. At the end of the campaign, reclaiming was performed followed by two days of CO_2 capture. The test series includes two weeks plant stop between test series 1 and 2 and a two days stop between test series 5-2- and 5-3. Stripper bottom pressure was typically maintained at around 0.95 barg.

Test series	Date (2015)	Stripper [-]	Absorber packing [m]	Flue gas flow [Sm^3/h]	CO_2 [dry,%]	Lean amine flow [kg/h]	Stripper bottom temp. [°C]
1	13.07-20.07	CHP	24	47,000	3.6	45,000 – 47,000	120 – 120.5
2	03.08-02.09	CHP	24	47,000	3.6	35,000 – 80,000	116.5 – 121
3-1	03.09-07.09	CHP	24	59,000	3.6	55,000 – 57,000	121
3-2 (IVP)	08.09-11.09	CHP	24	59,000	3.6	57,000	121
3-3	12.09-14.09	CHP	18	59,000	3.6	55,000 – 70,000	119 – 121
4 (Mist)	14.09-25.09	CHP/RFCC	18	30,000	3.6 – 13.6	30,000 – 91,000	120
5-1	25.09-26.10	CHP	18	59,000	3.6	65,000	120
5-2	26.09-03.10	RFCC	18	47,000 – 59,000	9	105,000 – 140,000	120 – 121
5-3	06.10-09.10	CHP	18	47,000	5	70,000 – 80,0000	120 – 121
5-4	09.10-12.10	CHP	24	47,000	3.6	43,000	121 – 121.5
Reclaiming	12.10-16.10	CHP	24	47,000	3.6	43,000 – 49,000	120.5 – 121.5
5-5	16.10-17.10	CHP	24-18	47,000	3.6	43,000	120

3. The amine plant

The amine plant was designed and constructed by Aker Solutions and Kværner. It is a generic and highly flexible plant allowing testing at different configurations and with a wide range of flue gas compositions and flow rates. The process flow diagram is shown in Figure 1. The plant capacity is about 80 and 275 tonnes of CO_2 per day for the CHP and RFCC flue gas operations respectively. The flue gas blower output capacity is up to about 270 mbar and 70,000 Sm^3/h. The flue gas is cooled by a direct contact cooler with wash water. Water saturated flue gas flows upwards the rectangular cross-section absorber tower where it comes into contact with falling lean solvent solution. The absorber has three beds of structured packing and column packing heights can be 24, 18 or 12 m. Liquid distributors, liquid collector trays and mist eliminators are installed at various locations in the tower. The flue gas depleted in CO_2 passes through two recirculating water wash stages before being emitted to the atmosphere. The process is operated with water balance. The water washes are used to control the depleted flue gas temperature and water content.

The CO_2 rich solvent solution is pre-heated by exchange with hot lean solution and pumped to the upper part of a stripper tower. The rich solution falls down the stripper packing section and comes into contact with rising steam and released CO_2. The lean solution is collected at the stripper bottom section and is circulated through a steam-heated thermosiphon reboiler system which provides the heat necessary to release the CO_2. The lean solution is pumped back to the top of the absorber packing.

The amine plant has two independent stripper columns with overhead condenser systems. Both columns have a total height of 30 m. The structured packing internals are of 8 m height. One stripper is designed for the CHP flue gas and measures 1.3 m in diameter while the other stripper is 2.2 m in diameter. The second stripper is suited for higher flow capacities and is utilized when testing flue gases of higher CO_2 content.

The CO_2 product stream leaves the stripper and is cooled with recovery of condensate that is returned to the stripper as a reflux. The cooled CO_2 stream is vented. When CHP flue gas is used it is possible to recycle a portion of the CO_2 to the CHP flue gas upstream of the direct contact cooler. This allows for testing a range of CO_2 concentrations in the inlet flue gas stream. More details on the plant design and equipment can be found in [1,2].

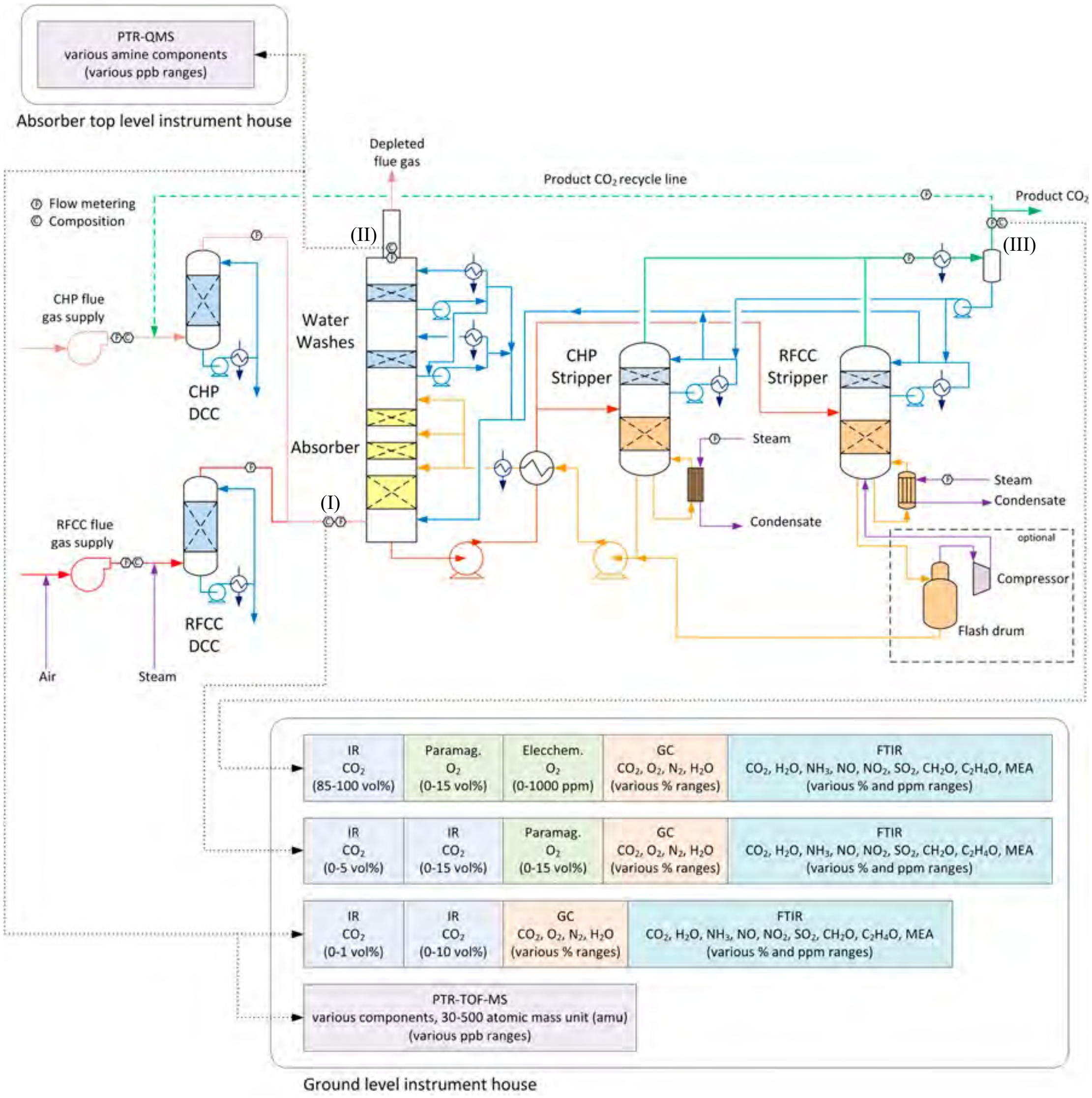

Figure 1. The TCM amine plant with two flue gas sources, CHP and RFCC, and the corresponding two strippers. Flue gas analyzers and flow meters are located at absorber inlet (I), outlet/depleted flue gas (II) and CO_2 product (III), see also section 4, Table 2 and Table 3. The sets of IR meters for absorber in and out, IR CO_2 (0 – 5 vol%)/IR CO_2 (0 - 15 vol%) and IR CO_2 (0 – 1 vol%)/IR CO_2 (0 - 10 vol%) are referred to as IR-low and IR-high in Table 3. The dotted green line shows that CO_2 can be recycled back to the absorber inlet for tests at elevated CO_2 concentration in the flue gas flow.

4. Mass balance closure (Series 1)

The amine plant is planned and equipped for conducting research and development activities and in 2015 TCM completed implementation of a major upgrade of the gas phase composition measurement equipment. The original set up was with one common FTIR analyzer that in 90 minute cycle shifted between measuring each of the tree gas streams [1]. Figure 1 shows the new gas composition measurement setup that includes multiple gas composition analyzers at each gas stream providing continuous measurements. The CO_2 measurements are based on fourier transform infrared spectroscopy (FTIR), infrared gas analysis (IR) and gas chromatography (GC). Absorber in and out have IR meters that cover both % and ppm range [3].

During the first part of the MEA 2015 test campaign the total- and CO_2-mass balance of the amine plant was checked carefully. There are two meters for the inlet flue gas flow rate, one meter for the flue gas flow out of absorber and two meters for the CO_2 product flow, see Table 2. The absorber out flue gas flow meter FT-2431 does not provide reliable measurements [1], thus flow out of absorber ($\dot{V}$) is also calculated from flow into the absorber assuming all components except water (C_{H2O}) and CO_2 (C_{CO2}) are conserved:

$$\dot{V}_{out} = \dot{V}_{in} \frac{100 - c_{H_2O}^{in} - c_{CO_2}^{in}}{100 - c_{H_2O}^{out} - c_{CO_2}^{out}} \qquad (1)$$

The mass balance is calculated as sum of absorber out and product flow divided by absorber in flow. This balance is based on 15 minutes averages of the measured gas flows in and out of the plant. No shift in time is applied, i.e. in order to take into account the residence time from gas phase absorber to gas phase stripper. Thus, stable operation is assumed. In Table 2 mass balance for four combinations of flow instruments, method A to D, are shown. Method A to C provide mass balances close to 100%. Method D which uses the absorber out pitot-based meter FT-2431 provides a mass balance around 95%, which suggests that this meter reports too low flow. For reference the CO_2 concentration (dry) into the absorber is shown. Around July 14 the CHP changed firing mode which resulted in a decrease in the CO_2 content in the flue gas and was stable for the rest of the week.

As shown in Figure 1 above there are four CO_2 analysers at the absorber inlet and at the outlet and three analysers at the product stream. Based on method A to C in Table 2 the CO_2 mass balance has been calculated using a combination of the CO_2 analyzers. Table 3 shows the cases investigated. For A1, A2, B1 and C1 the gas composition out of stripper is assumed to be only CO_2 and water were the latter is calculated from pressure and temperature assuming saturated conditions (f(T,p)). For A3 and A4 CO_2 concentration is based on GC and FTIR measurements. All three methods give wet CO_2 > 97 vol%.

Table 2. To the left instrumentation for absorber in (Abs. in) and out (Abs. out) and product flow. The absorber out flow (1) and (2) are marked with asterisks since these flows are calculated from absorber in flows by use of equation 1. Mass balance based on four combinations of instruments, methods A to D, are presented for one week of operation in the figure to the right. CO_2 concentration (dry) into the absorber is also shown.

Stream	Tag number	Instrument	Method			
			A	B	C	D
Abs. in (1)	FT-0150	Ultra-sonic	x	x		x
Abs. in (2)	FIC-0124	Multi-pitot tube			x	
Abs. out (1)	FT-0150*	Calculated (1)	x	x		
Abs. out (2)	FIC-0124*	Calculated (2)			x	
Abs. out (3)	FT-2431	Multi-pitot tube				x
Product (1)	FT-0010	Vortex	x		x	x
Product (2)	FT-2203A	Pitot		x		

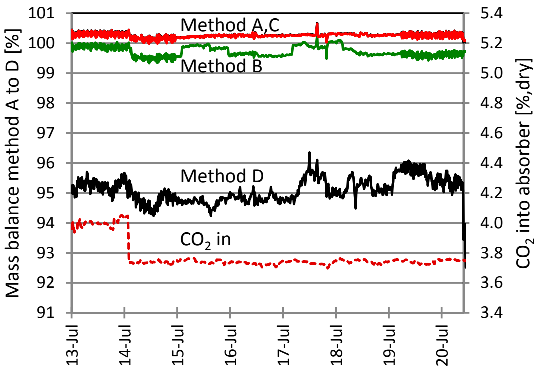

The CO_2 mass balance calculated as:

$$\%\dot{m}_{CO2,ballance} = \frac{\dot{m}_{CO2,abs.out} + \dot{m}_{CO2,product}}{\dot{m}_{CO2,abs.in}} \times 100 \qquad (2)$$

Figure 2 shows that method A1 to A4 and C1 results in CO_2 mass balance within 100 +/- 5%. Method B1 which is based on the gas flow rates of method B has a larger spread and is underestimating the CO_2 product flow resulting in an average CO_2 mass balance around 90%. In conclusion all composition meters results in an acceptable CO_2 mass balance, but flow should be based on method A or C.

Table 3. Instruments for CO_2 measurement at absorber in (Abs. in) and out (Abs. out) and product flow. With reference to Table 2 the measurements were combined with flow meters according to method A for four sets of instruments while method B and C were presented using the IR-low and CO_2 product concentration by difference from calculated moisture (f(T,p)).

Stream	Tag number	Instrument	Method					
			A1	A2	A3	A4	B1	C1
Abs. in (1)	AI-2003A	IR-low	x				x	x
Abs. in (2)	AI-2004A	IR-high		x				
Abs. in (3)	AI-2012A	GC			x			
Abs. in (4)	AI-2002A	FTIR				x		
Abs. out (1)	AI-2029A	IR-low	x				x	x
Abs. out (2)	AI-2030A	IR-high		x				
Abs. out (3)	AI-2036A	GC			x			
Abs. out (4)	AI-2046A	FTIR				x		
Product (1)	-	100-f(T,p)	x	x			x	x
Product (2)	AI-2037A	GC			x			
Product (3)	AI-2047A	FTIR				x		

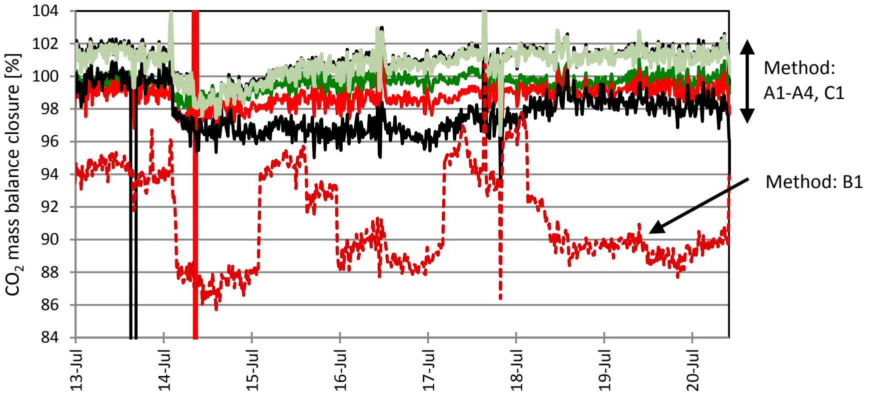

Figure 2. CO_2 mass balance based on method A1 to A4, B1 and C1 in Table 3.

5. Performance (Series 2)

One of the objectives was to investigate the plant performance under the improved control of heat and mass balances as explained above. A key question from the 2014 baseline testing [1] was whether the CHP stripper was operated under optimal conditions. Indicators of poor stripper performance are; fluctuating temperature sensors, a radial temperature gradient, and a reduced temperature gradient over the packing section. This results in higher temperatures above the stripper packing, 100 to 102°C, as well as higher pressure drop over the stripper packing section. Reasons for this behaviour could be moderate foaming or maldistribution over the packing section of the upcoming steam and/or the down coming liquid solvent. TCM had some earlier experience that adding anti-foam to the solvent flow could improve the situation.

In industrial amine units, anti-foam chemicals are often injected when operators suspect foaming to occur in the columns, which can lead to large solvent carry-over to the downstream overhead units. This could result in production turn down or worse, unplanned shutdown. The increase or rapid fluctuation of pressure drop over the amine column, and the unexpected level change in the amine unit (with rapid change of the control valve) are general indicators for foaming. Note that such foaming event in the TCM facility was likely not experienced during the campaign, and that the columns were operating within their design hydraulic operating window (i.e. no flooding).

This part of the test campaign repeated conditions from the 2014 tests at TCM [1] and included operation with and without the use of anti-foam. The main parameters used for creating u-curves and determining the optimum specific reboiler duty (SRD) under series 2 are given in Table 1 above. The tests were run at stable conditions with CO_2 inlet concentration about 3.6 vol %, dry. The stripper bottom pressure was held constant at 0.95 barg. The stripper bottom temperature was used as the controlling variable. For each selected temperature one point on the u-curve was created. The solvent flow rate was used to tune in the capture rate as close as possible to 85% at each test temperature before data collection.

The data for u-curves were prepared as shown in Figure 3 below. At a set stripper bottom temperature the lean solvent flow was tuned in order to achieve 85% capture rate. Rich and lean solvent was sampled during stable operation. Rich and lean loading data were obtained. The rich loading were always close to the equilibrium value of 0.50 mole CO_2/mole amine while the lean loading responded closely to the set stripper bottom temperature. The solvent flow rate was reduced in corresponding steps with the lean loading.

The test series started without the use of anti-foam. The main performance parameters are shown in Table 4 below. The SRD value is calculated based on the difference in steam enthalpy (ΔH) over the reboiler, the steam mass flow ($\dot{m}_{steam}$) and mass flow of CO_2 out of the product line ($\dot{m}_{CO2}$):

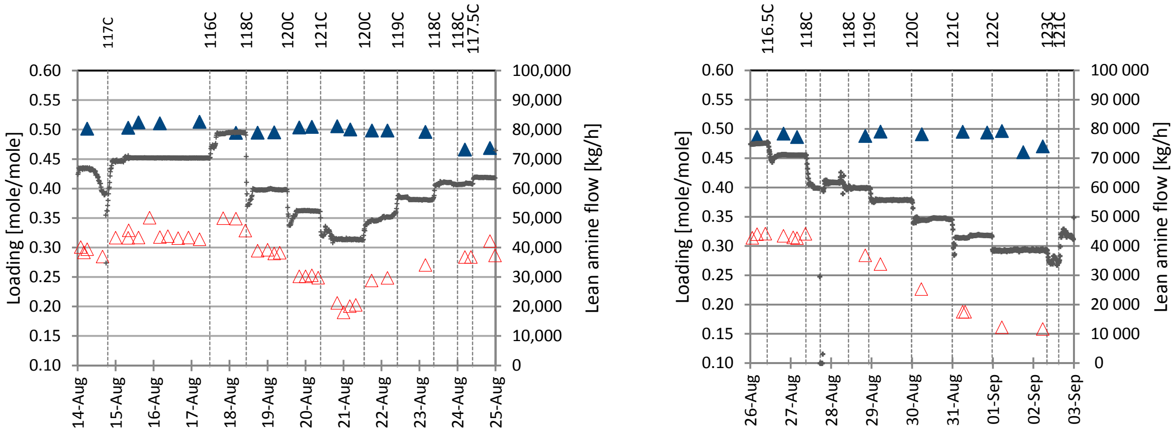

Figure 3. To the left tests without anti-foam and to the right tests with the use of anti-foam. Lean and rich loading are shown as filled blue and open red triangles, respectively. Lean amine flow (black points) is adjusted to get approximatively 85% CO_2 capture and then kept constant at each level of stripper bottom temperature. The latter is indicated as vertical dotted lines.

$$SRD = \frac{\Delta H \dot{m}_{steam}}{\dot{m}_{CO_2}} \tag{3}$$

The CO_2 capture rate is calculated based on a simplified expression using CO_2 concentration in and out of the absorber:

$$\xi = \left(1 - \frac{c_{CO_2}^{out}}{c_{CO_2}^{in}}\right) \times 100 \tag{4}$$

Table 4. Results for test cases without the use of anti-foam. The use of "A" and "B" (Test no) in Table 4 and Table 5 identifies tests without and with anti-foam, respectively. Loading is reported as mole CO_2/mole amine.

Test no	Stripper bottom temperature [°C]	Lean solvent flow [kg/h]	Lean amine loading [mole/mole]	Capture rate [%]	SRD [MJ/kg CO_2]
2A1	115.6	78,700	0.35	83.6	4.1
2A2	117.3	70,500	0.32	84.3	4.1
2A3	118.1	59,600	0.29	83.5	3.9
2A4	119.0	56,280	0.27	84.6	4.0
2A5	119.7	52,500	0.25	87.0	4.1
2A6	121.0	42,900	0.21	85.4	4.2

The stripper performance was observed by following the temperature profiles over the stripper packing section, the pressure drop over the packing and the temperature sensor placed above the stripper packing. All the indicators showed that the stripper was not performing optimal and therefore the anti-foam injection was decided. At August 26 four litre of anti-foam was added. After anti-foam had been injected all the indicators showed good stripper performance. The test series were continued in order to create a u-curve and determine optimum SRD value also for operation with the use of anti-foam. The strategy was to inject one litre of anti-foam if the indicators again showed signs of undesired behaviour to secure optimal performance for all the points on the u-curve. Figure 4 below illustrates how this operation was managed for the whole test series.

The most important performance parameters for the test cases with the use of anti-foam are shown in Table 5 below. Data from Table 4 and Table 5 were used to create the u-curves shown in Figure 5 below.

Table 5. Results for test cases with the use of anti-foam. The use of "A" and "B" (Test no) in Table 4 and Table 5 identifies tests without and with anti-foam, respectively. Loading is reported as mole CO_2/mole amine.

Test no	Stripper bottom temperature [°C]	Lean solvent flow [kg/h]	Lean amine loading [mole/mole]	Capture rate [%]	SRD [MJ/kg CO_2]
2B1	116.6	71,100	0.31	84.3	3.9
2B3	118.2	59,900	0.28	84.4	3.8
2B4	119.0	55,800	0.27	85.2	3.7
2B5	120.4	48,900	0.23	87.5	3.7
2B6	121.4	42,900	0.19	87.4	3.6
2B7	121.9	38,400	0.16	85.7	3.7

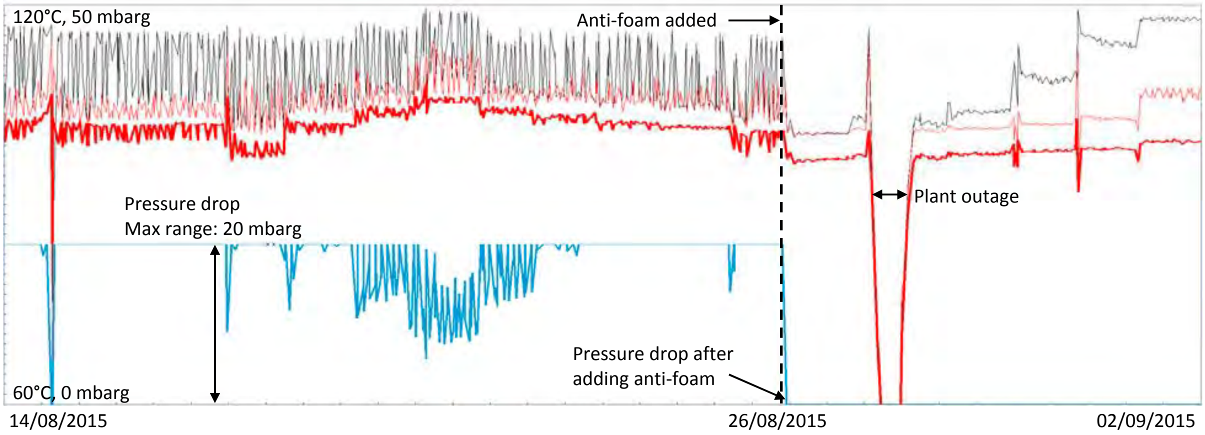

Figure 4. Stripper performance and result of using anti-foam is shown for the whole test series 2, see Table 1.The dashed vertical line shows the first use of anti-foam August 26 2015. The upper black and red thin lines show temperature sensors inside the stripper packing. The bold red and blue lines are temperature above the stripper packing and pressure drop over the stripper packing, respectively. Note that before adding anti-foam the pressure drop exceeded max range of 20 mbarg for the meter. Anti-foam resulted in immediate stabilising of temperatures and reduced the pressure drop over stripper. The further drop in temperature to the right of this is due to a short plant outage.

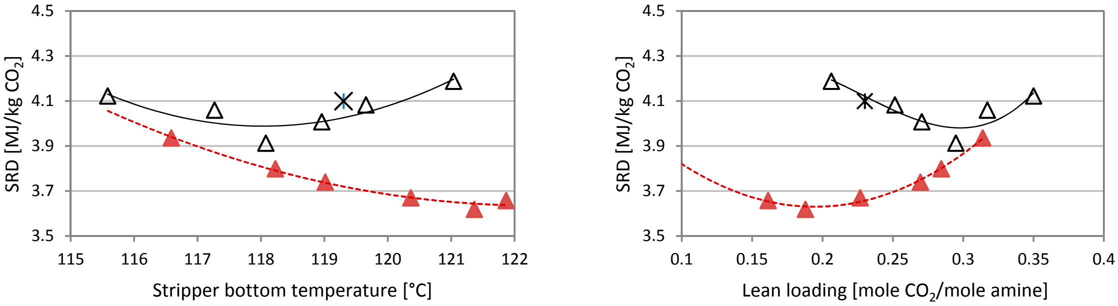

Figure 5. U-curves from series 2 and operation with anti-foam are shown as red filled triangles while results without the use of anti-foam are shown as open triangles. To the left SRD is given as function of stripper bottom temperature. To the right SRD is given as function of lean loading. The asterisk represents the 2014 baseline [1] made without the use of anti-foam.

The significant effect of anti-foam is clearly seen from the graphs. The stripper behaviour becomes much more optimal and the heat is no longer lost through the stripper overhead but used in efficient release of the CO_2 from the solvent amine. This leads to significantly lower specific reboiler duty and the optimum operation is shifted towards much leaner amine and less solvent circulation.

During test series 3 the independent verification protocol (IVP) and the 3rd party measurements were documented. Since the use of anti-foam allowed stable plant operation also at the full flue gas design capacity this operating condition was chosen for the verification testing, see series 3-1 (IVP) in Table 1. This test series established at 59,000 Sm^3/h flue gas flow will replace the baseline published in 2014 [1] and is reported in [3]. In Table 6 the main characteristics for the 2014 baseline are compared with test results from series 2. These tests were conducted at about the same flue gas flow of 47,000 Sm^3/h, CO_2 below 4 vol.% and with 24 meters of absorber packing. For comparison the table includes test “2A5” that have similar parameters as the 2014 baseline. The cases “2A3” and “2B6” represent optimum energy performance for operation without and with the use of anti-foam, see also Figure 5 above. The use of anti-foam gave about 20% reduction in lean amine flow rate and 12% reduction in SRD compared to the 2014 baseline.

Table 6. Comparison of the 2014 baseline and results from optimal performance testing. All tests are with 24 m absorber packing and around 3.6% dry CO_2 in flue gas from the CHP. Data sets "2A5" and "2A3" are without the use of anti-foam and are taken from Table 4, while "2B6" is with anti-foam and data are taken from Table 5. Loading is reported as mole CO_2/mole amine.

Name	Baseline [1]	2A5	2A3	2B6
Date	2014	19/08/2015	18/08/2015	31/08/2015
Flue gas flow [Sm^3/h]	46,970	46,900	46,900	46,900
FG temperature [°C]	25.0	29.0	28.2	28.0
Lean amine flow [kg/h]	54,900	52,500	59,600	42,900
Lean loading [mole/mole]	0.23	0.25	0.29	0.19
Rich loading [mole/mole]	0.48	0.50	0.49	0.50
Stripper bottom temp. [°C]	119.3	119.7	118.1	121.1
CO_2 capture [%]	90	87.0	83.5	87.4
SRD [MJ/kg CO_2]	4.1	4.1	3.9	3.6
Anti-foam	no	no	no	yes

6. **Parameter variations (Series 3 and 5)**

The test series 3 and 5 included tests made with 18 m absorber packing height and also tests at elevated CO_2 concentration in the flue gas flow into the absorber. These parameter variations will be discussed below.

With a new baseline established for full flue gas flow capacity (59,000 Sm^3/h) and use of 24 m absorber packing height [3] it was suggested to challenge the plant capacity even further with a test series at 18 m packing height. The flue gas flow rate was fixed at 59,000 Sm^3/h (3.6% CO_2 dry) and anti-foam was injected prior to the tests if needed. These results are presented in Table 7. In case "3A3" the absorber packing height was reduced from 24 to 18 m. The SRD value increased and rich loading decreased from 0.48 to 0.46, indicating that 18 m is not sufficient to give equilibrium. In case "3A4" the stripper bottom temperature was decreased from 121 to 119°C, resulting in a corresponding increase in lean loading from 0.20 to 0.26 and the capture rate decreased from 83 to 68%. In case "3A7" the stripper bottom temperature was increased to 120°C giving a lean loading of 0.23 and capture rate 76%. In case "3A8" the target was to achieve 85% capture rate at 120°C by changing the lean solvent flow rate. An increase in flow rate from 59,000 to 67,700 kg/h was required. For all these parameter variations the SRD was 3.6 to 3.9 MJ/kg CO_2.

Table 7. Parameter testing with 18m packing height compared to the new baseline (all with anti-foam). Loading is give as mole CO_2/mole amine.

Name	Baseline [3]	3A3	3A4	3A7	3A8
Date	2015	12/09/2015	12/09/2015	14/09/2015	14/09/2015
Packing height [m]	24	18	18	18	18
Flue gas flow [Sm^3/h]	59,400	59,500	59,400	59,500	59,600
FG temperature [°C]	29.8	30.2	30.4	31.2	31.7
Lean amine flow [kg/h]	57,400	59,200	59,200	59,000	67,700
Lean loading [mole/mole]	0.20	0.21	0.26	0.23	0.22
Rich loading [mole/mole]	0.48	0.46	0.48	0.46	0.45
Stripper bottom temp. [°C]	121	121.1	119.1	120.1	120.1
CO_2 capture [%]	83.4	83.1	68.1	75.5	84.7
SRD [MJ/kg CO_2]	3.6	3.8	3.7	3.8	3.9

Test series 5 also included tests at elevated CO_2 concentrations. The test series 5-2 and 5-3 started at stable conditions with 18 m packing height, flue gas flow 46,200 Sm^3/h and stripper bottom temperature 120.5°C. The objective was to investigate performance with increased CO_2 flue gas inlet concentration. At TCM the CO_2 inlet concentration can be varied by recycling CO_2 from the CO_2 product vent and back into the incoming flue gas. The CO_2 concentration was varied in controlled steps between nine and three percent (wet). The capture rate was kept close to 85% by adjusting the parameters stripper bottom temperature and lean solvent flow rate. The observed effects on SRD and solvent loading are shown in Figure 6 below.

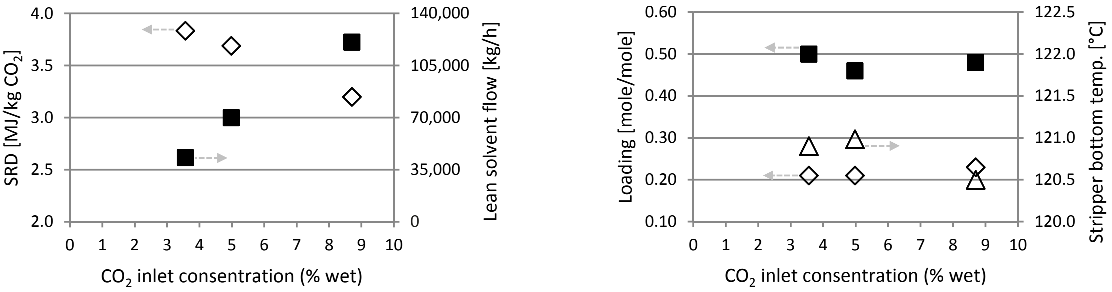

Figure 6. To the left SRD (diamonds) and lean solvent flow rate (squares) observed as function of inlet CO_2 concentration. To the right lean (diamonds) and rich (squares) solvent loading and stripper bottom temperature (triangles) observed as function of inlet CO_2 concentration. All with 18 m absorber packing height.

The testing started with CO_2 concentration about 9% wet and lean solvent flow 120,000 kg/h. The amount of captured CO_2 was 7,500 kg/h. When the CO_2 concentration was reduced to about 5% wet the lean solvent circulation was correspondingly reduced to 70,000 kg/h to reach 85% capture rate and the resulting amount of CO_2 captured was 3,900 kg/h. The baseline conditions were then tested with 3.6% wet CO_2 inlet concentration. The CO_2 captured was 2,700 kg/h.

The capture rate was within the range 85 to 88% for all the three selected test cases. From the right panel in Figure 6 it is seen that the stripper bottom temperature was only slightly adjusted between 120.5 and 121°C giving some minor changes in rich and lean loading.

As expected, the SRD increased with decreasing CO_2 inlet concentrations. It is interesting to further investigate the trade-off between CAPEX and OPEX parameters for operating conditions relevant for various gas power turbines and exhaust gas recycling systems in order to assess how total capture cost can be minimized.

7. Conclusion

The MEA 2015 campaign at TCM has provided a verification of mass balance over the plant and shown that the CO_2 mass balance based on gas phase can be maintained at a level better than +/- 5%. The plant performance presented in 2014 [1] has been revisited under operation with and without the use of anti-foam. Use of anti-foam enabled stable operation at lower lean solvent loading which resulted in lower lean amine flow rate and reduced SRD. Absorber packing height has been challenged and the results points towards operation at lower packing heights, but current tests also indicated that equilibrium was not achieved at reduced packing height. Tests at elevated CO_2 concentration showed as expected reduced SRD with increasing CO_2 concentration. The campaign has also resulted in reports on: new baseline [3], mist/aerosol induced emission to the air [4], emissions and degradation [5], reclaiming [6] and corrosion [7].

Acknowledgements

The authors gratefully acknowledge the staff of TCM DA, Gassnova, Statoil, Shell and Sasol for their contribution and work at the TCM DA facility. The authors also gratefully acknowledge Gassnova, Statoil, Shell, and Sasol as the owners of TCM DA for their financial support and contributions.

References

[1] Hamborg ES, Smith V, Cents T, Brigman N, Falk-Pedersen O, de Cazenove T, Chhaganl M, Feste JK, Ullestad Ø, Ulvatn H, Gorset O, Askestad I, Gram LK, Fostås BF, Shah MI, Maxson A, Thimsen D. Results from MEA testing at the CO_2 Technology Centre Mongstad. Part II: Verification of baseline results. Energy Procedia. Volume 63; 2014. p. 5994-6011.

[2] Thimsen D, Maxson A, Smith V, Cents T, Falk-Pedersen O, Gorset O, Hamborg ES. Results from MEA testing at the CO_2 Technology Centre Mongstad. Part I: Post-Combustion CO_2 capture testing methodology. Energy Procedia, Volume 63; 2014. p. 5938-5958.

[3] Faramarzi L, Thimsen D, Hume S, Maxson A, Watson G, Pedersen S, Gjernes E, Fostås BF, Lombardo G, Cents T, Morken AK, Shah MI, de Cazenove T, Hamborg ES. Results from MEA testing at the CO_2 Technology Centre Mongstad: Verification of baseline results in 2015. Energy Procedia (GHGT-13), Forthcoming 2017.

[4] Lombardo G, Fostås BF, Shah MI, Morken AK, Hvidsten OA, Mertens J, Hamborg ES. Results from aerosol measurement in amine plant treating gas turbine and residual fluidized catalytic cracker flue gases at the CO_2 Technology Centre Mongstad. Energy Procedia (GHGT-13), Forthcoming 2017.

[5] Morken AK, Pedersen S, Kleppe ER, Wisthaler A, Vernstad K, Ullestad Ø, Flø NE, Faramarzi L, Hamborg ES. Degradation and Emission Results of Amine Plant Operations from MEA Testing at the CO_2 Technology Centre Mongstad. Energy Procedia (GHGT-13), Forthcoming 2017.

[6] Flø NE, Faramarzi L, de Cazenove T, Hvidsten OA, Morken AK, Hamborg ES, Vernstad K, Watson G, Pedersen S, Cents T, Fostås BF, Shah MI, Lombardo G, Gjernes E. Results from MEA degradation and reclaiming processes at the CO_2 Technology Centre Mongstad. Energy Procedia (GHGT-13), Forthcoming 2017.

[7] Hjelmaas S, Storheim E, Flø NE, Thorjussen ES, Morken AK, Faramarzi L, de Cazenove T, Hamborg ES. Results from MEA amine plant corrosion processes at the CO_2 Technology Centre Mongstad. Energy Procedia (GHGT-13), Forthcoming 2017.

Results from MEA amine plant corrosion processes at the CO_2 Technology Centre Mongstad

(2017)

Available online at www.sciencedirect.com

ScienceDirect

Energy Procedia 114 (2017) 1166 – 1178

Energy Procedia

13th International Conference on Greenhouse Gas Control Technologies, GHGT-13, 14-18 November 2016, Lausanne, Switzerland

Results from MEA amine plant corrosion processes at the CO_2 Technology Centre Mongstad

Silje Hjelmaas[a,b], Erlend Storheim[a,b], Nina Enaasen Flø[a], Eva Svela Thorjussen[b], Anne Kolstad Morken[a,b], Leila Faramarzi[a,b], Thomas de Cazenove[a], Espen Steinseth Hamborg[a,b,]*

[a]CO_2 Technology Centre Mongstad (TCM DA), 5954 Mongstad, Norway
[b]Statoil ASA, PO Box 8500, 4035 Stavanger, Norway

Abstract

In 2015, the CO_2 Technology Center Mongstad (TCM DA), operated a test campaign using aqueous monoethanolamine (MEA) solvent at 30 wt%. The main objective was to demonstrate and document the performance of the TCM DA Amine Plant located in Mongstad, Norway. During the test period TCM DA monitored several indicators for corrosion, as well as analyzed corrosion coupons exposed to rich and lean solvent during the campaign. The results indicate unacceptable levels of corrosion for S235, coarse general corrosion for Inconel 600, and acceptable levels of corrosion for SS304L, SS316L, 22 Cr duplex SS, Stellite 6, Stellite 12 and EPDM. Some pitting was however observed on 316L stainless steel. No stress corrosion cracking was found on SS304L and SS316L.

© 2017 The Authors. Published by Elsevier Ltd. This is an open access article under the CC BY-NC-ND license (http://creativecommons.org/licenses/by-nc-nd/4.0/).
Peer-review under responsibility of the organizing committee of GHGT-13.

Keywords: Monoethanolamine; corrosion; pitting; metal ions.

1. Introduction

The CO_2 Technology Centre Mongstad (TCM DA) is located next to the Statoil refinery in Mongstad, Norway. TCM DA is a joint venture set up by Gassnova representing the Norwegian state, Statoil, Shell, and Sasol. The

---

* Corresponding author. Tel.: +47 56345220.
E-mail address: eham@tcmda.com

1876-6102 © 2017 The Authors. Published by Elsevier Ltd. This is an open access article under the CC BY-NC-ND license (http://creativecommons.org/licenses/by-nc-nd/4.0/).
Peer-review under responsibility of the organizing committee of GHGT-13.
doi:10.1016/j.egypro.2017.03.1280

facility run by TCM DA entered the operational phase in August 2012 and it is one of the largest post-combustion CO_2 capture test centres in the world. A unique aspect of the facility is that either a flue gas slipstream from a natural gas turbine based combined heat and power (CHP) plant or an equivalent volumetric flow from a residual fluidized catalytic cracker (RFCC) unit can be used for CO_2 capture. The CHP flue gas contains about 3.5% CO_2 and the RFCC flue gas contains about 13-14% CO_2. One of the main test plants at TCM DA is a highly flexible and well-instrumented amine plant. The amine plant was designed and constructed by Aker Solutions and Kværner to accommodate a variety of technologies, with capabilities of treating flue gas streams of up to 60,000 standard cubic meters per hour. The plant is being offered to vendors of solvent based CO_2 capture technologies to, among others, test; (1) the performance of their solvent technology, and (2) technologies aimed to reduce the atmospheric emissions and environmental impact of amines and amine based degradation products from such solvent based CO_2 capture processes. The objective of TCM DA is to test, verify, and demonstrate CO_2 capture technologies suitable for deployment at full-scale. Up to now the vendors Aker Solutions, Alstom, Cansolv Technologies Inc. and Carbon Clean Solutions Ltd. have successfully used the TCM DA facilities to verify their CO_2 capture technologies.

From July to October 2015 TCM DA, in collaboration with partners, operated a test campaign using the non-proprietary aqueous monoethanolamine (MEA) solvent at 30 wt%. A wide range of operational conditions were tested during this period to meet pre-set objectives and document the plant and solvent performance. Corrosion processes was monitored during the test campaign by installing and examining a variety of corrosion coupons, as well as measuring the metal ion and HSS content in the MEA solvent.

Corrosion is a major operational concern in amine treating plants for acid gas removal, which may lead to structural integrity issues and fouling. Amine carbamates are known complexing agents causing metal corrosion, and the following factors are closely associated with increased corrosion rates: operating temperature, CO_2 loading, amine type and concentration, and amine contaminants such as amine degradation products and heat stable salts [1,2]. Especially oxidative degradation products are known to cause corrosion of metal surfaces [3]. Oxidative degradation products are formed in presence of oxygen and are therefore expected to be a major contributor to corrosion in Post Combustion Capture (PCC) applications treating flue gases which generally contain higher levels of oxygen [4]. In addition to being corrosive themselves, formation of oxidative degradation products are also catalyzed by dissolved transition metals resulting from metal corrosion [4].

There exist several studies concerning corrosion in amine systems at laboratory scale [5]. However, investigations in more realistic CO_2 capture operating conditions with respect to variations in temperature, solvent concentrations, CO_2 loadings etc. are crucial in order to map required design specifications for PCC plants for commercial scale. Some work also exists for pilot scale investigation, but these are often limited concerning type of materials tested, examination methods and the length of test periods [2,4].

Kittel et al (2009) presents corrosion monitoring results for two different pilot plants, i.e. The International Test Centre for CO_2 Capture (ITC) at the University of Regina, Canada and the CASTOR pilot plant at Dong Energy in Esbjerg, Denmark [4]. Both pilot plants operated with 30wt% aqueous MEA solvent. The ITC pilot plant treated flue gas from a natural gas burner, while the Castor pilot plant treated flue gas from a coal power station. AISI 1018 (carbon steel) and AISI 316 or AISI 304 (stainless steel) corrosion coupons were installed at several locations in the Castor pilot plant for total exposure periods of 500 hours. The results confirm extremely high corrosion of carbon steel in the hot solvent exiting the stripper (4.5 – 8.5 mm/year), while good performance of carbon steel was observed in the hot solvent entering the stripper. Stainless steel exhibited excellent resistance for all locations of the pilot plant (corrosion rates below 0.005 mm/year). Corrosometer probes were used to monitor corrosion in the ITC plant. The highest corrosion rates were measured in the stripper overhead (0.535-0.538 mm/year) and at the stripper inlet (0.533-1.075 mm/year). The stripper bottom showed far less corrosion in this study (0.028-0.047 mm/year). The cool parts of the unit also showed low corrosion rates, in agreement with the results from Castor pilot plant.

Cousins et al. (2013) investigated corrosion in the Tarong Post Combustion Capture (PCC) pilot plant in Australia operating with 30 wt% aqueous MEA for 640 hours [6]. 4 different types of metal coupons (316L, 316L welded, C1018 and C1018 galvanized) were installed at 8 different locations in the pilot plant. The coupons were investigated by scanning electron microscopy (SEM), XRD analysis, and corrosion rates based on weight loss were calculated. The 316 stainless steel coupons exhibited extremely low corrosion rates (less than 0.003 mm/year) for all locations. The C1018 carbon steel coupons exhibited higher corrosion rates, with the highest measured in the stripper sump (0.800-1.6 mm/year).

The objectives of the present work are to present TCM DA's comprehensive corrosion evaluation during the 30 wt% aqueous MEA campaign conducted in 2015. A variety of corrosion coupons were installed and exposed to amine solution at two different locations in the plant, i.e. hot rich amine upstream the stripper column and hot lean amine upstream the rich/lean cross heat exchanger. Carbon and stainless steel, Inconel 600 and 22% Cr duplex materials were investigated for pitting corrosion by microscopy and the general corrosion rate was calculated based on weight loss and exposure time. Bent coupons of carbon and stainless steel were also inspected for stress corrosion cracking. In addition, Stellite was examined for decobaltification, and EPDM was investigated for degradation. The work included frequently analysis of metal ions and HSS in the solvent. Metals where monitored by ICP-OES, while total HSS by a titration procedure and IC for individual HSS anions.

Nomenclature

CHP	Combined heat and power
EPDM	Ethylene-propylene rubber
HSS	Heat Stable Salts
MEA	Monoethanolamine
PTFE	Polytetrafluoroethylene
RFCC	Residual fluidized catalytic cracker
TCM DA	CO_2 Technology Centre Mongstad
HSS	Heat Stable Salts
ICP-OES	Inductively coupled plasma optical emission spectronomy
IC	Ion Chromatography

2. Plant overview and test conditions

An illustration of the TCM DA Amine plant is shown in Figure 1. Flue gas containing CO_2 is contacted with the amine solvent in the absorber, leading CO_2 to react and be captured in the solvent. The rich solvent containing CO_2 is pre-heated by hot lean solvent in the lean/rich cross heat exchanger before it enters the stripper section. Additional heat is supplied by steam to the stripper reboiler in order to reverse the absorption reaction and release CO_2 from the solvent. The regenerated lean solvent leaving the stripper is cooled down in the lean/rich cross heat exchanger and lean cooler, before it is recirculated back to the absorber in order to capture CO_2 ones more. The depleted flue gas leaves the top of the absorber, while CO_2 is released to the atmosphere through the stripper section.

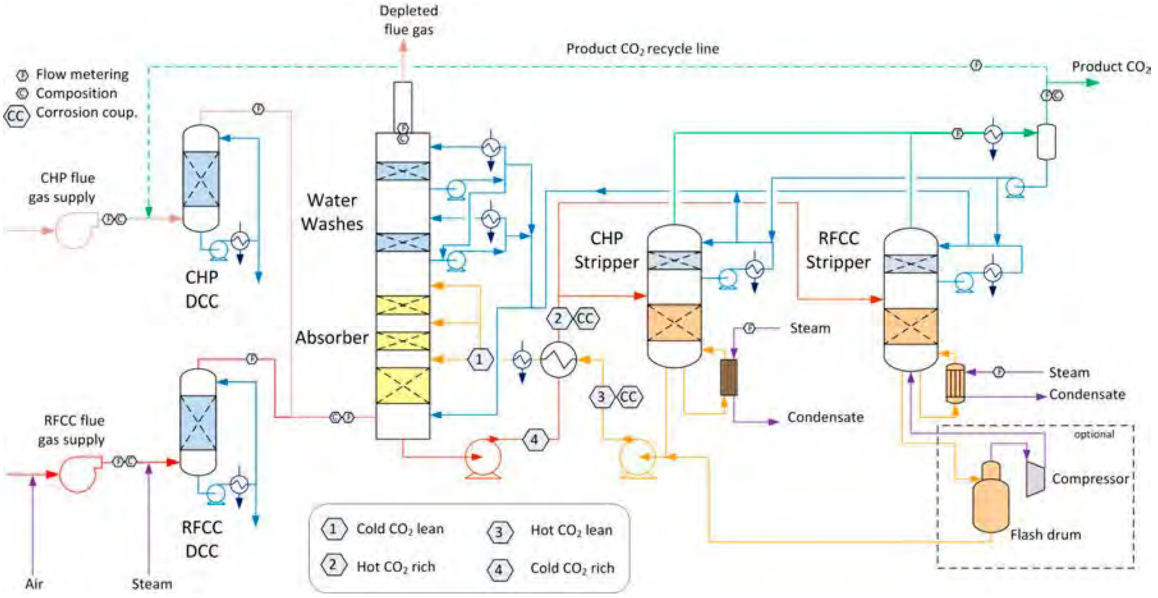

Figure 1: Illustration of TCM DA Amine plant and indication of rich and lean sections.

The test campaign was conducted from 06/07/2015 to 17/10/2015. During this period the plant treated mainly flue gas from the combined heat and power (CHP) plant. Separate testing were conducted for a period of 9 days from 16.09.2016 to 24.09.2016, where a mix of RFCC (0-10%) and CHP gas was utilized to study the effect of different flue gas conditions (CO_2 and gas impurity concentrations) on mist formation. Typical CHP and RFCC gas compositions to the Amine plant are presented in Table 1.

Table 1. Typical flue gas compositions to Amine plant.

Description	Units	CHP	RFCC
Flue gas flow (Sm3/h)	Sm3/h	<60.000	<45.000
Operating temperature (°C)	°C	25-50	15-50 ⁽¹⁾
Operating pressure (mbarg)	mbarg	Up to 250	Up to 250
N_2 (mole%)	mole%	73 - 79	73 - 79
O_2 (mole%)	mole%	13 - 14	3 - 8
CO_2 (mole%)	mole%	3.5 – 4.0 ⁽²⁾	13.0 – 14.5 ⁽³⁾
H_2O (mole%)	mole%	Saturated	Saturated
SO_2 (ppmv)	ppmv	<0.3	<5
NO_x (ppmv)	ppmv	<5	60
NH_3 (ppmv)	ppmv	<5	<1
CO (ppmv)	ppmv		<3
Particles (mg/Nm3)	mg/Nm3		⁽⁴⁾

Note:

1. With steam injection.
2. Facility is provided to enable CO_2 recycling, thereby allowing tests with CO_2 concentrations up to about 15 vol%.
3. Facility is provided to enable air dilution, thereby allowing tests with CO_2 concentrations down to about 2.5 vol %.

4. H_2SO_4: 10-25 mg/Sm^3; Other soluble salts
   $(NH_4)_2SO_4$+NH_4HSO_4+NaCl: 5-10 mg/Sm^3; Non water soluble salts
   SiO_2+Ca and other metals: 0-2 mg/Sm^3

The solvent used was 30 ± 2 wt % aqueous MEA. Pure MEA was diluted to desired concentration by adding demineralized water. An anti-foam agent was also used to reduce indication of foam in the stripper. Table 2 provides a comparative overview of compounds present in lean and rich solvent. Typical lean CO_2 loadings in the 30 wt% aqueous MEA solution were ranging from 0.15 to 0.25 mole CO_2 per mole MEA and typical rich CO_2 loadings were ranging from 0.48 to 0.50 mole CO_2 per mole MEA throughout the campaign.

Table 2. Components present in lean and rich solvent.

Compound	Lean	Rich
Molecular compounds MEA	High	Low
Ionic compounds*	Low	High

** Protonated MEA, carbamate, MEA carbonate and bicarbonate*

Typical process parameters for the MEA solvent in circulation are presented in Table 3. There were marginal changes in both temperature and pH during the campaign. The solvent flow was approximately 55 tons/hour, except for a period of approximately 20 days where the flow was 80 – 120 tons/hour. During the test campaign there were two shutdowns, the first for one day and the second for seven days. In addition, there were two short periods during the campaign when the flue gas was not in contact with the circulating solvent due to planned or unplanned stops. Total test period lasted for 123 days. Operational hours are counted as hours with both flue gas and solvent circulation. The campaign gave a total of 1960 hours of operation.

Table 3. Process parameters Amine circulation.

Process parameters	Unite	Hot lean	Hot Rich	Cold lean	Cold rich
Temperature	°C	120	110	35	35
Flow rate	Tons/hour	55-120	55-120	55-120	55-120
pH		10.2	9	10.2	9
Pipe size	Inches	8	6	8	6
Velocity	m/s	0.45-0.97	0.74-1.62	0.45-0.97	0.74-1.62

The main plant equipment and piping system in contact with amine consist of 22% Cr duplex. Gaskets used are mainly EPDM and PTFE. A few internal parts in valves are produced in Stellite and Inconel, while the absorber has packing and structure manufactured in SS 316L. The absorber is manufactured in concrete, but is internally lined with polypropylene material. These materials form the basis for the corrosion coupons chosen. Carbon steel nevertheless is included in the test program, although carbon steel is not used in the section in contact with amine. As a part of the internal TCM DA maintenance program, pipe spools in hot rich and lean section are inspected between each change of solvent inventory. Penetrant testing or x-ray is performed on pipe welding to check for any changes.

For corrosion several factors are important to monitor in the amine system; pH, temperature, velocity and heat stable salts[1].

3. Corrosion coupons and solvent analysis

3.1. Corrosion coupons

Table 4 presents the type of materials tested. The purpose and the locations in the plant are also listed.

Table 4. Corrosion coupons installed in the amine plant.

Coupon no.	Exposure location	Material	Manufacturer	Material type	Purpose
2,5	Hot lean	SS 304	Outokumpu	Austenitic stainless steel	Corrosion rate and pitting corrosion
9,10	Hot rich	1.4301 Type 304 1.437			
4,6	Hot lean	SS 316L			
7,8	Hot rich	1.4404 1.4401 Type 316L			
12,1	Hot lean	S235	Smith Stål	Carbon steel	
11,3	Hot rich				
13	Hot lean	Inconel 600	Yakin	Nickel based alloy	
14	Hot rich	ASTM B168 UNS N06600 (2011)			
17	Hot lean	22% Cr duplex	Aperam	Ferritic austenitic stainless steel	
18	Hot rich	UNS 32205/31803 DIN 4.4462 Type 2205			
19	Hot lean	22% Cr duplex with Stellite 6	Castoline Eutentic (stellite material)	Ferritic austenitic stainless steel with Stellite welding	Corrosion of Stellite and decobaltification
20	Hot rich				
21	Hot lean	22% Cr duplex with Stellite 12			
22	Hot rich				
23	Hot lean	SS 316L	Outokumpu	Austenitic stainless steel	Stress corrosion cracking
24	Hot rich	1.4404 1.4401 Type 316L (bent coupon)			
25	Hot lean	SS 304			
26	Hot rich	1.4301 Type 304 1.437 (bent coupon)			
27	Hot lean	S235 (bent coupon)	Smith Stål	Carbon steel	
28	Hot rich				
29	Hot lean	22% Cr duplex with EPDM	NA (EPDM material)	Ferritic austenitic stainless steel with synthetic rubber	Degradation of EPDM.
30	Hot rich				

The stainless steel, carbon steel and Inconel materials were cut out from larger plates using high pressure water. Stellite 6 and Stellite 12 were welded on duplex corrosion coupon surface according to supplier and welder recommendations. Purpose was to examine the corrosion resistance of the Stellite materials on duplex. Stellite is a cobalt-chromium alloy used as hard facing on machine parts. The EPDM material tested during the campaign was a gasket from equipment installed in the amine plant. A specific data sheet for the material is therefore not available. Coupons of SS 316, SS 304 and carbon steel where installed as both plain and bent coupons. The bent coupons were meant to simulate stress corrosion cracking [7]. Figure 2 and 3 presents the specimens mounted in the test rack exposed to the solvent.

Figure 2: Illustration of coupons installed in the rack. Flow direction from right to left.

Figure 3: Illustration of bent coupons installed in the rack. Flow direction from right to left.

The corrosion racks are of alloy 316L and are placed longitudinally in the pipe. This means that some specimens are placed at the top side of the piping, while others are located at the bottom of the pipe. Bent coupons are placed at the side of the rack. To ensure that there is no contact between each coupon and the rack, PTFE insulators are mounted between the two materials. Table 5 and Table 6 illustrates where in the rack each coupon is installed.

Table 5. Indicate coupon position in the lean rack, with number labelling. Flow direction from right to left.

Location	Materials					
Top side	EPDM (29)	Stellite 12 (21)	Stellite 6 (19)	SS304L (5)	empty	SS304L (2)
Bottom side	CS S235 (12)	Inconel 600 (13)	CS S235 (1)	SS316L (6)	Duplex (17)	SS316L (4)
Side of rack	SS304L (25)		SS316L (23)		CS S235 (27)	

Table 6. Indicate coupon position in the rich rack, with number labelling. Flow direction from right to left.

Location	Materials					
Top side	EPDM (30)	Stellite 6 (20)	Stellite 12 (22)	SS304L (9)	empty	SS304L (10)
Bottom side	CS S235 (11)	Duplex (18)	CS S235 (3)	SS316L (18)	Inconel 600 (14)	SS316L (7)
Side of rack	SS316L (24)		CS S235 (28)		SS304L (26)	

Before installation, all coupons were carefully prepared. Smergel 80-600 were used to polish the surface. Coupons were thoroughly water washed and dried with absolute alcohol. After 24 hours in exicator, weight measurements were performed. For each sample type, one additional coupon was stored in a clean and dry environment as an unexposed reference. After exposure, each coupon was washed and weight determid by the same procedure as before exposure.

3.2. Corrosion coupon analysis

The weight losses were used to calculate the general corrosion rate in mm/year. All corrosion coupons had the same dimensions before exposure. Equation 1 was used to calculate the corrosion rate in mm/year.

$$mm/year = \frac{Weight\ loss\ (g)\ x\ 365\frac{days}{year}\ x\ 10\ mm/cm}{\mathrm{Density}\left(\frac{\mathrm{g}}{\mathrm{cm3}}\right) x\ Area\ (cm2)\ x\ Exposure\ time\ (days)} \qquad (1)$$

The corrosion coupons were examined for local corrosion by microscopy at a magnification of 25X. The depth of the local corrosion was measured by use of Alicona scanning microscope.

The alloys Stellite 6 and Stellite 12 were examined by SEM (scanning electron microscopy) connected to EDS (Energy dispersive spectrometer) in order to identify “decobaltification”. The examination was performed at a magnification of 2000x.

The coupons prepared for stress corrosion cracking were examined for cracks by microscopy at a magnification of 40X and by use of dye penetrant fluid according to ASME B31.3.

Shore hardness, tensile testing (modulus and stress at break) and visual examination of fracture surfaces after tensile testing were performed on the EPDM material. Unexposed EPDM was examined as reference.

3.3. Evaluation criteria corrosion coupons

- General and pitting corrosion **:** The acceptance criterion for stainless steels for general corrosion based on weight losses is set to ≤ 0.1 mm/year and no pitting visible at a magnification of 25x. For carbon steel acceptance criterion is set to ≤ 0.1 mm/year and < 20 µm in local corrosion depths.

- Stress corrosion cracking: No visible cracking after dye penetrant testing is set as acceptable.

- EPDM: No significant difference in the results from the hardness and tensile testing of the unexposed and exposed EPDM.

- Stellite 6 and 12: No decobaltification shall be visible at a magnification of 2000x.

3.4. Solvent analysis

Previous experiences at TCM DA have shown an increase in iron, chrome and nickel ions measured in the circulating solvent. Monitoring the increase of metal ions in the solvent can therefore aid to discover possible corrosion attacks within the plant. Metal concentration was analyzed by ICP-OES frequently throughout the campaign. The solvent samples for analysis were taken from the cold lean amine.

The amount of HSS in the solvent is an important factor for corrosion evaluation in amine systems. Generally, low HSS concentration is recommended to keep amine CO_2-capture capacity high and corrosion rate low, 0.5-0.8 wt% for long term and reclamation at a certain wt% of total HSS [8,9,10]. The HSS concentrations were determined as described elsewhere. [11]

4. Results and discussion

4.1. Corrosion coupons and solvent analysis

Table 7 shows the general corrosion rates and depth of pitting corrosion found on the coupons. The green and red colour in the cells is explained below the table.

As shown in the table, the corrosion rate was far below 0.1 mm/year and no pitting observed on the corrosion coupons in alloy 304L and duplex stainless steel exposed to both lean and rich solvent.

All the coupons in alloy 316L had corrosion rate below 0.1 mm/year. No pitting was observed on 316L coupons exposed in lean solvent, while three pits were found on each of the 316L coupons exposed to the rich solvent. Figure 4 shows pictures of two pits found on these coupons. The maximum pitting depth was 51 µm, corresponding to 0.15 mm/year.

The Inconel 600 coupon exposed in lean solvent was attacked by coarse general corrosion with a corrosion rate of 0.84 mm/year. No pitting was observed. In rich solvent the same alloy showed corrosion rate far below 0.1 mm/year and no pitting. To verify that both coupons were Inconel 600, analysis with “Niton alloy analyser” was performed on these coupons. The analysis performed showed that both coupons were of the same alloy.

The carbon steel coupons in S235 disappeared during the exposure time due to total corrosion. The corrosion rate for carbon steel, S235, is calculated to be above or equal to 1.4 mm/year based on the total weight prior to exposure.

Table 7. General corrosion and pitting results.

Coupon no.	Materials	Exposure place	General corrosion mm/year	No. of pits	Max depth [µm]
2	SS304L	Hot lean	**<<0.1**	**No pitting found**	
5	SS304L	Hot lean	**<<0.1**		
9	SS304L	Hot rich	**<<0.1**		
10	SS304L	Hot rich	**<<0.1**		
4	SS316L	Hot lean	**<<0.1**		
6	SS316L	Hot lean	**<<0.1**		
7	SS316L	Hot rich	**<<0.1**	**3**	**36**
8	SS316L	Hot rich	**<<0.1**	**3**	**51**
1	S235	Hot lean	**>1.4**	**Not examined, coupon totally corroded.**	
12	S235	Hot lean	**>1.4**		
3	S235	Hot rich	**>1.4**		
11	S235	Hot rich	**>1.4**		
13	Inconel	Hot lean	**0.84**	**Coarse general corrosion, not pitting**	
14	Inconel	Hot rich	**<<0.1**	**No pitting found**	
17	Duplex	Hot lean	**<<0.1**		
18	Duplex	Hot rich	**<<0.1**		
	Acceptable		**Not acceptable**		

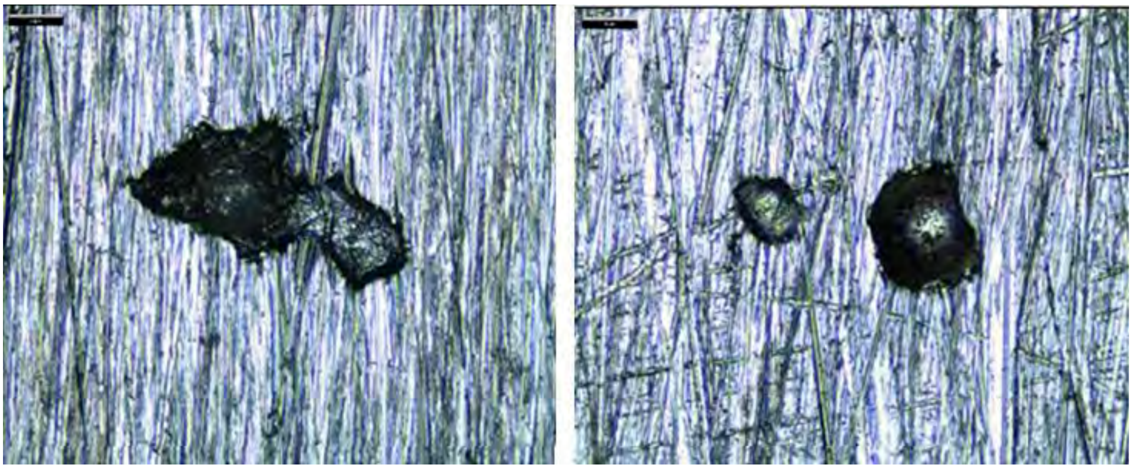

Figure 4. Pictures of pitting found on SS 316L coupon. Left picture illustrates pitting depth 51 µm at magnification 400x(coupon no. 8), while right illustrates depth 36 µm at magnification 160x(coupon no. 7). No similar pitting was found on the unexposed reference coupon..

No corrosion or degradation of the Stellite 6 and 12 material was observed in the SEM/EDS examination. There were no differences between the unexposed reference and the exposed coupons.

No stress corrosion cracking was observed on the 304L or 316L coupons after visual examination at a magnification of 40x nor after dye penetrant fluid examination.

There were insignificant differences between the unexposed reference and the exposed EPDM material based on the results from shore hardness and tensile testing. There was no visual difference in the fracture surfaces between the unexposed and exposed EPDM.

Figure 5 illustrates the ion concentration of metals in lean amine solvent. The aim of monitoring the metals in the solvent is to follow the increase of the metal ions. If a rapid increase would occur, inspection and evaluation of the cause(s) would have to be performed. In an amine plant some increase of metal ions is acceptable. Rennie (2006) informs that corrosion is typically worse at locations where the acid gases are flashed off, for example the regenerator reboiler [12]. In the reboiler and stripper section of the amine plant at TCM DA, fouling in the equipment and piping system is observed. This may be related to the boiling off of the solvent and the temperature at this location. The increase of metal ions might come from this hot section of the plant. However, internals within the absorber are manufactured in SS 316L, and might be affected by the process environment in the absorber. The flue gas from the CHP plant does not consist of considerable amount of metals. RFCC gas do contain a higher level of metals, but even with the mixed RFCC and CHP gas the metal ion concentration do not seem to have rapidly increased during the mixing period. This excludes that most of the metal ions measured in the solvent could originate from the flue gas during this MEA campaign.

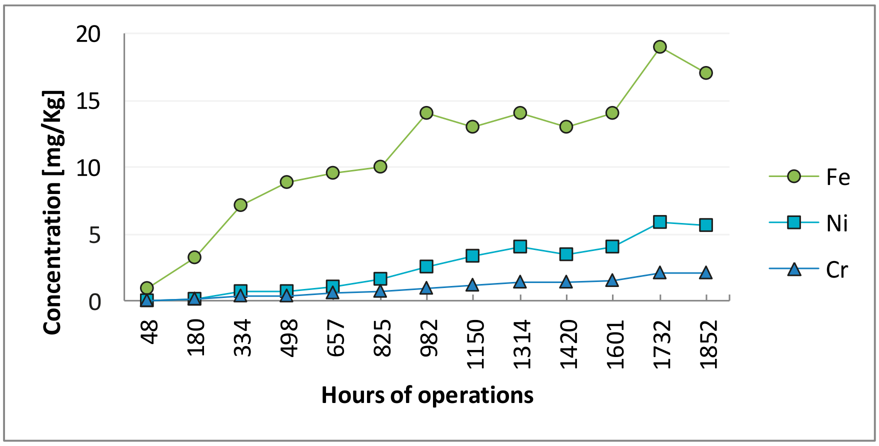

Figure 5: Metal ion concentration in lean solution. X-axis provides time of solvent analysis.

HSS are reported as the wt% of the equivalent amount of amine. This means if HSS concentration were 1 mole/kg (eq/Kg) of solution, it will be 6.1 wt% as MEA. Figure 6 illustrates the HSS wt% measured by titration during the campaign. Approximately 1.25 wt% HSS where measured at the end of the campaign, and the increase was close to linear.

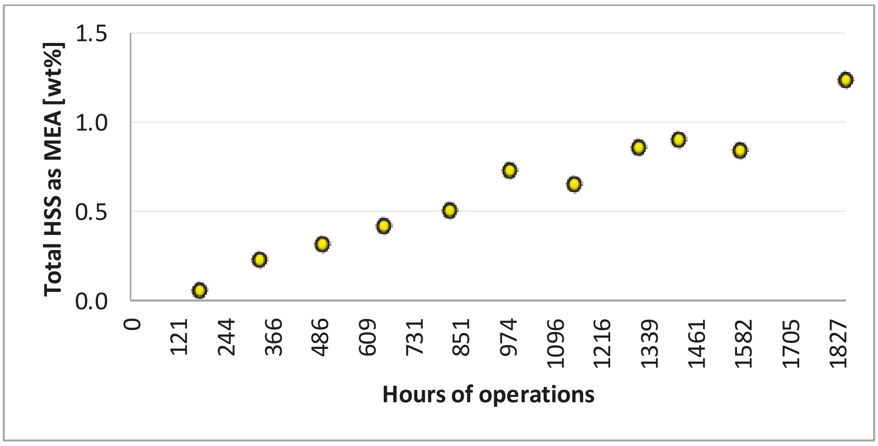

Figure 6. Heat stable salts measured by titration. X-axis provides time of solvent analysis.

The Inconel 600 coupon exposed in lean solvent was attacked by coarse general corrosion while in rich solvent the same alloy showed corrosion rate far below 0.1 mm/year. The reason for the high corrosion in lean solvent may be related to changes in chemical composition, pH or temperature. This campaign shows that Inconel 600 is not compatible with lean 30 wt% MEA at high temperatures (~120°C), but that the critical temperature for corrosion may be lower, somewhere between 50-120°C. No corrosion was observed in the hot rich section in the same operational period.

There were some mechanical damages on the coupons which made it difficult to analyze pitting corrosion. A few pits were found on the 316L coupons while no pitting was found on SS304L. SS316L is placed against the bottom while SS304L is placed against the top of the pipe coil. In periods without solvent circulation it may have been some deposits that have covered the surface of SS316L which can increase the corrosion attacks. However, the lean coupons have not been affected by the shutdown periods.

Erosion and the velocity of the fluid is a factor influencing the corrosion rate. As listed earlier in Table 3, the velocity during the campaign is highest in the rich section. Rennie (2006) informs that the velocity limit for carbon steel is maximum 1.5 m/s, and that for stainless steel it is often one upper and lower limit [12]. Based on the relatively low average velocity in the piping where the coupons have been installed, erosion is not the main reason for the corrosion results. However, the corrosion racks are designed such that turbulent flow will occur around the coupons, and it can affect the corrosion rate.

The location for the corrosion coupons is mainly chosen due to the high temperature at that section within the plant. For future work TCM DA will try to install corrosion coupons in the cold rich and lean section, as well as in the hot section. This can evaluate if there are larger differences between the corrosion rate in the hot and cold section. Inspections of equipment and piping system are also future work that can help understanding and conclude on the corrosion and corrosion mechanisms that occurs in amine plants.

5. Conclusions

After execution of 30 wt% aqueous MEA campaign at TCM DA amine plant from July to October 2015, the following conclusions can be made according to the work conducted:

- The coupons in alloy S235, carbon steel, was totally corroded during the test period. The corrosion rate for carbon steel, S235, is calculated to be above or equal to 1.4 mm/year.
- The corrosion rate was far below 0.1 mm/year for all the coupons in alloy 304L, 316L and 22 Cr duplex stainless steel.

- The Inconel 600 coupon exposed in lean solvent was attacked by coarse general corrosion with a corrosion rate of 0.84 mm/year. In rich solvent the same alloy showed corrosion rate far below 0.1 mm/year.
- Pitting was not observed on coupons in 304L, Inconel 600 and 22 Cr Duplex.
- A few pits were observed on the 316L coupons exposed to rich solvent with a maximum pitting depth of 0.15 mm/year. No pitting was found on the same alloy exposed to lean solvent.
- No corrosion or degradation of alloy Stellite 6 and Stellite 12 was observed.
- No stress corrosion cracking was found on the 304L or 316L coupons.
- No degradation of EPDM (Ethylene propylene elastomer) was observed.
- HSS and metal ions are similar to previous MEA campaigns, and are concluded to be within acceptable limits.

Acknowledgements

The authors gratefully acknowledge the staff of TCM DA, Gassnova, Statoil, Shell and Sasol for their contribution and work at the TCM DA facility. The authors also gratefully acknowledge Gassnova, Statoil, Shell, and Sasol as the owners of TCM DA for their financial support and contributions.

References

[1] Kohl A, Nielsen R. Gas Purification. 5th ed. Houston: Gulf Publishing Company; 1997.

[2] Pearson P, Hollenkamp A F, Meuleman E. Electrochemical investigation of corrosion in CO_2 capture plants – influence of amines. Electrochimica Acta 2013;110:514-516.

[3] Goff GS, Rochelle GT. Monoethanolamine Degradation: O_2 Mass Transfer Effects under CO2 Capture Conditions. Industrial & Engineering Chemistry Research 2004;43(20): 6400-6408.

[4] Kittel J, Idem R, Gelowitz D, Tontiwachwuthikul P, Parrain G, Bonneau A. Corrosion in MEA units for CO_2 capture: Pilot plant studies. Energy Procedia 2009;1:791-797.

[5] Verheyen TV, Adeloju SBO, Chaffee AL, Meuleman E. Primary sources and accumulation rates of inorganic and dissolved metals in a MEA absorbent during PCC at a brown coal-fired power station. International Journal of Greenhouse Gas Control 2015; 41:239-248.

[6] Cousins A, Ilyushechkin A, Pearson P, Cottrell A, Huang S, Feron PHM. Corrosion coupon evaluation under pilot-scale CO2 capture conditions at an Australian coal-fired power station. Greenhouse gases Science and Technology 2013;3:169-184.

[7] Field Corrosion Evaluation Using Metallic Test Specimens, NACE Standard RP0497-2004, Item No. 21083.

[8] Arthur L. Cummings, Scott W. Waite, Dennis K. Nelsen. Corrosion and Corrosion Enhancers in Amine Systems, MPR Services, 2005.

[9] Winyu Tanthapanichakoon, Amornvadee Veawab. Corrosion by heat-stable salts in amine-based CO_2 capture unit. University of Regina, 2003.

[10] E.R. Baumeister, R. C. Souza, Carlos Ihle Rusque. Amine contamination and associated problems in gas treating units, AVPG, 2010.

[11] Morken AK, Pedersen S, Kleppe ER, Wisthaler A, Vernstad K, Ullestad Ø, Flø NE, Faramarzi L, Hamborg ES. Degradation and Emission Results of Amine Plant Operations from MEA Testing at the CO2 Technology Centre Mongstad. Energy Procedia (GHGT -13), Forthcoming 2017.

[12] S. Rennie. Corrosion and material selection for amine service, Woodside Energy Ltd, 2006.

CATCHING OUR FUTURE

Results from aerosol measurement in amine plant treating gas turbine and Residue Fluidized Catalytic Cracker flue gases at the CO_2 Technology Centre Mongstad

(2016)

Available online at www.sciencedirect.com

ScienceDirect

Energy Procedia 114 (2017) 1210 – 1230

Energy Procedia

13th International Conference on Greenhouse Gas Control Technologies, GHGT-13, 14-18 November 2016, Lausanne, Switzerland

Results from aerosol measurement in amine plant treating gas turbine and Residue Fluidized Catalytic Cracker flue gases at the CO_2 Technology Centre Mongstad

Gerard Lombardo[ab]*, Berit F. Fostås[ac], Muhammad Ismail Shah[ab], Anne Kolstad Morken[a,c] Odd Arne Hvidsten[a,c], Jan Mertens[d], Espen Steinseth Hamborg[a,c]

[a]*CO_2 Technology Centre Mongstad (TCM DA), 5954 Mongstad, Norway*
[b]*Gassnova SF, Dokkvegen 10, 3920 Porsgrunn, Norway*
[c]*Statoil ASA, PO Box 8500, 4035 Stavanger, Norway*
[d]*Engie Research and Technologies, Simon Boulivardlaan 34, 1000 Brussels, Belgium*

Abstract

This work discusses the relation between flue gas particle content, mainly related to sulfuric acid aerosols and dust, and corresponding MEA emissions. The work lays grounds for future necessary pre-treatment options for various flue gases with high aerosol content in order to operate post-combustion amine plants with minimum emissions.

In 2015, the CO_2 Technology Center Mongstad (TCM DA), operated a test campaign using aqueous monoethanolamine (MEA) solvent at 30 wt%. The main objective was to demonstrate and document the performance of the TCM DA Amine Plant located in Mongstad, Norway. Two weeks were dedicated to the aerosol measurement testing.

© 2017 The Authors. Published by Elsevier Ltd. This is an open access article under the CC BY-NC-ND license (http://creativecommons.org/licenses/by-nc-nd/4.0/).
Peer-review under responsibility of the organizing committee of GHGT-13.

Keywords: Aerosols; monoethanolamine; MEA; emissions; mechanism; post combustion CO_2 capture; sufuric acid; mist

---

* Corresponding author. Tel.: +47 40 00 59 08
E-mail address: gl@gassnova.no

1876-6102 © 2017 The Authors. Published by Elsevier Ltd. This is an open access article under the CC BY-NC-ND license (http://creativecommons.org/licenses/by-nc-nd/4.0/).
Peer-review under responsibility of the organizing committee of GHGT-13.
doi:10.1016/j.egypro.2017.03.1377

1. Introduction

The CO_2 Technology Centre Mongstad (TCM DA) is located next to the Statoil refinery in Mongstad, Norway. TCM DA is a joint venture set up by Gassnova representing the Norwegian state, Statoil, Shell, and Sasol. The facility run by TCM DA entered the operational phase in August 2012 and it is one of the largest post-combustion CO_2 capture test centres in the world. A unique aspect of the facility is that either a flue gas slipstream from a natural gas turbine based combined heat and power (CHP) plant or an equivalent volumetric flow from a residual fluidized catalytic cracker (RFCC) unit can be used for CO_2 capture. The CHP flue gas contains about 3.5% CO_2 and the RFCC flue gas contains about 13-14% CO_2. One of the main test plants at TCM DA is a highly flexible and well-instrumented amine plant. The amine plant was designed and constructed by Aker Solutions and Kværner to accommodate a variety of technologies, with capabilities of treating flue gas streams of up to 60,000 standard cubic meters per hour. The plant is being offered to vendors of solvent based CO_2 capture technologies to, among others, test; (1) the performance of their solvent technology, and (2) technologies aimed to reduce the atmospheric emissions and environmental impact of amines and amine based degradation products from such solvent based CO_2 capture processes. The objective of TCM DA is to test, verify, and demonstrate CO_2 capture technologies suitable for deployment at full-scale. Up to now the vendors Aker Solutions, Alstom, Cansolv Technologies Inc. and Carbon Clean Solutions Ltd. have successfully used the TCM DA facilities to verify their CO_2 capture technologies.

TCM has so far not been able to operate the amine plant with the RFCC flue gas, due to amine emissions above the TCM emission permit. The high emissions are caused by sulfuric acid aerosols and dust particles present in the flue gas, which is a general phenomenon also observed in other amine plants [9]. To provide for testing with RFCC gas in the amine plant, TCM will install a Brownian Diffusion Filter (BD) to control the particle concentration in the RFCC flue gas and allow for testing at varying particle concentrations. In order to reduce risk, different types of BD filters have been tested in a pilot unit at TCM. Initial testing to evaluate the maximum aerosol number concentration acceptable for operation with a solvent based on MEA was also performed. Results from initial testing are reported in this paper. The relation between flue gas particle concentration and emissions of amine and amine degradation products will be further investigated by TCM.

From July to October 2015 TCM DA, in collaboration with partners, operated a test campaign with CHP flue gas using the non-proprietary aqueous monoethanolamine (MEA) solvent at 30 wt%. Two weeks of the campaign was dedicated to MEA aerosol testing with RFCC flue gas mixed with CHP flue gas.

Nomenclature

BD	Brownian Diffusion filter
FGD	Flue gas Desulfurisation
CHP	Combined heat and power plant
RFCC	Residue Fluidized Catalytic Cracker
TCM	CO_2 Technology Centre Mongstad
FTIR	Fourier Transform Infrared Spectroscope
PTR-TOF-MS	Proton Transfer Reaction -Time of Flight-Mass Spectroscope
$ELPI^+$	Electrical Low pressure Impactor
WESP	Wet Electrostatic Precipitator
MEA	Monoethanolamine

2. Amine plant overview

2.1. Flow diagram of the tests.

The amine plant test is performed with mixing of a controlled fraction of RFCC gas into the CHP (Combined Heat and Power) flue gas, while doing measurement of particle concentration in the gas upstream the absorber and continuous MEA emission measurement at the absorber outlet. The CO_2 concentration in the CHP flue gas is adjusted between 3.7% and 12.8% by a recycle of captured CO_2.

The flue gas bypass between RFCC and CHP flue gas is equipped with a flow measurement. The aerosol number concentration and particle size distribution is measured at the absorber inlet with an electrical low pressure impactor (ELPI$^+$, Dekati Ltd.)

The amine and other emissions out of the absorber stack were monitored by the following online analyzers:

- Fourier Transform Infrared Spectroscopy (FTIR), Model: Gasmet FCX
- FTIR, Model: Finetec Anafm 2000
- Proton Transfer Reaction – Time of Flight - Mass Spectrometry (PTR-TOF-MS), Model: PTR-TOF 8000

The analyzer at TCM are described in publication [22]

A Pilot Brownian filter is operated on a side stream of the RFCC flue gas (Figure 1) while doing measurement of particle concentration upstream and downstream the pilot filter with an electrical low pressure impactor (ELPI$^+$, DekatiLtd.).

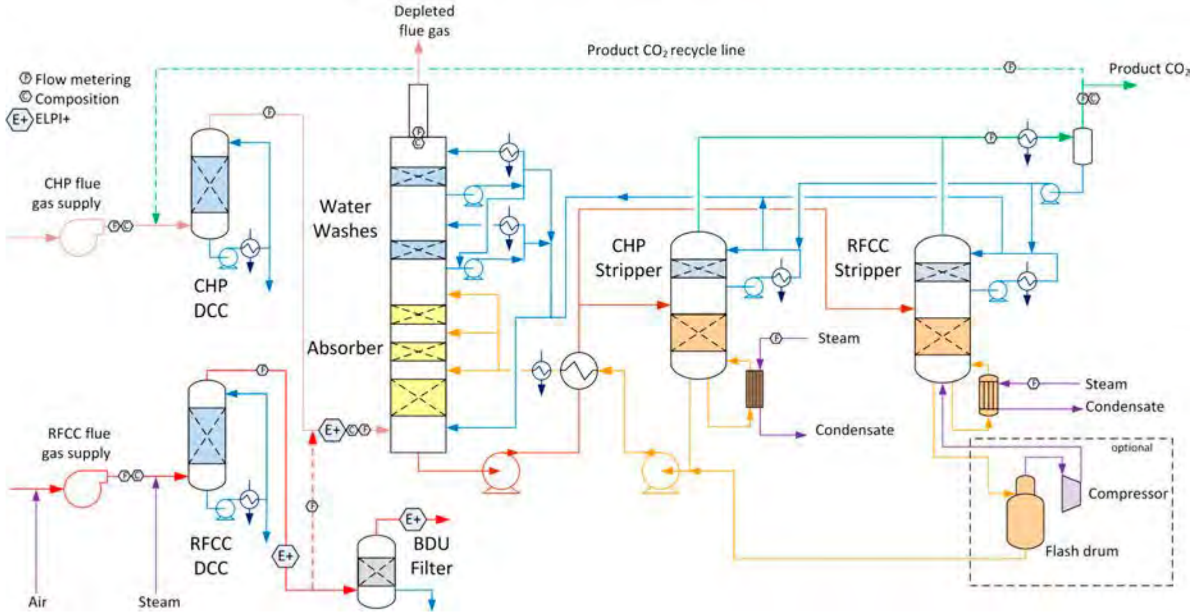

Figure 1. Simplified flow diagram for TCM amine plant prepared for aerosol tests.

2.2. Challenges related to aerosol emission measurements.

Aerosol measurements are more complex than gas composition measurements and require the comparison of multiple technologies in order to validate the results. The limitation and benefits of various systems tested at TCM are discussed:

- Online ELPI$^+$
- Online FTIR
- Online PTR-TOF-MS
- Isokinetic sampling [14]

For aerosols, the variable reliability of the various systems is documented [21].

2.2.1. Online ELPI$^+$

An Electrical Low pressure Impactor (ELPI$^+$) [6, 7, 21] measures the particle size distribution and total number concentration of the particles. As most of the particles above a critical size will grow in the absorber, the measurement of the particles upstream the absorber is a valuable data that may be correlated to the amine emissions at the top of the absorber at various process parameters and various solvents. As the flue gas is at saturation with a relative low water concentration and a relative high concentration in sulfuric acid in the aerosols, the measurement of the ELPI$^+$ is reliable and the influence of the dilution during the measurements is acceptable [7].

In the absorber beds, the water concentration of the flue gas is high and variable with possible supersaturation due to the absorber temperature bulge usually observed during CO_2 absorption. As a dilution of the sample is necessary for ELPI$^+$ measurement, the effect of the sample dilution may be substantial for high water concentrations in the flue gas. The results may be assessed at various dilution factors, but the measurement incertitude's remain significant at high water concentration in the flue gas.

The weight distribution of the particles and the concentration of amines in the droplets are necessary for an estimation of the aerosol growth in the absorber. As the concentration of amines in the aerosols is not available, an ELPI$^+$ is not suitable to estimate the weight of amines in the aerosols based on the calculated weight distribution of the particles.

At the stack of the absorber, ELPI$^+$ size distribution measurements are more reliable due to the lower water concentration in the flue gas. Based on the emission results from the FTIR or isokinetic sampling, the masse of amines in the aerosols may be calculated and compared to the weight distribution from the ELPI$^+$. From this comparison, an average concentration of the amine in the aerosols may be estimated.

In case of high emissions due to amines in aerosols, the measurement period is limited due to the accumulation of aerosols on the filters of the ELPI$^+$.

2.2.2. Online FTIR

A Fourier Transform Infrared Spectroscope (FTIR) does not directly measure aerosols but only gaseous compounds. The vaporization of the aerosols is therefore necessary for the quantification of amine emissions via aerosols.

At TCM the FTIR sample line is 101meter long. The line temperature is controlled and may be adjusted from 120ºC to 160ºC. The sample pump ensures under pressure (-0.4barg) in the sample line. This arrangement secures an adjustable vaporization of the aerosols in accordance to the amine properties.

General limitations of FTIR's:

- If a specific amine is present in both the aerosols and as a gaseous compound in the flue gas, the FTIR cannot distinguish if the emissions are cause by the aerosols or by the gaseous compound. The FTIR results will be limited to the total concentration of the vaporized amine in aerosols and gaseous compound in the flue gas.

- The vaporization of the amine in the aerosols may be highly variable with temperature, amine properties (surface tension), salts and other components that cannot be vaporized from the aerosols. A complete vaporization of the aerosols is usually not feasible.
- If a high temperature is required to vaporize most of the amines in the aerosols, amine decomposition products may be generated in the sample line to the FTIR.
- In case of high emissions, coalescence of aerosols on the sample line walls/bends and accumulation of liquid may occurs. Emissions are underestimated and may be detected after the end of the actual test.

2.2.3. Online PTR-TOF-MS

As a FTIR, the Proton Transfer Reaction Spectroscope does not directly measure aerosols but only gases. The same limitations as FTIR above apply.

2.2.4. Isokinetic sampling

Several procedures are applicable:

- Anderson Cascade Impactor (ACI): tests at TCM are described in a publication [13]. The procedure is complex and comprehensive and requires specific experience by trained operators. Emissions are quantified as mass of aerosols for a particle size distribution. Amine emissions via aerosols are usually not measured.
- Impingers with absorption in liquid: this procedure is described in publication [14]. Tests at TCM confirm that the results for aerosols are not reliable.

General limitations of isokinetic sampling's:

- The results are only known after the test period and as an average of a sampling period during stable operation. The consequences of the adjustment of operation parameters cannot be directly evaluated. The interpretation of the tests results is delayed and a prolonged test period is required.
- As the isokinetic sampling requires a sequence of several manual operations, the accuracy and repeatability may be limited. Several measurements are usually necessary to confirm an average value.

The following operations may affect the accuracy for aerosol measurements:

- Control of isokinetic sampling and sample flow measurement at low and variable velocity in the absorber
- Condensation/vaporization in sampling line/changing atmospheric conditions
- Control of the velocity in the impinger. Aerosols not captured in the impingers
- Transport of samples to laboratory and chemical reactions in transport period
- Analysis of the samples at the laboratory and calculation of the aerosols based on flow measurements and concentrations.

Isokinetic samplings are compulsory for the validation of the online instrumentation at the beginning of each campaign with a new amine solvent, new equipment or unproved process parameters. This validation is critical for the reliability and guarantee of the campaign results and compliance to the emission permit.

3. Purpose of the tests

3.1. Test 1: amine plant emissions

The purpose of the test is to evaluate the maximum aerosol number concentration acceptable for operation with a solvent based on MEA.

The emissions from the absorber with aqueous MEA solvent have been investigated by utilizing the high flexibility of the amine plant at TCM by variation of the following main parameters:

- Sulfuric acid aerosol in the inlet flue gas: number concentration and particle size distribution by mixing small fractions of the RFCC flue gas into the gas turbine flue gas
- CO_2 inlet flue gas concentration by CO_2 product stream recycling
- Lean MEA inlet temperature to the absorber and hence absorber temperature profile
- Water wash cooling temperature

3.2. Test 2: Pilot Brownian filter efficiency

A pilot Brownian filter was previously tested at TCM in collaboration with Aker Solutions [17].

Several types of pilot Brownian filters of 1000Sm^3/h of flue gas are now tested at TCM in order to assess the installation of a future Brownian filter unit capable of treating 35000 Sm^3/h of RFCC flue gas. The purpose of the future unit is to reduce and control the concentration of aerosols in the RFCC flue gas inlet to the amine absorber. This installation will allow TCM to remove almost all aerosols or adjust the aerosol concentration and particle size distribution at various CO_2 concentrations for future tests in order to investigate aspects such as:

- Sensitivity of a specific solvent to the aerosols
- Aerosol emissions due to degradation products
- Understanding of aerosol mechanism for various advanced solvents
- Recommendations for future flue gas treatment, amine absorber equipment and operation parameters.
- Assessment of the required flue gas treatment required for a specific coal power plant with a known range of aerosols, oxygen and CO_2 concentration.

The pilot is installed in order to check the efficiency of a Brownian filter based on the number particles and particle size distribution. The Brownian filter efficiency is usually reported by the mass of aerosols captured in the filter. This method is relevant for reporting sulfuric acid emissions, but is not sufficient to evaluate low concentration of aerosols downstream the filter and the consequences of aerosol growth in the absorber.

A Brownian filter is suitable for test purposes of the amine absorber at TCM for the RFCC flue gas:

- A high discharge pressure is available with the existing fan
- The concentration of particles/fly ashes is limited at TCM
- High concentrations of aerosols can be controlled by bypass of the Brownian filter

4. Results of the tests and parameters

4.1. Results of the amine emission tests

In this section, main results from MEA aerosol testing are summarized. The operating conditions for each sequence of test are described in the following paragraphs. The conditions are chosen close to the optimum operation conditions for an amine absorber with MEA as described in TCM DA publications [15, 16].

TCM DA received a temporary emission permit from the Norwegian Environmental Agency in order to conduct the given tests. The temporary permit allowed an increase of the MEA emissions from the current 6 ppmv to 500 ppmv for maximum 4 days of testing with RFCC flue gas. The limit of amine emission was not exceeded during the tests.

4.1.1. Properties of the CHP flue gas mixed with a fraction of RFCC flue gas

The particle size distribution of the aerosols is quite similar when different fractions of RFCC gas are mixed into the CHP as seen on Figure 2. The total number concentration is roughly proportional to the mixing ratio, but at lower RFCC flue gas flow, the number concentration of larger particles decreases due to the piping arrangement at the connection between the main RFCC duct and the bypass line to the CHP flue gas. At high velocity in the main RFCC duct and lower velocity in the bypass pipe, large particles remain in the main RFCC duct.

Typical Flue gas composition is given in Table 1.

Table 1. Typical Composition of the CHP flue gas with CO_2 recycle mixed with a fraction of RFCC flue gas.

Main components	Units	CHP +380m^3/h RFCC	CHP + 1100m^3/h RFCC
CO_2	mol%	3.6 to 13.6	3.6 to 13.6
O_2	mol%	13 to 13.8	13 to 13.8
H_2O (saturation at 30ºC)	mol%	4.2	4.2
N_2 & Argon	mol%	>65	>65
SO_2	ppmv	0.4	1.2
NOx	ppmv	<3	<9
Fly Ashes	mg/Sm^3	<0.02	<0.05
H_2SO_4 aerosols and ammonium sulfate salts	mg/Sm^3	<0.3	<0.9
Particle number concentration	Part./cm^3	0.25 million	0.9 million
Mass of aerosols guesstimate calculated with size distribution and spherical particles at water density.	mg/Sm^3	0.5	2.1

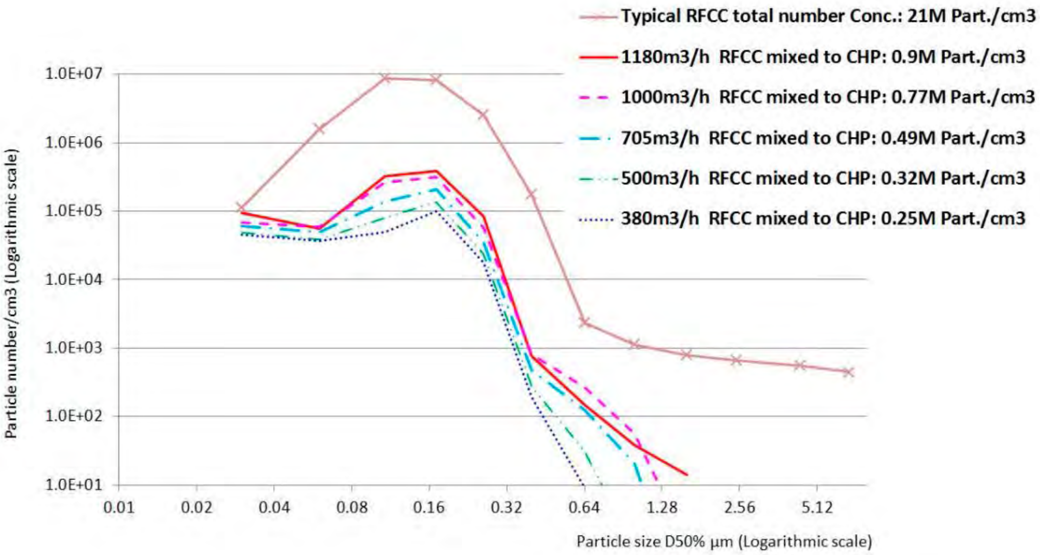

Figure 2. ELPI$^+$ measurements. Size distribution of the aerosols in the mixed RFCC flue gas flow ratios into 30 000 Sm^3/ of CHP

4.1.2. Correlation between particle concentration and MEA emissions

The correlation between particle concentration and MEA emissions was studied at three different CO_2 concentrations (3.7 %, 8% and 12.7% CO_2). At each concentration the effect of different particle concentrations was investigated by varying the mixing fraction of RFCC gas into the CHP gas. The lean amine temperature into the absorber was adjusted to keep the temperature difference between the maximum absorber bulge and the lean amine entering the absorber almost the same independent of CO_2 concentration. All test runs were performed at an absorber packing height of 18m. The upper 6 m of packing was not loaded with solvent. The parameter settings for each test are included in Table 2. Results of the correlation between particle concentration and MEA emissions are plotted in Figure 3.

At 3.7% CO_2 (no CO_2-recycling) and the process conditions given in Table 2, there is a linear correlation between particle concentration in the absorber inlet gas and MEA emissions as seen in Figure 3a (upper left). At particle concentrations <100 000 particles/cm^3, no MEA emissions was measured. The emission of MEA is below 3 ppmv at 150 000 particles/cm^3. When the concentration increases above 250 000 particles/cm^3, the regular discharge permit of 6 ppmv is exceeded.

The next test was conducted with CO_2-recycling to around 8 vol % CO_2 in the gas upstream the absorber. Results are plotted in Figure 3b (upper right). The MEA emissions correlates to the particle concentration and it is still linear up to around 500 000 particles/cm^3, then a nonlinear correlation is observed with higher emissions. However, at these process conditions the emission of MEA was still below 3 ppmv at around 500 000 particles/cm^3, indicating a higher tolerance to aerosols in the gas at 8% CO_2 compared to 3.7% CO_2. At close to 1 mill particles/cm^3 emission above 6 ppmv was observed.

Table 2. Parameter settings for testing effect of particle concentration in flue gas on MEA emissions.

Main components	Units	Test Conditions		
		a) 3.7% CO_2	b) 8.0% CO_2	c) 12.7% CO_2
Flue gas flow	Sm^3/h	30 000	30 000	30 000
Flue gas temperature	°C	27	27	27
CO_2 concentration, absorber inlet	mol%	3.7	8.0	12.7
CO_2 concentration, absorber outlet	mol%	0.6	1.3	2.3
CO_2 capture	%	79	74	76
Lean amine flow	kg/h	30 300	61 800	91 000
Lean amine temperature	°C	37	55	62
Max absorber bulge temperature	°C	52	66	75
ΔT(max absorber bulge-lean amine)	°C	15	11	13
Lean loading	mole CO_2/mole amine	0.21	0.21	0.22
Lower water wash temperature	°C	43	45	50
Temperature of gas out of absorber	°C	30	42	52

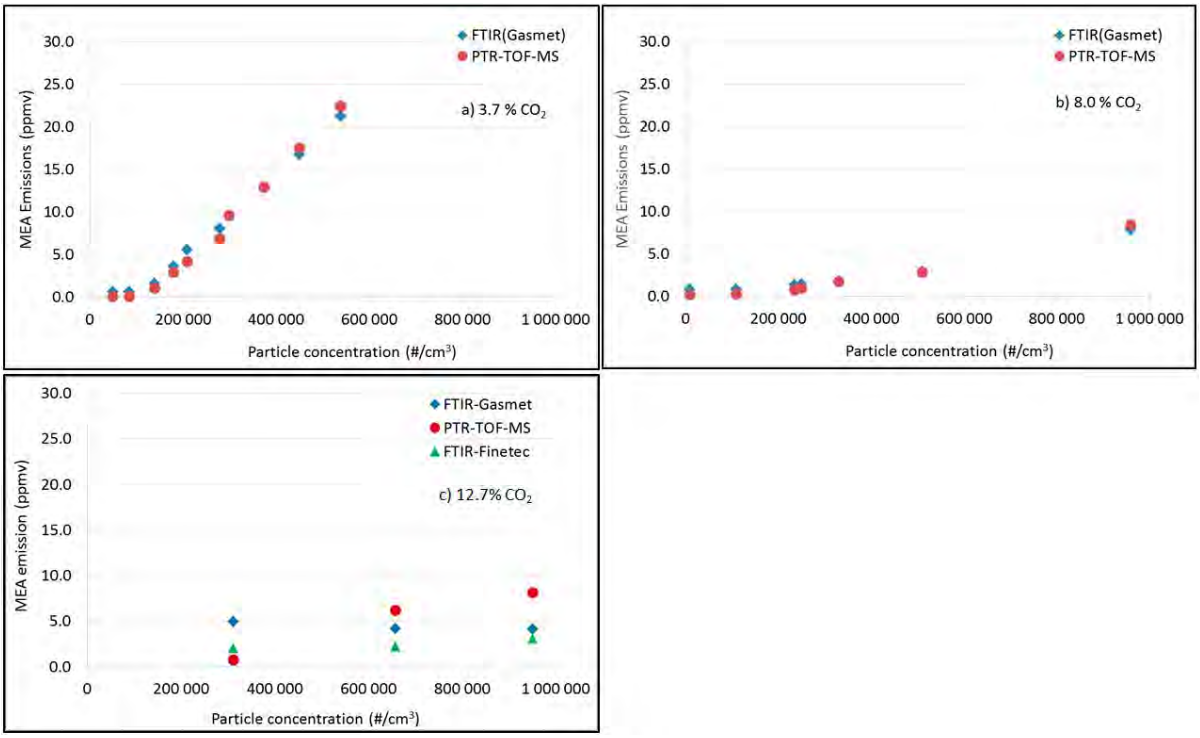

Figure 3. Correlation between particle concentration and MEA emissions at three different CO_2 concentrations. a) Upper left: Normal CHP absorber conditions with 3.7% CO_2. b) Upper right: CHP with CO_2-recycle to 8.0% CO_2. c) Lower left: CHP with maximum CO_2 recycle to 12.7% CO_2.

The CO_2-recycling was then increased to 12.7% CO_2, resulting in higher temperatures in the absorber due to more reactions taking place. Testing of the effect of particle concentrations in the flue gas on MEA emissions was conducted. Results are plotted in the Figure 3c lower left. As can be seen from the figure, there are more scattering in the data during this test. This is probably caused by analytical challenges due to the high temperature and water content of the gas leaving the absorber (refer to section 2.2). The effect of particle concentration on emission is comparable to what was observed at 8%, but again much less than at lower CO_2 concentration. At these conditions, the emission of MEA is below the 6 ppm limit at 600 000 particles/cm^3, and above 6 ppm at 1 mill particles/cm^3 in the absorber inlet gas, if the PTR-TOF-MS instrument is most trusted.

4.1.3. Effect of cooling the gas at the top of the absorber on MEA emissions

For each CO_2 concentration, the effect of increased cooling of the gas at the top of the absorber on the MEA emissions was investigated at a constant particle concentration in the gas. Cooling was done either by reducing the temperature of the lean solvent entering the absorber or by reducing the temperature in the lower water wash section. The effect of the lean amine temperature is shown in Figure 4. The effect of moving the cooling up to the lower water wash section was tested for the 8% CO_2 case only. Results are shown in Figure 5.

The particle concentration in the gas was kept constant at 540 000 particles/cm^3 for testing at 3.7% CO_2 and at 950 000 particles/sm^3 for testing at 8.0 and 12.7% CO_2. In each case, the lean amine temperature was changed step-vise to investigate impact on MEA emissions. The lower water wash temperature was kept constant at 30°C for the 3.7% CO_2 case and at 45°C for the cases with higher CO_2 concentrations. The other parameters were kept at the same levels as given in Table 2 above. However, the difference between the maximum absorber bulge temperature and the lean amine temperature increased as the lean amine temperature was step-vise reduced.

As can be seen in Figure 4, the MEA emissions increases when the temperature of the lean amine is reduced for tests with 3.7% CO_2 and 8% CO_2. For the 12.7% CO_2 case, there are more scattering in the data but no significant effect of reducing the lean amine temperature on MEA emissions was seen in the temperature window explored. However, at the end of the test when the lean amine temperature was further decreased to 30°C, a significant plume was observed and the on-line analyzers indicated MEA emissions above 20-30 ppmv.

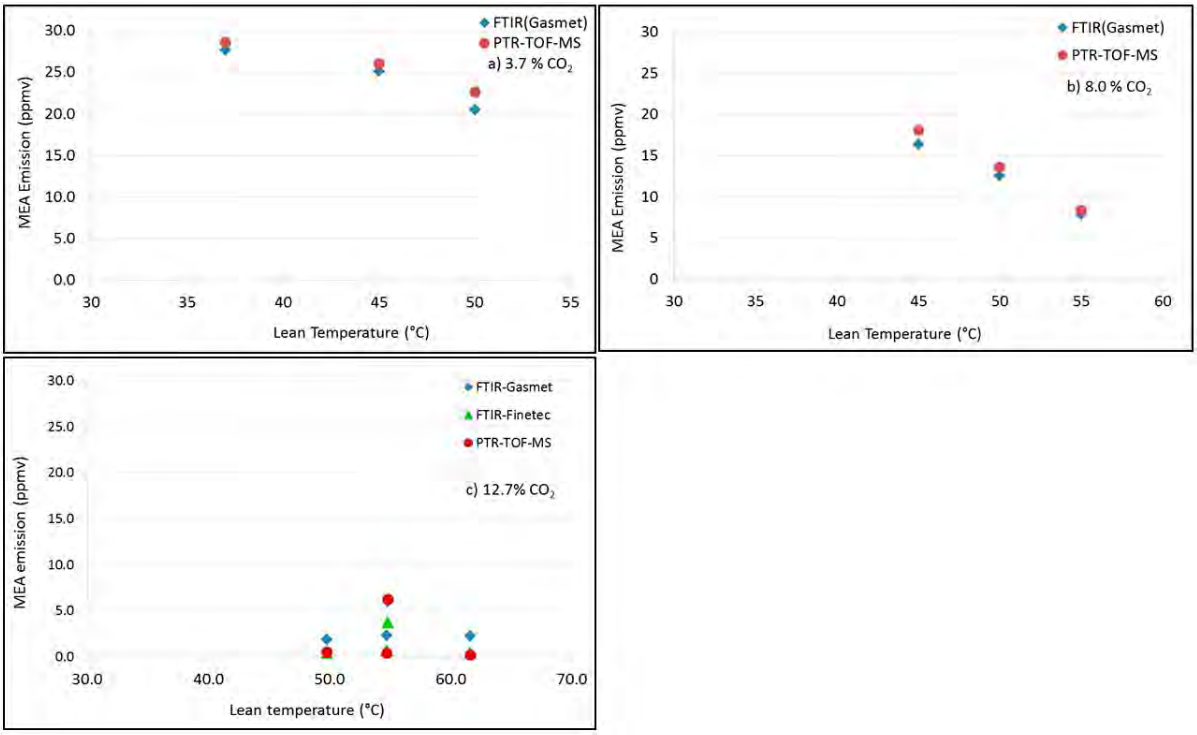

Figure 4 Effect of lean amine temperature on MEA emissions. a) Upper left: At 3.7% CO_2 and 540 000 particles/cm^3. b) Upper right: At 8.0% CO_2 and 950 000 particles/cm^3. c) Lower left: At 12.7% CO_2 and 950 000 particles/cm^3.

The effect of decreasing the temperature in the lower water wash on MEA emissions was then examined for the 8% CO_2 case at the same concentration of 950 000 particles/cm^3 in the gas. The lean amine temperature was set to 55°C, which is 11°C below the maximum absorber bulge temperature, resulting in a temperature of the gas into the lower water wash section of 60°C. The water wash section was operated at 45° and 35°C, respectively and MEA emissions were measured. Results are shown in Figure 5. There is a tendency of increased MEA emissions when the temperature of the water was reduced, however the effect is not as pronounced as when reducing the lean amine temperature (Figure 4b).

The effects of particle concentration, CO_2 concentration and temperatures in the absorber and water wash system on MEA emissions will be further investigated by TCM.

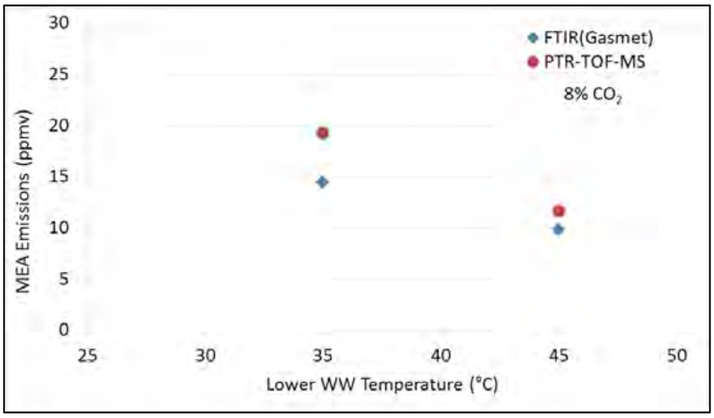

Figure 5 Effect of the temperature in the lower water wash on MEA emissions for case with 8% CO_2 and 950 000 particles/cm^3.

4.2. Results of the filter tests

4.2.1. Brownian diffusion filter description

In a fiber filter, particles may be captured by three collection mechanisms:

- Brownian diffusion: the smaller particles get random motion by collision with surrounding gas molecules. Higher random motion and longer residence time facilitates the capture of the particle to a fiber. Velocities between 5 and 10cm/s are necessary for high efficiency. Maximum velocity is 25cm/s.
- Interception: particles with higher momentum do not follow the gas stream around a fiber and are captured to the fiber by interception. Efficiency increases with the gas and particle velocity. Once a particle touches the surface of the collecting target, it adheres by weak Van Der Waals forces. Velocities between 0.2 and 1m/s are necessary for high efficiency.
- Direct impaction: The particle is intercepted from the gas stream if there is not enough space between two fibers or if the particle touches a fiber as it passes closed enough. Efficiency increases with the particle diameter and is constant for a velocity above 1m/s.

In a Brownian diffusion filter the main particle capture is achieved by the first collection mechanism.

A typical candle filter is illustrated in Figure 6. Small droplets will coalesce together in larger droplets until the collected liquid trends to flow in the same direction as the gas and fibers and drains out of the fiber bed by gravity to the bottom of the candle filter. A typical industrial candle is 600mm diameter and 3.6m height with a candle thickness between 50mm and 100mm. For practical application, the number of candle is increased until the required area and gas velocity are achieved.

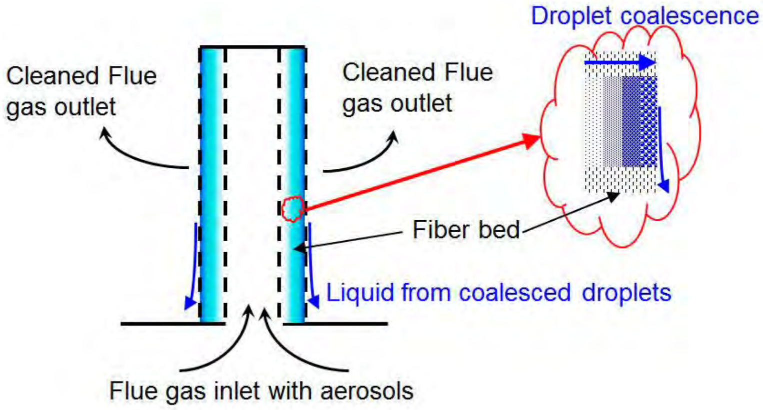

Figure 6. Typical Candle Filter

4.2.2. Flue gas Composition and aerosols upstream and downstream the Brownian filter

The efficiency of any flue gas treatment upstream an amine absorber cannot be evaluated by a single parameter, as for example, the "equivalent SO_3" concentration in the flue gas. The total number concentration, the size distribution of the aerosols and the composition of aerosols are the main critical parameters. For similar gas composition from various coal power plants, the aerosol properties may be highly variable from plant to plant and during the life time of each power plant.

Aerosols in the RFCC flue gas are mainly aqueous particles with some sulfuric acid, salts, catalyst particles and fly ashes. Scanning electron microscope analyses (SEM) performed at TCM confirms that fly ash concentration is low and has a similar composition as a typical flue gas from a coal power plant. At TCM, fly ashes are mainly found in aerosols in the range of 1µm diameter. The typical composition of the RFCC flue gas is defined in Table 3.

Table 3. Typical Composition of the RFCC flue gas upstream and downstream the BD filter.

Main components	Units	RFCC upstream BD filter	RFCC downstream BD filter at 7cm/s velocity
CO_2	mol%	14	14
O_2	mol%	3.2	3.2
H_2O (saturation at 30ºC)	mol%	4.2	4.2
N_2 & Argon	mol%	>78	>78
SO_2	ppmv	5	5
NO_x	ppmv	60	60
Fly Ashes	mg/Sm^3	0.5 to 2	0
H_2SO_4 as aerosols	mg/Sm^3	10 to 25	<0.3
Ammonium sulfate & soluble salts	mg/Sm^3	5 to 15	<0.2
Particle number concentration	$Part./cm^3$	15 to 25 million	0.35 million
Mass of aerosols guesstimate calculated with size distribution and spherical particles at water density.	mg/Sm3	180	4

As shown in Figure 7 the particle size distribution of the RFCC flue gas at TCM is close to coal power plant flue gases [19, 20].

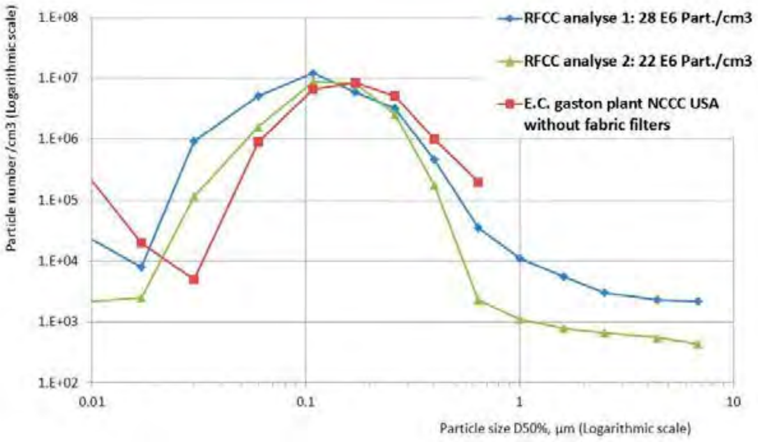

Figure 7. Comparison of RFCC flue gas and flue gas from a coal power plant

4.2.3. Overall efficiency

The overall efficiency of the Brownian diffusion filters tested at TCM is higher than 98% based on the particle number concentration. This efficiency is checked at TCM for several types of Brownian filters. The efficiency of a Brownian diffusion filter is variable with the particle size. Figure 8 illustrates that a lower velocity increases efficiency for smaller particle size. Higher velocity increases efficiency for larger particle size. This is in accordance with the three collection mechanisms of the filter candles:

- Brownian diffusion: requires high residence time/low velocities; high efficiencies for smaller particles (<0.1µm)
- Interception: requires higher velocities
- Impaction: high efficiency for larger particles (>0.5µm)

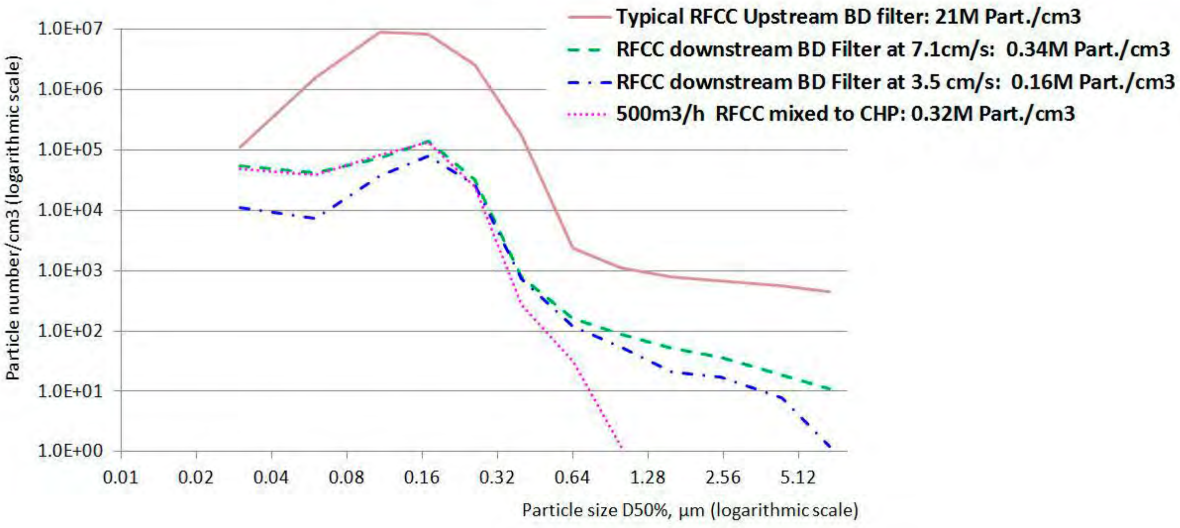

Figure 8. Size distribution upstream and downstream the BD filter and comparison with CHP mixed with RFCC flue gas

As illustrated in Figure 8 , the particle size distribution of the following flue gases is similar:

- CHP flue gas mixed with a fraction of RFCC flue gas
- RFCC flue gas after a Brownian diffusion filter

Above 0.5µm, the number of particles is negligible (<100particles/cm^3)

As illustrated in Figure 9, the efficiency of the various filters is variable. Some Brownian filters may reduce the number particles to less than the detection limit of the ELPI$^+$ (approximately 10 000 particles/cm^3). The main differences between the types of Brownian diffusion filter are the filter density, fiber diameter and fibers weave. Generally, more fibers and higher pressure drop will result in higher efficiency. Specific fibers weave and layers reduce pressure drop.

At the first start up the filter bed is dry and requires to be saturated with liquid from the aerosols. The pressure drop increases slightly during this period. After saturation, the pressure drop of Brownian diffusion filters is essentially proportional to the flue gas flow rate and velocity to the candle filters, due to the laminar flow inside the filter bed.

During 3 months of operation, the pressure drop of the test pilots at TCM was constant and no increase due to fly ashes or accumulation of solid particles in the filter bed was noticed.

The typical pressure drop is around 25mbar at an average velocity of 7cm/s based on the average of the inlet and outlet surface of the candle filters. The optimized velocity is specific to each type of candle filter/vendor and required efficiency.

As an example, for the candle filter from the Figure 9:

- Up from 3.5 to 7cm/s the efficiency decreases slightly, but the filter area required at 3,5cm/s is the double than at 7cm/s. The cost of the filter is almost proportional to the area required.
- From 7 to 10cm/s, the captured particles and efficiency are constant but pressure drop increases with the velocity.

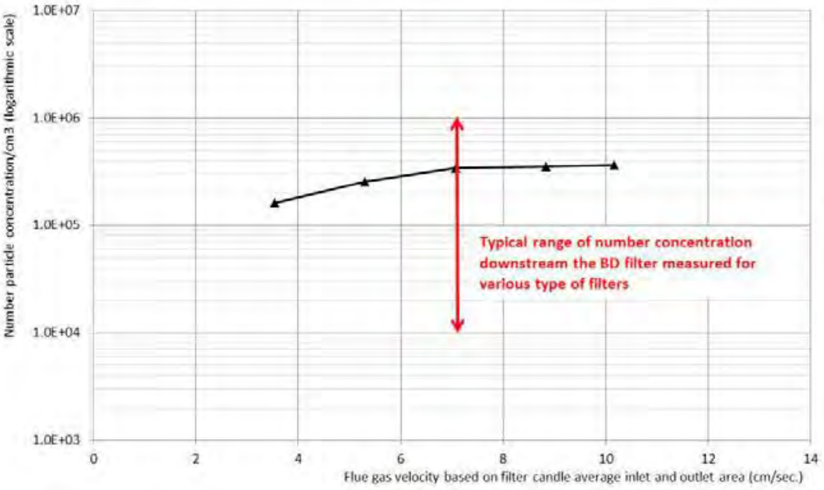

Figure 9. Typical particle total Number Concentration downstream the pilot BD Filter

The Brownian filter tests at TCM confirm that a suitable efficiency is achieved for the RFCC flue gas and testing with RFCC flue gas may be performed at TCM within the present emission permit.

The installation of Brownian filters may be applicable to specific refinery flue gases if the fly ash concentration is limited.

5. Aerosol emissions: discussions and interpretation of the results

5.1. Kelvin effect and literature

When an interface gas/liquid is flat, the condensation of gas to the liquid is generally given by the equilibrium concentration of vapor pressure at given temperature and pressure. The kelvin effect expresses that the vapor pressure over a curved interface is always higher for the same component than over a flat interface. The kelvin equation gives the critical particle size or minimum particle diameter of a liquid [2, 4, 18]:

d* is a function of the particles, gas composition and properties.

$$d^* = \frac{4\sigma M}{\rho RT \ln\left(p / po\right)} \tag{1}$$

Where:
d* = Particle diameter [m]
σ = Surface tension of liquid drop [N/m]
M = Average molecular weight of the condensable liquid [kg/Kmol.]
ρ = Liquid density [kg/m^3]
T = Temperature [ºK]
R = Universal gas constant [J/Kmol./ºK]
p = Sum of the partial pressures of all condensable components in the mixture [Pa]
p_0 = Corresponding sum of partial pressure when saturated (equilibrium conditions) [Pa]
The saturation of the gas mixture is $S = p/p_0$. The gas phase is supersaturated if $S > 1$

The kelvin equation indicates that:

- Very small droplets (for example < 0.1µm) are stable, and a large supersaturation is necessary for formation of new droplets or growth of existing droplets.
- Between 0.1µm and 1µm, aerosol growth may occur with supersaturation of water or amine vapor.
- Above 1µm, supersaturation is not necessary. These relatively large droplets may be considered as a flat surface. Aerosol growth may occur at once saturation is achieved.

5.2. Assumed aerosol mechanism

The challenge for amine absorbers is the evaluation of the chemical processes in the critical section where the flue gas that has been heated by chemical reactions, is cooled by the incoming lean amine (section 2 in Figure 11). The chemistry of the amine in the aerosols is similar to the lean solvent film of the packing, but the consequences of the variable aerosol diameter are new parameters. The experience acquired at TCM with MEA and various advanced solvents suggests that the chemical process in the aerosols is a major parameter. Similar aerosol mechanisms are described in multiple recent publications [1, 2, 3].

Figure 10 illustrates the assumed mechanisms for aerosols chemistry:

- Phase 1: Aerosol growth by water and eventual homogeneous nucleation in case of high supersaturation. The aerosol growth by water from gas phase is dependent of the supersaturation. The diameter of the aerosol increases in a short time, likely lower than 0.5second [18].
- Phase 2: Aerosol growth by amine. Due to the kelvin effect, the aerosol growth by amine from gas phase is dependent of the supersaturation and begins at once for large particles or as soon as a critical diameter is achieved (probably from 0.2µm to 1µm for MEA). The aerosol growth by amine may be continuous until equilibrium and saturation of amine in the aerosols.

- Phase 3: Large aerosols are considered as flat surfaces. Free amine with high activity like MEA captures CO_2 in the aerosols. Reaction kinetics is critical due to the short residence time.
- Phase 4: Due to the formation of salts, additional free amine is absorbed in the larger aerosols

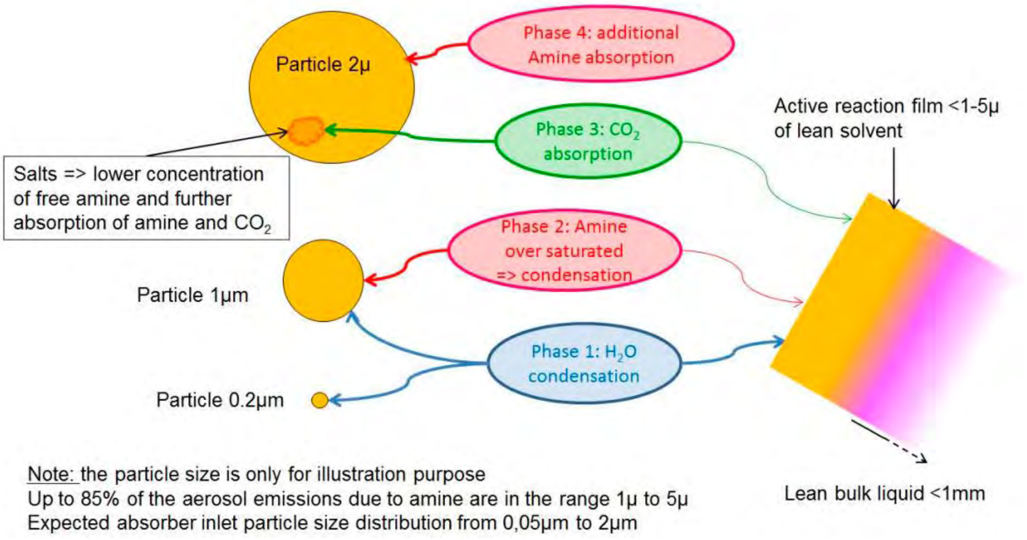

Figure 10. Description of assumed aerosol mechanisms

The major parameters for aerosol mechanisms are:

- The initial size of the aerosol and the growth rate with water is a major parameter. For example, a flue gas with large number of aerosols between 0.3µm and 1µm may cause high emissions.
- The difference of temperature between the lean and the flue gas is the main cause of the supersaturation of the components in the gas phase. The supersaturation of a component is not necessary related to the concentration of the component in gas phase. Without supersaturation, even with high concentration of amines (>1000ppmv) aerosols may not cause emissions. With supersaturation, even at low concentrations (<5ppmv), special amines may produce emissions. For advanced amines, decomposition products can typically be the cause of substantial aerosol emissions.
- The effect of lean solvent loading is probably significant but is not yet evaluated at TCM.
- Additional components in the aerosols may modify the chemistry and reaction kinetics: H_2SO_4, salts, fly ashes/catalyzer particles [10]

5.3. Amine absorber profile and main mechanism with MEA

As many parameters with opposite effects will modify the supersaturation in the amine absorber, the behavior of aerosols is complex. In order to illustrate the mechanisms in an amine absorber, the typical temperature profile of the amine absorber at TCM is described in Figure 11 and the main operation parameters are listed in Table 4.

Table 4. Operation condition of the absorber.

Main components	Units	CHP +1000m^3/h RFCC
Inlet flue gas CO_2	Mol %	12.8
Inlet flue gas flow	Sm^3/h	30 000
Particle number concentration	Part./cm^3	0.95 million
Lean solvent to the absorber	kg/h	91 000
Lean loading	mole CO_2/mole MEA	0.22
Lean solvent inlet temperature	ºC	50
CO_2 concentration in the flue gas outlet of the absorber	Mol %	2.3
CO_2 capture	%	80
Emissions due to MEA in aerosols	ppmv	3

The absorber upper packing for CO_2 absorption is not operated and the lean solvent feed is located above the middle packing of 6m height. The lower packing height is 12m. Temperature measurements are located every meter of the packing at four horizontal locations. This arrangement allows a suitable validation of the simulation models.

The aerosol mechanisms are specific in each of the following sections of the absorber:

- Section 1: In the packing under the bulge, 5000kg/h of CO_2 is absorbed and temperature increases in the lean solvent. The lean solvent heats the flue gas. Flue gas temperature is lower than the liquid solvent (7ºC to 1ºC). Up to 7000kg/h of water and 30kg/h of MEA are vaporized from the liquid. The larger aerosol droplets may also vaporize some water. Some limited mass of MEA may be absorbed in large aerosols (>1 µm) if saturation is achieved locally (cold walls, flue gas distribution, defective solvent distribution in the packing). It is expected that most of the aerosol composition remains unchanged.
- Section 2: starts from just below the maximum temperature in the absorber (bulge temperature) and finished at the elevation corresponding to a stable flue gas temperature. Below the lean solvent distributor, the relative cold solvent cools down the flue gas. Up to 2500kg/h of water and some solvent previously vaporized are condensed again in the liquid solvent. Due to sudden cooling, the concentration of condensable components in the gas phase exceeds the corresponding concentration in vapor–liquid equilibrium (VLE). The gas phase is supersaturated with high MEA concentration in gas phase. This section is critical, in a short residence time; the water particles diameter will increase with water and become saturated with amines. The chemistry in the droplets will be critical for the growth of the aerosols with amines. Above the lean feed, the temperature decreases until equilibrium conditions are achieved. The effect of the equilibrium condition is not yet evaluated in the tests, but may be critical for emissions.
- Section 3: Most of the remaining amines in vapor phase are absorbed in the lower water wash. Some water previously vaporized is condensed. Sudden cooling shall be avoided otherwise, the same mechanism as Section 2 occurs.
- Section 4: The last traces of amines in vapor phase are absorbed in the upper water wash. The remaining water previously vaporized is condensed. Sudden cooling is applied in order to keep the water balance of the plant. The aerosol diameter will increase with water but without additional amine capture.
- Stack: Most of the amine captured by aerosols in section 2 and eventually in section 3 will be emitted at the stack of the absorber. The typical efficiency of demisters and packing is poor or insignificant for such aerosols.

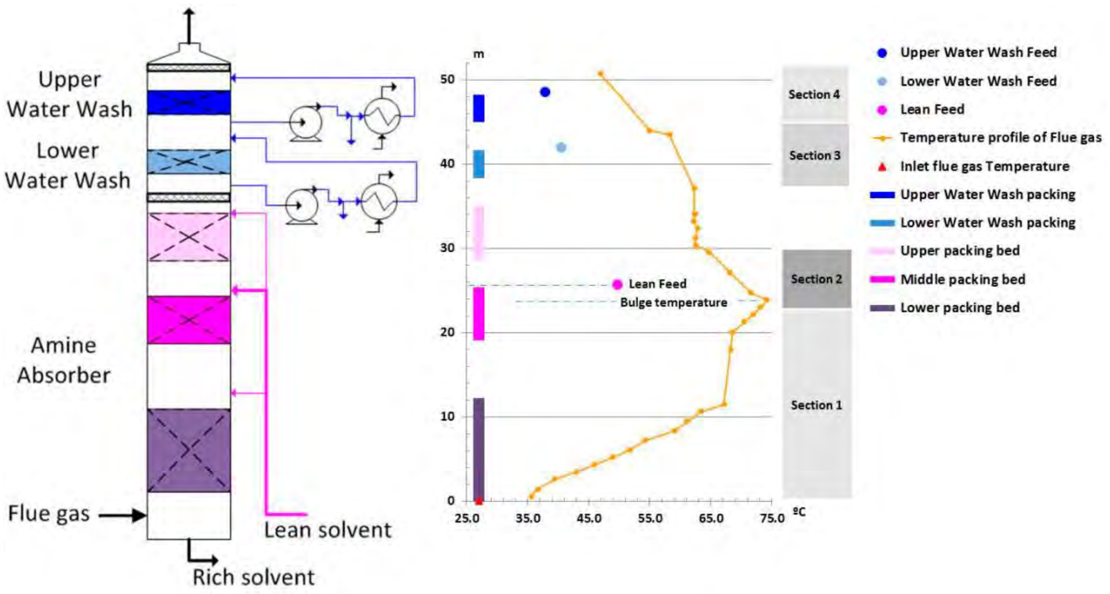

Figure 11. Temperature profile of the absorber at 12.8% CO_2 inlet

The results from testing show that the emissions of MEA increases as the particle concentration in the flue gas increases. This indicates that the extent of aerosol based emissions depends strongly on the number concentration of particles in the flue gas.

With the same particle concentration, the aerosol mechanisms are likely different for the cases at 3.7% CO_2 and 12.7% CO_2, see Table 2, test conditions a) and c):

- At 3.7% CO_2 the typical MEA concentration in the gas phase in the bulge area is 20 to 30 ppmv. The emissions due to aerosols are also 20 to 30 ppmv. It is likely that most of the MEA in gas phase is condensed in aerosols in section 2. Both homogeneous nucleation of MEA and a substantial condensation on aerosols may be considered.
- At 12.7% CO_2 the typical MEA concentration in the gas phase in the bulge area is 300 to 500 ppmv. The emissions due to aerosols are limited to less than 5 ppmv. The particle growth by water and MEA condensation are likely limited by the gradual temperature decrease above the bulge temperature.

Minor variations in dominant process parameters may increase or decrease aerosol emissions as several competitive mechanisms are involved. As illustrated in Figure 3, MEA emissions are lower at 8% CO2 and 12% in the flue gas than compared to the test at 3.7% CO2 concentration. This trend is dissimilar to published results obtained at slightly different process parameters [1, 2, 5, 12]. The higher emissions at low CO2 concentration were thus not expected. The following hypotheses are possible, but are not yet confirmed since advanced simulations are not available:

- The chemistry in the lean solvent solution may contribute to less amine condensed on the aerosols: at higher CO_2 concentration, kinetics and driving forces in the top of the absorber increases. Amine condensing from the vapor phase to the liquid lean reacts faster with CO_2, supersaturation decreases.
- The chemistry in the aerosol may also generate a decrease of emissions: at higher CO_2 concentrations, the solubility of CO_2 decreases with the higher flue gas temperature and less CO_2 is absorbed in the aerosols. The droplets are saturated in free amine and no more amines are absorbed.

6. Conclusions and recommendations

6.1. Conclusion of the tests at TCM

As described in this work, an appropriate description and composition of the flue gas is necessary to assess the risks of emissions associated to aerosols. The description should include gas components, aerosol size distribution and number concentration, and composition of the trace components in the aerosols, measured at the expected pressure and temperature of the flue gas at the inlet of the absorber.

Testing was conducted in the TCM amine plant to evaluate the maximum aerosol number concentration in the flue gas, acceptable for operation with MEA within TCM DA's emission permit. When operating the plant with flue gas from the natural gas fired power plant, no aerosol emission occurs. As a fraction of the flue gas from the residual fluidized catalytic cracker (RFCC) was added, the MEA emissions increased significantly. A strong correlation between particle concentration in the flue gas and MEA emission was found. The effect was more pronounced when the CO_2 concentration in the gas was reduced. The control of the lean amine temperature and the water wash temperature are effective measures to reduce the emissions. With the particle size distribution tested at TCM, a concentration of 500 000 particles/cm^3 is acceptable for operation of the RFCC flue gas. A Brownian Diffusion (BD) filter will be installed to reduce the particle concentration below this level and by-pass possibilities will enable for future testing at a large range of particle concentrations. Pilot testing at TCM has demonstrated high efficiency for BD filters with the RFCC flue gas.

6.2. Recommendation for future CO_2 capture plant based on MEA or advanced solvents

6.2.1. Operation parameters of CO_2 capture plants

As demonstrated in the test at TCM, in case of aerosols in the flue gas, the lean temperature and the water wash temperature requires to be optimized. The eventual energy penalty and mitigation design will be assessed in future works at TCM.

The effect of other operation parameters as CO_2 concentration, CO_2 capture rate or lean loading cannot be predicted by simple assessments. The validation of a simulation tool for aerosols specific to each solvent is essential for the extrapolation of the tests results from a pilot to a full-scale plant.

Tests results at TCM may be a basis for future works in order to validate simulations tools and confirm the major mechanisms of aerosol growth.

6.2.2. Process equipment for aerosol mitigation upstream the amine absorber

As illustrated for MEA in this work, the sensitivity of a specific solvent at various aerosol concentrations may be assessed. Based on sensitivity studies for a specific solvent, the works at TCM may contribute to specify the requirements downstream the flue gas treatments in order to minimize the risk of emissions. Typical flue gas treatments are as for example:

- Wet Electrostatic Precipitator (WESP) [8, 11]
- Flue gas desulfurization (FGD) [11]
- Bag house filter [19, 20]

6.2.3. Process equipment for aerosol mitigation in the amine absorber

The test results from the Brownian diffusion filters confirm a large variability of pressure drop an efficiency of the various fibers and the opportunity to improve the technology is confirmed. Future works are recommended in order to evaluate the pressure drop and efficiency of impaction candles and high efficiency demisters with coalescer materials and flushing systems. As these equipment's are specifically designed to remove particles between 1 and

5µm, they may reduce a large fraction of the aerosol emissions at a relatively low price. Such equipment's are currently not demonstrated in amine absorbers.

Future works at TCM will include specific high efficiency demisters.

6.2.4. Process equipment for aerosol measurements in the amine absorber

The works at TCM confirm the need for reliable measurements of emission due to aerosols. Based on the experience of the tests, the combination of the following measurements is recommended:

- Isokinetic sampling for the validation of the online instrumentation for aerosols.
- Sampling line to online instrumentation with temperature control suitable for an acceptable vaporization of the aerosols.
- FTIR for online measurements of amine from vaporized aerosols

An isokinetic sampling procedure based on a train of impinger jet was recently developed at TCM based on the experiences of the MEA campaign and further tests with advanced amines. This specific system is able to quantify both the vapor and aerosol emissions with reliable accuracy. Future test shall confirm the advantages of the specific procedure.

Acknowledgements

The authors gratefully acknowledge the staff of TCM DA, Gassnova, Statoil, Shell and Sasol for their contribution and work at the TCM DA facility. The authors also gratefully acknowledge Gassnova, Statoil, Shell, and Sasol as the owners of TCM DA for their financial support and contributions.

References

[1] Purvil Khakharia, Leonie Brachert, Jan Mertens, Christopher Anderlohr ,Arjen Huizinga, Eva Sanchez Fernandez, Bernd Schallert, Karlheinz Schaber,Thijs J.H. Vlugt, Earl Goetheer. Understanding aerosol based emissions in a Post Combustion CO_2 Capture process: Parameter testing and mechanisms. International Journal of Greenhouse Gas Control 34 (2015) 63–74.

[2] Purvil Khakhariaa, Jan Mertens, Thijs J.H. Vlugt, Earl Goetheer. Predicting Aerosol Based Emissions in a Post Combustion CO_2 Capture Process Using an Aspen Plus Model. Energy Procedia 63 (2014) 911 – 925.

[3] Hammad Majeed, Hanna Knuutila, Magne Hillestada Hallvard F. Svendsen. Characterization and Modelling of Aerosol Droplet in Absorption Columns. Ieaghg, 3rd Post Combustion Capture Conference (PCCC3)

[4] Steven M. Fulk, Gary T. Rochelle. Modeling aerosols in amine-based CO_2 capture. GHGT-11. Energy Procedia 37 (2013) 1706 – 1719

[5] Purvil Khakharia, Leonie Brachert, Jan Mertens, Arjen Huizinga, Bernd Schallert ,Karlheinz Schaber, Thijs J.H. Vlugt, Earl Goetheer. Investigation of aerosol based emission of MEA due to sulphuric acid aerosol and soot in a Post Combustion CO_2Capture process. International Journal of Greenhouse Gas Control 19 (2013) 138–144

[6] Jan Mertens; Leonie Brachert, Dominique Desagher, Bernd Schallert, Purvil Khakharia, Earl Goetheer. Predicting amine mist formation based on aerosol number concentration and size measurements in flue gas. Energy Procedia 63 (2014) 893 – 901.

[7] L. Brachert, J.Mertens, P.Khakharia, K.Schaber. The challenge of measuring sulphuric acid aerosols: Number concentration and size evaluation using a condensation particle counter(CPC) and an electrical low pressure impactor ($ELPI^+$). Journal of Aerosol Science 67 (2014) 21–27.

[8] Jan Mertens, C. Anderlohr, P. Rogiers, L. Brachert, P. Khakharia, E. Goetheer, K. Schaber. A wet electrostatic precipitator (WESP) as countermeasure to mist formation in amine based carbon capture. International Journal of Greenhouse Gas Control 31 (2014) 175–181.

[9] Takashi Kamijo, Yoshinori Kajiya, Takahiko Endo, Hiromitsu Nagayasu, Hiroshi Tanaka, Takuya Hirata, Takahito Yonekawa, Tatsuya Tsujiuchi. SO_3 impact on amine emission and emission reduction technology. Energy Procedia 37 (2013) 1793 – 1796.

[10] S. Sinanis, A. Wix, L. Ana, K. Schaber. Characterization of sulphuric acid and ammonium sulphate aerosols in wet flue gas cleaning processes. Chemical Engineering and Processing 47 (2008) 22–30.

[11] Peter Moser, Sandra Schmidt, Knut Stahl, Gerald Vorberg, Gustavo A. Lozano, Torsten Stoffregen, Frank Rösler. Demonstrating Emission Reduction – Results from the Post-combustion Capture Pilot Plant at Niederaussem. Energy Procedia 63 (2014) 902 – 910.

[12] Michael Imle, ErikvonHarbou, LeonieBrachert, KarlheinzSchaber, HansHasse. Predicting supersaturation by rate-based simulations of reactive absorption. Chemical Engineering Science 118(2014)41–49.

[13] De Cazenove T, Bouma RHB, Goetheer ELV, Van Os PJ, Hamborg ES. Aerosol Measurement Technique: Demonstration at CO_2 Technology Centre Mongstad. Energy Procedia 86 (2016) 160 – 170

[14] Morken AK, Nenseter B, Pedersen S, Chhaganlal M, Feste JK, Bøe Tyborgnes R, Ullestad Ø, Ulvatn H, Zhu L, Mikoviny T, Wisthaler A, Cents T, Bade OM, Knudsen J, De Koeijer G, Falk-Pedersen O, Hamborg ES. Emission results of amine plant operations from MEA testing at the CO_2 Technology Centre Mongstad. GHGT12. Energy Procedia 00 (2013) 000–000.

[15] Brigman N, Shah MI, Falk-Pedersen O, Cents T, Smith V, De Cazenove T, Morken AK, Hvidsten OA, Chhaganlal M, Feste JK, Lombardo G, Bade OM, Knudsen J, Subramoney SC, Fostås FB, De Koeijer G, Hamborg ES. Results of amine plant operations from 30 wt% and 40 wt% aqueous MEA testing at the CO_2 Technology Centre Mongstad. GHGT12. Energy Procedia 00 (2014) 000–000

[16] Gjernes E, Pedersen S, Cents T, Watson G, Fostås BF, Shah MI, Lombardo G, Desvignes C, Flø NE, Morken AK, de Cazenove T, Faramarzi L, Hamborg ES. Results from 30 wt% MEA performance testing at the CO2 Technology Centre Mongstad. Energy Procedia (GHGT-13), Forthcoming 2017.

[17] Bade OM, Knudsen JN, Gorset O, Askestad I. Controlling amine mist formation in CO_2 capture from Residual Catalytic Cracker (RCC) flue gas. GHGT12. Energy Procedia 63 (2014) 884 – 892

[18] Marco Tammaro, Francesco Di Natale, Antonio Salluzzo, Amedeo Lancia. Heterogeneous condensation of submicron particles in a growth tube. Chemical Engineering Science, Volume 74, 28 May 2012, Pages 124–134

[19] Justin Anthony, John Carroll. Advanced Technology Testing at the National Carbon Capture Center. Publication of National Carbon Capture Center (NCCC).

[20] Honghong Yi, Jiming Hao, Lei Duan, Xiaolong Tang, Ping Ning, Xinghua Li. Fine particle and trace element emissions from an anthracite coal-fired power plant equipped with a bag-house in China. ScienceDirect. Fuel 87 (2008) 2050–2057

[21] Jan mertens, Dominique Desagher, Marie-Laure Thielens, Han Huynh, Helene Lepaumier, Purvil Khakaria, Earl Goetheer. On- and off-line ethanolamine and ammonia emission monitoring in PCC. PCCC2 presentation Bergen September 2013

[22] Morken AK, Pedersen S, Kleppe ER, Wisthaler A, Vernstad K, Ullestad Ø, Flø NE, Faramarzi L, Hamborg ES. Degradation and Emission Results of Amine Plant Operations from MEA Testing at the CO2 Technology Centre Mongstad. Energy Procedia (GHGT-13), Forthcoming 2017

CATCHING OUR FUTURE

Degradation and Emission Results of Amine Plant Operations from MEA Testing at the CO_2 Technology Centre Mongstad

(2017)

Available online at www.sciencedirect.com

ScienceDirect

Energy Procedia 114 (2017) 1245 – 1262

Energy Procedia

13th International Conference on Greenhouse Gas Control Technologies, GHGT-13, 14-18 November 2016, Lausanne, Switzerland

Degradation and Emission Results of Amine Plant Operations from MEA Testing at the CO_2 Technology Centre Mongstad

Anne Kolstad Morken[a,b,*], Steinar Pedersen[b], Eirik Romslo Kleppe[a], Armin Wisthaler[d], Kai Vernstad[e], Øyvind Ullestad[a,b], Nina Enaasen Flø[a], Leila Faramarzi[a,b], Espen Steinseth Hamborg[a,b]

[a] *CO_2 Technology Centre Mongstad (TCM DA), 5954 Mongstad, Norway*
[b] *Statoil ASA, PO Box 8500, 4035 Stavanger, Norway*
[c] *Gassnova SF, Dokkvegen 10, 3920 Porsgrunn, Norway*
[d] *University of Oslo, Department of Chemistry, P.O. Box 1033 Blindern, 0315 Oslo, Norway*
[e] *Sintef Materialer og Kjemi, Avd Bioteknologi, Sem Sælands vei 2, 7034 Trondheim, Norway*

Abstract

In 2015, the CO_2 Technology Centre Mongstad (TCM DA), operated a test campaign using aqueous monoethanolamine (MEA) solvent at 30 wt%. The main objective was to demonstrate and document the performance of the TCM DA Amine Plant located in Mongstad, Norway. This paper will present several aspects concerning degradation of the solvent and atmospheric emissions from amine based CO_2 removal processes. The work aims to; (1) quantify the amounts and compositions of the degraded solvent (2) report results from atmospheric emissions measurements of amines and amine based degradation products; and (3) present Ambient Air measurement done during a 2 month campaign.

© 2017 The Authors. Published by Elsevier Ltd. This is an open access article under the CC BY-NC-ND license (http://creativecommons.org/licenses/by-nc-nd/4.0/).
Peer-review under responsibility of the organizing committee of GHGT-13.

Keywords: Monoethanolamine, MEA, Amine, Emission, Degradation, CO_2-capture

---

* Corresponding author. Tel.: +47 56 34 52 20.
E-mail address: akmo@tcmda.com

1876-6102 © 2017 The Authors. Published by Elsevier Ltd. This is an open access article under the CC BY-NC-ND license (http://creativecommons.org/licenses/by-nc-nd/4.0/).
Peer-review under responsibility of the organizing committee of GHGT-13.
doi:10.1016/j.egypro.2017.03.1379

1. Introduction

The CO_2 Technology Centre Mongstad (TCM DA) is located next to the Statoil refinery in Mongstad, Norway. TCM DA is a joint venture set up by Gassnova representing the Norwegian state, Statoil, Shell, and Sasol. The facility run by TCM DA entered the operational phase in August 2012 and it is one of the largest post-combustion CO_2 capture test centres in the world. A unique aspect of the facility is that either a flue gas slipstream from a natural gas turbine based combined heat and power (CHP) plant or an equivalent volumetric flow from a residual fluidized catalytic cracker (RFCC) unit can be used for CO_2 capture. The CHP flue gas contains about 3.5% CO_2 and the RFCC flue gas contains about 13-14% CO_2. One of the main test plants at TCM DA is a highly flexible and well-instrumented amine plant. The amine plant was designed and constructed by Aker Solutions and Kværner to accommodate a variety of technologies, with capabilities of treating flue gas streams of up to 60,000 standard cubic meters per hour. The plant is being offered to vendors of solvent based CO_2 capture technologies to, among others, test; (1) the performance of their solvent technology, and (2) technologies aimed to reduce the atmospheric emissions and environmental impact of amines and amine based degradation products from such solvent based CO_2 capture processes. The objective of TCM DA is to test, verify, and demonstrate CO_2 capture technologies suitable for deployment at full-scale. Up to now the vendors Aker Solutions, Alstom, Cansolv Technologies Inc. and Carbon Clean Solutions Ltd. have successfully used the TCM DA facilities to verify their CO_2 capture technologies.
From July to October 2015 TCM DA, in collaboration with partners, operated a test campaign using the non-proprietary aqueous monoethanolamine (MEA) solvent at 30 wt%.

2. The amine plant and operating conditions

The MEA campaign was started 6th of July 2015 with flue gas introduction to the amine plant. The campaign lasted to 17th of October 2015. Operational hours are counted as hours with both flue gas and solvent circulation. The entire campaign gave a total of 1960 hours of operation (figure 1).

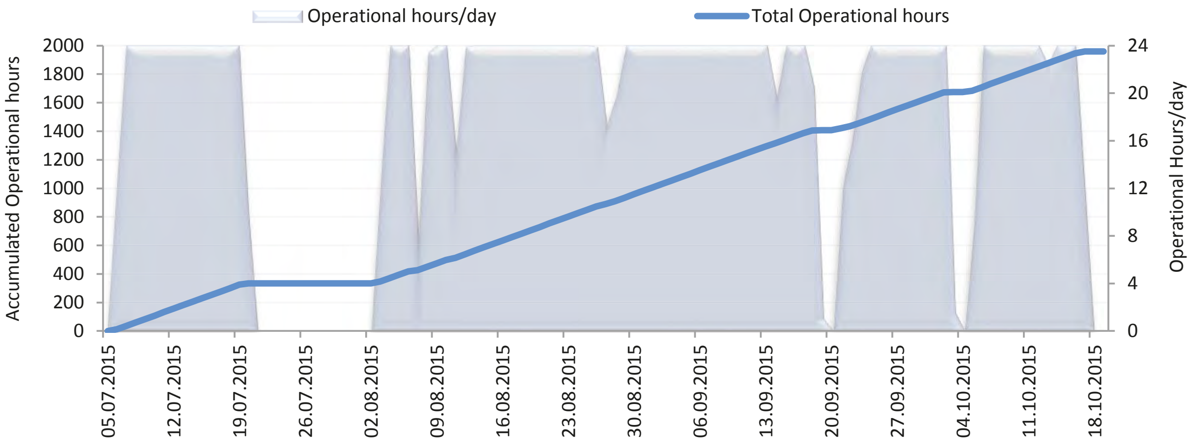

Figure 1. Overall MEA campaign operational hours, from 6th of July to 18th of October 2016.

A process flow diagram including sample points for the amine plant is given in figure 2. A more detailed description of the TCM DA amine plant and the TCM sample handling system can be found elsewhere [1,2,3]. Liquid and gas sampling, target component groups and analytical measurement techniques are described in sections 2.3 to 2.5 below.

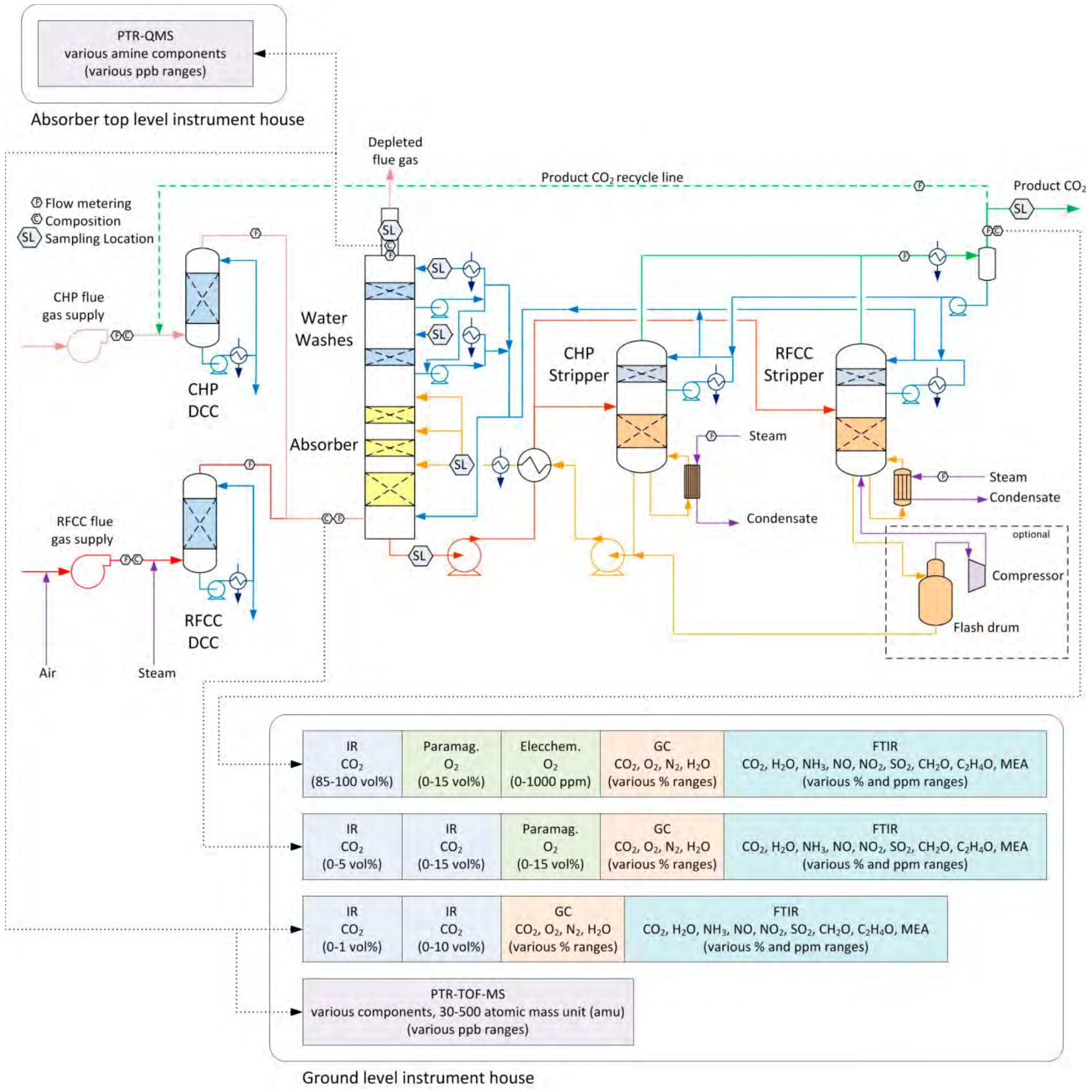

Figure 2. Process flow diagram for TCM, including online equipment's and manual sampling locations

Several operating conditions are important with respect to the solvent degradation and emission rates of amines and degradation products. Detailed information about the operating conditions and all the test activities and performance results from the MEA campaign, can be found in Gjernes et al [12].

The flue gas composition downstream the Direct Contact Cooler (DCC) from the CHP and the RFCC are providing a range of test conditions and the solvent will be exposed to a corresponding range in CO_2 and O_2 concentrations, as well as NOx, SOx and particles. Solvent amines react with the flue gas components and give rise to the degradation products as illustrated in figure 3. Degradation reactions of MEA and specific degradation products that where monitored during this campaign is given in section 3 below.

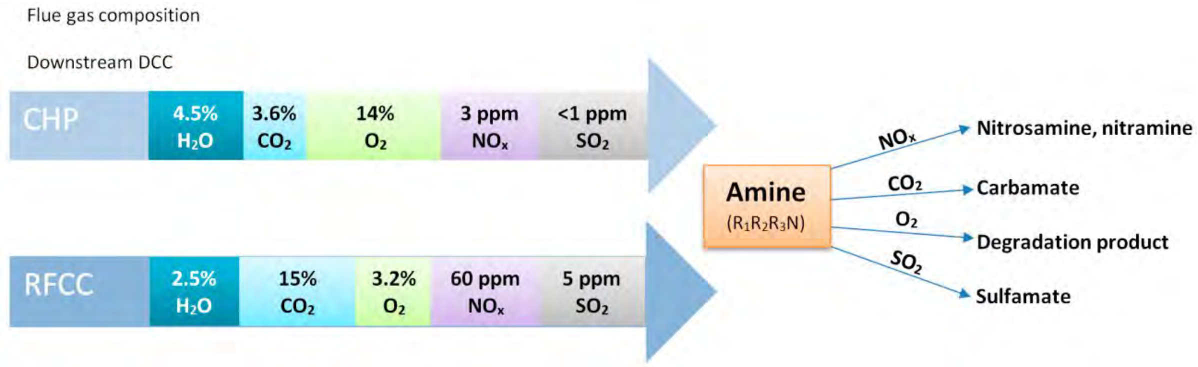

Figure 3. Typical flue gas composition influence of reaction with amines

When the solvent is exposed to higher temperatures in combination with the flue gas components, the degradation reactions are accelerated. Also the accumulation in the solvent of transition metal elements due to corrosion may contribute to degradation [11]. Process units with high temperature exposure are the stripper and reboiler system and the hot part of the solvent circulation loop. For more process details see Table 1. The inventory and the residence time of solvent in the hot areas are decisive for degradation, for more details regarding the inventory see Flø et al [13].

Table 1. Process parameters in the solvent circulation loop

Process parameters	Unit	Hot Lean Solvent	Hot Rich Solvent	Cold Lean Solvent	Cold Rich Solvent
Temperature	°C	120	110	35 - 37	30 - 40
Flow rate	Tons/hour	55 - 120	55 - 120	55 - 120	55 - 120
pH	-	10.4	9	10.4	9
Pipe size	Inches	8	6	8	6
Velocity	m/s	0.45-0.97	0.74-1.62	0.45-0.97	0.74-1.62

2.1. Liquid samples

The solvent amine, ammonia, and some degradation products were analyzed by TCM DA and Statoil Crude Oil and Products laboratories (CP Lab). Alkyl amines, aldehydes, ketone, generic nitrosamines, solvent specific nitrosamines and nitramines were analyzed by SINTEF laboratories. Total Nitrogen (Kjeldahl) was analyzed by LabNett Stjørdal, table 2 gives an overview of the different techniques used.

Organic acids and anions were measured by Ion Chromatograph (IC) and Total Heat Stable Salts (HSS) by ion exchange and following titration.

Table 2. Analytical measurements techniques

Component groups	Analysis methods	Supplier	Analysed by
Amines (solvent)	LC MS QQQ	Agilent	Statoil CP lab
Amines (alkyl)	LC MS QQQ	Agilent	Sintef
Ammonia	Cation chromatography, IC-ECD	Dionex	TCM Lab
Aldehydes	LS MS QQQ	Agilent	Sintef
Nitrosamines (TONO)	See *	-	Sintef
Nitrosamines (specific and generic)	LC MS QQQ	Agilent	Sintef
Nitramines	LC MS QQQ	Agilent	Sintef
Organic acids, anion	Anion chromatography, IC-ECD	Dionex	TCM Lab
Total Heat Stable Salts	Ion exchange and titration	Metrohm	TCM Lab
Total Nitrogen	-	-	LabNett Stjørdal

*TONO; Quench of solved nitrite followed by break of N-NO bond in a reaction chamber. Total NO released from the N-nitroso groups detected by chemiluminscence analyser.

2.2. Emission samples

TCM DA applies different measurement techniques to monitor and quantify the amounts and concentrations of emitted compounds. There are three different flue gas streams, flue gas inlet to the absorber (downstream DCC), absorber outlet and CO_2-stripper outlet. Online instruments are connected via heated sampling lines to sampling probes. The amine and other emissions were monitored and confirmed by isokinetic sampling and the following online analyzers in Table 3. A full description of emission monitoring at TCM is given in Morken et al [1]. For a more detailed description of the general online equipment see Lombardo and Gjernes [6,12].

Table 3. Online instrumentation for emission monitoring at TCM

Instrument	Gasmet FTIR FCX	FTIR Anafin2000	PTR-TOF-MS	PTR-QMS
Supplier	Gasmet Technologies Oy	Analect	Ionicon	Ionicon
Temp	Cell 180°C	Cell 85°C	Drift tube 100°C	Drift tube 100°C
Cell path length	5 m	7 m	-	-
Resolution	$8\ cm^{-1}$	$2\ cm^{-1}$	$(\Delta\ (m/z))/((m/z)) > 3000$	$\Delta\ (m/z) = 1$
Flow rate	120 – 600 L/h	100 L/h	30 L/h	30 L/h
Range	$900 – 4200\ cm^{-1}$	$500 – 7000\ cm^{-1}$	10-200	20-200
LOD	0.5 - 1 ppmv *	0.5 -1 ppmv *	0.0001 ppmv	0.001 ppmv
SD	*	*	± 20 %	± 20 %
Inlet Flue Gas		x		
CO_2-stack	x		x**	
Absorber	x	x**	x	x

*Limit of detection (LOD) value depends on compound, level of compound, the way of calculation and measurement time.

**Occasionally measurements on these streams for QA/QC and comparing different instruments.

2.3. Ambient Air measurements, instrumentation and locations

The ultra-sensitive proton-transfer-reaction quadrupole ion guide time-of-flight mass spectrometer (PTR-QiToF-MS) from IONICON was used for detecting trace gases at low pptv levels in ambient air in the vicinity of Technology Centre Mongstad. These novel ambient air measurements were performed in August and September 2015 by University of Oslo. Measurements were carried out in three different geographic locations, Sundsbø (60°46'10.1''N, 5°09'08.6''E), Sande (60°50'56.6''N, 5°00'21.0''E) and Mongstad West (60°48'45.7''N, 5°00'43.4''E). These sites were chosen from earlier measurement done by Norwegian Institute for Air Research (NILU) and dispersion models done by NILU [5]. For more technical details and results regarding this surveillance see Mikoviny et al [10].

3. MEA solvent and degradation theory

3.1. Oxidative and Thermal degradation

The degradation mechanisms for MEA have been extensively studied in the literature [4,5,8,11,14]. The main degradation reaction pathways with most important degradation products are indicated and proposed in figure 7 below. Oxidative degradation is induced by O_2 and produces oxidized fragments of the solvent. Organic acids, ammonia and aldehydes are the main products from this degradation route. Ammonia and aldehydes are observed in the emission samples. The organic acids react with MEA and various degradation products are formed in subsequent reactions. These products are identified in the solvent samples.

The carbamate degradation route requires CO_2 and fairly high temperatures. The thermal degradation of MEA occurs predominantly in the reboiler and stripper packing due to exposure to high temperature. While the initial products of thermal degradation have been identified, the kinetics of the thermal degradation pathways has not been clearly defined. Davis and Rochelle [14] indicate that thermal degradation is minor when reboiler temperature is held below 110°C but it accelerates above 130 °C. Carbamate polymerization due to high temperature is the main cause of thermal degradation of MEA. This degradation is also compounded when the CO_2 loading of the solution is increased. MEA concentrations can be kept at 30 wt % to minimize thermal degradation and prevent corrosion in industrial applications.

3.2. HSS components

Heat Stable Salts (HSS) are salts in the amine solution that is not affected by heat. The heat stable salt does not regenerate in the regenerator and remains in the circulating amine system. Total HSS are measured by a titration procedure which prepares the sample with a strong cation exchange resin. Individual HSS anions are measured by Ion Chromatography (IC). The different anions measured by IC are summarized in table 4.

Table 4. Heat stable salts anions analyzed by TCM laboratory using Ion Chromatography

Component	**Abb**	**CAS No**	**Mw**
Acetate	(AA^-)	71-50-1	59
Glycolate	(GA^-)	79-14-1	75
Formate	(FA^-)	71-47-6	45
Oxalate	(OA^{--})	144-62-7	125
Nitrate	(NO_3^-)	14797-55-8	62
Nitrite	(NO_2^-)	14797-65-0	46
Sulphate	$SO_4^{2-})$	14808-79-8	96
Propionate	$(C_2H_5COO^-)$	72-03-7	73

The identified anions are summed to provide a total HSS. In general, Total HSS by titration should be the same or larger than the sum of anions by IC, figure 6 (h). Total HSS are reported as the wt% of the equivalent amount of amine. This means if HSS concentration were 1 mole/kg (eq/kg) of solution, it will be 6.1 wt% as MEA (1).

$$\text{MEA} + \text{RCOOH} \rightarrow \text{MEAH}^{+} + \text{RCOO}^{-} \qquad (1)$$

3.3. Degradation components in solvent, from emission and in Ambient Air

The degradation components measured during the MEA campaign were based on information found from literature [4]. All components from solvent and emission samples in Table 5 were analyzed by Sintef. The analyzing measuring technique was primarily LC-MS-QQQ. The mixture of the different degradation components are hereafter called D-mix. Analysis of Ambient Air components were done by University of Oslo [10].

Table 5. Degradation products and measurements in solvent, emission from amine plant absorber stack and in Ambient Air.

Component	**Abb**	**CAS No**	**Mw**	**Solvent**	**Emission to Air**	**Ambient Air**
Monoethanolamine	MEA	141-43-5	61	x	x	x
Ammonia	NH_3	7664-41-7	17	x	x	
Formaldehyde	FA	50-00-0	30	x	x	
Acetaldehyde	AA	75-07-0	44	x	x	x
N-Nitroso-diethanol-amine	NDELA	1116-54-7	134	x	x	
N-(2-hydroxyethyl) acetamide	HEA	142-26-7	103	x		
1-hydroxyethane 1,1-diphosphonic acid	HEDP	2809-21-4	206	x		
N-(2-hydroxyethyl)ethylenediamine	HEEDA	111-41-1	104	x		
N-(2-hydroxyethyl)formamide	HEF	693-06-1	89	x		
N-(2-hydroxyethyl)glycine	HeGly	5835-28-9	119	x		
N-(2-hydroxyethyl)-2-(2-hydroxyethylamino)acetamide	HEHEAA	144236-39-5	162	x		
Pyrazine	-	290-37-9	80	x	x	
N-(2-hydroxyethyl)imidazole	HEI	1615-14-1	112	x		
N-(2-hydroxyethyl)imidazolidinone	HEIA	3699-54-5	130	x		
4-(2-hydroxyethyl)piperazin-2-one	HEPO	23936-04-1	144	x		
Dimetylamine	DMA	124-40-3	45	x	x	x
Methylamine (Monometylamine)	MA (MMA)	74-89-5	31	x	x	x
Ethylamine	EA	75-04-7	45	x	x	x
Diethylamine	DiEA	109-89-7	73	x	x	x
Morpholine	Mor	110-91-8	87	x	x	
Trimethylamine	TMA	75-50-3	59	x	x	x
4,4-dimethyl-2-oxazolidinone	4.4-DMO	26654-39-7	115	x	x	
N-Nitroso(2-hydroxyethyl)glycine	NO-HeGly	80556-89-4	148	x	x	
2-(Nitroamino)ethanol	NO2-MEA	74386-82-6	106	x	x	
N-methyl,N-nitroso-methanamine	NDMA	62-75-9	74	x	x	
N-nitro-N-methyl-methanamine	DMNA	4164-28-7	90	x	x	
N-Nitrosomethylethylamine	NMEA	10595-95-6	88	x	x	
N-Nitrosodiethylamine	NDEA	55-18-5	102	x	x	
N-Nitrosodi-n-propylamine	NDPA	621-64-7	130	x	x	
N-Nitrosodi-n-butylamine	NDBA	924-16-3	158	x	x	
N-Nitrosopyrrolidine	NPYR	930-55-2	100	x	x	
N-Nitrosopiperidine	NPIP	100-75-4	114	x	x	
N-nitrosodiethanolamine	NDELA	1116-54-7	134	x	x	
2-Oxazolidone	OZD	497-25-6	87	x	x	
Alkylpyrazine	-				x	
NN'-Bis(2-hydroxyethyl)oxamide	BHEOX	1871-89-2	176	x	x	
Diethanolamine	DEA	111-42-2	105	x	x	

4. Results and discussions

The first observable sign of degradation was color change of the solvent. The color of the solvent changed rapidly after the first contact with the flue gas. Samples taken before introduction of flue gas show a colorless solvent. Only hours after start up, the color started to change from colorless to yellow, and more and more orange and dark brown as seen in figure 4. After reclaiming 12th of October, the color is more like the color that appeared in the start of the campaign when the solvent was fresh.

Figure 4. Pictures of samples taken during the campaign. The color change gives an indication on how degraded the solvent is. The samples are from left to right after: 0, 1300, 1830, 1870 and 1920 hours of operation.

4.1. Heat stable salts in the solvent

Figure 5 and 6 shows how the levels of organic acids and anions developed during the entire campaign. Figure 5 shows overall heat stable salts development where 5a) are Total Heat Stable salts reported as wt% MEA, and 5b) results from individually IC results from each component. Figure 6 (a-g) shows more detailed development of all the individual components. The main anion formed is formate and the level of this component reach 3000 mg/L before reclaiming. Glyoxylic acid is assumed to be one of the formed organic acids during the degradation process [7]. It was not possible to analyze for this component as there were no available method at the time. An unknown component of significant response on the IC chromatogram was found. The area of the unknown component in the chromatogram was significant, and the component was calibrated with a mix of the other components. The result from this unknown component is rather uncertain, see figure 6 g). All other IC results have a repeatability uncertainty of ± 20%.

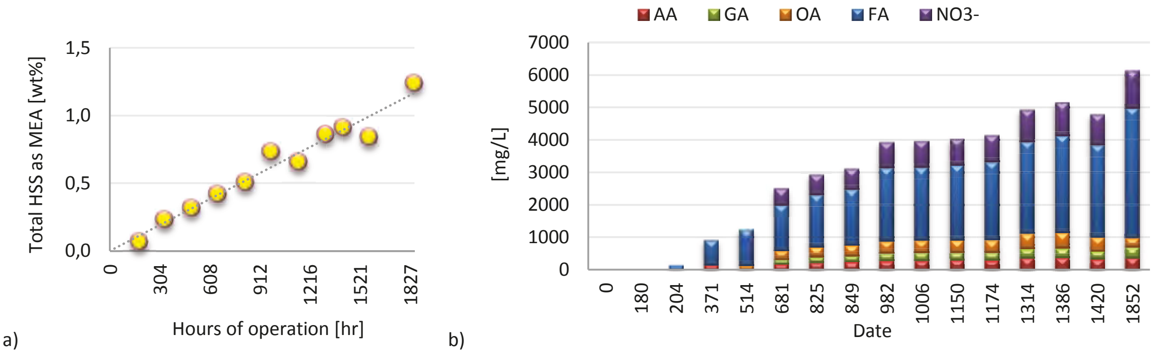

Figure 5. (a) Total Heat stable salt concentration; (b) Results from Anion IC analysis

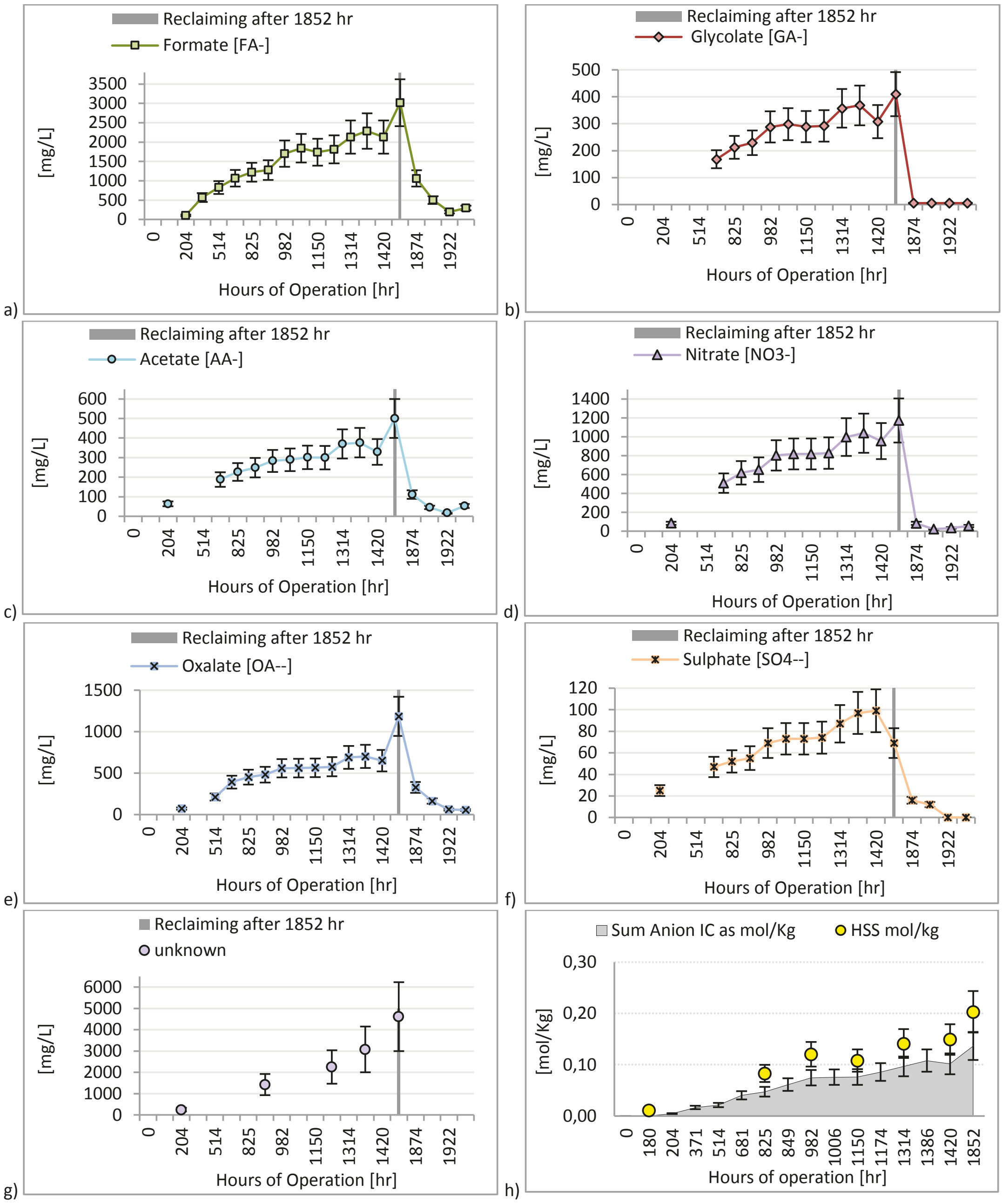

Figure 6. (a) Formate concentration, mg/L; (b) Glycolate concentration, mg/L; (c) Acetate concentration, mg/L; (d) Nitrate concentration, mg/L; (e) Oxalate concentration, mg/L; (f) Sulphate concentration, mg/L (g) unknown component, mg/L; (h) Total HSS and sum anions presented as mole/kg

Propionate ($C_2H_5COO^-$) and nitrite (NO_2^-) were not detected above 10 mg/L which is the limit of detection on the Ion Chromatograph.

4.2. Degradation products in the solvent

A simplified scheme for MEA degradation is proposed in figure 7. Oxidation reactions lead to formation of the organic acids and the emission products ammonia and aldehydes. This is indicated in the left blue square of the figure. Reactions between MEA and the organic acids, CO_2 and additional free MEA lead to formation of the degradation products identified in the lean solvent samples. This is indicated in the large red square of the figure. A nitrogen mass balance based on solvent analysis are presented and compared to literature data in section 4.5 below.

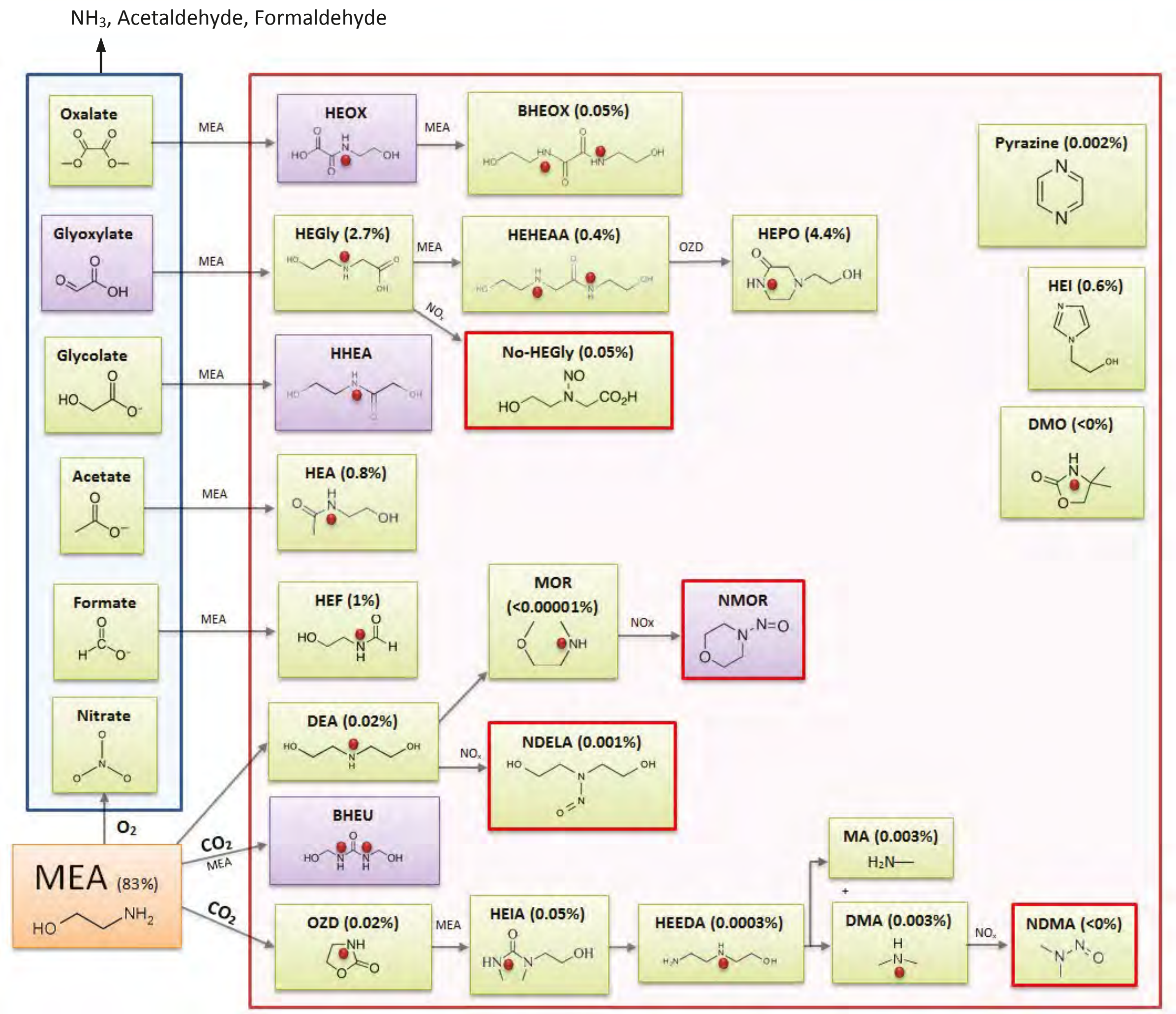

Figure 7. Proposed overall degradation scheme for monoethanolamine.
Scheme is simplified and intermediate amine compounds may form.

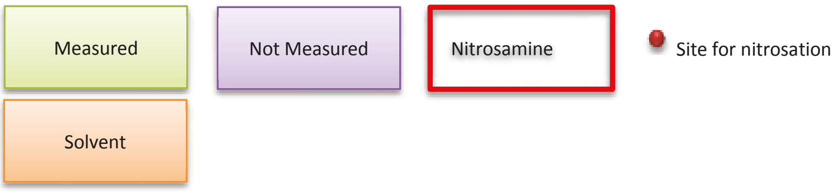

The rate of formation of the degradation products is a function of temperature (faster kinetics), CO2 loading (more carbamate present), and MEA concentration. The identified degradation products in the solvent samples and the accumulation of these as function of operational hours are shown in figure 8.TCM performed a MIST test after 1314 hours of operation and also did a CO2 recycling test with higher CO2 content in the CHP flue gas [12]. The results shown after 1314 hours are not consistent with the other samples and cannot be explained. Results from the reclaiming part of the 2015 MEA campaign is given in [13].

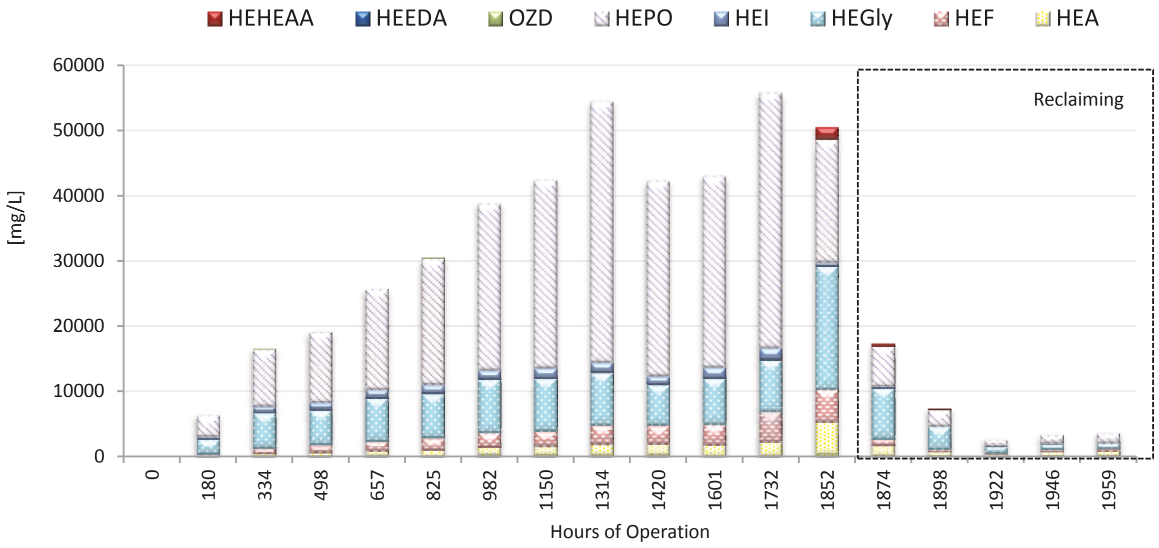

Figure 8. Main degradation products during the entire campaign. The component names and abbreviation is given in table 5 above.

It is seen that the dominant degradation products in the solvent are N-(2-hydroxyethyl)glycine (HeGly) and 4-(2-hydroxyethyl)piperazine-2-one (HEPO). This corresponds to the oxidation pathway via glyoxylate and subsequent reaction with MEA given in figure 7. The identification of the nitroso-compound nitroso-Hegly (No-HeGly) in the solvent further confirms this degradation route.

4.3. Nitroso- and Nitramines in solvent

Two solvent specific nitrosamines, N-nitrosodiethanolamine (NDELA) and N-nitroso-2-hydroxyethyl-glycine (Nitroso-HeGly), were detected in the solvent as the degradation process progressed. The total concentrations of nitrosamines (TONO) were measured to be 2351 µmol/L after 1850 hours of operation, see figure 9. Since MEA is a primary amine it is not expected to form a stable nitrosamine. The identified compounds are thus formed from secondary amines occurring as impurities in the solvent or being formed during the degradation reactions. As is shown in Figure 9 a), there are still some unidentified nitrosamines in the degraded solvent sample. These nitrosamines are formed from high molecular weight amines and have low volatility. Figure 9 b) shows a decrease in the level of total nitrosamines after reclaiming of the solvent.

Nitrosamines are formed after reaction with NOx in the flue gas [8]. During the MIST test, RFCC flue gas was used, and as this flue gas contains more NOx than flue gas from the Combined Heat and Power Plant, this could explain the higher amount of nitrosamines in this MEA2 campaign compared with the first MEA1 campaign from TCM [1].

The solvent specific nitramine (MEA-NO_2) was detected at a concentration of approximately 4 mg/L after 1850 hours of operation. Methylnitramine (MA-NO_2) and Dimethylnitramine (DMA-NO_2) were also analyzed, but the responses on the LC MS QQQ were below the limit of detection (< 0.1 mg/L).

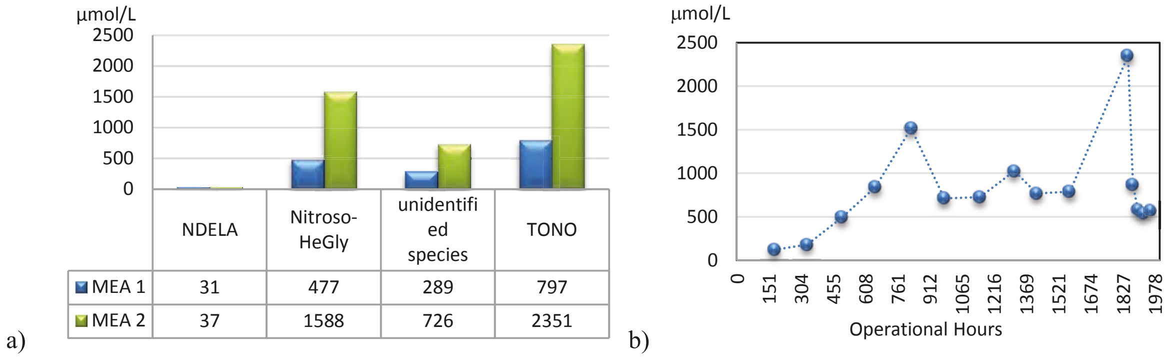

Figure 9. a) Nitrosamines in Lean MEA after 1850 operational hours. Results from the first MEA campaign (MEA 1) and this campaign (MEA 2) b) TONO measurements through the entire campaign

4.4. Nitrogen mass balance of the solvent

A nitrogen balance of the solvent was done after 1850 hours of operation, just before reclaiming, see table 6.

Table 6. A nitrogen mass balance of the solvent was done after 1850 operational hours

Component	mg/L	mg/Kg	tot Kg	mole N	µmole/L	%
MEA	326473		11263	184403		82.7
BHEOX	274		9.4	107		0.048
HEA	4963		171	1660		0.74
HEF	5062		175	1960		0.88
HEGly	18922		653	5480		2.46
HEI	1826		63	1124		0.50
HEPO	18788		648	8997		4.04
OZD	82		2.8	32		0.015
HEIA	181		6.3	96		0.043
HEEDA	1.0		0.03	0.7		0.00031
HEHEAA	1870		65	795		0.36
4.4-DMO	<1		<0.1	<1		<0.0004
Morpholine	<1		<0.1	<1		<0.0004
Bicine	62		2.1	13		0.0059
Pyrazine	8.0		0.3	3.4		0.0015
DEA	152		5.3	50		0.022
DMA	7.1		0.2	5.5		0.0024
DiEA	0.3		0.01	0.14		0.00006
MA	5.7		0.2	6.3		0.0028
EA	0.2		0.005	0.12		0.00005
Formamid	11		0.4	8.2		0.0037
Acetamid	12		0.4	7.0		0.0031
NDELA*	4.9		0.2	2.5		0.0011
No-HEGly*	235		8.1	110		0.049
TONO	306		11	162	2351	0.073
MEA-NO_2	4.0		0.1	2.6		0.0012
NO_3^-	1173		40	653		0.29
Sum Identified components			13116	205567		92.2
Unidentified				17397		7.80
Tot N		**83000**		**222964**		**100**

*NDELA and No-HeGly are included in the TONO results, and hence not summarized

Total Nitrogen in lean amine was measured to be 8.3 wt%, which give a total of 222964 mole N. The sum of the different degradation products found gives a total of 205567 moles. This gives 7.8 mole% of nitrogen that is not found by analysis, these components are hereafter called unidentified components. Some of the unidentified components are assumed to be long chain molecules. Dissolved ammonium and ammonia in the solvent were not measured; this means that they will presumably have some contribution to the amount of the unidentified components. Table 6 shows an overview of all the components that were analyzed, and the contributions of each component to the total amount of nitrogen.

4.5. Solvent loss

Excluding plant leakage, MEA loss can occur in the following ways:

- MEA emitted via Absorber (after water wash section)
- MEA emitted via stripper upper product after the condenser
- MEA degraded product via NH_3 formation, which is detected after the wash section and from the CO_2-product stream
- Liquid sampling, which was taken for analysis
- Unexpected loss due to leakage through joints and pumps
- Wash water (absorber, stripper)
- Reclaimer waste

Lab samples and reclaimer waste are a part of the total inventory calculation. MEA was charged into the amine makeup tank from trucks. From the amine make up tank, MEA can either be charged into the storage tank or directly to the process loop. A total of 30088 Kg of pure MEA was filled into the makeup tank, while a total of 23208 Kg of MEA was discharged from the plant after the end of campaign. This gave a total loss of 7622 Kg pure MEA. Total CO_2 capture in the campaign was 4941 ton, and this give a loss of 1.5 kg MEA/ton CO_2 captured.

A nitrogen mass balance of the total solvent system was also done. The accumulated NH_3 emission from the absorber and stripper corresponds to approximately 67% of the total MEA loss, while the nitrogen detected identified degradation compounds (D-mix) constitutes approximately 16% of the MEA loss. Table 7 gives a short summary of the degraded product produced per mole amine lost. These results are similar to the results reported by IEAGHG [11]. Total Nitrogen analysis was performed, and it is reasonable to assume that long-chain degradation compounds constitute some amount of the unidentified loss.

The nitrogen mass balance for the entire campaign gives a loss of MEA that corresponds to 1.6 kg MEA/ton CO_2 captured. There is a small gap between the two different methods of calculation, and average value is used. From this MEA 2 campaign it is concluded that the loss of solvent was 1.6 ± 0.1 kg/ton CO_2 captured.

Table 7. Stoichiometry of Products Produced per Mole of Degraded Amine

Product	Mole produced/mole amine lost	Mole produced/mole amine lost [a)]
Ammonia	0.67	0.67
Total formate + HEF	0.03	0.12
Oxalate + oxylamide	0.003 [b)]	0.01
Nitrate	0.005	0.01
HEI	0.01	0.06
HeGly	0.04	0.05
HEHEAA + HeGly + HEPO	0.12	-

[a)] Reported values from IEAGHG “Evaluation of reclaimer sludge disposal from post-combustion CO_2 capture”, 2015/02, March 2014 [11]

[b)] Oxylamide was not analyzed

5. Emissions of amines and amine based degradation products

5.1. Analysis of emission from depleted flue gas

Emission to Air from TCM DA amine plant has two sources, the amine absorber and the CO_2-stack. At TCM the CO_2 product stream is sent into the atmosphere, which will not be the case for a full-scale CO_2 capture plant. As the contribution from this stream is small considered to the absorber (1-3%), data from this stream is not given in this paper.

TCM DA applies different measurement techniques to monitor and quantify the amounts and concentrations of emitted compounds. A description of the TCM DA overall system for emission control and monitoring is given elsewhere [1]. The emission was followed up by FTIR, PTR-TOF-MS, PTR-QMS, isokinetic sampling and by 3rd party (FORCE Technology) [9].

MEA emissions are highly related to aerosols in the flue gas [6]. Even at low mass concentrations of aerosols, increased MEA emissions have been measured and reported. In September 2015 TCM investigated the relation between flue gas particle content, mainly related to sulphuric acid mist particles and dust, and corresponding MEA amine emissions. This “MIST test” was based on aerosol number concentration and size distribution, to evaluate the maximum aerosol number concentration acceptable for operation with a solvent based on MEA [6]. TCM received a temporary emission permit given for this campaign from the Norwegian environmental agency (NEA). The temporary permit gave allowance to increase MEA emission from 6 ppmV to 500 ppmV for maximum 4 days of testing.

The Mist test was a planned temporary campaign lasting for only two weeks. The rest of the MEA campaign were performed without issues regarding mist, impurities and aerosols, as flue gas from the combined heat and power plant does not contain particles and impurities. Detailed information about all the test activities and performance from the MEA campaign can be found in Gjernes et al [12].

Figures 10 - 13 provide the daily average ammonia, MEA, acetaldehyde and formaldehyde emissions and operational hours throughout the campaign. Some daily averages of ammonia emissions indicate higher emissions than allowed in the TCM DA emission permit. Any such emission peaks were communicated to the NEA. These incidents were administratively handled by NEA, and the campaign continued as planned. These higher levels were due to amine plant start-up activities, where molecular ammonia (or other amine compounds), i.e. ammonia (or other amine compounds) are unreacted with CO_2, are by convection transferred by the flue gas through the absorber and eventually emitted to atmosphere. The emissions follow a Gaussian like trend, i.e. an emission peak is observed until the emission levels settles at a lower steady state level. Test activities with increased CO_2-content in the flue gas combined with high temperatures in the solvent, water washes and flue gas, gave high ammonia emissions.

A start-up procedure conducted in the following order will reduce such start-up emission peaks;

- MEA solvent circulation starts at ambient temperatures
- Flue gas is introduced and the CO_2 loading process of the entire MEA solvent inventory occurs at ambient temperatures, until CO_2 in the MEA solvent are in equilibrium with CO_2 in the incoming flue gas (α = close to 0.5 mole CO_2 / mole MEA in the case of the CHP flue gas)
- Heat is applied to the stripper section in order start the continuous CO_2 removal process

By following the aforementioned start-up order, the amount of emitted molecular ammonia and amine compounds are decreased as the presence of these compounds in the gas phase inside the absorber is reduced, and hence less gaseous ammonia and amine compounds are transferred through the absorber by convection. 19th of May 2016, TCM received a new permanent emission permit from NEA allowing 100 ppmV ammonia emissions as a daily average.

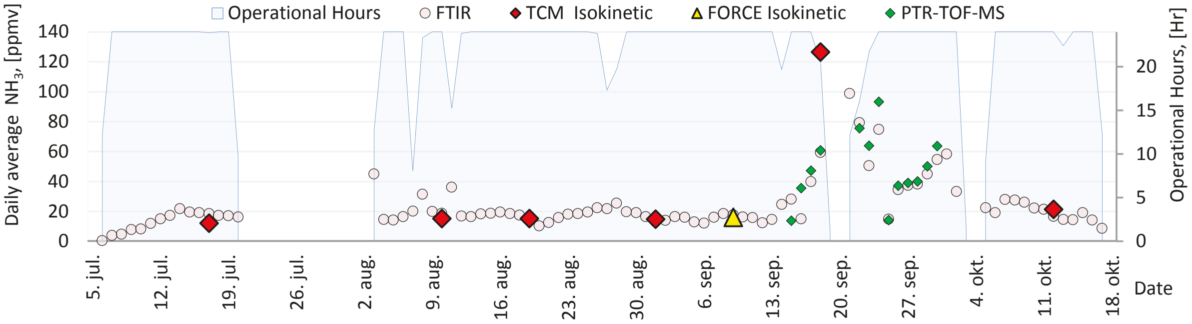

Figure 10. Daily average Ammonia (NH_3) ppmV emission from absorber measured by online FTIR, PTR-TOF-MS and isokinetic sampling, (isokinetic sampling is for a 2 hour period)

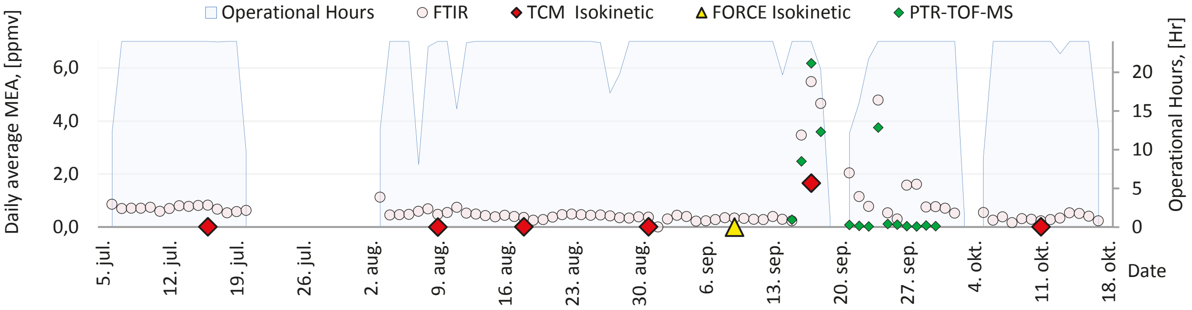

Figure 11. Daily average Monoethanolamine (MEA) ppmV emission from absorber measured by online FTIR, PTR-TOF-MS and isokinetic sampling, (isokinetic sampling is for a 2 hour period)

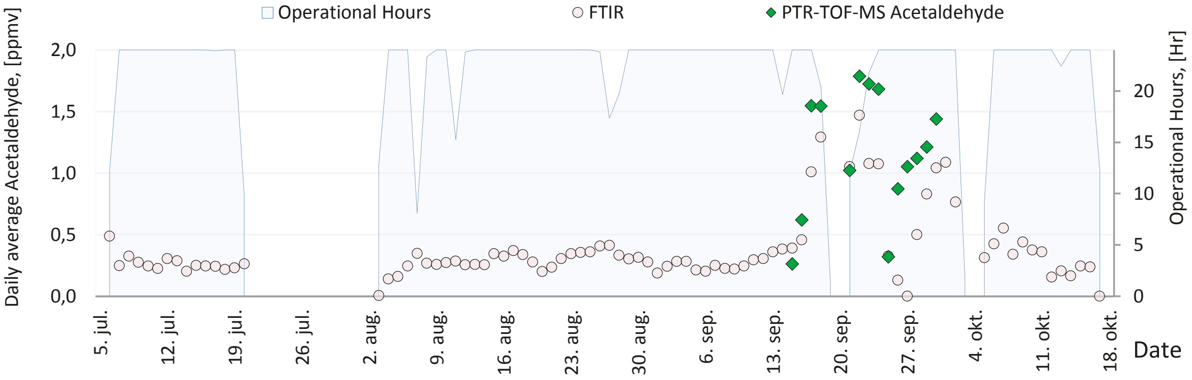

Figure 12. Daily average Acetaldehyde ppmV emission from absorber measured by online FTIR and PTR-TOF-MS

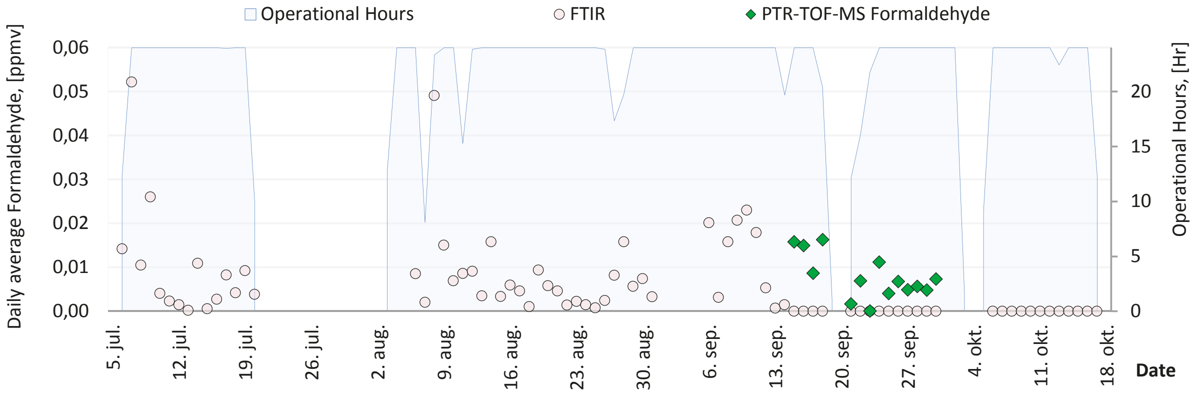

Figure 13. Daily average Formaldehyde ppmV emission from absorber measured by online FTIR and PTR-TOF-MS

For achieving the TCM objectives, it is important that variables are measured with high degree of accuracy. This will ensure that high quality data are obtained and thus a high quality of test results can be provided. This is significant not only for technology test reports but also for emissions reporting to the Norwegian Environmental Agency (NEA). A failure to estimate the inaccuracies of measurements will complicate the test planning, reporting to NEA and operation and maintenance of the test facility. Apart from accuracies of different variables, repeatability or precision of measurements for each of the variables on different streams also needs to be estimated. One quality assurance (QA) test is to compare different monitoring techniques. This was done during the MIST test, and depleted flue gas out of the absorber was measured by four different independent measurements; two FTIR's, PTR-TOF-MS and PTR-QMS. All the different measurement techniques showed very similar results. The result of this QA is shown in figure 14 and 15. TCM is a demo-plant where many types of online emission measurement equipment are tested, providing useful information for commercial projects.

Seven emission isokinetic sampling campaigns have been carried out in order to follow up on emissions form the absorber. Results from these measurements can be found in table 8. Overall the results are similar to the results reported by Morken et al [1].

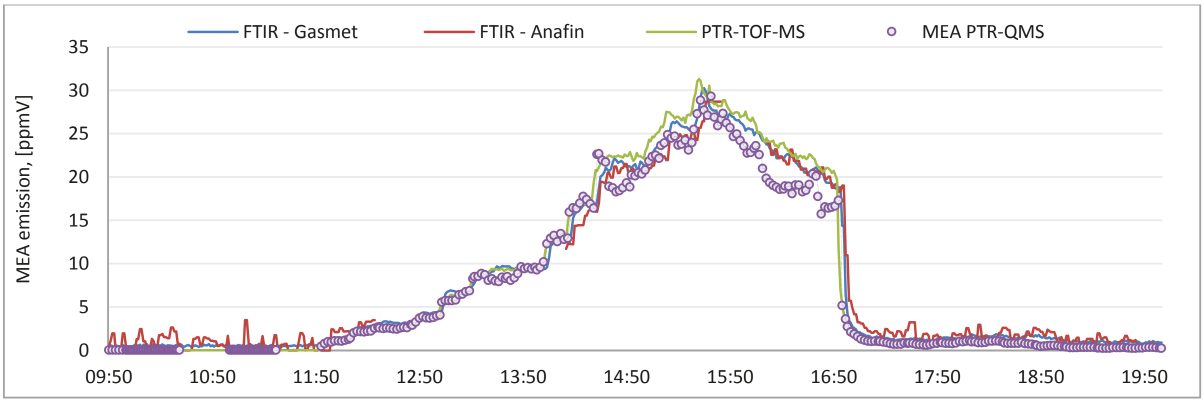

Figure 14. Simultaneously online measurement of MEA emission from amine absorber 16th of September 2015.
The online equipment's are two independent FTIR's, PTR-TOF-MS and PTR-QMS.

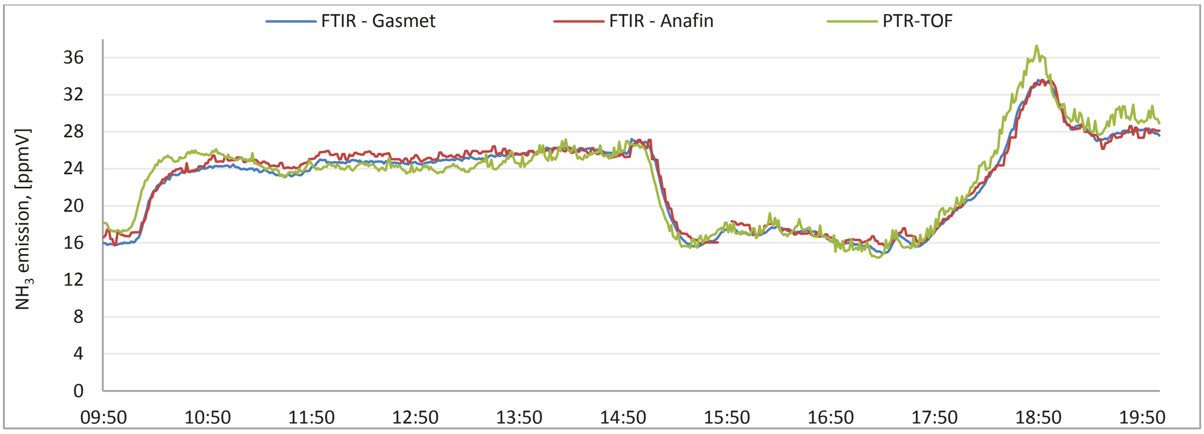

Figure 15. Simultaneously online measurement of ammonia (NH3) emission from amine absorber 16th of September 2015. The online equipment's are two independent FTIR's and PTR-TOF-MS.

TCM has shown earlier that the absorber wash water sections are found to effectively reduce possible atmospheric emissions from amine based solvent system [1]. Atmospheric emissions of monoethanolamine (MEA) were very low throughout the entire campaign, and determined to be in the parts per billion (ppb) ranges.

Atmospheric emissions of MEA amine based degradation products such as nitrosamines and nitramines were below detectable levels. Atmospheric emissions of alkyl amines in the low ppb range. Results from isokinetic measurements can be seen in table 8. These results confirm the emission results from earlier MEA campaign at TCM [1].

Table 8. Result from isokinetic gas emission measurements from the entire MEA campaign

Date	**17.07.2015**	**10.08.2015**	**19.08.2015**	**01.09.2015**	**09.09.2015***	**18.09.2015**	**12.10.2015**
MEA, µg/m^3	19.0	11.1	24.9	18.6	5.9	4281	18.5
MEA, ppmv	0.007	0.004	0.010	0.007	-	1.66	0.007
DMA, µg/m^3	56.4	35.4	42.2	35.4	37	228	494
DMA, ppmv	0.030	0.019	0.023	0.019	-	0.120	0.255
EA, µg/m^3	0.42	0.76	1.1	1.4	1.2	19.1	4.6
EA, ppmv	0.0002	0.0004	0.0006	0.0007	-	0.010	0.0024
MA, µg/m^3	29	11.2	17.8	33	30	238	166
MA, ppmv	0.022	0.008	0.014	0.025	-	0.181	0.124
DiEA, µg/m^3	0.025	0.065	0.062	0.032	9.7	0.428	<0.007
DiEA, ppmv	0.00001	0.00002	0.00002	0.00001	-	0.00014	<0.000002
EMA, µg/m^3	0.39	0.37	0.34	0.24	<0.8	2.2	3.0
EMA, ppmv	0.0002	0.0001	0.0001	0.0001	-	0.0009	0.0012
PA, µg/m^3	0.34	0.22	0.17	0.11	<0.8	1.3	1.1
PA, ppmv	0.00013	0.00009	0.00007	0.00004	-	0.00053	0.00041
NH_3, µg/m^3	9335	11667	11467	11370	13000	96329	16571
NH_3, ppmv	12.3	15.3	15.4	14.9	16	126.5	21.4

*Third party measurements done by FORCE Technology [9]. All other sampling and measurements are done by TCM.

Conclusions

During the MEA 2015 campaign at TCM the degradation products being formed in the solvent and released to the atmosphere were closely monitored. Based on an overall nitrogen mass balance it was concluded that less than 8% of total nitrogen introduced into the plant was not identified. The solvent loss calculated as pure MEA was 1.6 ± 0.1 kg/ton CO2 captured. The major contributors to the loss were ammonia emission (67% of loss) and identified degradation products in the solvent (16% of loss). Emissions to air from the absorber stack were monitored by five different independent on-line measurement instruments and by regular manual sampling. The four on-line methods provided very similar results. The manual sampling results confirmed results from earlier MEA campaign at TCM. The MEA and alkyl amines emissions are in the parts per billion ranges and nitrosamines and nitramines were below detectable levels.

Acknowledgements

The authors gratefully acknowledge the staff of TCM DA, Gassnova, Statoil, Shell and Sasol for their contribution and work at the TCM DA facility. The authors also gratefully acknowledge The TCM DA operation team, lab team at TCM DA and Statoil CP laboratory, Technology Committee, University of Oslo and Sintef for their contribution and work at the TCM DA facilities.

References

[1] Morken AK, Nenseter B, Pedersen S, Chhaganlal M, Feste J, Tyborgnes RB, Ullestad Ø, Ulvatn H, Zhu L, Mikoviny T, Wisthaler A, Cents T, Bade OM, Knudsen J, De Koeijer G, Falk-Pedersen O, Hamborg ES. Emission results of amine plant operations from MEA testing at the CO_2 Technology Centre Mongstad, Energy Procedia 63, 6023-6038.

[2] Thimsen D, Maxson A, Smith V, Cents T, Falk-Pedersen O, Gorset O, Hamborg E S. Results from MEA testing at the CO_2 Technology Centre Mongstad. Part I: Post-Combustion CO_2 Capture Testing Methodology. Energy Procedia 2014.

[3] Hamborg ES, Smith V, Cents T, Brigman N, Falk-Pedersen O, Chhaganlal M, Feste J K, Ullestad Ø, Ulvatn H, Gorset O, Askestad I, Gram L K, Fostås B F, Shah M I, Maxson A, Thimsen D. Results from MEA testing at the CO_2 Technology Centre Mongstad. Part II: Verification of baseline results. Energy Procedia 2014

[4] Da Silva EF, Hoff KA, Booth A; Emissions from CO2 capture plants; an overview, Energy Procedia 37 (2013) 784-790

[5] Lepaumier H, Picq D, Carrette P-L, New Amines for CO2 Capture. I. Mechanisms of Amine Degradation in the Presence of CO2, Ind. Eng. Chem. Res., 2009, 48 (20), pp 9061–9067

[6] Lombardo G, Fostås BF, Shah MI, Morken AK, Hvidsten OA, Mertens J, Hamborg ES. Results from aerosol measurement in amine plant treating gas turbine and residue catalytic cracker flue gases at the CO_2 Technology Centre Mongstad. Energy Procedia (GHGT-13), Forthcoming 2017.

[7] Vevelstad SJ, Eide-Haugmo I, Da Silva EF, Svendsen HF, Degradation of MEA; a theoretical study, Energy Procedia 4 (2011) 1608–1615

[8] Fostås B, Gangstad A, Nenseter B, Pedersen S, Sjøvoll M, Sørensen AL, Effects of NOx in the flue gas degradation of MEA, Energy Procedia 4 (2011) 1566–1573

[9] Faramarzi L, Thimsen D, Hume S, Maxson A, Watson G, Pedersen S, Gjernes E, Fostås BF, Lombardo G, Cents T, Morken AK, Shah MI, de Cazenove T, Hamborg ES. Results from MEA testing at the CO2 Technology Centre Mongstad: Verification of baseline results in 2015. Energy Procedia (GHGT-13), Forthcoming 2017.

[10] Mikoviny T, Nielsen C.J, Tana W, Wisthaler A , Zhu L, Morken A.K, Nilsen T.N, Ambient Measurements of Amines by PTR-QiTOF: Instrument Performance Assessment and Results from Field Measurements in the Vicinity of TCM, Mongstad, Forthcoming 2017.

[11] IEAGHG “Evaluation of reclaimer sludge disposal from post-combustion CO_2 capture”, 2015/02, March 2014

[12] Gjernes E, Pedersen S, Cents T, Watson G, Fostås BF, Shah MI, Lombardo G, Desvignes C, Flø NE, Morken AK, de Cazenove T, Faramarzi L, Hamborg ES. Results from 30 wt% MEA performance testing at the CO2 Technology Centre Mongstad. Energy Procedia (GHGT-13), Forthcoming 2017.

[13] Flø NE, Faramarzi L, de Cazenove T, Hvidtsten OA, Morken AK, Hamborg ES, Vernstad K, Watson G, Pedersen S, Cents T, Fostås BF, Shah MI, Lombardo G, Gjernes E. Results from MEA degradation and reclaiming processes at the CO_2 Technology Centre Mongstad. Energy Procedia (GHGT-13), Forthcoming 2017.

[14] Davis J, Rochelle G, Thermal degradation of monoethanolamine at stripper conditions, Energy Procedia 1 (2009) 327-333.

Results from MEA Degradation and Reclaiming Processes at the CO_2 Technology Centre Mongstad

(2017)

Available online at www.sciencedirect.com

ScienceDirect

Energy Procedia 114 (2017) 1307 – 1324

Energy Procedia

13th International Conference on Greenhouse Gas Control Technologies, GHGT-13, 14-18 November 2016, Lausanne, Switzerland

Results from MEA Degradation and Reclaiming Processes at the CO_2 Technology Centre Mongstad

Nina Enaasen Flø[a], Leila Faramarzi[a,b], Thomas de Cazenove[a], Odd Arne Hvidsten[a,b], Anne Kolstad Morken[a,b], Espen Steinseth Hamborg[a,b,]*, Kai Vernstad[c], Guillaume Watson[d], Steinar Pedersen[b], Toine Cents[e], Berit F. Fostås[b], Muhammad Ismail Shah[a,f], Gerard Lombardo[a,f], Erik Gjernes[f]

[a]*CO_2 Technology Centre Mongstad, 5954 Mongstad, Norway*
[b]*Statoil ASA, PO Box 8500, 4035 Stavanger, Norway*
[c]*SINTEF, Strindveien 4, 7034 Trondheim, Norway*
[d]*Shell Global Solutions International B.V., PO Box 663, 2501CR The Hague, The Netherlands*
[e]*Sasol Technology, PO Box 5486, Johannesburg 2000, South Africa*
[f]*Gassnova SF, Dokkvegen 10, 3920 Porsgrunn, Norway*

Abstract

In 2015, the CO_2 Technology Center Mongstad (TCM DA), operated a test campaign using aqueous monoethanolamine (MEA) solvent at 30 wt%. The main objective was to demonstrate and document the performance of the TCM DA Amine Plant located in Mongstad, Norway. As part of the test campaign, thermal reclaiming was performed in order to eliminate accumulated degradation products and improve the solvent performance. This paper presents results and discussions concerning formation and monitoring of amine degradation products along with experiences related to the thermal reclaiming process and its operational procedure. Evaluations of the efficiency of thermal reclaiming and the solvent improvement after reclaiming are also presented.

© 2017 The Authors. Published by Elsevier Ltd. This is an open access article under the CC BY-NC-ND license (http://creativecommons.org/licenses/by-nc-nd/4.0/).

Peer-review under responsibility of the organizing committee of GHGT-13.

Keywords: Thermal reclaiming; degradation monitoring; MEA reclamation; MEA degradation

---

* Corresponding author. Tel.: +47 56 34 52 20
E-mail address: eham@tcmda.com

1876-6102 © 2017 The Authors. Published by Elsevier Ltd. This is an open access article under the CC BY-NC-ND license (http://creativecommons.org/licenses/by-nc-nd/4.0/).

Peer-review under responsibility of the organizing committee of GHGT-13.
doi:10.1016/j.egypro.2017.03.1899

1. Introduction

The CO_2 Technology Centre Mongstad (TCM DA) is located next to the Statoil refinery in Mongstad, Norway. TCM DA is a joint venture set up by Gassnova representing the Norwegian state, Statoil, Shell, and Sasol. The facility run by TCM DA entered the operational phase in August 2012 and it is one of the largest post-combustion CO_2 capture test centres in the world. A unique aspect of the facility is that either a flue gas slipstream from a natural gas turbine based combined heat and power (CHP) plant or an equivalent volumetric flow from a residual fluidized catalytic cracker (RFCC) unit can be used for CO_2 capture. The CHP flue gas contains about 3.5% CO_2 and the RFCC flue gas contains about 13-14% CO_2. One of the main test plants at TCM DA is a highly flexible and well-instrumented amine plant. The amine plant was designed and constructed by Aker Solutions and Kværner to accommodate a variety of technologies, with capabilities of treating flue gas streams of up to 60,000 standard cubic meters per hour. The plant is being offered to vendors of solvent based CO_2 capture technologies to, among others, test; (1) the performance of their solvent technology, and (2) technologies aimed to reduce the atmospheric emissions and environmental impact of amines and amine based degradation products from such solvent based CO_2 capture processes. The objective of TCM DA is to test, verify, and demonstrate CO_2 capture technologies suitable for deployment at full-scale. Up to now the vendors Aker Solutions, Alstom, Shell Cansolv Technologies Inc. and Carbon Clean Solutions Ltd. have successfully used the TCM DA facilities to verify their CO_2 capture technologies.

From July to October 2015 TCM DA, in collaboration with partners, operated a test campaign using the non-proprietary aqueous monoethanolamine (MEA) solvent at 30 wt%. After testing a variety of process conditions for a total of 1843 hours, clear evidence of solvent degradation was observed. The test campaign proceeded with thermal reclaiming of the solvent in order to eliminate accumulated degradation products and demonstrate improvement of solvent performance. This work presents results concerning MEA degradation monitoring and reclaiming operation at TCM DA. Various design and operational factors that affect degradation rates are discussed, the efficiency of thermal reclaiming is estimated and experiences related to the reclaiming process and its operational procedure is shared.

1.1. Solvent degradation mechanisms

Amine solvents degrade due to exposure to heat (thermal degradation), presence of oxygen (oxidative degradation) and reactions of the amine with flue gas contaminants such as SO_x, NO_x, halogenated compounds, hydrocarbons and other impurities. Thermal degradation occurs mainly in the stripper section and is strongly dependent on the stripper operating temperature. The main thermal degradation products in MEA are Oxazolidin-2-one (OZD), MEA urea, HEIA, HEEDA [1]. The rate of formation of these products depend on the operating temperature (faster kinetics), CO_2 loading (more carbamate present) and MEA concentration. Oxidative degradation is mainly an issue for post-combustion CO_2 capture where the solvent is exposed to oxygen present in the flue gas. This occurs mainly in the absorber, where the level of oxygen is significant. Amine oxidation is also shown to be catalyzed by transition metal ions and will typically results in formation of ammonia and different organic acids [2]. In a second step, the organic acids will form heat stable salts (HSS) which are difficult to regenerate under normal regeneration conditions (atmospheric pressure and temperature around 120°C) [1]. These salts will therefore remain and accumulate in the circulated solvent. Amine degradation may also be induced by flue gas contaminants such as sulfur, polysulfide and CO. This issue has become especially evident for oil refinery flue gases such as gas originating from RFCC units [2]. Nonvolatile contaminants causing amine degradation can also arise from other sources such as make-up water, anti-foam agents, lubricants and corrosion inhibitors [2].

Several degradation processes often occur simultaneously to produce a wide range of degradation products. Accumulation of amine degradation products affects the solvent properties. They are known to increase the solvent viscosity and surface tension which again affects heat transfer coefficients, diffusion coefficients, and mass transfer rates [3]. This will again lead to loss of solvent capacity and increased energy numbers. Further, degradation products might lead to corrosion, fouling and foaming [2], which again increases operational and maintenance costs and might cause long-term technical integrity issues. Dissolved metal elements originating from corrosion are also as mentioned above expected to contribute as catalysts for oxidative degradation [1].

1.2. Solvent refreshing options

In order to reduce the impact of unwanted impurities and minimize the operational and maintenance issues listed above, a number of techniques have been suggested. Wang et al. (2015) have published an extensive review of amine reclaiming technologies and other techniques to handle this issue, including purging (bleed and feed), neutralization, ion exchange, adsorption, electrodialysis, and different thermal reclamation techniques [4]. Dumée et al. (2012) also presents a thorough comparison of the most promising techniques [1]. A summary is provided below.

- **Bleed and feed**

Bleed and feed is a simple operational procedure where a portion of the degraded solvent is continuously or periodically purged and replaced with fresh solvent. However, amine replacement and disposal might make this technique rather costly, particularly for specialized and expensive solvents. Further, a certain level of degradation products needs to build up before effecting bleed and feed in order to minimize replacement and disposal costs.

- **Neutralization**

Neutralization converts amine HSS to sodium or potassium HSS by addition of NaOH or KOH, according to the following reaction using NaOH as an example:

$$\text{NaOH} + [\text{AmineH}^+\ \text{RCOO}^-] \rightarrow \text{Amine} + \text{H}_2\text{0} + [\text{Na}^+\ \text{RCOO}^-] \qquad (1)$$

Neutralization maintains the amine capacity; however, there is no reduction in salt content of the solvent. The amine becomes more and more contaminated by salts that contribute to higher solvent density and viscosity, reduced surface tension, and possibly foaming and fouling. Eventually, the solvent needs to be discarded.

- **Ion exchange**

Ion exchange is a technology where the amine HSS ion is replaced with a friendlier ion. For example, an anion exchange removes HSS anions, replacing them with hydroxide ions, which frees the amine and let it return together with water to the process. The HSS anions are later removed from the resin by regeneration with NaOH. The practice of removing HSS from amine systems by ion exchange has presented many technical and operational challenges, and several researchers report doubt in the practical efficiency for amine applications. High consumption of chemical and water for resin regeneration together with generation of large amounts of waste are mentioned as other disadvantages. Further, ion exchangers are not capable of removing uncharged contaminants, i.e. degradation products originating from thermal degradation. It is still regarded a relatively economical method, especially for low levels of contaminants. However, if poorly designed and/or operated it can cause significant solvent losses and sodium slippage into the main amine process.

- **Adsorption**

Adsorption on activated carbon is a widely used method to remove high-boiling or surface active organic compounds [5]. However, activated carbon it is not able to remove significant amount of degradation products [2].

- **Electrodialysis**

Electrodialysis has also been suggested as a method to purify amine solutions. It uses a stack of alternating anionic and cationic ion-exchange membranes to selectively remove charged contaminants from the solvent [1]. The main disadvantage also for this method is inability to remove uncharged amine degradation products originating from thermal degradation and hydrocarbons [2].

- **Thermal reclaiming**

Thermal reclaiming is usually conducted on a small slipstream extracted from the stripper reboiler on a semi-continuous basis [2, 5]. The amine solution is vaporized in the reclaimer vessel and returned as vapour to the main process, while the less volatile degradation products and other contaminants accumulate in the reclaimer vessel bottoms. Stoichiometric addition of NaOH during thermal reclaiming allows recovery of the amine from the amine heat stable salts by conversion to sodium salts, according to Reaction (1). Thermal reclaiming has long been a recognized reclamation method for MEA. Compared with secondary and tertiary amines, MEA has a low normal boiling point allowing it to vaporize without degrading significantly. For other amines with higher boiling points vacuum might be required in order to prevent thermal degradation during reclaiming. The fact that MEA reclaiming units can be operated at the stripper pressure eliminates the need for a separate condenser for the reclaiming system and reduces the overall energy demand. In this approach the reclaimer product vapour which contains MEA is directly sent to the stripper [1, 5]. A major disadvantage of thermal reclaiming is the formation of an aqueous slurry waste whose disposal poses a challenge for the CO_2 capture process. The amount of waste depends on various parameters such as the flow rate of the slip stream fed to the reclaimer, the amount of basic solution used to liberate

MEA from heat stable salts, solvent conditions and overall operating conditions of the plant. According to the International Energy Agency (IEA) about 3.2 kg of amine reclaimer waste is generated per ton of CO_2 captured from coal fired flue gases using MEA [3]. However, depending on gas pre-treatment, combustion fuel, the type of amine used and the capture process itself, the reclaimer waste generation can vary in the range of 0.1-14.9 kg waste/ ton CO_2 [3]. Collecting representative samples of reclaimer waste is complicated and so far there is limited information in the public domain that fully represents amine reclaiming waste for CO_2 capture processes. Using the Flour Econamine FG^{SM} system as a reference, Nurrokhmah et al. (2013) have investigated methods to characterize MEA reclaiming waste along with possible waste treatment and reuse options. Thermal reclaiming is also mentioned to be energy extensive. However, alternative reclaiming technologies such as ion exchange and electrodialysis are not able to remove metals and non-ionic products and the potential efficiency of HSS removal is not as high as for thermal reclaiming [1].

Nomenclature

CHP	Combined Heat and Power
DCC	Direct Contact Cooler
HSS	Heat Stable Salts
IBC	Intermediate Bulk Container
IEA	International Energy Agency
MEA	Monoethanolamine
MP	Medium Pressure
RFCC	Residue Fluidized Catalytic Cracker
SRD	Specific Reboiler Duty
TCM	CO_2 Technology Centre Mongstad

2. The TCM DA amine plant

An illustration of the TCM DA amine test unit is presented in Figure 1, and a short description is given in the following. Flue gas is cooled down and saturated with water in a direct contact cooler (DCC) before it enters the absorber. At TCM DA there are two possible sources of flue gas, i.e. exhaust gas originating from the natural gas fired combined heat and power plant and industry gas originating from the residue fluidized catalytic cracker. Both flue gas sources have their individual flue gas fans and DCCs as illustrated in Figure 1. Product CO_2 can also be recirculated back to the CHP gas absorber inlet to adjust the CO_2 content. For RFCC gas there is an option of mixing in air to adjust the CO_2 content. The conditioned flue gas is contacted counter-currently with the amine solvent in the absorber tower. CO_2 from the flue gas is absorbed yielding a solvent rich in CO_2 and a depleted flue gas with low CO_2 content. The depleted flue gas is released to the atmosphere after passing two sections of water wash. Typical absorber conditions are close to ambient pressure and temperatures of 40 - 80 °C, depending on the CO_2 content in the incoming flue gas. The CO_2 rich solvent is pre-heated in the lean/rich cross heat exchanger before it enters the stripper column where the chemical reactions are reversed to desorb CO_2 and regenerate the solvent. Heat is provided through steam in a thermosiphon reboiler to maintain regeneration conditions, i.e. 100 - 120 °C and pressure around 1 barg. The product CO_2 is released to the atmosphere, while the regenerated lean solvent is pumped back to the absorber via the lean/rich cross heat exchanger and the lean cooler.

The TCM DA amine test unit is also equipped with a thermal reclaimer which treats a slip stream of the lean solvent coming from the stripper. The thermal reclaimer uses additional heat provided by steam to separate the useful solvent from the degradation products which are accumulated in the solvent over time. The reclaimer vapour contains useful solvent which is recycled back to the main process, while the waste remains in the reclaimer and is periodically discharged. Water and NaOH can be added to the reclaimer unit on demand. The operating pressure corresponds to the stripper pressure.

The reclaiming system consists of a flash vessel and a steam heater, as illustrated in Figure 1. The dimensions of the reclaimer vessel is 2.3m x 3.0 m (IDxTT) and it is designed for an operating volume of 1 – 7 m^3, which corresponds to approximately 2 – 14 % of the total solvent inventory of the plant.

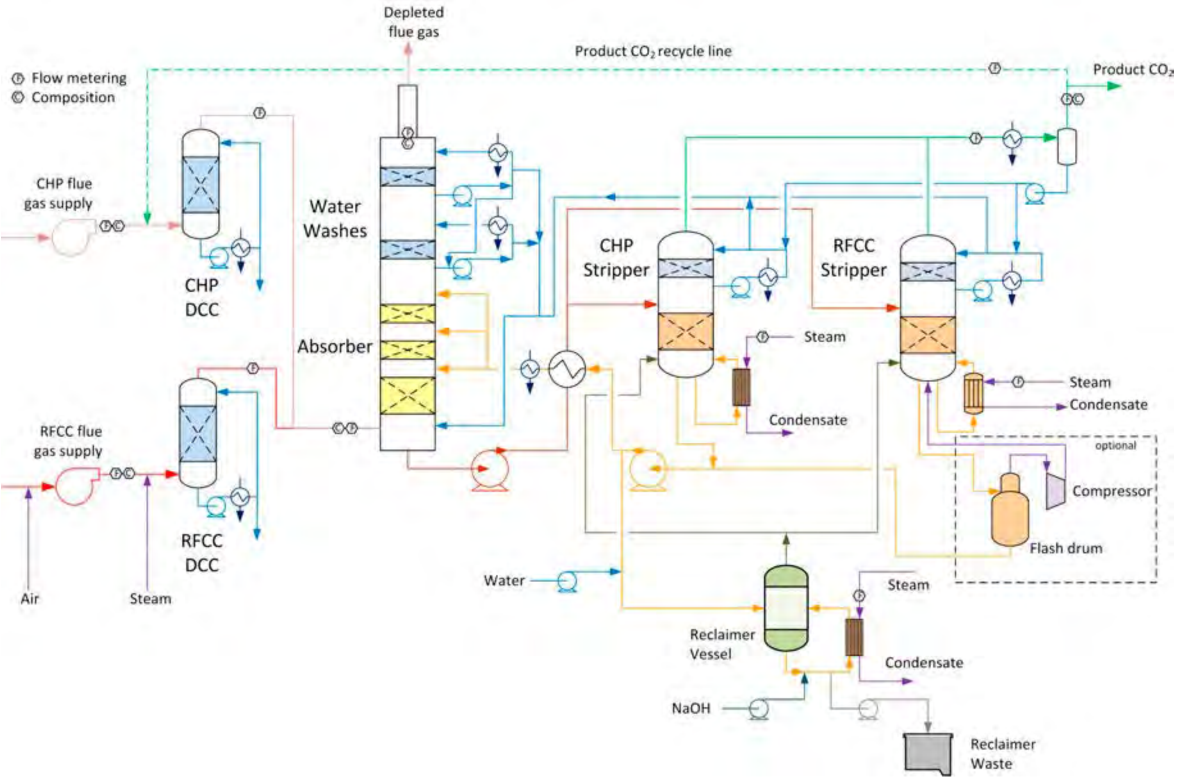

Figure 1: Schematic illustration of the TCM DA amine plant

2.1. MEA campaign overview

The MEA test campaign was conducted from 06/07/2015 to 17/10/2015. During the total 1960 hours of operation a wide range of operational process conditions were executed and a total of 4941 tons of CO_2 was captured. The variation of gas and solvent flow rates and stripper bottom temperatures are presented in Figure 2, while further details on typical operating process conditions are presented in Table 1 of Gjernes et al. (2017) [7]. The test campaign was operating on 30 ± 2 wt% MEA and the ranges of the lean and rich CO_2 loadings during the campaign was 0.19 - 0.29 and 0.46 - 0.53 mol CO_2/mol MEA, respectively. The majority of the campaign was operated with CHP flue gas; however, for a shorter period of 9 days from 16/09/2015 to 24/09/2015 it was operated on a mixture of CHP and RFCC gas, as indicated in Figure 2. Thermal reclaiming was performed towards the end of the campaign, after 1838 hours of operation. Reclaiming was performed for 92 hours, and the plant was run for an additional 28 hours after the reclaiming period before the campaign was concluded 17/10/2015.

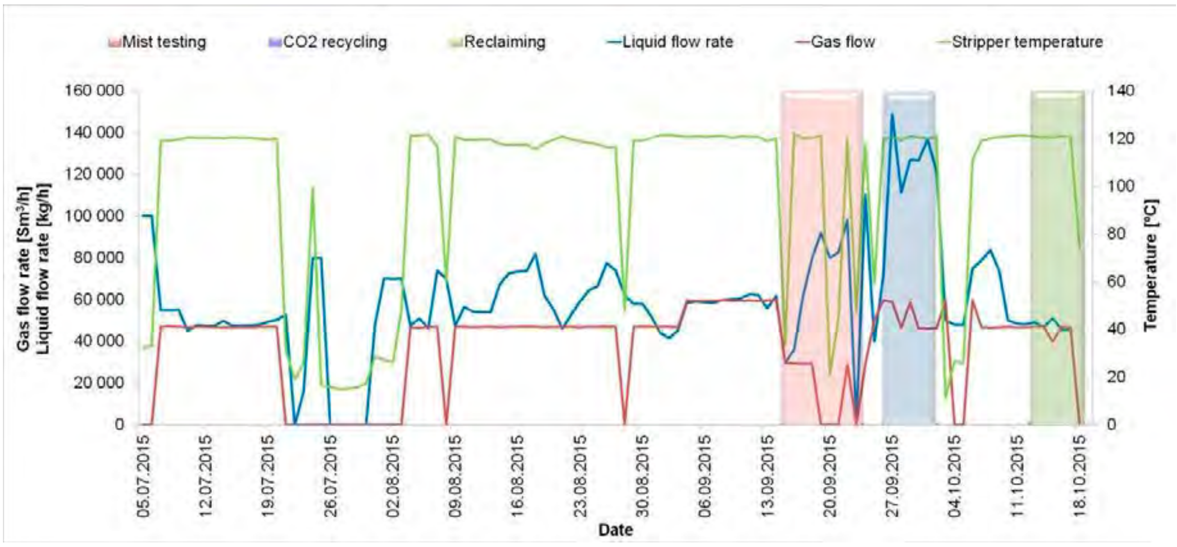

Figure 2: Overview of the daily gas and solvent flow rates and stripper temperatures during the MEA test campaign

3. Solvent degradation during the test campaign

3.1. Process conditions that influenced solvent degradation

The MEA test campaign was conducted by executing a wide range of process conditions with frequent operational set-point changes. Such a shifting operating environment might accelerate solvent degradation. The average stripper bottom temperature was 120 °C, with a maximum of 122.5 °C. Superheated MP steam in the temperature range of 130 - 150 °C was used as heat source in the stripper reboiler. The reboiler skin temperature for which the solvent is exposed to, can therefore be assumed to be around 130°C. The solvent will undergo thermal degradation when exposed to temperatures at this level.

The majority of the campaign was operated with CHP flue gas. However, as part of specific mist testing where the aim was to induce formation of aerosols and study its effect on emissions, the plant was operated on a mixture of CHP and RFCC gas [8]. The mist testing where more specifically conducted by;

1. Increasing the concentration of CO_2 in the feed flue gas up to 12 vol% by recycling parts of the captured CO_2 to the absorber flue gas inlet.
2. Mixing portions of the RFCC flue gas with the CHP flue gas.

Up to 10 % mixing of RFCC gas in CHP gas was tested. Typical CHP and RFCC gas concentrations downstream the DCCs are presented in Table 1. As seen in the table, the CHP flue gas contains significant amounts of oxygen which causes oxidative degradation. Exposure to higher concentrations of CO_2 and RFCC gas impurities during the mist testing accelerated the rate of solvent degradation. Further, metal particulate material present in the RFCC gas might have contributed as catalysts for oxidative degradation.

Table 1: Typical CHP and RFCC flue gas conditions downstream DCC conditioning at TCM DA.

Description	Unit	Conditioned CHP gas	Conditioned RFCC gas
Temperature	°C	25 - 50	15 - 50 (1)
Pressure	mbar g	Up to 250	Up to 250
Nitrogen	mol %	73 - 79	73 - 79
Oxygen	mol %	13 - 14	3 - 8
CO_2	mol %	3.5 - 4.0 (2)	13.0 - 14.5 (3)
H_2O	mol %	Saturated	Saturated
SO_2	ppmv	<0.3	<5
NO_x	ppmv	<5	60
NH_3	ppmv	<5	<1
CO	ppmv		<3
Particulates	mg/Nm^3		(4)

Note:

1. With steam injection.
2. Facility is provided to enable CO_2 recycling, thereby allowing tests with CO_2 concentrations up to about 15 vol%.
3. Facility is provided to enable air dilution, thereby allowing tests with CO_2 concentrations down to about 2.5 vol %.
4. H_2SO_4: 10-25 mg/Sm^3; Other soluble salts $(NH_4)_2SO_4$+NH_4HSO_4+NaCl: 5-10 mg/Sm^3; Non water soluble salts SiO_2+Ca and other metals: 0-2 mg/Sm^3

3.2. The impact of process design on solvent degradation

As mentioned above, the main factors causing solvent degradation was elevated operating temperature in the stripper section and exposure to oxygen and contaminants in the flue gas. The effect of thermal and oxidative degradation will not only depend on these factors themselves, but also on the solvent residence times in the sections of the plant where these factors are significant, i.e. the part of the plant where the solvent is exposed to higher temperatures and oxygen and gas contaminants.

The hot solvent inventory (desorber packing, desorber sump, reboiler, hot part of the lean/rich cross heat exchanger and the hot lean and rich solvent piping) calculated for CHP baseline operating conditions are presented in Table 2. For details about the CHP baseline operating conditions it is referred to Faramarzi et al. (2017) [9]. The total of 13.4 m^3 hot solvent inventory is quite significant and corresponds to about 35% of the total solvent inventory. The corresponding solvent residence time is about 20 minutes for CHP baseline operating conditions. The main contributor to the hot solvent inventory is clearly the rather long hot lean solvent pipe, which contributes to 60% of the total hot solvent inventory. The reboiler itself has a rather low solvent residence time; however, the beforementioned reboiler skin temperature of about 130 °C might also contribute to significant thermal degradation as degradation increases exponentially with the temperature.

The solvent inventory exposed to oxygen and the corresponding oxygen exposure time is also presented in Table 2. It is expected that the largest effect of oxygen exposure is seen in the absorber packing, where the actual inventory and exposure time is estimated to about 8 m^3 and 12 minutes, respectively, considering CHP baseline operating conditions. This abovementioned exposure time is also relevant for flue gas contaminants when operating on CHP/RFCC gas mixture.

In order to minimize solvent degradation it is clearly of interest to perform plant design such that the exposure times to oxygen and elevated temperatures are limited. For scale-up purposes it is therefore of specific importance to minimize solvent hold-up in hot parts of the plant.

Table 2: Estimated solvent inventory and residence times for solvent exposed to oxygen and elevated temperatures based on CHP baseline operating conditions (for details about the CHP baseline conditions it is referred to Faramarzi et al (2017) [9].

Section of the plant	Solvent inventory [m^3]		Exposure/residence time [min]	
	Exposed to oxygen	Exposed to temperature > 100°C	Oxygen	Temperature > 100°C
Absorber packing	7.8		11.5	
Absorber sump	9.0		13.3	
Desorber packing		0.9		1.3
Desorber sump		2.3		3.4
Reboiler		0.4		0.6
Lean/rich cross heat exchanger		0.5		0.7
Hot rich solvent piping		1.1		1.6
Hot lean solvent piping		8.2		12.1
Total	16.8	13.4	24.8	19.8

3.3. Monitoring of solvent degradation

Solvent degradation was observed and monitored by a number of parameters during the test campaign. Lean and rich solvent samples were frequently withdrawn for solvent analysis. The analytical methods are described by Morken et al (2017) [10]. Firstly the physical properties of the solvent changed during the campaign as shown by the increase of solvent viscosity in Figure 3. The viscosity was measured in TCM DA lab and reported at two different temperatures (30°C and 60°C) and a clear increase of about 50% is observed from the test campaign start until reclaiming started on 12/10/2015.

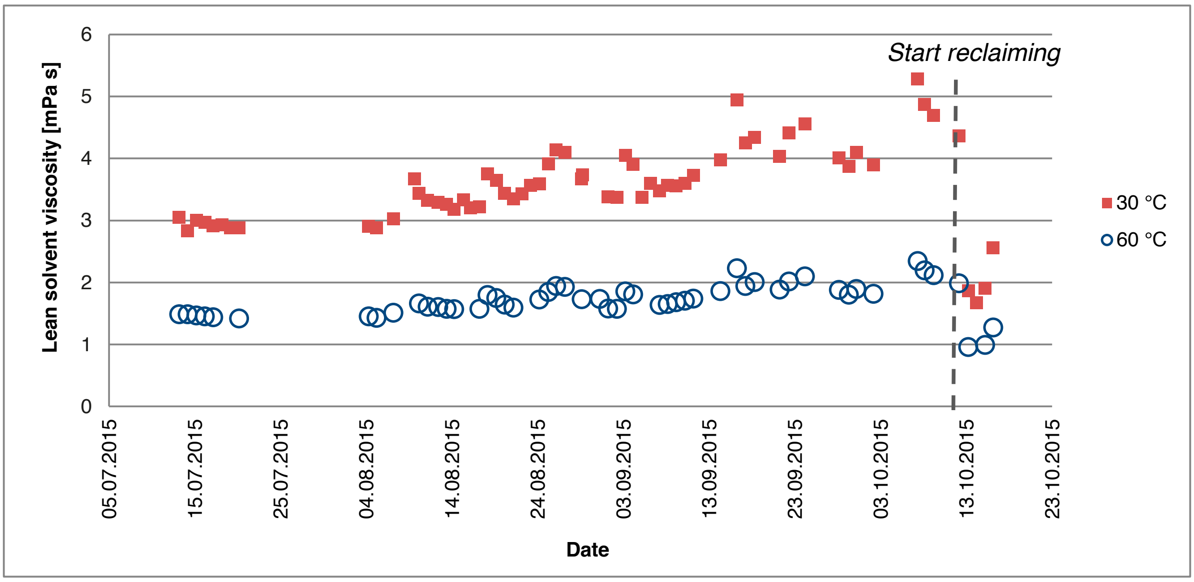

Figure 3: Change in solvent viscosity during the MEA test campaign

A clear observation of solvent degradation was also the change of solvent color during the test campaign. The fresh 30 wt% MEA solvent started out as a clear liquid, which changed color quite fast after contact with flue gas. The solvent became gradually darker during the campaign, until it reached the dark brown color illustrated by the third sample glass from 11/10/2015 in Figure 4.

Figure 4**:** Picture of solvent samples taken during the campaign. The color change indicates solvent degradation.

Further, the level of volatile degradation products in the gas phase increased significantly during the period of Mist testing. Morken et al (2017) presents detailed results regarding ammonia emissions, which is associated with presence of ammonia in the solvent originating from solvent degradation [10]. Emission of ammonia is also highly dependent on operating conditions; however the observed build-up of ammonia in the solvent is regarded as a clear sign of solvent degradation.

Heat stable salts started building up in the solvent as shown in Table 3 before it reached a maximum of 0.203 mol/kg just before reclaiming started on 12/10/15. More detailed results concerning HSS analysis are presented by Morken et al (2017) [10]. The concentration of main degradation products was also monitored continuously and shows a significant increase as the test campaign progressed. It is referred to Morken et al (2017) for details [10].

Table 3: Total concentration of heat stable salts (HSS) during the campaign.

Date	Concentration of heat stable salts (HSS) [mol/kg]
13.07.2015	0.011
20.07.2015	0.038
10.08.2015	0.052
17.08.2015	0.069
24.08.2015	0.083
31.08.2015	0.120
07.09.2015	0.108
14.09.2015	0.141
21.09.2015	0.149
28.09.2015	0.138
12.10.2015	0.203

Additional parameters which are important to monitor during operation of the amine plant are solvent foaming tendency and metal ion concentration. The latter gives indications of plant corrosion and was also monitored during the test campaign. The results are presented by Hjelmaas et al. (2017) [11].

4. Reclaiming procedure and operational experience.

The reclaimer was operated in a semi-continuous operation mode, meaning that solvent was continuously fed to the reclaimer vessel, while the reclaimer waste was allowed to accumulate and was only disposed at the end of the test campaign. The process was operated continuously for 3 days with exception of one unexpected plant stoppage for about 3 hours on the 13/10/2015.

The reclaimer vessel was initially filled with water. Water circulation and steam heating was started before the solvent feed to the reclaimer vessel. The rather large volume of initial water evaporated during the reclaiming operation and resulted in dilution of the solvent as shown in Figure 5.

The reclaimer liquid was circulated in the reclaiming system loop through the steam heat exchanger at a circulation rate of approximately 165 m^3/h. No boiling occurs in the steam heater, but the liquid flashes when it enters the evaporator vessel. The evaporating level was controlled by adjusting the steam rate supply. As the liquid became more concentrated, its boiling temperature increased and the rate of evaporation was reduced. The percentage of degradation products in the reclaimer, and the resulting temperature were slowly increasing. Upon reaching high temperature, high viscosities and high amounts of precipitates, the reclaimer feed was stopped.

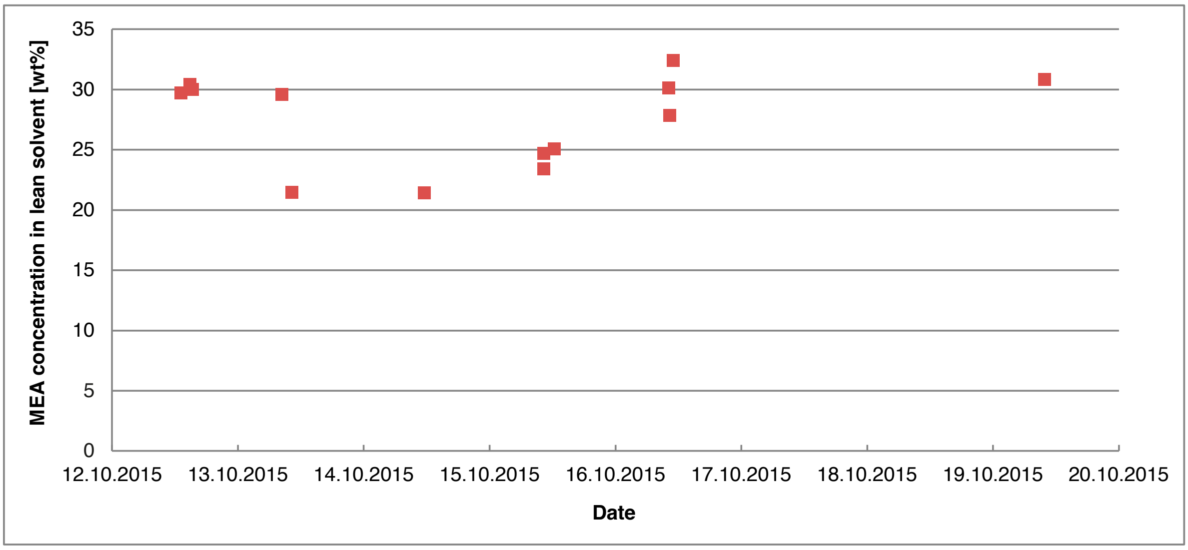

Figure 5: MEA concentration in the lean solvent during reclaiming

4.1. Solvent and water feed rate.

The reclamation unit was fed with a continuous slip stream of the lean amine solvent from downstream the stripper. The reclaimer was also fed simultaneously with water in order to control the boiling temperature of the reclaimer fluid below 160 °C. Figure 6 presents the solvent and water flow rates along with the reclaimer liquid temperature.

The solvent slip stream corresponded to 4 - 5 % of the lean solvent circulation and was up to a maximum of about 3 000 kg/h as illustrated in Figure 6. A total accumulated amount of 46 000 kg solvent was fed to the reclaimer during the whole period of 3 days. This corresponds to about 110 % of the total solvent inventory.

4.2. Steam consumption

The reclaimer heat duty variations were according to the changing amount of the lean solvent slip stream directed to the reclaimer vessel. As shown in Figure 7, in order to vaporize MEA in the reclaimer a significant amount of heat was required. At times, the amount of heat used for reclaiming was almost equal to the heat used to regenerate the solvent in the stripper. As reclamation of MEA is energy intensive, it is important to optimize the amount of lean amine slip stream sent to the reclamation unit. However, as shown in Figure 6 the flow of slip stream varied due to the fluctuations in the process conditions and it was not possible to achieve a constant flow during the reclaiming procedure.

The reboiler heat duty increased significantly when the reclaimer was brought on stream and then plateaued at about 2 500 kW. This was due to the large amount of water that was initially added to reclaimer unit, which evaporated from the reclaiming vessel and caused dilution of the solvent. The concentration of MEA was consequently reduced to about 21 wt% as shown in Figure 5. Thus the amount of water to be boiled off in the stripper was much larger, causing higher energy numbers.

The reclaimer liquid circulation and steam heating continued for 2 days after the solvent feed was stopped in order to evaporate as much as possible of the useful MEA solvent and concentrate the waste.

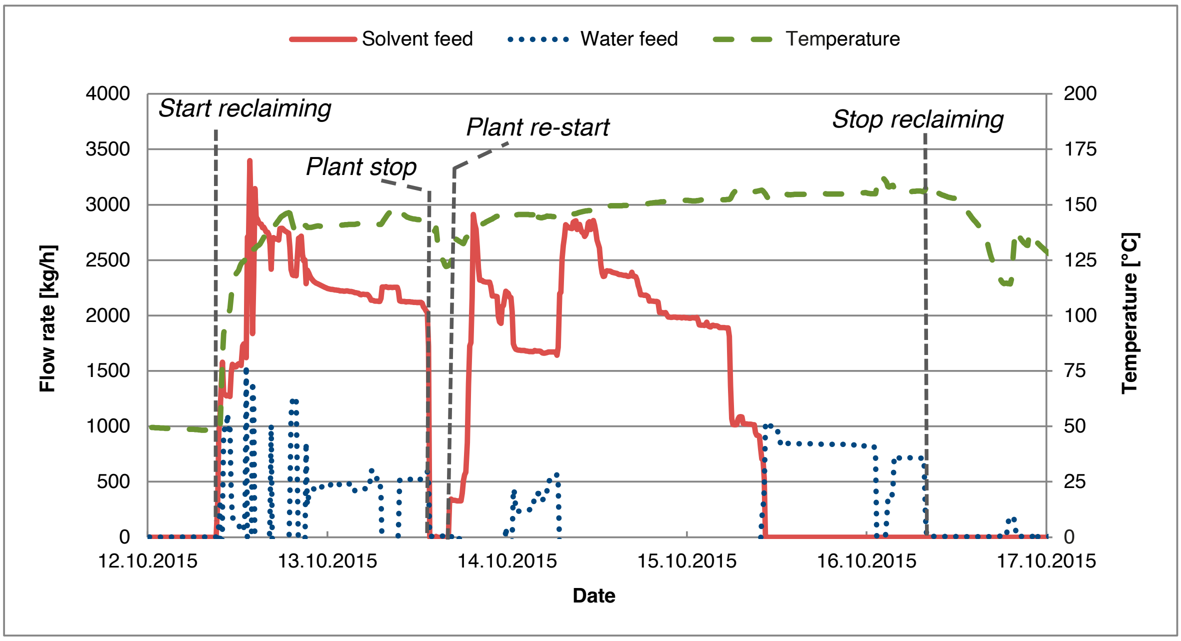

Figure 6: Reclaimer solvent slip stream, water feed rate and reclaimer liquid temperature.

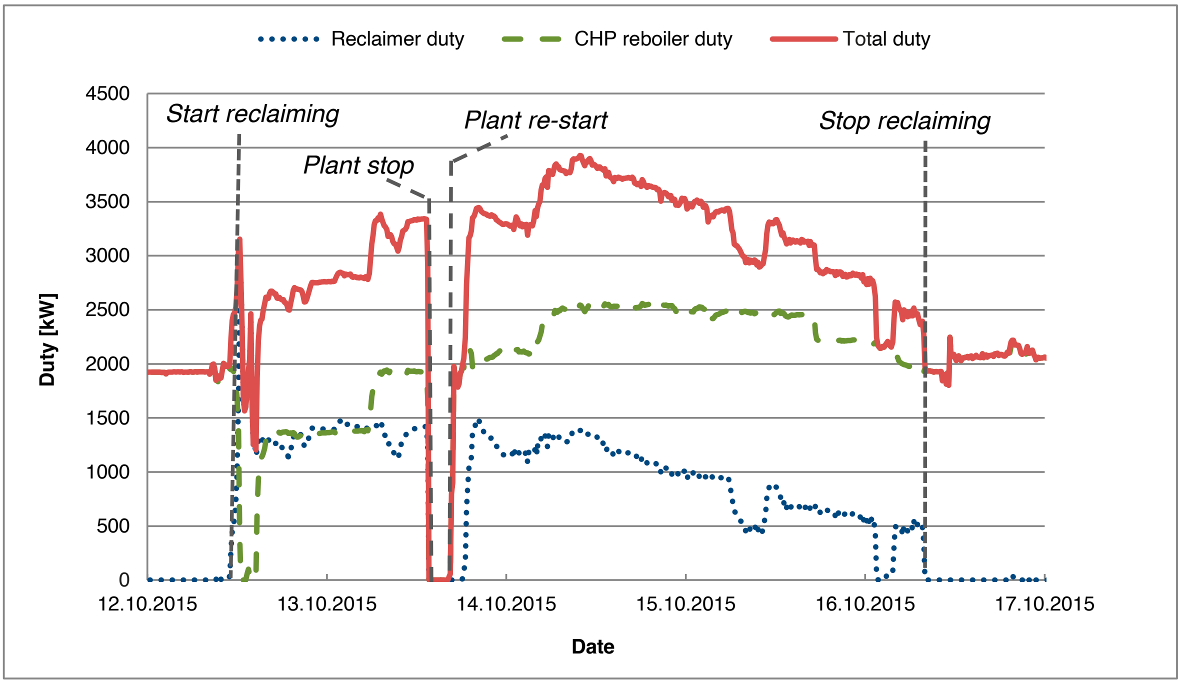

Figure 7: Steam consumption during reclaiming.

4.3. Dosage of NaOH

Aqueous solution of 50 wt% NaOH was added to the reclaimer vessel via the reclaimer liquid circulation loop in order to stabilize anions of amine heat stable salts by converting them to sodium salts and liberating the amine according to Reaction (1). The recovered amine and water vapor was returned to the stripper sump.

A dosage rate of 3 L NaOH/m^3 solvent was applied during reclaiming based on previous experience at TCM DA. In total 227 liters 50% NaOH was added, which corresponds to 4299 mol Na^+.

According to Reaction (1), the stoichiometric ratio of NaOH to HSS should ideally be 1:1. This is a very rough estimate since the actual ratio depends on the electrical charge of the anions. The concentration of HSS components was 0.203 mol MEA-eq/kg solvent at the point of reclaiming start 12.10.15 (see Table 3). With a total solvent inventory of 40 800 kg in the plant at the time, this corresponds to 8282 mol HSS. A stoichiometric check shows excess HSS compared to NaOH, which might cause additional MEA loss in the reclaimer waste.

4.4. Reclaimer waste

After the reclaiming operation was concluded the majority of the concentrated waste was drawn off to the flushing line and passed through the sea water cooler to the IBC (Intermediate Bulk Container) drainage system. The reclaimer fluid was quite concentrated and viscous at the time, thus some water was added in order to dilute the waste and enable unloading of the vessel. The total concentrated waste was collected in IBCs and added up to a total of about 6 m^3. This corresponds to about 1.3 kg reclaimer waste/ton CO_2 captured during the overall campaign, which is well below reported numbers in the literature. Further, the reclaiming process was initiated when HSS concentration reached 0.203 mol/kg, as beforementioned. The actual necessity of reclaiming at this level of HSS must be considered based on the actual solvent condition and potential plant corrosion issues, i.e. at this moment the reclaiming campaign was not necessary but rather conducted for demonstration purposes in the test campaign. The waste/ton CO_2 capture would thus be even lower in an actual necessary reclaimer case. The reclaimer vessel and piping was afterwards flushed with water.

5. Efficiency of thermal reclaiming

In order to investigate the reclaiming efficiency and demonstrate how the solvent quality is recovered and maintained by the reclaiming process, samples were frequently taken from the lean amine solvent, the reclaimer liquid and reclaimer vapor. The samples were analyzed for MEA, degradation products, HSS and metals, and the results are summarized in Table 4.

The concentration of degradation products in lean amine was analyzed throughout the test campaign and the results are presented by Morken et al (2017) [10]. Figure 8 below shows the concentration of degradation products in the lean amine solvent during the reclaiming operation. It is seen that the degradation products is efficiently cleaned from the lean amine and about 95% percent of the degradation products was removed. A small increase in concentration from day three indicates that degradation is significant during reclaiming, likely due to thermal degradation due to operation at elevated temperatures inside the reclaimer vessel.

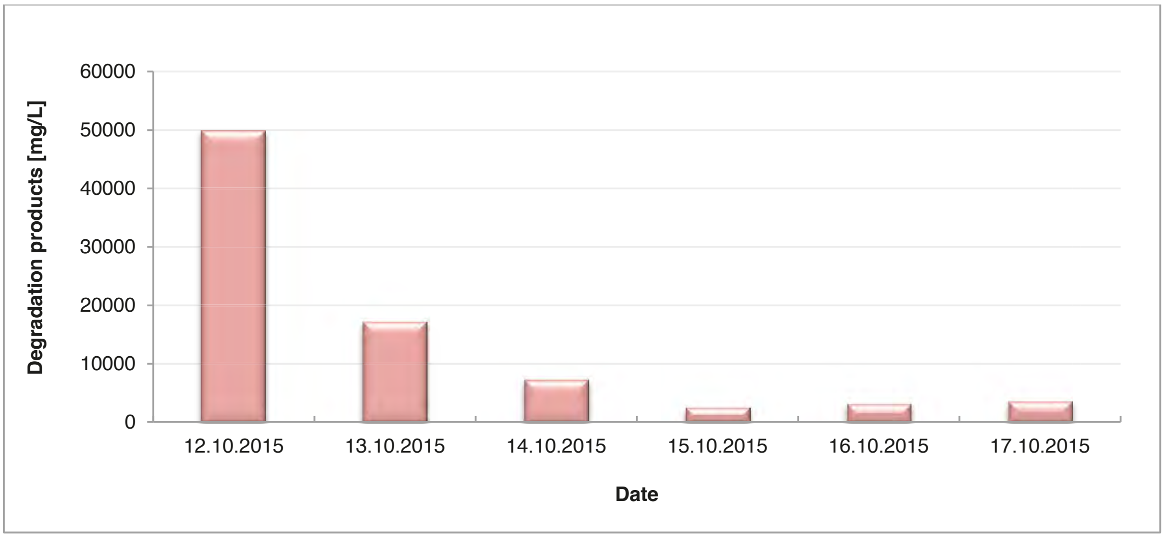

Figure 8: Concentration of degradation products (D-mix) in lean amine during reclaiming

A very similar trend is seen for the concentration of metal elements iron (Fe), Nickel (Ni) and Chromium (Cr) in Figure 9 below. The concentration is reduced by more than 95% after reclaiming.

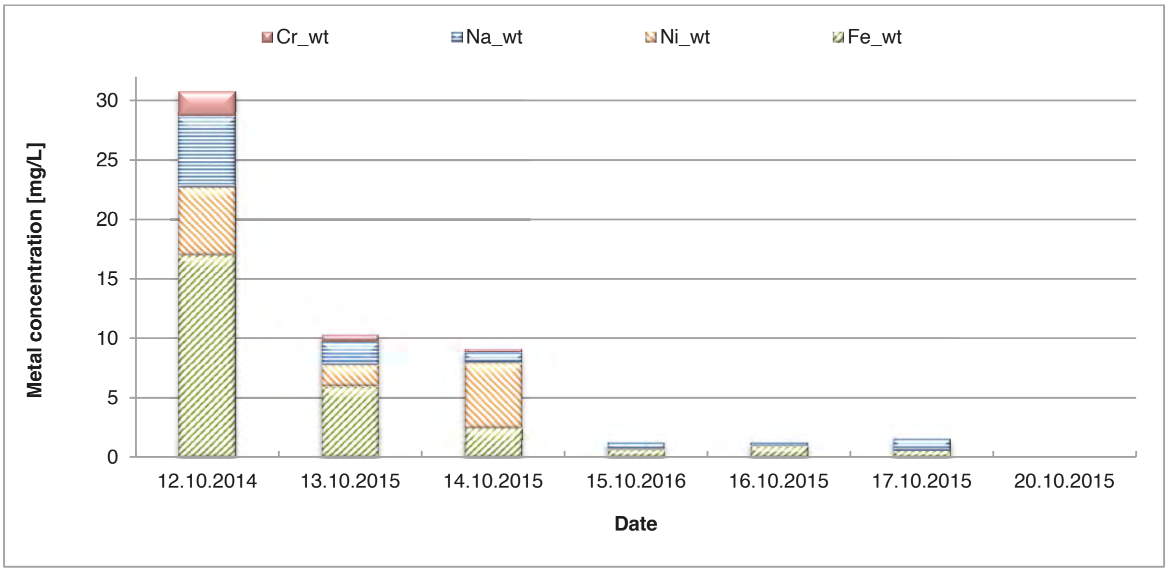

Figure 9: Concentration of metal elements in lean amine during reclaiming

The trends for heat stable salts in the lean solvent, reclaimer liquid and the reclaimer vapor are shown in Figure 10. Again, the concentration of HSS in lean amine is rapidly reduced to less than 5% of the start concentration, as shown by the blue columns in the graph. The accumulation of HSS in the reclaimer liquid is also clearly seen by the red columns. HSS could not be detected in the reclaimer vapor return to stripper, as expected. Figure 11 presents the concentration of MEA, NaOH and HSS in the reclaimer liquid during the reclaiming process. Most of the MEA is evaporated during the period as seen in the figure. HSS and Na^+ is accumulated, however MEA seems to be in excess, also at the end of the reclaiming.

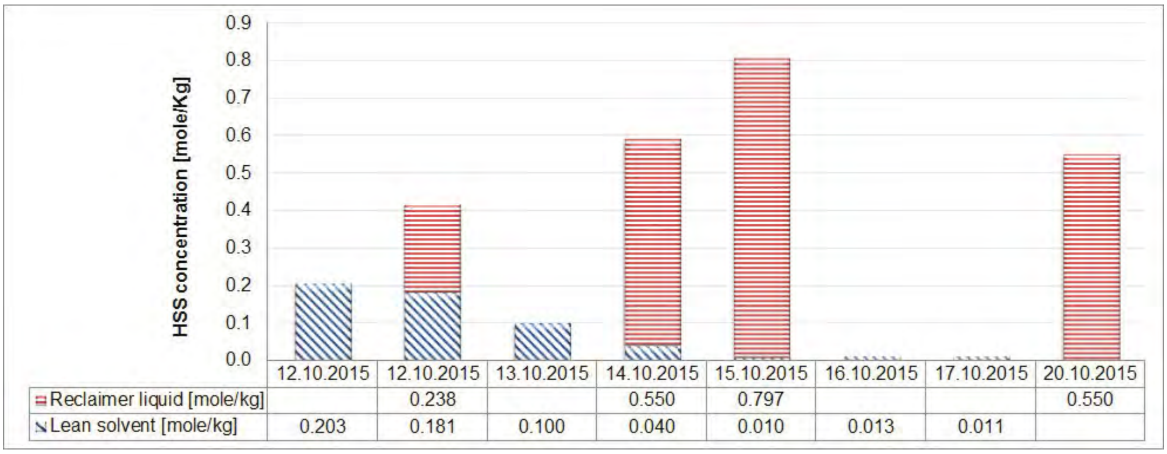

	12.10.2015	12.10.2015	13.10.2015	14.10.2015	15.10.2015	16.10.2015	17.10.2015	20.10.2015
Reclaimer liquid [mole/kg]		0.238		0.550	0.797			0.550
Lean solvent [mole/kg]	0.203	0.181	0.100	0.040	0.010	0.013	0.011	

Figure 10: Concentration of HSS in lean amine and the reclaimer liquid

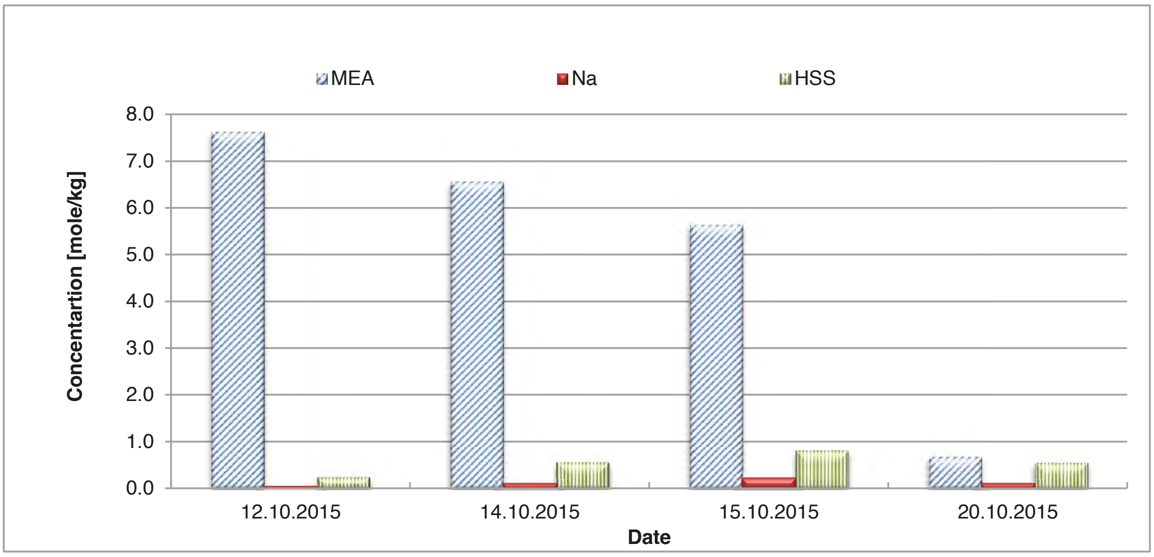

Figure 11: Concentration of MEA, NaOH and HSS in the reclaimer liquid

The color of the solvent changed back to a lighter color after reclaiming as illustrated by the fifth sample glass from 15/10/2015 in Figure 4. Based on analysis of the reclaimer waste and assessment of the total MEA inventory in the plant before and after reclaiming, it is estimated that about 500-550 kg MEA was lost to waste during reclaiming. This corresponds to 4% of the total inventory (according to Table 4) and 0.11 kg MEA/ton CO_2 captured.

Table 4: Amount of HSS, degradation products and metals removed from the solvent and MEA lost in reclaimer waste

		12.10.2015 Before reclaiming	17.10.2015 After reclaiming	Removal
Total solvent inventory	[kg]	40800	37600	
MEA	[kmol]	199	191	4 %
HSS	[mol]	8280	413	95 %
Degradation products	[kg]	1837	129	93 %
Metals	[g]	1133	56	95 %

6. Solvent performance after reclaiming

After the reclaiming operation had been concluded the plant was operated for another 28 hours at a flue gas flow rate of 47,000 Sm^3/h. Two test cases were conducted during this period, and these are used for comparison to other similar tests conducted previously in the campaign with a fresh solvent. The two test cases after reclaiming is designated “T4” and “T5”, while the optimum energy case with the use of anti-foam (case 2B6) from previously in the campaign is used for comparison. The total operating hours at the point in time when case 2B6 was conducted was approximately 950 hours. The overall 2015 MEA campaign and the entire specific test series carried out to investigate the capture plant performance is described by Gjernes et al. (2017) [7].

Figure 12 summarizes the operation before and after reclaiming. T4 and T5 were operated with 24 and 18 m absorber packing height, respectively. During T4 the amine plant was a bit unstable while there were stable conditions during T5. Case 2B6 was operated with 24 meters of packing height. The plant performance after reclaiming was comparable to the optimum performance achieved earlier in the campaign and there were no significant indications of reduced solvent quality.

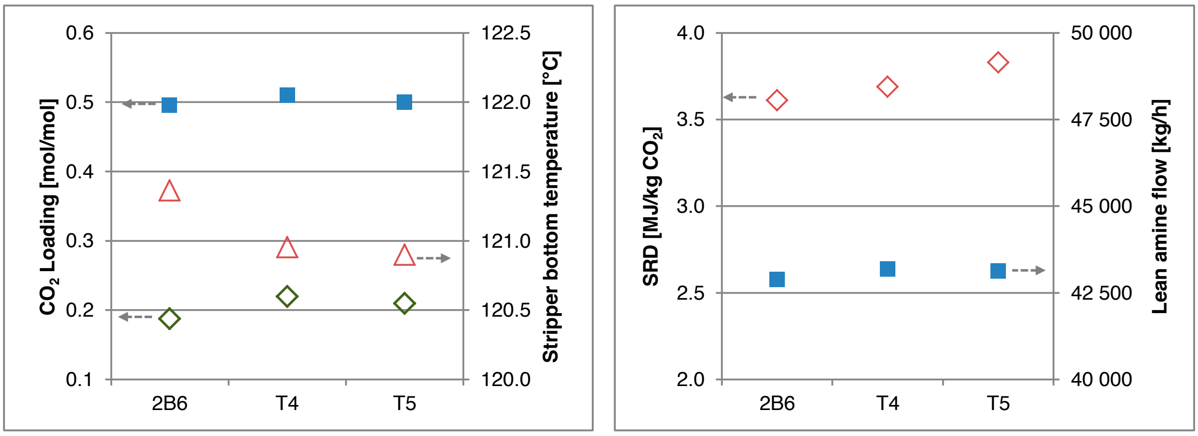

Figure 12: Results for test cases 2B6, T4 and T5: To the left rich- (squares) and lean-loading (diamonds) and stripper bottom temperature (triangles) and to the right SRD (diamonds) and lean amine flow (squares).

7. Discussion and future work

Monitoring the amine concentration and CO_2 loading is very important for optimal operation. At TCM DA the solvent concentrations are mainly followed on a daily basis with manual samples and analysis. Further, a number of analyzers are available for real-time online monitoring, i.e. conductivity, density and pH analyzers. These online results can be correlated to enable a closer follow-up of the solvent condition.

As an effect of reclaiming start-up, the solvent in the main process was diluted by water evaporating from the reclaimer vessel. In future campaigns, extra care will be taken not to disrupt the main process during reclaiming. The deviation in solvent concentration could have been corrected at an earlier stage with an online estimate of solvent concentration.

The reclaiming environment is very harsh to the solvent due to high temperatures (up to 160 °C). The elevated temperatures represent a risk of additional thermal degradation. Care must therefore be taken in order to limit the residence time of the reclaimer solvent and thereby unnecessary degradation. Thus frequent manual solvent sampling or online analyses are required in order to monitor the progress of reclaiming and terminate the reclaiming process when the target is reached. In this test campaign it was very successfully demonstrated a 95 % cleaning efficiency when circulation a 4-5 % slip stream through the reclaimer for three days, which added up to an accumulated reclaimed volume of about 110% of the total solvent inventory.

The total HSS analysis indicates that the amount of NaOH added during reclaiming was on the stoichiometric low side to limit the MEA loss in the reclaimer waste. It is therefore reason to believe that additional MEA was lost in HSS to the waste. Thus, the total MEA loss of 4% could be reduced even further by optimizing the NaOH dosage. However, the actual effect of NaOH addition on MEA release from HSS should be investigated more in detail.

There is little information available in the literature that addresses how the build-up of impurities impacts the energy demand for regenerating MEA in the stripper i.e. reboiler heat duty. However, the density and viscosity of the solvent increased with the increasing level of contaminants as discussed in Section 3. This will cause reduction of the solvent heat transfer coefficient and consequently the heat transfer efficiency in the reboiler. The impact of accumulation of the contaminants on the specific heat capacity of amines is also very little addressed in the literature. However, it is expected that degraded MEA has higher specific heat capacity than MEA which in turn could increase the sensible heat needed to regenerate the solvent in the stripper. It is recommended to investigate these effects in the future.

As the amine plant was only operated for 28 hours after solvent reclaiming, a very limited investigation of the effect of removing the aqueous phase contaminants on the energy requirement of the stripper reboiler was performed. In future tests, sufficient time should be allowed to investigate in detail and compare the solvent performance at the beginning of the test campaign to the performance just before reclaiming and just after reclaiming.

In order to further optimize the process and reduce disposal problems both the reclaiming procedure itself and the collection and drainage of the reclaimer waste can be improved. The rapid cleaning of the lean solvent suggests running the reclaimer more frequently for shorter time periods (for example 12 hours a week) as one option to avoid degraded solvent to accumulate in lean amine. In this way the acceleration of degradation reactions could also be minimized. The draining and flushing operation can be improved by using less water or even small amounts of steam for keeping the reclaimer vessel fit for purpose. This will reduce the amounts of waste.

8. Conclusions

A test campaign with 30 wt% MEA has been conducted for a total of 1960 hours at the CO_2 Technology Centre Mongstad. The present paper discusses main causes of solvent degradation and various parameters for monitoring degradation products. Further, the effect of process design and operating conditions on solvent degradation is discussed, and thermal reclaiming is evaluated as a technique for removal of degradation products and other contaminants in the MEA solution.

The solvent condition was closely monitored during the test campaign and several observations such as increasing solvent viscosity and darker solvent color indicated solvent degradation. Solvent exposure to oxygen and flue gas contaminants in the absorber and operation at elevated temperatures (above 100 °C) in the stripper section are highlighted as main causes for degradation. When performing scale-up to commercial CO_2 capture units it is recommended to minimize the hot solvent residence time in the plant, in order to minimize solvent degradation.

Thermal reclaiming has demonstrated an efficient clean-up of the MEA solvent. The cleaning efficiency was about 95% with respect to degradation products, HSS and metal elements. The solvent viscosity returned to normal values and the solvent color was normalized to a clearer and more yellow appearance. The quality recovery of the solvent was further assessed by an evaluation of the capture process after the reclaiming was concluded by comparing the solvent performance to results obtained at earlier stages of the test campaign and there were no significant indications of reduced solvent quality.

Acknowledgements

The authors gratefully acknowledge the staff of TCM DA, Gassnova, Statoil, Shell and Sasol for their contribution and work at the TCM DA facility. The authors also gratefully acknowledge Gassnova, Statoil, Shell, and Sasol as the owners of TCM DA for their financial support and contributions.

References

[1] Dumée L, Scholes C, Stevens G, Kentish S. *Purification of aqueous amine solvents used in post combustion CO_2 capture: A review*. International journal of Greenhouse Gas Control 10 (2012): 443-455.

[2] Abdi MA, Golkar MM. *Improve contaminant control in amine systems*. Hydrocarbon Processing 63 (2011): 102C – 102-I.

[3] IEAGHG, *"Evaluation of Reclaimer Sludge Disposal from Post-Combustion CO_2 Capture"*, 2014/02 (March 2014).

[4] Wang T, Hovland J, Jens, KJ. *Amine reclaiming technologies in post-combustion carbon dioxide capture*. Journal of Environmental Science 27 (2015): 276 – 289.

[5] Kohl AL, Nielsen RB. Gas purification. Gulf publishing Company, Houston, Texas, USA, 5th edition (1997).

[6] Nurrokhmah L, Mezher T, Abu-Zahra MRM. *The evaluation of monoethanolamine-based CO_2 post-combustion capture process waste handling approaches considering the regulations in UAE*. Energy Procedia 37 (2013): 751 – 758.

[7] Gjernes E, Pedersen S, Cents T, Watson G, Fostås BF, Shah MI, Lombardo G, Desvignes C, Flø NE, Morken AK, de Cazenove T, Faramarzi L, Hamborg ES. *Results from 30 wt% MEA performance testing at the CO_2 Technology Centre Mongstad*. Energy Procedia (GHGT-13), Forthcoming 2017.

[8] Lombardo G, Fostås BF, Shah MI, Morken AK, Hvidsten OA, Mertens J, Hamborg ES. *Results from aerosol measurement in amine plant treating gas turbine and residue fluidized catalytic cracker flue gases at the CO2 Technology Centre Mongstad*. Energy Procedia (GHGT-13), Forthcoming 2017.

[9] Faramarzi L, Thimsen D, Hume S, Maxson A, Watson G, Pedersen S, Gjernes E, Fostås BF, Lombardo G, Cents T, Morken AK, Shah MI, de Cazenove T, Hamborg ES. *Results from MEA testing at the CO_2 Technology Centre Mongstad: Verification of baseline results in 2015*. Energy Procedia (GHGT-13), Forthcoming 2017.

[10] Morken AK, Pedersen S, Kleppe ER, Wisthaler A, Vernstad K, Ullestad Ø, Flø NE, Faramarzi L, Hamborg ES. *Degradation and Emission Results of Amine Plant Operations from MEA Testing at the CO_2 Technology Centre Mongstad*. Energy Procedia (GHGT-13), Forthcoming 2017.

[11] Hjelmaas S, Storheim E, Flø NE, Thorjussen ES, Morken AK, Faramarzi L, de Cazenove T, Hamborg ES. *Results from MEA amine plant corrosion processes at the CO_2 Technology Centre Mongstad*. Energy Procedia (GHGT-13), Forthcoming 2017.

CATCHING OUR FUTURE

Dynamic process model development and validation with transient plant data collected from an MEA test campaign at the CO_2 Technology Center Mongstad

(2016)

Available online at www.sciencedirect.com
ScienceDirect
Energy Procedia 114 (2017) 1538 – 1550
Energy Procedia

13th International Conference on Greenhouse Gas Control Technologies, GHGT-13, 14-18 November 2016, Lausanne, Switzerland

Dynamic process model development and validation with transient plant data collected from an MEA test campaign at the CO_2 Technology Center Mongstad

Rubén M. Montañés[a]*, Nina E. Fløb[b], Rohan Dutta[a], Lars O. Nord[a], Olav Bolland[a]

[a]*Department of Energy and Process Engineering, NTNU - Norwegian University of Science and Technology, NO-7491 Trondheim, Norway.*
[b]*CO_2 Technology Center Mongstad (TCM DA), 5954 Mongstad, Norway.*

Abstract

This work focuses on the development and validation of a dynamic process model of the post-combustion CO_2 chemical absorption process with temperature swing absorption (TSA) using aqueous monoethanolamine (MEA) as solvent. A new set of steady-state and transient cases were generated during an MEA test campaign at the amine pilot plant at CO_2 Technology Center Mongstad (TCM DA). Nine steady-state cases comprising a wide range of operating conditions of the plant and two transient tests consisting of flue gas volumetric flow rate step-changes were utilized for the purpose of dynamic process model validation of the overall pilot plant process model. It is concluded that the dynamic process model is capable of estimating the absorber and stripper columns temperature profiles with good accuracy after tuning of model parameters. An over-prediction of the model for lean and rich CO_2 loadings has been reported, being mean percentage errors <1.5% for lean loading and <6.7% for rich loading. In addition, an under prediction of CO_2 product flow rate has been observed (<5%). The process model is capable of predicting the variability of lean and rich loadings for the range of steady-state operating conditions. The main process dynamics of the pilot plant under flue gas volumetric flow rate set-point step changes is captured by the process model.

© 2017 The Authors. Published by Elsevier Ltd. This is an open access article under the CC BY-NC-ND license
(http://creativecommons.org/licenses/by-nc-nd/4.0/).
Peer-review under responsibility of the organizing committee of GHGT-13.

Keywords: Post-combustion; natural gas; transient data; rate-based model; model validation; pilot plant; dynamic modeling; Modelica.

---

* Corresponding author. Tel.: +47 735093722;
E-mail address: ruben.m.montanes@ntnu.no

1876-6102 © 2017 The Authors. Published by Elsevier Ltd. This is an open access article under the CC BY-NC-ND license
(http://creativecommons.org/licenses/by-nc-nd/4.0/).
Peer-review under responsibility of the organizing committee of GHGT-13.
doi:10.1016/j.egypro.2017.03.1284

1. Introduction

Post-combustion CO_2 capture (PCC) with amines is considered one of the more mature technologies that can contribute to reduce anthropogenic CO_2 emissions to the atmosphere from fossil-fueled thermal power plants. It is considered that thermal power plants with CO_2 capture and storage (CCS) might be operated as load-following units in future energy systems with higher integration of variable renewable energy sources [1]. The Carbon Capture and Storage update 2014 concludes that the financial case for CCS requires that it operates in a flexible manner, and considers load-following ability as extremely important to the long-term economics [2]. Therefore, interest has grown in the field of operational flexibility of thermal power plants with CCS. A key aspect of operational flexibility of power plants with post-combustion CO_2 capture using amines is the transient behavior of the capture process, i.e. the time dependent behavior of the PCC plant when varying operating conditions. Pilot plant testing allows analyzing flexible operation of the process [3-5]. Nevertheless, pilot plant testing requires expensive resources and normally a limited amount of transient testing can be conducted during test campaigns.

The scarcity of published transient performance data from pilot plants together with the limited operational experience from commercial-scale post-combustion capture plants, claims for an interest within the research community for the development of dynamic process simulation models. Dynamic process models are considered as invaluable tools that can help studying different aspects of the transient behavior of PCC plants. The models allow studying various transient events, as well as developing and implementing optimal control strategies. In addition, computational tools and process models can contribute to identify process bottlenecks and develop useful knowledge that will contribute to technology development and ease process scale-up. However, the reliability of results from dynamic simulations might be questioned if the dynamic process models have not been validated against experiments or pilot plant transient data. Thus, validation of dynamic process models is necessary [6-9]. According to Bui et al. [10], further research must focus on producing transient pilot plant data for increasing knowledge on real plant transient performance and for dynamic process model validation in order to ensure reliability of simulation results.

The objectives of this work were:

- Generate a set of steady-state and transient plant data that can be used for dynamic process model validation.
- Develop and validate a dynamic process model of the amine-based TSA plant at CO_2 Technology Center Mongstad for flue gas from a natural gas fueled power plant.

Steady-state and dynamic experiments were conducted by TCM DA during an MEA test campaign at the post-combustion amine pilot plant at TCM DA treating flue gas from a natural gas fueled power plant. The steady-state data sets reflect a wide range of operating conditions while the dynamic experiments consist of set-point changes in exhaust gas volumetric flow rate fed to the absorber. In this work, a dynamic process model of the amine-based plant at TCM DA was built with the open physical modeling language Modelica [11], by means of the commercial tool Dymola [12]. After processing the pilot plant data, validation of the overall process model has been conducted with the steady-state and transient data by comparing the prediction of the overall process model of the PCC plant with the pilot plant data. In this paper, the validation with nine steady-state cases and two transient events is presented.

Nomenclature

TSA	Temperature swing absorption
MEA	Monoethanolamine
TCM DA	CO_2 Technology Center Mongstad
PCC	Post combustion CO_2 capture
CCS	CO_2 Capture and Storage
CHP	Combined heat and power
FMI	Functional Mock-up Interface
FMU	Functional Mock-up Unit

2. TCM DA amine pilot plant configured for CHP flue gas treatment

CO_2 Technology Centre Mongstad has an installed pilot-scale amine-based temperature swing absorption (TSA) process plant next to the Statoil refinery in Mongstad, Norway. TCM DA has recently conducted a test campaign with 30% aqueous monoethanolamine (MEA), operated from 6 July until 17 October 2015. The work is part of the continuous effort of TCM DA on generating better understanding of the performance of the non-proprietary aqueous MEA solvent system. From TCM DA's perspective, one of the objectives of MEA test campaigns is to provide understanding of the transient operations of the amine plant [13]. A detailed description of the flexible and fully instrumented TCM DA plant can be found in Hamborg et al. [14]. In the following it is presented a brief description of the TCM DA PCC pilot plant configured for flue gas cleaning from natural gas fueled power plant.

The exhaust gas, with a CO_2 content of about 3.5 vol%, comes from the natural gas combined heat and power plant (CHP) placed next to the TCM DA facility. The amine pilot plant treats a fraction of about 3% of the total exhaust gas originating from the two GE 9001E gas turbines operating at design load at the CHP plant. The total capacity of the pilot plant for CHP flue gas is 60000 Sm^3/hr and it is capable of capturing around 80 ton CO_2/day. Figure 1 shows a simplified process flowsheet for TCM DA amine plant operated with CHP flue gas. An induced draft blower is present at the plant to overcome pressure drops and blow the flue gas flow. It has variable speed drives that allow manipulating the flue gas volumetric flow rate fed to the absorber. The flue gas flows through a direct contact cooler that cools down and saturates the flue gas by a counter-current water flow.

The absorber column consists of a rectangular polypropylene-lined concrete column with a cross-section of 3.55 x 2 m and a total height of 62 m. It has three absorber packed sections consisting of Koch Glitsch Flexipac 2X structured stainless-steel packing of 12 m, 6 m and 6 m. Two water-wash systems are operated in the upper part of the absorption tower, consisting of two sections of Koch Glitsch Flexipac 2Y HC structured stainless-steel packing. The absorber in TCM DA has the flexibility option to use different packing heights (12, 18 or 24 m). During the tests presented in this paper, 24 m of absorber packing were utilized (12 bottom + 6 middle + 6 top). There are 4 temperature sensors radially distributed in the absorber column per meter of absorber packing in the axial direction. This makes a total of 96 temperature sensors within packed segments.

The CHP stripper with overhead condenser system consists of a 1.3 m diameter column of Koch Glitsch Flexipac 2X structured stainless-steel packing of 8 m, and a rectifying water-wash region with Koch Glitsch Flexipac 2Y HC structured stainless-steel packing of 1.6 m of height. There are 4 temperature sensors radially distributed in the

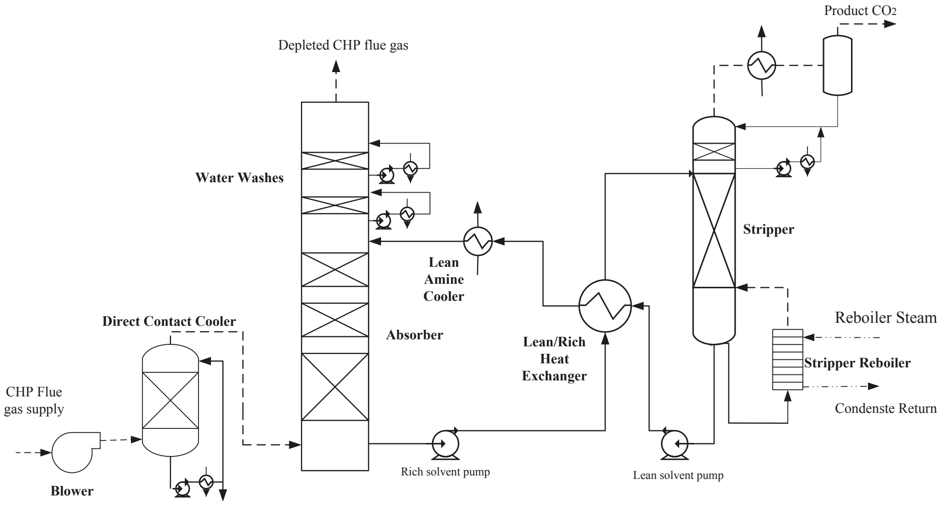

Figure 1. Simplified flowsheet of the TCM amine plant for CHP flue gas.

absorber column per meter of absorber packing in the axial direction. The total number of temperature sensors within packed segments is therefore 28. The stripper reboiler consists of a thermosiphon steam-driven system that provides the required heat for the stripping process. A plate and frame heat exchanger allows heat integration between the absorber and stripper columns, where the hot lean amine solution coming from the stripper heats up the rich amine solution. In addition, a lean amine cooler is utilized to control the lean solution temperature introduced at the top of the absorber packing sections.

3. Steady-state and transient operating cases from the MEA test campaign

With the purpose of dynamic model validation under steady-state operating conditions, a set of nine steady-state plant operation cases from the MEA test campaign were utilized. The tests were conducted with 30 wt% aqueous MEA, and comprise a wide range of operating conditions with various combinations of rich solvent flow rate and reboiler duty. Table 1 shows the steady-state cases generated during the test campaign that are used in this work. Cases 1 to 5 were obtained by varying rich solvent mass flow rate when operating the absorber at 80% volumetric flue gas flow rate capacity with a CO_2 capture target of 85%. The mass based L/G ratios on the absorber range from 1.34 to 0.75 for cases 1 to 5. Cases 6 to 9 were obtained from the steady-state operation of the plant achieved in between the four transient tests (refer to Table 2).

A transient event happens when the plant is brought from one operating point to another. During transient testing key manipulated variables (inputs) of the plant are changed to observe how the process variables evolve over time from one steady-state operating point until a new steady-state operating point is reached. The purposes of these experiments are to increase knowledge of the process under transient conditions and to generate a set of data for assessing the validity of dynamic process models at the plant scale. It is desirable that the transient data represents the main dynamics of the plant. Table 2 includes the test matrix for the set-point change experiments conducted during the autumn 2015 MEA test campaign at TCM DA. The experiments consist of set-point changes in main inputs to the pilot plant, i.e., rich solvent flow rate, flue gas volumetric flow rate into the absorber and steam flow rate to reboiler. In this paper, tests 2 and 3 are presented for the purpose of dynamic process model validation. These two tests represent set point step-changes in flue gas volumetric flow rate fed to the absorber.

The responses and performance of the pilot plant was logged. The data was extracted every 30 seconds in order to reduce the data load. Logged data includes:

- Gas analyzers at the inlet of the absorber, outlet of the absorber, and CO_2 rich to stack.
- Main liquid and gas flow rates.
- Main process temperatures, including absorber and stripper temperatures.
- Pressures and pressure drops at different components of the plant.
- Online solvent analysis measurements include pH, density and conductivity, at the inlet and outlet of the absorber (lean and rich solvent).
- Liquid hold-ups distribution at different components of the plant.
- Main active controller set-points and tuning parameters.

Solvent samples were taken during steady-state conditions at the inlet and outlet of the absorber for posterior analysis in the lab, in order to obtain the CO_2 lean and rich solvent loadings. Actual reboiler duty was estimated based on logged measurement data of steam temperatures, pressures and mass flow rate as indicated in Thimsen et al. [15]. In order to assess the validity of the process model, temperature profiles of the absorber and stripper columns were utilized. Each of the measured temperature points included in the steady-state absorber temperature profiles is the average over time during steady-state conditions, of the averaged 4 temperature measurements of the sensors radially distributed within the absorber column, at the given axial position of the column.

The tests were run with a total inventory of aqueous MEA of about 38.2 m^3. For process simulations, it is of importance to understand how the solvent inventory is distributed within the different components of the plant. Therefore, liquid hold-ups at different parts of the plant were registered for the steady-state operating cases.

Table 1. Steady-state data for the nine operating cases selected from the MEA test campaign. The plant was operated with 30 wt% aqueous MEA and 24 meters of absorber packing. Note that standard conditions are 15 ºC and 1 atm. The tag IDs for the instrumentation utilized are included.

Case	1	2	3	4	5	6	7	8	9
Gas flow rate [Sm^3/hr] (8610-FT-0150)	47000	47000	47000	47000	47000	47000	47000	40000	47000
Rich solvent [kg/s] (8611-FIC-2004)	20.56	17.50	16.11	12.74	11.46	13.04	14.16	14.17	13.06
Reboiler duty [kW] (estimated [15])	2156.2	2093.3	2104.4	2102.8	2137.3	3901.3	3698.7	3549.7	2929.2
Absorber inlet CO_2 [%](8610-ai-2036a)	3.60	3.62	3.62	3.62	3.62	3.47	3.48	3.48	3.46
Absorber inlet O_2 [%](8610-ai-2036b)	15.30	15.48	15.49	15.51	15.52	14.70	14.74	14.84	14.77
Absorber inlet H_2O [%](8610-ai-2036c)	3.80	3.36	3.46	3.52	3.43	4.19	4.11	3.66	4.23
Absorber inlet N_2 [%](8610-ai-2036d)	78.18	78.88	78.94	79.06	78.96	75.51	75.53	75.87	75.40
Loading rich [mol/mol] (lab samples)	0.47	0.49	0.49	0.49	0.49	0.43	0.42	0.37	0.43
Loading lean [mol/mol] (lab samples)	0.34	0.33	0.31	0.26	0.23	0.21	0.19	0.18	0.17
CO_2 Product [kg/s] (C-8615-FT-0010)	0.74	0.74	0.75	0.77	0.76	0.80	0.80	0.70	0.82

Table 2. Test matrix for the set-point change experiments conducted during the Autumn 2015 MEA test campaign at TCM DA. The tag IDs for the instrumentation used is included.

Input	Test 1	Test 2	Test 3	Test 4
Rich amine mass flow rate [kg/hr] (8611-FIC-2004)	47000 51000	51000	51000	47000
Flue gas volumetric flow rate [Sm^3/hr] (8610-FT-0150)	47000	47000 40000	40000 47000	47000
Steam flow rate [kg/hr] (8655-FI-2368B)	5300	5300	5300	5300 4615

4. Dynamic process models of the CO_2 chemical absorption process with aqueous MEA

A dynamic process model of the amine-based TSA plant at TCM DA was built with the open physical modeling language Modelica [11], by means of the commercial modeling and simulation tool Dymola [12]. Modelica allows for component-based modeling, and the component models consist of systems of differential and algebraic equations. The overall plant model consists of models for the absorber and stripper columns, sumps, internal heat exchanger, reboiler, condensers, flow resistances, pumps, valves, measurements and controllers. The process models were obtained from a Modelica library from Modelon AB [16] and have been presented elsewhere [17, 18]. In this work, the component models were configured, parameterized and modified in order to obtain a dynamic process model of the TSA plant at TCM DA considering the main process equipment, size, geometry, material and solvent inventory during the experiments. In addition, the regulatory control layer of the plant was implemented in the process model, considering the control structure at the PCC pilot plant.

Absorption and desorption columns are modeled considering the two-film theory approach, thus thermodynamic equilibrium is assumed at the liquid and gas interface. Packed sections consider rate-based approach for modeling interface mass transfer, with mass transfer coefficients for CO_2 and H_2O by Onda et al. [19], and enhanced mass transfer due to chemical reactions is implemented via a pseudo-first order enhancement factor [7]. Chemical equilibrium is considered in all model parts, both at interface and liquid bulk, with chemical equilibrium constants obtained empirically from Bötinger [20].

Heats of reaction are inferred from the equilibrium constant via the van't Hoff equation. Sensible heat transfer between phases is correlated to gas-phase mass transfer coefficient (Cohilton-Colburn analogy), while heat of solution and evaporation is calculated as a function of temperature but is constant with solvent loading. Ideal gas law applies to the gas phase, which is only composed of CO_2, O_2, H_2O and N_2. The pressure of the system p is determined by gas phase pressure drop from a known operating point and a quadratic correlation with gas velocity.

A simplified washer component is included in the head of the column. It is modelled as a simple volume with phase separation. Its purpose is to cool down the gas flow to a temperature given as an input signal and condense as much vapor as required to reach saturation in the gas phase. Water balance is ensured by a make-up water source in the absorber sump that controls the H_2O mass balance of the plant. Note that in this model MEA is considered non-volatile, which means that it is only present in the liquid phase. This implies that MEA make-up source is not required in the overall dynamic process model. This is not the case for the real plant, where MEA make-up is required for operation.

The numerical solver DASSL was selected in Dymola for solution of the resulting system of differential and algebraic equations. The process model was exported as a co-simulation Functional Mock-up Unit (FMU) via FMI technology (Functional Mockup Interface) [21]. Simulations and validation were carried out in Microsoft Excel® environment via a FMI-add-in for Excel® [22].

5. Dynamic model validation results

5.1. Dynamic model validation using steady-state operational data.

The approach to overall PCC plant model development and validation followed in this work was to initially separate the plant in three main parts: absorber, lean/rich cross heat exchanger and stripper with reboiler. Proper boundary conditions were specified for each part of the process. Steady-state data measured at the pilot plant were used as inputs to the boundary conditions of each section of the process, and the main outputs from the model were compared with the plant data. This involves checking absorption and desorption rates, temperature profiles in the absorber and stripper, and lean and rich CO_2 loadings. The task required tuning of uncertain model parameters (tuners) in order to obtain a better agreement between measured plant performance and behavior predicted by the model. Uncertain parameters include enhancement factors and pre-multiplying factors for adjustment of effective interface area correlations. Then, the overall PCC plant process model was closed by connecting the different sections of the process and implementing the suitable regulatory control layer. The main model outputs were compared with measured plant data in steady-state for the overall plant. In the following, the results from the overall plant process model validation are presented.

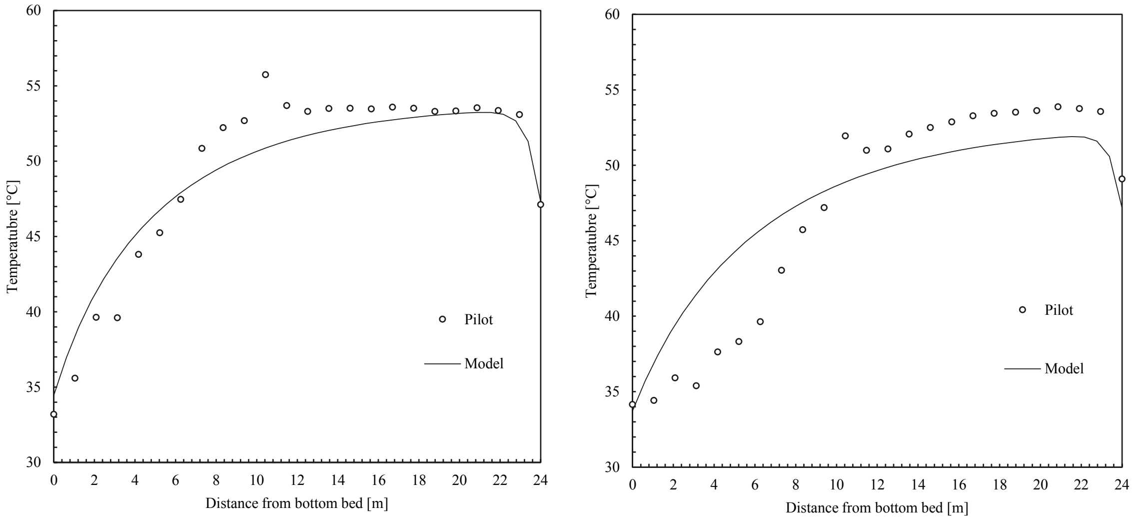

Figure 2. Examples of temperature profiles in absorber and stripper columns during steady-state operating conditions. Left: Case 8. Right: Case 9.

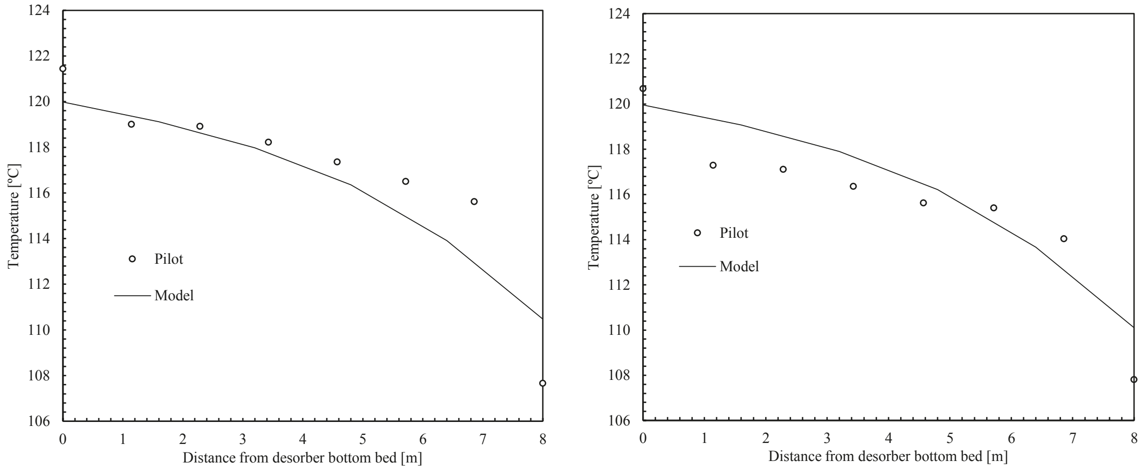

Figure 3. Examples of stripper temperature profiles for two steady-state operating conditions of the PCC pilot plant. Left: Case 8. Right: Case 9 (refer to Table 1).

Examples of temperature profiles within the absorber are shown in Figure 2. Figure 2 (left) shows the absorber temperature profile for the case 8, whereas Figure 2 (right) shows the absorber temperature profile for case 9. Figure 3 (left) shows temperature profiles in the stripper for case 8, whereas Figure 3 (right) shows temperature profiles for stripper in case 9. Note that for cases 8 and 9 the PCC plant is operated with 67 and 80 % flue gas volumetric flow rate capacity in the absorber respectively. Absorber temperature profiles predicted by the model show a good agreement with plant data, especially for case 8. The model is capable to predict properly the trends in temperature along the column. An over prediction is observed in case 9, at the bottom packing below the temperature bulge, while an under prediction is observed from the temperature bulge, within the middle and upper packing. The stripper temperature profile predicted by the process model shows also good agreement with plant data, as illustrated with steady-state cases in Figure 3.

Figure 4 shows the parity plot for lean and rich solvent loadings for the nine steady-state operating cases. It can be observed that the model over predicts the lean and rich loading when compared with the experimental data. The mean percentage error for lean loading is 1.4% and for rich loading 6.7%. There are two steady-state cases where the model shows an under prediction of lean solvent loading. This could be explained by the fact that these two steady-state cases are obtained prior to the injection of anti-foam solution in the plant (cases 6 and 7). Anti-foam is periodically used during MEA test campaigns at TCM to tackle the unideal phenomena in the stripper, and has a direct impact in the performance of the stripper [13]. From the results shown in Figure 4 it can be concluded that the dynamic process model is capable to predict the variability in solvent loading for the steady-state operating cases. The CO_2 product flow is under predicted with an average percentage error of 5% for the simulated cases.

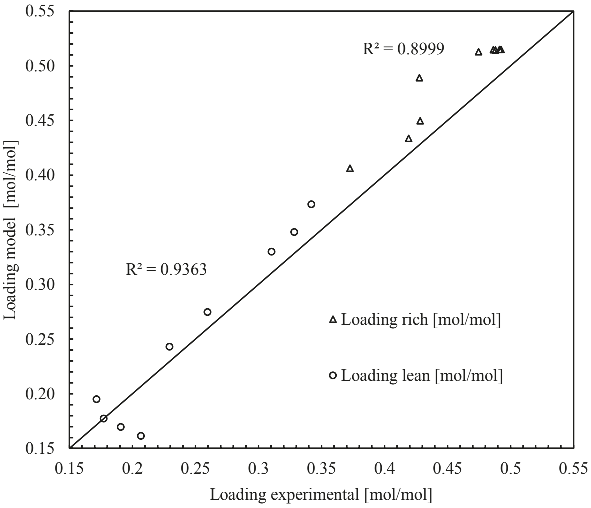

Figure 4. Lean and rich amine CO_2 loading parity plots. Model results from overall pilot plant model for nine steady-state operating cases. The mean percentage error for lean loading is 1.4% and for rich loading is 6.7%.

5.2. Dynamic model validation using transient operational data.

Once the steady-state estimation performance of the dynamic process model is validated for the full plant model, the dynamic process model is validated with transient plant data. Transient performance of this process is characterized by long dead times and large lag times in main process variables, resulting in relatively large total stabilization times. This means that this process is considered slow, when it is compared with a change in load in the steam cycle of a power plant. During the test campaign four transient tests were conducted, here two of them involving flue gas volumetric flow rate ramp-down and ramp-up will be presented.

5.2.1. Flue gas volumetric flow rate reduction

The test consisted of set-point reduction of the exhaust gas volumetric flow rate fed to the absorber, from 80% to 67% of the plant capacity, i.e. 47000 Sm^3/hr to 40000 Sm^3/hr. The purpose was to change the flue gas volumetric flow rate while keeping the rest of the plant process variables constant. Figure 5 shows the three main inputs of the plant for this test. The main controlled drifting variables of the plant during the test were kept constant by the action of the controllers of the regulatory control layer of the plant.

The plant was disturbed by manipulating the speed of the induced draft blower located upstream the direct contact cooler. The blower speed was changed in order to set the flue gas volumetric flow rate at the inlet of the absorber. Step set-point reduction in flue gas volumetric flow rate was applied. As shown in Figure 5, this has resulted in an oscillatory flue gas volumetric flow rate as disturbance to the plant, due to the fact that the blower speed/volumetric flue gas flow rate controller is a PI controller. Steam mass flow rate was maintained constant, while the solvent mass flow rate had small amplitude oscillations around the set-point. In order to compare the transient plant data with the actual plant data, the measured flue gas volumetric flow rate was introduced as an input trajectory to the dynamic process model. This means that the same disturbance applied to the plant during the test campaign, was applied to the dynamic process model for simulation. In addition, averaged value of the time series of the measured rich solvent mass flow rate and the estimated reboiler duty was applied as input to the dynamic process model.

Figure 6 shows the response on CO_2 product flow rate to the plant input. It was observed an input/output dead time of 40 minutes between flue gas volumetric flow rate and CO_2 product mass flow rate. This means that for a change in the flue gas flow rate input to the plant, no changes are observed in the product CO_2 flow until around 40 minutes later. Therefore, the system acts as a buffer to load change driven by flue gas volumetric flow rate change at absorber inlet. In addition, it takes around 4 hours to reach the new steady-state operating point. In addition, a significant lag time was found in stabilization of temperature profiles in the absorber (1 hour) and stripper columns (3-4 hours), not shown. It can be observed in Figures 6 and 7 that the process model is capable of predicting the main process dynamics for CO_2 product mass flow rate and rich and lean solvent CO_2 loadings.

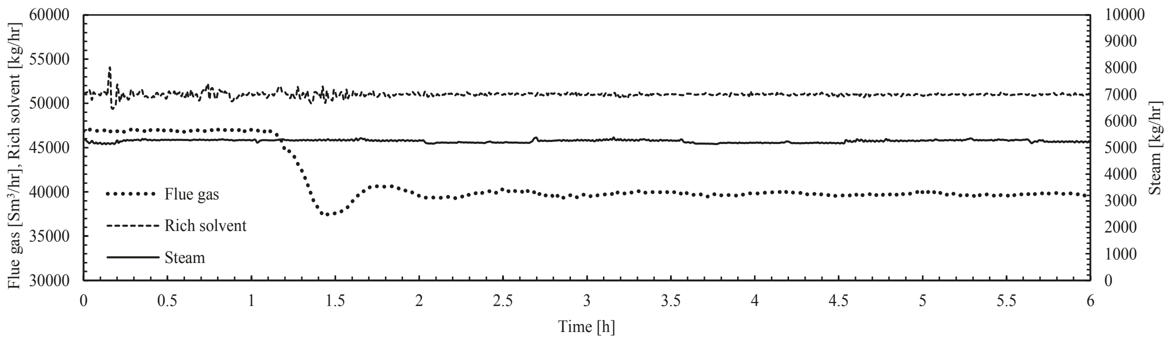

Figure 5. Main inputs to the plant for test with flue gas volumetric flow rate set-point reduction from 47000 [Sm3/hr] to 40000 [Sm3/hr] (8610-FT-0150). Rich solvent flow rate from absorber [kg/hr] (8611-FIC-2004) and steam flow to reboiler [kg/hr] (8655-FI-2368).

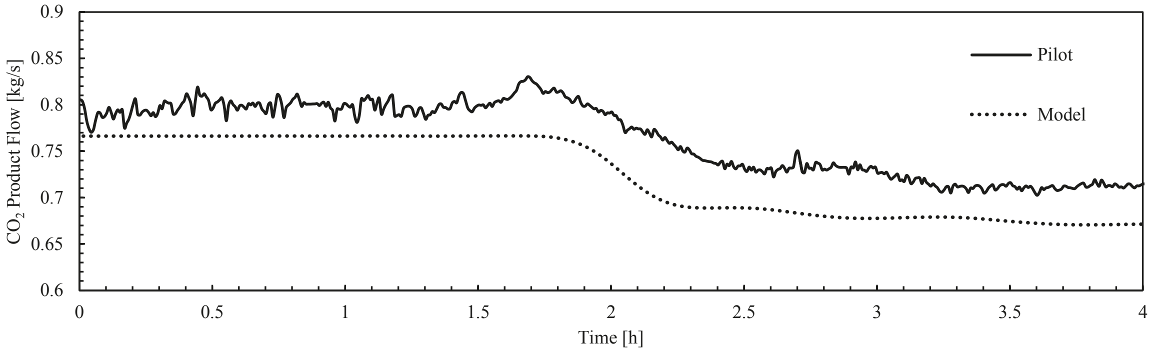

Figure 6. CO_2 Product flow rate [kg/s] (C-8615-FT-0010).

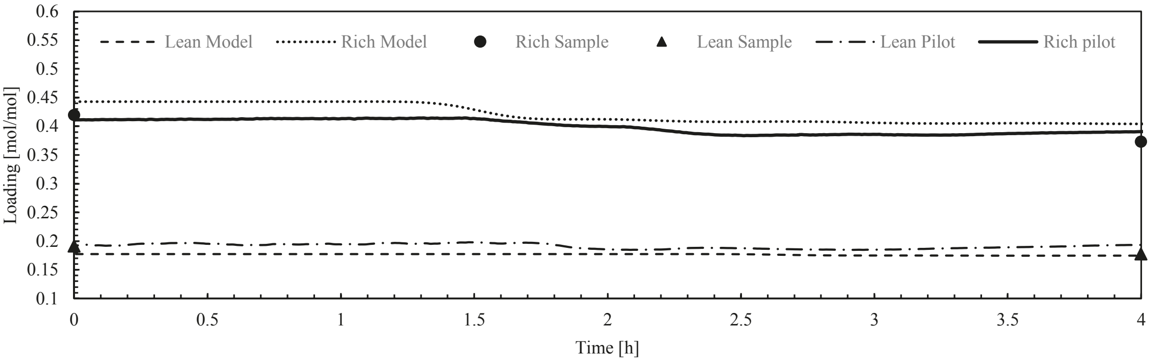

Figure 7. CO_2 lean and rich solvent loadings during test 2 (refer to table 2). Lean and rich pilot curves are based on a correlation for total alkalinity, density and temperature of the solvent, measured online at the plant. Lab samples were taken before and after the test.

5.2.2. Flue gas volumetric flow rate increase.

This test consist of set-point increase of the flue gas volumetric flow rate fed to the absorber, from 67% to 80% of the plant capacity, i.e. 40000 Sm^3/hr to 47000 Sm^3/hr. Figure 8 shows the three main inputs of the plant during the test. As in the previous test, an oscillatory behavior of the flue gas volumetric flow rate around the new set point is observed. The same approach with the measured input to the plant as input trajectory to the dynamic process model was applied. The plant acts as a buffer for flue gas volumetric flow rate changes as shown in Figure 9. Around 20 minutes dead time input/output from flue gas volumetric flow rate to CO_2 product mass flow rate was observed. Figure 9 shows the CO_2 product flow for the model and the pilot plant data and Figure 10 shows the plant and model response for this disturbance in terms of CO_2 lean and rich solvent loadings. A mismatch of 15 min for CO_2 product flow rate predicted by the process model is observed. A similar offset as in the previous test is observed, with a steady-state under prediction of CO_2 product flow rate. Despite of the steady-state offset shown on solvent CO_2 loadings prediction, it is observed a good prediction of the main dynamics, refer to Figure 10. It can be concluded that the process dynamics are well captured by the process model.

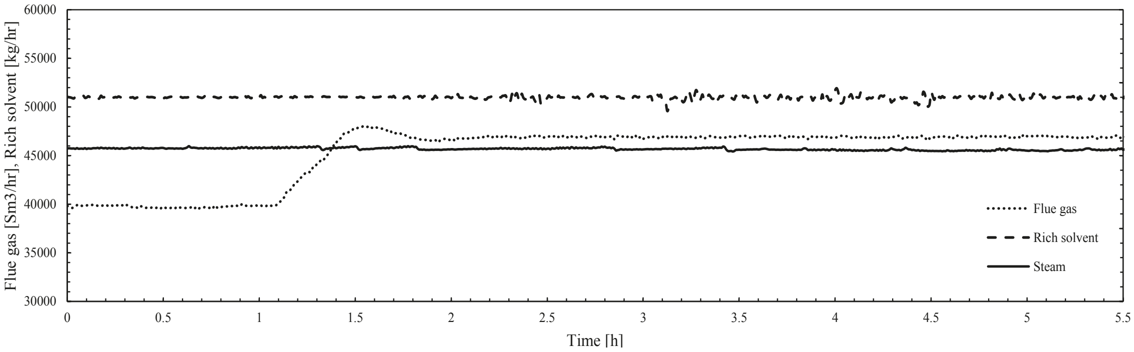

Figure 8. Main inputs to the plant. Flue gas volumetric flow rate set-point change from 47000 [Sm^3/hr] to 40000 [Sm^3/hr] (8610-FT-0150). Rich solvent flow rate from absorber [kg/hr] (8611-FIC-2004) and steam flow to reboiler [kg/hr] (8655-FI-2368).

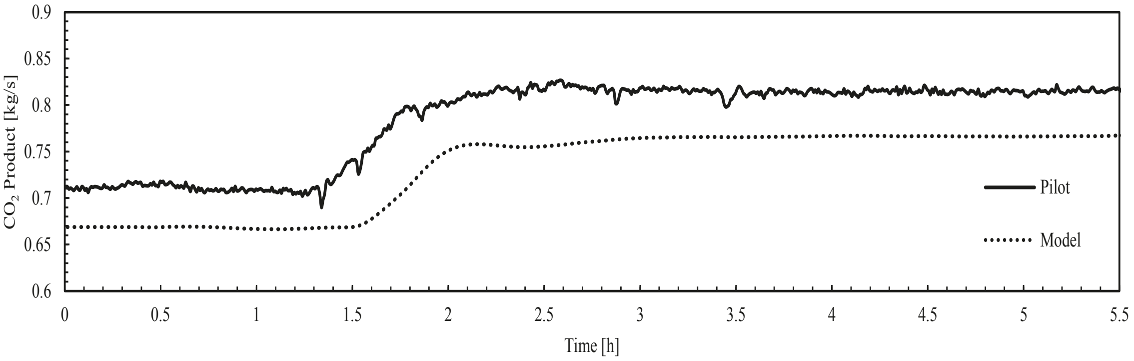

Figure 9. CO_2 product [kg/hr] (C-8615-FT-0010). Results from test 3 on flue gas volumetric flow rate set-point increase (refer to Table 2).

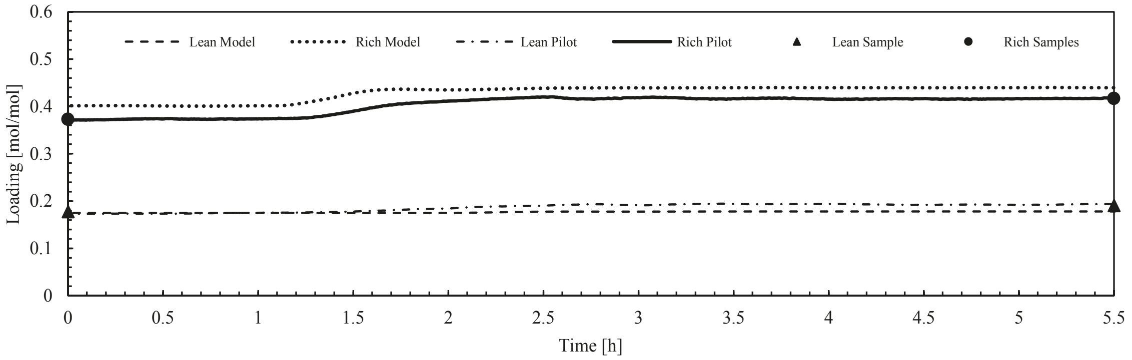

Figure 10. CO_2 lean and rich solvent loadings during test 3 (refer to Table 2). Loading pilot curves are based on a correlation for total alkalinity, density and temperature of the solvent, measured at the plant. Lab samples were taken before and after the test.

6. Discussion

The task of dynamic process model validation of the post-combustion CO_2 absorption with aqueous MEA requires the generation of suitable data sets including both steady-state and transient data. Ideally, the steady-state data should reflect a wide range of operating conditions of the PCC plant. The steady-state data utilized in this work consists of a wide range of operating conditions achieved by changing rich solvent mass flow rate and reboiler heat duty. As shown in Table 1, nine steady-state cases were gathered from the MEA test campaign. The cases include operation of the PCC plant with mass based L/G ratios on the absorber ranging from 1.34 to 0.75, when operating the absorber at 80% capacity and with a capture rate of 85% (cases 1 to 5).

During campaigns at TCM with 30% aqueous MEA, unideal behaviour occurs in the stripper bed and it is handled by addition of anti-foam solution. As shown in literature [13], the addition of anti-foam solution has a significant effect on stripper temperature profile at TCM DA pilot plant for CHP, and especially on specific reboiler duty at low lean amine loadings. Cases 6 and 7 were run before the addition of the anti-foam solution and it has been shown in Figure 4 that the model prediction under estimates lean loading only for these two specific cases. It is advised to check if anti-foam solution was used during the tests, if the data is to be used for process model validation. Anti-foam was introduced in the plant between the transient tests presented in this paper. If required, sufficient time between the tests should be allowed so that steady-state conditions are reached before and after adding anti-foam solution.

The post-combustion TSA process design with solvent recirculation from the stripper to the absorber in a closed-loop makes modeling and validation of the full plant challenging. Modeling errors and inaccuracies in one component of the plant will easily propagate towards other parts of the process. Therefore, a systematic approach is recommended beginning with validation of the separate models of absorber, stripper with reboiler, and heat exchanger sections. In this work, the overall process model is finally developed by joining the different sections and validated with the steady-state and transient pilot data. The intended application of the process model is for transient estimation and plantwide control studies.

Column temperature profiles accurate prediction is of importance since temperature affects phase equilibrium calculation at the gas-liquid interface and liquid phase. In addition, several model parameters and thermophysical properties depend on temperature. These include heat capacity, CO_2 solubility, water heat of condensation, heats of reaction and equilibrium constants. The pilot plant absorber and stripper columns temperature profiles are calculated as an averaged value of the temperature measurements from the sensors distributed in the radial plane at the given axial position of the column. The individual temperature measurements are considered reliable, and the resulting temperature profiles are clear and reasonable. Nevertheless, it should be mentioned that some sensors are closer to the wall while some are closer to the center of the packing, thus a small maximum variation (<6 ºC) is observed between the measurements at a given radial position. The variation is different for different operating conditions of the columns and radial planes. The aggregated effect of above-mentioned aspects makes validation of the absorber temperature profiles challenging. Based on the results presented in Figures 2 and 3, it is considered that the dynamic process model is capable of predicting temperature profiles of both absorber and stripper columns with good accuracy for the purpose considered in this work. Tuning of the pre-multiplying factor of the mass transfer enhancement factor has been required (0.2 in absorber and 0.09 in stripper).

Lean and rich CO_2 loadings are over-predicted by the dynamic process model. Lean and rich loadings are dependent of each other, and modeling errors will easily propagate. In addition, actual reboiler heat duty has been estimated from steam measurements in the plant as suggested by Thimsen et al. [15]. Nevertheless, that value is not truly representative of regeneration energy due to external factors such as changes in ambient conditions and heat loses through non-insulated pipes and equipment [5]. An under-prediction of lean loading is found on cases 6 and 7. It is believed that this is because the plant was operated before addition of anti-foam solution during these cases as well as due to small deviations on MEA concentration from 30 wt% during that period. The mean percentage error for lean loading is 1.4 % and for rich loading 6.7%. It can be concluded that the process model is capable of predicting the variability in lean and rich loading for the range of operating conditions of the PCC plant. The process model under-predicts CO_2 product mass flow rate within <5% for all steady-state cases, being the precision uncertainty of the product CO_2 flow measurement 1% (Vortex FT-0010) [13]. This under prediction is illustrated in the transient cases (Figures 6 and 9).

Dynamic process validation with the two tests involving volumetric flue gas flow rate reduction and increase has been presented in this paper. The experiment shows that the system acts as a buffer to load change driven by flue gas volumetric flow rate change at absorber inlet, and long dead times input/output in terms of CO_2 product flow are observed (around 20-40 minutes). The results from the model show that the model development has been successful to predict the main process dynamics. This includes CO_2 lean and rich loadings and CO_2 product flow response to the disturbances.

7. Conclusions

A dynamic process model of the overall amine-based TSA plant at TCM DA was built for the purpose of model validation with a new set of steady-state and transient plant data. It is concluded that the dynamic process model is capable of estimating the temperature profiles of absorber and stripper columns with good accuracy for the purpose of application. Tuning of the pre-multiplying factor for calibration of the enhancement factor has been required. An over prediction of the model for lean and rich CO_2 loadings has been reported, being mean percentage errors <1.5% and <6.7%. The process model is capable of predicting the variability of lean and rich loadings for a wide range of steady-state operating conditions. In addition, an under prediction of CO_2 product flow rate has been observed (<5%). The main process dynamics of the pilot plant under flue gas volumetric flow changes is captured by the process model.

The validated process model developed in this work will be used to analyze the TCM plant transient performance and expanded to a full-scale plant model to predict transient performance of a natural gas combined cycle power plant integrated with post-combustion CO_2 capture.

Acknowledgements

The authors acknowledge TCM DA and the Department of Energy and Process Engineering at NTNU-Norwegian University of Science and Technology for funding this project. The Faculty of Engineering Science NTNU-Statoil Publication Grant 2016 is also acknowledged. The authors want to acknowledge Espen S. Hamborg from TCM DA for his contribution to establish the ongoing collaboration between TCM DA and the Thermal Energy Research Group at the Department of Energy and Process Engineering at NTNU.

References

[1] R.M. Montañés, M. Korpås, L.O. Nord, S. Jaehnert, Identifying Operational Requirements for Flexible CCS Power Plant in Future Energy Systems, Energy Procedia, 86 (2016) 22-31.

[2] M.E. Boot-Handford, J.C. Abanades, E.J. Anthony, M.J. Blunt, S. Brandani, N. Mac Dowell, J.R. Fernandez, M.-C. Ferrari, R. Gross, J.P. Hallett, R.S. Haszeldine, P. Heptonstall, A. Lyngfelt, Z. Makuch, E. Mangano, R.T.J. Porter, M. Pourkashanian, G.T. Rochelle, N. Shah, J.G. Yao, P.S. Fennell, Carbon capture and storage update, Energy & Environmental Science, 7 (2014) 130-189.

[3] R. Faber, M. Köpcke, O. Biede, J.N. Knudsen, J. Andersen, Open-loop step responses for the MEA post-combustion capture process: Experimental results from the Esbjerg pilot plant, Energy Procedia, 4 (2011) 1427-1434.

[4] P. Tait, B. Buschle, I. Ausner, P. Valluri, M. Wehrli, M. Lucquiaud, A pilot-scale study of dynamic response scenarios for the flexible operation of post-combustion CO_2 capture, International Journal of Greenhouse Gas Control.

[5] M. Bui, I. Gunawan, V. Verheyen, P. Feron, E. Meuleman, Flexible operation of CSIRO's post-combustion CO_2 capture pilot plant at the AGL Loy Yang power station, International Journal of Greenhouse Gas Control.

[6] N. Enaasen Flø, H. Knuutila, H.M. Kvamsdal, M. Hillestad, Dynamic model validation of the post-combustion CO_2 absorption process, International Journal of Greenhouse Gas Control, 41 (2015) 127-141.

[7] H.M. Kvamsdal, J.P. Jakobsen, K.A. Hoff, Dynamic modeling and simulation of a CO_2 absorber column for post-combustion CO_2 capture, Chemical Engineering and Processing: Process Intensification, 48 (2009) 135-144.

[8] C. Biliyok, A. Lawal, M. Wang, F. Seibert, Dynamic modelling, validation and analysis of post-combustion chemical absorption CO_2 capture plant, International Journal of Greenhouse Gas Control, 9 (2012) 428-445.

[9] J. Gaspar, A.-M. Cormos, Dynamic modeling and absorption capacity assessment of CO_2 capture process, International Journal of Greenhouse Gas Control, 8 (2012) 45-55.

[10] M. Bui, I. Gunawan, V. Verheyen, P. Feron, E. Meuleman, S. Adeloju, Dynamic modelling and optimisation of flexible operation in post-combustion CO_2 capture plants—A review, Computers & Chemical Engineering, 61 (2014) 245-265.

[11] Modelica Association, https://www.modelica.org/.

[12] Dassault Systems, Dymola, http://www.3ds.com/products-services/catia/products/dymola.

[13] N. Brigman, M.I. Shah, O. Falk-Pedersen, T. Cents, V. Smith, T. De Cazenove, A.K. Morken, O.A. Hvidsten, M. Chhaganlal, J.K. Feste, G.

Lombardo, O.M. Bade, J. Knudsen, S.C. Subramoney, B.F. Fostås, G. de Koeijer, E.S. Hamborg, Results of Amine Plant Operations from 30 wt% and 40 wt% Aqueous MEA Testing at the CO_2 Technology Centre Mongstad, Energy Procedia, 63 (2014) 6012-6022.

[14] E.S. Hamborg, V. Smith, T. Cents, N. Brigman, O.F. Pedersen, T. De Cazenove, M. Chhaganlal, J.K. Feste, Ø. Ullestad, H. Ulvatn, O. Gorset, I. Askestad, L.K. Gram, B.F. Fostås, M.I. Shah, A. Maxson, D. Thimsen, Results from MEA testing at the CO_2 Technology Centre Mongstad. Part II: Verification of baseline results, Energy Procedia, 63 (2014) 5994-6011.

[15] D. Thimsen, A. Maxson, V. Smith, T. Cents, O. Falk-Pedersen, O. Gorset, E.S. Hamborg, Results from MEA testing at the CO_2 Technology Centre Mongstad. Part I: Post-Combustion CO_2 capture testing methodology, Energy Procedia, 63 (2014) 5938-5958.

[16] Modelon, Post-combustion capture with amine solutions. http://www.modelon.com/industries/energy-process/carbon-capture-and-sequestration/.

[17] K. Prölß, H. Tummescheit, S. Velut, J. Åkesson, Dynamic model of a post-combustion absorption unit for use in a non-linear model predictive control scheme, Energy Procedia, 4 (2011) 2620-2627.

[18] S.Ó. Garðarsdóttir, F. Normann, K. Andersson, K. Prölß, S. Emilsdóttir, F. Johnsson, Post-combustion CO_2 capture applied to a state-of-the-art coal-fired power plant—The influence of dynamic process conditions, International Journal of Greenhouse Gas Control, 33 (2015) 51-62.

[19] K. Onda, H. Takeuchi, Y. Okumoto, Mass transfer coefficients between gas and liquid phases in packed columns, Journal of Chemical Engineering of Japan, 1 (1968) 56-62.

[20] W. Böttinger, NMR-spektroskopische Untersuchung der Reaktivabsorption von Kohlendioxid in wässrigen Aminlösungen, VDI-Verlag, 2006.

[21] Functional Mock-up Interface. https://www.fmi-standard.org/.

[22] Modelon, FMI-Add-In for Excel. http://www.modelon.com/products/fmi-tools/fmi-add-in-for-excel/.

CATCHING OUR FUTURE

Aerosol Measurement Technique: Demonstration at CO_2 Technology Centre Mongstad

(2016)

Available online at www.sciencedirect.com
ScienceDirect
Energy Procedia 86 (2016) 160 – 170
Energy Procedia

The 8th Trondheim Conference on Capture, Transport and Storage

Aerosol Measurement Technique: Demonstration at CO_2 Technology Centre Mongstad

Thomas de Cazenove[a], Richard H.B. Bouma[b], Earl L.V. Goetheer[b], Peter J. van Os[b], Espen Steinseth Hamborg[a,c,]*

[a] CO_2 Technology Centre Mongstad (TCM DA), 5954 Mongstad, Norway,
[b] TNO Science and Industry, Leeghwaterstraat 46, Delft, Netherlands
[c] Statoil ASA, P.O. Box 8500, 4035 Stavanger, Norway

Abstract

There are two main routes for amine emission. The first one is connected to volatile amine emission. The second route is amine emission via aerosols. Recently, it has been observed that under certain conditions and at specific test locations significant aerosol formation and emission can occur. To distinguish between the two routes for amine emission, a novel methodology has been developed. This methodology is based on the separation of the aerosols from the vapour phase in a controlled isothermal modus. To be able to do this, the design of the probe and the sampling procedure should fit to the operational circumstances and is of crucial importance to guarantee isokinetic sampling. The separation of the aerosols is done via an impactor. Using an impactor, not only the total mass of aerosols can be determined, but also the size distribution.

At the end of 2013 and at the beginning of 2014, two aerosol measurement campaigns were performed at CO_2 Technology Centre Mongstad, Norway. The measurements indicate that small amounts of aqueous aerosols with a broad aerosol size distribution are present in the flue gas stream from gas turbine operations. The presence of aqueous aerosols does not necessarily imply significant amine emission from the amine process. Analysis of the aqueous aerosols indicates low amine content present in the aerosol fractions, and it seems evident that amines present in the gaseous phase inside the absorber column have not been transferred to the aqueous aerosols and by such the total amine emissions are very low.

© 2016 The Authors. Published by Elsevier Ltd. This is an open access article under the CC BY-NC-ND license (http://creativecommons.org/licenses/by-nc-nd/4.0/).
Peer-review under responsibility of the Programme Chair of the 8th Trondheim Conference on CO_2 Capture, Transport and Storage

Keywords: CO_2 capture; aerosol; analysis; monoethanolamine; amine emissions

---

* Corresponding author. Tel.: +47 56 34 52 20.
E-mail address: eham@tcmda.com

1876-6102 © 2016 The Authors. Published by Elsevier Ltd. This is an open access article under the CC BY-NC-ND license (http://creativecommons.org/licenses/by-nc-nd/4.0/).
Peer-review under responsibility of the Programme Chair of the 8th Trondheim Conference on CO_2 Capture, Transport and Storage
doi:10.1016/j.egypro.2016.01.017

1. Introduction

CO_2 Technology Centre Mongstad (TCM DA), located next to the Statoil refinery near Mongstad, Norway, is one of the largest post-combustion capture test facilities in the world. TCM DA is a joint venture between Gassnova, Statoil, Shell, and Sasol. The purpose of this facility, which started operation in August 2012, is to allow vendors of suitable amine formulations and other carbon capture processes to test their technology and collect performance data to support full-scale design and anticipate the associated performance and operating costs. A unique aspect of the facility is that either a slipstream from a natural gas-fired combined heat and power (CHP) plant or an equivalent volumetric flow from a refinery residue fluid catalytic cracker (RFCC), whose higher CO_2 content (about 12.9% compared with about 3.5% for the natural gas-based flue gas) is closer to that seen in coal flue gas, can be used for CO_2 capture. In the CHP plant, the natural gas is combusted in a gas turbine and the flue gas content and characteristics are similar to those of a combined cycle gas turbine (CCGT) power plant.

One of the testing facilities in place at TCM DA is a highly flexible and well-instrumented generic amine plant, designed and constructed by Aker Solutions and Kværner, aimed to accommodate a variety of technologies with capabilities of treating flue gas streams of up to 60,000 Sm^3/hr. This plant is being offered to vendors of solvent-based CO_2 capture technologies to primarily test: (1) the performance of their solvent technology; and (2) technologies aimed to reduce the atmospheric emissions of amines and amine-based degradation products from such solvent-based CO_2 capture processes.

Between December 2013 and February 2014, a monoethanolamine (MEA) solvent campaign was performed as part of Aker Solutions' test campaigns at TCM DA treating CHP flue gases. During this period, two aerosol measurement campaigns were performed as a collaboration between TNO and TCM DA in order to investigate amine emissions via the mechanisms of aerosols and the effectiveness of commercially available knitted wire mesh demisters.

This work is part of a continuous effort of gaining better understanding of the performance potential of the non-proprietary aqueous MEA solvent system, conducted by TCM DA and its affiliates and owners, in order to test, verify, and demonstrate CO_2 capture technologies.

2. Aerosol Emission: mechanism and impact

Volatile amine emission can be considered as well understood, and is usually related to the volatility of the amine compound(s), gas to liquid flow ratios in the absorber column, etc. Countermeasures such as water wash and acid wash sections can be properly designed in order to mitigate such volatile amine emissions [1]. However, recently it has been seen that under certain conditions significant amine emission can occur via aerosols. Although the detailed mechanism is not yet fully understood, it is generally accepted that a gas phase mass transfer mechanism of amines into aerosols present in the flue gas results in increased amine emissions. The size, number, and types of particles present in the flue gas before the absorber are important parameters [2-4]. Condensation or adsorption of amines and water on particle surfaces or (physical) absorption of amines into aqueous particles may contribute to the increased emissions [5]. Typically, this would lead to sub-micron sized aerosols containing amines [6]. Traditional countermeasures like demisters and water or acid washes are not suitable to remove such aerosols. Amongst others, options such as electrostatic precipitator (ESP) and Brownian demister units have been studied, but these options would lead to significant additional cost [7,8]. To be able to design more cost effective countermeasures, it is needed to improve the understanding of the mechanism of aerosol formation. TNO has been working on a new methodology for the isolation of the aerosols from flue gas, given in details below. By creating more knowledge on the size and composition of these aerosols, steps can be made for developing detailed models. This methodology has been demonstrated at the TCM DA amine plant.

The flow schematics for the TCM DA amine plant treating CHP flue gas is shown in Fig. 1 and a picture of the amine plant is shown in Fig. 2.

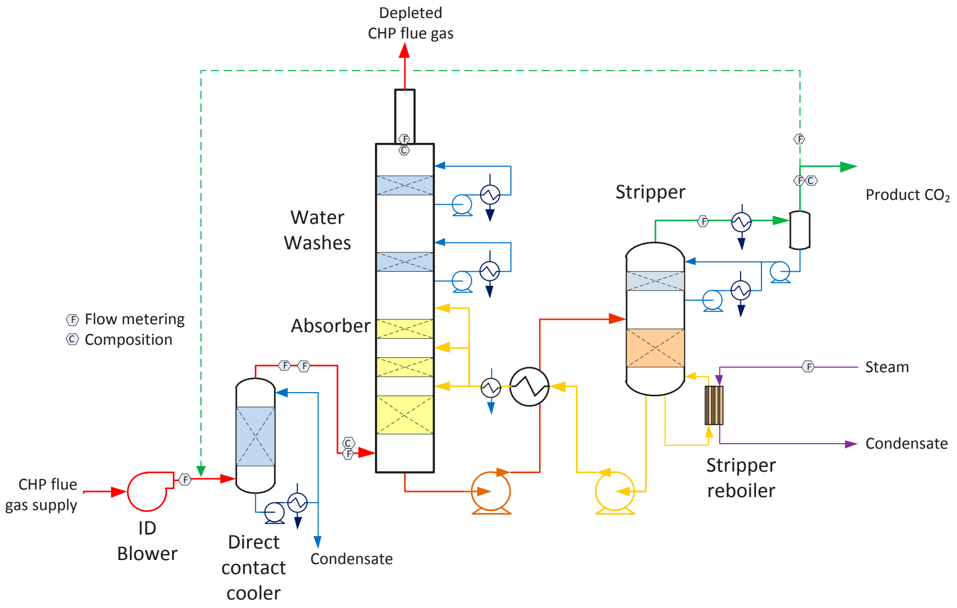

Fig. 1. Simplified flow schematic for TCM DA amine plant treating CHP flue gas.

Fig. 2. TCM DA amine plant. The direct-contact cooler is situated to the right, the concrete absorber tower in the middle, the two stripper columns to the left, and the lean vapor compressor system to the far left. The platforms towards the upper part of the absorber towers indicate the access location for the sample ports for the aerosol measurements.

The nominal characteristics of flue gas from the CHP source both before and after the direct-contact cooler (DCC) treatment are shown in Table 1. The primary purpose of the DCC is to temperature control and water saturate the flue gas, in addition to scrub the flue gas with process water. The CHP flue gas is typical of high excess air combustion turbine exhaust.

Table 1. Nominal characteristics of CHP flue gas supplied to TCM DA CO2 capture plant.

		Flue gas before DCC	Flue gas after DCC
Temperature	°C		20–50
Flow rate	Sm^3/hr		0–60.000
N_2 + Ar	mol%, dry		81-83
O_2	mol%, dry		14–15
CO_2	mol%, dry		3.5–4
H_2O			saturated
SO_2	ppmv, dry	not detected	
SO_3	ppmv, dry	not detected	
NO_X	ppmv, dry	< 5	
CO	ppmv, dry	unknown	
NH_3	ppmv, dry	< 5	
Particulates	mg/Nm^3	unknown	

The direct-contact cooler (DCC) system initially quench and lower the temperature and saturate the incoming flue gas by a counter-current flow water in order to improve the efficiency of the absorption process and provide pre-scrubbing on the flue gas. The DCC column designed for CHP flue gas operations has a 3-m diameter and a total height of 16 m. The section where water counter currently contacts the flue gas is of 3.1 m height with Flexipack 3X structured stainless-steel packing of Koch Glitsch. Above the contact section is a 0.2 m Meshpad demister type 412 of FMC Technologies with an overhead water sparging system.

The purpose of the absorber is to remove CO_2 from the flue gas using solvent. The absorber has a rectangular polypropylene-lined concrete column with a cross-section measuring 3.55 x 2 m of a total of 62 m of height. The lower regions of the tower, where the amine solution contacts the flue gas, consist of three sections of Koch Glitsch Flexipac 2X structured stainless-steel packing of 12 m, 6 m, and 6 m of height, respectively. Water-wash systems are located in the upper region of the tower to scrub and clean the flue gas particularly of any solvent carry over, and consist of two sections of Koch Glitsch Flexipac 2Y HC structured stainless-steel packing of both 3 m of height. The process is operated to be water neutral in order to maintain water balance, i.e. the recirculating water washes at the top of the absorber are used to temperature control the depleted flue gas for water content control. If water accumulates in the absorber-stripper loop, the flue gas temperature leaving the absorber is allowed to increase, increasing the water vapor content of the depleted flue gas, and vice versa.

The absorber tower includes two demisters located above the absorption section: one is installed below the lower water wash section to reduce the amount of amine entrained with the flue gas exiting the absorption section, and the other one is installed above the upper water wash section to reduce amine contaminated water entrainment released to air with the flue gas. Both demisters are 0.3 m knitted wire mesh demisters type 172 of Koch Glitsch.

The CO_2 depleted flue gas exits the absorber column to the atmosphere through a 1 m diameter nozzle stack located at the top of the absorber column in order to increase the flue gas velocity and lift.

The TCM amine plant is described in further details elsewhere [9-12].

3. Design and Construction of Aerosol Emission Detector

The design of the aerosol sampling equipment was made specific for the conditions at TCM DA. A superficial velocity of 2 m/s was taken as the reference, with an anticipated variation of this velocity in the range of 1.5 m/s to 2.5 m/s during the measurement campaign. The aerosols were to be sampled at a typical distance of 0.6-1.0 meter from the inside of the absorber wall, and equipment had to fit to a standard ASME B16.5 size flange on site. The pressure at the top of the demister was atmospheric, and within the absorber of typically 10-40 mbar excess pressure. These data were used to set design requirements for the aerosol sampling equipment. Construction of the equipment and settings of flow and temperature during experiments were then as close as reasonably practical to the design requirements derived from the above conditions.

The basic design of the sampling system consisted of 1) a probe with nozzle inserted into the absorber tower, 2) a piece of glassware that splits the incoming flow, and 3) an Anderson Cascade Impactor (ACI) that separates the aerosol in different particle size ranges. Some of the sampling system is shown in Fig. 3. The flow exiting the glassware (in Fig. 3) downwards is towards the ACI and should be 28.3 l/min, whereas the flow exiting to the right is to adjust the flow profile near the nozzle of the probe in order to operate close to iso-kinetic conditions. The nozzle of the probe and the tube inside the flow splitting section, are tapered in order not to disturb the flow profile.

Fig. 3. Glassware that directs part of the incoming flow towards the impactor and an additional flow to match the sampling system to the probed conditions and operate under near-isokinetic sampling conditions (left). Demounted Anderson Cascade Impactor with 8 stages each containing a nozzle plate and a tray for aerosol collection (right).

The ACI is a standard measurement device to determine aerosol particle size distributions. The challenges of this application are 1) the transfer of the aerosol from within the absorber towards the ACI positioned outside the absorber and without deposition of aerosols in this flow path or a change in particle size distribution, 2) collection of liquid instead of solid aerosol particles from a (nearly) saturated vapor, and 3) handling the ACI with associated equipment and shielding those against the influence of weather and temperature conditions on experimental results.

The ACI requires a precise flow of 28.3 l/min, and collects the aerosol particles on 8 different trays (stages). Meeting the flow requirement means that particles sizes are collected in the following ranges: > 9 µm in stage 1, 5.8-9.0 µm, 4.7-5.8 µm, 3.3-4.7 µm, 2.1-3.3 µm, 1.1-2.1 µm, 0.65-1.1 µm and 0.43-0.65 µm in stage 8. As the Stokes number, the particle stopping distance divided by the nozzle radius, is a constant for each tray, one can derive from the impactor design equations in [13] that with an increase of the actual flow particles of smaller diameter are caught on each tray. Abovementioned particle ranges change with actual flow Q_{actual} according to

$$28.3 l/\min d^2_{particleACIspecification} = Q_{actual} d^2_{actual\ particle\ size}. \qquad (1)$$

The additional flow to create horizontal streamlines within the flow splitting section of Fig. 3. can be calculated from the dimensions of the inner tube ($\varnothing_{int}$=13 mm, $\varnothing_{ext}$=13 mm) and the outer tube ($\varnothing_{int}$=26 mm). The additional flow is 58.9 l/min, yielding a total flow of (28.3 + 58.9) l/min = 87.2 l/min.

With an internal diameter of the probe of 12.4 mm, it follows that 87.2 l/min will lead to a flow velocity in the probe of 12.0 m/s. The probe has a nozzle with 25.4 mm internal diameter and was chosen to be close to the iso-kinetic sampling condition as demonstrated in Tab. 2, by comparison of the upward flow through a 25.4 mm diameter area and the 87.2 l/min total flow drawn in through the nozzle.

The condition of horizontal streamlines in the flow splitting section is preferred over iso-kinetic sampling, because of the sampling over a large particle size interval. The upward flow is somewhat smaller than the flow through the probe, indicating that the flow near the probe nozzle must be slightly convergent.

Table 2. Comparison of upward flow in tower with flow of 87.2 l/min towards the aerosol sampling equipment, and based on dimensioning of probe and nozzle, and based on superficial velocity in the tower.

$\varnothing_{nozzle}$ mm	V_{tower} m/s	Upward flow l/min	$\varnothing_{probe}$ mm	V_{probe} m/s	F_{total} l/min
25.4	**1.5**	**45.6**	**12.4**	**12.0**	**87.2**
25.4	**2.0**	**60.8**	**12.4**	**12.0**	**87.2**
25.4	**2.5**	**76.0**	**12.4**	**12.0**	**87.2**

The transport efficiencies due to settling in the tubes are calculated, as well as the concentration variation across the nozzle due to non-isokinetic sampling. Transport efficiencies should be close to 1 (i.e. 100% of aerosol particle transfer along the probe length), and concentration variation across the nozzle should be negligible. Both transport efficiency and concentration variations can be evaluated as function of aerosol particle size by using the equations provided in [14]. The transport efficiency $\eta_{probe,grav}$ for aerosol transport along the probe which accounts for gravitational deposition, is calculated using

$$\eta_{probe,grav} = 1 - \frac{2}{\pi}\left[2k\sqrt{1-k^{\frac{2}{3}}} - k^{\frac{1}{3}}\sqrt{1-k^{\frac{2}{3}}} + arcsin\left(k^{\frac{1}{3}}\right)\right] \tag{2}$$

with

$$k = \frac{3}{4}\left(\frac{L_{probe}}{d_{probe}}\right)\left(\frac{V_{ts}}{V_{gas\,in\,probe}}\right)\cos(\theta)$$

and

$$V_{ts} = \frac{\rho_{particle} d_{particle}^2 C_c g}{18\mu}.$$

In eq. (1) L_{probe} is the length of the probe, d_{probe} the inside diameter of the probe, V_{ts} the terminal settling velocity of particles, V_{gas} the velocity of the gas in the probe, and θ the inclination of the probe. The terminal settling velocity is a function of the aerosol particle density ρ, the particle diameter $d_{particle}$, the Cunningham slip correction factor C_c, gravitational acceleration g, and the flue gas viscosity μ.

The aspiration efficiency accounting for concentration change at the inlet nozzle is calculated using

$$\frac{C}{C_0} = 1 + \left(\frac{V_{absorber}}{V_{inlet\,probe}} - 1\right)\left(1 - \frac{1}{1+\left(2+0.617\frac{V_{inlet\,probe}}{V_{absorber}}\right)Stk}\right) \tag{3}$$

with

$$Stk = \frac{V_{ts}V_{absorber}}{g d_{inlet\,probe}}.$$

In eq. (2) C is the particle size dependent concentration in the inlet of the probe, C_0 is the particle size dependent concentration of the aerosol in the absorber, $V_{absorber}$ is the superficial velocity of the flue gas in the absorber tower, $V_{inlet\,probe}$ is the velocity of the gas in the nozzle at the inlet probe and which has a diameter $d_{inlet\,probe}$. and Stk the Stokes number.

The product of eqs. (1) and (2) gives the expected ratio of the concentration at the inlet of the impactor and the aerosol concentration in the absorber.

$$\frac{C_{impactor}}{C_0} = \eta_{probe,grav} \cdot \frac{C}{C_0}. \tag{4}$$

Calculations results are shown here for superficial velocities of 1.5, 2.0 or 2.5 m/s, a nozzle internal diameter of 25.4 mm, a probe diameter of 12.4 mm and probe length of 1.0 or 2.0 m and a velocity in the probe of 12.0 m/s.

Calculations were performed for an aerosol in air, a temperature of 40 °C, and a pressure of 101.2 kPa. The Reynolds number in the probe is 9850 and is just in the turbulent regime. The calculated transport efficiencies according to laminar flow or to turbulent flow, are approximately the same. Note that the ACI measures in the range 0.43 – 11 µm.

The length of the probe has a relatively large influence on the transport efficiency. For a 1 m probe more than 97% of 10 µm particles will be transported (i.e. less than 3% will settle in the tube), while for a 2 m probe still 95% of 10 µm particles will be transported, see Fig. 4.

With a flow velocity of 1.5, 2.0 and 2.5 m/s, respectively, more than 97%, 98% and 99% of the 10 µm particle concentration in the absorber, will be present inside the inlet of the probe, see Fig. 5.

The overall effect (concentration change at the inlet, and transport efficiency through the tube) indicates that for 10 µm particles between 92% (1.5 m/s, 2.0 m) and 97% (2.5 m/s, 1.0 m) will reach the ACI, see Fig. 6. For smaller aerosol particles the figures will be better. For 3 µm particles, one calculates that more than 99% will reach the ACI.

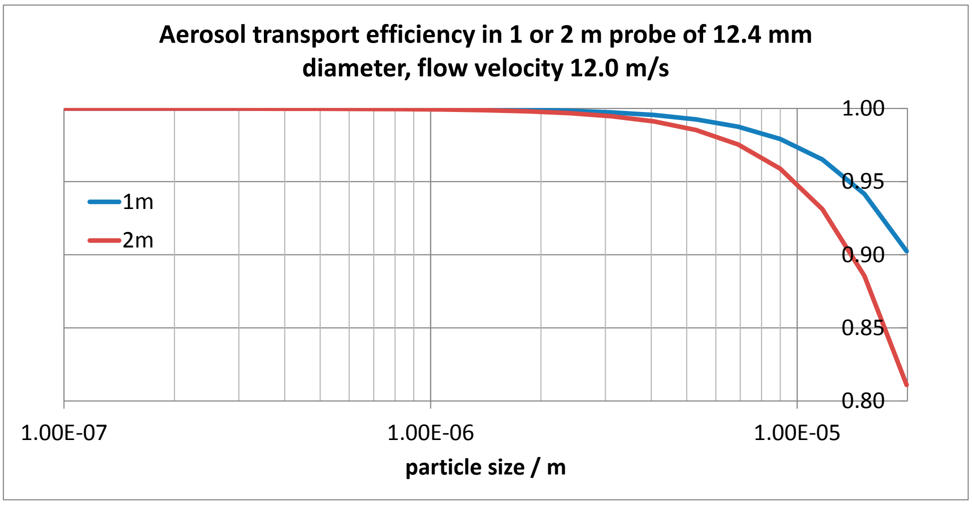

Fig. 4. Aerosol transport efficiency as function of particle diameter, for two different probe lengths.

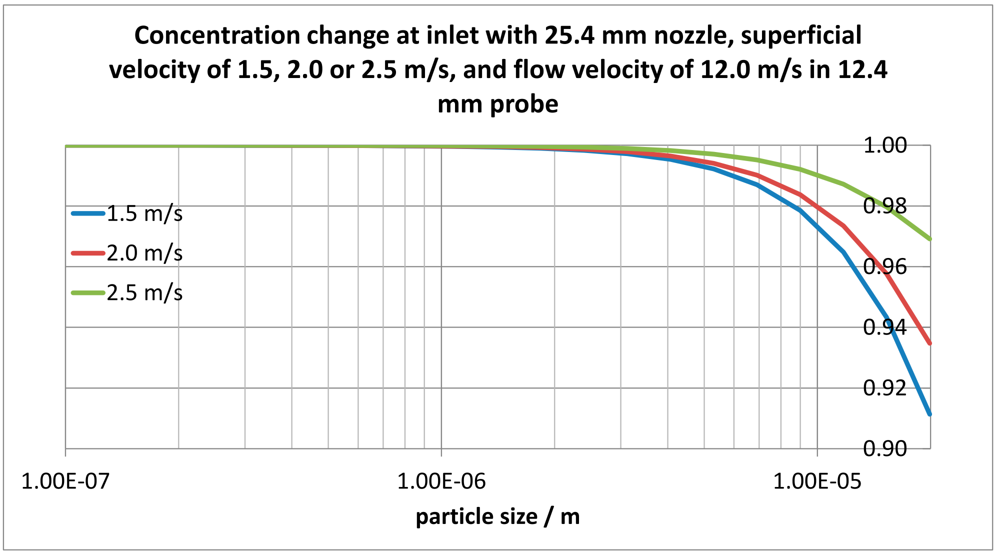

Fig. 5. Concentration change at nozzle inlet as function of particle diameter, due to non-isokinetic sampling conditions.

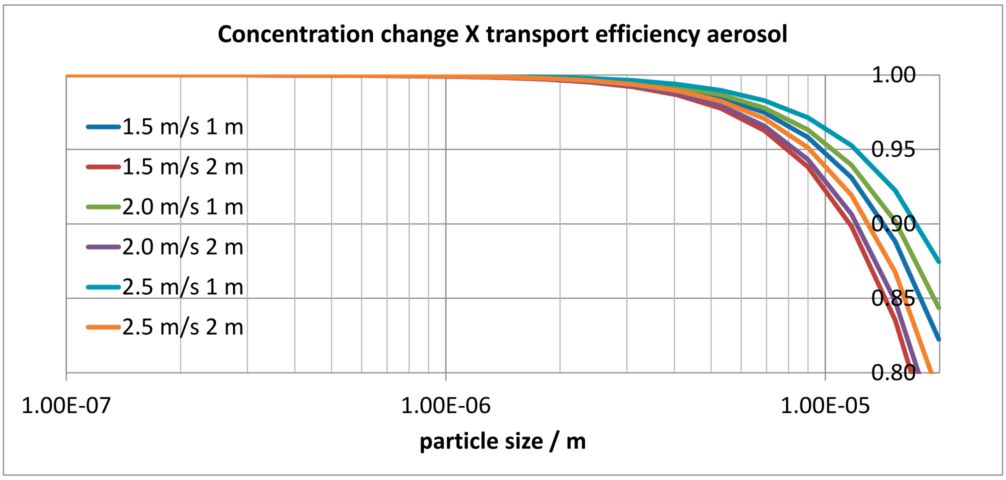

Fig. 6. Ratio of measured aerosol particle size distribution and true aerosol particle size distribution, as function of particle diameter. The ratio depends on probe length as well as near-isokinetic sampling conditions.

Even though it is clear one should minimize the probe length for a better aerosol capture, a minimum length is needed to bridge distance in practice. The minimum probe length is 191 cm, based upon a measurement 60 cm into the absorber, a 50 cm absorber concrete wall thickness, 71 cm from wall to spool tee, and 10 cm external to spool tee. The data in Fig. 4 and Fig. 6 corresponding to a 2 meter probe length are therefore relevant to the experiments.

The glass probe was mounted with thermocouple for measurement of the local absorber temperature, and with heat tracing into a metal tube. The metal tube can be inserted at the various measurement locations available at the absorber tower. The flow split section with ACI was located in an isolated box with temperature control, which was connected to the nozzle, see Fig. 7. In the experimental campaign the logged temperature in the aerosol box was maintained 2 to 4.4 °C above the temperature at the sample point, because of the finding under laboratory conditions that aerosol collection from a saturated vapor will lead to condensation on the impactor surface starting at the lowest nozzle plates with the smallest holes. This condensation should not spill over to the collection trays inside the impactor and thus limits the duration of a vapor collection experiment.

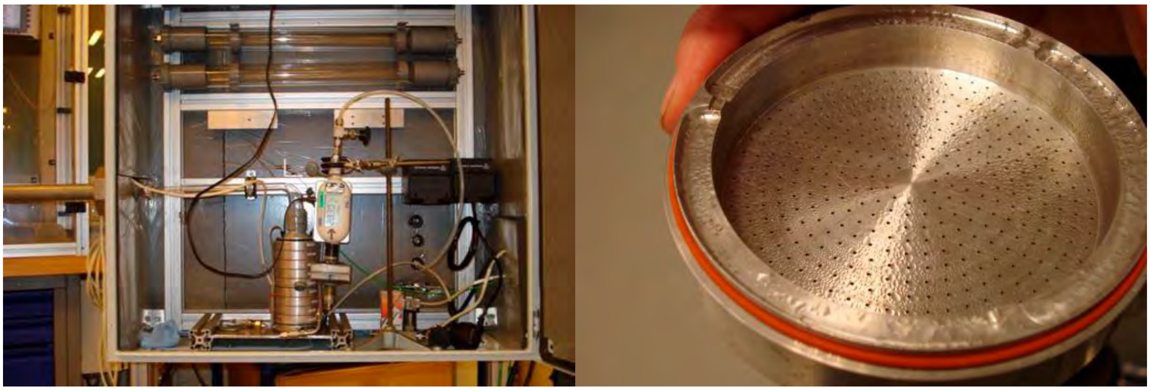

Fig. 7. Aerosol box with impactor, mass flow controllers, temperature control and desiccant, during laboratory testing phase (left). Condensation of a vapor from a saturated vapor flow with aerosol particles onto one of the impactor nozzle plates (right).

4. Results at Technology Centre Mongstad

There is a demister above the absorption section and a demister above the water wash section in the absorber tower. A total of four sampling locations were available for aerosol sampling, upstream and downstream the two demisters. Sampling location 1 and 2 are respectively upstream and downstream the lower demister, i.e. located above the absorption section, and sampling location 3 and 4 are respectively upstream and downstream the upper demister, i.e. located above the upper water wash section.

Measurements were performed in two campaigns, in December 2013 and in February 2014. The sampling locations, temperatures in the absorber and measurement durations are indicated in Tab. 3. In the four experiments in December it was noticed that liquid was collected in the flow splitting section in the aerosol box. It seems that the cold environment and the long external tube lowered the temperature of the probe, even though the flue gas may circulate around the probe and despite the short contact time of the sampled gas in the probe. An external heating band was added to the 2 meter long probe for the last two experiments, with trace heating controlled by the temperatures measured at the tip of the probe and halfway the probe.

An important aspect is the collection of filter papers from the ACI. In contrast to a laboratory environment the experiment is carried out in the open and at high elevation. It was decided to transfer the ACI from the absorption tower to a remote location and there disassemble the ACI, weigh, and store the filter papers.

Table 3. Location of aerosol sampling, temperature in the absorber tower, and measurement duration for each of 6 experiments.

Date	Exp nr	Location	Temperature in absorber	Measurement duration
11/12/2013	1	3	25 °C	1 hr
11/12/2013	2	3	45 °C	1 hr
12/12/2013	3	2	25 °C	1 hr
12/12/2013	4	2	25 °C	12 min
18/2/2014	5	4	25 °C	1 hr
18/2/2014	6	3	25 °C	1 hr

The total mass of aerosols collected by the ACI and the calculated aerosol concentration are given in Tab. 4, for the experiments with trace heating of the probe. Further to the intended aerosol sampling, 5 mL/min of the flow leaving the ACI and thus free from aerosols, was passed through a series of three aqueous sulfuric acid filled impingers. The vapor concentration calculated from the measured weight increase of the flasks with aqueous sulphuric acid is presented in Tab. 4, as well as the amine content of the vapor determined by LC-MS. The vapor concentration in experiment 5 is below $21 \cdot 10^3$ mg/Nm^3; the latter value corresponding to the maximum amount of condensable water vapor at the process temperature. The MEA emissions in the vapor phase as found by chemical analysis by LC-MS in the current work, are similar to the reported MEA emissions in the order of 10^{-2} mg/Nm^3 by Morken *et al.* [12]. This reference reports absorber stack emission results from the MEA campaign applying iso-kinetic gas measurements.

Table 4. Total mass of aerosol (water and amine) collected by the ACI and the calculated aerosol concentration, as well as the total vapour concentration (water and amine) calculated from weight increase impinger, during 1 hour experiment.

Exp nr	Location	Total mass on impactor g	Total aerosol concentration mg/Nm^3	Total vapor concentration mg/Nm^3	Amine concentration in liquid of first impinger mg/L	Calculated amine concentration in vapour mg/Nm^3
5	4	0.13*	74	$6.0 \cdot 10^3$	0.1	0.03
6	3	0.30	177		<0.05	<0.02

* On stage 8 a wet spot is observed on the filter paper. This stage is discarded in the result as the spot is due from vapor condensed at the impactor structure and has dropped onto the tray with the filter paper.

The particle size distributions are given in Fig. 8. Series 6 is a measurement of the aerosol particle distribution directly above the wash section and before the demister. Aerosols have a size in the range of 0.43 to 4.7 µm. The measurement on stage 7 seems too high; and one should note that in the laboratory condensation was noticed starting at the lower nozzle plates, with the risk of droplets falling down on the tray below, see Fig. 7.

Series 5 is a measurement of the aerosol as in series 6 only after passing the demister. Broadly the same particle size range is observed, from 0.65 to 4.7 µm, with a maximum near 3 µm. This is expected as a demister would be effective typically at particle sizes of 10 µm and above.

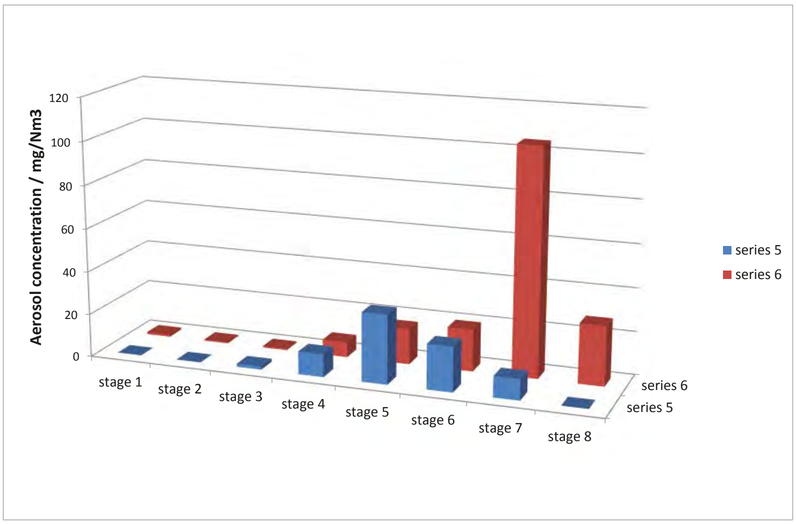

Fig. 8. Particle size distributions in series 5 and 6, with particle size decreasing towards higher stage number.

5. Conclusions and recommendations

The following conclusions can be drawn from the aerosol measurement campaign.

- One can design and optimize aerosol transfer and aerosol collection devices from aerosol kinetics theory. Effective transfer of aerosols with particle sizes up to 10 µm and over a 2 meter distance should result in a loss of aerosol particles of at most 8 % (i.e. for the largest particles size) for the designed equipment and under flow conditions.
- Aerosol collection from a nearly saturated vapor stream requires strict control over impactor temperature, and limits the duration of aerosol collection. Also the probe requires temperature tracing to avoid preliminary conditions during aerosol transfer.
- Small amounts of aerosols are present with particles up to 4.7 µm. The total concentration on mass basis is around 100 mg/Nm^3.
- The aerosols contain for the largest part water. Total amine emissions, emissions based on volatility and aerosol formations, are very low.

A recommendation for future experiments is to analyze the amine concentration of the aerosol samples by directly transferring the filter papers put on individual stages of the impactor into vials with a known quantity of an aqueous sulfuric acid solution. The extent of evaporation is thus minimized, and samples can safely be analyzed at a later moment for example with LC-MS, providing an amine concentration per particle size range. This, however, would be at the expense of determining the total mass of water and amine per particle size range.

The measurements presented here are in the absorber tower. In a risk assessment of amine plants for CO_2 capture, the relation between discharge rates from the absorber at TCM Mongstad and downstream concentrations in air and drinking water were compared to NIPH guidelines values [15]. Nitrosamine and amine discharge values were considered acceptable.

References

[1] Khakharia, P., Huizinga, A., Jurado Lopez, C., Sanchez Sanchez, C., De Miguel Mercader, F., Vlugt, T.J.H., Goetheer, E. Acid wash scrubbing as a countermeasure for ammonia emissions from a postcombustion CO2 Capture Plant (2014) Industrial and Engineering Chemistry Research, 53 (33), pp. 13195-13204.

[2] Kamijo, T., Kajiya Y., Endo, T., Nagayasu, H., Tanaka, H., Hirata, T., Yonekawa, T., Tsujiuchi, T. SO2 impact on amine emissions and emission reduction technology (2013) Energy Procedia 37, pp. 1793-1796.

[3] Bade, O. M., Knudsen, J. N., Gorset, O., Askestad, I. Controlling amine mist formation in CO2 capture from Residual Catalytic Cracker (RCC) flue gas (2014) Energy Procedia 63, pp. 884-892.

[4] Khakharia, P., Brachert, L., Mertens, J., Anderlohr, C., Huizinga, A., Fernandez, E.S., Schallert, B., Schaber, K., Vlugt, T.J.H., Goetheer, E. Understanding aerosol based emissions in a Post Combustion CO2 Capture process: Parameter testing and mechanisms (2015) International Journal of Greenhouse Gas Control, 34, pp. 63-74.

[5] Khakharia, P., Brachert, L., Mertens, J., Huizinga, A., Schallert, B., Schaber, K., Vlugt, T.J.H., Goetheer, E. Investigation of aerosol based emission of MEA due to sulphuric acid aerosol and soot in a Post Combustion CO2 Capture process (2013) International Journal of Greenhouse Gas Control, 19, pp. 138-144.

[6] Mertens, J., Brachert, L., Desagher, D., Thielens, M.L., Khakharia, P., Goetheer, E., Schaber, K. ELPI+ measurements of aerosol growth in an amine absorption column (2014) International Journal of Greenhouse Gas Control, 23, pp. 44-50.

[7] Mertens, J., Anderlohr, C., Rogiers, P., Brachert, L., Khakharia, P., Goetheer, E., Schaber, K. A wet electrostatic precipitator (WESP) as countermeasure to mist formation in amine based carbon capture (2014) International Journal of Greenhouse Gas Control, 31, pp. 175-181.

[8] Khakharia, P., Kvamsdal, H.M., Da Silva, E.F., Vlugt, T.J.H., Goetheer, E. Field study of a Brownian Demister Unit to reduce aerosol based emission from a Post Combustion CO2 Capture plant (2014) International Journal of Greenhouse Gas Control, 28, pp. 57-64.

[9] Thimsen D, Maxson A, Smith V, Cents T, Falk-Pedersen O, Gorset O, Hamborg E S. Results from MEA testing at the CO_2 Technology Centre Mongstad. Part I: Post-Combustion CO_2 capture testing methodology. Energy Procedia 63 (2014) 6012–6022.

[10] Hamborg E S, Smith V, Cents T, Brigman N, Falk-Pedersen O, De Cazenove T, Chhaganlal M, Feste J K, Ullestad Ø, Ulvatn H, Gorset O, Askestad I, Gram L K, Fostås B F, Shah M I, Maxson A, Thimsen D. Results from MEA testing at the CO_2 Technology Centre Mongstad. Part II: Verification of baseline results. Energy Procedia 63 (2014) 6012–6022.

[11] Brigman N, Shah M I, Falk-Pedersen O, Cents T, Smith V, De Cazenove T, Morken A K, Hvidsten O A, Chhaganlal M, Feste J K, Lombardo G, Bade O M, Knudsen J, Subramoney S C, Fostås B F, De Koeijer G, Hamborg E S. Results of amine plant operations from 30 wt% and 40 wt% aqueous MEA testing at the CO_2 Technology Centre Mongstad. Energy Procedia 63 (2014) 6012–6022.

[12] Morken A K, Nenseter B, Pedersen S, Chhaganlal M, Feste J K, Tyborgnes R B, Ullestad Ø, Ulvatn H, Zhu L, Mikoviny T, Wisthaler A, Cents T, Bade O M, Knudsen J, De Koeijer G, Falk-Pedersen O, Hamborg E S. Emission results of amine plant operations from MEA testing at the CO_2 Technology Centre Mongstad. 63 (2014) 6012–6022.

[13] Marple, V.A., Willeke, K., Impactor design, Atmospheric Environment Vol 10 (1976) 891-896.

[14] Chapter 6, Sampling and transport of aerosols, J.E. Brockmann, in Aerosol Measurement, Principles Techniques and Applications, eds. K. Willeke and P.A. Baron.

[15] De Koeijer, G., Randgaard Talstad, V., Nepstad, S., Tønnessen, D., Falk-Pedersen O., Maree, Y., Nielsen, C., Health risk analysis for emissions to air from CO2 Technology Centre Mongstad, International Journal of Greenhouse Gas Control 18 (2013) 200–207.

Results from MEA testing at the CO_2 Technology Centre Mongstad. Part I: Post-Combustion CO_2 capture testing methodology

(2014)

Available online at www.sciencedirect.com
ScienceDirect
Energy Procedia 63 (2014) 5938 – 5958
Energy Procedia

GHGT-12

Results from MEA testing at the CO_2 Technology Centre Mongstad. Part I: Post-Combustion CO_2 capture testing methodology

David Thimsen[a,]*, Andrew Maxson[a], Vian Smith[b,c], Toine Cents[b,c], Olav Falk-Pedersen[b,d], Oddvar Gorset[e], Espen S. Hamborg[b,f]

[a]*Electric Power Research Institute, 3420 Hillview Avenue, Palo Alto, CA 94304, USA*
[b]*CO_2 Technology Centre Mongstad (TCM DA), 5954 Mongstad, Norway*
[c]*Sasol Technology, PO Box 5486, Johannesburg 2000, South Africa*
[d]*Gassnova SF, Dokkvegen 10 3920 Porsgrunn, Norway*
[e]*Aker Solutions, PO Box 222, 1326 Lysaker, Norway*
[f]*Statoil ASA, P.O. Box 8500, 4035 Stavanger, Norway*

Abstract

This paper lays out a generic CO_2 capture testing methodology that has been applied at multiple sites providing details on the procedure, its key performance indices and their associated specifications, as well as the required pre-test work. Specific application of the methodology for the CO_2 Technology Centre Mongstad site, a CO_2 capture testing facility located in Norway that performed CO_2 capture tests using MEA, is shown as an illustrative example.

© 2014 The Authors. Published by Elsevier Ltd. This is an open access article under the CC BY-NC-ND license
(http://creativecommons.org/licenses/by-nc-nd/3.0/).
Peer-review under responsibility of the Organizing Committee of GHGT-12

Keywords: CO_2 capture; EPRI; MEA; Post-combustion capture; CO_2 Technology Centre Mongstad; TCM DA

---

1. Introduction

At the beginning of the 21st century, increasing political and technological focus is being given to minimizing carbon dioxide (CO_2) emissions to the atmosphere. As the combustion of fossil fuels at large industrial facilities is a significant source of CO_2 entering the atmosphere, reducing CO_2 emissions from existing and new fossil-fired plants

---

* Corresponding author. Tel.: +1-651-766-8826; fax: +1-651-765-6375.
E-mail address: dthimsen@epri.com

1876-6102 © 2014 The Authors. Published by Elsevier Ltd. This is an open access article under the CC BY-NC-ND license
(http://creativecommons.org/licenses/by-nc-nd/3.0/).
Peer-review under responsibility of the Organizing Committee of GHGT-12
doi:10.1016/j.egypro.2014.11.630

will be critical. A principal method proposed for accomplishing this reduction is to capture the CO_2 produced by separating it from the flue gas into a relatively pure stream and then injecting the purified CO_2 into acceptable underground geological reservoirs for long-term storage.

Currently the only CO_2 capture technologies sufficiently mature to apply at full scale are temperature swing absorption (TSA) processes that remove the relatively dilute CO_2 from flue gas (common in processes that use air for combustion and produce significant nitrogen that dilutes the flue gas) by chemical absorption into an alkaline solvent at low temperature. The solvent is then heated to release the CO_2 in a relatively pure stream for subsequent geological storage. Aqueous amine solutions at high concentration are leading near-term solvent candidates.

The use of amines to remove CO_2 from various industrial and fuel gas streams is a relatively mature technology. There is less experience using amines to remove CO_2 from flue gases, which contain significant levels of oxygen. In addition, the full-scale application of amine post-combustion capture (PCC) processes for removing CO_2 from flue gas would be conducted at a scale approximately an order of magnitude larger than industrial amine-based TSA processes currently deployed.

Supply of the utilities required by a TSA process (thermal, electrical, and cooling) will have a significant impact on the operations of the host plant producing the flue gas being treated. Perhaps the greatest focus of PCC development is identifying processes that minimize the use of these utilities, particularly the thermal utility.

The Electric Power Research Institute (EPRI) has developed a generic independent verification protocol (IVP) to assess the performance of amine-based TSA processes. This IVP has already been tailored to and applied during EPRI-led CO_2 capture testing at the following facilities:

- **AEP's Mountaineer Plant –** 20-MWe demonstration of Alstom's chilled ammonia process during 2011–2012
- **Alabama Power's Plant Barry –** 500 tonnes/day demonstration of MHI's KM-CDR advanced amine process; testing began in 2012 and is still ongoing
- **EDF's Le Havre –** 2.0-MWe demonstration of Alstom/Dow's Advanced Amine Process (AAP) during 2014
- **We Energies' Pleasant Prairie Power Plant –** 1.7-MWe demonstration of Alstom's chilled ammonia process during 2008.

CO_2 Technology Centre Mongstad (TCM DA) has installed pilot-scale amine-based TSA process equipment next to the Statoil refinery in Mongstad, Norway. The purpose of this facility is to allow vendors of suitable amine formulations and other PCC processes to test their process and collect performance data to support full-scale design and anticipate the associated performance and costs.

This work is part of a continuous effort of gaining better understanding of the performance potential of the non-proprietary aqueous MEA solvent system, conducted by TCM DA and its affiliates and owners, in order to test, verify, and demonstrate CO_2 capture technologies [1, 2, 3]. As part of an overall program of CO_2 capture testing, EPRI worked with TCM DA, which operates the TCM DA facility and led the testing effort, and Aker Solutions to customize the IVP for TCM DA. Details on that customization are provided within this paper.

2. Independent verification protocol purpose and scope

2.1. Amine process description

Flue gas can be supplied to the TCM DA PCC amine plant from either the on-site natural gas-fired combined heat and power (CHP) plant or from the Statoil refinery residue fluid catalytic cracker (RFCC). As the testing work that this report discusses pertains to using the CHP flue gas, details on the RFCC will not be provided here. In the CHP plant, the natural gas is combusted in a gas turbine and the flue gas content and characteristics are similar to those of a combined cycle gas turbine (CCGT) power plant.

The flow schematic for the TCM DA pilot plant when treating CHP flue gas is shown in Fig. 1 and a photo of the amine plant is shown in Fig. 2.

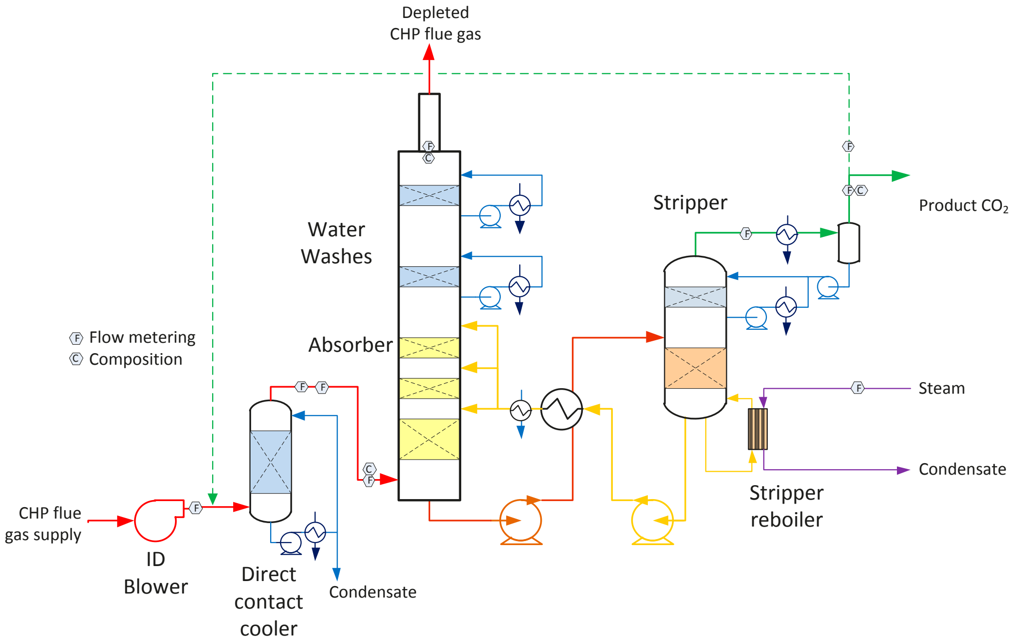

Fig. 1. Simplified flow schematic for TCM DA CO_2 capture of CHP flue gas

Fig. 2. TCM DA amine plant. The direct-contact cooler is situated to the right, the concrete absorber tower in the middle, the two stripper columns to the left, and the lean vapour compressor system to the far left.

The nominal characteristics of flue gas from the CHP source both before and after the direct-contact cooler (DCC) are shown in Table 1. The CHP flue gas is typical of high excess air combustion turbine exhaust.

Table 1. Nominal characteristics of CHP flue gas supplied to TCM DA CO_2 capture plant

		Flue gas before DCC	Flue gas after DCC	
Temperature	°C		20–50	
Flow rate	Sm^3/hr		0–60.000	
N_2 + Ar	mol%, dry		81-83	
O_2	mol%, dry		14–15	
CO_2	mol%, dry		3.5–4	
H_2O			saturated	
SO_2	ppmv, dry	not detected		
SO_3	ppmv, dry	not detected		
NO_X	ppmv, dry	< 5		
CO	ppmv, dry	unknown		
NH_3	ppmv, dry	< 5		@ 15% O_2
Particulates	mg/Nm^3	unknown		Nm^3 at 101.3 kPa and 0°C

The raw flue gas may be cooled by direct contact with wash water. By these means, plant operators have the capability of controlling the temperature of the flue gas (saturated with water) delivered to the absorber.

The saturated flue gas rises in the rectangular cross-section absorber tower and comes into contact with falling lean solution in one of up to three beds of structured packing. The flue gas, depleted in CO_2, then passes through up to 2 recirculating water wash stages to remove solvent vapors before being emitted to the atmosphere in a 1-meter diameter duct. The solution flow through the absorber tower is “once-through”; there is no recirculation of rich solution from the tower sump back to the top of the absorber section.

The solution rich in CO_2 is pumped to the top of a stripper tower. Rich solution entering the stripper is pre-heated by exchange with hot lean solution being returned to the absorber. The falling rich solution comes into contact with rising steam/CO_2. The lean solution at the bottom of the stripper is circulated through a steam-heated reboiler to provide the heat necessary to drive the endothermic CO_2-releasing reactions.

The raw product CO_2 leaving the stripper is cooled with recovery of condensate that is returned to the stripper as a reflux. The cooled product CO_2 is vented. During CHP flue gas operations, a portion of the product CO_2 can be recycled to the CHP flue gas upstream of the DCC to increase the CO_2 content of the CHP flue gas for test purposes.

The process is operated to be water neutral. The recirculating water washes at the top of the absorber are used to control the depleted flue gas temperature/water vapor content. If water accumulates in the absorber-stripper loop, the flue gas temperature leaving the absorber is allowed to increase, increasing the water vapor content of the depleted flue gas, and vice versa.

2.2. Testing to support process characterization

The key performance indices are those features of the PCC process that are of interest when designing and planning for a full-scale implementation of the technology. Some of these indices can be modeled using chemical/thermodynamic/physical design data. A primary function of pilot-plant operations is to provide measured data such that uncertainties in the model can be reduced by comparison of model results with measured results.

The key performance indices are dependent parameters that can be expected to vary with changes in the process independent parameters. Performance data collected when changing the independent parameters during pilot-plant operations can be used to calibrate the process model, which can then be used to identify a set of independent parameters that “optimize” the key performance indices.

Pilot-plant operations can also be used to quantify those key performance indices that are not readily amenable to modeling including the effects of trace constituents of the flue gas supply. There are also intermittent and long-term performance indices that cannot be effectively modeled and must be assessed from many hours of pilot-plant operations (typically 1000s of hours) including: heat exchanger fouling, mass transfer packing fouling, foaming, material corrosion, solvent quality control measures, solvent loss/replacement, etc.

2.3. Pertinent independent parameters

The independent parameters are those temperatures, pressures, flows, compositions, and physical design parameters readily subject to control by the plant operators. Changing these parameters can be expected to affect the key performance indices (dependent parameters). The most important independent parameters for the purposes of modeling the process installed at TCM DA are listed below.

- Inlet flue gas characteristics
  - CO_2 content
  - Flow rate
  - Temperature
  - With/without flue gas pre-treatment for SO_X and particulates (future).
- Solution characteristics
  - Amine concentration
  - Circulation rate
  - Lean solution CO_2 loading.
- Equipment design characteristics
  - Absorber height
  - Lean solution flash/compression use
  - Number of water washes
  - Rich/lean heat exchanger effectiveness.
- Operating options
  - Stripper pressure.

2.4. Modeled key performance indices (dependent parameters)

The set of key performance indices that can be modeled and quantified by pilot-plant operations at TCM DA are listed below.

- CO_2 capture performance
  - % CO_2 captured / produced / emitted.
- Utility use
  - Cooling duty
  - Electrical power
  - Steam thermal.
- Depleted flue gas amine/degradation product content.

2.5. Key performance indices not modeled (dependent parameters)

While it is fairly straightforward to model the heat and mass transfer associated with the PCC process, there are key performance indices that are less straightforward to model. It is more expedient to quantify these indices, which are listed below, by measurements during pilot-plant operations.

- Depleted flue gas trace constituents
  - Mercury and air toxics

  - Particulates
  - SO_2–SO_3–NO_X
  - Total hydrocarbons (HC) – Amine/degradation products not modeled.
- Product CO_2 trace constituents
  - O_2
  - SO_2–SO_3–NO_X
  - Total HC–Amine/degradation products not modeled.
- Continuous waste streams
  - DCC blowdown.

2.6. Long-term process/plant monitoring

There are also key performance indices that can only be assessed over many hours of operation. These include chronic effects as well as intermittent operations as shown below.

- Material uses
  - Amine make-up
  - Water make-up/blowdown.
- Intermittent waste streams
  - Amine reclaim waste
  - Lean-solution filter cake
  - Spent activated carbon.
- Heat exchanger fouling/corrosion
- Gas-liquid contactor fouling/corrosion/foaming
- Accumulation/emission of degradation/corrosion products.

2.7. Key outcomes

Key outcomes of pilot-plant operations are:

1. A stand-alone model that predicts key performance indices within the uncertainty in actual measurements made during pilot-plant operations (or other clearly stated uncertainty) when only the independent parameters listed above are the variable inputs to the model
2. One or more sets of formal performance test results collected during "base-case" operations that include, in addition to the modeled key performance indices, empirical measurement of the key performance indices not modeled. These "base-case" operations can be expected to be conducted under a set of independent parameters that have been determined to "optimize" the key pre-defined performance indices.

3. Performance testing principles

3.1. General performance testing guidelines

There is no accepted procedure for assessing PCC plant performance. There are, however, reference-testing procedures that are similar in scope and provide guidance for specifying the protocols under which the performance of PCC plants can be verified. These include:

- **Overall power plant performance –** Steam-boiler operations are comparable in complexity to PCC plant operations. Flow, temperature, and pressure, and composition data must be collected over the test period and are used to calculate a number of key performance indices such as steam temperature, pressure, and flow, fuel quality, flue gas flow rate and composition, sensible and latent heat losses in the flue gas, auxiliary power use, gross generation, net generation, etc. The overall power plant performance test code will also make extensive reference to companion test codes for measuring temperature, pressure, flow, gas composition, electrical and other power flows, and sub-component performance (boilers, air heaters, turbines, etc.). The American Society of Mechanical Engineers (ASME) publishes and maintains performance test codes for a wide range of equipment that have a long history of successful use [4].

- **Quantifying flue gas emissions –** The U.S. Environmental Protection Agency (EPA) has published reference methods for quantifying emissions from stacks for the purpose of demonstration conformance with the site air emission permit. These reference methods have a long history of use in the U.S. and have achieved wide acceptance. Appendix A lists the pertinent U.S. EPA reference methods. The European Commission has published similar reference methods.

The performance testing protocols presented here draw heavily on these two sources.

3.2. Base-case performance testing/process verification

Results from the base-case testing will be used to assess the steady-state performance of the process for the purposes of designing the full-scale plant and estimating capital and operating costs. For this reason, base-case performance testing should be conducted with measurement uncertainty as low as can be reasonably achieved. Therefore, test protocols consistent with well-developed reference methods should be incorporated as much as possible.

3.3. Parametric performance testing

The primary objective of parametric performance testing is to observe the effects on the key performance indices of incremental changes in the various independent variables. While accuracy in measurement is always desired, some bias error in measurements can be tolerated in parametric testing as long as the measurements achieve adequate precision; i.e., the measurement instruments give repeatable values. This condition can usually be met without strict adherence to reference methods that can be very costly to use as frequently as is required for a parametric performance testing program.

4. Test conduct and data collection procedures

4.1. Instruments and methods of measurement

4.1.1. Temperature

Process temperatures are generally not key performance parameters for a PCC plant. Nonetheless, temperature measurements are process condition indicators and care should be taken in their measurement.

No review of process temperature instrumentation was conducted in support of this study. In general, thermocouple or resistance temperature detectors are commonly deployed for process monitoring. These are usually precise enough to give acceptable repeatability without re-calibration. However, care should be exercised in ensuring that electrical temperature measurement signals are correctly wired, correct calibration algorithms are employed, and the resulting temperature is correctly logged and displayed to the operators.

4.1.2. Pressure

Process pressures are generally not key performance parameters for a PCC plant without a pipeline gas compressor. (Pipeline compressor discharge pressure would be a key performance parameter.) Nonetheless, several pressure measurements are process condition indicators and care should be made in their measurement. These include absolute and differential pressures at flow metering installations, absorber flue gas pressure drop, liquid distribution spray pressures, and stripper operating pressure.

No review of process pressure instrumentation was conducted in support of this study. In general pressure transmitters are commonly deployed for process monitoring. The key pressure transmitters, at a minimum, should be recalibrated according to manufacturer's specifications prior to the onset of parametric testing. Pressure transmitters supporting primary flow measurement calculations should be recalibrated during base-case testing.

4.1.3. Flow

The standard used for flow metering is ASME PTC 19.5 Flow Measurement. Note that high accuracy may not be required for parametric testing where the incremental effect on key performance indices with incremental changes in process conditions is measured. In this case high precision (repeatability) may be an adequate substitute for high accuracy.

The flow meters installed in the PCC plant at TCM DA supporting CHP flue gas are listed in Table 2, respectively. The flow metering locations were indicated in Fig. 1. TORBAR pitot tube-style flue gas flow meters are the predominant choice implemented with single installation of an ultrasonic flow meter (after the DCC). Vortex flow meters are used to measure steam flows to the reboiler. A vortex flow meter is used to meter final CO_2 product flow, which is redundant to the TORBAR flow meter.

The flow metering installations have been internally analyzed in detail at TCM DA, identifying the sources of uncertainty in each flow metering location.

Table 2. Gas and steam flow metering for CHP flue gas applications at TCM DA

Stream	Flow meter tag	Flow meter type	Duct dimension
Flue gas supply			
Raw CHP after blower	8610-FT-0104	TORBAR pitot tube	991 mm
CHP after DCC	8610-FT-0150	Ultrasonic	991 mm
CHP after DCC	8610-FT-0124	TORBAR pitot tube	991 mm
Absorber flue gas flows			
Inlet	8610-FT-2039	TORBAR pitot tube	991 mm
Outlet	8610-FT-2431	TORBAR pitot tube	991 mm
Product CO_2 flows			
Cooled product CO_2	8610-FT-2203	TORBAR pitot tube	311 mm
Cooled product CO_2	8615-FT-0010	Vortex	254.5 mm
CO_2 recycled to CHP	8615-FT-2206	TORBAR pitot tube	
Stripper reboiler steam flow			
Reboiler	8655-FT-2386	Vortex	

4.1.3.1. TORBAR pitot tube flow meters

The uncertainty in the flow measurements using the TORBAR flow meters was estimated to be slightly greater than 2.5%. Of this, 2% was associated with installation of the TORBAR flow meters, by far the largest uncertainty component. This uncertainty component is a measure of the sensitivity of bias error introduced into the differential pressure indication by misalignment of the flow element in radial dimension and rotational orientation to the flow. The uncertainty associated with installation cannot be effectively estimated short of performing an in-situ flow calibration against a primary standard, and the assignment of 2% uncertainty to this component is somewhat arbitrary; misalignment could result in higher bias errors. Thus, while the flow reading calculated from the TORBAR measured pressure differential, absolute pressure, and temperature may have a precision of approximately 1.8% (precision excludes installation uncertainty), the uncertainty in accuracy may be significantly more than the estimate. The uncertainty associated with installing this class of flow meters generally disqualifies them for use in applications requiring predictable accuracy unless a relative accuracy test audit (RATA) has been performed for the field installation.

4.1.3.2. Vortex flow meter

A vortex meter is installed to meter product CO_2. The vortex meter is redundant to a TORBAR meter located nearby. Vortex flow meters are shipped with a flow factor which, when multiplied by the vortex shedding frequency (an internal meter measurement) and fluid density, gives mass flow. The density must be derived from temperature, pressure, and composition measurements. These meters cannot be recalibrated short of performing an in-situ flow calibration against a primary standard.

A vortex flow meter is also used to meter steam flow to the reboiler. It is a linear device that indicates mass flow; thus the calibration range is based on mass flow. This meter is suitable for high accuracy mass flow measurements if it is calibrated under the following conditions:

- Steam flow over the full range expected during operations
- Calibration temperatures and pressures close to the operating temperature/pressure
- Calibration against standards traceable to the National Institute of Standards & Technology (NIST) or equivalent.

4.1.4. Composition

The standard recommended here for high-accuracy gas composition measurements is the use of reference standards commonly employed to monitor compliance with air emissions regulations. Where possible, the use of continuous emissions monitoring (CEM) methods is recommended.

It is recognized that the Fourier Transform Infrared (FTIR)-based systems installed at TCM DA will continue to be used. The relative locations for the sampling points are indicated in Fig. 1. The gas compositions reported by these instruments may be sufficiently accurate and precise to meet the requirements of the standards indicated, but this should be demonstrated against the instruments and procedures in the respective reference methods. The reference methods indicated below should be employed during all base-case testing unless there is clear evidence that the FTIR system gives results that duplicate the reference methods.

4.1.4.1. Flue gas supply and depleted flue gas

Table 3 lists the several flue gas components and the recommended reference methods for quantifying the components. CEMs are available for all non-condensable, non-soluble flue gas components. The condensable/soluble flue gas components and particulate matter require extractive sampling reference methods.

Table 3. Flue gas composition sampling and analysis reference methods

Component	Reference method	Notes
O_2	EPA method 3a	CEMs, dried sample from common sampling point
CO_2	EPA method 3a	
SO_2	EPA method 6c	
NO_X	EPA method 7e	
Total HC	EPA method 8a	CEMs, wet sample from common sampling point
Particulates	EPA method 5	Extractive traverse
Particulate metals	EPA methods 5 and 29	
SO_3	NCASI method 8a	
NH_3	EPA conditional test method 027	
Gaseous organics (amines and amine degradation products)	See Appendix B	See Appendix B
Aldehydes	SW846-0011: Sampling Method 8315: Analysis	This is essentially the same as that practiced by TCM DA at present

4.1.4.2. Product CO_2

Table 4 lists the several product CO_2 components and recommended reference methods for quantifying the components. CEMs are available for all components except NH_3.

Table 4. Product CO_2 composition sampling and analysis reference methods

Component	Reference method	Notes
O_2	EPA method 3A	Dried sample from common sampling point. Analyze with polarographic trace O_2 analyzer.
CO_2	EPA method 3A	CEMs, dried sample from common sampling point
SO_2	EPA method 6C	
NO_X	EPA method 7E	
Total HC	EPA method 8A	CEMs, wet sample from common sampling point
NH_3	EPA conditional test method 027	Extractive single point

The most critical parameters for delivery of the product CO_2 to receiving pipelines are likely to be O_2 content and moisture content. Measurement of trace O_2 in any gas stream is challenging. In-situ O_2 analyzers commonly used for measurement of flue-gas O_2 at levels, which are typically above a few % (vol), are not sufficiently sensitive to accurately quantify trace levels of O_2. Trace O_2 levels may be quantified by polarographic (fuel cell) analyzers. Paramagnetic analyzers or gas chromatography may also be used but these are likely to add complexity and/or expense without significantly increasing accuracy. All of these techniques require extraction of a gas sample to the analyzer. Care must be exercised to exclude sampling system and instrument air in-leaks and to completely purge the sampling system of air on start-up and after calibrations; even small residues of air (containing 210,000 ppmv O_2) will result in erroneously high analyses. Certified trace O_2 calibration gases are also required. Moisture control will be part of a pipeline compression package that is not a part of the pilot plant at TCM DA.

Note that CO_2 monitoring in the product CO_2 stream is for reference only. Instrument readings near 100% cannot be relied on for accuracy at the 99.99% (vol) readings expected. Nitrogen is a likely diluent that can only be quantified by gas chromatography. An N_2/O_2 ratio cannot be assumed in the product CO_2 equal to that in air. Dissolution of O_2 in the aqueous amine solution or transfer of flue gas micro-bubbles with release in the stripper cannot be ruled out.

4.2. Instrumentation recommendations

4.2.1. Temperature measurements

- No pre-test calibrations required
- Loop checks should be made on temperature instruments supporting flue gas flow meters and product CO_2 flow meters during parametric testing.

4.2.2. Pressure measurements

- Loop checks should be made on pressure instruments during parametric testing
- Pressure transmitters supporting flow meters and product CO_2 flow meters should be recalibrated prior to or during all base-case test campaigns.

4.2.3. Flow measurements

- A RATA (see Appendix C) should be conducted, calibrating the three (3) flow metering installations for the CHP flue gas flow between the DCC and the absorber during each base-case test campaign. During this test, data may also be collected at the absorber outlet to calibrate the TORBAR flow metering installation at this location.
- Reboiler steam condensate orifice flow elements should be used to quantify reboiler steam use
- One of the following should be accomplished during base-case testing:
  - A RATA (see Appendix C) to calibrate within 2% accuracy the TORBAR flow meter installed to meter the product CO_2 flow
  - A differential flow element consistent with ASME PTC 19.5 should be at an applicable location to achieve CO_2 flow measurement within 2% uncertainty.

4.2.4. Composition measurements

- The FTIR analyzer system should be calibrated against primary calibration standards weekly or on a frequency that results in instrument drift of no more than 2% on calibration gases
- Gas stream sampling and analysis consistent with reference methods indicated in Table 3 and Table 4 should be employed during all base-case test campaigns
- Flue gas sampling ports should be used to sample from the duct near the existing flue gas flow meters
- The depleted flue gas sample should be taken from a probe extending at least 50 cm in from the absorber wall.

5. Calculation and reporting of key performance indices

Performance data collected during operations at TCM DA pilot plant fall generally into two broad classes: 1) data collected during parametric testing to support process model development and identify optimal operating conditions, and, 2) base-case data collected during operation under optimized conditions to verify the performance of the process, modeled parameters, and those key performance indices that are not modeled.

A complete test results report includes:

- List of independent parameters; those parameters under the more or less direct control of the operators that describe the process conditions imposed for the test
- Several key performance indices; dependent parameters that are uniquely determined by the process design and the independent parameters established by the operators.

5.1. Independent parameters

Table 5 lists the measured independent parameters that are likely to influence the key performance indices and should be included as test conditions in any report of process performance.

Table 5. Measured independent parameters

Parameter	Instrument/Comment
A. Flue gas source and flow rate	- Calibrated meter flow, composition at the absorber inlet or recommended sample ports near flue gas flow meters
B. Flue gas supply bulk composition	- Wet-basis (flowing) composition to include CO_2, O_2, N_2/Ar by difference. Wet-basis water content saturated at the measured temperature.
C. Flue gas temperature inlet to the absorber	- Plant instrumentation
D. Amine composition or identification	- Vendor supplied
E. Lean-amine concentration	- Lab analyses
F. Lean-amine CO_2 loading	- Lab analysis
G. Lean-amine flow rate	- Plant instrumentation
H. Lean-amine temperature	- Plant instrumentation
I. Water-wash flow rate	- Plant instrumentation
J. Water-wash operation	- Number in service **Note**: Water-wash temperature is a dependent variable that maintains the water balance in the lean/rich solution loop.
K. Rich-amine temperature inlet to the stripper (achieved by bypassing rich/lean cross-over heat exchanger)	- Plant instrumentation
L. Active absorber height	- Packed beds in service / aggregate height in service
M. Stripper outlet pressure	- Plant instrumentation
N. Stripper reboiler steam (enthalpy) flow	- **Parametric testing:** Condensate flow meters or existing vortex flow meters - **Base-case testing:** Condensate flow meters
O. Lean vapor compression system operation	- On/off
P. Trace flue gas supply/depleted flue gas composition	- **Base-case testing:** NO_X, SO_2, SO_3, total HC, amines/aldehydes/NH_3

Table 6 lists pertinent independent parameters derived from the measured independent parameters that are likely to be more instructive than the parameters from which they are calculated.

Table 6. Derived independent parameters

Parameter	Calculation
A. Operating capacity	• Inlet flue gas flow rate as a % of design inlet flue gas flow rate
B. Absorber liquid-to-gas ratio	• Lean-amine flow divided by flue gas flow rate
C. Stripper liquid-to-gas ratio	• Rich-amine flow divided by stripper overhead CO_2 flow
D. Cross-over heat exchanger effectiveness	Calculated from: • Lean amine TCM DA instrumentation: FT2045, TT2114, TT2110 • Rich amine TCM DA instrumentation: TT2003, TT2111

5.2. Test period data results

Test period data include dependent variables that are directly measured parameters as well as key performance indices that are pertinent to calculations of measured values and independent parameters. Table 7 lists the important measured dependent parameters.

Table 7. Measured dependent parameters

Parameter	Instrument/Comment
A. Depleted flue gas temperature	• Plant instrumentation
B. Depleted flue gas bulk composition	• CO_2, O_2, N_2/Ar (by difference), H_2O (saturated). **Parametric testing:** Plant instrumentation; **Base-case testing:** CEMs data.
C. Depleted flue gas amines / aldehydes / NH_3 / SO_3	• During tests varying water wash operations and base-case tests
D. Depleted flue gas flow	• Plant instrumentation or calculated from composition
E. Absorber pressure drop	• Plant instrumentation
F. Product CO_2 flow rate	• TORBAR or recommended differential flow meter during parametric testing; recommended differential flow meter during base-case testing.
G. Product CO_2 trace composition	• O_2, SO_2, NO_X, H_2O (saturated), and CO_2 (by difference). Amines / aldehydes / NH_3 during base-case testing.
H. Reboiler steam flow	• **Parametric testing only:** Vortex meter
I. Reboiler steam temperature	• Plant instrumentation
J. Reboiler steam pressure	• Plant instrumentation
K. Reboiler condensate flow	• **Base-case testing:** Condensate orifice flow meter(s)
	Base-case testing:
L. Rich solution CO_2 content and inventory at the beginning and end of the test	• Laboratory analyses and sump levels
M. Lean solution CO_2 content and inventory at the beginning and end of the test period	• Laboratory analyses and sump levels
N. Pumping power use	• Plant instrumentation
O. Depleted flue gas trace components	• **Base-case testing:** SO_2, SO_3, NO_X, total HC, NH_3, particulates, and HAPs

Table 8 lists the key performance indices. Each test period report should include these data.

Table 8. Calculated key performance indices

Performance index	Calculation/Definition
A. CO_2 stored in solution	• Difference between solution CO_2 inventory at the end and the beginning of the test period (solution CO_2 inventory = CO_2 content times liquid inventory)
B. CO_2 capture	• Sum of CO_2 produced (product flow meter) and CO_2 stored in solution, all divided by the product of flue gas supply flow rate and flue gas supply CO_2 mass fraction
C. CO_2 recovery	• Sum of product CO_2 flow and CO_2 stored in solution divided by the difference between CO_2 entering in flue gas (mass flow times mass fraction) and the CO_2 leaving in the depleted flue gas (mass flow times mass faction). CO_2 recovery measures the degree to which CO_2 flows balance. This factor should be within 95% to 105%.
D. SO_2 and NO_X removal	• The difference between mass flows in the flue gas supply and the depleted flue gas divided by the mass flow in the flue gas supply
E. Specific thermal use	• **Base-case testing:** M_{steam} from condensate flow meter(s) or vortex meters. Enthalpies from steam tables at measured stream temperature and pressure. Product CO_2 flow rate from recommended differential flow meter. • **Parametric testing:** Base-case procedure or M_{steam} from vortex meter. Product CO_2 flow rate from the vortex or TORBAR flow meter.
F. Specific power use	• See Section 5.5
G. Specific cooling duty	• Plant instrumentation for aggregate sea water flow and temperature differential and heat capacity • Alternative – Sum similar calculations around pertinent sea water-cooled heat exchangers

5.3. CO_2 capture performance

Fig. 3 lays out the general CO_2 flows. Note that CO_2 leakage to atmosphere is included as a flow. As leakage flows cannot be measured directly, it does not enter into the calculations. Its inclusion here is simply to acknowledge that leakage flow is a possibility. CO_2 accumulation is the amount of CO_2 stored within the amine pilot-plant boundaries over the course of a test; CO_2 may accumulate in (or be released from) the rich/lean solution over the course of a test period.

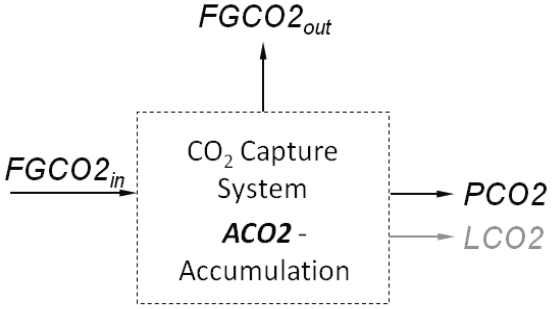

- *$FGCO2_{in}$* = CO_2 mass flow entering in the flue gas
- *$FGCO2_{out}$* = CO_2 mass flow leaving in depleted flue gas
- *PCO2* = CO_2 exported as product
- *ACO2* = Net CO_2 accumulation in the CO_2 capture system
- *LCO2* = CO_2 leakage to atmosphere from the CO_2 capture system

Fig. 3. CO_2 capture flow diagram

Three general methods of calculating CO_2 capture efficiency are:

1. The ratio of measured high-purity product CO_2 flow to the CO_2 entering the absorber in the flue gas is given by:

$$\frac{PCO2}{FGCO2_{in}}$$

2. The ratio of measured high-purity product CO_2 flow to the sum of the high-purity product CO_2 flow and the CO_2 flow leaving the absorber in the depleted flue gas is given by:

$$\frac{PCO2}{FGCO2_{out}+PCO2}$$

3. The ratio of the difference between the CO_2 entering the absorber in the flue gas and the CO_2 leaving the absorber in the depleted flue gas to the CO_2 entering the absorber in the flue gas is given by:

$$\frac{FGCO2_{in}-FGCO2_{out}}{FGCO2_{in}}$$

The relative uncertainties in CO_2 capture by these three methods, using various combinations of flow meter data, were assessed. The conclusion is that uncertainty in CO_2 capture is minimized in Method 2 above, assuming that the CO_2 entering the capture plant is the sum of the two measured CO_2 flows out of the plant: 1) PCO2 – High-Purity Product CO_2 and 2) $FGCO2_{out}$ – CO_2 Emitted in the Depleted Flue Gas Leaving the Absorber.

As the specific thermal use and specific cooling duty will be calculated using the measured product CO_2 flow, the CO_2 capture should also make use of the measured CO_2 product flow. This recommends against Method 3, which uses only flue gas CO_2 flows.

Key independent parameters that characterize CO_2 capture plant performance include inlet flue gas flow rate as a % of design and absorber liquid/gas ratio, both of which use measured inlet flue gas flow rate. To the extent that absorber operation details are to be assessed and reported as key performance indices, corresponding reported CO_2 capture should also be based on the measured inlet flue gas CO_2 flow. This recommends against Method 2 despite its identification as the least uncertain method. In any event, sufficient data will be collected during operations to calculate and report CO_2 capture by all methods.

Note that a 4th method might be considered using only dry-basis CO_2 concentrations for the absorber inlet and depleted flue gas streams and assuming all dry components other than CO_2 pass through the absorber unchanged. This 4th method requires no flow measurements and is given by:

$$E_{CO2}=1-\frac{O}{I}\frac{(1-I)}{(1-O)}$$

where: E_{CO2} = CO_2 capture efficiency fraction
O = CO_2 concentration at absorber inlet dry mol fraction
I = CO_2 concentration at the absorber outlet dry mol fraction.

For all test periods, CO_2 recovery should be reported. This parameter is an indicator for the overall uncertainty in test results:

$$CO_2\,Recovery=\frac{PCO2+FGCO2_{out}+ACO2}{FGCO2_{in}}$$

CO_2 emissions are not included in the key performance indices listed in Table 8. Measuring CO_2 emissions for the purposes of meeting air emissions regulations will likely require traverse sampling for composition and velocity from the stack.

CO_2 emissions may be estimated by subtracting the sum of the (direct-measured) product CO_2 flow (*PCO2*) and the CO_2 stored in solution (*ACO2*, calculated) from the flue gas supply CO_2 flow ($FGCO2_{in}$). Note that this method of calculating CO_2 emissions is a comparatively small difference in two large numbers and carries considerable uncertainty.

5.4. Specific thermal use

Specific thermal use is the heat supplied by imported steam, primarily to the stripper reboiler, divided by the product CO_2 flow. The calculation for this parameter:

$$Q_{reboiler} = \frac{M_{steam}\left(h_{gi}\left(T_g, P_g\right) - h_{fo}\left(T_f, P_f\right)\right)}{M_{CO2}}$$

Details on each term in this equation are given in Table 9.

Table 9. Specific thermal use calculation details

Item	Units	CHP operation	Notes
$Q_{reboiler}$	kWth		Calculation result
M_{steam}	kg/s	Option 1: FT-2386 Option 2: FT 2051 Option 3: new	Medium-pressure (MP) steam flow to reboiler High-pressure (HP) steam flow to plant Condensate return flow from regenerator reboiler.
T_g	ºC	TT2387	
P_g	bar	PT-2389	
T_f	ºC	TT-2388	
P_f	bar	PT-2392	
h_{gi}	kJ/kg		Steam enthalpy from steam tables
h_{fo}	kJ/kg		Condensate enthalpy from steam tables
M_{CO2}	kg/s		From calibrated flow meter

5.5. Electrical utility use

The primary auxiliary power uses for PCC are the induced draft (ID) fan (to overcome flue gas pressure drops in the plant), the aggregate of solution and water pumping inside the plant, and the CO_2 compressor (to deliver at pipeline pressure; the TCM DA pilot plant does not have a CO_2 pipeline compressor). The ID fan use will correlate most closely to flue gas flow rate. The internal pumping power loads will correlate loosely with CO_2 production. Thus, it is unlikely that any single parameter will be useful in describing process auxiliary power use. In practice, pumping power differences from varying the independent parameters during parametric testing are likely to be insignificant. ID fan load will change with flue gas supply flow rate and, possibly, liquid flows in the absorber tower. Both of these factors are included in the ID fan pressure rise and flue gas flow rate. Auxiliary power use for a full-scale process can be estimated by:

- Summing the full-scale pumping loads
- Modeled ID fan power use from design flow rate and required pressure rise measured at pilot scale
- Modeled compressor power used to compress the product CO_2 from stripper column overhead pressure and specified compressor discharge pressure to deliver to the receiving pipeline.

These can be developed from parameters included in Table 7 and a specified receiving pipeline pressure.

6. Conclusions

A generic CO_2 capture testing methodology that has been applied at multiple sites providing details on the procedure, its key performance indices and their associated specifications, as well as the required pre-test work has been presented. Specific application of the methodology for the CO_2 Technology Centre Mongstad site, a CO_2 capture testing facility located in Norway that performed CO_2 capture tests using MEA, is shown as an illustrative example.

Acknowledgements

The authors gratefully acknowledge the staff of TCM DA, Gassnova, Statoil, Shell, Sasol, and Aker Solutions for their contribution and work at the TCM DA facility.

The authors also gratefully acknowledge Gassnova, Statoil, Shell, and Sasol as the owners of TCM DA and Aker Solutions for their financial support and contributions.

Appendix A. Pertinent flue gas monitoring reference methods

Table 10 lists reference methods used, their associated title, what is measured, and its units.

Table 10. Reference methods

Reference method	Title	Sampling/Analysis result	Units
EPA method 1	Sample and velocity traverses for stationary sources		
EPA method 2	Determination of stack gas velocity and volumetric flow rate (Type S pitot tube)	Stack velocity profile and aggregate volumetric flow rate	volume flow rate
EPA method 3A	Determination of oxygen and carbon dioxide concentrations in emission from stationary sources (instrumental analyzer procedure)	O_2, CO_2	% vol, dry
EPA method 5	Determination of particulate matter emissions form stationary sources	Total particulate matter	Mass per unit volume flue gas
EPA method 6C	Determination of sulfur dioxide emissions from stationary sources (instrumental analyzer procedure)	SO_2	ppmv, dry
EPA method 7E	Determination of nitrogen oxides emissions from stationary sources (instrumental analyzer procedure)	NO_X	ppmv, dry as NO_2
EPA method 25A	Determination of total gaseous organic concentration using a flame ionization analyzer	Total gaseous organic concentration	ppmv propane equivalent
EPA CTM-027	Procedure for collection and analysis of ammonia in stationary sources	NH_3	ppmv, dry
EPA method 29	Determination of metals emissions from stationary sources	Sb, As, Ba, Be, Cd, Cr, Co, Cu, Pb, Mn, Mg, Ni, P, Se, Ag, Hg	Mass per unit volume flue gas
NACSI method 8A	Determination of sulfuric acid vapor or mist and sulfur dioxide emissions from Kraft recovery furnaces	H_2SO_4 and SO_3	ppmv, dry

Appendix B. Flue gas amine / amine degradation product sampling

Background

TCM DA is planning to operate the PCC test unit at the facility with MEA solvent and no additives or amine blending. The solvent will be continuously cycling through the system for 1440 hours (60 days). Testing will be performed for a variety of operational parameters, including chemical characterization of the air and liquid waste streams. In particular, air emissions testing of the solvent and potential degradation products (amines, nitrosamines, and aldehydes) will be performed. This will be done during selected operational periods, including base-case testing.

Recommendations

Although other PCC tests have been performed with longer solvent cycling times, published studies suggest the presence of complex mixes of solvent degradation products that are emitted into the flue gas streams, even after shorter operational times. At least several days' worth of 'later' samples should be taken near the end of the 2-month period, during normal operations, in addition to the samples planned during the parametric and base-case testing.

Any testing undertaken for these solvent and degradation products should be performed isokinetically. A variety of sample collection processes can be of use, including impingers that are empty or charged with acidic solution.

NH_3 should be measured regularly as a frequently-observed high emission rate product. This is often done with FTIR, especially in situations where operations are expected to change quite substantially over time. Thus it can be a proxy for operational tracking as well as for the purposes of emission rate quantification. During stable operations, other methods which can have lower detection limits (such as an EPA Method 5 / Method 17 approach, collection with impinger, and analysis by ion chromatography) can be used on samples collected from various impinger approaches.

Due to its relevance and high abundance in the mist observed in several PCC test facilities, SO_3 should also be measured at the absorber outlet. Submicron mist and aerosols may form in the absorber as a result of heterogeneous condensation followed by dissolution and enrichment with the highly soluble amines in the mist. Several studies have shown that high quantities of mist composed partly of SO_3 can be observed. The mist may be a large sink of nitrogenous compounds of interest (primarily the amines as opposed to degradation products) due to their alkalinity.

A recent EPRI report contains details, features, and difficulties with multiple options for sampling and analysis of each compound class [6]. It should be noted that it is likely that only a subset of chemicals with a given compound class can be analyzed with any particular technique. Knowledge of the specific target compounds of interest, or a desire to measure as much of the total mass of the compounds class, is needed to recommend any particular suite of methods. Specific issues of importance include the need for very stable elevated temperatures of the entire sampling train (no unheated tubing gaps) and appropriate elimination or addressing of sampling and analytical interferences from water.

Amine sampling could be attempted with FTIR but it is possible to likely that any emissions would fall below detection limits due to chemical interferences. Thus manual sampling is recommended, with approaches similar to EPA Method 5 [6].

Nitrosamine sampling must be done manually; sufficient testing and use of continuous methods is not available to justify its use for this purpose. The most reasonable approaches at this time center on cartridges loaded with Thernosorb/N, with later extraction and analysis by HP liquid chromatography or gas chromatography following, or slightly modified from, the OSHA 27 method. It is likely that multi-stage sampling trains will be required to obtain the suite of desired nitrosamines. Both aqueous and vapor phases should be collected. If water removal methods are used, condensed phase must also be collected and analyzed.

Whatever methods are chosen to be applied must include multiple field blanks collected under conditions as close to those used for sampling full operations as possible. Serious consideration should be given to the feasibility of undertaking method validation tests at the stack (such as spike tests at the sample train inlets in order to estimate potential sample losses through the sampling train, as they can be quite high for the types of compounds of interest).

Appendix C. Relative accuracy test audits

The CHP flue gas supply and product CO_2 flow meters installed do not conform to ASME PTC 19.5, Standard for Flow Measurement [7]. It is recommended here that these flow meters be subjected to a RATA prior to or during base-case testing. Three options for conducting such an audit are described below.

Note that use of one of these RATA calibration methods for CHP flue gas flow could provide calibrations for the flow meters described in Table 11.

Table 11. RATA methods for CHP flow meters

Meter location	RATA method	Meter type
CHP after DCC	8610-FT-0150	Ultrasonic
CHP after DCC	8610-FT-0124	TORBAR pitot tube
Absorber inlet	8610-FT-2039	TORBAR pitot tube
Absorber outlet	8610-FT-2431	TORBAR pitot tube

Use of these RATA/calibration methods for product CO_2 flow could provide simultaneous calibrations for the product CO_2 flow meters given in Table 12.

.

Table 12. RATA methods for product CO_2 flow meters

Meter location	RATA method	Meter type
Product CO_2	8615-FT-0010	Vortex
Product CO_2	8615-FT-2203	TORBAR pitot tube

Pitot tube traverse method

The unobstructed CHP flue gas duct lengths allow pitot tube traverses to be used to calibrate the CHP flow meters. ASME PTC19.5 describes how such a pitot tube traverse for flow is to be conducted. The practice in the US is to conduct a minimum of nine (9) separate flow traverses during which the challenged flow meter data is also collected. A maximum of three (3) of the flow traverse data sets may be discarded as outliers. The calibration flow and uncertainty are then calculated from remaining flow traverse data sets. The procedure is summarized in Section 2 of EPRI publication TR-104527 [8]. Duct nozzles allowing the use of traversing pitot tubes would need to be installed in the CHP flow duct to accomplish the flow traverses.

Dilution method

The flow meters may be calibrated by a dilution procedure. This is not a reference method, but it can be acceptable if the injection flow and concentrations are measured with sufficient accuracy. The general approach is to inject a tag gas far upstream of the flow meter (to allow for good mixing) and measure the concentration of the tag gas at the flow meter. The calibrated flow is then calculated by:

$$q_{meter} = q_{tag} \frac{C_{tag}}{C_{tag,meter}}$$

where: q_{meter} = mass flow rate at the metering location
q_{tag} = measured mass flow rate of the tag gas injected
C_{tag} = measured concentration of tag gas injected
$C_{tag,\ meter}$ = measured concentration of tag gas at the flow meter.

A suitable tag commonly used is helium in air. The tag gas is supplied in high pressure gas bottles. A certified concentration of helium is required from the supplier. The tag gas is metered through a critical orifice (upstream pressure greater than ~2.5 bar). The flow through the orifice is directly proportional to the upstream (absolute) pressure. The concentration of helium can be measured at the flow meter using a thermal conductivity detector. A second cylinder of helium in air at the anticipated span concentration is required to calibrate the detector as is a helium-free air zero gas. Thermal conductivity detectors for helium are available from a number of manufacturers (and rental companies). These are normally used to detect helium leaks in lab equipment but are suitable also for sampling. Typical detection limit is 25 ppmv. In order to achieve ~1% uncertainty in the measured concentration, a measured concentration at the flow meter would be 2500 ppmv (0.25%).

Using this procedure to calibrate the flow meter at the absorber outlet would require a separate C_{tag}, concentration measurement at the absorber outlet flow meter location.

Radioactive tracer method

The flow meters may also be calibrated by a procedure to measure transit time of a radioactive tracer. The method is described in a British Standard [9]. By this method, a radioactive tracer is pulse-injected upstream and radiation detectors are located a measured distance apart downstream. The method reports average velocity by measuring the transit time of the radiation pulse between the injection and detector locations. Mass flow is then calculated by multiplying the measured velocity, the pipe cross section and the gas density:

$$q_{meter} = \frac{d\rho\pi D^2}{4t}$$

where:
q_{meter} = mass flow rate
d = distance between radiation detectors
ρ = gas density
D = duct diameter
t = time of radiation pulse transit.

Particular care must be taken in locating the injection point, and the radiation detectors. All three locations should be located on a long straight pipe run with minimal obstructions and no side taps. Conduct of this calibration procedure requires careful attention to a number of design and operating factors and should be undertaken only by personnel experienced in conduct of the procedure.

References

[1] Hamborg E S, Smith V, Cents T, Brigman N, Falk-Pedersen O, De Cazenove T, Chhaganlal M, Feste J K, Ullestad Ø, Ulvatn H, Gorset O, Askestad I, Gram L K, Fostås B F, Shah M I, Maxson A, Thimsen D. Results from MEA testing at the CO_2 Technology Centre Mongstad. Part II: Verification of baseline results. Energy Procedia; 2014.

[2] Brigman N, Shah M I, Falk-Pedersen O, Cents T, Smith V, De Cazenove T, Morken A K, Hvidsten O A, Chhaganlal M, Feste J K, Lombardo G, Bade O M, Knudsen J, Subramoney S C, Fostås B F, De Koeijer G, Hamborg E S. Results of amine plant operations from 30 wt% and 40 wt% aqueous MEA testing at the CO_2 Technology Centre Mongstad. Energy Procedia; 2014.

[3] Morken A K, Nenseter B, Pedersen S, Chhaganlal M, Feste J K, Tyborgnes R B, Ullestad Ø, Ulvatn H, Zhu L, Mikoviny T, Wisthaler A, Cents T, Bade O M, Knudsen J, De Koeijer G, Falk-Pedersen O, Hamborg E S. Emission results of amine plant operations from MEA testing at the CO_2 Technology Centre Mongstad. Energy Procedia; 2014.

[4] Performance test code on overall plant performance. ASME PTC-46. ASME. New York, NY; 1996.

[5] Certification of calibration traceable to the NIST. Colorado Engineering Experiment Station, Inc. 10EHA-0001_1: 24; August 2010.

[6] Working group review of sampling and analytical methods for amines and amine degradation products in post-combustion carbon capture technologies. EPRI. Palo Alto, CA; 2012; 1026867.

[7] PTC 19.5 flow measurement. ASME. New York, NY; 2004.

[8] Guidelines for flue gas flow rate monitoring. EPRI. Palo Alto, CA: 1995; TR-104527.

[9] Fluid flow in closed conduits using tracers: Measurement of gas flow by transit time using radioactive tracers. BS 5857-2.4; 1980.

Results from MEA testing at the CO_2 Technology Centre Mongstad. Part II: Verification of baseline results

(2014)

Available online at www.sciencedirect.com

ScienceDirect

Energy Procedia 63 (2014) 5994 – 6011

Energy Procedia

GHGT-12

Results from MEA testing at the CO_2 Technology Centre Mongstad. Part II: Verification of baseline results

Espen S. Hamborg[a,b], Vian Smith[a,c], Toine Cents[a,c], Natasha Brigman[a,c], Olav Falk-Pedersen[a,d], Thomas De Cazenove[a], Milan Chhaganlal[a,b], Jane K. Feste[a,b], Øyvind Ullestad[a,b], Helge Ulvatn[a,b], Oddvar Gorset[e], Inga Askestad[e], Lars K. Gram[f], Berit F. Fostås[b], Muhammad I. Shah[d], Andrew Maxson[g], David Thimsen[g,]*

[a]CO_2 Technology Centre Mongstad (TCM DA), 5954 Mongstad, Norway
[b]Statoil ASA, P.O. Box 8500, 4035 Stavanger, Norway
[c]Sasol Technology, P.O. Box 5486, Johannesburg 2000, South Africa
[d]Gassnova SF, Dokkvegen 10, 3920 Porsgrunn, Norway
[e]Aker Solutions, P. O. Box 222, 1326 Lysaker, Norway
[f]FORCE Technology, Park Allé 345, 2605 Brøndby, Denmark
[g]Electric Power Research Institute, 3420 Hillview Avenue, Palo Alto, CA 34304, USA

Abstract

Independent verification protocol (IVP) work has been conducted at the CO_2 Technology Centre Mongstad (TCM DA) during treatment of flue gas from a natural gas-fired combined heat and power (CHP) plant. The testing applied an aqueous 30 wt% monoethanolamine (MEA) solvent system treating flue gases with a flow rate of about 47.000 Sm^3/hr and a CO_2 content of about 3.5%. The CO_2 capture rate was about 90% and the thermal steam consumption was about 4.1 GJ/t CO_2. Emissions of MEA were very low and MEA-related degradation products were all below detection levels, and all within the emission limits set by the Norwegian environmental authorities. The current work may be considered an independently verified baseline for a non-proprietary post-combustion amine based solvent system carried out at an industrial-scale plant facility.

Long-term performance indices, such as material corrosion, MEA solvent degradation, etc., have not been considered in the current IVP work. Additional minor process adaption to the aqueous MEA solvent system, such as increased MEA concentrations, the use of anti-foam solutions, etc., may lead to lower thermal steam consumptions than aforementioned.

© 2014 The Authors. Published by Elsevier Ltd. This is an open access article under the CC BY-NC-ND license (http://creativecommons.org/licenses/by-nc-nd/3.0/).
Peer-review under responsibility of the Organizing Committee of GHGT-12

---

* Corresponding author. Tel.: +1-651-766-8826; fax: +1-651-765-6375.
E-mail address: dthimsen@epri.com

1876-6102 © 2014 The Authors. Published by Elsevier Ltd. This is an open access article under the CC BY-NC-ND license (http://creativecommons.org/licenses/by-nc-nd/3.0/).
Peer-review under responsibility of the Organizing Committee of GHGT-12
doi:10.1016/j.egypro.2014.11.634

Keywords: CO_2 capture; EPRI; MEA; Post-combustion capture; CO_2 Technology Centre Mongstad; TCM DA

1. Introduction

CO_2 Technology Centre Mongstad (TCM DA), located next to the Statoil refinery near Mongstad, Norway, is one of the largest post-combustion capture (PCC) test facilities in the world. TCM DA is a joint venture between Gassnova, Statoil, Shell, and Sasol. The purpose of this facility, which started operation in August 2012, is to allow vendors of suitable amine formulations and other PCC processes to test their technology and collect performance data to support full-scale design and anticipate the associated performance and operating costs. A unique aspect of the facility is that either a slipstream from a natural gas-fired combined heat and power (CHP) plant or an equivalent volumetric flow from a refinery residue fluid catalytic cracker (RFCC), whose higher CO_2 content (about 12.9% compared with about 3.5% for the natural gas-based flue gas) is closer to that seen in coal flue gas, can be used for CO_2 capture. In the CHP plant, the natural gas is combusted in a gas turbine and the flue gas content and characteristics are similar to those of a combined cycle gas turbine (CCGT) power plant. One of the testing facilities in place at TCM DA is a highly flexible and well-instrumented generic amine plant, designed and constructed by Aker Solutions and Kværner, aimed to accommodate a variety of technologies with capabilities of treating flue gas streams of up to 60,000 Sm^3/hr. This plant is being offered to vendors of solvent-based CO_2 capture technologies to primarily test: (1) the performance of their solvent technology; and (2) technologies aimed to reduce the atmospheric emissions of amines and amine-based degradation products from such solvent-based CO_2 capture processes.

An independent verification protocol (IVP) has been developed by the Electric Power Research Institute (EPRI) to be used as part of the overall performance assessment of amine-based TSA processes, as described in details elsewhere [1]. The IVP is designed to provide a structured testing procedure for assessing thermal and environmental performance of PCC processes under normal operating conditions.

The IVP has been applied during base-case testing done 6–10 January 2014 on the TCM amine plant using aqueous 30 wt% monoethanolamine (MEA) as the solvent while treating flue gas at a flow rate of about 47.000 Sm^3/hr from the CHP plant. The IVP project was performed jointly between TCM DA, Aker Solutions, FORCE Technology, and the Electric Power Research Institute (EPRI), and the base-case testing is part of Aker Solutions' test campaigns at TCM DA.

This work is part of a continuous effort of gaining better understanding of the performance potential of the non-proprietary aqueous MEA solvent system, conducted by TCM DA and its affiliates and owners, in order to test, verify, and demonstrate CO_2 capture technologies [1, 2, 3]. The purpose of the current work is to provide the results of the IVP done for aqueous 30 wt% MEA, which provides a baseline that can be commensurately compared against other (solvent-based) PCC processes. This work may thus be considered the baseline for a non-proprietary PCC amine-based solvent system treating low CO_2 partial pressure flue gases at a significant flow rate from the combustion of natural gas in a gas turbine.

2. Project overview

The TCM pilot-scale amine plant was designed and constructed by Aker Solutions and Kværner. The amine plant was designed to be flexible to allow testing of different configurations, and has respective capacities of about 80 and 275 tonnes-CO_2/day for CHP and RFCC flue gas operations. The TCM DA amine plant process flow diagram showing high-level equipment contained within the plant along with key extant instrumentation and the nominal CHP flue gas characteristics is given elsewhere [1]. The major systems include:

- An induced draft (ID) blower to overcome pressure drops and blow the flue gas through the plant with a blower output capacity of up to about 270 mbar and 70,000 Sm^3/hr.
- A direct-contact cooler (DCC) system to initially quench and lower the temperature and saturate the incoming flue gas by a counter-current flow water in order to improve the efficiency of the absorption process and provide pre-scrubbing on the flue gas. The DCC system has two individually operated packed columns for operations with respectively the CHP flue gas and the flue gas from the refinery cracking unit. The DCC column designed

for CHP flue gas operations has of a 3-m diameter and a total of 16 m of height. The section where water counter currently contacts the flue gas is of 3.1 m of height with Flexipack 3X structured stainless-steel packing of Koch Glitsch. The DCC column designed for the flue gas from the refinery cracking unit has a diameter of 2.7 m and a total height of 16 m. The section where water counter currently contacts the flue gas is of 3 m of height with Intalox Snowflake random polypropylene packing of Koch Glitsch.

- An absorber to remove CO_2 from the flue gas using solvent. The absorber has rectangular polypropylene-lined concrete column with a cross-section measuring 3.55 x 2 m of a total of 62 m of height. The lower regions of the tower, where the amine solution contacts the flue gas, consist of three sections of Koch Glitsch Flexipac 2X structured stainless-steel packing of 12 m, 6 m, and 6 m of height, respectively. Water-wash systems are located in the upper region of the tower to scrub and clean the flue gas particularly of any solvent carry over, and consist of two sections of Koch Glitsch Flexipac 2Y HC structured stainless-steel packing of both 3 m of height. The water wash system is also used to maintain the water balance of the solvent system by adjusting the temperature of the circulating water of the upper water-wash section. Liquid (re-)distributors, liquid collector trays, and mesh mist eliminators by Koch Glitsch are located at various locations in the tower. The CO_2 depleted flue gas exits the absorber column to the atmosphere through a stack located at the top of the absorber column.
- Stripper columns to recover the captured CO_2 and return CO_2-lean solvent to the absorber. The amine plant consist of two independent stripper columns with overhead condenser systems; one measuring 1.3 m in diameter and a total of 30 m of height, the second measuring 2.2 m in diameter and also a total of 30 m of height. The lower regions of both stripper column, where the amine solutions is stripped, consist of Koch Glitsch Flexipac 2X structured stainless-steel packing of 8 m of height, and in the upper regions of the strippers consist of a rectifying water-wash section of Koch Glitsch Flexipac 2Y HC structured stainless-steel packing of 1.6 m of height. Liquid (re-)distributors, liquid collector trays, and mesh mist eliminators by Koch Glitsch are located at various locations in the strippers. Each stripper column is connected to its respective stream-driven thermosiphon reboiler system, providing the necessary heat required for the stripping process. The two stripper columns are operated independently considering the CO_2 content in the flue gas, due to column design and hydraulics and gas velocities effects, i.e., the smaller diameter stripper column is utilized when treating CHP flue gas, whereas the large diameter column is utilized when treating flue gases of higher CO_2 content.
- A set of pumps used to move the CO_2-lean and CO_2-rich solvent streams between the absorber and stripper and through a cross-flow heat exchanger to recover heat from the lean stream.
- A reflux drum, condenser, and pumps to dry the product CO_2 that exits from the stripper. A portion of the product CO_2 can also be recycled back to the inlet of the DCC to increase the concentration of the CO_2 in the inlet flue gas stream.

The roles and responsibilities of the organizations that conducted the current IVP project are as follows:

- **TCM DA** is the prime on the project and its personnel organized the field testing including contracting to do gas sampling during the test period. Personnel from TCM DA and TCM DA owner organizations were responsible for planning and setting the test program for the base-case testing, and also operating the plant throughout. TCM DA personnel collected samples during the base-case testing for quantification of trace species in the depleted flue gas stream.
- **Aker Solutions** is the technology vendor testing its solvent-based PCC technologies at TCM DA. A part of Aker Solutions' test period was to conduct a campaign based on the non-proprietary MEA solvent system, which was intended to be used as a reference for future testing. The base-case testing done 6–10 January 2014 was consequently a part of Aker Solutions' test campaigns at the TCM DA amine plant.
- **FORCE Technology** brought a single sampling crew on-site during the base-case testing to extract and analyse samples from the CHP flue gas supply, depleted flue gas, and product CO_2 streams. This sampling was conducted sequentially with a single set of continuous emissions monitors (CEMs). FORCE Technology also collected gas samples for off-site analysis of particulate, SO_2/SO_3, and amine-related compounds.
- **EPRI** was contracted to develop the IVP and help apply it during the base-case MEA testing. Two EPRI engineers were on-site during the testing to observe the conduct of the tests. EPRI is also the lead on the current IVC work.

3. Independent verification protocol approach

Base-case testing of the performance of the TCM amine plant using a nominal 30% MEA as the solvent was conducted the week of 6 January 2014 after approximately 6 weeks of operating the amine plant with the 30% MEA solution. The plant was operated at steady state through the entire week. (Note: The MEA solution concentration did drift down approximately 1 percentage point during the week of base-case testing.) The only operational abnormality was a short loss of flue gas flow for about 15 minutes at 15:00 hrs on 8 January 2014 from which operations were quickly restarted.

FORCE Technology was on-site to manually collect samples sequentially from the flue gas supply, depleted fuel gas, and product CO_2. During all sampling periods the following sample data were collected:

- CO, CO_2, NO_X, O_2, SO_2, and N_2 (by difference) concentrations in vol%
- Flow rate, pressure, and temperature.

The sampling time periods and sampling period designator are shown in Table 1 along with additional sampling undertaken on each day. Data logs for all sampling periods containing pertinent flows, temperatures, pressures, and concentrations measured by permanent plant instruments were supplied by TCM DA.

Table 1. FORCE Technology sampling periods

Stream sampled	Date	Start time / Stop time	Sampling results reported	Test designator
Depleted flue gas	6 January 2014	14:13 / 17:43	Major gases, flow	C1-1a
		10:28 / 13:50	Acetone, aldehydes amine degradation products, NH_3	C1-1b
Depleted flue gas	7 January 2014	7:58 / 11:23	Cl^-, H_2SO_4, NH_4^+, particulate, salts, SO_2, SO_4^{2-}	C1-2
Product CO_2	8 January 2014	11:50 / 15:07	Major gases, flow	C1-3a
		17:02 / 20:10	Acetone, aldehydes amine degradation products, NH_3	C1-3b
Flue gas supply	9 January 2014	9:12 / 12:55	Cl^-, H_2SO_4, NH_4^+, SO_4^{2-}, salts	C1-4a
		13:05 / 16:14	NH_3	C1-4b

4. Instrument assessment

This section assesses the quality of the instrumentation installed for measuring the respective compositions and flow rates. There are two measures of instrumentation quality:

- Accuracy / bias – Measure of the difference between the instrument reading (or average of a set of readings under unchanging process conditions) and the true value of the parameter. The “true value” must be determined by means other than the measurement in question. This is usually accomplished by simultaneous measurement of the parameter by the plant instrument and a reference method or instrument with calibration that can be traced to primary standards.
- Precision – Variability of the instrument reading when stream conditions do not change. Precision is a measure of the random error associated with the measurement.

The aggregate uncertainty in a measurement includes both precision error and bias error. Absent a calibration against primary standards, the uncertainty published by the instrument supplier is only the precision error.

Note also that precision is a measure of repeatability when the process parameter being measured does not change. It is often the case that the process parameter (flow, pressure, and temperature) does change over the measurement period. Thus, measurements over long periods of time (greater than process time constants) will also include an error term related to process uncertainty.

4.1. Gas phase compositions

The CO_2 and O_2 content of the flue gas supply, depleted flue gas, and CO_2 product stream is routinely determined by the respective plant Fourier Transform Infrared (FTIR) (Applied Instrument Technologies and Finetech, model: Anafin 2000) and O_2 (Siemens, model: Oxymat 6) sampling and analysis system. The sampling system admits the gas stream, sampled from various single points as given by Thimsen et al [1]. The sample is continuously drawn by a selection system serving the analyzer. The gas supply samples are diverted to the common analyzers in a 90-minute cycle, i.e., the analyzer cycles between flue gas supply for 15 minutes, depleted flue gas for 30 minutes, and CO_2 product stream for 15 minutes. In each sampling, the analyzer sampling lines and cells are sufficient flushed with the gas to be measured and, after a certain time, wet-gas concentration for every 1½ minutes for a total of 10 concentrations are reported. The plant control system displays to the operators the most recent concentration report. Thus, the last report of the 10 is displayed for approximately 75 minutes until the next sampling cycle for the flue gas supply and CO_2 product stream and approximately 60 minutes for the depleted flue gas.

The flue gas supply, depleted flue gas, and CO_2 product stream compositions were analyzed by FORCE Technology during the base-case operations. The measurements reported by FORCE Technology were on a dry basis. (The sample is dried before analysis.) These dry-basis data were converted to wet basis by assuming that the flue gas supply is saturated with water at the temperature and pressure measured by the plant data acquisition system. The recalculated FORCE Technology data are given in Fig. 1 and Fig. 2, and compared to the values determined by the FTIR system. Details include:

- Fig. 1 displays the CHP flue gas supply CO_2 and O_2 concentration data over the test campaign. The agreement between FORCE Technology O_2 measurements and those measured by TCM DA O_2 analyzer on 9 January are as good as the agreement in respective CO_2 measurements. These data show that for the last 2½ days of the campaign, CHP flue gas supplied to the pilot plant was of relatively uniform composition. This is probably not the case for the first 1½ days of the campaign. The variability in CO_2 and O_2 concentrations are significantly greater than the precision uncertainty in the measurements indicating that the changes in measured concentration represent real changes in CHP flue gas composition.
- Fig. 2 displays the depleted flue gas CO_2 and O_2 concentration data over the test campaign. The FORCE Technology O_2 data collected on 6 January differ significantly from the TCM DA O_2 data for the first half of the sampling period, but are in general agreement over the last half of the sampling period. The relative uniformity of the FORCE Technology data on 6 January suggests that the TCM DA O_2 data above 15% O_2 may be spurious and not a result of process changes. There was significant variation in the depleted flue gas FORCE Technology CO_2 and TCM DA FTIR concentration data for the sampling period. The precision error for this measurement is in excess of 20%. In addition, there was a significant positive bias in the FTIR data compared to FORCE Technology data taken simultaneously on 6 January. The bias could be corrected by multiplying the FTIR data by 0.7 over this time period. Although the bias is significant, the error was about 0.1% points.
- The product CO_2 composition data reported by FORCE Technology include O_2 content between 1–2%. It is difficult to imagine a mechanism by which the product CO_2 stream (stripper overhead) can contain this much oxygen, and it is therefore presumed that this oxygen is due to air in-leakage into the sampling system, thereby disqualifying the data. For the purposes of calculating CO_2 removal and recovery, it is assumed here that the product CO_2 stream consists only of CO_2 saturated with water at the measured temperature and pressure.

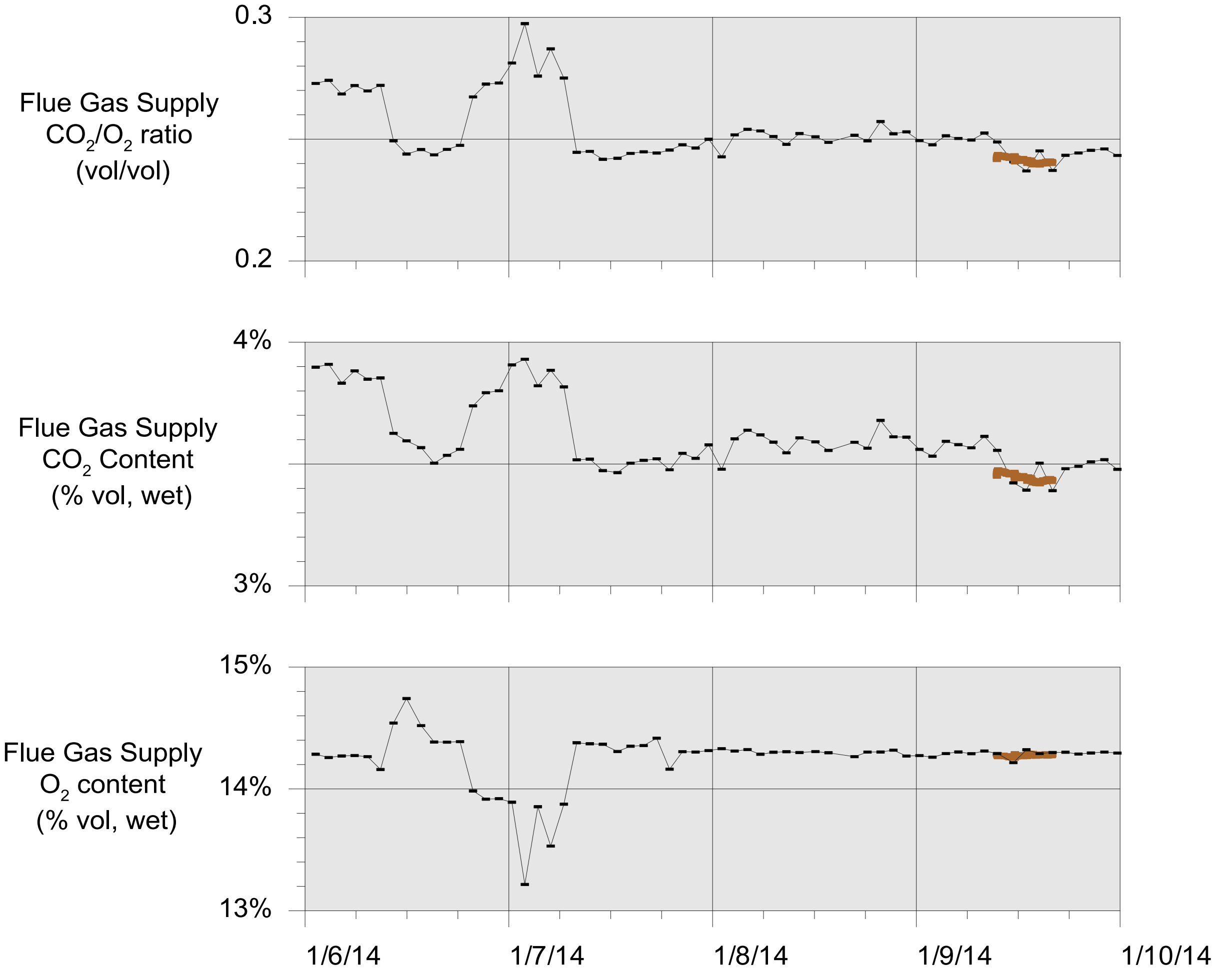

Fig. 1. CHP flue gas supply CO_2 and O_2 data. FTIR and O_2 analyzer data are averaged over analysis circles. Data collected by FORCE Technology on 9 January are also shown.

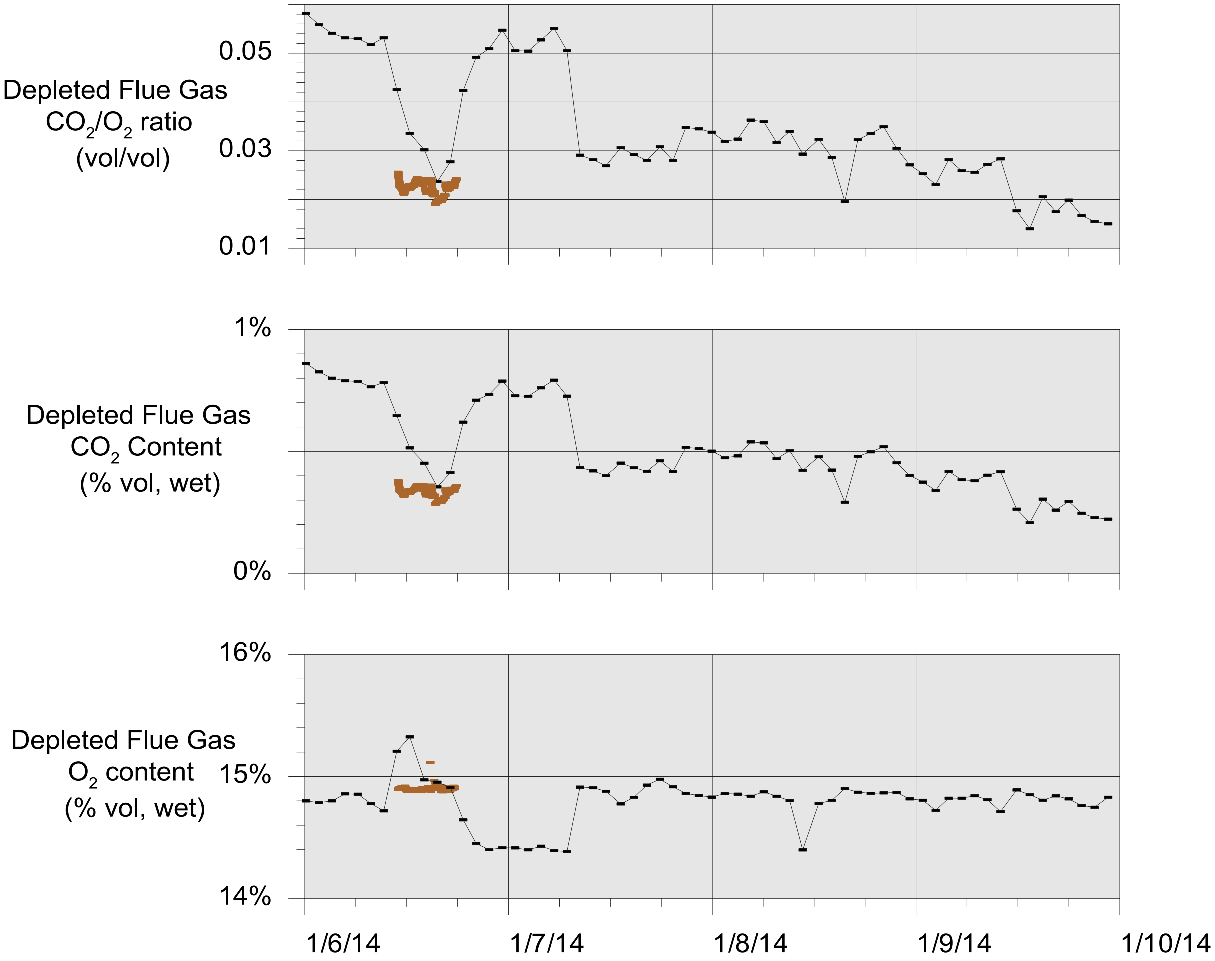

Fig. 2. Depleted flue gas CO_2 and O_2 data. FTIR and O_2 analyzer data are averaged over analysis cycles. Data collected by FORCE Technology on 6 January are also shown.

4.2. Gas phase flow rates

The flow rates of the flue gas, depleted flue gas, and CO_2 product stream are continuously determined by plant instrumentation. The TCM DA amine plant facility is particularly well instrumented for determining the flue gas supply flow rate, with several different types of flow meters in series.

The flue gas, depleted flue gas, and CO_2 product stream flow rates were determined by pitot-tube traversing during the base-case operations by FORCE Technology and the results compared to plant instrumentation are discussed below:

- The CHP flue gas supply flow is measured by two instruments, an ultra-sonic flow meter (FT-0150) and a multi-pitot-tube flow meter (FIC-0124), which are characterized in Table 2. The data from these flow meters are shown in Fig. 3. The flow rates are defined standard conditions of 15 °C and 1 atmosphere. The CHP flue gas flow was very steady over the test week with the exception of a 15-minute period on 8 January when the flow went to zero due to a trip of the ID blower. FORCE Technology made an independent measurement of flow on 9 January as indicated in Fig. 3. The difference between the value measured by FORCE Technology and that measured by the plant instruments is less than 1%. This result must be tempered by the reported uncertainty in the FORCE

Technology measurement of 10%. The test period flow averages used for all calculations are the data reported by the ultrasonic flow meter (FT-0150).

- The depleted flue gas flow is measured by a single multi-pitot tube flow meter whose characteristics are listed in Table 2. The depleted flue gas flow rate of this instrument varies in a fashion that is uncorrelated with any known operational parameter rendering this data of little use for the purposes of the base-case testing. Investigation of this has indicated variation of the measured flue gas flow rate with the ambient air pressure. This may be related to the physical installation position of the instrument; however, exact cause for this flow rate variation is not yet understood. FORCE Technology measured a flow of 47.000 Sm^3/hr (±10%) at this location on 7 January 2014.
- The key product CO_2 flow meters are listed in Table 2. The product CO_2 flow measured by the vortex flow meter (FT-0100) is the primary flow meter used by TCM operators. The data from this flow meter are shown in Fig. 4. The product CO_2 flow was relatively steady over the test week with the exception of the 15-minute period on 8 January 2014 when the flow went to zero due to an ID blower trip. FORCE Technology made an independent measurement of flow on 8 January as indicated in Fig. 4. The difference between the value measured by FORCE Technology and that measured by the plant instruments is approximately 6%, within the uncertainty reported by FORCE Technology measurement of 10%.

Table 2. Key flow instrumentation. Precision uncertainties are based internal instrument assessment by TCM DA.

Stream	Tag number	Instrument type	Primary flow measurement	Precision uncertainty
CHP flue gas supply	FIC-0124	Multi-pitot tube	Differential pressure	2.5%
	FT-0150	Ultra-sonic	Flowing volume	1.3%
Absorber outlet depleted flue gas	FT-2431	Multi-pitot tube	Differential pressure	5.4%
Product CO_2	FT-0010	Vortex	Flowing volume	1.0%

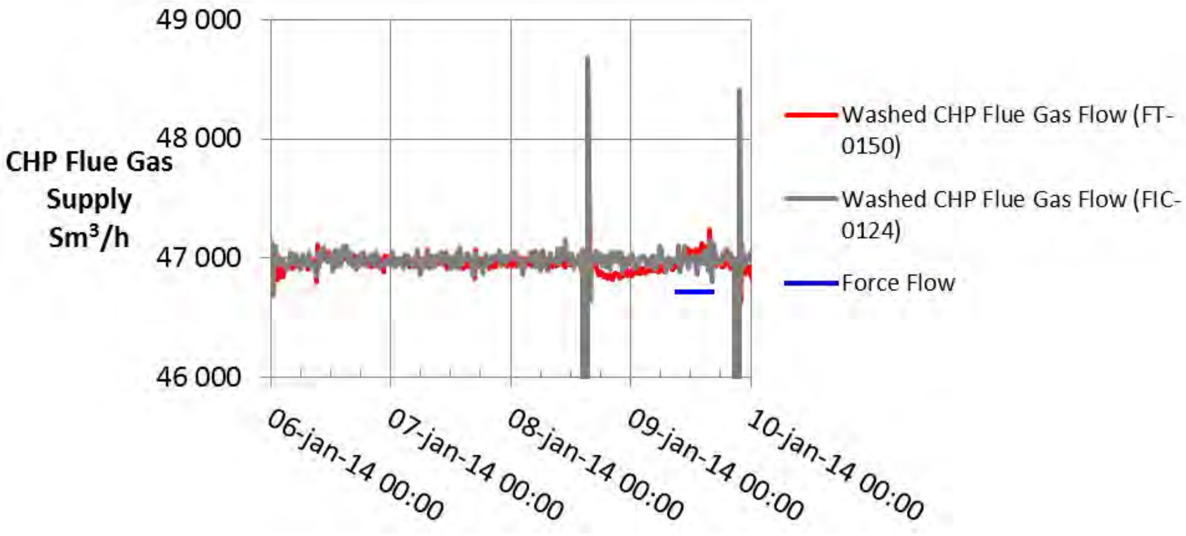

Fig. 3. CHP flue gas supply flow measurements

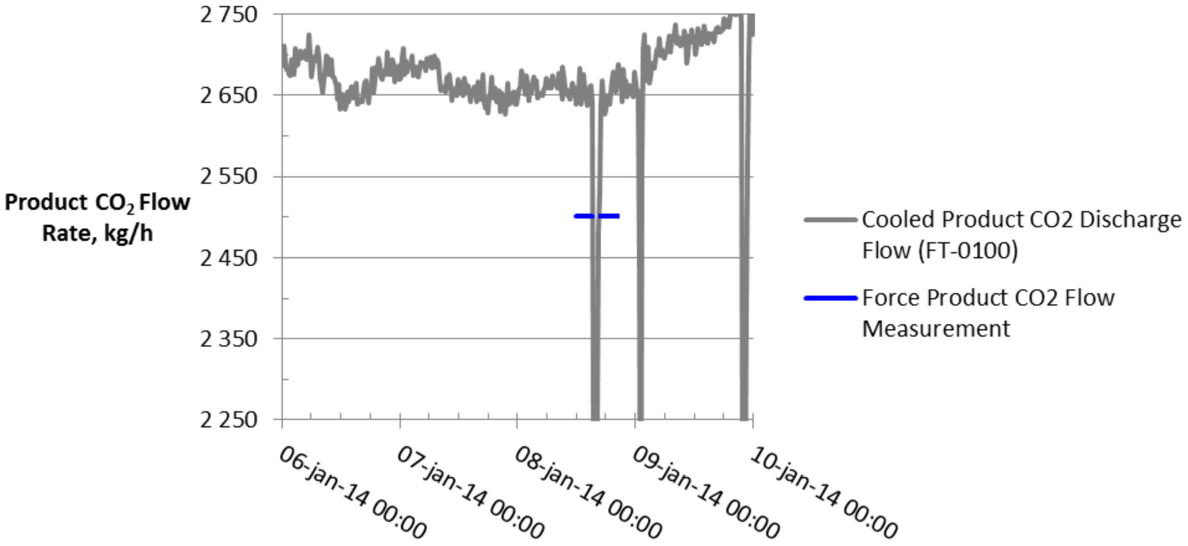

Fig. 4. Product flue gas flow rate and test period averages

4.3. Steam and condensate flow rates

A schematic of the system supplying steam to the stripper reboiler is shown in Fig. 5. High-pressure (HP) steam is delivered from the refinery to the TCM amine plant at a pressure of approximately 30 bars, superheated to approximately 240°C to 310°C. The HP steam is throttled to a pressure near the stripper reboiler steam pressure at approximately 5 bars and then desuperheated with condensate. The stripper reboiler condensate collects in a receiver from which it is returned to the refinery. A small amount of medium-pressure (MP) steam is reduced to a lower pressure for use in steam heat tracing. The low-pressure (LP) steam condensate is returned to the same receiver as the stripper reboiler condensate.

The parameter of interest is the steam flow to the reboiler. A check on this parameter is the HP condensate flow returned to the refinery. The condensate return flow should be the sum of the reboiler steam flow and any condensate flow produced in steam heat tracing. Fig. 5 shows these two parameters. The condensate return flow indicated (FT-2455) is consistently higher than the reboiler steam flow (FT-2386) by typically 2% to 8%. This difference is in the correct direction when heat tracing condensate (not measured by the reboiler steam flow meter) is entering the condensate receiver.

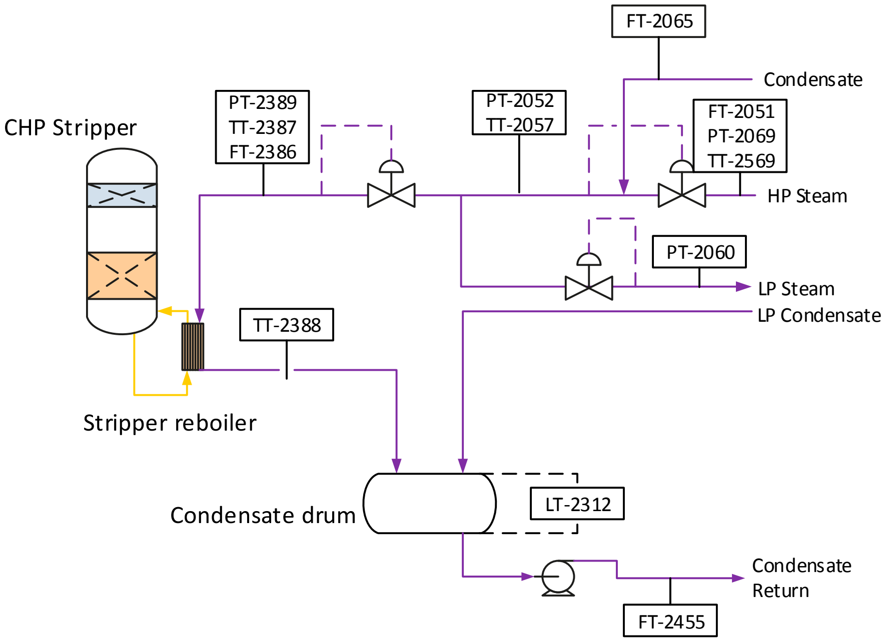

Fig. 5. Stripper reboiler steam supply flow schematic

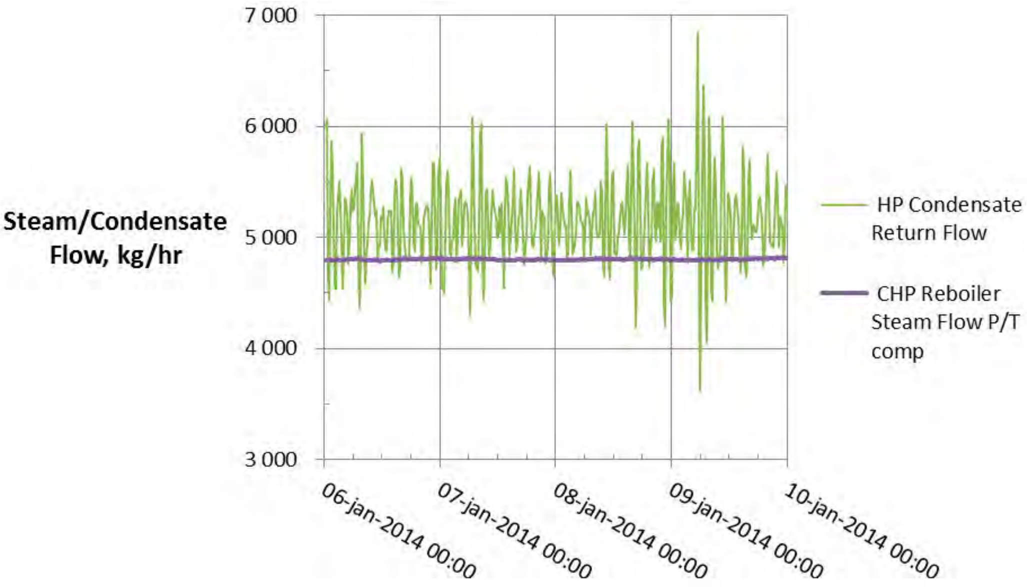

Fig. 6. Reboiler steam flow and HP condensate return flow

5. Results and discussions

5.1. CO_2 capture efficiency and recovery

CO_2 capture efficiency can be quantified in four ways as described by Thimsen et al. [1] and indicated in Table 3. In addition, the CO_2 recovery calculation is given in Table 3. The CO_2 recovery is a measure of the CO_2 mass balance.

Table 3. CO_2 capture efficiency and recovery calculations

Term	Description	Formula
CO_2 capture efficiency: Method 1	CO_2 product flow as a ratio to the CO_2 flow in the flue gas supply	$=\frac{CO_2(product)}{CO_2(supply)}$
CO_2 capture efficiency: Method 2	CO_2 product flow as a ratio to the sum of the CO_2 product flow and the CO_2 flow in the depleted flue gas	$=\frac{CO_2(product)}{CO_2(product)+CO_2(depleted)}$
CO_2 capture efficiency: Method 3	Ratio of the difference between the CO_2 flow in the flue gas supply and the CO_2 in the depleted flue gas to the CO_2 flow in the flue gas supply	$=\frac{CO_2(supply)-CO_2(depleted)}{CO_2(supply)}$
CO_2 capture efficiency: Method 4	Ratio of the depleted flue gas CO_2 per unit O_2+N_2 to the flue gas supply CO_2 per unit O_2+N_2	$=1-\frac{O_{CO_2}}{(1-O_{CO_2})}\frac{(1-I_{CO_2})}{I_{CO_2}}$ O_{CO2} = Depleted flue gas CO_2 content, dry basis I_{CO2} = Flue gas supply CO_2 content, dry basis
CO_2 recovery	Ratio of the sum of the CO_2 flow in depleted flue gas and the product CO_2 flow divided by the CO_2 flow in the flue gas supply	$=\frac{CO_2(depleted)+CO_2(product)}{CO_2(supply)}$

The depleted flue gas flow measurement is not yet a reliable measurement. A value can be calculated for the depleted flue gas flow by assuming that the oxygen and nitrogen entering the absorber with the flue gas supply leaves in the depleted flue gas. The depleted flue gas temperature may be used to calculate saturated water content. The depleted flue gas CO_2 concentration may be used to calculate CO_2 flow. Note that these are essentially the same assumptions as those used for Method 4, hence the Method 3 and Method 4 calculations result in essentially identical CO_2 capture rates. Using the calculated flow of depleted flue gas allows an estimate of the CO_2 recovery to be calculated.

Table 4 shows the four calculations of CO_2 capture and recovery for the base-case test periods (using the calculated value for depleted flue gas flow). The first thing to note is that all calculated CO_2 captures were fairly steady for the first three days of operation (test periods C1-1a to C1-3b). The CO_2 capture on the last day (C1-4a, C1-4b) was significantly higher by approximately 3–4 percentage points. The CO_2 recovery (mass balance) was neither greater than 95.5% nor as low as 91.3%. Note also that the CO_2 capture calculated by Method 1 is always less than the CO_2 capture calculated by Methods 2, 3, and 4. These two facts suggest that either quantification of CO_2 flow in the CHP flue gas supply is biased high or that calculation of CO_2 flow in the product is biased low.

Table 4. CO_2 capture and CO_2 recovery results

Test period	Method 1	Method 2	Method 3	Method 4	CO_2 recovery
S-Supply D-Depleted P-Product	$=\frac{P}{S}$	$=\frac{P}{P+D}$	$=\frac{S-D}{S}$	$=1-\frac{O_{CO_2}}{\left(1-O_{CO_2}\right)}\frac{\left(1-I_{CO_2}\right)}{I_{CO_2}}$	$=\frac{D+P}{S}$
C1-1a	83.5%	90.8%	91.5%	91.5%	91.3%
C1-1b	85.8%	90.8%	91.3%	91.3%	94.0%
C1-2	86.5%	90.8%	91.3%	91.3%	94.8%
C1-3a	84.8%	90.8%	91.5%	91.5%	92.8%
C1-3b	83.7%	90.1%	90.8%	90.8%	92.2%
C1-4a	88.7%	93.8%	94.1%	94.1%	94.2%
C1-4b	90.8%	94.8%	95.0%	95.0%	95.5%

The uncertainty in measurement of flow and composition propagate into uncertainty in the CO_2 capture. The uncertainty calculations and representative results from the each of the calculation methods are shown in Table 5. The following assumptions are used:

- Flow metering uncertainties are those theoretically estimated and calculated by internal work at TCM DA for the indicated flow meters [1]
- Concentration uncertainties for the flue gas flows are those aforementioned
- Concentration uncertainty for the product CO_2 is arbitrarily assigned to be 2%, which allows for actual CO_2 content as low as 98%
- CO_2 capture percentage of 90% is representative of that measured during base-case testing. (The calculation is not particularly sensitive to this parameter between 85 and 95%.)

A few notes on the CO_2 capture uncertainty results:

- The uncertainty in CO_2 capture is almost all due to uncertainty in CO_2 content of the CHP flue gas supply for the assigned total flow uncertainties. The CO_2 capture uncertainty is relatively insensitive to both the product CO_2 content uncertainty and the depleted flue gas CO_2 content uncertainty.
- The fact that CO_2 recovery is less than 100% suggests that one or more of the flows has a significant bias error than calculated from instrument specifications. Hence the need for a relative accuracy test audit of the pertinent flow meters to assign more realistic uncertainties. These are likely to be higher than the calculated values, which will increase overall CO_2 capture uncertainty above that indicated in Table 5.

Table 5. Uncertainty in CO_2 capture as a function of flow/composition measurement uncertainty (Nominal CO_2 capture of E_{CO2} = 90%)

CO_2 capture calc. method	Stream	Uncertain in:				CO_2 capture uncertainty equation
		Total flow	CO_2 content	CO_2 flow	CO_2 capture	
1	Product	1.1%	2%	U_{CO2P}=2.3%	5.6%	$\sqrt{(U_{CO2S})^2+(U_{COSP})^2}$
	Supply	1.3%	5%	U_{CO2S}=5.2%		
2	Product	1.1%	2%	U_{CO2P}=2.3%	2.5%	$(1-E_{CO2})\sqrt{(U_{CO2D})^2+(U_{COSP})^2}$
	Depleted	1.3%	25%	U_{CO2D}=25%		
3	Supply	1.3%	5%	U_{CO2S}=5.2%	2.8%	$\frac{(1-E_{CO2})}{E_{CO2}}\sqrt{(U_{CO2S})^2+(U_{COSD})^2}$
	Depleted	1.3%	25%	U_{CO2D}=25%		

5.2. Thermal energy use

The heat released in the reboiler is calculated as the difference between steam enthalpy at the measured reboiler inlet temperature (T) and pressure (P) and saturated water enthalpy at the reboiler condensate temperature. The pertinent data are given in Table 6.

Table 6. Stripper reboiler thermal use calculation

	Reboiler steam				Reboiler condensate				
	Flow	T	P	Steam enthalpy	T	Enthalpy	Reboiler heat duty	CO_2 flow	Specific thermal use
Test Period	kg/hr	°C	bara	kJ/kg	°C	kJ/kg	MJ/hr	kg/hr	GJ/t CO_2
C1-1a	4793	168.1	5.43	2782.8	118.9	498.9	10,946	2629	4.16
C1-1b	4803	169.0	5.43	2784.8	118.9	498.9	10,980	2631	4.17
C1-2	4802	168.8	5.43	2784.4	118.8	498.7	10,976	2639	4.16
C1-3a	4801	170.0	5.43	2787.2	119.0	499.7	10,983	2635	4.17
C1-3b	4802	170.2	5.43	2787.7	119.1	500.2	10,985	2633	4.17
C1-4a	4802	169.8	5.43	2786.6	119.2	500.3	10,978	2696	4.07
C1-4b	4801	170.1	5.43	2787.3	119.2	500.5	10,978	2702	4.06

The thermal steam consumption data give in Table 6 are based on aqueous 30 wt% MEA solvent system without the addition of any anti-foam solution. Upon addition of anti-foam solution and increase of the MEA solvent concentration during the MEA test campaign at TCM DA, the steam consumption was further reduced during CHP flue gas treatment, as described by Brigman et al [2]. Those tests were not a part of the current IVP work. Additionally, TCM DA has a LVC system installed; however, this system was not operated during Base-Case test and is consequently also not a part of the current IVP work. LVC systems have previously been showed by Knudsen et al. [4] to substantially decrease the thermal steam consumptions during amine plant operations with the aqueous MEA solvent systems.

5.3. Process contaminants

FORCE Technology measured gas-phase concentrations of the compounds listed below and the results are provided in Table 7. During the base-case testing time period, the CHP plant received refinery gas from the Mongstad refinery, which was, to some extent, co-fired with the natural gas.

- SO_2 concentrations were measured on different days. The CHP flue gas supply SO_2 concentrations are very low as are concentrations in the other streams.
- H_2SO_4 concentrations were measured in the two flue gas streams on different days. The flue gas H_2SO_4 concentrations are very low as are concentrations in the other streams. The H_2SO_4 concentrations were determined by extracting aqueous H_2SO_4 containing droplets, referred to as SO_3 mist droplets, on a heated filter.
- NO_x concentrations were below detectable limits for all streams
- Total particulates concentrations were measured on different days. The CHP flue gas supply total particulate concentrations are very low and were below detection limit in the depleted flue gas.
- Acetone, acetaldehyde, and formaldehyde were measured in the depleted flue gas and the product CO_2 stream on separate days. The emissions concentrations of acetone and the aldehydes are higher in the product CO_2 than the depleted flue gas, likely due to the low temperature boiling point nature of these compounds.
- NH_3 concentrations were measured for both depleted flue gas and product CO_2. The results indicated emissions of NH_3, likely arising from MEA degradation process occurring in the solvent system.

- MEA concentrations were determined by iso-kinetic sampling conducted by TCM DA personnel and further sample analysis by the TCM DA laboratories. The MEA concentrations in the depleted flue gas are very low, and were below the emission limits set by the Norwegian environmental authorities (Miljødirektoratet). [3]
- MEA degradation products were determined by iso-kinetic sampling from the depleted flue gas and product CO_2 by FORCE Technology and further laboratory analysis. The concentrations of any nitrosamines and nitramines were all below detection limits for both the depleted flue gas and the CO_2 product. [3] The emissions of MEA degradation products were below the emission limits set by the Norwegian environmental authorities.

Table 7. Gas-phase concentrations

Test period ID			C1-1a	C1-1b	C1-2	C1-3a	C1-3b	C1-4a	C1-4b
Item / *S*-Supply / *D*-Depleted / *P*-Product									
SO_2	*S*	ppmv						0.043	
	D				0.042				
	P						0.093		
H_2SO_4	*S*	mg/Sm^3 (dry)						0.0088	
	D				0.0036				
	P								
NO_X	*S*	mg/Sm^3 (dry)						< 10	
	D				< 10				
	P						< 10		
Particulate	*S*	mg/Sm^3 (dry)						0.060	
	D				< 0.053				
	P								
Acetone	*D*	mg/Sm^3 (dry)	< 0.07						
	P					0.91			
Formaldehyde	*D*	mg/Sm^3 (dry)	< 0.07						
	P					0.19			
Acetaldehyde	*D*	mg/Sm^3 (dry)	0.30						
	P					13.0			
NH_3	*D*	mg/Sm^3 (dry)	7.7						
	P					16			
MEA*	*D*	µg/Sm^3 (dry)							22.5
	P								
Total nitrosamines	*D*	µg/Sm^3 (dry)	< 0.80						
	P						< 0.07		
Total N-nitrosdimethylamine	*D*	µg/Sm^3 (dry)	< 0.08						
	P						< 0.07		
Total nitramines	*D*	µg/Sm^3 (dry)	< 0.20						
	P						< 0.10		

* FORCE Technology measurements of MEA gas phase concentrations for both depleted flue gas and product CO_2 were unsuccessful. The value given in Table 7 for the depleted flue gas was iso-kinetically sampled and analyzed by TCM DA. The MEA gas-phase concentration for the product CO_2 was not measured by TCM DA.

5.4. Process stream information

Additional amine plant process information for the base-case test is given in Appendix A. This information is not covered by the current IVP work, but is given for the convenience of the reader.

6. Conclusions

IVP work has been conducted at CO_2 Technology Centre Mongstad during treatment of flue gas from a natural gas-fired combined heat and power (CHP) plant. The testing is referred to as the base-case testing, applying an aqueous 30 wt% MEA solvent system treating flue gases with a flow rate of about 47.000 Sm^3/hr and a CO_2 content of about 3.5%. For the base-case considered, the CO_2 capture was about 90% and the thermal steam consumption was about 4.1 GJ/t-CO_2. Emissions of MEA were very low and MEA related degradation products were all below detection levels, and all within the emission limits set by the Norwegian environmental authorities. The current work may be considered an independently verified baseline for a non-proprietary PCC amine-based solvent system.

The following process aspects were not considered in the current IVP work:

- Long-term performance indices such as heat exchanger fouling, mass transfer packing fouling, foaming, material corrosion, solvent quality control measures, solvent loss/replacement, etc.
- Use of anti-foam solution, which has proven to reduce the thermal steam consumptions at TCM DA
- Use of the installed lean vapor compressor system at TCM DA.

These aspects warrant further (IVC) work and studies in order to gain better understanding of the performance potential of the aqueous MEA solvent system as a non-proprietary PCC system.

Acknowledgements

The authors gratefully acknowledge the staff of TCM DA, Gassnova, Statoil, Shell, Sasol, and Aker Solutions for their contribution and work at the TCM DA facility.

The authors also gratefully acknowledge Gassnova, Statoil, Shell, and Sasol as the owners of TCM DA and Aker Solutions for their financial support and contributions.

Appendix A. Amine plant process information

Table 8 provides the amine plant main process information averaged over the base-case test time period. Process fluctuations, generally attributed to fluctuations in the CO_2 content of the CHP flue gas, cannot be derived from the given values.

Table 8. Typical amine plant process information during Base-Case testing

Process parameter	Units	Value
Operating capacity	%	80
CHP flue gas supply rate	Sm^3/hr	46970
CHP flue gas supply temperature	°C	25.0
CHP flue gas supply pressure	barg	0.063
CHP flue gas supply CO_2 concentration (wet)	vol%	3.7
CHP flue gas supply O_2 concentration (wet)	vol%	13.6
Depleted flue gas temperature	°C	24.7
Lean MEA concentration	wt%	30
Lean CO_2 loading	mol CO_2 / mol MEA	0.23
Lean amine supply flow rate	kg/hr	54900
Lean amine supply temperature	°C	36.5
Lean amine density	kg/m^3	1067
Active absorber packing height	m	24
Temperature, upper absorber packing – 6	°C	45.4
Temperature, upper absorber packing – 5	°C	51.1
Temperature, upper absorber packing – 4	°C	51.2
Temperature, upper absorber packing – 3	°C	50.3
Temperature, upper absorber packing – 2	°C	49.6
Temperature, upper absorber packing – 1	°C	48.5
Temperature, middle absorber packing – 6	°C	46.7
Temperature, middle absorber packing – 5	°C	45.2
Temperature, middle absorber packing – 4	°C	43.5
Temperature, middle absorber packing – 3	°C	41.7
Temperature, middle absorber packing – 2	°C	40.6
Temperature, middle absorber packing – 1	°C	39.0
Temperature, lower absorber packing – 12	°C	38.4
Temperature, lower absorber packing – 11	°C	39.1
Temperature, lower absorber packing – 10	°C	35.0
Temperature, lower absorber packing – 9	°C	33.7
Temperature, lower absorber packing – 8	°C	32.2
Temperature, lower absorber packing – 7	°C	30.4
Temperature, lower absorber packing – 6	°C	29.8
Temperature, lower absorber packing – 5	°C	29.3
Temperature, lower absorber packing – 4	°C	28.1
Temperature, lower absorber packing – 3	°C	28.4
Temperature, lower absorber packing – 2	°C	27.6
Temperature, lower absorber packing – 1	°C	27.2

Rich solution return temperature	°C	27.7
Temperature above upper absorber packing	°C	38.1
Wash water 1 supply flow rate	kg/hr	55000
Wash water 1 inlet temperature	°C	28.4
Wash water 1 withdrawal temperature	°C	43.9
Temperature above Wash Water 1	°C	36.2
Wash water 2 supply flow rate	kg/hr	62000
Wash water 2 inlet temperature	°C	23.5
Wash water 2 withdrawal temperature	°C	35.0
Temperature above Wash Water 2	°C	24.7
Rich CO_2 loading	mol CO_2 / mol MEA	0.48
Rich solution supply flow rate	kg/hr	57200
Rich solution supply temperature	°C	108.6
Lean solution return temperature	°C	119.1
Rich amine density	kg/m^3	1114
Reboiler steam flow rate	kg/hr	4800
Reboiler steam temperature	°C	169
Reboiler steam pressure	barg	4.42
Reboiler condensate temperature	°C	118.8
Reboiler condensate pressure	barg	4.11
Stripper overhead pressure	barg	0.90
Stripper overhead temperature	°C	99.8
Stripper overhead reflux flow rate	kg/hr	1370
Stripper overhead reflux temperature	°C	23.3
Stripper sump temperature	°C	119.3
Reboiler solution temperature	°C	122.3
Lean vapour compressor system	-	off
Product CO_2 flow rate	kg/hr	2670
Product CO_2 discharge temperature	°C	17.7
Product CO_2 discharge pressure	barg	0.023

References

[1] Thimsen D, Maxson A, Smith V, Cents T, Falk-Pedersen O, Gorset O, Hamborg E S. Results from MEA testing at the CO_2 Technology Centre Mongstad. Part I: Post-Combustion CO_2 capture testing methodology. Energy Procedia; 2014.

[2] Brigman N, Shah M I, Falk-Pedersen O, Cents T, Smith V, De Cazenove T, Morken A K, Hvidsten O A, Chhaganlal M, Feste J K, Lombardo G, Bade O M, Knudsen J, Subramoney S C, Fostås B F, De Koeijer G, Hamborg E S. Results of amine plant operations from 30 wt% and 40 wt% aqueous MEA testing at the CO_2 Technology Centre Mongstad. Energy Procedia; 2014.

[3] Morken A K, Nenseter B, Pedersen S, Chhaganlal M, Feste J K, Tyborgnes R B, Ullestad Ø, Ulvatn H, Zhu L, Mikoviny T, Wisthaler A, Cents T, Bade O M, Knudsen J, De Koeijer G, Falk-Pedersen O, Hamborg E S. Emission results of amine plant operations from MEA testing at the CO_2 Technology Centre Mongstad. Energy Procedia; 2014.

[4] Knudsen J N, Andersen J, Jensen J N, Biede O. Evaluation of process upgrades and novel solvents for the post combustion CO2 capture process in pilot-scale. Energy Procedia 2011;4:1558-1565.

CATCHING OUR FUTURE

Results of amine plant operations from 30 wt% and 40 wt% aqueous MEA testing at the CO_2 Technology Centre Mongstad

(2014)

Available online at www.sciencedirect.com

ScienceDirect

Energy Procedia 63 (2014) 6012 – 6022

Energy Procedia

GHGT-12

Results of amine plant operations from 30 wt% and 40 wt% aqueous MEA testing at the CO_2 Technology Centre Mongstad

Natasha Brigman[a,b], Muhammad I. Shah[c], Olav Falk-Pedersen[a,c], Toine Cents[a,b], Vian Smith[a,b], Thomas De Cazenove[a], Anne K. Morken[a,d], Odd A. Hvidsten[a,d], Milan Chhaganlal[a,d], Jane K. Feste[a,d], Gerard Lombardo[a,c], Otto M. Bade[e], Jacob Knudsen[e], Shalendra C. Subramoney[b], Berit F. Fostås[d], Gelein de Koeijer[d], Espen S. Hamborg[a,d,*]

[a]*CO_2 Technology Centre Mongstad (TCM DA), 5954 Mongstad, Norway*
[b]*Sasol Technology, P.O. Box 5486, Johannesburg 2000, South Africa*
[c]*Gassnova SF, Dokkvegen 10, 3920 Porsgrunn, Norway*
[d]*Statoil ASA, P.O. Box 8500, 4035 Stavanger, Norway*
[e]*Aker Solutions, P. O. Box 222, 1326 Lysaker, Norway*

Abstract

An amine plant campaign has been performed at the CO_2 Technology Centre Mongstad applying the aqueous 30 wt% and 40 wt% monoethanolamine (MEA) solvent systems for treatment of flue gas from a combined heat and power (CHP) plant. CHP flue gas flow rates were ranging from about 40.000 Sm^3/h to 60.000 Sm^3/h and the CO_2 content was about 3.5 vol%.

Minimum specific reboiler duties (SRD) of respectively 4.0 MJ/kg CO_2 and 3.7 MJ/kg CO_2 were obtained for the aqueous 30 wt% MEA solvent system without and with the addition of anti-foam solution. A minimum SRD of 3.4 MJ/kg CO_2 was obtained for the aqueous 40 wt% MEA solvent system. Lower SRD and absorber liquid to gas (L/G) ratios were obtained with higher concentration MEA solvents.

Increased absorber packing heights resulted in lower SRD. Variation in flue gas supply flow rates and corresponding variations in solvent flow rates, i.e. constant L/G ratios, did not yield any significant variations in SRD. Decreased flue gas supply temperatures resulted in lower SRD.

For any future large scale post-combustion capture (PCC) amine plant, engineering aspects such as the flue gas supply temperature and instrumentation monitoring CO_2 content in the flue gas must be evaluated to avoid the chemical equilibrium pinch behavior. Engineering and environmental aspects related to the use of anti-foam solutions for future large scale PCC amine plants must also be considered.

---

* Corresponding author. Tel.: +47 56 34 52 20.
E-mail address: eham@tcmda.com

1876-6102 © 2014 The Authors. Published by Elsevier Ltd. This is an open access article under the CC BY-NC-ND license (http://creativecommons.org/licenses/by-nc-nd/3.0/).
Peer-review under responsibility of the Organizing Committee of GHGT-12
doi:10.1016/j.egypro.2014.11.635

© 2014 The Authors. Published by Elsevier Ltd. This is an open access article under the CC BY-NC-ND license
(http://creativecommons.org/licenses/by-nc-nd/3.0/).

Peer-review under responsibility of the Organizing Committee of GHGT-12

Keywords: Amine plant operations; 30 wt% monoethanolamine; 40 wt% monoethanolamine

1. Introduction

The CO_2 Technology Centre Mongstad (TCM DA) is the one of the world's largest and most advanced facilities for testing and improving CO_2 capture technology. The facility enables vendors of suitable amine formulations and other post-combustion capture processes to test their process, collecting performance data to support full-scale design. The vendors can then anticipate the associated performance and operating costs of their amine formulations and capture processes. As a result, one of the main objectives of TCM DA is to investigate and demonstrate the flexibility of post-combustion amine based solvent systems with respect to load changes, variations in flue gas composition, variations in amine plant operations and solvent system compositions in order to achieve optimal and environmentally safe operating conditions. The flue gas utility system allows for flue gas supplies with varying temperatures, flow rates, and CO_2 content and also different types of flue gases with various trace components from either a combined heat and power (CHP) plant or a refinery catalytic cracker. In the CHP plant, the natural gas is combusted in a gas turbine and the flue gas content and characteristics are similar to those of a combined cycle gas turbine (CCGT) power plant. The amine plant at TCM DA is a highly flexible and well instrumented generic amine plant, designed and constructed by Aker Solutions, aimed to accommodate a variety of technologies with capabilities of treating flue gas streams of up to 60.000 Sm^3 per hour. The flexibility of the amine plant allows for handling of a wide range of flue gas flow rates, temperatures, and CO_2 content in the flue gas, and also a wide range of various operational parameters, i.e. solvent flow rates, absorber packing heights, stripper pressures, reboiler heat duties, lean amine and cross heat exchanger duties, absorber water wash temperatures and flow rates with or without acid injections, anti-foam solution injections, etc. [1, 2]

The campaign described in the current paper was conducted at TCM DA in the period December 2013 to February 2014 as a part of Aker Solutions' test period. In general, during the campaign the aqueous 30 wt% monoethanolamine (MEA) solvent system was applied treating the flue gas from the CHP plant. The primary purposes and goals of the campaign were:

- Generate results from CHP plant operations with CO_2 capture
- Generate an independently verified TCM DA amine plant base case while treating CHP plant flue gas with the aqueous 30 wt% MEA solvent system [3, 4]
- Investigate the performance potential of higher MEA concentration solvents
- Verify design capacities and flexibilities of the TCM DA amine plant and specific functionalities
- Gain better understanding of scale-up, performance, and emission aspects and transient operations of the TCM DA amine plant
- Verify and improve process simulation models
- Test and improve various online analyser for emission monitoring [5]
- Scientific dissemination of some results

These purposes and goals are aimed for gaining experience and knowledge for future large scale carbon capture and storage (CCS) projects.

This work is part of a continuous effort of gaining better understanding of the performance potential of the non-proprietary aqueous MEA solvent system, conducted by TCM DA and its affiliates and owners, in order to test, verify, and demonstrate CO_2 capture technologies. [3, 4, 5] The purpose of the current work is to provide results of various operational conditions of the TCM DA amine plant, and hence demonstrating some capacities, flexibilities, and performances of the plant while treating CHP flue gases.

2. Testing Philosophy

An overview of the TCM DA amine plant has been given elsewhere. [3, 4, 5]

The test philosophy during the current campaign was to adjust one operational parameter at a time, e.g. the solvent flow rate, the gas flow rate, etc., whilst subsequently allowing the amine plant to reach steady-state operations and simultaneously manually controlling the CO_2 capture rate to a specific value. The CO_2 capture rate was controlled to about 85% for most of the campaign by manually adjusting the reboiler steam flow rate. The response time of the amine plant was up to about 3 hours, depending on the varied operational parameter. The plant was operated for at least an additional 3 hours of steady-state operations after an operational parameter change before the plant was considered to provide representative process values. Any solvent sampling for laboratory analysis was conducted once representative process values were obtained. Certain transient operations were conducted during the campaign, and the aforementioned test philosophy was adapted in order to accommodate such operations. During Base-Case testing, as described elsewhere [3, 4], the amine plant was operated at steady-state operations for about 1 week.

Table 1 provides the main operational parameters and ranges adjusted during the campaign. Approximately 150 different operating conditions were conducted during the campaign, and the results of some of these are presented in the current work.

Table 1: MEA campaign overview

Adjusted operational parameter		Range
Flue gas flow rate	Sm^3/h	30.000 - 60.000
Flue gas temperature	°C	20 – 50
Flue gas CO_2 concentration	vol%	3.2 – 11.0
Lean solvent flow rate	m^3/h	30 – 150
Lean solvent temperature	°C	20 – 45
L/G ratio	kg liquid / kg gas	0.5 – 2.5
CO_2 capture rate	%	60 – 95
MEA concentration	wt%	25 – 45
Absorber packing height	m	12 – 24
Stripper pressure	bara	1.9 – 2.5
Stripper reboiler duties	MW	2.5 – 6

The calculations procedures for the various performance indices presented in the current work are as described by Thimsen et al. [3] and Hamborg et al. [4].

3. Chemicals

MEA [CAS: 141-43-5] was supplied by AkzoNobel, and was diluted to a desired solvent concentration by addition of demineralized water. Anti-foam solution was supplied from KCC Basildon.

4. Results and Discussion

4.1. Mass recovery and MEA solvent concentrations

The total mass and CO_2 mass recovery also referred to as the total mass and CO_2 mass balances, for the complete campaign, were determined as described by Thimsen et al. [3] and displayed in Figure 1. The total mass recovery is, as expected, close to 100% during the complete campaign. The CO_2 mass recovery is however scattered, and this may be attributed to inadequate instrumentation for monitoring of the CO_2 gas phase concentrations in the flue gas supply and depleted flue gas. The gas phase concentrations of CO_2 in the flue gas streams were monitored by the installed Fourier transform infrared spectroscopy (FTIR) analyzer, and accuracy and precision challenges with respect to this FTIR analyzer setup has been described by elsewhere. [4] The scattering of the CO_2 mass recovery displayed in Figure 1 leads to uncertainties in the CO_2 capture rates, whereas the specific thermal use, as derived in the current work, is independent of the FTIR analyzer system. [4]

The MEA solvent concentrations, based on sampling and laboratory analysis of the lean amine, are displayed in Figure 2. The MEA solvent concentration was maintained at about 30 wt% during most of the campaign, and was increased to above 40 wt% towards the end. The MEA solvent water balance was maintained by adjusting the depleted flue gas temperature to the flue gas supply temperature, and, if necessary, addition of demineralized water to the MEA solvent. Due to the rapid change of operational parameters and conditions and additional time consuming sampling and laboratory analysis, the MEA solvent concentration could not be maintained at constant values throughout the campaign.

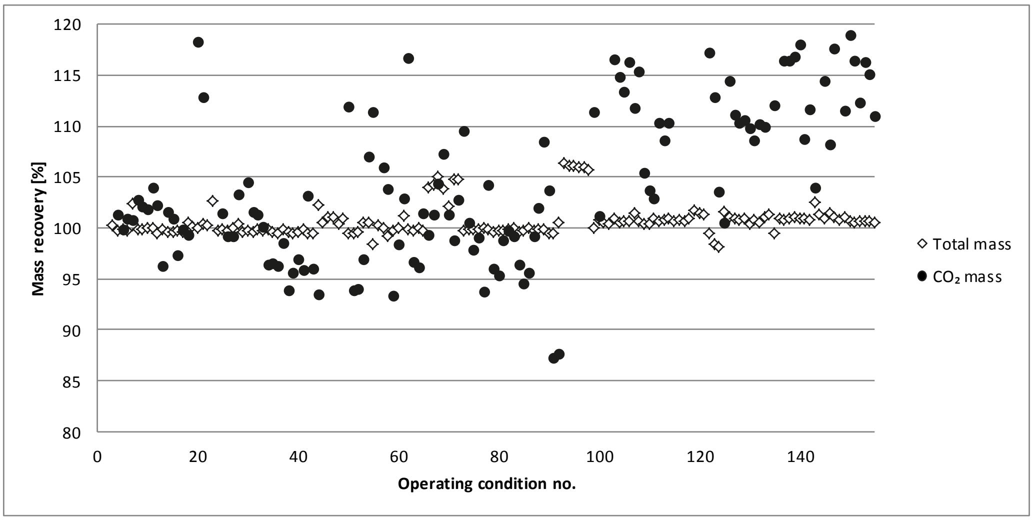

Figure 1: Total and CO_2 mass recovery at various operating conditions

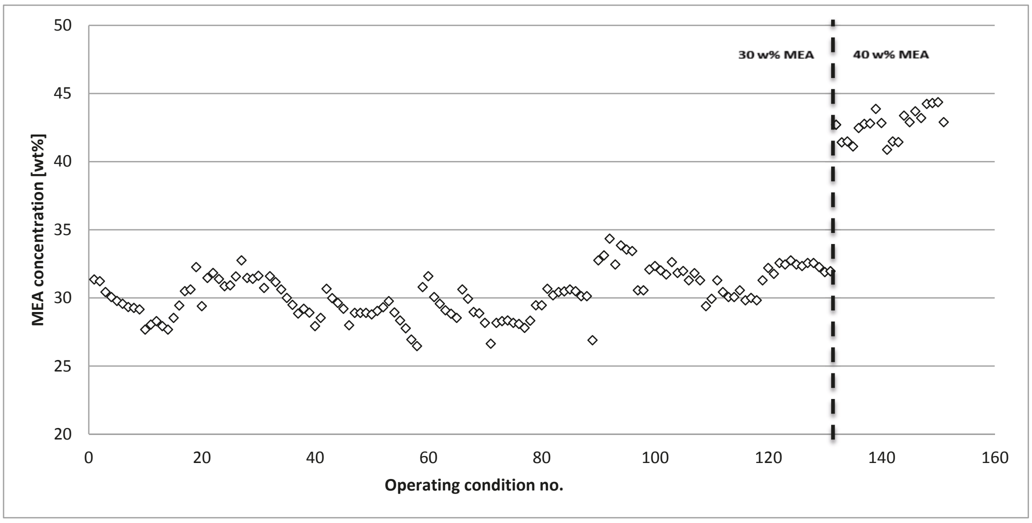

Figure 2: MEA concentrations at various operating conditions

4.2. Overall energy performances

Figure 3 displays the specific reboiler duties (SRD) for the aqueous 30 wt% MEA solvent system with and without the use of anti-foam solutions. The plant was operated with 24 meters of absorber packing heights, 1.9 bara stripper pressure, and a flue gas flow rate of about 47.000 Sm^3/h at 25 °C. The CO_2 capture rate was kept at about 85 %. The results in Figure 3 show a clear minimum in the SRD of about 4.0 MJ/kg CO_2 at a lean amine loading of about 0.25 for operations without anti-foam solutions added. Results refer to Base-Case testing as presented elsewhere [4] provided a SRD of 4.1 MJ/kg CO_2 and is displayed in Figure 3. For operations with addition of anti-foam solutions, the minimum SRD is shifted towards lower lean CO_2 loadings, and the cause for this behavior is described later. The minimum SRD for these operations with anti-foam addition may have not been achieved. The lean amine CO_2 loading can be assumed closely proportional to the MEA solvent circulation rate, assuming steady-state plant operations, and in these specific cases solvent circulation rates approached the minimum achievable due to solvent pump limitations. Lower solvent flow rates could have been achieved with the use of the solvent filtration system however this was not tested during operations with addition of anti-foam solutions. The minimum SRD obtained for operations with anti-foam solutions added was approximately 3.7 MJ/kg CO_2.

Figure 4 displays the SRD for the aqueous 40 wt% MEA solvent system. The plant was operated with 24 meters of absorber packing heights, 1.9 bara stripper pressure, and a flue gas flow rate of about 59.000 Sm^3/h at 25 °C. The CO_2 capture rate was kept at about 85 %. The results in Figure 4 show a minimum in the SRD of about 3.4 MJ/kg CO_2 at lean amine loadings ranging between 0.2 and 0.25. A batch of anti-foam solutions were added several days prior to these tests, and the effect of the anti-foam solution was likely present during these operating conditions.

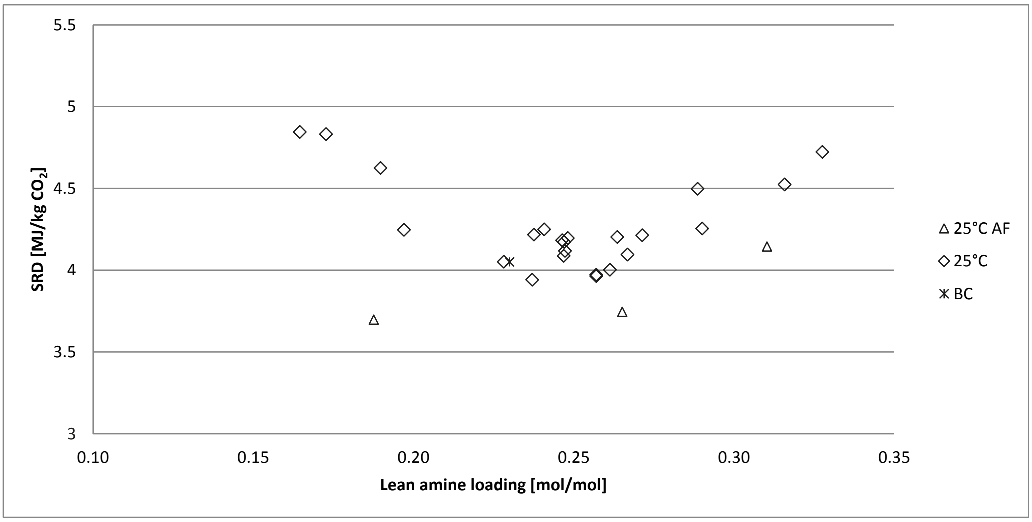

Figure 3: SRD for the 30 wt% aqueous MEA solvent system as a function of the lean amine CO_2 loading. AF indicates operations with anti-foam solutions injected into the aqueous MEA solvent system. BC indicates the Base-Case operation as in described by Hamborg et al. [4]

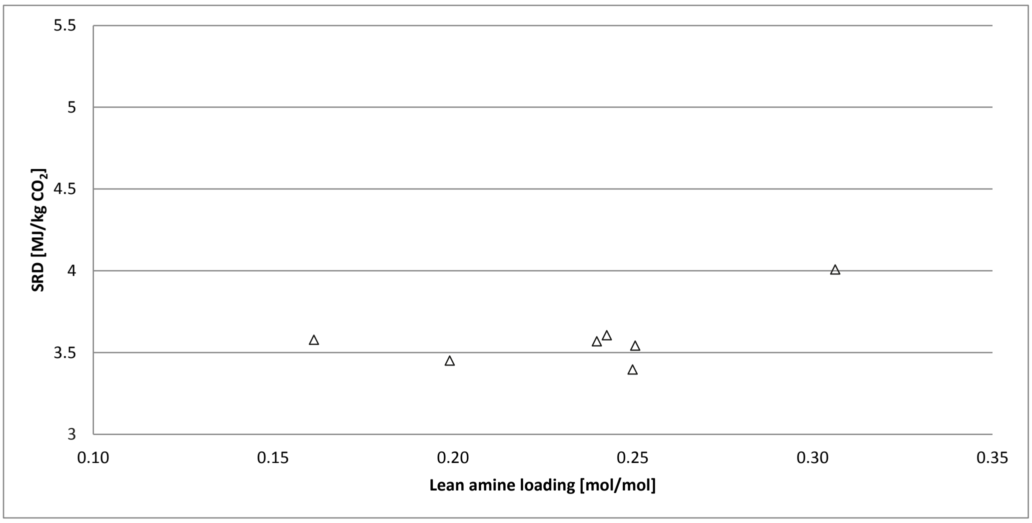

Figure 4: SRD for the 40 wt% aqueous MEA solvent system as a function of the lean amine CO_2 loading.

Figure 5 displays a comparison of the results presented in Figure 3 and Figure 4 as a function of the ratio of solvent flow rate to the flue gas supply rate on mass basis (L/G ratio). Operations with the 40 wt% aqueous MEA solvent system clearly provide lower values of the SRD and L/G ratios. The use of 40 wt% or higher MEA concentrations must however be considered with respect to higher solvent degradation rates, as described by Morken et al. [5], and possible material corrosion rates. The latter is however irrelevant for the TCM DA amine plant as it is constructed primarily of high grade stainless steel and polypropylene plastic material for absorber lining. The metal ion concentrations were monitored during the MEA campaign, and no significant increase in ion concentration was observed for 40 wt% operations.

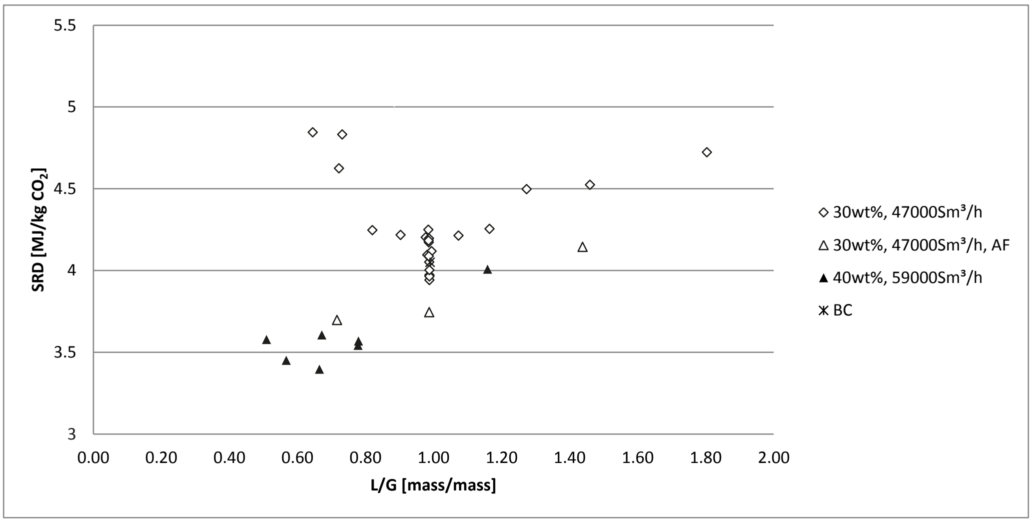

Figure 5: SRD for the 30 wt% and 40 wt% aqueous MEA solvent system as a function of L/G ratios

4.3. Effects of absorber packing heights

Figure 6 displays the effects of absorber packing heights. The SRD obtained with 24 meters of absorber packing heights of about 4.0 MJ/kg CO_2 are lower than those of 18 meters of about 4.5 MJ/kg CO_2. The plant was operated at 1.9 bara stripper pressure and a flue gas flow rate of about 47.000 Sm^3/h at 25 °C. The CO_2 capture rate was kept at about 85 %.

It is well known that MEA is considered an amine with a relatively high kinetic reaction rate towards CO_2, and equilibrium conditions could be expected in the absorber bottom section. Solvent sampling and laboratory analysis resulted in rich solvent CO_2 loadings of about 0.44 and 0.48 for respective 18 meters and 24 meters of absorber packing heights, whereas the expected CO_2 equilibrium loading for the aqueous MEA system was approximately 0.50. Preliminary simulation work has indicated that it is most likely the kinetic rate which limits the approach to equilibrium in the test runs.

Similar trends, as displayed in Figure 6, were observed with the 40 wt% aqueous MEA solvent system at different absorber packing heights.

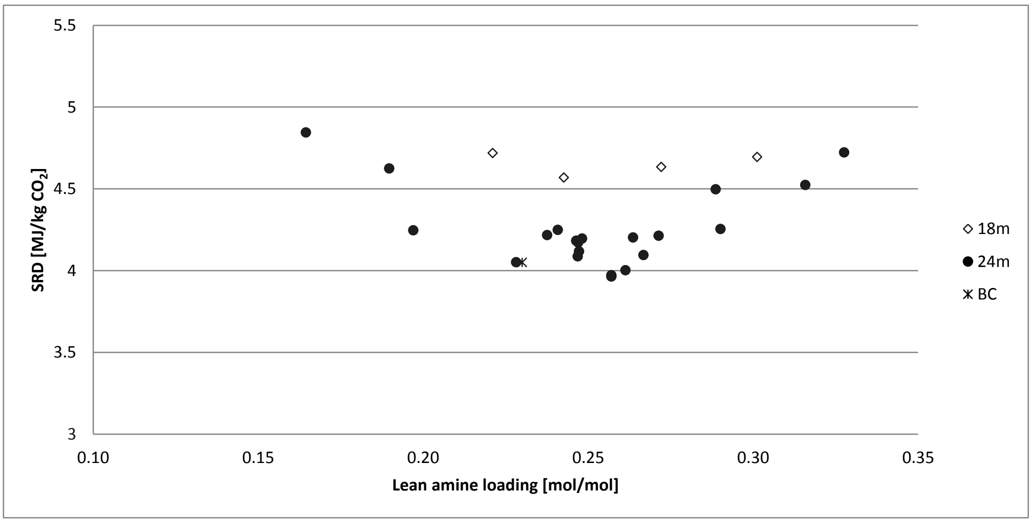

Figure 6: SRD for the 30 wt% aqueous MEA solvent system as a function of the lean amine CO_2 loading and absorber packing heights

4.4. Effect of flue gas supply flow rates

Figure 7 displays the effects of flue gas supply flow rates. The flue gas supply rate shows no significant effect on the SRD at specific lean amine loadings. The plant was operated with 24 meters of absorber packing heights, 1.9 bara stripper pressure, and a flue gas supply temperature of 25 °C. The CO_2 capture rate was kept at about 85 %. At specific lean amine loadings it can be assumed that the amine plant was operated at close to identical conditions for the various flue gas supply flow rates, except the correlated adjustment of the solvent flow rate. This would ideally create a constant L/G ratio for the various flue gas supply flow rates at a certain lean amine loading. The minor differences in the SRD between the various flue gas supply flow rates at a certain lean amine loading must therefore be attributed to normal operational variations of the various amine plant unit operations.

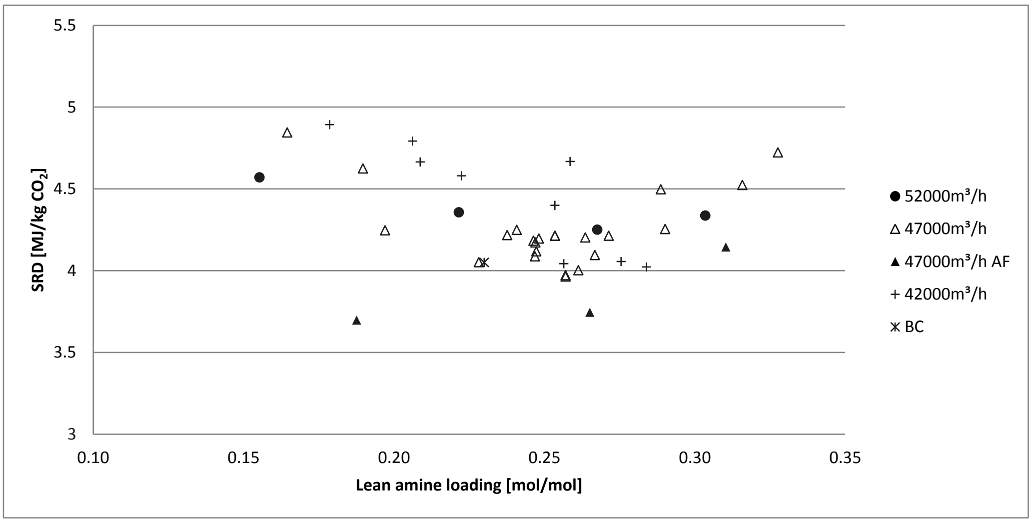

Figure 7: SRD for the 30wt% aqueous MEA solvent system as a function of the lean amine CO_2 loading and flue gas supply flow rates

4.5. Effect of flue gas supply temperatures

Increased SRD were observed when increasing the flue gas supply temperatures from 25 °C to about 50 °C. The SRD was determined to be about 4 MJ/kg CO_2 for the 30 wt% aqueous MEA solvent system at 25 °C flue gas supply temperatures, whereas the SRD was determined to be about 5.0 MJ/kg CO_2 for 50 °C flue gas supply temperatures. Some increase is expected due to the temperature dependent CO_2 vapor liquid equilibria behavior in the absorber bottom, leading to a lower rich amine loading at increased absorber bottom temperature, and the fact that the partial pressure of CO_2 is slightly lower in the flue gas supply stream of 50 °C than 20 °C leading to decreased mass transfer driving forces. However, the more important aspect encountered during these test conditions at elevated flue gas supply temperatures was chemical equilibrium pinching of the upper section of the absorber. This was encountered when the lean amine loading was not sufficiently low, i.e. the CO_2 equilibrium pressure in the lean amine solvent entering the absorber is close to or identical to the actual CO_2 partial pressure in the gas phase of the upper section of the absorber. At such conditions little mass transfer will occur in the upper section of the absorber, as mass transfer driving forces are low. In order to avoid such chemical equilibrium pinching, the lean amine loading would need to be lowered by e.g. increasing the stripper bottom temperature. Aspects around this are described further below.

The chemical equilibrium pinch behavior, as aforementioned, was encountered primarily as a result of the very low targeted depleted flue gas CO_2 partial pressure, as is a consequence of CO_2 capture from low partial CO_2 pressure CHP flue gases. Assuming flue gas supply CO_2 content of about 3.5 vol% and a corresponding partial pressure of about 35 mbara by assumption of ideal gas law behavior, the depleted flue gas CO_2 partial pressure would be about 5 mbara at 85 % CO_2 capture rate. In order to avoid and control such chemical equilibrium pinching behavior for any future large scale PCC amine plants in the upper section of the absorber, engineering considerations such as e.g. flue gas supply temperatures and sufficient instrumentation for monitoring of the CO_2 content in the depleted flue gas should be taken into account.

4.6. Effect of stripper behavior

Figure 8 and Figure 9 displays the effect of addition of anti-foam solution to the solvent. The effect of anti-foam solution addition on the SRD is more pronounced at lower lean amine loadings. The plant was operated at 1.9 bara stripper pressure and a flue gas flow rate of about 47.000 Sm^3/h at 25 °C. The CO_2 capture rate was kept at approximately 85 %.

Addition of anti-foam solutions showed no impact on the absorber temperature profile as displayed by Figure 8, but showed a considerable impact on the stripper temperature profile as displayed by Figure 9. The temperature values displayed in the Figure 8 and Figure 9 are the average value of four temperature sensors in the radial plane at each axial column position. For operations without anti-foam solutions, the stripper temperature profile shows relatively high temperatures in the upper section of the stripper of about 115 °C. It is well known that such will lead to excessive amounts of water vapor leaving the stripper and being further directed to the overhead condenser, which will lead to an unnecessarily high SRD. Upon analysis of the stripper temperature profiles in the radial plane and axial direction, it was concluded that transient channeling in the stripper bed occurred during operations without addition of anti-foam solution. This resulted in poor gas liquid distribution and contact, and condensation of the stripping gas and water vapor occurred in the overhead condenser rather than inside the stripper bed. Addition of anti-foam solution reduced the channeling behavior in the stripper, and well defined as expected stripper temperature profiles were obtained in the axial direction, as displayed by Figure 9, and minor temperature differences were observed in the radial plane. At these stripper operating conditions, only moderate amounts of water vapor, as defined by chemical phase equilibria, will leave the stripper and be further directed to the overhead condenser. This is defined as optimal stripper behavior. The exact cause of the observed transient steam channeling is not yet clearly understood, however it may be caused by the solvent foaming. Engineering aspects related to this and the use of anti-foam solutions for future large scale PCC amine plants must be considered. Environmental aspects of the use of anti-foam in such amine plants where the depleted flue gas may be emitted to air must also be considered.

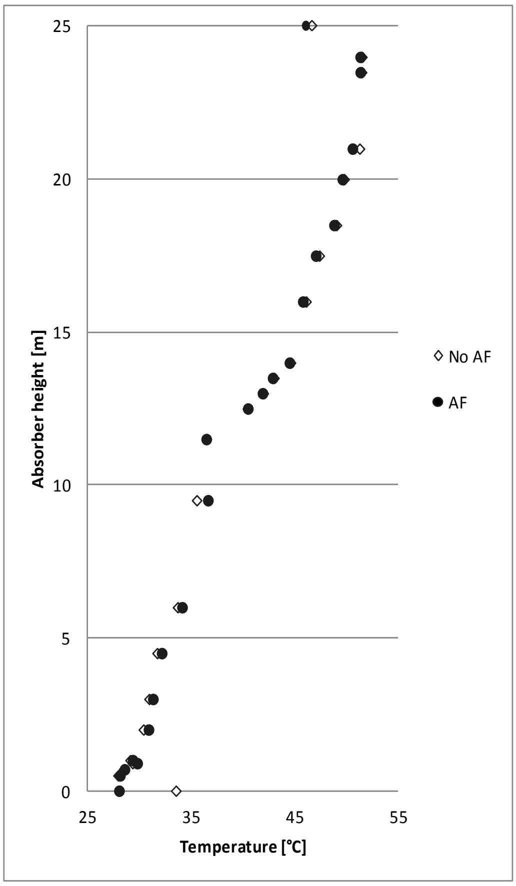

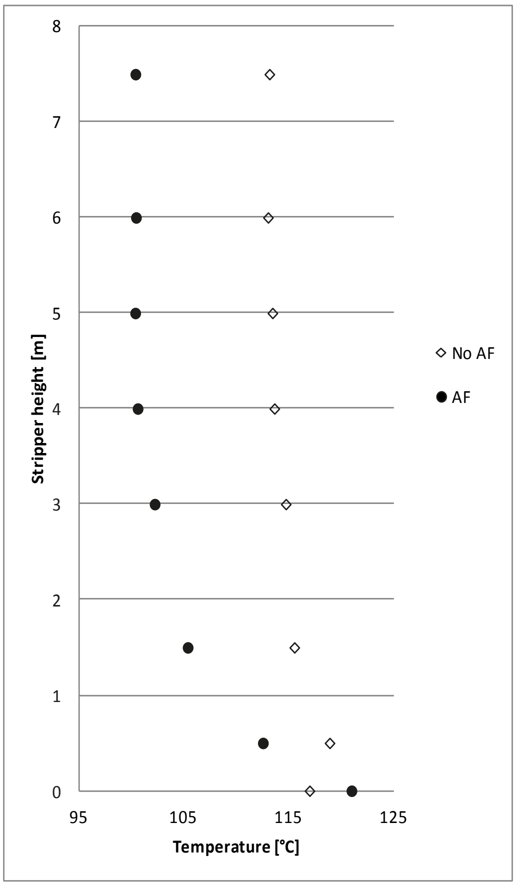

Figure 8: Absorber temperature profile with and without antifoam

Figure 9: Stripper temperature profile with and without antifoam

5. Conclusion

A campaign has been performed in the amine plant at the CO_2 Technology Centre Mongstad applying the aqueous 30 wt% and 40 wt% MEA solvent systems for treatment of flue gas from a combined heat and power (CHP) plant. CHP flue gas flow rates were ranging from about 40.000 Sm^3/h to 60.000 Sm^3/h and the CO_2 content was about 3.5 vol%.

Minimum steam reboiler duties (SRD) of respectively 4.0 MJ/kg CO_2 and 3.7 MJ/kg CO_2 were obtained for the aqueous 30 wt% MEA solvent system without and with addition of anti-foam solution. Minimum SRD of 3.4 MJ/kg CO_2 was obtained for the aqueous 40 wt% MEA solvent system. Lower SRD and absorber liquid to gas (L/G) ratios could be obtained with the higher concentration MEA solvents.

Increased absorber packing heights resulted in lower SRD. Variation in flue gas supply flow rates and corresponding variations in solvent flow rates did not yield any significant variations in SRD. Decreased flue gas supply temperatures resulted in lower SRD, as rich amine loadings increased and chemical equilibrium pinch behavior in the upper section of the absorber was limited.

Engineering aspects such as flue gas supply temperatures and instrumentation for gas phase monitoring of the CO_2 flue gas contents must be considered for any future large scale PCC amine plant in order to avoid chemical equilibrium pinch behavior during treatment of CHP flue gases. Engineering and environmental aspects related to the use of anti-foam solutions for future large scale PCC amine plants must also be considered.

Acknowledgements

The authors gratefully acknowledge the staff of TCM DA, Gassnova, Statoil, Shell, Sasol, and Aker Solutions for their contribution and work at the TCM DA facility.

The authors also gratefully acknowledge Gassnova, Statoil, Shell, and Sasol as the owners of TCM DA and Aker Solutions for their financial support and contributions.

References

[1] Andersson V, Wittmeyer K. Operational Experience and Initial Results from the First Test Period at CO_2 Technology Centre Mongstad. Energy Procedia; 2013; 37:6348-6356

[2] de Koeijer G, Enge Y. CO_2 Technology Centre Mongstad – Design, functionality and emissions of the amine plant. Energy Procedia; 2011; 4:1207-1213

[3] Thimsen D, Maxson A, Smith V, Cents T, Falk-Pedersen O, Gorset O, Hamborg E S. Results from MEA testing at the CO_2 Technology Centre Mongstad. Part I: Post-Combustion CO_2 capture testing methodology. Energy Procedia; 2014

[4] Hamborg E S, Smith V, Cents T, Brigman N, Falk-Pedersen O, De Cazenove T, Chhaganlal M, Feste J K, Ullestad Ø, Ulvatn H, Gorset O, Askestad I, Gram L K, Fostås B F, Shah M I, Maxson A, Thimsen D. Results from MEA testing at the CO_2 Technology Centre Mongstad. Part II: Verification of baseline results. Energy Procedia; 2014

[5] Morken A K, Nenseter B, Pedersen S, Chhaganlal M, Feste J K, Tyborgnes R B, Ullestad Ø, Ulvatn H, Zhu L, Mikoviny T, Wisthaler A, Cents T, Bade O M, Knudsen J, De Koeijer G, Falk-Pedersen O, Hamborg E S. Emission results of amine plant operations from MEA testing at the CO_2 Technology Centre Mongstad. Energy Procedia; 2014.

CATCHING OUR FUTURE

Emission results of amine plant operations from MEA testing at the CO_2 Technology Centre Mongstad

(2014)

Available online at www.sciencedirect.com

ScienceDirect

Energy Procedia 63 (2014) 6023 – 6038

Energy Procedia

GHGT-12

Emission results of amine plant operations from MEA testing at the CO_2 Technology Centre Mongstad

Anne K. Morken[a,b], Bjarne Nenseter[b], Steinar Pedersen[b], Milan Chhaganlal[a,b], Jane K. Feste[a,b], Rita Bøe Tyborgnes[a,b], Øyvind Ullestad[a,b], Helge Ulvatn[a,b], Liang Zhu[c], Tomas Mikoviny[c], Armin Wisthaler[c], Toine Cents[a,d], Otto M. Bade[e], Jacob Knudsen[e], Gelein de Koeijer[b], Olav Falk-Pedersen[a,f], Espen S. Hamborg[a,b,*]

[a]CO_2 Technology Centre Mongstad (TCM DA), 5954 Mongstad, Norway
[b]Statoil ASA, P.O. Box 8500, 4035 Stavanger, Norway
[c]University of Oslo, Department of Chemistry, P.O. Box 1033 Blindern, 0315 Oslo, Norway
[d]Sasol Technology, PO Box 5486, Johannesburg 2000, South Africa
[e]Aker Solutions, P. O. Box 222, 1326 Lysaker, Norway
[f]Gassnova SF, Dokkvegen 10, 3920 Porsgrunn, Norway

Abstract

Extensive atmospheric emission monitoring has been conducted at the CO_2 Technology Centre Mongstad (TCM DA) during amine based post-combustion CO_2 capture. The TCM DA amine plant was operated with an aqueous monoethanolamine (MEA) solvent system, treating flue gas from a combined heat and power (CHP) plant. Emission monitoring was conducted by a Fourier Transform Infrared (FTIR) Spectroscopy analyzer, a Proton Transfer Reaction Time-of-Flight Mass Spectrometry (PTR-TOF-MS) analyzer, and manual isokinetic sampling followed by off-line analysis in the laboratory.

Atmospheric emissions of MEA were very low throughout the entire campaign, ranging from a few to a few hundred parts per billion (ppb, 1 ppb = 10^{-9} v/v). Atmospheric emissions of MEA amine based degradation products such as nitrosamines and nitramines were below detectable levels. Atmospheric emissions of ammonia (NH_3) were in the low ppm range. Methylamine was emitted at low ppb range.

Absorber wash water sections were found to effectively reduce atmospheric emissions from amine based solvent system.

---

* Corresponding author. Tel.: +47 56 34 52 20.
E-mail address: eham@tcmda.com

1876-6102 © 2014 The Authors. Published by Elsevier Ltd. This is an open access article under the CC BY-NC-ND license (http://creativecommons.org/licenses/by-nc-nd/3.0/).

Peer-review under responsibility of the Organizing Committee of GHGT-12
doi:10.1016/j.egypro.2014.11.636

© 2014 The Authors. Published by Elsevier Ltd. This is an open access article under the CC BY-NC-ND license
(http://creativecommons.org/licenses/by-nc-nd/3.0/).

Peer-review under responsibility of the Organizing Committee of GHGT-12

Keywords: MEA, monoethanolamine, atmospheric emission, nitrosamine, nitramine, amine degradation products

1. Introduction

The CO_2 Technology Centre Mongstad (TCM DA) has in collaboration with partners undertaken several months test using the non-proprietary aqueous monoethanolamine (2-aminoethanol, MEA) solvent system at 30 wt% and 40 wt% in an attempt to characterize the performance and atmospheric emissions from such operations [1,2,3]. The operations were carried out at a considerably large scale of about 50.000 Sm^3/h of flue gas supply flow rates from a combined heat and power (CHP) plant, as described elsewhere [1,2,3]. In the CHP plant, the natural gas is combusted in a gas turbine and the flue gas content and characteristics are similar to those of a combined cycle gas turbine (CCGT) power plant. TCM DA has made significant investment in equipment and instrumentation for monitoring of stack emissions. Continuous efforts are being done to improve sampling methods, sampling lines and the instrumental analysis.

Quantitative emission data from a representative CO_2 capture plant is one remaining knowledge gap in the assessment of health and environmental risks posed by the amine-based post combustion capture (PCC) technology [4]. A health risk analysis for the emissions to air from the amine plant TCM DA was recently published [5]. The emission permit granted to TCM DA by the Norwegian Environmental Agency (Miljødirektoratet) in November 2011 regulates the emission levels for solvent amines, alkylamines, aldehydes and ammonia [6]. It also sets requirements for online monitoring and how to calculate the nitrosamine and nitramine environmental concentrations by a dispersion calculation method. The air and drinking water concentrations of 0.3 ng/m^3 and 4 ng/L respectively were associated with negligible excess risk level for cancer (10^{-6}) after lifelong exposure to nitrosodimethylamine (NDMA). Since all amines that are emitted to air from the absorber stack may undergo photo-oxidation in the atmosphere and be converted to nitramines or nitrosamines they will contribute to the environmental concentrations as calculated by the dispersion simulation method. In the granted permit the total sum of nitrosamines and nitramines must be below the given limits. Therefore both amine emissions and direct emissions of nitrosamines and nitramines will contribute to the total environmental budget of the harmful compounds.

Although sampling and analysis of flue gases in general are well known, the wet flue gas containing solvent amine, amine degradation products and other trace components give many sampling and analytical challenges. Very limited standard methods are established for such a task. Several studies were undertaken by international experts for the, now terminated, Carbon Capture Plant Mongstad (CCM) project, and much of the work is available for the public [7]. The CCM project developed a toolbox for qualifying amine based solvent technologies, consisting of the steps liquid sampling, isokinetic gas sampling, sample preservation and sample logistics, sample work-up and analytical procedures, atmospheric chemistry including dry and wet deposition, dispersion modelling including local Mongstad weather conditions, toxicology assessment of major degradation products as nitramines and nitrosamines, solvent degradation rig and test protocol for solvent stress testing as well as process emission reducing technologies. The analytical measurement chain was essential in the toolbox and it is also the basis for the current work.

This work is part of a continuous effort of gaining better understanding of the performance potential of the non-proprietary aqueous MEA solvent system, conducted by TCM DA and its affiliates and owners, in order to test, verify, and demonstrate CO_2 capture technologies [1, 2, 3]. The purpose of the current work is to provide results which quantify the amounts and the compositions of atmospheric emissions sampled and analyzed during amine plant operations treating CHP flue gases. A thorough overview and discussion of available equipment and instrumentation for monitoring of stack emissions will be given. The results are believed to provide realistic emission figures for emission monitoring and control for any future large scale carbon capture and storage (CCS) project due to the considerable size of the TCM DA amine plant.

2. Instrument and analysis

A description of the TCM DA amine plant is given elsewhere [1,2,3].

2.1 Overall system description and instrument position

Removing CO_2 from flue gas by using post-combustion amine based CO_2 capture reduces the emission of greenhouse gases to the atmosphere, but inevitably causes some emissions of amines and amine related degradation products to the atmosphere. Thus, qualitative and quantitative analysis of the emitted components is very important, but this task is far from trivial. For practical purposes, analytical instruments are preferably placed at ground level, but in that case a long sampling line (often >50 m) is required to direct the treated flue gas from the top of the absorber into the apparatus at ground level. This sample line has to be heated to well above the dew point of the gas to avoid condensation and possibly unwanted adsorption and/or reaction of emitted components.

TCM DA applies different measurement techniques to monitor and quantify the amounts and concentrations of emitted compounds. Some of the analyzer techniques currently applied on a permanent basis are;

- Fourier Transform Infrared (FTIR) Spectroscopy
- Proton Transfer Reaction Time of Flight Mass Spectrometry (PTR-TOF-MS)
- Manual isokinetic sampling technique with impingers and subsequent off-line laboratory analysis (carried out by TCM DA, Statoil CP Laboratory, SINTEF and Ramboll)

Online gas phase concentration measurements are also performed at ground level (via a sample line) using a Fourier Transform Infra-Red (FTIR) Spectroscopy instrument and a Proton Transfer Reaction – Time of Flight – Mass Spectrometry (PTR-TOF-MS) device. This online equipment is placed in an analyzer house at ground level. At the absorber top, isokinetic sampling is performed on a regular basis. There is an analyzer house and a shelter on the top of the amine absorber where all the equipment is located, as seen in Figure 1.

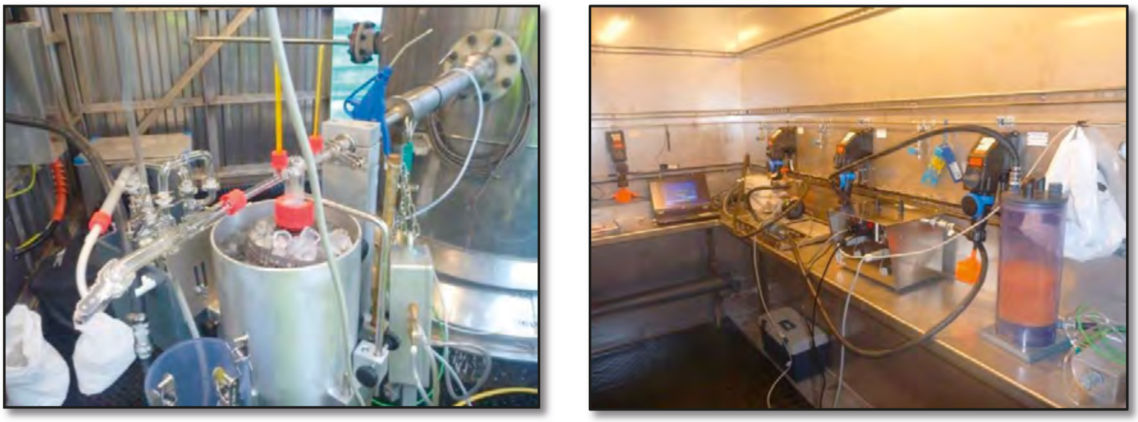

Figure 1: Emission sampling set-up on the top of the amine absorber. Stack configuration (left) and sampling control from analyzer house (right)

Extracted gas is sampled from the stack through an impinger train containing absorption liquids. By onsite measurement of the gas flow and laboratory analysis of the impinger liquids, the gas phase concentration of different components can be determined. The measurement system is shown schematically in Figure 2 and the techniques are further explained in the sections below.

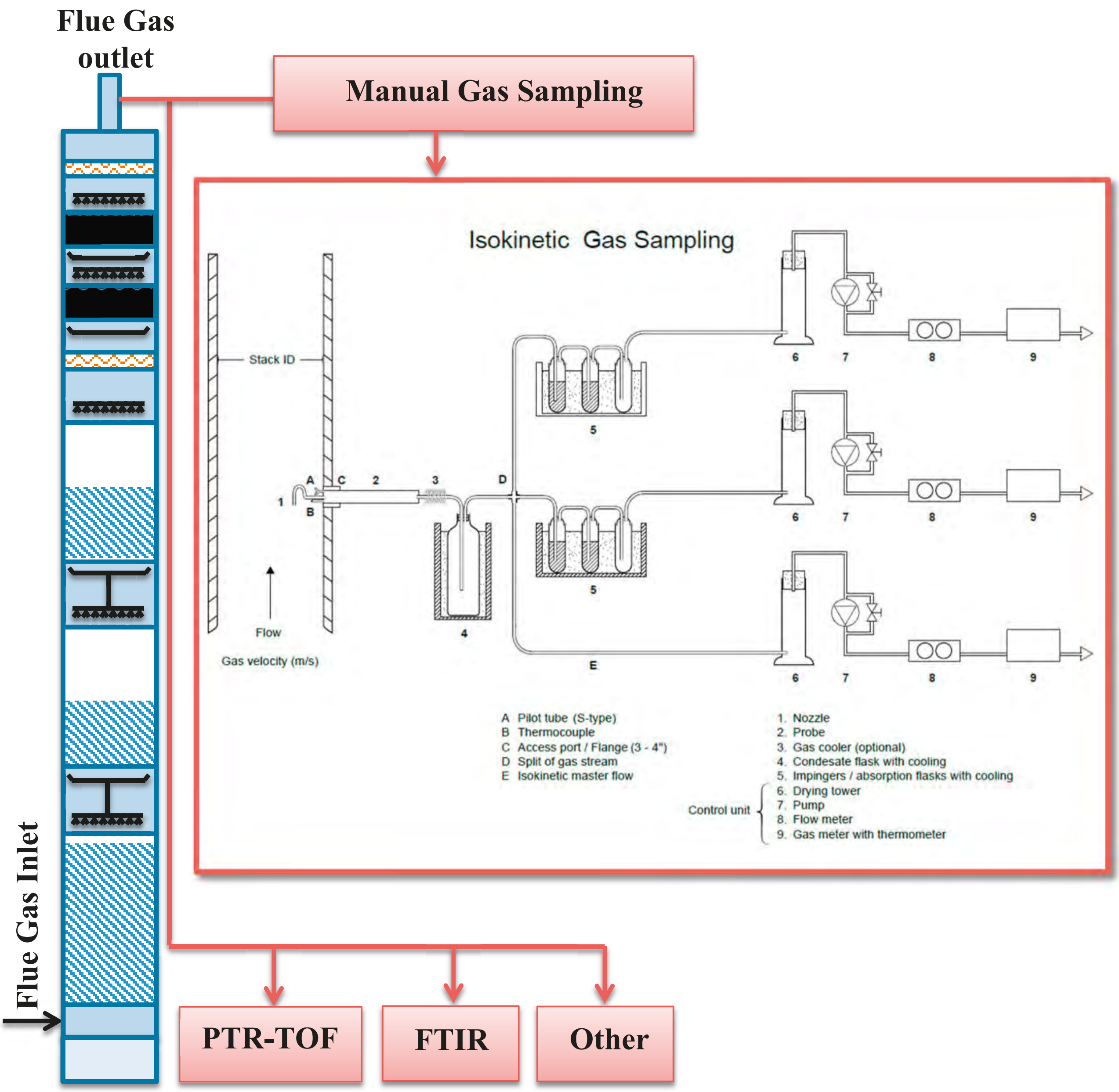

Figure 2: Schematic drawing of the emission monitoring set-up at the TCM DA amine plant

2.2 Sampling lines

The sampling line bundle installed at TCM DA is 101 meters long. It consists of 3 separate lines made from the following materials, respectively:

- PFA Teflon®
- Electro-polished stainless steel
- Sulfinert®-treated passivated stainless steel

All lines can be heated to 140 °C. Sample transfer via a heated sampling line has several benefits over placing the equipment at the top of the absorber:

- Easy access to the analyzer for maintenance and calibration and to utilities such as power, gas supplies, etc.
- Increased physical space for the analyzer
- Safer operations

Some negative aspects are however:

- Delayed analyzer response
- Potential degradation reactions and adsorption effects in the sampling line

Potential sample line effects are rarely reported in open literature. It is generally accepted is that the sample path should be kept as short as possible, and that the line temperature should be well above the dew point. However, increasing the temperature too much may lead to unwanted decomposition, to potential formation of nitrosamines, and to other sampling artefacts. Switch between different sample lines should be avoided due to memory effects. The effects of different sample lines were investigated by Cents et al [8].

2.3 FTIR analyzer

The FTIR model Anafin 2000 is employed at TCM DA to measure standard gas phase components (CO_2, water, NO_x, SO_x) as well as amines, aldehydes and ammonia. The analyzer operates at wave numbers between 500 and 7000 cm^{-1}, with a resolution of 2 cm^{-1}. The path length is 7 meters. The detection limit for amines, aldehydes and ammonia is on the order of 1 ppmv. According to the discharge permit from the Norwegian Environmental Agency (Miljødirektoratet), TCM DA is allowed to emit 6 ppmv of total amines as a daily average [6]. For this purpose, the detection limit of the FTIR instrument is satisfactory.

The FTIR is connected via heated sampling lines to sampling probes at the absorber inlet (downstream DCC), absorber outlet and desorber overhead condenser outlet. An automatic stream selector makes it possible to program the plant's control system to alternate between the different measuring locations as desired. The FTIR is calibrated for a list of standard flue gas pollutants, including CO_2, SO_2, NH_3, etc., as well as solvent amines and some volatile degradation products e.g. aldehydes. The instrument is not set up for measuring alkyl amines, nitrosamines and nitramines.

The FTIR technique has the advantage that the sample is measured without any preconditioning, hence reducing the risk for analytical artefacts. To avoid water condensation, the FTIR gas cell is heated to 85°C and the sampling lines are heated to 120°C. Target compounds contained in mist or droplets are likely to be evaporated at these temperatures. The FTIR monitor thus measures the total content of analytes in the flue gas. A draw-back of the FTIR technique is the interference from water vapor which results in a relatively high detection limit. The experience is that NH_3 and amines can be detected down to 1 ppm levels. This is also in accordance with earlier measurements of gaseous emissions in post combustion carbon capture [9, 10].

2.4 PTR-TOF-MS analyzer

The PTR-TOF-MS (model PTR-TOF 8000) used is manufactured by Ionicon Analytik (Innsbruck, Austria). The PTR technique has been widely used for environmental volatile compound measurements for over a decade. Its measurement principle is based on soft ionization, via proton transfer, followed by high mass resolution mass spectrometric analysis. At TCM DA, the PTR-TOF-MS instrument subsamples from the main sample line through a heated (100-130°C) Siltek inlet line. The sample flow is diluted by a factor of 10 to 20 with bottled synthetic (zero) air, to avoid ion signal titration caused by high ammonia levels. The PTR-TOF-MS is able to measure amines, ammonia, aldehydes, ketones, carboxylic acids, nitramines and nitrosamines which are all important target compounds in amine based CO_2 capture. The analytical setup at Mongstad is described in recent publications by Zhu et al. [11, 12].

2.5 Manual gas emission sampling

The analytical value chain applied for manual gas emission sampling and analysis is schematically shown in Figure 3. This value chain governs the measurement and is described in details below.

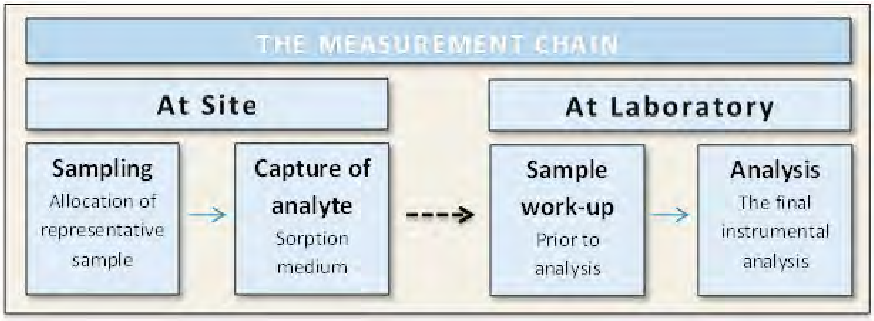

Figure 3: Schematic drawing of the emission measurement value chain

Sampling. The TCM DA stack is designed to achieve flow conditions suitable for isokinetic flue gas sampling as specified in the standard EN 15259:2007. The stack is insulated to minimize condensation. Sampling nozzles are located at a level 2 meters below the stack exit. A sampling system from Paul Goethe GmbH in Germany is used for allocation of a gas emission sample. The equipment is operated from an associated control unit (iTES). The special sampling equipment configuration is assembled for amine emissions based on experiences from the CCM project [7]. Isokinetic gas sampling principles are used to secure representative sampling from a ducted gas stream where two-phase conditions (particles or droplets with diameter > 1 μm) are present or may occur. From an amine absorber the presence of droplets in the flue gas has to be considered, hence isokinetic gas sampling is an assurance for representative samples.

Capture of analyte. The double tube sampling probe was cooled with pressurized air in order to start condensation of the extracted gas sample stream. Typical amine emission analytes are captured by two principles, condensation and liquid absorption. It is experienced that the main sampling step is condensation. The condensate flask is kept cool in an ice bath and has a size and design to maximize the condensation capacity. In this way the gas is dried and further downstream split to subsequent impinger trains or solid adsorbents. It is further experienced that only for the most volatile components like NH_3, small alkyl amines and aldehydes the second trap based on stepwise liquid absorption or solid phase adsorption is significant. In case of mist formation in the absorber, submicron aerosols will enter the sampling train. It is known that aerosols potentially can have limited retention through liquid sampling systems. In order to improve the capture of aerosols, a high capacity condensation step is followed by jet-impinger flasks to force agglomeration. However mist is normally not associated with the CHP flue gas.

The condensates were preserved with sulfamic acid at site directly after sampling to avoid potential nitrosation of secondary amines [7]. Ammonia and the different amines were absorbed in 0.05 M sulphuric acid, the aldehydes and ketones were adsorbed on DNPH cartridges (Sep-Pak DNPH-Silica Long Body Cartridges, Waters). For nitrosamines and nitramines 10 g/L sulfamic acid solutions were used as second sampling step.

Sample work-up. Samples were brought to TCM laboratory and immediately cooled or frozen for storage until analysis. As a principle the condensate sample was prepared for analysis first and subsequent absorbent solutions were prepared and analyzed secondly, with various experimental techniques (Table 1). This often includes extensive laboratory work.

Analysis. Expected degradation and emission products from a MEA based solvent system, were assessed from a recent study using the solvent degradation rig for stress testing of MEA [13]. The target analytes for the current work is given in Table 1. These compounds cover the requirements set forth by the Miljødirektoratet in the emission permit.

Table 1. TCM DA sampling and analysis configuration and principle for different parameters / component groups

Parameters/ component groups	**Sampling**	**Analysis**
Amines (solvent)	Condensate + 2x 0,05M sulphuric acid impingers + empty flask	LC MS QQQ
Amines (alkyl)	Condensate + 2x 0,05M sulphuric acid impingers + empty flask	UPLC-MS/MS (Ramboll [7])
Ammonia	Condensate + 2x 0,05M sulphuric acid impingers + empty flask	Cation chromatography, IC-ECD
Aldehydes	Condensate + 2x DNPH cartridges	LS MS QQQ
Nitrosamines* (Specific, generic and TONO)	Condensate + 2x 10 g sulfamic acid impingers + empty flask	See * (Ramboll [7])
Nitramines	Condensate + 2x 10 g sulfamic acid impingers + empty flask	UPLC-MS/MS or GC-HRMS (Ramboll [7])
pH**	-	pH-paper [7]
Nitrite (NO_3^-)**	-	Anion chromatography, IC-ECD [7]

*Specific; CLLE extraction followed by UPLC-MS/MS or GC-HRMS . Generic; LLE followed by analysis on GC-HRMS. TONO; Quench of soluted nitrite followed by break of N-NO bond in a reaction chamber. Total NO released from the N-nitroso groups detected by chemiluminscence analyzer.
**For sample preservation and work-up.

Amines, nitrosamines, and aldehydes were analyzed using an LC MS-MS QQQ (Agilent). The condensate from the first impinger was analyzed directly on the LC MS, the acidic impinger solutions were diluted before analysis. Ammonia was analyzed on an ion chromatograph (IC).

2.6 Additional analyzer techniques: Voice200 and PTR-QMS

TCM DA also tested a Voice200 analyzer from SYFT Technologies and a PTR-QMS 300 analyzer from Ionicon. These instruments operate on the same measurement principle as the PTR-TOF-MS but include cheaper and less specific quadrupole mass analyzers. Results from both analyzers compared well with the PTR-TOF-MS data. The results are not presented in this paper.

3. Results and Discussions

3.1 Analysis of Solvent samples

Solvent degradation processes were monitored during the course of the entire MEA campaign. The solvent amine, ammonia, and some degradation products were analyzed by TCM DA and Statoil CP laboratories. Alkyl amines, aldehydes, ketone, generic nitrosamines, solvent specific nitrosamines and nitramines were analyzed by Ramboll and SINTEF laboratories.
The concentration of the solvent amine was observed to remain stable over the extended period of the campaign indicating reasonable degradation rates of the solvent amine. The main degradation products of MEA were found to be amides, amino acids and other amines. Heat stable salts were also measured through the entire campaign, anions (OA, GA, FA, NO_3^-) by IC and total heat stable salts (HSS) by ion exchange and titration. Figure 4 displays the evolution of various degradation products and heat stable salts in the solvent. The components and amounts found were expected from an aqueous based MEA solvent system [9].

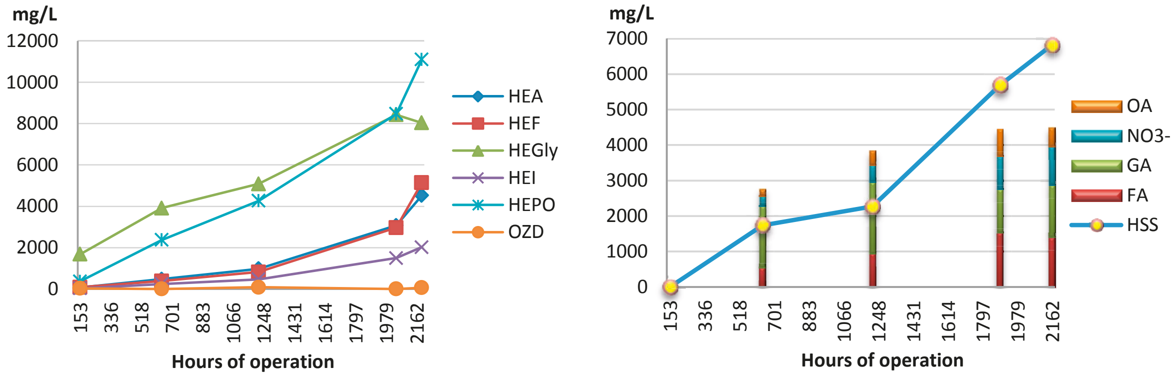

Figure 4: Results from some major degradation components (left figure) and heat stable salt formations (right figure) in the aqueous MEA solvent system during treatment of CHP flue gas

Two solvent specific nitrosamines, N-nitrosodiethanolamine (NDELA) and N-nitroso-2-hydroxyethyl-glycine (Nitroso-HeGly), were detected in the solvent as the degradation process progressed (Figure 5). The total concentrations of nitrosamines (TONO) were measured to be 797 µmol/L.

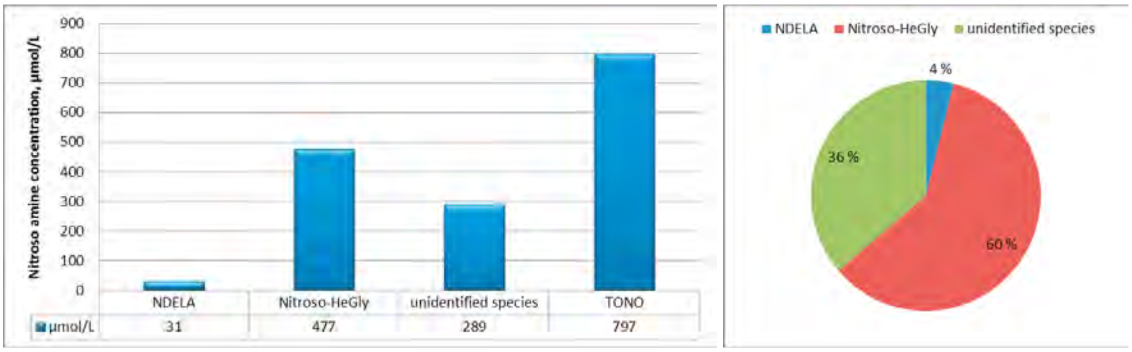

Figure 5: Results from degradation of solvent amine MEA (04.02.2014) [13]

Since MEA is a primary amine it is not expected to form a stable nitrosamine. The identified compounds are thus formed from secondary amines occurring as impurities in the solvent or being formed during the degradation reactions. As is shown in Figure 5, there are still some unidentified nitrosamines in the used solvent sample. These nitrosamines are formed from high molecular weight amines and have low volatility. Only in the first water wash stage low quantities of nitrosamines were found (see below).

The solvent specific nitramine (MEA-NO_2) was detected at a concentration of approximately 2 mg/L (Table 3).

3.2 Analysis of wash water samples

MEA was periodically measured in the wash water from both water wash sections. The wash water sections are specifically designed to physically absorb gaseous and entrained aqueous MEA before the depleted flue gas is emitted to atmosphere. Figure 6 shows that the liquid phase concentration in the first wash water section (Lower wash water – right y-axis) was about 100 times higher than the upper section (Upper Water Wash – left y-axis). The results from 16/12-2013 show higher results, the temperature in the flue gas was 47°C and this will give higher MEA concentrations. Going from 30 to 40 wt% MEA in the solvent, will also give higher MEA concentrations in the water wash sections and this is measured at 19/2-2014, where the solvent MEA concentration was 40 wt%. Methylamine and minor amounts of ethylamine were also found in water wash samples, as presented in Table 3.

Figure 6 clearly demonstrates the effectiveness of two water wash sections.

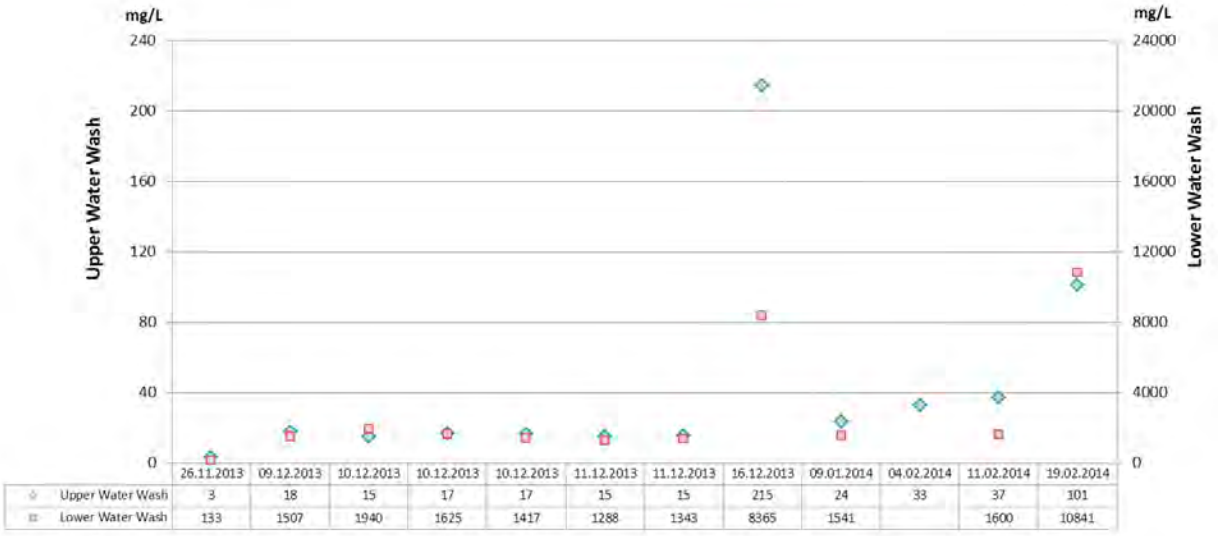

	26.11.2013	09.12.2013	10.12.2013	10.12.2013	10.12.2013	11.12.2013	11.12.2013	16.12.2013	09.01.2014	04.02.2014	11.02.2014	19.02.2014
◇ Upper Water Wash	3	18	15	17	17	15	15	215	24	33	37	101
□ Lower Water Wash	133	1507	1940	1625	1417	1288	1343	8365	1541		1600	10841

Figure 6: MEA concentrations in wash water 1 and 2.

The concentration of alkylamines, nitrosamines and nitramines in wash water samples are given in Tables 2 and 3. TONO were above detection limit only in the first water wash section, in one of two samples. This clearly indicates that nitrosamine volatility is low and that nitrosamines escaping from the solvent are efficiently captured in the first water wash section. No generic or solvent specific nitramines were found in either of the wash water sections.

Methylamine and minor amounts of ethylamine were found in low concentrations (µg/L) and it is seen that the water wash also has effect of these volatile compounds. No generic or solvent specific nitramines were found in either of the wash water sections.

Table 2. TONO (Total nitrosamines) measurement, measured by Ramboll (flue gas, wash water) and Sintef (lean MEA).

Date	Sample	TONO, µmol/L	Operational Conditions
11.02.2014	Wash water 2	<0.05	30 wt% MEA
11.02.2014	Wash water 1	0.13	30 wt% MEA
04.02.2014	Lean MEA	797	30 wt% MEA

Table 3. Degradation components in solvent and wash water measured by Ramboll

Compound	Unit	Wash water 1	Wash water 2	Lean MEA
		11.02.2014	11.02.2014	04.02.2014
Methylamine (MA)	µg/L	3700	1600	-
Dimethylamine (DEA)	µg/L	<50	<500	-
Ethylamine (EA)	µg/L	270	<500	-
Diethylamine (DiEA)	µg/L	<50	<50	-
Ethylmethylamine (EMA)	µg/L	<100	<1000	-
MEA	mg/L	1600	37	-
DEA	mg/L	<0.05	<0.5	-
Morpholine	mg/L	5.8	<1	-
MEA-NO2	µg/L	<1	<1	2120
Dimethylnitramine	µg/L	<0.2	<0.2	<2
Diethylnitramine	µg/L	<0.4	<0.4	<4
NDMA	µg/L	<0.1	<0.1	<1
NMEA	µg/L	<0.1	<0.1	<1
NDEA	µg/L	<0.1	<0.1	<1
NDPA	µg/L	<0.1	<0.1	<1
NPYR	µg/L	<0.1	<0.1	<1
NMOR	µg/L	<0.2	<0.2	<2
NPIP	µg/L	<0.1	<0.1	<1
NDBA	µg/L	<0.1	<0.1	<1
NDELA	µg/L	<1	<1	4200

3.3 Analysis of gas emission samples

Thirteen manual isokinetic sampling emission campaigns were conducted during the MEA-campaign. All emission samples were collected by TCM DA, except one which was performed by FORCE Technology. The amine plant operating conditions and detailed emission results are given in Tables 4 to 6. All nitrosamine and nitramine emissions were below detection limits. Emissions of alkyl amines were limited and only methylamine is quantified in the low ppb range. Possible emission of unknown compounds has been investigated via PTR-TOF-MS. A list of identified or tentatively identified compounds is given in Table 7. No alkylamines, nitrosamines and nitramines were detected by PTR-TOF-MS.

Table 4. List of emission measurements during the MEA campaign

Date and time	Start	Stop	Flue Gas volume, m^3/h	Temp. gas out, °C	Operational Conditions	Operational hours*
26.11.2013	09:14	11:14	58.000	46	30 wt% MEA	50
09.12.2013	10:33	12:33	50.000	25	30 wt% MEA	350
09.12.2013	13:33	15:33	50.000	25	30 wt% MEA	350
16.12.2013	10:38	12:38	47.000	43	30 wt% MEA	500
08.01.2014	12:11	14:11	49.000	25	30 wt% MEA	1000
08.01.2014	14:35	16:53	49.000	25	30 wt% MEA	1000
08.01.2014	17:12	19:12	49.000	25	30 wt% MEA	1000
09.01.2014	10:20	12:20	49.000	25	30 wt% MEA	1030
09.01.2014	12:40	14:40	49.000	25	30 wt% MEA	1030
27.01.2014	12:25	14:25	61.000	25	30 wt% MEA	1260
04.02.2014	11:53	13:53	62.000	27	30 wt% MEA	1390
11.02.2014	08:15	10:15	49.000	26	30 wt% MEA	1540
14.02.2014	10:50	12:50	62.000	25	40 wt% MEA	1600

* Operating hours counted as hours with CO_2 capture

Table 5. Result from isokinetic gas emission measurements during the MEA campaign

Date	MEA, $\mu g/m^3$	MEA, ppmv	NH_3, $\mu g/m^3$	NH_3, ppmv	Formaldehyde, $\mu g/m^3$	Formaldehyde, ppmv	Acetaldehyd, $\mu g/m^3$	Acetaldehyd, ppmv
26.11.2013	848	0.323	6413	8.3	-	-	-	-
09.12.2013	78	0.030	4907	6.3	-	-	-	-
09.12.2013	59	0.022	5242	6.8	-	-	-	-
16.12.2013	29	0.011	8907	11.5	-	-	-	-
08.01.2014	14	0.005	6336	8.2	-	-	-	-
08.01.2014	21	0.008	9611	12.4	-	-	-	-
08.01.2014	36	0.014	6452	8.3	-	-	-	-
09.01.2014	38	0.014	6729	8.7	-	-	-	-
09.01.2014	3.5	0.001	6806	8.8	-	-	-	-
27.01.2014	14	0.005	-	-	3.1	0.002	18.1	0.009
04.02.2014	12	0.004	-	-	4.4	0.003	31.7	0.017
11.02.2014	21	0.008	-	-	4.3	0.003	31.7	0.016
14.02.2014	22	0.008	10031	13	-	-	-	-

Figure 6 and Figure 7 display atmospheric emission results of MEA and NH_3 from absorber outlet over the entire campaign. Figure 6 display emission results from the FTIR and PTR-TOF-MS analyzer in comparison with results from manual isokinetic sampling and analysis. The MEA FTIR results are not considered to be reliable in the low ppm range, since they are below/around the detection limit. The first measurement (performed on the 26th of November) showed emissions above 300 ppb. The reason for the higher amine emission in the first measurement is related to amine plant operating conditions. The NH_3 emissions were reasonably low and as expected for MEA.

According to TCM DA experience the aldehyde concentrations were varying from low ppbv to several hundred ppbv during operations. Results found in this campaign and earlier campaigns are in agreement, and they are confirmed by third party. The FTIR is not measuring aldehydes below 1 ppm, but PTR TOF gives a good agreement to results found by isokinetic sampling and analysis, see tables 7 and 8. The PTR TOF is a good candidate for a reliable online analyzer of aldehydes in the ppb range.

Comparison of emission results from three sampling and analysis methods is somewhat tricky as there are some fundamental differences like; sampling point, sample extraction principles and sample transfer to the collecting or detection units. In this case manual samples are collected on the top of absorber using isokinetic extraction principles while the online methods are extracted non-isokinetic and switched in through a 101 meter long sampling line. Hence a comparison of MEA emission data can reflect differences in the sampling configuration. The analytical differences are first of all related to instrumental detection limits. Taking sampling and analytical differences into account the comparison of results is summarized and illustrated in figure 6. It is clear that the FTIR data is affected by high detection limit and by then increased uncertainty for this low ppm to ppb-level. Results from manual sampling and online PTR-TOF-MS are first of all according to both methods reported in a low concentration level (0,001 – 0,3 ppmv). The variation between the two data sets is significant and in general manual sampling reflects lower values than online PTR-TOF-MS results. Based on TCM-experience it is likely that the different sampling set-up explain this. TCM has experienced during this MEA campaign, that switch between different sampling points and long heated sampling lines are challenging and need to be tested more and further optimized to secure stable and representative gas composition.

The manual isokinetic sampling and analysis is considered to be a reference method for TCM DA. Isokinetic sampling and analysis is verified by two independent third party companies (during earlier campaigns by Kema/SGS and FORCE, and in this MEA campaign by FORCE).

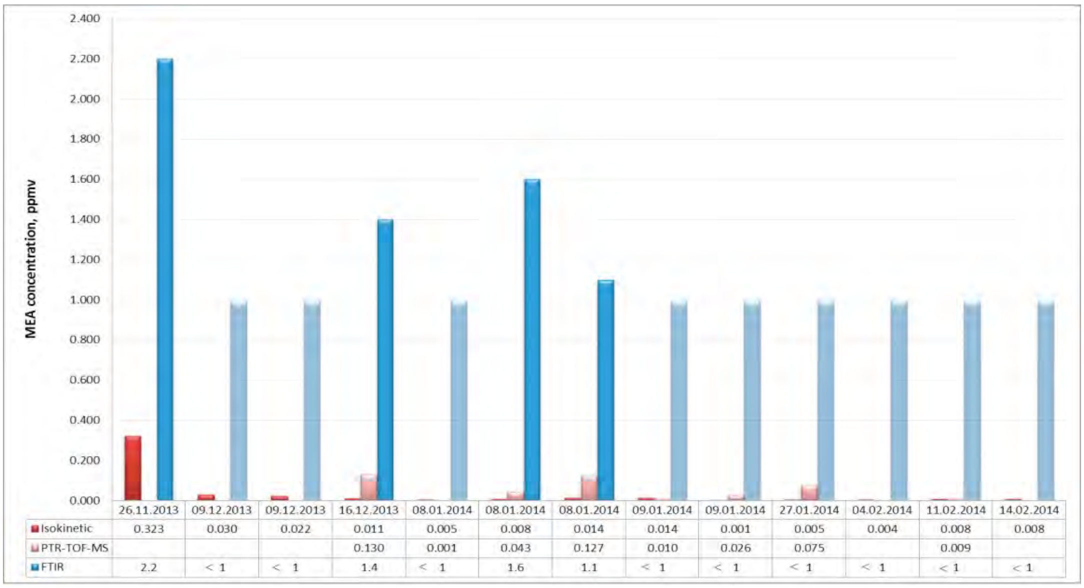

	26.11.2013	09.12.2013	09.12.2013	16.12.2013	08.01.2014	08.01.2014	08.01.2014	09.01.2014	09.01.2014	27.01.2014	04.02.2014	11.02.2014	14.02.2014
■ Isokinetic	0.323	0.030	0.022	0.011	0.005	0.008	0.014	0.014	0.001	0.005	0.004	0.008	0.008
■ PTR-TOF-MS				0.130	0.001	0.043	0.127	0.010	0.026	0.075		0.009	
■ FTIR	2.2	< 1	< 1	1.4	< 1	1.6	1.1	< 1	< 1	< 1	< 1	< 1	< 1

Figure 6: MEA emissions determined by different analyzer techniques during the campaign. Results on the FTIR below detection limit (<1 ppmv) are colored lighter blue.

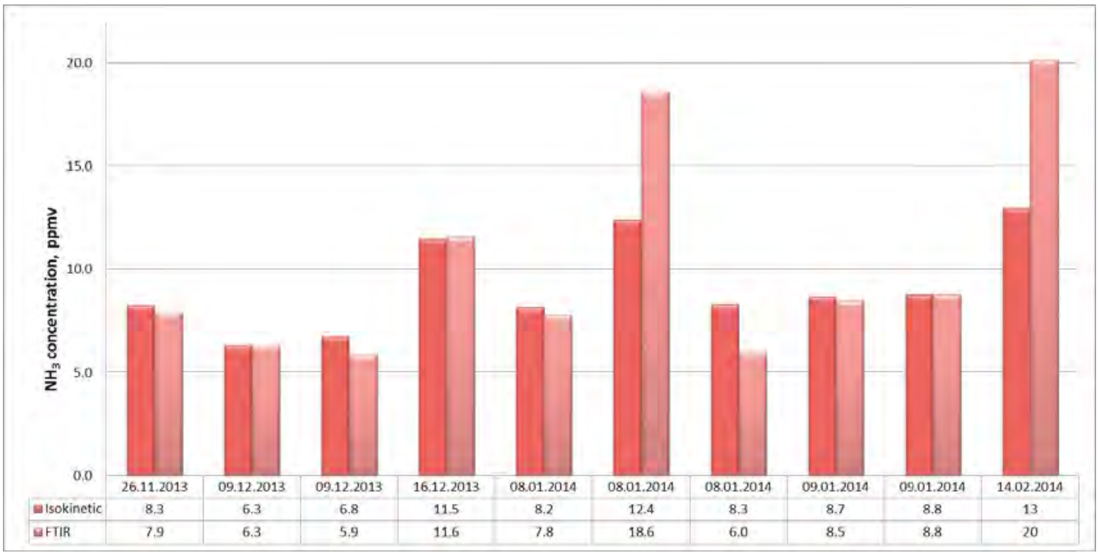

Figure 7: NH_3 emissions determined by different analyzer techniques during the campaign

Table 6. Degradation components in Flue gas out of absorber from isokinetic gas emission measurements.

	04.02.2014	04.02.2014	10.02.2014	10.02.2014
Compound	µg/m³	ppbv	µg/m³	ppbv
Methylamine	2.6	2	3.6	3
Dimethylamine	<1.1	<1	<1.1	<1
Ethylamine	<1.1	<1	<1.1	<1
Diethylamine	<1.1	<0.3	<1.1	<0.3
Ethylmethylamine	<2.2	<1	<2.1	<1
MEA	13	5	17	6
DEA	<1.1	<0.2	<1.1	<0.2
Morpholine	<2.2	<1	<2.1	<1
MEA-NO2	<0.01	<0.002	<0.01	<0.002
Dimethylnitramine	<0.002	<0.0006	<0.002	<0.0006
Diethylnitramine	<0.004	<0.001	<0.004	<0.001
NDMA	<0.001	<0.0003	0.001	0.0004
NMEA	<0.001	<0.0003	<0.001	<0.0003
NDEA	<0.001	<0.0002	<0.001	<0.0003
NDPA	<0.001	<0.0002	<0.001	<0.0002
NPYR	<0.001	<0.3	<0.001	<0.3
NMOR	<0.002	<0.0004	<0.002	<0.0004
NPIP	<0.001	<0.0002	<0.001	<0.0002
NDBA	<0.001	<0.0002	<0.001	<0.0002
NDELA	<0.01	<0.002	<0.01	<0.002
TONO*	<0.2	<0.04	<0.2	<0.04

*Converted from molar to mass basis, using M_w 130 g/mol

PTR-TOF-MS was also used for screening of potential other emissions. A list of identified or tentatively identified compounds is given in Table 7. It is noted that PTR-TOF-MS did not detect any emissions of alkylamines, nitrosamines or nitramines.

Table 7. Results from PTR-TOF-MS measurements on 11.02.2014, 08:15-10:15. Estimated uncertainty in measurements is ±20%.

Name	Formula	ppbv	Structure	m/z
2-aminoethanol	$H_2NCH_2CH_2OH$	8.9		62.060
Ammonia	NH_3	18265.7		18.034
Formaldehyde	HCHO	43.1		31.018
Acetaldehyde	CH_3CHO	454.9		45.033
Acetone	$(CH_3)_2CO$	88.2		59.049
Aceticacid	CH_3COOH	12		61.028
Formamide*	$CHONH_2$	13		46.028
Acetamide*	NH_2CH_2CHO	14.1		60.044
Methane,nitro*	CH_3NO_2	19.8		62.024
Ethane,nitro*	$CH_3CH_2NO_2$	0.8		73.039
Pyrrole*	C_4H_4NH	5.2	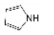	68.049
Pyrazine*	$C_4H_4N_2$	107.1		81.044
Pyrazinemethyl*	$C_4H_3N_2CH_3$	23.2		95.060
Pyrazinedimethyl*	$C_4H_2N_2(CH_3)_2$	7.1		109.079

* Tentative interpretation based on chemical formula, temporal profile or possible chemical pathway of formation.

3.4 Third party gas emission measurement

One third-party emission measurement was done on January 6. FORCE Technology carried out isokinetic sampling onto a solid sorbent (Thermosorb/N) in combination with condensate collection in an impinger. The condensate was analyzed separately. Analysis of collected samples was done by Isconlab GmbH. The results show that all nitrosamine and nitramine emissions were below detection limits.

Table 8. Results from third part measurement on 6th of January, done by FORCE Technology

Compound	µg/m^3
Total nitramine	<0.2
Total nitrosamine	<0.08
NDMA (N-nitrosodimethylamine)	<0.08
Formaldehyde	<70
Acetaldehyde	310

4. Conclusion

Extensive atmospheric emission monitoring has been conducted at the CO_2 Technology Centre Mongstad (TCM DA) during amine based post-combustion CO_2 capture. The TCM DA amine plant was operated with the aqueous MEA solvent system treating flue gas from a combined heat and power plant (CHP). Emission monitoring was conducted by a Fourier Transform Infrared (FTIR) Spectrometry analyzer, a Proton Transfer Reaction Time-of-Flight Mass Spectrometry (PTR-TOF-MS) analyzer, and manual isokinetic sampling followed by off-line analysis in the laboratory.

Atmospheric emissions of monoethanolamine (MEA) were very low throughout the complete campaign, and determined to be in the parts per billion (ppb) range. Atmospheric emissions of MEA amine based degradation products such as nitrosamines and nitramines were below detectable levels. Atmospheric emissions of ammonia (NH_3) were in the low ppm range, and alkyl amines in the low ppb range.

Absorber wash water sections were found to effectively reduce possible atmospheric emissions from amine based solvent system.

Acknowledgements

The authors gratefully acknowledge the staff of TCM DA, Gassnova, Statoil, Shell, Sasol, and Aker Solutions for their contribution and work at the TCM DA facility, and the staff of the Statoil CP laboratory for their contribution and work with the LC-MS measurements.

The authors also gratefully acknowledge Gassnova, Statoil, Shell, and Sasol as the owners of TCM DA and Aker Solutions for their financial support and contributions.

Appendix A. Abbreviations

AA	Acetic acid
CLLE	Continuous Liquid Liquid Extraction
DCC	Direct Contact Cooler
DiEA	Diethylamine
DMA	Dimetylamine
DMNA	N-nitro-N-methyl-methanamine
DMO	4,4-dimethyl-2-oxazolidinone
EA	Ethylamine
FA	Formic acid
GA	Glycolic acid
GC-HRMS	Gas Chromatography-High Resolution Mass Spectrometry
HEA	N-(2-hydroxyethyl) acetamide
HEF	N-(2-hydroxyethyl)formamide
HeGly	N-(2-hydroxyethyl)glycine
HEI	N-(2-hydroxyethyl)imidazole
HEIA	N-(2-hydroxyethyl)imidazolidinone
HEPO	4-(2-hydroxyethyl)piperazin-2-one
HSS	Heat Stable Salt
IC-ECD	Ion Chromatography-Electric Conductivity Detection
LC MS QQQ	Liquid Chromatography Mass Spectrometry Triple Quadrupole
LLE	Liquid Liquid Extraction
MA	Methylamine

NDBA	N-Nitrosodi-n-butylamine
NDEA	N-Nitrosodiethylamine
NDMA	N-methyl,N-nitroso-methanamine
NDPA	N-Nitrosodi-n-propylamine
NMEA	N-Nitrosomethylethylamine
NO2-MEA	2-(Nitroamino)ethanol
NO-HeGly	N-Nitroso(2-hydroxyethyl)glycine
NPIP	N-Nitrosopiperidine
NPYR	N-Nitrosopyrollidine
OA	Oxalic acid
TONO	Total Nitroso amines
UPLC-MS/MS	Ultra Performance Liquid Chromatography – Mass Spectrometry / Mass Spectrometry

References

[1] Thimsen D, Maxson A, Smith V, Cents T, Falk-Pedersen O, Gorset O, Hamborg E S. Results from MEA testing at the CO_2 Technology Centre Mongstad. Part I: Post-Combustion CO_2 capture testing methodology. Energy Procedia; 2014.

[2] Hamborg E S, Smith V, Cents T, Brigman N, Falk-Pedersen O, De Cazenove T, Chhaganlal M, Feste J K, Ullestad Ø, Ulvatn H, Gorset O, Askestad I, Gram L K, Fostås B F, Shah M I, Maxson A, Thimsen D. Results from MEA testing at the CO_2 Technology Centre Mongstad. Part II: Verification of baseline results. Energy Procedia; 2014

[3] Brigman N, Shah M I, Falk-Pedersen O, Cents T, Smith V, De Cazenove T, Morken A K, Hvidsten O A, Chhaganlal M, Feste J K, Lombardo G, Bade O M, Knudsen J, Subramoney S C, Fostås B F, De Koeijer G, Hamborg E S. Results of amine plant operations from 30 wt% and 40 wt% aqueous MEA testing at the CO_2 Technology Centre Mongstad. Energy Procedia; 2014.

[4] Eirik Falck da Silva, Karl Anders Hoff, Andy Booth; Energy Procedia 37 (2013) 784-790

[5] Gelein de Koeijer, Vibeke Randgaard Talstad, Sissel Nepstad, Dag Tønnesen, Olav Falk-Pedersen, Yolandi Maree, Claus Nielsen; International Journal of Greenhouse Gas Control 18 (2013) 200-207

[6] In: Norwegian Climate and Pollution Agency (Ed.), Tilllatelse til virksomhet etter forurensningsloven for TCM DA (Norwegian only), Norwegian Climate and Pollution Agency, Oslo, Norway (Now: Norwegian Environmental Agency (Miljødirektoratet))

[7] http://www.gassnova.no/en/ccs-projects/full-scale-mongstad/results-from-the-second-round-of-studies-of-the-health-and-environmental-issues-of-amines

[8] Toine Cents, Øyvind Ullestad, Anne Kolstad Morken, Olav Falk-Pedersen, Otto Bade, Gunnar Schade, Liang Zhu, Claus Nielsen. Measurement of emissions from the amine based CO2 capture plant at CO2 Technology Centre Mongstad. TWELFTH ANNUAL CONFERENCE ON CARBON CAPTURE, UTILIZATION AND SEQUESTRATION May 13 – 16, 2013 • David L. Lawrence Convention Center • Pittsburgh, Pennsylvania

[9] Jan Mertens, Marie-Laure Thielens, Jacob Knudsen and Jimmy Andersen. Monitoring and impacting gaseous emissions in post combustion carbon capture. IEAGHG PCCC1, 1st Post Combustion Capture Conference

[10] Jan Mertens, Dominique Desagher, Marie-Laure Thielens, Han Huynh Thi Ngoc, Helene Lepaumier, Purvil Khakaria and Earl Goetheer. On- and off-line ethanolamine and ammonia emission monitoring in PCCC. IEAGHG PCCC2, 2nd Post Combustion Capture Conference.

[11] Zhu, L., Schade, G. W. & Nielsen , C. J. Real time monitoring of emissions from monoethanolaminebased industrial scale carbon capture facilities. Environmental Science & Technology 47, 14306-14314 (2013)

[12] Zhu, L., Schade, G. W. & Nielsen , C. J. TCM emission measurements: results from PTR-ToF-MS measurements during use of MEA 2012. (2013).

[13] Aslak Einbu, Eirik DaSilva, Geir Haugen, Andreas Grimstvedt, Kristin Giske Lauritsen, Kolbjørn Zahlsen, Terje Vassbotn, Energy Procedia 37 (2013) 717-726.

Scale-up and Transient Operation of CO_2 Capture Plants at CO_2 Technology Centre Mongstad

(2014)

This article is behind a paywall.

SPE 171873

Scale-up and Transient Operation of CO2 Capture Plants at CO2 Technology Centre Mongstad

G.M. de Koeijer, Statoil ASA, K.I. Aasen, Statoil ASA, E.S. Hamborg, TCM DA

Copyright 2014, Society of Petroleum Engineers

This paper was prepared for presentation at the Abu Dhabi International Petroleum Exhibition and Conference held in Abu Dhabi, UAE, 10–13 November 2014.

This paper was selected for presentation by an SPE program committee following review of information contained in an abstract submitted by the author(s). Contents of the paper have not been reviewed by the Society of Petroleum Engineers and are subject to correction by the author(s). The material does not necessarily reflect any position of the Society of Petroleum Engineers, its officers, or members. Electronic reproduction, distribution, or storage of any part of this paper without the written consent of the Society of Petroleum Engineers is prohibited. Permission to reproduce in print is restricted to an abstract of not more than 300 words; illustrations may not be copied. The abstract must contain conspicuous acknowledgment of SPE copyright.

Abstract

The CO_2 Technology Centre Mongstad (TCM) is the world's largest facility for testing and improving technologies for CO2 capture. The knowledge gained will prepare the ground for full scale CO_2 capture initiatives to combat climate change. TCM is a joint venture between the Gassnova, Statoil, Shell and Sasol. It is located at the West coast of Norway, north of the city Bergen. This paper will discuss the scale-up and transient operation of amine based post-combustion CO_2 capture plants in general, and presents some typical results. Scale-up and transient operation are typically among the last topics to be assessed in the technology development process because it requires bigger plants. Results from the monoethanolamine (MEA) campaign that was executed in fall/winter 2013/2014 were used. Normalized transient data were presented for 7 important variables during a plant stop and restart and a sudden stop case. Stable CO_2 product flow could be obtained after 3-4 hours, while stable emissions and CO_2 product temperature took 1-2 hours more. NH_3 emissions showed a peak after restart due to accumulation in the solvent during the stop. It was concluded that amine based CO_2 capture plants should be able to follow their power plants without significant additional CO_2 emissions. Furthermore, the discussion on scale-up showed that the process of upscaling is ongoing and that emissions, material choice, construction method, vapour/liquid distribution and reclaiming are important technical aspects of this process. The main non-technical learning for efficient upscaling is to systematically learn from previous projects on how to build and operate cheaper.

For futher information: https://onepetro.org/SPEADIP/proceedings-abstract/14ADIP/3-14ADIP/D031S045R003/210190

CATCHING OUR FUTURE

Real-Time Monitoring of Emissions from Monoethanolamine-Based Industrial Scale Carbon Capture Facilities

(2013)

This article is behind a paywall.

Environmental Science & Technology
Article
pubs.acs.org/est

Real-Time Monitoring of Emissions from Monoethanolamine-Based Industrial Scale Carbon Capture Facilities

Liang Zhu,[†] Gunnar Wolfgang Schade,[†,‡] and Claus Jørgen Nielsen*[,†]

[†]Department of Chemistry, University of Oslo, P.O. Box 1033 Blindern, 0315, Oslo, Norway

Supporting Information

ABSTRACT: We demonstrate the capabilities and properties of using Proton Transfer Reaction time-of-flight mass spectrometry (PTR-ToF-MS) to real-time monitor gaseous emissions from industrial scale amine-based carbon capture processes. The benchmark monoethanolamine (MEA) was used as an example of amines needing to be monitored from carbon capture facilities, and to describe how the measurements may be influenced by potentially interfering species in CO_2 absorber stack discharges. On the basis of known or expected emission compositions, we investigated the PTR-ToF-MS MEA response as a function of sample flow humidity, ammonia, and CO_2 abundances, and show that all can exhibit interferences, thus making accurate amine measurements difficult. This warrants a proper sample pretreatment, and we show an example using a dilution with bottled zero air of 1:20 to 1:10 to monitor stack gas concentrations at the CO_2 Technology Center Mongstad (TCM), Norway. Observed emissions included many expected chemical species, dominantly ammonia and acetaldehyde, but also two new species previously not reported but emitted in significant quantities. With respect to concerns regarding amine emissions, we show that accurate amine quantifications in the presence of water vapor, ammonia, and CO_2 become feasible after proper sample dilution, thus making PTR-ToF-MS a viable technique to monitor future carbon capture facility emissions, without conventional laborious sample pretreatment.

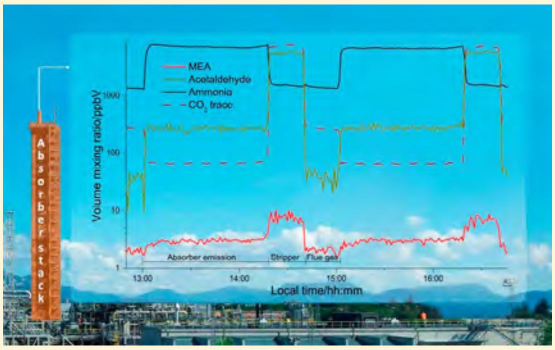

Futher information: https://pubs.acs.org/doi/10.1021/es4035045

Received: August 8, 2013
Revised: October 2, 2013
Accepted: November 11, 2013
Published: November 11, 2013

© 2013 American Chemical Society

CATCHING OUR FUTURE

Operational Experience and Initial Results from the First Test Period at CO_2 Technology Centre Mongstad

(2013)

Available online at www.sciencedirect.com

SciVerse ScienceDirect

Energy Procedia 37 (2013) 6348 – 6356

Energy Procedia

GHGT-11

Operational Experience and Initial Results from the First Test Period at CO_2 Technology Centre Mongstad

Vibeke Andersson[a*], Kristina Wittmeyer[b], Oddvar Gorset[a],
Yolandi Maree[b], Knut Sanden[a]

[a]*Aker Clean Carbon, N-1360, Oslo, Norway*
[b]*TCMDA, N-5954, Norway*

Abstract

The CO_2 Technology Centre Mongstad (TCM) is currently regarded as the largest CO_2 capture technology test center for testing and improving CO_2 capture. The aim of the TCM facility is to provide a platform for improving CO_2 capture processes by establishing the means for technology providers to further develop and verify their technologies on a larger scale, thereby promoting the application of CO_2 capture processes at full scale, worldwide.

The amine plant at TCM came on-line during the second quarter of 2012. This paper outlines the main functionalities of the amine plant and presents some operational experiences and initial results from the first operation period with MEA. Further testing in the plant over the next 15 months is dedicated to qualification programs aimed towards full third-party facilitated qualifications for large scale plants with ACC technology.

© 2013 The Authors. Published by Elsevier Ltd.
Selection and/or peer-review under responsibility of GHGT

Keywords: CO_2 technology demonstration; MEA; post combustion carbon capture; amine plant operation experience

---

* Corresponding author. Tel.: +47 928 56 744
E-mail address: vibeke.andersson@akersolutions.com

1876-6102 © 2013 The Authors. Published by Elsevier Ltd.
Selection and/or peer-review under responsibility of GHGT
doi:10.1016/j.egypro.2013.06.564

Nomenclature

ACC	Aker Clean Carbon
CCM	CO_2 Capture Mongstad (full scale project)
CHP	Combined Heat and Power
EPC	Engineering, Procurement and Construction
MEA	Mono Ethanol Amine
MTU	Mobile Test Unit
RFCC	Residue Fluid Catalytic Cracker
SRD	Specific Reboiler Duty
TCM	Technology Centre Mongstad
TCMDA	Technology Centre Mongstad Joint Venture

1. Technology Centre Mongstad

The CO_2 Technology Centre Mongstad (TCM) is currently regarded as the largest CO_2 capture technology test center for testing and improving CO_2 capture processes. The facility is owned by TCMDA - a joint venture between Gassnova (the Norwegian state) (75%), Statoil (20%), Shell (2.4%) and Sasol (2.4%) [1]. The facility's total capacity is 100 000 tons of CO_2 captured per year, and the test results will be valid for direct scale-up to full scale CO_2 capture plants. The design and functionality is described in detail elsewhere [2].

The aim of the TCM facility is to provide a platform for improving CO_2 capture processes by establishing the means for technology providers to further develop and verify their technologies on a larger scale, thereby influencing the applicability of CO_2 capture processes worldwide.

There are two capture plants installed at TCM, one utilizing amine technology, designed and delivered by Aker Clean Carbon (ACC), and the second utilizing a chilled ammonia technology, designed and delivered by Alstom.

The two technologies will both be tested on two different flue gas sources. One of the sources is off-gas from the Residue Fluid Catalytic Cracker (RFCC) at the Mongstad Refinery. In addition to being a typical refinery emission gas this source exhibits similar characteristics and properties as flue gas from coal fired plants. The other source is exhaust gas originating from the Combined Heat and Power plant (CHP) at Mongstad.

As part of the EPC contract awarded by TCMDA to ACC, ACC was allocated the right - upon delivery of the plant to TCMDA - to lease the facility for the first period of operation. In essence, ACC being the user of the facility will specify the test program for the first 15 months of operation. TCM DA has the responsibility of operations of the facility including the obtaining of emission permit [3], as well as provision of operational support. Detailed results from testing with ACC proprietary solvents are owned by ACC.

2. Amine Plant

2.1. Absorber and Regeneration units

The purpose of the absorber tower and the associated water wash sections is to absorb a minimum of 85 % of the CO_2 in the flue gas, to maintain the water balance in the plant and to minimize amine and amine degradation products in the treated flue gas before exiting the tower.

The absorber tower in the amine plant is more flexible than commercial CCS plants, with three absorption sections - each with a separate lean amine inlet and a total of 60 temperature sensors, thus enabling thorough investigation of solvent reaction rates and distribution. Results to date have shown clear temperature profiles in the areas of reactions when feeding at all of the three inlets, both horizontally as well as vertically over the packing. This, in turn, provides a comprehensive understanding of the packing height requirements while confirming proper liquid distribution throughout the column.

In the sides of the rectangular-shaped absorber tower, four columns are installed through which gamma radiation sources are fitted (on an ad-hoc basis) to provide a scan of the column internals [4]. This scan has been performed twice; the first serving as a base-line scan and the second was performed shortly after full load of the plant was achieved (flue gas and solvent load). The scans showed no abnormalities, and good liquid distribution profile through the tower. A third scan is planned after a few months of operation to assess if any blockages or mal-distribution have occurred.

Figure 1 : Absorber and regeneration units in the amine plant

The two water wash systems each consist of a three meter packing section, a holding tank, a pump and a cooler. The top washing section may be utilized as an acid wash section. Two demisters are installed - one above the last absorption section and one above the upper water wash packing section. Both water wash systems have been operated at full load (50 t/h and 60 t/h respectively) without acid addition. Very low levels of amines have been detected from the absorber flue gas (below 1ppm) which verifies that the current water wash system was appropriately designed for the MEA specific runs.

To accommodate for the difference in CO_2 concentration in the two flue gas sources, two strippers (desorbers) are installed. The strippers are installed with different types of reboilers, one is a plate and frame reboiler and the other is a shell and tube reboiler. This enables validation of reboiler suitability in various operating scenarios. The welded plate and frame reboiler has proven to be sensitive towards steam/water hammer, subsequently leading to micro-cracking of the internals. While this was being attended to, the RFCC reboiler was put in operation with no further difficulties experienced. The CHP reboiler is expected to be back in service for testing with the ACC propriety solvent soon.

Figure 1 shows a picture from the 3D model of the amine plant, illustrating the absorption and desorption sections.

2.2. Data collection and laboratory

To be able to ensure good technology qualification, a vast amount of data is collected from more than 1000 online instruments in the amine plant and more than 1100 in the utility plant. In addition, there are multiple sampling points for liquid sampling throughout the amine plant. A laboratory has been established as part of the TCMDA infrastructure to analyze the liquid samples using state-of-the-art technologies. As the analytical procedures for many of the measurements required for particularly emissions related activities are in the development phase, extensive amount of time has been spent in establishing methods within the TCM laboratory. This process is on-going as improvements to existing methods are made by outside research organisations. In conjunction to analyses, methods for physical sampling also had to be established. This relates in particular to the isokinetic sampling at the absorber tower exhaust.

Properties such as conductivity, pH and density are measured online in the amine streams and these data can also be verified by lab analyses. Also, emissions monitoring is mainly done online and is regularly verified by isokinetic sampling and lab analyses.

To establish the mass balances and to monitor emissions to air, an FTIR analyzer is installed, measuring various components in the inlet flue gas stream, the treated flue gas stream out of the absorber and the CO_2 product stream out of the regenerator. The FTIR analyzer is the main piece of equipment used for emissions reporting to the authorities, especially for amine, ammonia and aldehyde components [2]. All data is logged and stored in an IP21 data management system.

3. Utilities

The TCM plant provides its own utilities and also receives some utilities from the adjacent Mongstad refinery and the CHP plant. Utilities such as cooling water (seawater), demineralised water, plant and instrument air and nitrogen are provided from the TCM facility directly. The imported utilities include process (raw) water, fire water, potable water and high-pressure steam, which is provided at 30 Barg and 335 C. Both the technology plants have their own steam let-down systems to medium- and low pressure steam. The plants also have their own steam condensate receiving system from where the condensate is returned directly to the Mongstad refinery.

The two flue gas sources are first run through a separate blower to obtain enough transport pressure to reach the TCM plant. The RFCC flue gas is also run through a sea water cyclone for particle removal. The flue gas from the CHP has a CO_2 concentration of ca. 3.5 mole%. There is a possibility to recycle CO_2 when the CHP flue gas source is in use, to boost the CO_2 content up to 9 mole%. It is a relatively clean flue gas with small amounts of NOx, SOx and ammonia, see Table 1.

Table 1: Typical flue gas compositions

	CHP		RFCC	
Component	Concentration (mole %)	Concentration (ppmv)	Concentration (mole %)	Concentration (ppmv)
N_2	78.6		79.5	
CO_2	3.6		12.9	
H_2O	2.5		2.5	
O_2	14.4		4.2	
Ar	0.9		0.9	
NO_x		5		75
CO		3		3
SO_x		0.3		25
NH_3		5		

The online FTIR is set to measure the quality of the flue gas entering the system, but difficulties were experienced in the calibration of the instrument at low levels of NOx. The estimated detection limit of NO (as NOx) is 5ppm at this stage as interferences with water peaks were observed. The result was that the instrument read 0ppm for levels below 5ppm during most of the MEA specific run.

4. General operational experience at TCM

Hot commissioning of the plant was carried out with MEA and flue gas from the CHP. A successful stability test conducted as part of commissioning marked the hand-over of the plant from Aker Clean Carbon to TCMDA and at the same time marked the start-up of the ACC test period at TCM. The initial tests in this test period was also carried out with MEA and flue gas from CHP.

By the end of August 2012, the plant had been in operation capturing CO_2 for approx. 500 hours. Figure 2 below shows the time trend of the flue gas flow into the Absorber. The trend illustrates the operational period with CO_2 capture, during this time frame. It is worth noting that significant time during this period was dedicated to different commissioning-related activities, and several periods of down-time were necessary due to these activities, as evident from the figure. Figure 3 below shows both the accumulated operating hours of the amine plant and the accumulated CO_2 capture for this period.

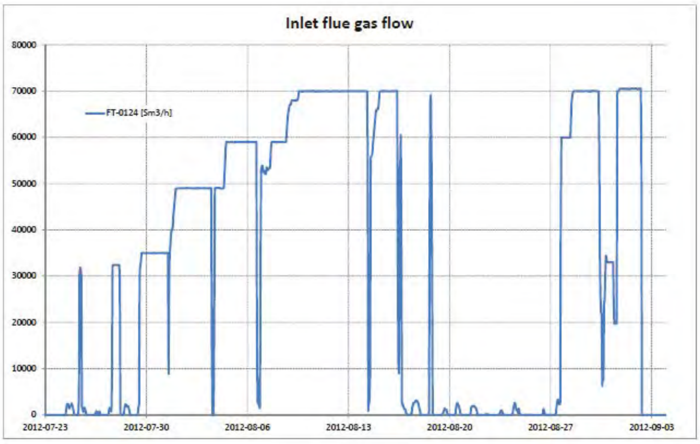

Figure 2: Inlet flue gas flow indicating operational periods, i.e.periods with CO_2 capture.

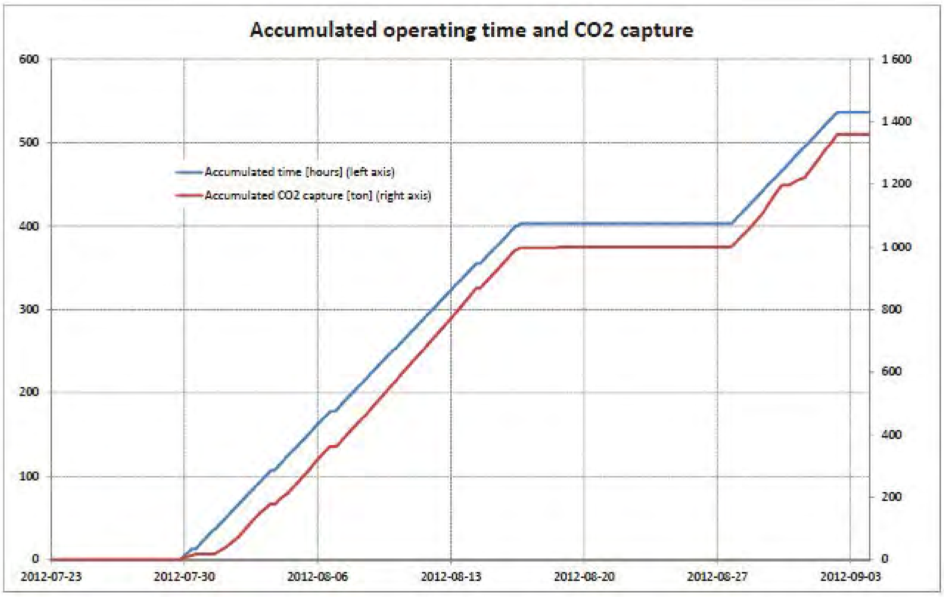

Figure 3: Accumulated hours of operation and CO_2 captured.

It *was* expected that a plant of such complexity in terms of amount of instrumentation would require substantial effort before normal operation was established. This has proven to be the case. The main operational focus this far has therefore been related to tuning of the plant, especially tuning of flow instruments and gas analyzers.

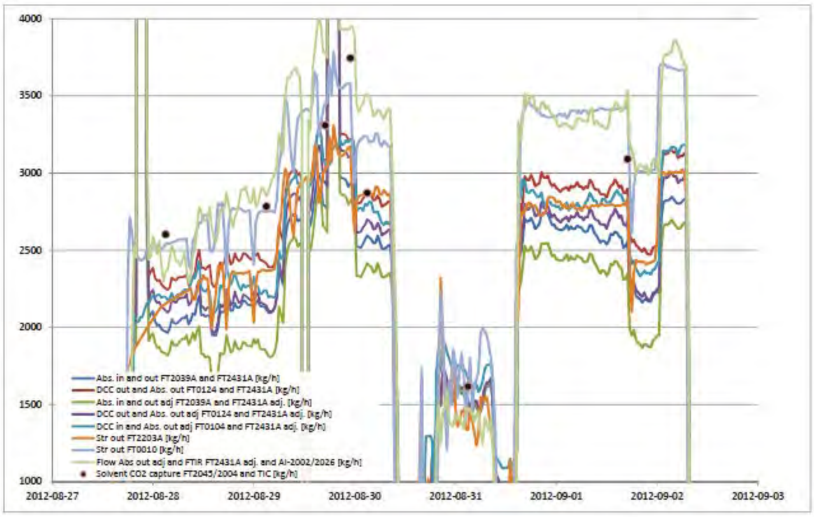

Figure 4: Illustration of mass-balance challenge

Figure 4 illustrates the challenge of mass balance closure, through different measured readings of the captured CO_2. A total of 8 online measurements as well as solvent analysis are available for calculating the CO_2 capture, and as seen, the readings had a discrepancy of ~40%. Through thorough investigations and testing of the flow meters set-up, we have now decreased the discrepancy and are able to close the balances to acceptable levels. Establishing and verification of the mass and heat balances, both in-house and by independent third party is still on-going at TCM.

5. Initial Results

5.1. CO_2 capture degree

During the initial start-up period, it was not our focus to maintain a constant CO_2 capture degree, or to maximize this. As seen from Figure 5, the capture degree has varied between 68% and close to 100% during operation. However, operational experience has now shown that the capture degree can be set at the required level and maintaining the capture at required 85-90% is achievable.

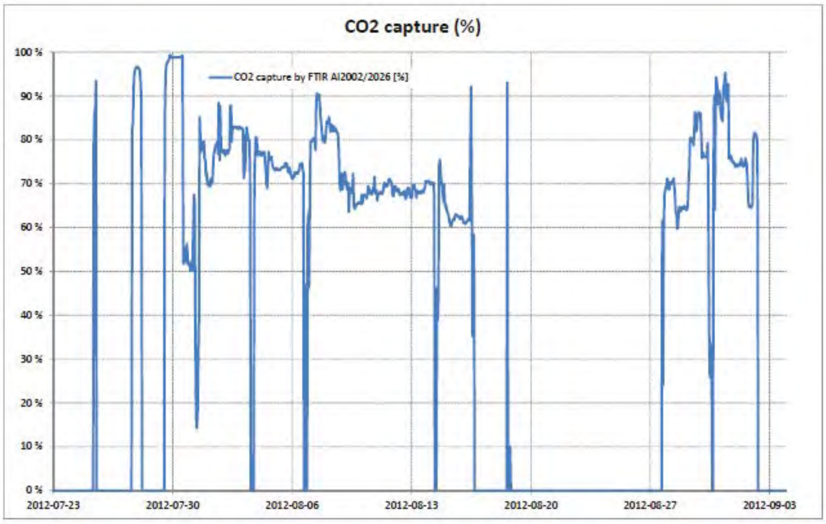

Figure 5: CO_2 capture degree throughout the period

5.2. Energy Consumption

The calculated Specific Reboiler Duty (SRD) in terms of MJ thermal/kg CO_2 captured is shown in Figure 6. Also in the figure, the measured steam consumption and the CO_2 capture is shown. The initially achieved SRD lies between 4.1 and 5 MJ/kg CO_2 and is within what we expected for MEA for these operational conditions, based on earlier experiences.

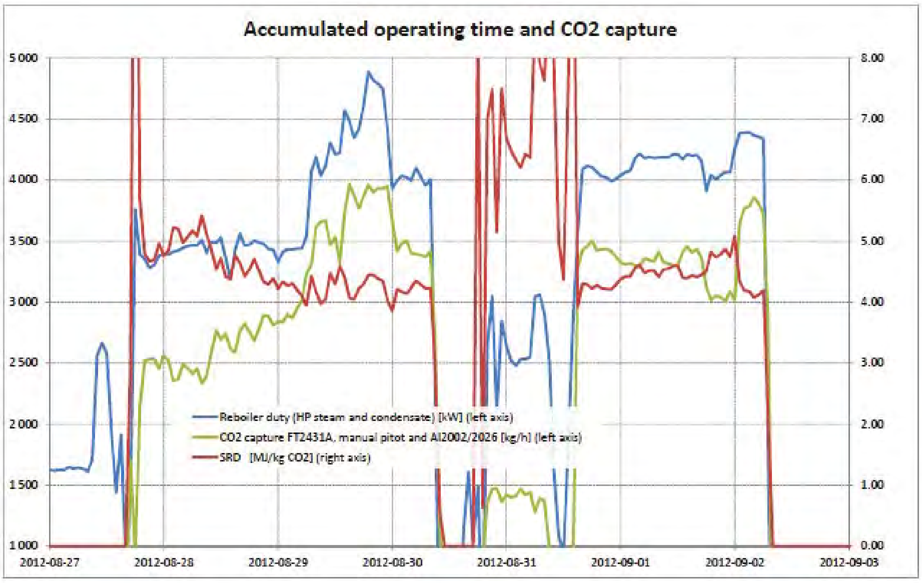

Figure 6: Measured energy consumption

5.3. Emissions

The surveillance and minimization of emission from the TCM plant was and remains top priority [2,3]. The emission from the amine plant is closely monitored through online measurements, isokinetic sampling and lab analysis. In Figure 7, the emission of MEA throughout the period as measured by the online FTIR instrument is shown. It is seen that during this first operational period, low levels of MEA emissions were detected with the online measurements, well within the expectation level and emission permit [2]. Superimposed on the graph are points representing the results from isokinetic sampling and laboratory analysis of MEA. As seen from the figure, these manual measurements have confirmed the readings from the online instrumentation.

6. Future Testing

ACC is responsible for developing a test program at TCM during the Test Period and will utilize the plant for their proprietary solvent development and technology qualification.

Recently, the MEA has been replaced with one of ACC's proprietary amines and for the next months, operation of the plant will be dedicated to a qualification program for the full-scale Mongstad project (CCM) using one of ACC's proprietary amine developed to minimize environmental impact and steam consumption The amine plant at TCM, ACC's Mobile Test Unit (MTU), testing at supplier and laboratory testing are all inputs to this program.

Following completion of the ongoing qualification program, a reference run with MEA (Baseline Reference Case) will be conducted, providing more details and confidence to the data presented as the first initial results. Subsequent to the reference case, ACC will continue to utilize the TCM plant for further testing of their proprietary solvent using both the CHP and RFCC flue gas source.

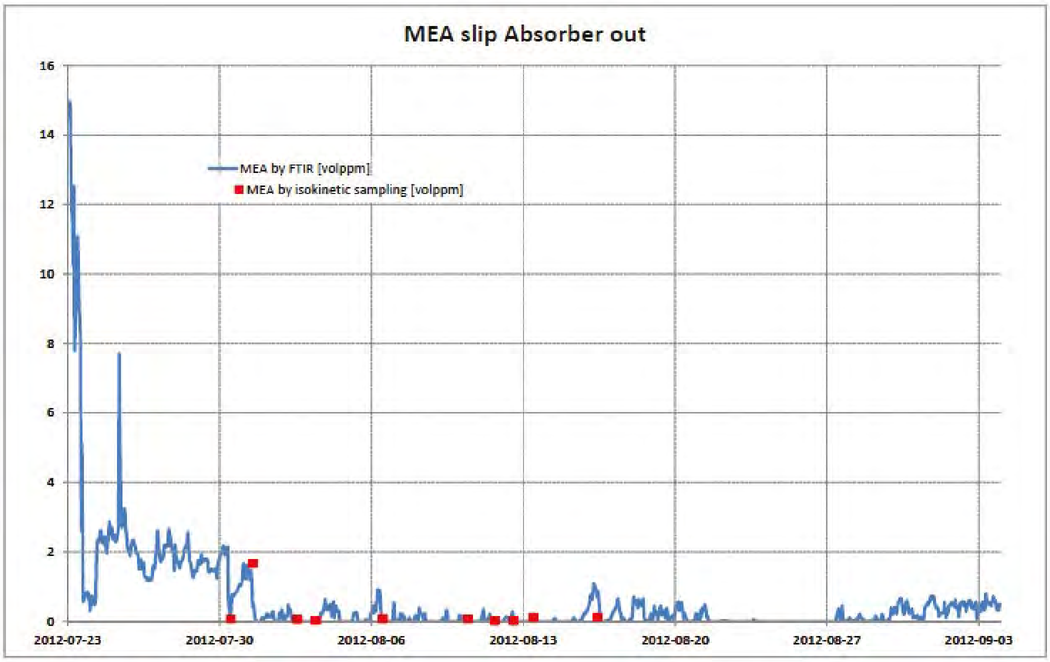

Figure 7: Emission profile as measured by online instrumentation as well as isokinetic sampling.

7. References

[1] www.tcmda.com

[2] De Koeijer G, Enge, Y., Sanden, K., Graff, O.Fr., Falk-Pedersen-, O., Amundsen, T. and Overå, S.; CO_2 Technology Mongstad – Design, Functionality and Emissions of the Amine Plant, GHGT10

[3] Maree Y, Nepstad S, De Koeijer G, Establishment of knowledge base for Emission Regulation for the CO_2 Technology Centre Mongstad. 2012.

[4] Gallon A, TRACERCO Diagnostics^{TM} Tower Scan of the Flue Gas Absorber, TCM unit, Mongstad – August 2012 [Restricted report]

Technology Centre Mongstad (TCM) is the largest and most flexible test centre for verification of CO_2 capture technologies and a world leading competence centre for CCS.

Here is an overview of the main topics where TCM has gathered together its professional contributions:

01	TCM Design & Construction
02	Operational Experience & Results
03	TCM Verified Baseline Results
04	Emissions – Limits, Measurements and Mitigation
05	Aerosols & Mist
06	Solvent Degradation, Management and Reclaiming
07	Process modelling, Scale-up and Cost reduction
08	Transient / Dispatchable operation & Process control
09	Corrosion & Materials
10	CESAR 1 Solvent
11	MEA Solvent

tcmda.com